

BIRLA CENTRAL LIBRARY

PILANI (Rajasthan)

Class No...5325

Book No...H 90.E

Accession No. 64578

Engineering Applications of Fluid Mechanics

Engineering Applications of Fluid Mechanics

By J. C. HUNSAKER

*Department of Aeronautical Engineering
Massachusetts Institute of Technology*

and B. G. RIGHTMIRE

*Department of Mechanical Engineering
Massachusetts Institute of Technology*

McGRAW-HILL BOOK COMPANY, INC.

NEW YORK AND LONDON

1947

ENGINEERING APPLICATIONS OF FLUID MECHANICS

COPYRIGHT, 1947, BY THE
MCGRAW-HILL BOOK COMPANY, INC.

PRINTED IN THE UNITED STATES OF AMERICA

*All rights reserved. This book, or
parts thereof, may not be reproduced
in any form without permission of
the publishers.*

x

31290

PREFACE

This book has grown out of some 12 years' experience with a course in fluid mechanics for an undergraduate class in the mechanical engineering department of the Massachusetts Institute of Technology.

The controlling importance of flow phenomena in nearly every type of machine and process led to the conversion of a traditional course in hydraulics into a more fundamental treatment of the action of fluids generally. The authors were more anxious that the student understand flow phenomena than that he be familiar with details of many practical devices. They attempted to give unity to the subject by the careful development, at an adult level, of the mechanics of fluids and to provide interest and utility by condensed treatment of selected types of engineering application.

The course is essentially an introduction to a field of engineering science that includes important subjects for later professional study. An introductory course should lay an adequate foundation for advanced work and should, therefore, deal both with mathematical reasoning and with experimental results. Recent advances in the efficiency of machines and engines have resulted from a better understanding of their operation. This understanding requires not so much the determination of over-all performance in terms of a few pressure and temperature measurements as a detailed exploration of flow conditions.

In such investigations fluid mechanics is of first importance, both in machines actually handling fluid, such as compressors and turbines, and also in engines, where controlled flow of air, fuel, and combustion gases is essential.

The application of Newton's laws of mechanics to fluids with the aid of the tools of mathematics gives an exact description of flow phenomena for certain idealized cases but only an approximate description for many practical cases. The greatest difficulty comes in real fluids from the effect of friction and the resulting turbulence and separation from the boundary surfaces designed to guide the flow. When the type of flow is too confused to be postulated with any confidence, mathematical analysis from first principles is usually hopeless.

First the naval architect and later the aeronautical engineer have been brilliantly successful in the use of models to solve such complicated problems. For this, a theory of similitude is necessary to ensure that the model experiments shall predict full-scale performance under the desired conditions. In view of the increasing importance of controlled experiments in

mechanical engineering, in this text the authors have gone into the theory of dimensions and physical similitude with some care. They believe that the student is entitled to a full explanation of the apparently simple rules for conducting model experiments.

The theoretical behavior of an ideal frictionless fluid has been discussed in order to introduce the student to basic concepts governing pressure and velocity distribution. While no real fluid is frictionless, in many engineering problems friction in the main flow may be neglected. At the same time, friction can be the controlling factor near solid boundaries, as Prandtl showed in his theory of the boundary layer. The student is expected to appreciate the simplicity and elegance of the mathematical treatment of the ideal fluid and also the validity and logic of the simplifying assumptions on which the treatment of frictional flow is based. For these reasons, the authors have given more weight to hydro-mechanics and boundary-layer theory than might be expected in an introductory text.

An explanation should perhaps be made of what may appear in the early chapters to be an overelaborate analysis of self-evident phenomena, such as the conditions of static equilibrium. A mathematical formulation of very simple physical relations is developed with some care to ensure familiarity with certain powerful methods of analysis needed later. For example, the device of a potential function is introduced as the potential energy of a gravity field, in anticipation of the later use of a velocity potential to describe a velocity field. Teaching experience indicates that the calculus needs restatement when applied to physical quantities.

The material in Chaps. I to VIII is essentially that presented during the first term of a two-term course in fluid mechanics. Parts of the remaining chapters are covered in the second term, with emphasis on topics in Chaps. X, XI, XII, XIV, XV, and XVII. The students for whom this material is intended have had 2 years of physics and mathematics, including differential equations, and 1 year of applied mechanics.

Since the student is taking a parallel course in thermodynamics at the same time, certain topics that might logically be included have been omitted. Furthermore, the class is also engaged in a sequence of laboratory exercises involving instrumentation, fluid measurements, and determination of the operating characteristics of many examples of machinery. While this book is designed to illuminate such laboratory work, it is in no sense a laboratory manual nor is it descriptive of current practice.

The treatment of servomechanisms is included for use in a separate one-term elective course.

Acknowledgment is made of valuable help from those who have given the course, notably R. von Mises, C. B. Millikan, and H. Peters. The chapters on lubrication were largely written by J. T. Burwell. M. Raus-

cher helped with the material on jets, and C. E. Grosser with that on hydraulic transmissions. The authors, however, are responsible for the end product.

J. C. HUNSAKER

B. G. RIGHTMIRE

CAMBRIDGE, MASS.

October, 1947

CONTENTS

PREFACE	v
I Introductory Survey.	1
II Statics	15
III Kinematics and Continuity.	54
IV Dynamics of an Ideal Fluid	62
V Energy Relations for Steady Flow	79
VI Momentum Relations for Steady Flow.	87
VII Dimensional Analysis and Similitude	98
VIII Incompressible Flow in Closed Conduits	122
IX Compressibility Phenomena	160
X Drag	182
XI Wing Theory	217
XII Hydrodynamic Lubrication.	278
XIII Boundary Lubrication	315
XIV Hydraulic Turbines	341
XV Pumps, Fans, and Compressors	360
XVI Propellers and Jets	381
XVII Fluid Couplings and Torque Converters	404
XVIII Hydraulic Transmissions and Controls.	414
APPENDIX	449
PROBLEMS	453
INDEX	489

CHAPTER I

INTRODUCTORY SURVEY

1.1. Definition. Fluid mechanics is the special branch of general mechanics that applies its fundamental principles to fluids. These principles are Newton's laws of motion, the conservation of energy, and the indestructibility of matter. Fluid mechanics can describe and predict the behavior of fluids to the extent that we know their physical properties and to the extent that practicable methods of applied mathematics can be found.

1.2. Objective. The primary objective of fluid mechanics for a mechanical engineer is twofold, (1) to explain the facts of experience by the deduction of general rules and (2) to apply such general rules to predict, at least to a practical approximation, the fluid phenomena involved in the performance of ships, airplanes, engines, compressors, turbines, pipe lines, and wherever a working fluid is involved in the operation of machinery. The rules of fluid mechanics are also fundamental to lubrication, convective heat transfer, ballistics, oceanography, and meteorology, where important modern developments have taken place as a result of analysis of observed facts. In nearly all actual cases, some simplifying assumptions must be made as to the physical properties of the fluid or as to the character of the flow.

1.3. Fluids and Solids. The word "fluid" (from Latin *fluidus*) means a substance having particles that readily change their relative positions. Fluid refers, therefore, to both gases and liquids, as opposed to solids.

Solids and fluids behave differently under the action of an applied force. The force necessary to produce deformation of a solid depends mainly on the amount of the deformation, as, for example, in the case of a spring. The force must be maintained in order to hold the deformation. In the case of a fluid the force depends primarily on the speed with which a deformation is produced. Such force tends to vanish when the speed of deformation approaches zero. The increased resistance accompanying any increase in the speed of a solid body moving through a fluid illustrates this characteristic.

1.4. Viscosity. A fluid has the property of resisting deformation in proportion to the rate of deformation. Experiment shows that in a flooded journal bearing in which the shaft and bearing are concentric the following proportionality holds:

$$\frac{F}{2\pi aL} \sim \frac{V}{h}$$

1

where F is the tangential force acting on the lubricant at the surface of the shaft and the other quantities are shown in Fig. 1.1. Since it is known that a fluid does not slip at a boundary, the ratio V/h measures the rate of deformation of the oil in the bearing. The ratio $F/2\pi aL$ is the shear force

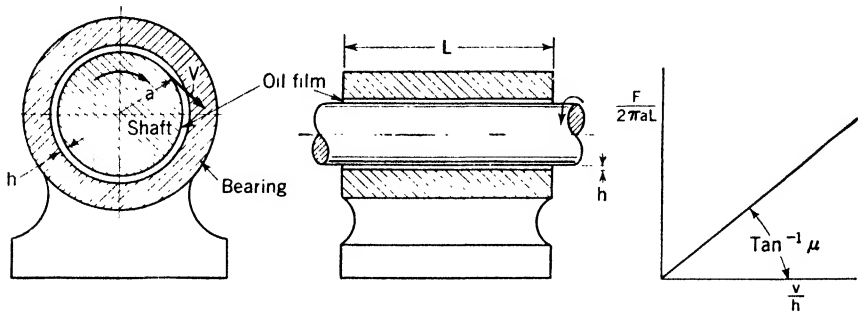


FIG. 1.1. — Oil viscosity causes shearing stress on the shaft of a flooded journal bearing.

per unit area, or shear stress exerted on the oil. The factor of proportionality between shear stress and rate of deformation is a property of the lubricating fluid and is called the “coefficient of viscosity” or, simply, “viscosity.” The defining equation for viscosity of the lubricant in the journal bearing of Fig. 1.1 is

$$\text{Shear stress} = \frac{F}{2\pi a L} = \mu \frac{V}{h} \quad (1.1)$$

where μ is the viscosity. It is seen that the shear stress persists as long as the ratio V/h is greater than zero.

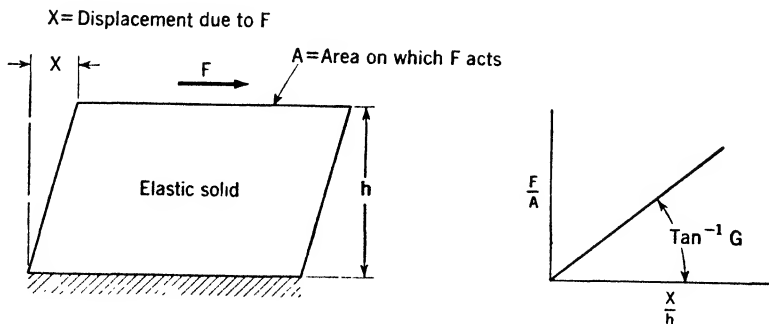


FIG. 1.2. — Shearing stress is proportional to deformation of an elastic solid.

Many substances, like metals, become true fluids when heated, while quasi solids, like jelly, pitch, and grease, may behave like fluids of very high viscosity.

For an elastic solid deformed by a shear force F the following equation holds:

$$\text{Shear stress} = \frac{F}{A} = G \frac{x}{h} \quad (1.2)$$

where G is a property of the solid called the "shear modulus" and the other quantities are shown in Fig. 1.2. The analogy between Eqs. (1.1) and (1.2) is obvious.

1.5. Plasticity. Metals heated just short of the melting point or strained beyond the elastic limit no longer behave as elastic solids but deform continuously under a constant load. This phenomenon of creep is characteristic of the plastic state of many solids. A metal in the plastic state is still polycrystalline and is not a fluid until melted. Hot metal in the rolling mill is plastic; so is cold metal under the very great local forces involved in wire drawing, press-forming, or cold-riveting. A yielding material that does not resist shear in proportion to the rate of shear is sometimes called a "non-Newtonian liquid." Heavy grease at low temperatures may exhibit a definite yield point and act like a plastic rather than like a true liquid.

The methods of fluid mechanics are ordinarily inapplicable to substances in the plastic state.

1.6. Perfect Fluid. Since real substances may partake of the fluid state to various degrees depending on conditions of temperature and pressure, application of the principles of fluid mechanics can be greatly simplified if the analysis is first made for an imaginary perfect fluid that is nonviscous, *i.e.*, for one that is subject to no shearing stress during motion. The assumption of such a frictionless fluid, under many circumstances, leads to very fair approximations to the behavior of real fluids of low viscosity, such as, for example, air, water, and alcohol.

It should be noted that in problems of statics, since there is no motion, it is unnecessary to postulate a perfect fluid because the effect of viscosity is nil.

1.7. Liquids and Gases. A fluid may be either a gas or a liquid. A gas completely fills the region within given boundaries regardless of the amount of gas enclosed, while a definite amount of liquid is required to fill a given region. A smaller amount of liquid will fill only part of the region, a free surface being formed as one boundary. In the words of Sir Oliver Lodge: "A solid has volume and shape, a liquid has volume but no shape, a gas has neither."

The most important difference between a liquid and a gas, from the viewpoint of fluid mechanics, is the fact that a liquid, like a solid, is practically incompressible under ordinary conditions, while a gas can be readily compressed. When the change in density of a gas is small, however, it can often be treated as an incompressible fluid to a good approximation.

A vapor is a gas that condenses to a liquid under lowered temperature or increased pressure. The pressure at which vapor begins to condense at any given temperature is called the "vapor pressure" or "saturation pressure." This pressure forms a limit below which laws applicable to gases cannot be used. Strictly speaking, all gases are vapors, since they can be condensed under extreme conditions. Vapors, however, behave like true gases under conditions sufficiently far removed from the saturation pressure.

In this study of fluid mechanics the treatment will ordinarily be restricted to practically incompressible fluids, with consideration given to compressibility only in special cases.

1.8. Concepts. The behavior of fluids is extremely difficult to describe or to observe in detail because there are no separate elements to be seen. In the mechanics of solid bodies we deal with separate entities of known dimensions and motions. A fluid, however, is continuous throughout a space, though its motion may be different at every point. Pressure, density, and temperature may vary throughout the space. Sometimes the flow seems to be regular, as if in layers, or laminar, and at other times it is confused and turbulent. Under some conditions large whirls or eddies occur.

Analysis is hopeless unless we can distinguish the conditions that are associated with the various types of behavior. Our method will be first to observe characteristic situations and then to devise simple idealized conditions that give an approximation of what has been observed. This method leads to a further classification, not as to the properties of the fluid itself, but rather as to the conditions under which the fluid is acting. Certain concepts will be required to define these conditions.

1.9. Continuity. The most conspicuous feature of fluids is that they generally exist and move as a continuous body of substance without voids. We postulate for analysis continuous flow such that at no place is fluid created or destroyed. We, in effect, affirm conservation of matter. Furthermore, we observe that in general, as in a river, the velocity, pressure, temperature, and density vary continuously from point to point at a given instant of time but at a given point may vary with time if the flow is not steady.

1.10. Continuum. This observation leads to the idealized conception of a continuum in which the quantities characterizing the flow, such as velocity, pressure, and density, are continuous functions of time and position. It then remains to consider under what conditions such a continuum represents our experience and also what meaning to attach to such ideas as pressure, density, and velocity at a point. When we examine these questions later, we shall conclude that gas in a vacuum tube contains too few molecules to be treated as a continuum. We shall see also that, under

some conditions of flow, velocity is not a continuous function of position but may change suddenly at a so-called "surface of discontinuity" which separates, for example, a jet of air from the surrounding atmosphere.

1.11. Statics. We may greatly simplify our analysis if we first confine our attention to fluid at rest. It is common knowledge that liquids come to equilibrium with less dense fluid on top. We also know that the barometric pressure on a mountain peak is less than in a valley and that a deep-sea diver is subjected to greater pressure as he goes deeper. Furthermore, the phenomenon of convection, due to heating lower layers of fluid, is a rupture of a previous condition of stable equilibrium. From the principles of statics we can explain why a ship floats, why balloons rise in the air, and why other phenomena concerned with the stability of fluid at rest occur as they do.

1.12. Dynamics. Since flowing fluid is subjected to dynamic forces due to the motion, the distribution of pressure and density in the continuum, as determined by static conditions, can be greatly modified by the motion. By the principle of the conservation of energy we can predict the interchanges between kinetic and potential energy as a flow proceeds, and by means of a special form of Newton's second law of motion we can predict the dynamic forces exerted by the fluid.

In the mechanics of solids Newton's second law relates the force on a body of known mass to the rate of change in its momentum. In fluid mechanics individual masses are not distinguishable, and it is necessary to deal with a portion of the continuum contained within imaginary fixed boundaries. The resultant external force exerted on the fluid that at any instant lies inside this fixed "control volume" equals the rate of change of momentum of this fluid. Under certain conditions this force simply equals the difference between the rates of outflow and inflow of momentum across the boundary of the control volume.

1.13. Compressible and Incompressible Gases. We may simplify both the static and the dynamic problems of fluid mechanics by the assumption of constant density throughout the continuum. This is exactly what has been done in hydraulics, which deals exclusively with liquids. We know from experience that liquids are practically incompressible. Only when we deal with pressure waves in a liquid are we concerned with its compressibility.

Gases, however, are easily compressed, and substantial volume changes are produced in various types of machinery. For moderate changes in level the atmosphere behaves like an incompressible fluid, and appreciable density change requires an increase in altitude of the order of a mile. Likewise, for ordinary velocities (less than 250 mph) the density change produced by the motion is only a small fraction of the normal density. For velocities approaching the speed of sound (about 750 mph) compressibility is very important.

The facts of experience, therefore, tell us that liquids and atmospheric air may be treated as incompressible fluids in many practical cases. Air need be treated as a compressible fluid only where great density changes are brought about, as by great change in height, by machinery, or by extreme velocity.

For any object moving through a fluid there is some place on its surface where the relative velocity of the fluid is substantially higher than the velocity of translation. Consequently it is possible for this local velocity to reach the velocity of sound while the translatory velocity is subsonic.

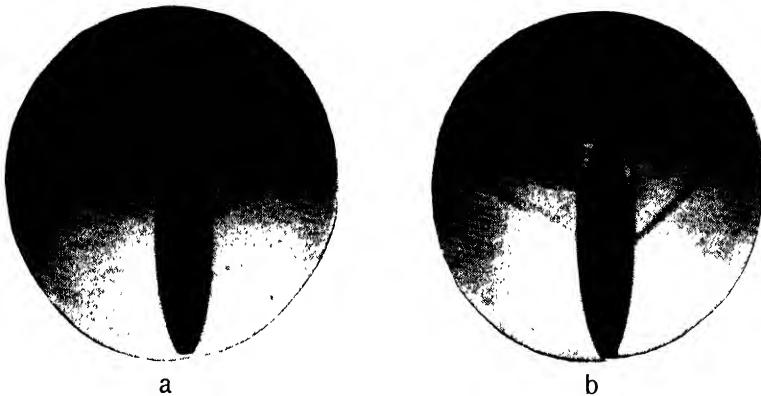


FIG. 1.3. — *a*. Flow past an airfoil at a speed well below that of sound. *b*. Flow in which sound velocity is reached locally in a region below the slanting dark lines (shock waves). The flow is upward in both pictures.

The velocity of translation at which local sonic velocity is encountered determines a critical speed for the particular shape of body, marked by the presence of standing compression waves.

Figure 1.3*a* is a photograph of the upward flow of air past an airfoil at a speed of 0.422 sound velocity. Figure 1.3*b* shows the flow pattern for the critical air speed at 0.776 sound velocity. The photographic method used makes visible variations in air density. In Fig. 1.3*a* the airflow is relatively smooth, and no marked discontinuity of density can be observed except close to the tail, where the flow separates to form a turbulent wake. At critical speed, Fig. 1.3*b* shows a great change. The dark lines across the airflow indicate regions of rapid change in density. Behind these lines the flow separates from the airfoil, and a broad wake is formed. The critical speed is marked by a large and abrupt increase in resistance.

The difference in the flow for the two photographs is a consequence of compressibility. At critical speed the airflow next to the thickest part of the model has reached the speed at which a pressure wave is propagated. Hence, pressure changes on the rear of the model cannot influence the flow over the forward part since a pressure change cannot be propagated upstream. To preserve equilibrium a discontinuity of pressure (and density)

occurs in the form of standing waves, or "compression shocks," shown by the dark lines. The very sharp increase in pressure at the compression shocks forces the flow to separate from the model, leaving a broad wake. In general, a critical flow is unsteady, and the position of the compression shocks fluctuates with time.

The technical measure of high speed is the Mach number M , defined as the ratio of the general flow velocity to the velocity of sound in the fluid. Subsonic velocity is indicated by $M < 1$ and supersonic velocity by $M > 1$. Airplanes fly at subsonic velocity but may reach a critical speed in a dive with consequent serious effects on control and structural integrity. Propellers, superchargers, and other machinery frequently handle air at critical speeds and higher. Bombs dropped from a great height may attain and pass through a critical velocity. Projectiles are fired with an initial supersonic velocity.

In the discussion of the dynamics of fluid motion, compressibility cannot be neglected when the Mach number approaches unity.

1.14. Steady Motion. The simplest case of flow is a steady motion whose pattern is the same at all times. Such a flow is seen in the steady jet from a nozzle, the steady current in a river, or the steady wind at a good height above the ground. Mathematically we express this statement that the velocity field is independent of time and depends only on the space coordinates x, y, z thus:

$$V = f(x, y, z)$$

Steady motion may be incompressible or not, depending on whether the density is constant or a function of location.

1.15. Boundary Layer. When one looks over the side of a vessel proceeding in smooth water, a belt of so-called "friction eddies" is seen, made visible by day because of air released and often by night by phosphorescence in the water. Just outside this belt the flow seems to be steady and of the order of the velocity of the ship. Since the water wets the ship and is carried along with it, there is, close to the ship's hull, a high velocity gradient that makes viscosity important and creates a strong frictional drag on the hull (see Fig. 1.4).

Outside the boundary layer the velocity gradients are small; hence, for this steady motion, friction or viscosity should be unimportant. The fluid outside the boundary layer seems to flow in a steady and frictionless manner.

Accordingly, to approximate the complicated motion of real fluids, it has been found generally useful to consider the continuum as made up of two distinct and separate portions, the boundary layer and wake, where friction controls the motion, and the region outside, where friction can be neglected. The justification for this concept, due to Prandtl, is its evident

resemblance to the observed state of affairs and the useful practical results that can be obtained from analyses based on it.

Observation of real fluids shows no discontinuity in velocity through

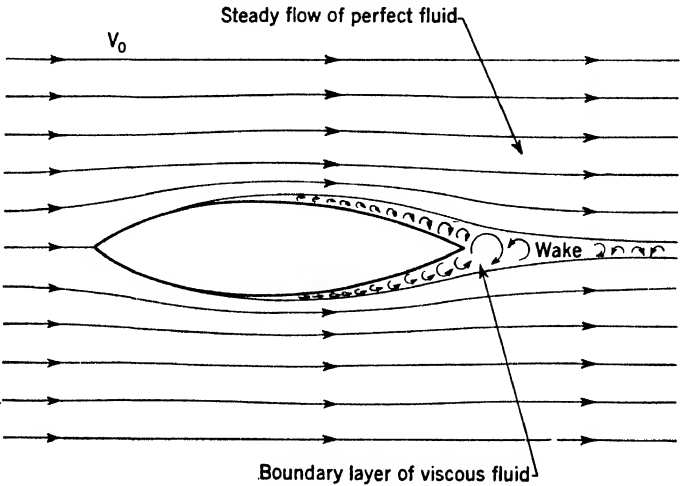


FIG. 1.4. — Fluid particles entering the boundary layer adjacent to a body are set into rotation by the action of viscosity.

the boundary layer. Figure 1.5 indicates a rapid but smooth transition of velocity from zero to V_0 in passing out from the ship's side through a boundary layer such as is represented in Fig. 1.4.

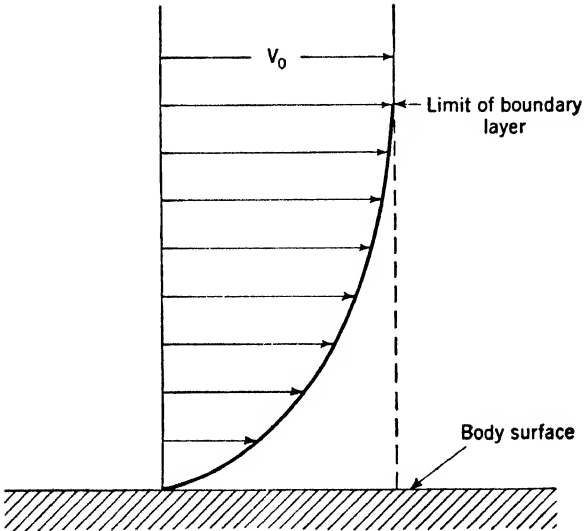


FIG. 1.5. — Velocity distribution in a boundary layer.

1.16. Discontinuity. Where a sharp corner projects into the flow, the steady stream of fluid would be thrown clear, as in Fig. 1.6a. On one side of DD there is dead water and on the other the full velocity of the stream. There is consequently a discontinuity of velocity, but not of fluid. The

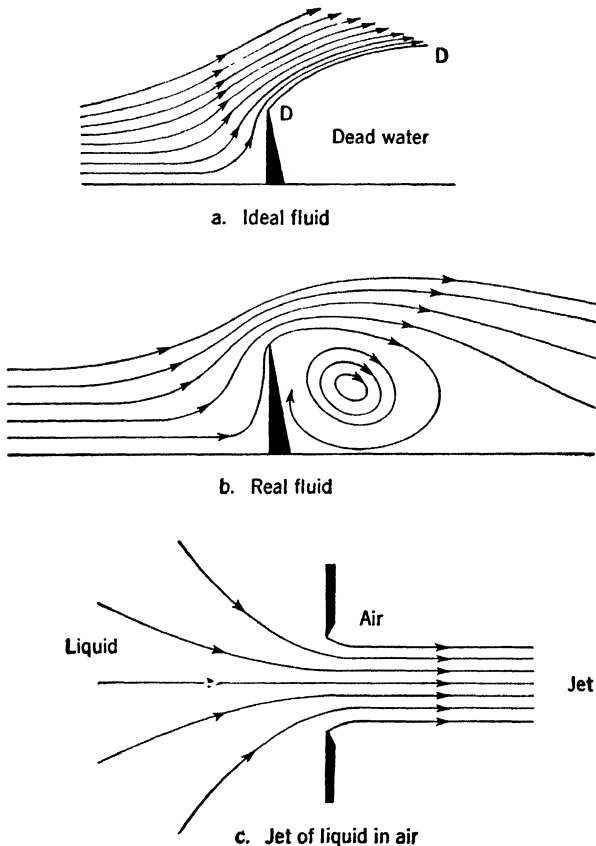


FIG. 1.6. — Surfaces of discontinuity in velocity.

velocity gradient is, for an ideal fluid, infinite at such a “surface of discontinuity.”

For real fluids having friction the abrupt change in velocity (high velocity gradient) causes large frictional forces tangential to the direction of motion. The dead water is set into rotation by the stream. The eddy that builds up is indicated in Fig. 1.6b.

A liquid jet in air, as from a nozzle, is surrounded by a surface of discontinuity. Here the liquid continuum may be considered to extend throughout the tank and the jet but not to cross the surface of the jet into the air (see Fig. 1.6c).

Observed phenomena frequently show a distinct separation of the flow from the object about which it flows. Such separation appears to be associated with a rapid change in contour, which the fluid will not follow. Flow separation involves a surface of discontinuity that breaks up into eddies. The ideal concept of a continuum can represent only the region not containing a surface of discontinuity.

Flow separation is of great technical importance because smooth flow is destroyed and energy losses become very large. An airplane stalls when the flow separates from the wing flown at too high an angle of incidence.

1.17. Laminar and Turbulent Flow. Observation shows that fluid flowing very slowly through a pipe or flowing through a very small capillary tube moves steadily in parallel layers having different speeds. This kind of motion is called "laminar flow." The boundary layer on a smooth object in a free stream may likewise show laminar flow for low speeds.

In pipes of sufficient size and at sufficient velocity the flow breaks up into a confused turbulence. A similar transition from laminar to turbulent flow, depending on flow conditions, is observed generally in boundary layers.

It is helpful to classify any flow in the region of a boundary or in a pipe as either laminar or turbulent and to develop an analysis for each. Each is observed in nature and must be accounted for in any theory that pretends to predict natural phenomena.

1.18. Rotation. In the flow of real fluids it is observed that abrupt deflection of the flow by a solid object often gives rise to separation, followed by whirling eddies, or vortices. Parts of the fluid are evidently set into rotation of a peculiar sort, which persists for an appreciable time. A surface of discontinuity seems to be unstable and to roll up into a vortex. Another sort of rotation of fluid is an obvious feature of centrifugal pumps and hydraulic turbines.

We, therefore, must examine the nature of rotation in a fluid continuum. For this purpose a farther classification of fluid phenomena will be discussed, *viz.*, irrotational and rotational flow, corresponding somewhat to the appearance of what is observed.

1.19. Circulation. When a solid body, submerged in a fluid stream, is placed in such an attitude as to deflect the stream, a force is created transverse to the stream. On an airplane wing this force is called a "lift"; on a propeller blade it is called a "thrust." Experiment has shown that the pressure on the surface of a deflector is higher than normal over the face and lower than normal over the back, evidently giving rise to the lifting force observed. There is also experimental evidence to indicate that the flow is speeded up along the back of the deflector and slowed down along the face. This observed speeding up and slowing down can be accounted for if we imagine an idealized case in which there is a circulation of fluid

about the deflector which combines with the transverse flow to produce the velocity distribution observed in nature. This concept of circulation leads to a useful theory of lift applicable to machinery, making use of dynamic forces transverse to the general direction of fluid flow.

1.20. Density. Newton's second law states that the product of mass times acceleration equals the sum of all external forces acting on the body under consideration. To apply this statement to a fluid requires careful consideration of the concept of mass with special relation to a fluid continuum.

A fluid mass distributes itself throughout a continuum in such a manner that there are no voids; consequently, there is fluid at every point. We can consider the quotient obtained by dividing the mass Δm , within a small element of volume enclosing the point, by the volume ΔV of this element. The result is in terms of mass per unit volume and is called the "average density" of Δm .

It is a basic assumption of a fluid continuum (without voids) that every element of volume ΔV contains a definite mass of fluid Δm , and it follows that the density must have a definite value at every point. We define density at a point, therefore, as the limit of $\Delta m/\Delta V$ as $\Delta V \rightarrow 0$, or $\rho = dm/dV$.

Since a finite mass $m = \int dm$, it follows that $m = \int \rho dV$.

The density may vary in a continuous manner from point to point. If the fluid flow is unsteady, the density at a given point may also vary with time. In general, for the idealized continuum, density is a single-valued continuous function of time and position, or

$$\rho = \frac{dm}{dV} = f(x, y, z, t)$$

Density has no physical significance if ΔV , as it approaches zero, momentarily contains no molecules. We therefore restrict our concept of a continuum to apply to fluids in which there is a large number of molecules in any volume element which is small relative to the extent of fluid. Thus for air at atmospheric pressure a volume element of $1/10^9$ cu mm contains some 3×10^7 molecules.

Although molecular agitation causes molecules continually to pass in and out of a fixed element of volume, the average number contained in such an element will remain substantially constant and the fluid can be treated as a continuum with a definite density at every point. The concept of density at a point as a statistical quotient also applies to the analogous concept of temperature, which is measured by the mean value of the kinetic energy of the molecules per unit volume.

In a vacuum tube the mean free path of the molecules may be of the order of the size of the tube, and density at a point can have no mean-

ing. The concept of a continuum does not apply to problems of high vacua.

In a real fluid, volume elements lose identity through interchange of molecules by diffusion, but the continuum approximates a state of affairs that exists for an appreciable period of time. The interchange of molecules between volume elements is also responsible for internal friction or viscosity (interchange of momentum between layers of fluid in relative motion) and for heat conduction (interchange of molecular kinetic energy).

In an ideal fluid continuum we ignore molecular agitation. Observed large-scale phenomena such as viscous shear and heat conduction are satisfactorily accounted for by assigning to the continuum the properties of viscosity and thermal conductivity, which vary continuously with position and time. We choose to overlook the molecular origin of these properties.

1.21. Pressure. In fluid mechanics not only density, but also pressure, has special significance and requires precise definition. It is obvious that any portion of a fluid must experience a force acting on it due to the surrounding fluid. If this were not the case, a portion of the fluid could move under the influence of gravity and there would be no state of rest or equilibrium. We must, therefore, accept the compulsory hypothesis of external forces proportional to the surface area. There will also be body forces proportional to the mass of the element of volume in consideration, *e.g.*, its weight.

In addition to external surface and body forces there will be internal forces within any volume element; but, as is the case for solid bodies, the internal forces mutually cancel.

As the element of volume is imagined to contract toward zero, the body forces, which are proportional to volume and hence to the third power of a linear dimension, become negligible with respect to the surface forces, which are proportional to the surface and hence to the square of a linear dimension.

Consequently, we have left for consideration only the external surface forces, which must be in equilibrium among themselves for a sufficiently small portion of a fluid.

For an ideal fluid without friction the surface force on an element of fluid must be perpendicular to the surface on which it acts. For a real fluid at rest the surface force is also perpendicular since, when there is no motion, there is no friction. This conclusion applies only to a true fluid whose viscosity is defined by the Newtonian relation between force and rate of deformation.

We now examine the meaning of "pressure at a point" in a fluid at rest in the light of the two conclusions that the surface forces on a sufficiently small element of volume are in equilibrium and are perpendicular to the surfaces on which they act.

Pressure is defined as stress, or surface force per unit area,

$$p = \lim_{\Delta A \rightarrow 0} \frac{\Delta F}{\Delta A} = \frac{dF}{dA}$$

Since we may choose a volume element of any form, consider a small prism as shown in Fig. 1.7 near a point O in a fluid at rest. We choose the volume so small that body forces can be neglected; hence the element to be in equilibrium must have no resultant horizontal or vertical surface force acting on it.

Hence,

$$p_3 dy dz = p_2 dy \sqrt{dx^2 + dz^2} \sin \alpha$$

and

$$p_1 dy dx = p_2 dy \sqrt{dx^2 + dz^2} \cos \alpha$$

But

$$\cos \alpha = \frac{dx}{\sqrt{dx^2 + dz^2}}$$

and

$$\sin \alpha = \frac{dz}{\sqrt{dx^2 + dz^2}}$$

Therefore

$$p_3 = p_2 = p_1$$

Since the volume element may be chosen with any orientation and since we may make the element as small as we please, we may say that the pressure p at or near the point O is independent of the orientation of the surface element on which it acts. The name "hydrostatic pressure" is given to p , a scalar quantity expressed as force per unit area.

We may consequently define p as a continuous function of position.

$$p = f(x, y, z)$$

This statement is true for all fluids at rest. For a viscous fluid in motion there is friction, and the force on a surface element near any point depends on the orientation of the surface element with respect to the motion. Therefore, to describe the stress distribution at a point, we need a sphere for a fluid at rest, and an ellipsoid for a viscous fluid in motion, identical with the ellipsoid of stress for a solid. For an ideal fluid the pressure at a point is independent of the direction of the surface element on which it acts, regardless of whether the fluid is at rest or in motion.

1.22. Concluding Remarks. The foregoing discussion is intended as a general survey of the problem of fluid flow. It is to be noted that the

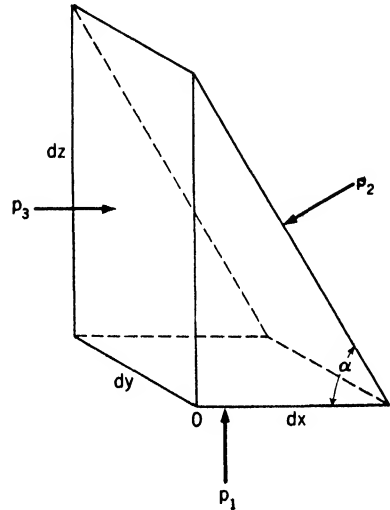


FIG. 1.7.

problem can have many aspects, each characterized by a concept peculiar to a recognizable type of flow. These concepts are justified only to the extent that they lead to useful approximations.

Historically, the science of fluid mechanics stems from Archimedes, who understood statics. Euler developed the concept of the ideal fluid continuum and the dynamic equations of motion. He may fairly be credited with establishing the dynamics of ideal fluids, or the science of hydromechanics, which was notably extended in the nineteenth century by the theoretical work of Helmholtz, Kirchhoff, Kelvin, Lamb, and Rayleigh. However, it was not until after the stimulation given experimental research by aeronautics, in the present century, that the behavior of real fluids began to be understood. To one man more than to any other, L. Prandtl of Göttingen, belongs the credit for illuminating the facts of observation by application of the general principles of mechanics.

Three fundamental concepts, defining simplifying assumptions, mark the renaissance of nineteenth-century classical hydromechanics into the practical fluid mechanics of today. The first is the concept of the boundary layer surrounded by an ideal continuum, due to Prandtl. The second, independently proposed by Lanchester and Kutta and later developed into useful form by Joukowski and Prandtl, is the circulation theory, by means of which forces on wings and propeller blades may be predicted. A third concept, of great practical utility, is the theory of dimensions, which we shall discuss in connection with experimental work. Though dimensional theory was not new to physics, Lord Rayleigh showed how it could be used to generalize the results of empirical but controlled model experiments to yield information needed for the design of airplanes, ships, machinery, and many other engineering applications of fluid mechanics. Where the actual flow is too complex for theoretical analysis, tests with a scale model can often guide the designer to a practical solution of his problem.

CHAPTER II

STATICS

The equilibrium and stability of a fluid at rest will be developed from the fundamental concept of a fluid continuum in which the pressure at any point has a single positive value $p = f(x, y, z)$. The fluid may be viscous, but if so it must be of so-called "Newtonian" character. The statement regarding pressure could also be made regarding the density at any point $\rho = f(x, y, z)$, since pressure and density are related by a simple physical law, the equation of state. The concept of mass will be required in the discussion of dynamics of a fluid, but it is not essential to statics. We are, however, directly concerned with the weight of the fluid since weight is the primary cause of hydrostatic pressure.

Under what conditions does a fluid remain in equilibrium? We define equilibrium as a state in which each particle or portion is at rest or has no velocity with respect to a suitable system of reference. Consequently, there can be no relative motion between adjacent portions of the fluid. As a suitable system of reference for practical problems of engineering we can use a system either rigidly connected to the earth or having a uniform translation with respect to the earth. In either case the fluid under consideration has no acceleration with respect to the earth. The absence of acceleration is identical with the condition that the sum of forces is zero. Thus we can say that equilibrium is a state in which the resulting force on each portion of the fluid is zero.

There are two kinds of force to be considered, one due to gravity, the other due to the interaction between neighboring particles, the hydrostatic pressure. There are no frictional or tangential forces in the absence of relative motion between portions of the fluid.

2.1. Gravity Force. Gravity acts toward the center of the earth, but in engineering problems we can assume that all gravity forces are parallel. The magnitude of the gravity force, or weight, acting on an element of volume dV is γdV , where γ , the weight per unit volume, or specific weight, is equal to ρg , the product of density times the acceleration g . There are few cases in engineering in which the decrease of g at high altitudes is important.

2.2. Pressure Force. The problem in the theory of equilibrium of fluids is to find an expression for the resulting force on the surface of an element of volume dV due to the surrounding fluid. Consider an element of cylindrical shape (Fig. 2.1). The cross section of the small cylinder is dA , and its length is dx . The orientation of the cylinder is arbitrary, so that we may choose as its direction that of our x axis. The volume of the

element $dV = dA \, dx$. There are three groups of pressure forces acting on the cylinder, (1) the pressure forces acting on the convex surface, which have different directions but which are all perpendicular to the x axis; (2) the pressure force on the left-hand base, which has the x direction; and (3) the pressure force on the right-hand base, which has the opposite, or the minus, x direction. If we confine ourselves to the x component of the resulting force, we may disregard forces 1 and consider only the difference between force 2 and force 3. If p is the pressure at the center of the left-

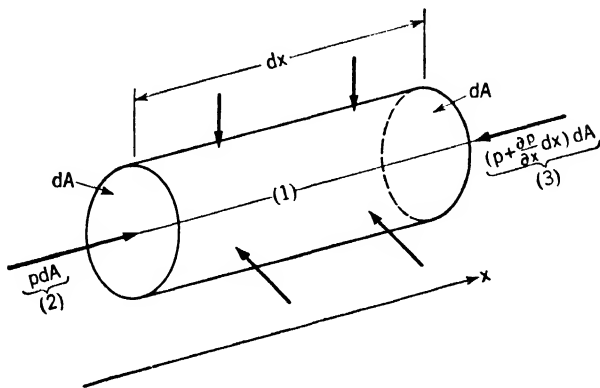


FIG. 2.1.

hand base, we can say that $p \, dA$ is the magnitude of force 2. We really assume that p may be treated as constant over an infinitesimal area.

The pressure at the center of the right-hand base will in general be different from p . Let us call this pressure $p + dp$. But since p is a function of the location of a point in the fluid, or of x, y, z , the notation dp by itself is not clear. The change in p is not the same for each direction when we proceed from a given point. What we need to know is the change in p that corresponds to proceeding a distance dx along the x direction. It is usual to denote the rate of increase of a variable p by $\partial p / \partial x$ when the point in consideration is moved in the x direction. ($\partial p / \partial x$ = partial derivative of p with respect to x .) Therefore our dp , which measures the increase of p from one point to a neighboring one on the x axis, is written $(\partial p / \partial x) \, dx$. It follows that the resulting force in the x direction is given by

$$p \, dA - \left(p + \frac{\partial p}{\partial x} dx \right) dA = - \frac{\partial p}{\partial x} dx \, dA \quad (2.1)$$

If we divide this expression by the volume $dV = dx \, dA$, we obtain the resulting pressure force in the x direction per unit of volume

$$- \frac{\partial p}{\partial x} \frac{dx \, dA}{dV} = - \frac{\partial p}{\partial x} \quad (2.2)$$

The x component of the resultant of all pressure forces acting upon an infinitely small element has, per unit of volume, the value $-\partial p/\partial x$, that is, the negative partial derivative of p with respect to x .

The expression " x direction" is used here quite arbitrarily; we could replace it by any other, such as y direction or z direction. In each case the component of the resulting pressure force per unit of volume is determined by the negative partial derivative of p in the corresponding direction. If we use the ordinary rectangular coordinate system with x , y , and z axes, calling K_x , K_y , K_z the resulting pressure forces per unit of volume in the x , y , and z directions, we have

$$\left. \begin{aligned} K_x &= -\frac{\partial p}{\partial x} \\ K_y &= -\frac{\partial p}{\partial y} \\ K_z &= -\frac{\partial p}{\partial z} \end{aligned} \right\} \quad (2.3)$$

In vector analysis, the gradient of a scalar function is the vector whose components parallel to the three axes are the partial derivatives of the function with respect to the three coordinates x , y , z . (Gradient means rate of increase. We may concisely state that the *resulting pressure force per unit of volume is the negative gradient of p* where p is considered a function of x , y , and z . Note that the hydrostatic pressure p at any point is a scalar quantity without direction, while the resulting force per unit volume due to hydrostatic pressure is a vector having a definite direction determined by the gradient of p .

Consider, for example, a pressure distribution that is a linear function of x , y , z : $p = ax + by + cz$. Here the partial derivatives of p are $\partial p/\partial x = a$, $\partial p/\partial y = b$, $\partial p/\partial z = c$. The resulting pressure force per unit of volume has therefore the constant value $\sqrt{a^2 + b^2 + c^2}$, and its direction is determined by the constant ratios $a/b/c$. The pressure is constant in each plane the equation of which is given by $ax + by + cz = \text{constant}$. The normal to this plane is again given by the ratio $a/b/c$. According to the well-known formulas of analytic geometry these are the ratios of the three direction cosines, $\cos \alpha/\cos \beta/\cos \gamma$. The same direction is the direction of the force vector whose components are a , b , and c . From this example we can make the general statement that the resulting pressure force is perpendicular to the surface on which p has a constant value. Such surfaces are called "isobars," and the resulting pressure force is normal to the isobar passing through a point and is directed toward the isobars with smaller pressure values [because of the minus sign in Eq. (2.3)].

All this becomes clearer if we consider the special case in which the constants a and b are zero and p is simply equal to cz . Then $\partial p/\partial x = 0$,

$\partial p / \partial y = 0$, and $\partial p / \partial z = c$. The xy planes are the isobars, or surfaces of constant pressure. The resultant pressure force, or the gradient of p , is parallel to the z axis since its x and y components are zero. If the positive z direction is assumed to be upward, the z component of the resultant force is directed vertically downward for a positive value of c , and vice versa.

In the present discussion it does not matter whether the fluid is compressible or incompressible. In either case the resultant pressure force per unit of volume at any point has the components $-\partial p / \partial x$, $-\partial p / \partial y$, $-\partial p / \partial z$.

2.3. Conditions of Equilibrium. When the expression for the resultant pressure force is known, there is no difficulty in setting up the conditions of equilibrium for a fluid. As was mentioned before, the only forces acting on a fluid particle are due to gravity and hydrostatic pressure. The gravity force per unit volume (or specific weight) has the magnitude γ and is directed vertically downward. The pressure force per unit volume has the components $-\partial p / \partial x$, $-\partial p / \partial y$, $-\partial p / \partial z$, and its direction at any point is normal to the isobar passing through the point and is directed toward decreasing values of p . In a coordinate system of arbitrary orientation the components of the weight per unit volume may be called γ_x , γ_y , γ_z , and the equilibrium conditions at any point, x , y , z , will be

$$\left. \begin{aligned} \gamma_x - \frac{\partial p}{\partial x} &= 0 \\ \gamma_y - \frac{\partial p}{\partial y} &= 0 \\ \gamma_z - \frac{\partial p}{\partial z} &= 0 \end{aligned} \right\} \quad (2.4)$$

Usually it will be convenient to use a coordinate system where the z axis is vertical and the positive z direction is upward. In this case gravity has no x or y components, and its z component is negative.

$$\gamma_x = 0 \quad \gamma_y = 0 \quad \gamma_z = -\gamma \quad (2.5)$$

With respect to such a coordinate system the three equilibrium conditions simplify to

$$\frac{\partial p}{\partial x} = 0 \quad \frac{\partial p}{\partial y} = 0 \quad \frac{\partial p}{\partial z} = -\gamma \quad (2.6)$$

or, in words: A fluid mass is in equilibrium if the isobars are horizontal planes and if the pressure increases downward at the rate γ . The fact that $\partial p / \partial x$ and $\partial p / \partial y$ are zero means that p is a function of z alone. It follows that $\partial p / \partial z$ can be written in the form dp / dz in this case. The pressure gradient dp / dz , or the resultant pressure force per unit of volume, has, therefore, a constant value in each horizontal plane.

We draw an important conclusion from the fact that dp/dz is constant for each horizontal plane. Since Eq. (2.6) shows that $-dp/dz = \gamma$, the specific weight and consequently the density ρ must be constant in a horizontal plane if the fluid is in equilibrium. (We assume that variations in $g = \gamma/\rho$ are negligible.) This statement is of course of no interest for an incompressible fluid, where density has the same value everywhere, but it is important for gases or other compressible fluids. For this latter case we have established the fact that a fluid mass can be in equilibrium only if the density is constant along horizontal isobars. A mixture of insoluble liquids at rest becomes stratified with lighter liquid on top.

If we took the spherical shape of the earth into account, the isobars would be concentric spheres with centers at the center of the earth. In the case of a compressible fluid like the atmosphere, the density would be constant over all such spherical surfaces if the fluid mass were in perfect equilibrium.

When the vertical distance z alone appears in the equations of equilibrium, we do not need a three-coordinate system. We shall use the letter h (height) instead of z to denote the vertical distance of a point above an arbitrarily chosen level.

We can now summarize the conditions for static equilibrium in the following three statements:

1. Pressure is constant in each horizontal plane.
2. Pressure decreases upward at the rate γ , or

$$\frac{dp}{dh} = -\gamma \quad (2.7)$$

3. In the case of compressible fluids, density is constant in each horizontal plane.

Note that in the theory of static equilibrium there is no difference between ideal and viscous fluids. The three above-stated equilibrium conditions are valid for both cases.

2.4. Potential. It will later be necessary in the discussion of dynamics to introduce a potential function to facilitate the analysis. For statics the concept of potential in a gravity field is especially simple owing to its identity with potential energy.

For a fluid at rest under gravity, the weight per unit volume is $\gamma = g\rho$, acting downward. The acceleration of gravity is a vector of constant magnitude, and unit mass of fluid has the same weight g regardless of position.

Define a potential function P of h such that

$$\frac{dP}{dh} = -g$$

Therefore

$$P = -g \int_{h_0}^h dh = -g(h - h_0)$$

where h and h_0 are heights above some arbitrary datum level and the value of P at h_0 has been arbitrarily taken as zero. Note that, for a given elevation, P is constant and that the gradient of P in the direction of h gives the gravity force $-g$ in the same direction. Define potential energy per unit mass at height h with respect to height h_0 as the work done in lifting unit mass from h_0 to h ,

$$E_1 = -g(h - h_0)$$

Since E_1 and P are identical, we can state that the numerical value of the potential function at any level is equal to the potential energy of unit mass of fluid at that level.

The kinetic energy of unit mass after falling freely a distance $h - h_0$ has the same numerical value,

$$E_2 = \frac{1}{2}(V^2) = \frac{1}{2}[\sqrt{2g(h - h_0)}]^2 = g(h - h_0)$$

2.5. Equilibrium of Incompressible Fluids (Hydrostatics). Water, oil, and similar liquids can be considered as incompressible and the density as constant throughout the continuum. Under this condition the basic

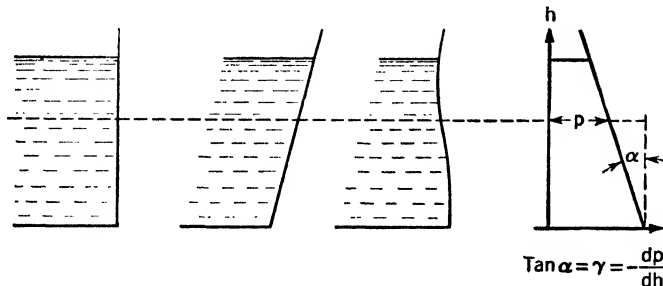


FIG. 2.2. — Pressure in a vessel is independent of the shape of the wall.

equation of equilibrium, Eq. (2.7), can easily be integrated. From $dp/dh = -\gamma$ follows

$$p + \gamma h = \text{constant} \quad \text{or} \quad \frac{p}{\gamma} + h = \text{constant} \quad (2.8)$$

Pressure is evidently a linear function of h , increasing downward at a rate γ . The pressure diagram that has h as a vertical coordinate consists, therefore, of an oblique straight line as shown in Fig. 2.2.

Along the side wall of a vessel filled with liquid the pressure increases from its value at the top to its value at the bottom according to the linear law as shown. The shape of the wall has no influence on the pressure at a given level.

The lighter the fluid, the smaller the angle α between the oblique straight line and the vertical.

In the ordinary problems of hydrostatics, we shall often have as reference level the free surface of the liquid exposed to the atmosphere. The vertical pressure gradient of the atmosphere is $dp/dh = -\gamma_a$, where γ_a is the specific weight of air. Since the density of air is very small compared with the density of liquids, we shall be justified in neglecting it. Therefore, within a restricted region we can assume a constant atmospheric pressure p_0 , regardless of elevation of the liquid surface.

Where the liquid touches the atmosphere, the pressure in the liquid must equal the atmospheric pressure p_0 . It follows that the boundary between liquid and atmosphere is an isobar

$p = p_0$; and since all isobars are horizontal planes, we have proved the well-known fact that the free surface of a liquid in equilibrium is a horizontal plane.

Two exceptions may be mentioned. (1) In problems involving very large dimensions, such as an expanse of ocean, the free surface will be a spherical one with the center at the center of the earth, and the isobars will be spherical surfaces. (2) In certain problems involving very small dimensions additional molecular forces exerted on the liquid particles by a wall must be considered.

The general condition of equilibrium for incompressible fluids as given in Eq. (2.8) can also be written in the form

$$p + \gamma h = p_1 + \gamma h_1 = p_0 + \gamma h_0 \quad (2.9)$$

where the pairs p, h ; p_1, h_1 ; and p_0, h_0 refer to three different levels in the fluid. We may take, as in the case of Fig. 2.3, the bottom of the tank as the level of reference, calling this level 1. Then the height h_0 , which is equal to the depth of the water, refers to the top where the pressure p_0 is the atmospheric pressure. At an arbitrary height h or at a depth $h_0 - h$ the pressure is p , and Eq. (2.9) shows that

$$p + \gamma h = p_1 = p_0 + \gamma h_0$$

or

$$p - p_0 = \gamma(h_0 - h) \quad \text{and} \quad p_1 - p_0 = \gamma h_0 \quad (2.10)$$

The last equation can be read as follows: The pressure increase from the surface to any point within the fluid equals the product of γ times its depth below the free surface. It is convenient in many cases to use as the measure of pressure the pressure difference $p - p_0$, that is, the absolute

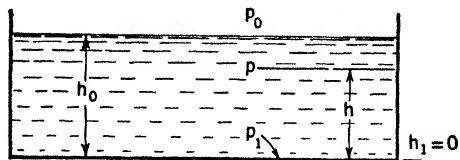


FIG. 2.3.

pressure minus the atmospheric pressure. This difference is often called the "gauge" pressure, or overpressure.

Let us now consider the second form of the equilibrium equation as given in Eq. (2.8)

$$\frac{p}{\gamma} + h = \text{constant}$$

The quotient p/γ should have the dimensions of a length; otherwise it could not be a term summed up with h . But it is evident that, since p has the dimensions force/length² and γ the dimensions force/length³, p/γ has the dimension of length. This length p/γ has an immediate physical significance, which can be illustrated by an example.

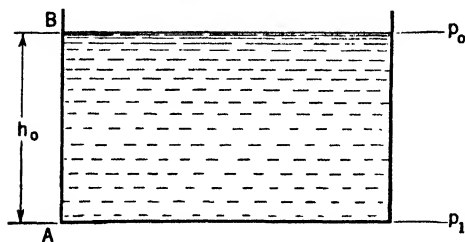


FIG. 2.4.

Consider a vertical column of fluid from A to B (Fig. 2.4), where B is a free surface. Then

$p_1 - p_0 = \gamma h_0$, where h_0 is the length AB . It follows that

$$AB = h_0 = \frac{p_1 - p_0}{\gamma}$$

We see that, if $p_1 - p_0$ is the gauge pressure at the bottom of the column, then the height of the column is $(p_1 - p_0)/\gamma$. In this way pressure values can be visualized by lengths, *i.e.*, heights of columns with a free surface and a certain pressure value at the bottom. In hydraulics it is usual to call the quotient p/γ the pressure head corresponding to p .

2.6. Some Applications of the Hydrostatic Equation. *a. Communicating Vessels.* The pressure in a fluid is a function of height only, and at the

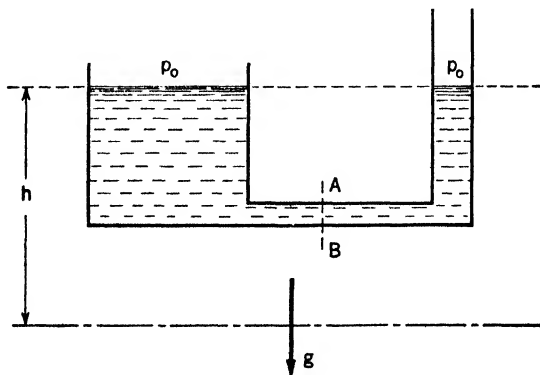


FIG. 2.5.

free surfaces is equal to the general atmospheric pressure. Therefore, the free surfaces in all communicating vessels are at the same height.

It has been mentioned that the equilibrium conditions within a fluid mass are in no way altered by the shape of the vessel which contains the fluid. As long as the fluid forms a continuum, the equation $p + \gamma h = \text{constant}$ applies to all its parts. If the vessel in Fig. 2.5 is filled with a liquid,

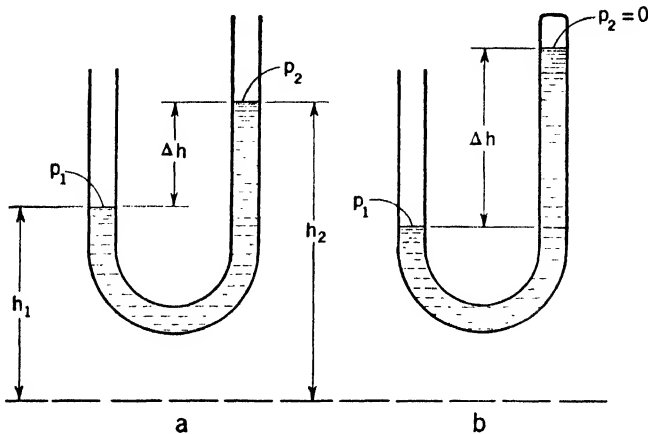


FIG. 2.6. — a. Manometer. b. Barometer.

the level of the free surface in each leg is the same. Also, the pressure p in any horizontal plane is the same in each leg. Nothing could be said about the levels and pressures if the fluid were separated by a wall along the line AB .

b. Barometer and Liquid Manometer. Referring to Fig. 2.6 we see that, in the manometer, at h_1 ,

$$p = p_1$$

while at h_2 ,

$$p = p_2$$

$$p_1 - p_2 = \gamma \Delta h$$

In the barometer,

$$p_1 = p_0$$

$$p_2 = 0, \text{ approximately}$$

$$p_1 - p_2 = p_0 = \gamma \Delta h$$

In the barometer, p_2 is nearly zero if the instrument is carefully filled with mercury initially. The right-hand leg is open, so that there the atmospheric pressure p_0 acts on the mercury. If γ_{Hg} designates the specific weight of mercury (848 lb per cu ft) and p_0 the atmospheric pressure, the equilibrium condition yields the equation

$$p_0 = \gamma_{Hg} \Delta h$$

Since γ_{H_0} is known, the reading of the distance Δh indicates the atmospheric pressure. The pressure of the atmosphere is often expressed in terms of pressure head of mercury. The usual average value for sea level is 760 mm, or 29.92 in., Hg.

c. Hydraulic Press. A well-known application of the laws of hydrostatics is made in the hydraulic press, as shown in Fig. 2.7. In order to exert a large force F on the piston of area A , it is sufficient to produce the

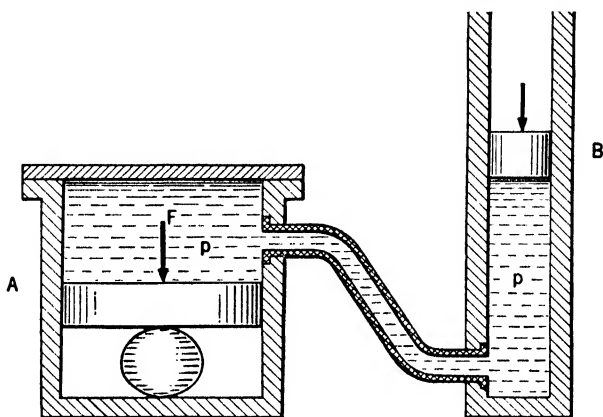


FIG. 2.7. — Hydraulic press.

pressure $p = F/A$ above the piston. This can be done according to the law of communicating vessels by producing the same pressure p in the smaller cylinder of area B , which requires only the force $pB = FB/A$. The small differences in height are neglected here, and so are friction and inertia forces, as we assume very slow motion of the pistons. If the body underneath the piston A has its height reduced by ϵ , the work done is $F\epsilon = pA\epsilon$. This movement requires a transition of a volume of liquid $A\epsilon$ from the small cylinder to the large one. It follows that the small piston B must move a distance $\epsilon_1 = \epsilon A/B$. The work done by the piston B is $pB\epsilon_1 = pB\epsilon A/B = pA\epsilon$, equal to the work done by the large piston in compressing the body below it. The small piston has the greater motion, but a small force on B can balance a large force on A .

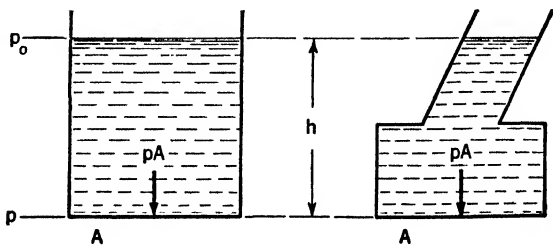


FIG. 2.8.

d. Pressure on Floors;

Hydrostatic Paradox. Since the pressure p_0 at the free surface is the same for both vessels of Fig. 2.8, the pressures at the same depth in

each are equal provided that both are filled with fluid of the same density. Hence if the areas of the bottoms A are equal, the total force pA is the same on the bottom of each vessel in spite of the obvious difference in the total weights of liquid contained.

c. Pressure on Walls. Let h be the distance, or "head," measured down-

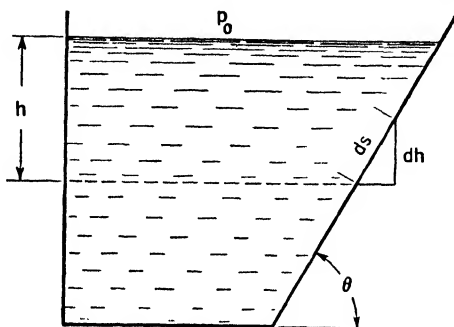


FIG. 2.9.

ward from the free surface of Fig. 2.9. Then, at depth h , $p = p_0 + \gamma h$, and the normal force per unit width of a vertical wall,

$$F = \int_0^h (p_0 + \gamma h) dh$$

The normal force per unit width of a sloping wall,

$$F_s = \int_0^{h/\sin \theta} (p_0 + \gamma h) ds = \int_0^h (p_0 + \gamma h) \frac{dh}{\sin \theta} = \frac{F}{\sin \theta}$$

when θ is constant.

The horizontal component of the force on the sloping wall is $F = F_s \sin \theta$. In general, the horizontal component of the total force due to hydrostatic pressure on a wall of any slope or shape is equal to that on a vertical wall of the same depth.

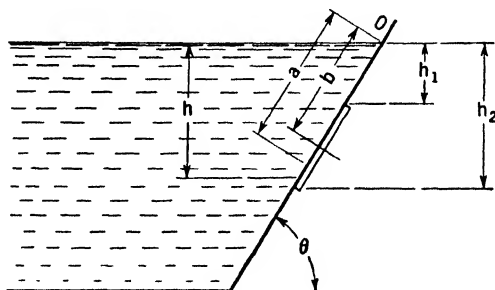


FIG. 2.10.

j. Force on an Area. We first compute the total hydrostatic force on the water gate in the sloping dam shown in Fig. 2.10.

$$\text{Area of gate} = A = \int_{h_1}^{h_2} dA$$

$$\text{Force on gate} = F = \int_{h_1}^{h_2} (p - p_0) dA = \gamma \int_{h_1}^{h_2} h dA$$

Let b be the distance measured along the face of the dam to the center of gravity of the area of the gate. The moment of the area A about O is

$$Ab = \frac{1}{\sin \theta} \int_{h_1}^{h_2} h dA = \frac{1}{\sin \theta} \frac{F}{\gamma}$$

and

$$F = A\gamma b \sin \theta$$

But the pressure at the center of gravity of A is

$$p_c = \gamma b \sin \theta$$

Therefore,

$$F = Ap_c$$

The general rule follows that the total force due to hydrostatic pressure on an inclined plane surface is equal to the area of the surface times the pressure at its center of gravity. This force is independent of the inclination of the surface.

g. Center of Pressure. Referring again to Fig. 2.10, we ask for the point on the gate of area A through which passes the line of action of the force F . Call this point the center of pressure, and let it be a distance a from O . The moment of F about O is Fa .

The pressure at the center of an element of area dA is γh , and the normal force on the element is $\gamma h dA$. The moment of this force about O will be $\gamma h dA (h/\sin \theta)$, and the moment of all such forces will be the sum, or integral, of such elementary moments.

Then, taking the moment of F about O and remembering that F is normal to the gate, we find

$$\begin{aligned} Fa &= \int_{h_1}^{h_2} \gamma h dA \frac{h}{\sin \theta} = \int_{h_1}^{h_2} \gamma dA \left(\frac{h}{\sin \theta} \right)^2 \sin \theta \\ &= \gamma I \sin \theta \end{aligned}$$

where I is the moment of inertia of A about O . But $F = \gamma b \sin \theta A$; and, by substitution for F in the above equation,

$$a = \frac{I}{bA} = \frac{\text{moment of inertia about } O}{\text{moment of area about } O}$$

If I_g is the moment of inertia of the gate about its center of gravity, $I = I_g + b^2A$ and $a - b = I_g/bA$, which is always positive. The center of pressure, therefore, lies below the center of gravity.

Note that the location of the center of pressure relative to the center of

gravity is independent of the density of the fluid and depends only on the geometry.

h. Convection. Suppose a chimney of height h discharges smoke and warm air into the atmosphere at pressure p_c corresponding to the level of the chimney top of Fig. 2.11. Let the pressure in the fireplace be p_f and the pressure in the air outside be p_0 . Assume the average specific weight of the warm gases in the chimney to be γ_c and that of the cool air outside to be γ_a . The warm gas is lighter, and $\gamma_a > \gamma_c$. Neglecting any acceleration of the air, we find by the hydrostatic equation

$$p_f - p_c = \gamma_c h \quad p_0 - p_c = \gamma_a h$$

and

$$p_0 - p_f = h(\gamma_a - \gamma_c)$$

This approximate analysis, based on the assumption of equilibrium, shows that the two columns of equal height are actually not in equilibrium and air will flow into the fireplace. A rising column of fluid caused by unequal heating is called a "convection current." It is not necessary to have a fireplace and chimney to start convection. Any local heating of a portion of fluid in a continuum will destroy the previously established condition of equilibrium. The convective currents tend to establish a new state of equilibrium.

Convection in the atmosphere due to unequal heating of the surface of the ground may be very marked over a region with adjoining areas of bare ground, forest, and lakes. On a clear summer day an airplane's flight may be very rough although no evidence of disturbance of the air is visible.

2.7. Pressure Measurement.

If we wish to know the pressure at any point P in a liquid, we attach a tube as shown in Fig. 2.12. This tube may be filled with any liquid that does not mix with and that has a

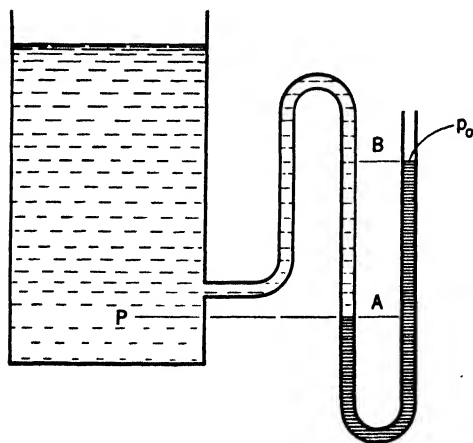


FIG. 2.12.

greater density than the liquid in the vessel. We must take care that the liquid in the tube is in equilibrium. Then the distance AB between the

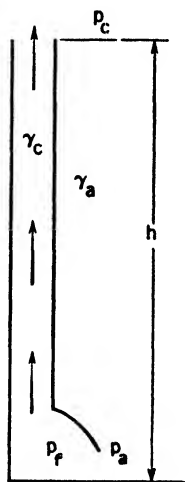


FIG. 2.11.

level of P and the free surface in the tube multiplied by the specific weight of the manometer liquid equals the overpressure at P .

The precision of such a manometer can be seriously impaired if the tube containing the liquid is so small that capillarity comes into play. Furthermore, if the inner surface of the tube near A is clean and near B is dirty

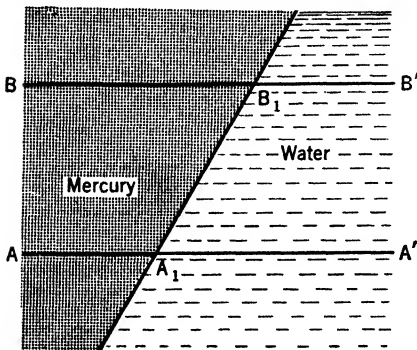


FIG. 2.13.

or otherwise of different nature, the wetting of the tube surface by the liquid may be so different as to affect seriously the observed pressure reading. For very small pressure differences the ordinary U-tube type of manometer is inadequate.

In some pressure-measuring arrangements different liquids are in contact, for example, water and oil, water and mercury, mercury and alcohol. It is assumed, of course, that the liquids do not mix. Within one kind of liquid the isobars are horizontal planes, and the pressure difference between two planes equals the specific weight times the distance between the planes. It follows that the interface of two fluids can be only a horizontal plane; for if it were inclined as shown in Fig. 2.13, the pressure difference between A and B would be $\gamma_{Hg} \overline{AB}$ and the pressure difference between A' and B' would be $\gamma \overline{A'B'}$. The consequence would be that either at A_1 or at B_1 a pressure difference would exist across the interface. But a pressure difference is impossible in the case of equilibrium. It follows that, if no rigid wall is put between the two fluids, an interface which is not horizontal is physically impossible. This statement may not be true for the part of the fluids very close to a vertical wall, where the fluid interface is usually curved as a result of surface tension.

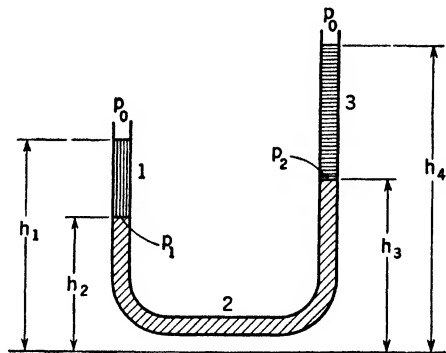


FIG. 2.14.

Let us assume, as shown in Fig. 2.14, that there are three kinds of liquid in a U-tube with respective specific weights γ_1 , γ_2 , and γ_3 . The pressure at the top levels of fluid 1 and fluid 3 is atmospheric, and the pressure at the interface of 1 and 2 is p_1 and at the interface of 2 and 3 is p_2 . If h_1 , h_2 , h_3 , and h_4 are the different heights as shown in the figure, the

equilibrium conditions for each of the three fluids supply the following equations:

$$\frac{p_1 - p_0}{\gamma_1} = h_1 - h_2$$

$$\frac{p_1 - p_2}{\gamma_2} = h_3 - h_2$$

$$\frac{p_2 - p_0}{\gamma_3} = h_4 - h_3$$

Pressure measurements based on the use of a liquid manometer depend directly on precise knowledge of the weight of unit volume of the fluid used and on precise observation of the levels at which the fluid stands. The measurement of very small pressure differences is obviously difficult, and various modifications of the simple manometer have been devised to suit special cases.

a. Three-liquid Manometer. In Fig. 2.15 a manometer is sketched that contains three nonmiscible liquids of densities γ_1 , γ_2 , and γ_3 . The unknown pressure p is communicated to a closed vessel by a tube as shown. The manometer is filled through the stopcock X .

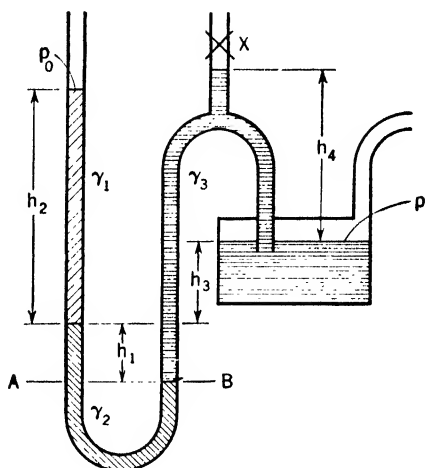


FIG. 2.15. — Three-liquid manometer.

By observing h_1 , h_2 , and h_3 and knowing the values of γ_1 , γ_2 , and γ_3 , p can be computed. Note that the weight of air or other gas that transmits the pressure p to the closed vessel is neglected.

At level AB , pressures are equal in each tube, and hence

$$p_0 + h_2\gamma_1 + h_1\gamma_2 = p + h_3\gamma_3 + h_1\gamma_3$$

and

$$p - p_0 = h_1(\gamma_2 - \gamma_3) + h_2\gamma_1 - h_3\gamma_3$$

b. Two-liquid Manometer. If γ_2 represents water γ_w , and γ_1 and γ_3 are both kerosene γ_k , we can adjust the filling of the manometer to make h_2 equal to h_3 for the pressure to be measured and have

$$p - p_0 = h_1(\gamma_w - \gamma_k)$$

The head h_1 to be measured is now larger than would be the case for a simple water manometer, $p - p_0 = h\gamma_w$. The amplification is greater the nearer the two liquids are to the same density.

Note that, when both γ_1 and γ_3 are air γ_a , $\gamma_w - \gamma_a \approx \gamma_w(1 - 1/800) \approx \gamma_w$ and the weight of air in the connecting tubes can be neglected.

c. *Inclined-liquid Manometer (Draft Gauge).* When $p = p_0$, liquid stands at level A (Fig. 2.16). For a pressure difference $p - p_0$, liquid in the inclined tube rises to level B . The change in level of the large reservoir is negligible if its cross section is made very large compared with that of the tube. Provided that the tube is straight,

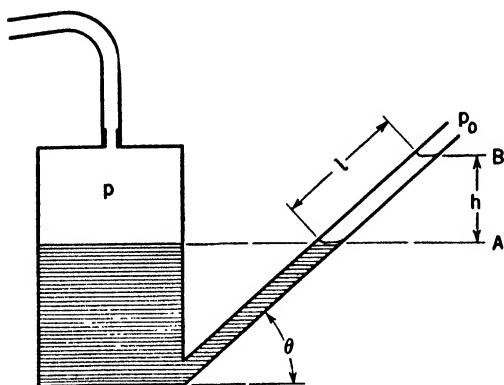
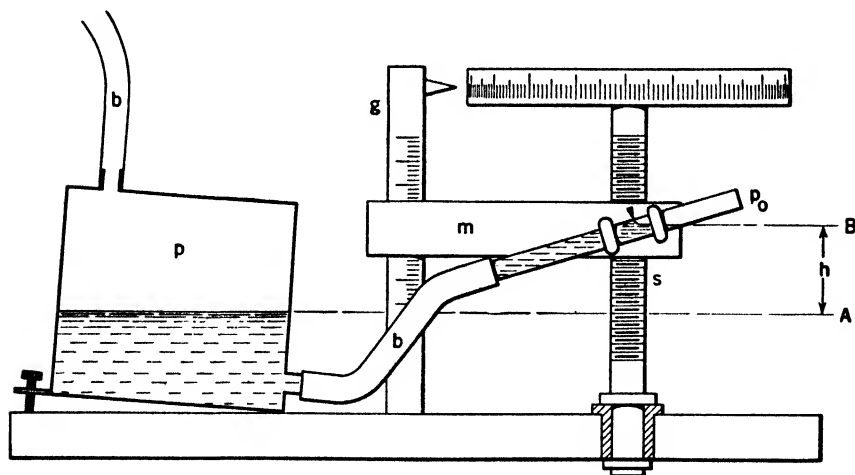


FIG. 2.16. — Inclined-liquid manometer.

$$p - p_0 = \gamma h = \gamma l \sin \theta$$

The distance l can be observed with precision. The amplification of h is $1/\sin \theta$ for a given liquid. If further amplification is desired, a lighter liquid can be used provided that it makes a clear meniscus with clean glass.

The effect of capillarity in the tube is presumed to be the same at B as at A and not to affect the distance l . The tube is thus assumed to have a uniform bore and surface condition.



(b) Rubber tubing; (m) metal block carried by screw (s) and sliding on guide post (g)

FIG. 2.17. — Krell, or Prandtl, manometer.

d. *Krell, or Prandtl, Manometer.* Errors due to capillarity and to change in reservoir level are eliminated by having the liquid meniscus

always at the same marked place in the glass tube of Fig. 2.17. The inclined tube is carried parallel to itself by a low-pitch screw with micrometer head. When $p = p_0$, the level is noted at A . When $p - p_0 = \gamma h$, the value of h is read from the micrometer head. Only one reading is necessary to determine h . The inclination of the tube determines the sensitivity of the manometer, and very small deviations from a desired pressure can be detected. The number of turns of the screw needed to bring the meniscus back to a reference mark on the tube measures this deviation.

e. Inverted-cup Manometer. In Fig. 2.18 the pressure difference $p - p_0$ is measured by the force tending to lift the cup,

$$p - p_0 = \frac{b}{a} \frac{F}{A}$$

If the cup is large, a small pressure is measured by a substantial force.

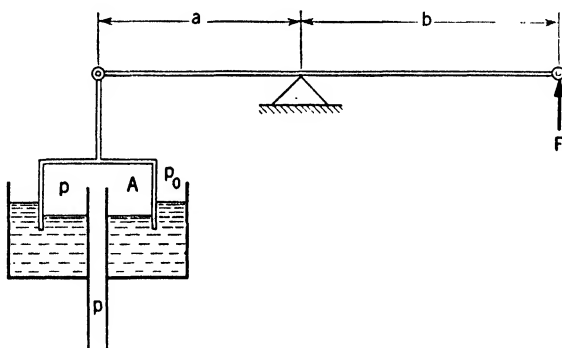


FIG. 2.18. — Inverted-cup manometer.

f. Spring-type Gauges. All such pressure gauges separate two regions of static pressure, p and p_0 , by an elastic solid whose deformation depends on the spring constant of the apparatus. These gauges must be calibrated

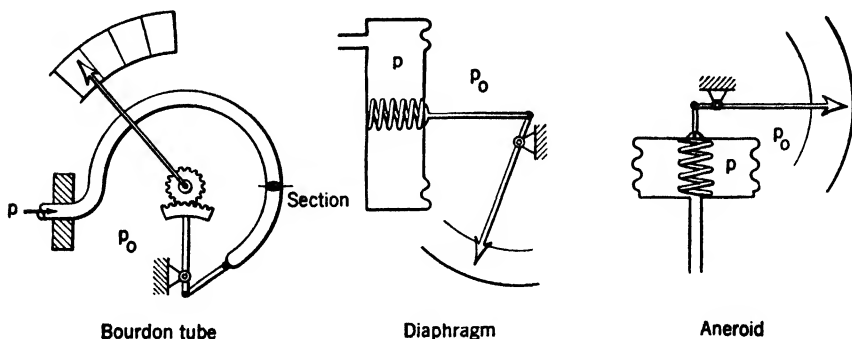


FIG. 2.19. — Spring-type gauges.

against some type of manometer whose indications are based on the hydrostatic equation. Some well-known examples are shown in Fig. 2.19.

2.8. Archimedes' Principle. The theory of flotation and fluid displacement originated with Archimedes, and its formal statement is still called "Archimedes' principle."

Consider the solid body of Fig. 2.20 suspended by a thread below the surface of a liquid. Since the body and all parts of the liquid are at rest, the pressure distribution throughout the liquid and on the surface of the body is described by the hydrostatic equation.

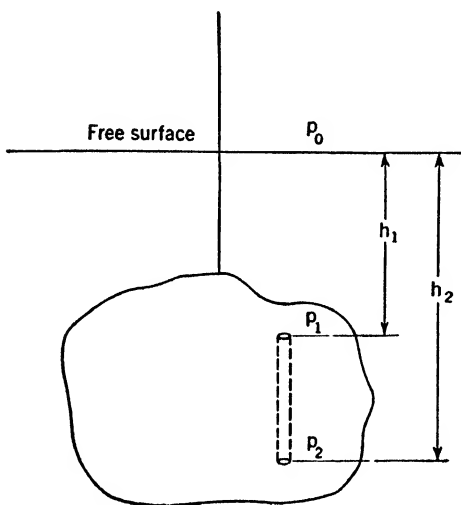


FIG. 2.20.

Assume a small vertical cylinder of cross-sectional area dA cut through the body as shown, extending from depth h_1 at the top to depth h_2 at the bottom. As dA is small, the pressures on the exposed, or wetted, ends of the cylinder may be taken as p_1 and p_2 . The force due to the hydrostatic pressure is normal to the surface of each wetted end. The

vertical components of these forces are independent of the inclinations of the surfaces and are of magnitudes $p_1 dA$ and $p_2 dA$.

Since $p_2 > p_1$, there will be an upward force $(p_2 - p_1) dA$ on each element of volume $(h_2 - h_1) dA$ and the total lift, or buoyancy, of the hydrostatic pressures all over the wetted surface of the body will be

$$B = \int_A (p_2 - p_1) dA = \int_A \gamma(h_2 - h_1) dA$$

But the volume of the body is

$$V = \int_A (h_2 - h_1) dA$$

and hence $B = \gamma V$. The weight of the body, if of average specific weight γ_b , is

$$W = \gamma_b V$$

The apparent weight on the suspension is therefore

$$W - B = V(\gamma_b - \gamma)$$

The effect of the horizontal components of the forces on the wetted surface may be dismissed, as the body is hanging at rest. An analogous

analytical procedure could be undertaken to show that the pressure forces on the ends of small horizontal cylindrical volume elements are equal and opposite, because they are at the same level. Consequently, the integral over the wetted surface of all horizontal forces is zero.

Archimedes' principle may now be stated thus: A submerged body is subject to a buoyancy equal to the weight of fluid displaced.

A further conclusion of importance can also be drawn. We know that the resultant of the gravity forces on a body passes through a certain point called the center of gravity. Since the buoyancy is the sum of a number of elementary forces, each equal in magnitude to the weight of a small cylindrical portion of fluid, it follows that the line of action of the buoyancy must pass through the center of gravity of the fluid mass which we can imagine put in place of the solid body. In other words, the center of buoyancy is the center of gravity of the displaced fluid.

2.9. Stability of Submerged Bodies. A completely submerged body, such as a submarine (Fig. 2.21), can remain in equilibrium at rest only if the buoyancy B is equal to the weight W and if the center of gravity (C.G.)

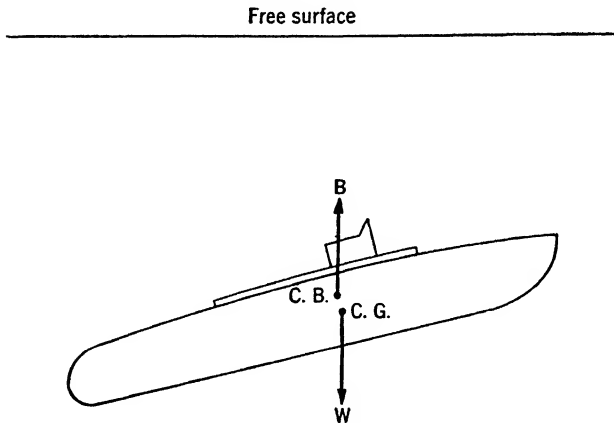


FIG. 2.21.

lies directly below the center of buoyancy (C.B.). Submarines must use balancing tanks to make $B = W$ and trimming tanks to bring the C.B. over the C.G. An airship similarly must use ballast or let out gas to keep in balance and trim as fuel is consumed or weight changed by rain or ice.

The equilibrium of a submerged body is stable with the C.G. below the C.B.; for if the body is rotated through a small angle θ , there is a righting moment, as shown in Fig. 2.22,

$$R = Wa \sin \theta = Wa\theta$$

The body thus tends to return to its original position. In general, an equilibrium position is said to be stable if a small change of this position arouses forces that oppose the change.

The period of the rolling oscillation T evidently depends primarily on the relative magnitudes of the righting moment and the moment of inertia of the body. We might neglect, for a first approximation, the frictional damping of the water. For a given body the righting moment depends on

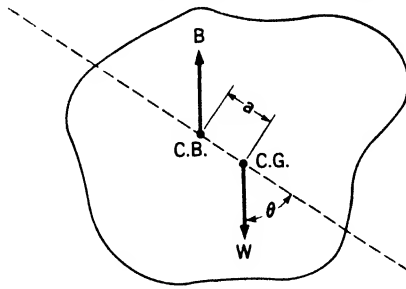


FIG. 2.22.

$W a \theta$, while $I = (W/g)k^2$, where k is the radius of gyration of the body with respect to the axis of roll. Their ratio is $ga\theta/k^2$, and we assume that T is some function of this quantity, or

$$T = f\left(\frac{ga\theta}{k^2}\right)$$

We might further assume that the function is approximated by

$$T = C \left(\frac{ga\theta}{k^2}\right)^x$$

where C is a constant. But T has dimensions $[T]$ and $(ga\theta/k^2)^x$ has dimensions

$$\left[\left(\frac{L \cdot L}{T^2 \cdot L^2}\right)^x\right] = \left[\frac{1}{T^{2x}}\right],$$

where the brackets indicate that the dimensions only of the enclosed quantity are represented. Consequently, for both sides of the equation to be of the same dimensions, x must equal $-1/2$. Then

$$T = C \frac{k}{\sqrt{ga}} f_1(\theta) = \frac{k}{\sqrt{ga}} f_2(\theta)$$

where $f_2(\theta)$ is an unknown function. Note that the power of θ cannot be determined by balancing the dimensions because θ is already a dimensionless variable. Experiments show that $f_2(\theta)$ is practically constant for small values of θ . It is seen that T is directly proportional to k and inversely proportional to the square root of a .

The equilibrium of a submerged body is unstable if the C.G. lies above the C.B. because the body will tend to move away from its original position if slightly disturbed. The equilibrium is neutral if the C.G. and C.B. coincide.

In general, if the equilibrium is stable, the stability is said to be positive; if the equilibrium is unstable, the stability is negative; and if the equilibrium is neutral, the stability is zero.

2.10. Floating Bodies. Archimedes' principle can be applied to bodies that are partly submerged and floating on the free surface of a liquid. Consider a body as shown in Fig. 2.23 submerged to a certain extent in an incompressible fluid of specific weight γ . Above the free surface the

atmospheric pressure is p_0 . To find the vertical force exerted by the fluid on the solid body, we proceed as before, subdividing the body into small vertical cylinders of cross-sectional area dA . In this case we find that the

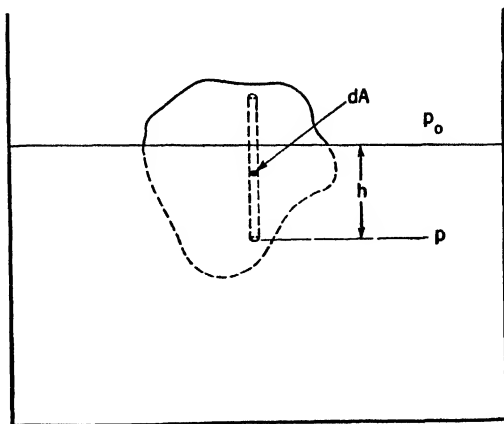


FIG. 2.23.

vertical force acting on each small cylinder whose upper end is above the fluid surface is $(p - p_0) dA$. The hydrostatic equation gives $p - p_0 = \gamma h$. Thus we see that the vertical force $\gamma h dA$ equals the weight of a fluid cylinder of cross section dA and of height h . The vertical force on a completely submerged small cylinder is the same as in the case of a totally submerged body. The total buoyancy exerted by the fluid upon the solid body has, therefore, the magnitude of the weight of the fluid displaced by the submerged part. The further steps of the argument concerning the horizontal components of the hydrostatic forces and the position of the C.G. can be repeated in exactly the same way as for the case of the fully submerged body. We arrive at the following conclusions: A body partly submerged in an incompressible fluid is subjected to a buoyancy that equals in magnitude the weight of the fluid displaced by the body and that also has the same line of action as this weight.

According to the principle just stated, equilibrium requires that the total weight of the body equal the weight of the displaced fluid and that the C.G. of the body lie on the same vertical line as the C.G. of the displaced fluid.

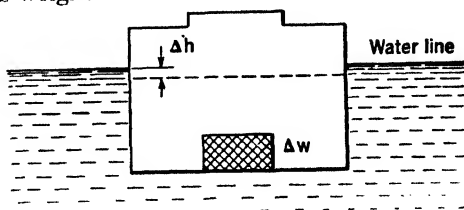


FIG. 2.24.

A floating body to which a weight ΔW is added will sink sufficiently to increase its displacement a corresponding amount (Fig. 2.24). If ΔW is small

with reference to the total weight, $\Delta W = \gamma A \Delta h$, where Δh is the sinkage caused by ΔW and A is the area of the horizontal section at the water-line plane. With ΔW expressed in tons and Δh in inches, the ratio $\Delta W/\Delta h$ is called by naval architects "tons per inch immersion." This is an important characteristic of a vessel, since it is constant for small changes in draft. The captain, for instance, can check by observation of the change in draft the weight of fuel reputedly placed on board by a contractor.

Consider as an example a short wooden cylinder of circular cross section with radius a and height b floating in water. What is the relation between the densities γ and γ_b and the depth of submergence? First assume that the axis of the cylinder remains vertical. If t denotes the depth of the submerged part, the principle of Archimedes yields the equation $\gamma a^2 \pi t = \gamma_b a^2 \pi b$. Therefore $t/b = \gamma_b/\gamma$. If, for example, the density of the body is one-half that of water, half of the cylinder will be submerged.

2.11. Stability of a Floating Body. A cylinder with a large ratio of length to diameter will not float with axis vertical but will lie flat on the water. Each position of the cylinder, vertical or horizontal, is, however, an equilibrium position. One of the two equilibrium positions is stable, while the other is unstable.

A submerged body is in stable equilibrium when the C.G. lies below the C.B. A floating body, on the contrary, may be in stable equilibrium (against rolling over) when the C.G. lies considerably above the C.B. It is a well-known fact, however, that a vessel has a very limited range of stable locations for the C.G. The criterion of the initial stability of a floating body is the position of a fictitious point, the metacenter, discovered by the French naval architect Bouguer in the eighteenth century to be inherent in the form of the submerged portion of the hull. This portion of the hull is called the "carene."

The concept of the metacenter is illustrated by the pair of sketches of Fig. 2.25. The left-hand sketch represents a cross section of a vessel floating upright at water-line level WL , in equilibrium. The right-hand sketch represents the same vessel inclined through an angle of roll θ and held over at this inclination by some external agency as by a sail. The new water line is marked $W'L'$. For convenience, the former water line and the former vertical axis are also indicated.

The C.G. of the vessel with all weights on board is assumed to be at G . If none of the cargo shifts, the C.G., when the vessel is inclined, will remain at G .

However, the C.B. will not remain fixed with reference to the vessel as it heels over. Recall that the C.B. has been shown to be at the C.G. of the displaced fluid. This is the center of volume of the carene. But the carene has a different shape when the vessel is inclined. The volume of fluid displaced is decreased on the high side by the wedge-shaped portion marked 2

in the figure and increased on the low side by the corresponding wedge marked 1. Since the weight of the vessel is unchanged, the displacement 2 lost on the high side must be equal to the displacement 1 gained on the low side. Consequently, there is a shift of the C.B. to the low side. As the vessel is progressively inclined, the C.B. moves from B to a succession of positions toward the low side and reaches a definite location B' for the

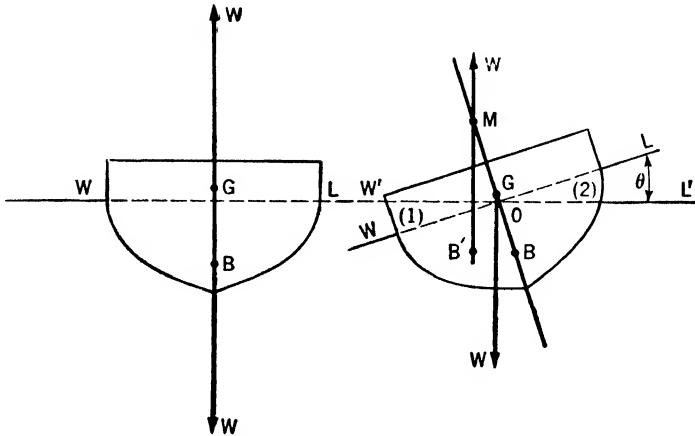


FIG. 2.25.

inclination shown. Note that the location of B' is a function only of θ and the outer form of the hull.

In the upright position, the vessel floats in equilibrium with weight W and buoyancy W , acting along the vertical axis.

In the inclined position, the weight W acts downward through G , but the buoyancy W now acts upward through B' , fortunately well to the low side of the vessel. The intersection of the vertical through B' with the axis of symmetry of the vessel (the vertical through B and G in the upright position) is at M . M is named the metacenter.

Now it is apparent that, as long as M lies above G , the couple of the two forces W is of a nature to resist the inclination and to restore the vessel to the upright position. Conversely, if M should fall below G , the couple would roll the vessel over.

The magnitude of the righting moment at a given inclination, or heel, could be readily computed if we knew the location of M . For if the distance \overline{GM} is known, the arm of the couple would be $\overline{GM}\theta$, for a small angle. Then the righting moment would be

$$R = W\overline{GM}\theta$$

2.12. Metacentric Height. Naval architects name the length \overline{GM} the "metacentric height" and make careful estimates of its value under various

conditions of loading and damage before the design of a vessel is accepted. In the previous section it was noted that the righting moment was proportional to the metacentric height. However, if the righting moment can be computed without knowledge of the metacentric height, then the metacentric height can be found.

We observe that the moment of buoyancy of the carene about B in the upright case is zero, while this moment about the same point becomes $W\overline{BB'}$ when the vessel is inclined. This change of moment of the buoyant forces due to a shift of the C.B. from B to B' is caused by a shift of the displacement of wedge 2 on the high side to wedge 1 on the low side. We may then equate the moment due to the shift of the C.B. to the moment of the couple due to the shift of displacement from wedge 2 to 1.

Since the moment of a couple is the same for any point in its plane, the moment of the wedges may be taken about point O for convenience in computation.

Let V be the volume displaced by the vessel, or $V\gamma = W$. Let x be the distance from the center line of the vessel to an element of volume as shown in Fig. 2.26. The element has transverse thickness dx , height θx , and

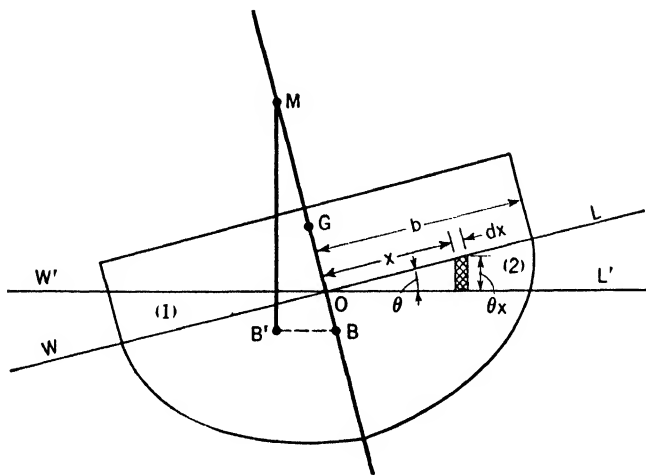


FIG. 2.26.

length l . Assume θ to be a small angle. Then the moment of the displacement of wedges 1 and 2 about O will be the sum of the moments of the weight of fluid in each such element of volume, $l\theta x dx$,

$$\text{Moment of wedges} = \gamma\theta \int_{-b}^{+b} lx^2 dx = \gamma\theta I$$

where I is the moment of inertia of the water-plane area, the horizontal section of the vessel cut by the plane of WL .

Since the moment of this couple about O and B is the same, we may, as was mentioned before, equate it to the moment about B due to the shift of the buoyancy from B to B' . Therefore, $W\overline{BB'} = \gamma V \overline{BM} \theta = \gamma \theta I$, and $\overline{BM} = I/V$. Since $\overline{BM} = \overline{GM} + \overline{BG}$,

$$\overline{GM} = \frac{I}{V} - \overline{BG}$$

It is of particular importance to note that we have obtained an expression for the metacentric height that is independent of the specific weight of the fluid γ and of the inclination θ .

The metacentric radius $\overline{BM} = I/V$ depends on the geometry of the vessel and can be computed from its plans. \overline{BM} also depends on the draft, as both I and V change with the water line corresponding to the loading of the vessel. For a vessel of parallel sides, I will remain constant, but V becomes less as load is removed. \overline{BM} should, therefore, increase.

The stability of the vessel, however, depends very much more on the location of the C.G. If cargo is removed from a deep hold, the C.G. in light condition is relatively higher, while at light draft the C.B. is relatively lower. Consequently, \overline{BG} may increase so much at light draft that the metacentric height (and consequently the stability) may vanish.

It is evident from the expression $\overline{GM} = I/V - \overline{BG}$ that to gain stability the C.G. should be low (\overline{BG} small) and the beam wide (I large).

In the discussion of stability in terms of metacentric height, it must be remembered that θ is assumed to be a small angle. Therefore only the initial stability of a floating body is indicated by this analysis.

The initial metacentric height is 1 to 2 ft for passenger steamers and 3 to 4 ft for naval vessels and sailing ships. Experience shows that the period of roll is shorter and rolling is more uncomfortable for a large metacentric height.

2.13. Period of Rolling. The applied moment $W\overline{GM}\theta$ and the mass moment of inertia of the vessel about the axis of roll are the most important factors on which the period of roll depends. The frictional damping is a second-order effect. Denoting the mass moment of inertia by $(W/g)k^2$, where k is the radius of gyration of the vessel, we find by an analysis like the one of Art. 2.9 that the period $T = (k/\sqrt{g\overline{GM}})\phi(\theta)$, where $(\phi\theta)$ is an unknown function. $\phi(\theta)$ is found experimentally to be constant for small values of θ .

We conclude, as has the practical seaman, that large \overline{GM} produces quick rolling. River steamers, not designed for a seaway, customarily have relatively great beam (large I/V), a high C.B. (small \overline{BG}), and a metacentric height of as much as 20 per cent of the beam.

A floating cylinder has zero stability; M lies on G , and $\overline{GM} = 0$

(Fig. 2.27). A vertical side or, even better, a flare is required for stability. "Tumble home" as on some whaleback steamers and on submarines awash can give doubtful stability.

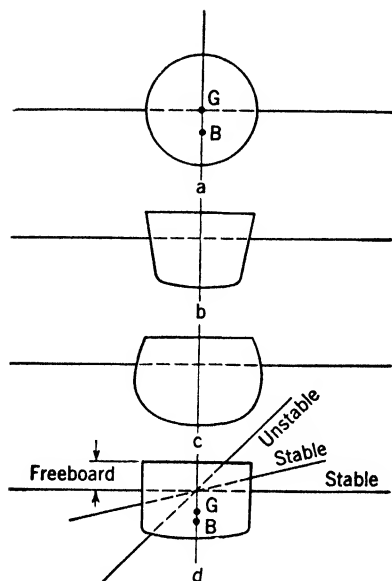


FIG. 2.27. — Floating bodies having varying degrees of stability. *a.* Circular cylinder — zero stability. *b.* Hull with flared sides — very stable. *c.* Hull with "tumble home" — doubtful stability. *d.* Range of stability of a typical hull form depends on the freeboard.

the metacentric height of the vessel is lowered by an amount equal to i/V , where i is the moment of inertia of the free surface about its center line and V , as above, is the volume of the carene. In damaged condition, a vessel with several compartments open to the sea may capsize before it sinks.

A fair \overline{GM} initially is not enough to give safety, as stability may vanish when the deck edge dips because I decreases abruptly. To preserve a "range of stability" through a large inclination, adequate freeboard is required.

2.14. Inclining Experiment. To determine \overline{GM} experimentally in order to verify the safety of a loaded barge or other vessel is a common precaution. A weight F is moved across the deck a distance x (Fig. 2.28). The change of moment Fx causes an observed heel, or list, θ balanced by a righting moment $W\overline{GM}\theta$. W can be computed from the plans of the vessel corresponding to the observed draft. Then

$$W\overline{GM}\theta = Fx \quad \text{and} \quad \overline{GM} = Fx/W\theta$$

2.15. Free-surface Effect. It can be shown, by methods identical with those used to compute the position of the metacenter, that, if any compartment of a ship has a free liquid surface, the

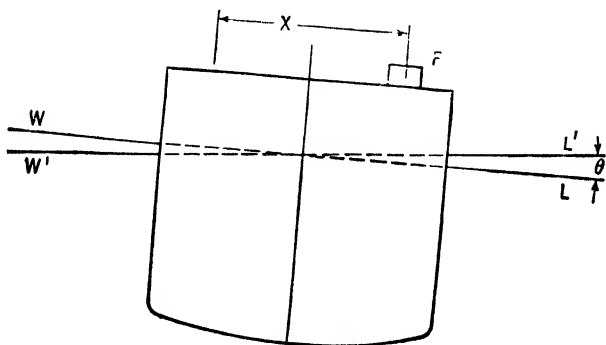


FIG. 2.28.

2.16. Statics of Moving Systems. When the entire continuum is in uniform rectilinear motion, our conclusions regarding the statics of a fluid in the gravity field of force apply without change. This follows from Newton's fundamental concept that force results from change of motion. When there is uniform motion of all particles of a system, there is no change of motion for any of them, and hence no change in the forces that would act on them when at rest.

Consequently, we may ignore a uniform velocity of translation and write as before for the hydrostatic equation.

$$p - p_0 = \gamma h$$

2.17. d'Alembert's Principle. Consider a particle or small portion of fluid of mass m in a continuum, located at x, y, z , and moving at a given time with an acceleration whose components are d^2x/dt^2 , d^2y/dt^2 , and d^2z/dt^2 . The presence of such an acceleration implies, from Newton, that the resultant force acting on the particle has effective components equal to $m(d^2x/dt^2)$, $m(d^2y/dt^2)$, and $m(d^2z/dt^2)$. Now the resultant force acting on the fluid particle is the sum of the external surface and body forces. Let its components be X, Y, Z . Note that the resultant external force is acting in the direction of the resultant acceleration.

The equations of motion for the particle are thus:

$$X = m \frac{d^2x}{dt^2} \quad Y = m \frac{d^2y}{dt^2} \quad Z = m \frac{d^2z}{dt^2}$$

or

$$X - m \frac{d^2x}{dt^2} = 0 \quad Y - m \frac{d^2y}{dt^2} = 0 \quad Z - m \frac{d^2z}{dt^2} = 0$$

The latter form of the equations of motion is identical in appearance with the three equations of equilibrium for a particle without acceleration. It is therefore obvious that, if a fictitious force with components $-m(d^2x/dt^2)$, $-m(d^2y/dt^2)$, $-m(d^2z/dt^2)$ is considered to act on the particle in addition to the real forces, then this system of fictitious and real forces is in equilibrium. The fictitious force is called the "inertia force," and the fictitious equilibrium is called "dynamic equilibrium."

The principle of d'Alembert is embodied in the last paragraph. It is seen that this principle enables us to reduce a problem of motion to one of equilibrium simply by taking into account the inertia forces which act on the masses involved.

2.18. Uniform Rectilinear Acceleration. Consider the liquid in an open tank moving with constant acceleration a in a horizontal direction as shown in Fig. 2.29. By d'Alembert's principle, we may consider the liquid at rest in the tank in a field of force determined by g units of force per unit mass downward and a units horizontally, toward the left. The

resultant force vector is $\sqrt{a^2 + g^2}$ and is directed away from the vertical by $\theta = \tan^{-1} a/g$. The direction and magnitude of the force vector are the same at all points.

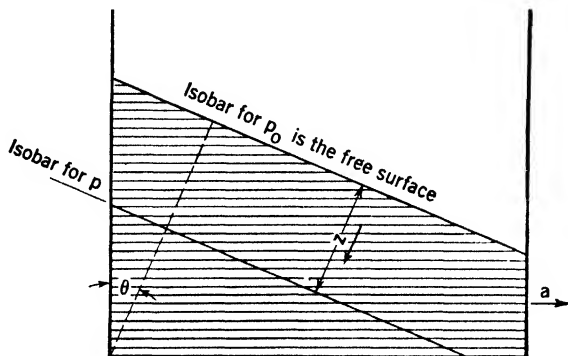


FIG. 2.29.

The force on unit volume of fluid that when at rest is $\gamma = \rho g$ is now $\gamma' = \rho\sqrt{a^2 + g^2}$, and the hydrostatic equation becomes

$$p - p_0 = \gamma' z = \rho\sqrt{a^2 + g^2} z = \frac{\rho g z}{\cos \theta} \quad (2.10a)$$

where z is measured normal to a surface of constant pressure, as shown in Fig. 2.29.

The free surface at $z = 0$ and $p = p_0$ is inclined to the horizontal at an angle $\theta = \tan^{-1} a/g$. If the horizontal acceleration is g , the liquid banks up at a 45-deg angle. The surfaces of constant pressure are parallel to the

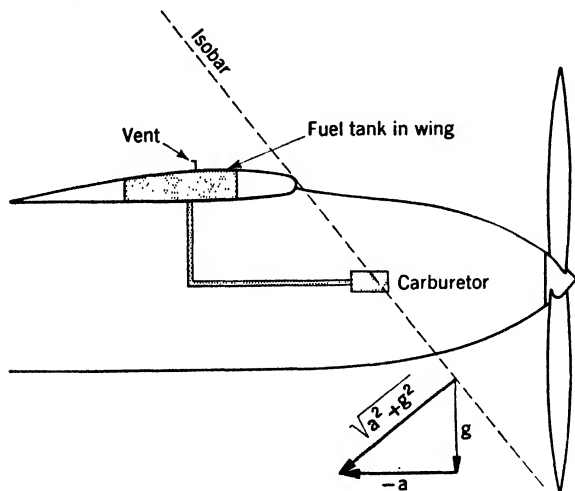


FIG. 2.30. — A catapulted airplane may be momentarily starved of fuel.

free surface. The maximum pressure is at the corner of the tank where z is a maximum.

This type of analysis applies to the design of a tank truck where brakes may be applied roughly or to a tank car for a railway. An interesting example (Fig. 2.30) is furnished by the fuel system of an airplane launched by catapult (with a horizontal acceleration usually greater than g). A gravity feed will not operate; instead, the carburetor may be drained back into the tank, and fuel may pour out of the vent of the main tank. Obviously, a check valve is required, or a pressurized fuel tank.

2.19. Uniform Spin. When a body of fluid rotates uniformly as a whole without relative motion of its parts, each particle moves in a circle as do elements of a rigid body.

Let the constant angular velocity be ω , and let ρ be the density of the liquid. Choose polar coordinates with z and r as shown in Fig. 2.31. The centripetal acceleration of a particle at radius r is $\omega^2 r$. Consider the dynamic equilibrium of the particle by d'Alembert's principle. In the horizontal plane the pressure must increase radially to balance the centrifugal force $\rho \, dr \, dz \, dn \, \omega^2 r$. In the vertical plane the pressure must increase with depth to balance the weight $\rho g \, dr \, dz \, dn$, as for a fluid at rest. Therefore,

$$\rho \, dr \, dz \, dn \, \omega^2 r = \frac{\partial p}{\partial r} \, dr \, dn \, dz \quad \text{or} \quad \rho \omega^2 r = \frac{\partial p}{\partial r}$$

$$- \rho \, dr \, dz \, dn \, g = \frac{\partial p}{\partial z} \, dz \, dr \, dn \quad \text{or} \quad - \rho g = \frac{\partial p}{\partial z}$$

Since p depends only on r and z , we can write that

$$dp = \frac{\partial p}{\partial z} \, dz + \frac{\partial p}{\partial r} \, dr = - \rho g \, dz + \rho \omega^2 r \, dr$$

or

$$p = \int_{z_0}^z - \rho g \, dz + \int_0^r \rho \omega^2 r \, dr = - \rho g (z - z_0) + \frac{\rho \omega^2 r^2}{2} + p_0$$

At the free surface where $p = p_0$, $z = z_0 + (\omega^2/2g)r^2$, a paraboloid of revolution.

Surfaces of constant pressure are similar paraboloids of revolution with common axis,

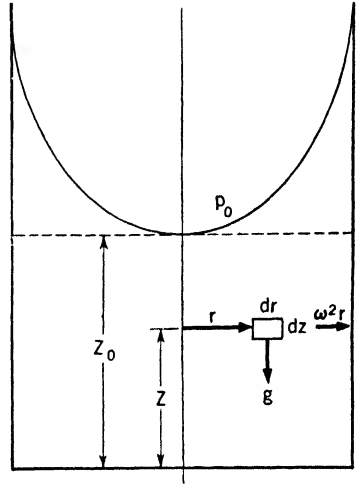


FIG. 2.31.

$$z - z_0 = \frac{\omega^2}{2g} r^2 - \frac{p - p_0}{\rho g}$$

Where $r = 0$, the variation of pressure is as in a fluid at rest,

$$p - p_0 = -\rho g(z - z_0)$$

Note that, for constant z , p increases as r^2 . A centrifugal pump and a centrifuge make use of this principle. An enclosed mass of water is whirled rapidly to create a great difference in pressure between its center and its periphery.

2.20. Overshot Water Wheel. On unit mass of water in a bucket as shown in Fig. 2.32, the force field can by d'Alembert's principle be con-

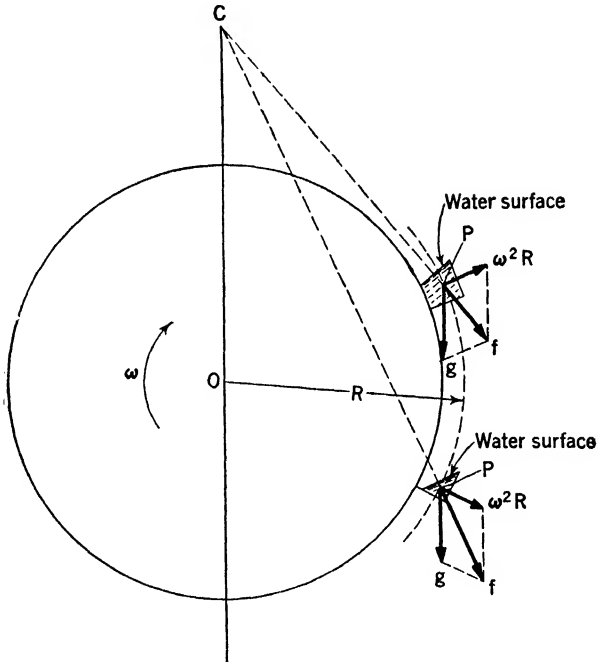


FIG. 2.32. — Overshot water wheel.

sidered as made up of a component g due to gravity and a component $\omega^2 R$ due to centrifugal force as shown. The resultant force f cuts the vertical at C .

$$\frac{OC}{OP} = \frac{OC}{R} = \frac{g}{\omega^2 R}$$

or

$$OC = \frac{g}{\omega^2} = \text{constant}$$

Consequently, C is a fixed point for all buckets, and the water in each is in equilibrium under a force field directed along a line CP . The free surface of water in each bucket will be normal to CP for all positions.

2.21. Statics of Compressible Fluids. The general condition for the equilibrium of a fluid at rest holds for both compressible and incompressible cases, *i.e.*, the pressure gradient equals the specific weight and is directed vertically downward. For the usual coordinate system, with the h axis upward, we have from Eq. (2.7)

$$\frac{dp}{dh} = -\gamma \quad (2.7)$$

The surfaces of constant pressure are horizontal planes as in the case of the incompressible fluid, and p is a function of h alone. From the relation $dp/dh = -\gamma$ we also conclude that γ (or ρg) depends on h . In the incompressible case, density is constant, but for a compressible fluid the density, which obviously decreases with pressure, must also decrease with h and must be constant over each horizontal plane.

If we knew the relation between height and density of the fluid, we could predict the pressure change between level h_1 and a higher level h by integrating the equation to obtain

$$p - p_1 = - \int_{h_1}^h \gamma \, dh$$

or

$$h - h_1 = - \int_{p_1}^p \frac{dp}{\gamma}$$

2.22. Physical Properties of Liquids and Gases. For practical problems, however, we are usually able to relate density or specific weight only to pressure and temperature. For liquids, the relation between specific weight and pressure is usually given in the form

$$dp = \beta \frac{d\gamma}{\gamma} = -\beta \frac{dv}{v} \quad (2.11)$$

where β , called the "bulk compression modulus," is practically constant over a large range of pressures; and v , the reciprocal of γ , is called the "specific volume."

For water, $\beta = 310,000$ lb per sq in., for usual hydraulic work where temperatures are not near freezing or boiling and pressures are less than 10,000 lb per sq in. Thus for a pressure increase of 1,000 lb per sq in. there is an increase in specific weight or density of 0.32 per cent and a decrease in specific volume of the same amount.

Water is peculiar in its change of density with temperature. For moderate pressures there is an increase in density of about 8 per cent at the change from ice to liquid. There is a further increase to a maximum density at 4 C (39 F) and then a density decrease of about 4 per cent up to the boiling point. At the transition from liquid to steam the density decreases by a factor of 1,700.

The following table shows the variation of specific gravity in the sea as a function of depth. The last column, headed *With compression*, gives the actual specific gravity resulting from the effects of both temperature and pressure. The adjacent column, headed *Without compression*, gives the effect on specific gravity of temperature alone. Note that there is little change in specific gravity (and hence in density) even at immense depths.

Depth, ft	Temperature, deg F	Specific gravity	
		Without compression	With compression
0	80.8	1.02220	1.02220
1,000	40.1	1.02739	1.03215
10,000	36.7	1.02768	1.07123

For engineering purposes, water may be considered incompressible, provided that neither ice nor steam is involved and further provided that it is not subject to severe acceleration giving rise to compression waves (water hammer). Other liquids likewise may be treated as incompressible, and the ordinary hydrostatic equation applied.

$$p_2 - p_1 = -\gamma(h_2 - h_1)$$

For the permanent gases, however, substantial density changes accompany changes of both pressure and temperature. At a height between 3 and 4 miles, where pressure and temperature are considerably lower than at the earth's surface, the atmosphere has but half the density at sea level. The well-known equation of state for a perfect gas is sufficiently accurate for most engineering purposes,

$$pv = RT \quad (2.12)$$

where R is the gas constant for the gas in question and T is the absolute temperature. R has the dimensions of a length divided by a temperature, as shown by Eq. (2.12),

$$[R] = \left[\frac{pv}{T} \right] = \left[\frac{F}{L^2} \frac{L^3}{F} \frac{1}{\theta} \right] = \left[\frac{L}{\theta} \right]$$

A second relationship that applies to the permanent gases is the polytropic equation, connecting specific weight (or volume) and pressure,

$$\frac{p}{\gamma^n} = pv^n = \text{constant} \quad (2.13)$$

where n is a constant. The value of n depends on the process and on the gas. For a process in which friction and heat transfer are negligible (reversible adiabatic process) it is found, to a good approximation, that $n = c_p/c_v$, where c_p and c_v are the specific heats at constant pressure and constant volume, respectively. The ratio c_p/c_v is here denoted by k .

The following table gives the values of R , k , and γ for a few gases:*

Gas	k	R		γ	
		M/deg C	Ft/deg F	Kg/m ³	Lb/ft ³
Helium . .	1.66	212.0	386.5	0.1785	0.01114
Air	1.40	29.27	53.35	1.2928	0.08071
Oxygen . .	1.40	26.50	48.31	1.4289	0.08921
Nitrogen .	1.40	30.26	55.20	1.2505	0.07807
Hydrogen	1.41	420.6	766.5	0.08987	0.005611

2.23. Isothermal Equilibrium. The general equilibrium condition for a compressible fluid, $dp/dh = -\gamma$, cannot be integrated to obtain the pressure distribution unless γ can be eliminated. This can be done by means of the equation of state,

$$pv = \frac{p}{\gamma} = RT \quad \text{or} \quad \gamma = \frac{p}{RT}$$

Substituting for γ , we have

$$\frac{dp}{p} = -\frac{dh}{RT} \quad (2.14)$$

For the isothermal case, T is constant. Accordingly, we find by integration of Eq. (2.14), if h is measured above a reference level h_1 where the pressure is p_1 , that

$$\left. \begin{aligned} \log p - \log p_1 &= \log \frac{p}{p_1} = \frac{h_1 - h}{RT} \\ \text{or} \quad p &= p_1 e^{(h_1 - h)/RT} \end{aligned} \right\} \quad (2.15)$$

This is the pressure distribution for isothermal equilibrium of a permanent gas. It may be noted that it corresponds to and replaces the simpler formula $p = p_1 + \gamma(h_1 - h)$ for an incompressible fluid. The two expressions become identical if $(h_1 - h)/RT$ becomes small, that is, for an elevation of the order of 250 ft. For if x is small, $e^x = 1 + x$ (the first two terms of the power-series expansion for e^x). In this case we can write Eq. (2.15) as

$$p = p_1 \left(1 + \frac{h_1 - h}{RT} \right) = p_1 + \frac{p_1}{RT} (h_1 - h) = p_1 + \gamma_1 (h_1 - h)$$

substituting $\gamma_1 = p_1/RT$ from the equation of state.

For the measurement of height from a knowledge of the pressures p_1 and p , Eq. (2.15) is put in the form of the so-called "barometric formula." Since barometer heads b_1 and b correspond directly to p_1 and p , we can take $b_1/b = p_1/p$ and write Eq. (2.15) in the form

$$h - h_1 = RT \log \frac{b_1}{b} \quad (2.16)$$

for the isothermal case.

* At 760 mm, 0 C or 29.92 in. Hg, 32 F.

As an example, suppose a mercury barometer is observed to stand at 29.8 in. at the foot of a hill and at 24.6 in. at the top. It is assumed that the average temperature of the air is 50 F. (Note that we neglect the temperature gradient up the hill. For a high mountain this would not be justified.) Then $T = 50 + 460 = 510$ F abs, and from Eq. (2.16)

$$h - h_1 = 53.3 \times 510 \log 1.21 = 2,256 \text{ ft}$$

2.24. Lapse Rate in the Atmosphere. In applying the barometer to the measurement of a great altitude, allowance must be made for the decrease in temperature with elevation. For the first few miles above the ground the rate of decrease has been found to be nearly constant. Assume such a constant rate of temperature decrease, and let $dT/dh = -\lambda$, the constant lapse rate.

The equation of state (2.12) and the fundamental condition of equilibrium (2.7) have already been combined to give Eq. (2.14). Eliminating dh by combining Eq. (2.14) with $dT/dh = -\lambda$, we get

$$\frac{dp}{p} = \frac{1}{\lambda R} \frac{dT}{T}$$

The last equation can be integrated to give $\log p = (1/\lambda R) \log T + C$ or

$$\frac{p^{\lambda R}}{T} = C = \frac{p_1^{\lambda R}}{T_1} \quad (2.17)$$

where p_1 and T_1 are an arbitrary pair of values of p and T . Substitution of $p/R\gamma$ for T , from the equation of state, gives

$$\frac{p^{\lambda R R \gamma}}{p} = C$$

or

$$\frac{p}{\gamma^{1/(1-\lambda R)}} = \left(\frac{R}{C}\right)^{1/(1-\lambda R)} = \text{constant} \quad (2.18)$$

Comparison of Eqs. (2.13) and (2.18) shows that the assumption of a constant lapse rate is equivalent to the assumption of a polytropic relation between p and γ for which the exponent

$$n = \frac{1}{1 - \lambda R} \quad (2.19)$$

If n is taken as being equal to k for air, the corresponding value of λ is called the "adiabatic lapse rate,"

$$\lambda_{ad} = \left(\frac{1}{R}\right) \left[1 - \left(\frac{1}{k}\right)\right] = \left(\frac{1}{53.3}\right) \left[1 - \left(\frac{1}{1.4}\right)\right] = 0.00535 \text{ F per ft}$$

or about 5 F per 1,000 ft (1 C per 100 m).

In the real atmosphere the lapse rate is usually about half of this value ($\lambda \approx \lambda_{ad}/2 = 0.0027$ F per ft), and thus the corresponding value of $n = 1/(1 - \lambda R) = 1/(1 - 0.0027 \times 53.3) = 1.17$.

To find the pressure distribution in the atmosphere or the relation between pressure and altitude, we substitute in Eq. (2.17) for T its value from $T - T_1 = \lambda(h_1 - h)$, which is merely the integrated form of $dT/dh = -\lambda$. Thus we find, after solving for $h - h_1$,

$$h - h_1 = \frac{T_1}{\lambda} \left[1 - \left(\frac{p}{p_1} \right)^{\lambda R} \right] \quad (2.20)$$

If the gradient λ and a set of corresponding values of h_1 , p_1 , T_1 are given, this formula can be used for determining the altitude h from a barometer reading p . If we have for instance at the ground $h_1 = 0$, $T_1 = 540$ F abs, and $p_1 = 29.92$ in. Hg, a barometer reading $p = 17.5$ in. Hg gives, for $\lambda = 0.0027$,

$$h = \frac{540}{0.0027} \left[1 - \left(\frac{17.5}{29.92} \right)^{0.144} \right] = 14,900 \text{ ft}$$

It is evident that the selection of the lapse rate has an important effect on the altitude estimated from Eq. (2.20). An alternative form of the barometric equation requires the selection of a suitable value of n , corresponding to the probable lapse rate.

Substituting in Eq. (2.20) for λ its value from Eq. (2.19), we find

$$h - h_1 = RT_1 \frac{n}{n-1} \left[1 - \left(\frac{p}{p_1} \right)^{(n-1)/n} \right] \quad (2.21)$$

This is a general formula for determining height from an observation of two pressures p and p_1 provided that n is known.

A corresponding formula connecting height with temperature drop has already been obtained by integration of $dT/dh = -\lambda$,

$$h - h_1 = \frac{1}{\lambda} (T_1 - T)$$

or

$$h - h_1 = R \frac{n}{n-1} (T_1 - T) \quad (2.22)$$

2.25. Height of the Atmosphere. *a. Adiabatic Case.* Taking $n = k = 1.4$ for dry air, $R = 53.4$ ft per deg F, and $T_1 = 592$ F abs at the ground level, we find from Eq. (2.21) that p will be zero when

$$h - h_1 = RT_1 \frac{k}{k-1} = 92,000 \text{ ft}$$

or about 17 miles.

We know that the atmosphere does not stop at 17 miles but extends, with diminishing density, for hundreds of miles. However, we also know

that the troposphere, or the part of the atmosphere next the earth, has an approximately adiabatic lapse rate for 6 or 7 miles and that thereafter an isothermal stratosphere extends to a considerable height. Let us examine the extent of a hypothetical isothermal atmosphere to see whether a large extent is compatible with static equilibrium.

b. Isothermal Case. The equilibrium condition for this case is embodied in Eq. (2.15), $h - h_1 = RT \log (p_1/p)$, from which h is seen to be infinite if $p = 0$. An isothermal atmosphere would extend outward indefinitely, as seems to be the case with the actual atmosphere, although it is now known not to be isothermal.

c. Constant-density Case. The height of a column of air of uniform density necessary to create the pressure under which we live, or the "head" of air, can be computed from the hydrostatic equation [Eq. (2.9)]. If the assumed value of density corresponds to $p = 29.92$ in. Hg and $T = 32$ F, the height of the column for $p = 0$ is found to be about 5 miles.

2.26. Remarks on the Equilibrium of the Atmosphere. The lower part of the atmosphere, or troposphere, is constantly being mixed by convection. Water vapor is being taken up and again precipitated, and there are great movements of polar air and of tropical air into the temperate regions. In the tropics, owing to intense heating of the ground, air is rising. This produces a general circulation of air from the temperate regions toward the tropics (trade winds) and a drift near the top of the troposphere from the tropics toward the poles. Cold air aloft settles toward the earth to maintain continuity. This general mixing of the atmosphere is due to unequal heating of the earth's surface, caused by variation of solar intensity with latitude and by unequal heat-absorptive qualities of land and water areas. As a result, the troposphere is kept in some average thermal and mechanical equilibrium whose disturbance we know as weather. This varies from day to day or even from hour to hour in an irregular manner.

Climate is determined by the average weather at a given place over a long period of time. Thus climatology predicts from past records the safe date for planting crops. Meteorology predicts tomorrow's weather from a knowledge of the present condition of the atmosphere near a given locality. The convective mixing of the troposphere tends to establish a stable equilibrium, and there is a certain degree of continuity in our weather.

That the lower atmosphere should have an approximately adiabatic temperature gradient is suggested by the fundamental nature of convection. Air next the ground that is heated more in one locality than elsewhere will rise like warm air in a chimney. Colder and denser air will flow in to take its place. The rising air cools adiabatically, for air is a poor conductor.

It is interesting to observe that the natural temperature lapse rate makes for stability of the lower atmosphere; *i.e.*, an air mass, displaced vertically from any cause, tends to return toward its original level. Con-

sider a mass of air rising by convection because it became slightly unstable at ground level owing to local heating. This air will cool adiabatically 1 C per 100 m. At any level it will be subject to the same pressure as the surrounding atmosphere. Hence, if the atmospheric lapse rate is but 0.6 C per 100 m (the usual case), the displaced air mass will be denser than its surroundings and will tend to fall back.

In general, when the atmospheric lapse rate exceeds the adiabatic rate of 1 C per 100 m, the air is unstable. Under usual conditions the air is stable, and large-scale convection does not occur. Thunderstorms arise in an unstable atmosphere in which the lapse rate is temporarily excessive from abnormal heating of the ground and the lower strata of the air. This condition frequently occurs in summer. In winter, when the ground is covered with snow, the lower strata are cold, the lapse rate is low, and the air is likely to be stable. On a clear summer night the ground cools quickly by radiation, and the lower stratum of air may become cooler than that lying above it. Here the lapse rate may be zero or even reversed. This is called "temperature inversion" and makes for very great stability.

The troposphere is found to extend upward with a fairly constant lapse rate until the temperature has fallen to about -50°C . This temperature may be reached at a height of about 7 miles in our latitude. From there on to 12 or 13 miles, the stratosphere extends as an isothermal blanket.

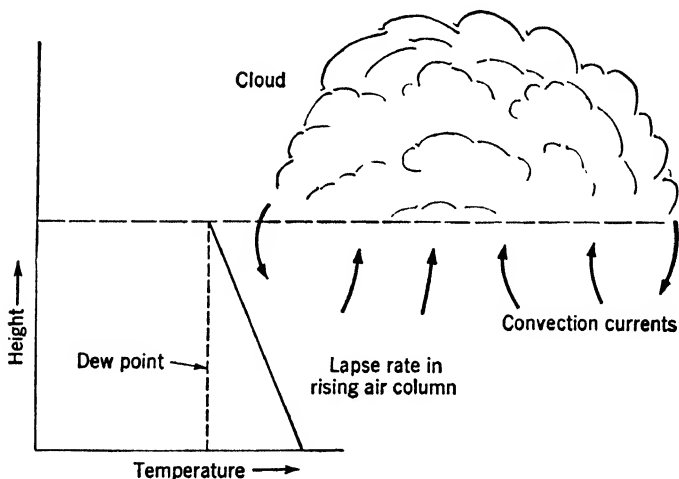


FIG. 2.33. — Cloud formation by condensation of water vapor carried upward in a rising column of air.

Above the stratosphere, there is evidence of a temperature maximum of about 80°C at a level of 30 to 40 miles. Above 50 miles, the atmosphere is strongly ionized and is known as the "ionosphere." It has properties of great importance to radio-wave propagation by reflection. There is

evidence from auroral measurements of the presence of an upper atmosphere to 750 miles.

The formation of cumulus clouds and thunderstorms is a result of instability. Warm, moist air next to the ground becomes unstable and rises, cooling adiabatically until the dew point is reached, when condensation of water vapor makes a cloud form (Fig. 2.33). If the initial uprush is violent, the rising air may overshoot its altitude of equilibrium. If there is an inversion or a stable layer of air at this elevation, further upward motion is stopped. However, if the upper air is neutral or slightly unstable, the

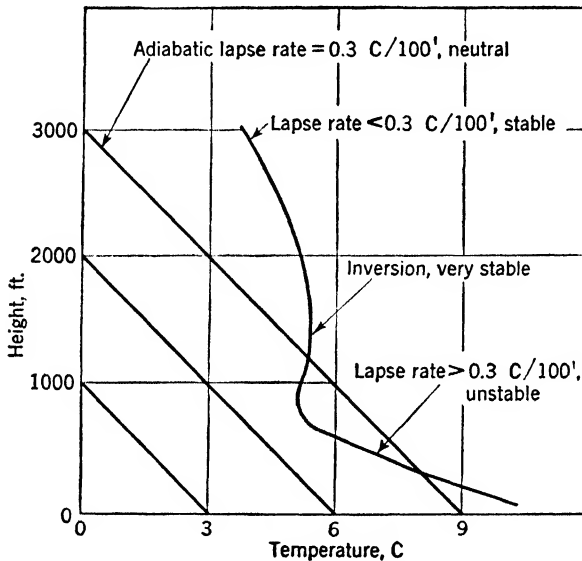


FIG. 2.34. — Relation between lapse rate and stability of the atmosphere.

latent heat released by condensation may be enough to carry the convection current to greater heights. Aviators have occasionally found storm clouds extending to 35,000 ft, but usually the air is clear above 20,000 ft. Figure 2.34 shows how the actual lapse rate may be stable or unstable depending on whether it is greater or less than the adiabatic (neutral) rate.

2.27. Balloons. *a. Taut Balloon.* A balloon is said to be taut if it is completely filled with gas. Since the bag of a balloon can support only negligible internal overpressure, a safety valve is provided, which allows gas to escape as the balloon rises, thus maintaining nearly equal internal and external pressures. If we assume the balloon rises so slowly that the internal and external temperatures are equal at every instant, the equation of state [Eq. (2.12)] yields $\gamma_g/\gamma_a = R_a/R_g = \text{constant}$. Subscript g refers to the gas and subscript a to the atmosphere.

For a balloon of volume V rising at uniform velocity the buoyant force

$V(\gamma_a - \gamma_g)$ is just counterbalanced by the weight W of the structure and load, plus the air resistance D ,

$$W + D = V\gamma_g\left(\frac{\gamma_a}{\gamma_g} - 1\right) = V\beta \quad (2.23)$$

As γ_a/γ_g is constant, β will vary as γ_g . The buoyancy of the balloon will therefore diminish as γ_g becomes smaller, *i.e.*, as altitude is increased.

At the maximum height the velocity, and hence the drag D , will be zero, and $\beta = \beta_m = W/V$. Note, however, that, if the balloon overshoots the maximum level by virtue of its kinetic energy, too much gas will be lost and the rest condition cannot be attained. Instead, the balloon will fall under the action of a constant downward force since the weight of gas $V\gamma_g$ will now be constant. The balloon will therefore accelerate downward until the condition $W - D = V\beta$ is satisfied.

If the balloon is anchored to the ground, the drag D of Eq. (2.23) will be replaced by the tension F in the mooring cable. Letting $\beta = \beta_0$ at ground level, we find that $\beta_0 = (W + F)/V$. Therefore, the ratio $\beta/\beta_0 = \gamma_a/\gamma_{a_0} = (p/p_0)^{1/n} = (W + F)/W$. From a table of the standard atmosphere one may pick out h corresponding to any value of p/p_0 , or h can be computed from an assumed average temperature change. Hence, for a known value of the ballast necessary to hold a balloon on the ground, one may estimate the height to which it can rise.

b. Flabby Balloon. If the balloon is only partly filled at the start, it will rise under the action of a constant buoyant force until it is completely filled, for the weight of gas $V\gamma_g$ remains unchanged. The level at which gas starts to escape is called the "pressure height." For elevations greater than the pressure height the rising balloon is taut and behaves as described above.

2.28. Superchargers. At 20,000 ft the density of air is less than half that at sea level. The oxygen in the air intake per cylinder volume of an airplane engine is therefore only about half that needed to burn the fuel required to develop full power. If a compressor is used to supply air to the engine at sea-level density, the full power is restored. Such compressors, known as superchargers, are gear-driven from the engine or driven by an exhaust turbine. An engine may not safely be supercharged at ground level because the compression ratio is presumably already as high as the fuel will tolerate without detonation.

Human beings resemble the internal-combustion engine in that a fixed lung capacity and a fairly constant frequency of respiration require a fixed amount of oxygen per stroke. Above 12,000 ft human beings need extra oxygen enrichment of the thin air they breathe or else the equivalent of supercharging (supercharged cabin).

CHAPTER III

KINEMATICS AND CONTINUITY

3.1 Relative Motion. Kinematics is concerned only with space-time relationships, without regard to force. We shall deal with a continuum in which there are no voids and such that nowhere in it is fluid either created or destroyed. The mathematical description of the motion is complete if we have an expression which gives, for every point, the magnitude and direction of the fluid velocity at that point, at any instant of time.

Velocity is measured relative to some coordinate system, either fixed or moving. We might choose a coordinate system fixed in space, past which the fluid flows, *e.g.*, an observer sitting on the bank of a stream. Alternatively, we might choose a coordinate system attached to a particular part of the fluid and moving with it, *e.g.*, a swimmer allowing himself to be carried along with the stream. For reasons of simplicity we shall adopt the first system of coordinates, following Euler, and describe fluid velocity V in terms of the time for every point x, y, z , fixed with reference to a stationary coordinate system. Thus $V = f(x, y, z, t)$.

In this connection a type of relativity discussed by Newton will be helpful in keeping our mathematics simple in form. Suppose we are interested in the flow around a solid body moving with velocity V through a large expanse of fluid that is at rest at a great distance from the body. The fluid is disturbed by the passage of the body and, relative to the body, moves past it and closes in behind, preserving the continuity of the fluid. Since the fluid motion is due only to the relative motion of the body and the continuum, the velocities and accelerations relative to the body would be exactly the same at all points in the continuum if we considered the body at rest in an infinite expanse of fluid moving past it with a velocity of $-V$. We shall, in general, consider cases of flow past solid objects as if the object were at rest in a stream of fluid.

We literally adopt this procedure in the wind tunnel, in which a model on a force-measuring balance is exposed to a stream of air. But for testing models of ships, the model is towed through a channel or tank of water at rest. To observe the flow pattern relative to the ship's model it is necessary to fix a camera to the carriage that tows the model. A short time exposure will make a record of the flow pattern, provided that one puts sawdust in the water or otherwise makes visible the motion of individual particles. To observe the flow pattern in the wind tunnel a stationary camera is used to record the appearance of air flow made visible by smoke.

With the moving camera in the tank experiment we have in effect chosen a set of coordinates fixed in the body. The camera sees the water as if flowing past the model with a relative velocity equal but opposite to that of the model.

3.2. Streamlines. If we knew the direction of the velocity at each point x, y, z at a given instant of time, we could make a record of the flow by drawing lines everywhere tangent to the particle velocities. Such lines are technically named "streamlines." When we take a short time exposure of the surface of the water in the ship's model tank referred to above, each of the distinguishable particles of water will be represented on the developed plate by a short streak, whose slope indicates the direction and whose length indicates the relative magnitude of the fluid velocity at this point. We can then draw a series of streamlines tangent to these experimentally determined velocity vectors and obtain a streamline picture, or flow pattern.

3.3. Path Lines. If, on the other hand, we take a long time exposure, the long streaks on the plate will register the paths of the different visible particles of fluid. Such lines are called "path lines" (after Prandtl). They do not necessarily give information about the velocity, as they record an observation of the change in the position of particles, which takes place from time t_1 to a later time t_2 . Obviously, the streamline picture at time t_2 may be very different from that at time t_1 . The path lines may crisscross and present a tangled picture impossible to interpret in terms of velocity.

3.4. Steady Flow. If the velocity at every point remains the same at all times the motion is said to be steady; $V = f(x, y, z)$ and is independent of time, that is, $\partial V / \partial t = 0$ everywhere. For such steady motion, the streamline pattern is "stationary," and all streamline photographs will be identical. Steady motion is often called "stationary flow." In this case, the path lines and the streamlines, as here defined, are identical. Under certain conditions one can show that a steady velocity implies steady pressure, density, and temperature. It will be assumed in all cases that these conditions are fulfilled. A steady flow will therefore be defined as one in which not only velocity but also pressure, density, temperature, and any other fluid property are all independent of time at any fixed point.

3.5. Stream Tubes. Since a streamline is, by construction, everywhere tangent to particle velocities, in steady motion the flow follows the streamlines. Consequently, no fluid crosses a streamline. In an ideal continuum the velocity for steady motion is a continuous function of the space coordinates, and every streamline is a continuous line beginning at an infinite distance upstream and extending an infinite distance downstream. When the continuum is bounded by solid walls, such as is the case in a hydraulic system, we may consider the streamlines as starting in the reservoir where

fluid is at rest and extending through the entire system to the ultimate discharge. Streamlines in a steady flow represent the paths of particles; and since matter in the continuum is neither created nor destroyed, a streamline can, theoretically, have no ends. It either extends to infinity in both directions or is a closed line.

Through any point in the fluid only one streamline can be drawn, extending up- and downstream. The streamlines through all points on a closed curve define a stream tube. The fluid inside such a stream tube remains inside the tube since no fluid can cross a streamline. Extending the concept we can imagine the entire flow composed of stream tubes, drawn through some arbitrarily selected net or mesh stretched across the flow.

3.6. Conservation of Mass — Equation of Continuity. The mathematical statement of the fact that fluid is neither created nor destroyed in a

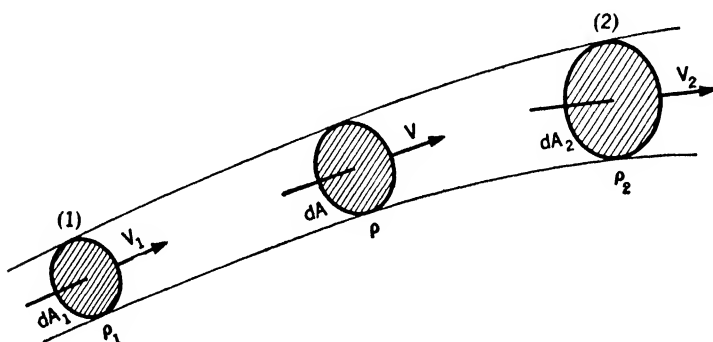


FIG. 3.1. — Flow in a stream tube of infinitesimal cross section.

continuum is called the “equation of continuity.” For steady flow in a stream tube of infinitesimal cross section, this equation is

$$\frac{dm_1}{dt} = \frac{dm_2}{dt} = \frac{dm}{dt} = \text{constant}$$

where dm/dt is the rate of mass flow through the stream tube at an arbitrary point. The equation has this form because in steady flow there is nowhere a change in density with time. Hence no accumulation of mass can occur inside the stream tube, and the same amount must pass all cross sections in unit time. Since the rate of mass flow across area dA is equal to $\rho V dA$ (Fig. 3.1), the above equation may be written

$$\rho_1 V_1 dA_1 = \rho_2 V_2 dA_2 = \rho V dA = \text{constant} \quad (3.1)$$

For a stream tube of finite cross section this can be integrated to give

$$\int_A \rho V dA = \text{constant} \quad (3.2)$$

where dA is normal to the velocity V at every point (Fig. 3.2). If ρ and V are assumed constant over every cross section, Eq. (3.2) reduces to

$$\rho VA = \text{constant} \quad (3.3)$$

Equation (3.3) is sufficiently exact for many engineering problems. If the fluid can be considered incompressible (as can water in ordinary pipe flow, or air in many aerodynamic problems), Eq. (3.3) becomes

$$VA = \text{constant} \quad (3.4)$$

We now develop a more general form of the continuity equation, which will apply both to steady and to unsteady flow. The method used here for continuity will be useful in later chapters in the treatment of energy and momentum.

We imagine to be drawn in the fluid a volume of arbitrary shape, which is at rest with respect to a convenient frame of reference. We call this the "control volume" \mathcal{V} and its surface the "control surface" A . Fluid will in general be flowing across some parts of the control surface. At an arbitrary time t_a there is a definite mass m occupying the control volume. This may comprise both fluid and solid bodies, as shown in Fig. 3.3a.

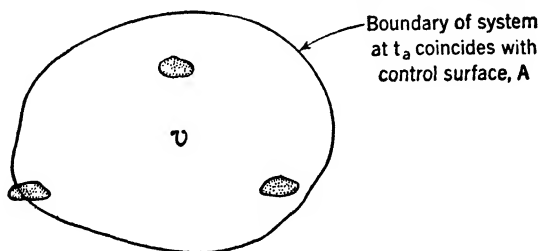


FIG. 3.3a.

After a time interval $dt = t_b - t_a$, the boundary of the mass system will in general no longer coincide with the control surface but will be as shown by the dotted line in Fig. 3.3b.

The mass of that part of the system lying outside of \mathcal{V} at time t_b we call dm_{out} , and the mass of the new matter inside of \mathcal{V} at t_b but not included in the system we call dm_{in} . Representing the entire mass inside \mathcal{V} at any time by m' we can express the mass of the system in two ways, $m = m'_a$ and $m = m'_b + dm_{\text{out}} - dm_{\text{in}}$. Eliminating m and dividing by dt , we get

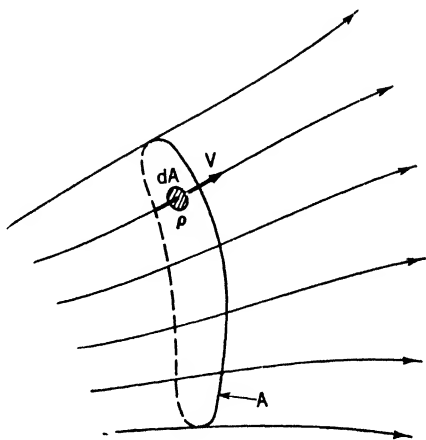


FIG. 3.2. — Flow in a stream tube of finite cross section.

$$0 = \frac{m'_b - m'_a}{dt} + \frac{dm_{\text{out}} - dm_{\text{in}}}{dt} \quad (3.5)$$

Equation (3.5) is a general statement of the continuity condition. The first term represents the rate of accumulation of mass inside the control

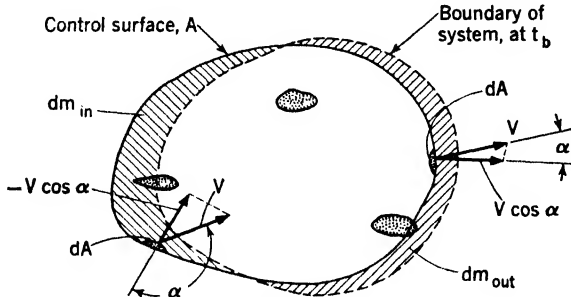


FIG. 3.3b.

volume, while the second represents the net rate of outflow of matter through the control surface.

The special cases already discussed are readily handled by means of Eq. (3.5). If, for example, we let \mathcal{V} coincide with a section of stream tube (Fig. 3.1), we get

$$\frac{dm_{\text{out}}}{dt} = \rho_2 V_2 dA_2$$

$$\frac{dm_{\text{in}}}{dt} = \rho_1 V_1 dA_1$$

If, furthermore, the flow is steady relative to \mathcal{V} , the mass inside \mathcal{V} will not change with time, that is, $m'_b = m'_a$. Equation (3.5) thus reduces to $\rho_2 V_2 dA_2 = \rho_1 V_1 dA_1$, which is identical with Eq. (3.1).

For future use it will be helpful to express the net rate of mass outflow across the control surface in another form. The mass that crosses an element dA of the control surface in time dt is equal to $\rho V \cos \alpha dA dt$, where $V \cos \alpha$ is the component of velocity normal to dA (Figs. 3.3b and 3.4). We stipulate that α be the angle between V and the outward-drawn surface normal, so that outward-flowing matter is automatically positive, while inward-flowing matter is negative. Therefore,

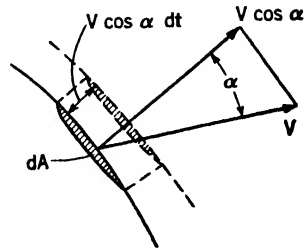


FIG. 3.4.

$$dm_{\text{out}} - dm_{\text{in}} = dt \int_A \rho V \cos \alpha dA \quad (3.6)$$

where the integral is taken over the entire control surface A . The time interval dt is of course the same for all area elements and has therefore been taken out from under the integral sign. Equation (3.5) thus becomes

$$\frac{m_b - m_a}{dt} + \int_A \rho V \cos \alpha \, dA = 0 \quad (3.7)$$

and for steady flow

$$\int_A \rho V \cos \alpha \, dA = 0 \quad (3.8)$$

It is readily seen also that if the fluid is incompressible ($\rho = \text{constant}$), $m_a = m_b$ and Eq. (3.7) reduces to

$$\int_A V \cos \alpha \, dA = 0 \quad (3.9)$$

In most problems, the control surface can be chosen so that $\cos \alpha$ has one of the three values 1, 0, or -1 everywhere on the surface. Furthermore, there will usually be flow across the surface at only a few areas, over each of which the density and velocity can be considered uniform. The integral of Eq. (3.7) or (3.8) thus reduces to the sum of only a few terms. The simplest case has already been discussed, *viz.*, a stream tube or a length of pipe in which the velocity and density can be considered uniform over a cross section. For steady flow in a branched pipe we find, referring to Fig. 3.5 and using Eq. (3.8),

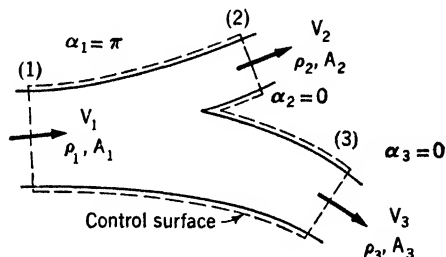


FIG. 3.5.

$$\int_A \rho V \cos \alpha \, dA = \rho_2 A_2 V_2 + \rho_3 A_3 V_3 - \rho_1 A_1 V_1 = 0$$

3.7. Two-dimensional Flow. When the flow is identical in all planes parallel to a plane of reference (the plane of the paper in the illustrations that follow), the flow is said to be two-dimensional. For steady motion, $V = f(x, y)$ only. This restriction greatly simplifies the study of many common flow patterns, but the same methods apply to the general case of three-dimensional flow, although a graphical representation is not easy to devise. Consider an incompressible flow in the x, y plane as shown in Fig. 3.6, with identical conditions in every plane parallel to it. Let the flow be represented by a streamline pattern in which the spacing between streamlines is n at any place. Well upstream, if the flow is uniform and

parallel there, we might space points a, b, c, d, e at equal intervals, indicating an equal flux entering each rectangular stream tube, of height n_0 in the y direction and of unit width in the z direction normal to the plane of the paper. Let the streamlines through a, b, c, d, e be as shown. Then the

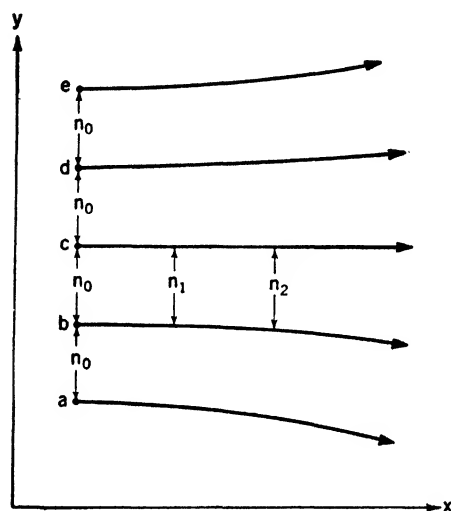


FIG. 3.6. — Two-dimensional flow.

area of each stream tube is numerically equal to n , the spacing of the streamlines. From the condition of continuity for incompressible fluid, $V_0 n_0 = V_1 n_1 = Vn = \text{constant}$.

The velocity is thus inversely proportional to the streamline spacing. Where the streamlines are spread apart, the velocity is lower and, where spreading, the flow is slowing down. Consequently, the streamline pattern gives information as to both the direction and the magnitude of the velocity at every point.

The mathematical problem of hydromechanics is to find the function $V = f(x, y)$ that maps the velocity field. We shall, however, find that many simple problems of steady two-dimensional flow of incompressible fluid can be solved approximately by a simple graphical construction.

For example, consider the flow through the square nozzle in Fig. 3.7.

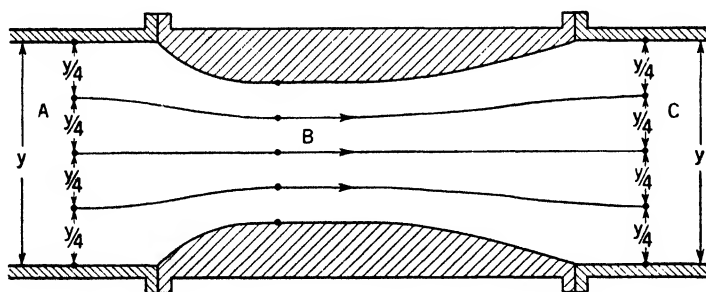


FIG. 3.7. — Flow through a square nozzle treated as two dimensional.

Neglecting friction, the velocity at sections A and C , where the pipe walls are parallel, will be parallel and uniform across the section. We can, therefore, indicate points on several streamlines at each section, as shown. At the throat section B , the velocity is also parallel and uniform across the section. We can thus locate another point on each streamline by dividing

the throat section into four equal spaces. The streamlines are then faired through these points. The resulting picture is an approximation only, for but three points on each streamline have been determined. This problem can be solved exactly by use of more advanced methods.

In making a sketch of streamlines based on continuity requirements, we assume a steady flow of a frictionless liquid that follows the boundaries of a solid without separation. For real fluids we may expect the flow picture to be seriously different from the idealized case if the flow is controlled by a body of such abrupt form as to cause the flow to separate from the boundaries. A body of such easy form that a real flow passes smoothly along it is called a "streamline body." The word "streamlining" is popularly applied to efforts to fair, or smooth, surfaces exposed to flow.

CHAPTER IV

DYNAMICS OF AN IDEAL FLUID

The dynamic equations of motion for a fluid particle lead, when integrated, to a generalized statement of the mutual relation between the nature of the flow and the forces acting. The basis for such a relation lies in Newton's second law of motion, which can be stated thus: The component in any direction of the resultant external force acting on a given mass is equal to the product of the mass and the component of its acceleration in that direction. To apply this law to a fluid continuum it will be necessary to choose some particular element or particle of fluid located with reference to time and space coordinates. We must also choose some convenient shape for the volume of this element of fluid. The procedure will be first to determine the external forces acting on the particle and next its accelerations along the axes of the space coordinates and then to write down an equation of motion for each of the axes by the application of Newton's second law.

To facilitate integration of these equations of motion it is necessary to make the simplifying assumption that we deal only with an ideal frictionless fluid. For such a fluid, since there can be no tangential or shearing forces, the only external forces acting are due to pressure and gravity. This assumption, which is fundamental to classical hydrodynamics, has been found by experience to represent to a very fair approximation the behavior of a real fluid in many practical engineering problems.

The development and integration of the equation of motion can be further simplified if we assume steady flow. Again this represents practical conditions in most engineering problems dealing with the steady motion of ships and airplanes and the continuous operation of machinery.

Finally, when the fluid in question is a liquid, it will be permissible to consider the fluid as incompressible. For the flow of air or gas at moderate velocities the assumption of incompressibility, while an approximation, may also be justified.

The circumstances of the case will determine which assumptions should be made. In a later chapter consideration will be given separately to the effect of viscosity on the dynamics of real fluids.

4.1. Accelerations. Consider first a steady flow where the streamline pattern is stationary and each fluid particle moves along a streamline. For this simple case it is possible to state the position of the particle in terms of the distance s that the particle has moved along the streamline, from an original reference position.

The particle is assumed to be at point O initially and to move with the steady flow a distance ds in time dt to point O' , as shown in Fig. 4.1. The acceleration of the particle will be the change in its velocity at point O' from its velocity at point O , divided by the infinitesimal element of time dt . It is convenient to choose as space axes the tangent to the streamline at O and the normal to that streamline. Then the accelerations required for the two equations of motion corresponding to these two axes will be the component a_s tangent to the streamline and the component a_n normal to a_s and directed toward the local center of curvature of the streamline.

Let V represent the initial velocity of the particle at O , tangent to the streamline by definition of a streamline. When the particle reaches O' , the

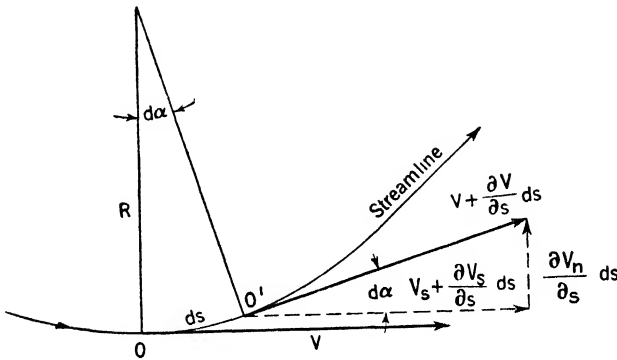


FIG. 4.1.

velocity is tangent to the streamline at that point, its direction having changed through an infinitesimal angle $d\alpha = ds/R$, for which $\cos d\alpha = 1$ and $\sin d\alpha = d\alpha$.

The magnitude of the velocity along the streamline has increased from V at O to $V + (\partial V/\partial s) ds$ at point O' . The component of velocity at O' in the direction of the tangent at O is, by geometry,

$$V_s = \left(V + \frac{\partial V}{\partial s} ds \right) \cos d\alpha = V + \frac{\partial V_s}{\partial s} ds$$

and consequently

$$\frac{\partial V_s}{\partial s} = \frac{\partial V}{\partial s}$$

Taking note that $ds/dt = V$, we can write down the acceleration in the s direction as

$$a_s = \frac{V + (\partial V_s/\partial s) ds - V}{dt} = \frac{\partial V_s}{\partial s} \frac{ds}{dt} = V \frac{\partial V}{\partial s}$$

The velocity normal to the streamline at O is zero. From Fig. 4.1, the velocity at O' in this same direction will be

$$V_n = 0 + \frac{\partial V_n}{\partial s} ds = \left(V + \frac{\partial V}{\partial s} ds \right) \sin d\alpha = \frac{[V + (\partial V/\partial s) ds] ds}{R} = V \frac{ds}{R}$$

since $\sin d\alpha = ds/R$ and the term in ds^2 is negligible. Therefore,

$$\frac{\partial V_n}{\partial s} = \frac{V}{R}$$

Then the acceleration in the direction of V_n is

$$a_n = \frac{0 + (\partial V_n/\partial s) ds - 0}{dt} = \frac{\partial V_n}{\partial s} \frac{ds}{dt} = \frac{V^2}{R}$$

For a steady flow, therefore, the two components of acceleration at any point O are

$$a_s = V \frac{\partial V}{\partial s}$$

and

$$a_n = \frac{V^2}{R} \quad (4.1)$$

For an unsteady flow the velocity at a fixed point changes with time, and account must be taken of this fact in computing the acceleration. At a fixed point the rate of change of velocity with respect to time is represented by $\partial(\text{velocity})/\partial t$. At the instant one particle is at O with tangential velocity V , another particle is at O' with velocity components V_s and V_n as discussed for the case of steady flow. After time dt the particle that was at O arrives at O' and then will have velocity components containing an additional term due to the elapsed time dt .

$$\begin{aligned} V + \frac{\partial V_s}{\partial s} ds + \frac{\partial}{\partial t} \left(V + \frac{\partial V_s}{\partial s} ds \right) dt &= V + \frac{\partial V_s}{\partial s} ds + \frac{\partial V}{\partial t} dt \\ V_n + \frac{\partial V_n}{\partial s} ds + \frac{\partial}{\partial t} \left(V_n + \frac{\partial V_n}{\partial s} ds \right) dt &= \frac{\partial V_n}{\partial s} ds + \frac{\partial V_n}{\partial t} dt \end{aligned}$$

where we neglect terms in $ds dt$, take $V_n = 0$, but admit that $\partial V_n/\partial t$ need not be zero.

Substituting previously determined values $\partial V_s/\partial s = \partial V/\partial s$ and $\partial V_n/\partial s = V/R$, we find for the acceleration components when the flow is unsteady

$$\begin{aligned} a_s &= V \frac{\partial V}{\partial s} + \frac{\partial V}{\partial t} \\ a_n &= \frac{V^2}{R} + \frac{\partial V_n}{\partial t} \end{aligned} \quad (4.2)$$

4.2. External Forces. To form the equations of motion we must determine the components of the resultant of all external forces in the direc-

tions of the accelerations a_s and a_n that they produce. Since the shape of the fluid particle is arbitrary, we choose a rectangular element of volume having an infinitesimal length ds in the direction of s and a height dn in the direction of the normal. The width of the particle (in the direction at right angles to the plane of the paper) is taken as unity, so that the volume is $ds dn$, the mass $\rho ds dn$, and the weight $\rho g ds dn$.

Figure 4.2 shows the diagram of external forces acting in the s and n

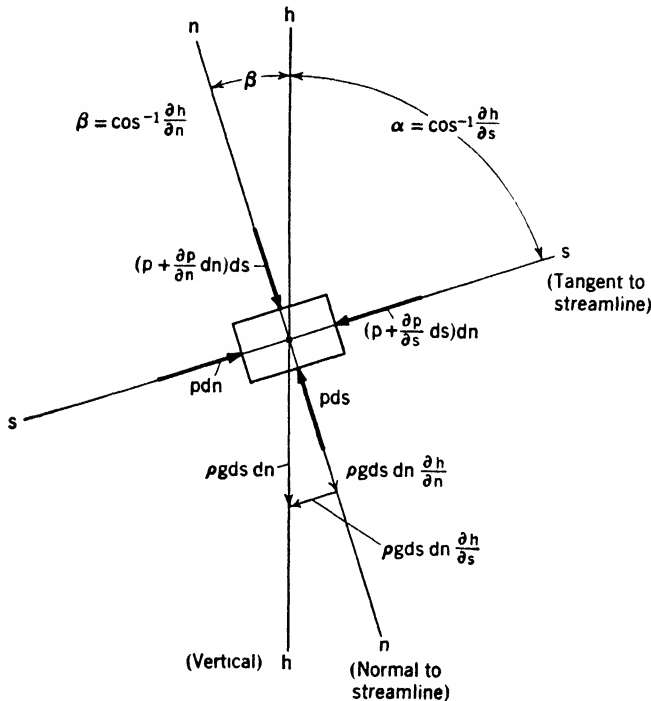


FIG. 4.2.

directions. Recall that we are dealing with a frictionless fluid, so that the only forces are those due to pressure and gravity.

The resultant of pressure forces on the two ends of the particle and the component of the weight along the axis of s give the resultant force in the s direction.

$$F_s = p dn - \left(p + \frac{\partial p}{\partial s} ds \right) dn - \rho g ds dn \frac{\partial h}{\partial s} = - \left(\frac{\partial p}{\partial s} + \rho g \frac{\partial h}{\partial s} \right) ds dn$$

In a similar way the algebraic sum of forces in the n direction is made up of the pressure forces on the top and bottom of the particle and the component of the weight in the n direction.

$$F_n = p ds - \left(p + \frac{\partial p}{\partial n} dn \right) ds - \rho g ds dn \frac{\partial h}{\partial n} = - \left(\frac{\partial p}{\partial n} + \rho g \frac{\partial h}{\partial n} \right) ds dn$$

The above components of weight are obtained as follows: From Fig. 4.2,

$$s \text{ component} = - \rho g ds dn \cos \alpha$$

$$n \text{ component} = - \rho g ds dn \cos \beta$$

The change in the height h depends on both s and n . For arbitrary small increments ds and dn , the change

$$dh = dh_s + dh_n = \cos \alpha ds + \cos \beta dn,$$

as shown in Fig. 4.3. But dh equals the rate of change of h with respect to s times ds plus the rate of change with n times dn .

$$dh = \frac{\partial h}{\partial s} ds + \frac{\partial h}{\partial n} dn$$

Therefore, $\cos \alpha = \partial h / \partial s$ and $\cos \beta = \partial h / \partial n$, and the components of weight are $-\rho g (\partial h / \partial s) ds dn$ and $-\rho g (\partial h / \partial n) ds dn$.

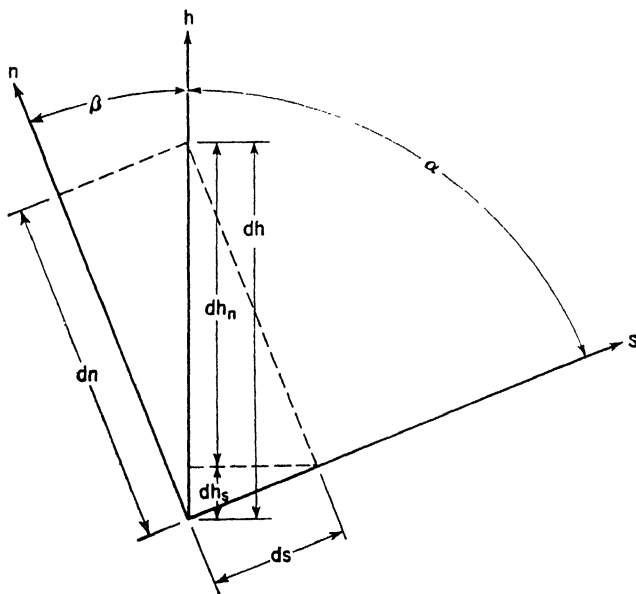


FIG. 4.3.

For clarity in Figs. 4.2 and 4.3, h is shown in the s, n plane although this is not generally true. The expressions for the weight components are not affected by this simplification.

4.3. Equations of Motion. We may now apply Newton's second law by equating these forces to the product of mass and acceleration for the directions s and n .

$$F_s = \rho \, ds \, dn \, a_s$$

and

$$F_n = \rho \, ds \, dn \, a_n$$

Substituting the values found for F_s , F_n , a_s , and a_n , and dividing through by $\rho \, ds \, dn$, we get

$$-\frac{1}{\rho} \frac{\partial p}{\partial s} - g \frac{\partial h}{\partial s} = V \frac{\partial V}{\partial s} + \frac{\partial V}{\partial t} \quad (s \text{ direction}) \quad (4.3)$$

$$-\frac{1}{\rho} \frac{\partial p}{\partial n} - g \frac{\partial h}{\partial n} = \frac{V^2}{R} + \frac{\partial V_n}{\partial t} \quad (n \text{ direction}) \quad (4.4)$$

4.4 Euler's Equation. If we multiply Eq. (4.3) by ds , an element of length of a streamline at a given instant of time ("instantaneous streamline"), we can integrate with respect to s and obtain Euler's general equation for the motion of an ideal fluid.

$$\int \frac{\partial V}{\partial t} ds + \int V \frac{\partial V}{\partial s} ds + \int \frac{1}{\rho} \frac{\partial p}{\partial s} ds + g \int \frac{\partial h}{\partial s} ds = f(t) \quad (4.5)$$

or

$$\int \frac{\partial V}{\partial t} ds + \frac{V^2}{2} + \int \frac{1}{\rho} \frac{\partial p}{\partial s} ds + gh = f(t) \quad (4.6)$$

It is important to notice that in the derivation of Euler's equation only the restriction to an ideal (frictionless) fluid is involved. The equation, therefore, applies to both steady and unsteady motion and to both compressible and incompressible cases.

Steady flow requires that V , p , and ρ be independent of time. In this case Euler's equation reduces to

$$\left. \begin{aligned} \frac{V^2}{2} + \int \frac{1}{\rho} \frac{\partial p}{\partial s} ds + gh &= \text{constant} \\ \frac{V_2^2 - V_1^2}{2} + \int_1^2 \frac{1}{\rho} \frac{\partial p}{\partial s} ds + g(h_2 - h_1) &= 0 \end{aligned} \right\} \quad (4.7)$$

A fluid is said to be homogeneous if the density is a function only of pressure. Experience shows that in most problems of interest to mechanical engineers the working fluid is homogeneous, so that the second term of Eq. (4.7) can be integrated. The so-called "polytropic formula" usually applies, $p/\rho^n = p_0/\rho_0^n$, where n is a constant and p_0 and ρ_0 are the pressure and density at a specified point.

4.5. Bernoulli's Formula. For liquids and for gases where high pressures and velocities are not involved the density can be assumed to remain constant to a good approximation. In the case of steady motion of an incompressible fluid, Euler's equation is further simplified to the relation between velocity, pressure, and elevation attributed to Daniel Bernoulli

and known in hydraulics as Bernoulli's formula. Bernoulli is considered to be the father of hydraulics, largely as a result of the clarification of hydraulic phenomena that followed the application of this formula.

Making ρ constant in the steady-flow form of Euler's equation, we find

$$\left. \begin{aligned} \frac{1}{2} V^2 + \frac{p}{\rho} + gh &= \text{constant} \\ \text{or} \quad \frac{1}{2} (V_2^2 - V_1^2) + \frac{p_2 - p_1}{\rho} + g(h_2 - h_1) &= 0 \end{aligned} \right\} \quad (4.8)$$

It should be noted particularly that the Euler equation and the Bernoulli formula as well apply to the one streamline along which the integration is taken. For another streamline the constant may have a different value. In the special case for which the streamlines start in a reservoir where V , ρ , p , and h are the same for all, the constant will be the same for all streamlines. Likewise, in a hydraulic system where all the fluid passes through some region, such as an inlet pipe where ρ , p , h , and V are constant across the section, the same constant applies to all streamlines. In the case of a mass of fluid rotating like a rigid body it will be shown later that the constant varies with the distance from the axis of rotation. Such change is to be expected since both the velocity and the pressure are greater for a greater radius.

4.6. Interpretation of the Equations of Motion. In Eq. (4.7) each term has the dimensions of work or energy per unit mass. Since $-(1/\rho)(\partial p/\partial s)$ is the pressure force on unit mass in the s direction, $-(1/\rho)(\partial p/\partial s) ds$ is the work done by the pressure force on unit mass of fluid as it moves a distance ds . Similarly, $-g(\partial h/\partial s) ds$ is the work done by gravity on unit mass during the same motion. For steady flow the corresponding change in kinetic energy of unit mass is $V(\partial V/\partial s) ds = [\partial(V^2/2)/\partial s] ds$. Equation (4.7), therefore, states that in steady flow of an ideal fluid the change in kinetic energy of unit mass between any two positions equals the work done on the mass by pressure and gravity forces. The Bernoulli formula [Eq. (4.8)] is the same statement for unit mass of incompressible fluid.

Since the work done by gravity on a given mass depends only on the initial and final levels, we can assign to the mass a "gravity potential energy," the change in which between any two levels is defined as the negative of the work done by gravity. An alternative statement of Eq. (4.7) is, therefore, that the sum of the changes in kinetic and potential energy equals the work done on the unit mass by the pressure force.

4.7. Applications of Bernoulli's Equation. The examples discussed here are ones in which friction is known from experiment to play only a minor role. Therefore, the results given by Bernoulli's equation require only small corrections, even if high precision is necessary.

a. Sharp-edged Circular Orifice. In Fig. 4.4 is shown a tank in which the water level is maintained at a height h above the center of a sharp-edged circular orifice. The cross section of the tank is so large that the velocity is negligible, except near the outlet. Bernoulli's equation [Eq. (4.8)] can be applied between the water surface 1 and the section of minimum jet diameter 2. The result is that

$$V_2 = \sqrt{2gh} \quad (4.9)$$

which is called "Torricelli's formula," after Torricelli, who discovered it in 1640, a century before Bernoulli's equation was known.

The jet reaches its minimum cross section, the "vena contracta," at a distance of about one orifice diameter from the outlet. The "contraction coefficient" C_c is equal to A_2/A_1 , by definition. The experimental value of C_c , found by measuring the jet diameter, is about 0.61 or 0.62, which checks well with the value 0.61, obtained by ideal-fluid theory.

If frictional effects were wholly negligible, the discharge rate $Q = A_2 V_2$ would be equal to $C_c A \sqrt{2gh}$. Experiment shows, however, that Q is slightly less than $C_c A \sqrt{2gh}$. It is customary to define a "discharge coefficient" C_d by the formula

$$Q = C_d A \sqrt{2gh} \quad (4.10)$$

The average of many experiments on water at ordinary temperatures indicates that the best value of C_d is about 0.60, provided that $h \geq 1.5$ ft and the orifice diameter $d \geq 0.2$ ft. The value of C_d increases if these limits are exceeded or if the kinematic viscosity of the liquid is increased.

Comparison of Eqs. (4.9) and (4.10) shows that a "velocity coefficient" C_v should be introduced into Eq. (4.9) to account for the effect of friction on the velocity.

$$V_2 = C_v \sqrt{2gh} \quad (4.11)$$

The value of C_v is found to lie between 0.98 and 0.99.

Gravity causes the jet to bend downward soon after leaving the orifice. The path of the stream being approximately a parabola. We have, however, assumed that the effect of gravity on the velocity and pressure in the vena contracta is negligible. This assumption is justifiable only if $d\sqrt{C_c} g/V_2^2$ is small compared with unity, as can be shown by writing

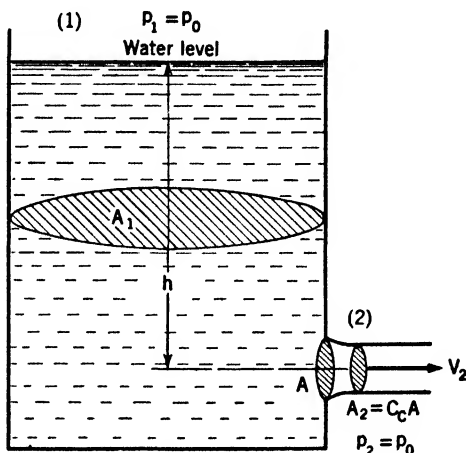


FIG. 4.4. — Steady flow out of a tank.

Bernoulli's equation for the highest and lowest points of the vena contracta. Experiment shows that errors caused by gravity are negligible provided that $d\sqrt{C_c}g/V_2^2 \leq 0.2$.

If there is no inflow to maintain the level in the tank constant, the time t needed for the head to be reduced from h_0 to h is found from the fact that $Q = -A_1(dh/dt) = A_2V_2$. The acceleration at a fixed point caused by the decreasing head is very small compared with the acceleration of the fluid approaching the outlet. Thus, although the flow is not perfectly steady, Eq. (4.11) applies, since $\partial V/\partial t$ is negligible. Using the value of V_2 from Eq. (4.11) one finds $-dh/dt = (A_2/A_1)C_v\sqrt{2gh} = (AC_c/A_1)C_v\sqrt{2gh} = (AC_d/A_1)\sqrt{2gh}$. Integrating and solving for t ,

$$t = \sqrt{\frac{2}{g}} \frac{A_1}{AC_d} h_0^{1/2} \left[1 - \left(\frac{h}{h_0} \right)^{1/2} \right] \quad (4.12)$$

b. Pitot Tube. A small tube pointing directly upstream and connected to a manometer, as shown in Fig. 4.5, provides a means for measuring the velocity anywhere in a straight parallel flow. Such an instrument is called

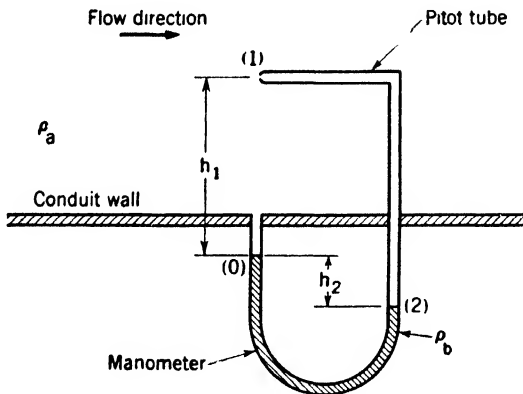


FIG. 4.5. — Pitot tube.

a "pitot tube," after its inventor Pitot, who performed his experiments about the year 1732.

The Bernoulli constant at an arbitrary point 1 is unaffected by the presence of the pitot tube, but the velocity there is reduced to zero (stagnation point). Equating the Bernoulli constants at 1 for the two conditions, with and without the tube, and letting primed symbols represent values with the tube in place, we find

$$\frac{p_1}{\rho_a} + \frac{V_1^2}{2} + gh_1 = \frac{p'_1}{\rho_a} + \frac{V_1'^2}{2} + gh_1$$

whence, since $V'_1 = 0$,

$$V_1 = \sqrt{\frac{2}{\rho_a} (p'_1 - p_1)} \quad (4.13)$$

By use of Eq. (4.4) the pressure difference $p'_1 - p_1$ can be expressed in terms of the manometer reading h_2 and the fluid densities ρ_a and ρ_b . Let the pitot tube be removed from the flow. Then for any direction n , lying in a vertical plane perpendicular to the streamlines and passing through 1, Eq. (4.4) reduces to $(1/\rho_a)(\partial p/\partial n) + g(\partial h/\partial n) = 0$, since the radius of curvature R is infinite.* The pressure is seen to vary hydrostatically over the section. The pressure near the small opening in the conduit wall is unaffected by the pitot tube, and the pressure varies hydrostatically inside the tube and the manometer. The pressure at point 0 is thus equal to $p_1 + \rho_a g h_1$, provided that the manometer-tube opening is flush with the conduit wall, so that no disturbance is set up at this point. The pressure at point 2 is $p'_1 + \rho_a g(h_1 - h_2)$; and $p'_1 - p_1 = g h_2(\rho_b - \rho_a) = \rho_b g h_2[1 - (\rho_a/\rho_b)]$. Equation (4.13), therefore, becomes

$$V_1 = \sqrt{2gh_2 \frac{\rho_b}{\rho_a} \left(1 - \frac{\rho_a}{\rho_b}\right)} \quad (4.14)$$

If the ratio ρ_a/ρ_b is negligible compared with unity, as for an airflow measured by a water manometer, Eq. (4.14) simplifies to

$$V_1 = \sqrt{2gh_2 \frac{\rho_b}{\rho_a}} \quad (4.15)$$

c. Pitot-static Tube. The pitot-static tube shown in Fig. 4.6 has both an impact-pressure opening 1' and a static-pressure opening 1. Between 1 and 1', differences in level and effects of friction are negligible. At point 1' the velocity is zero, while for a properly designed instrument the velocity at 1 is that of the undisturbed stream. Bernoulli's equation yields

$$V_1 = \sqrt{\frac{2}{\rho_a} (p'_1 - p_1)}$$

Inside the tube the velocity is everywhere zero, and the hydrostatic equation applies, so that

$$p'_1 - p_1 = g h_2 \rho_b \left(1 - \frac{\rho_a}{\rho_b}\right)$$

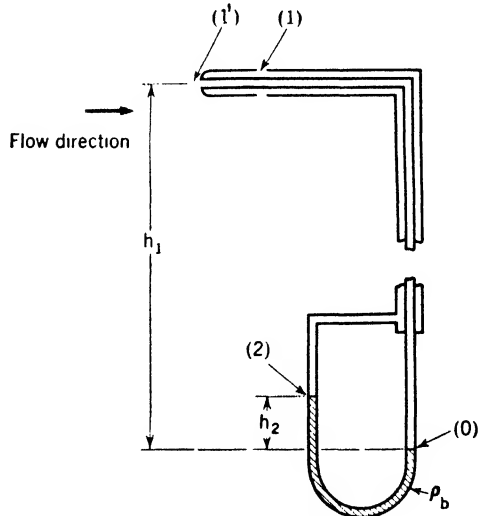


FIG. 4.6. — Pitot-static tube.

* This demonstration is valid only in the absence of friction, since it is based on Eq. (4.4); but the result holds also for a real fluid, as is shown both by experiment and theory.

The relation between the stream velocity and the manometer reading is the same as for the pitot tube.

Equation (4.15), which applies to both the pitot tube and the pitot-static tube, requires no empirical correction. Properly designed instruments can be used without calibration.

4.8. Application of Euler's Equation. In this article Euler's equation [Eq. (4.7)] will be applied to computation of the pressure at a stagnation

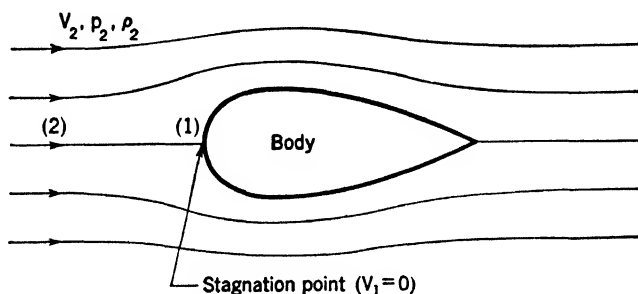


FIG. 4.7. — Body immersed in a steady parallel flow.

point on a body immersed in a steady flow of compressible fluid that has a uniform parallel velocity distribution far from the body. Changes in elevation will be neglected.

Referring to Fig. 4.7, we see that Eq. (4.7) reduces to

$$\frac{V_2^2}{2} + \int_1^2 \frac{dp}{\rho} = 0 \quad (4.7a)$$

In this equation the symbol dp is used as an abbreviation of $(\partial p / \partial s) ds$ to denote the difference in pressure between two points near together on the same streamline.

It has been found that in such a flow the compression of the fluid is adiabatic and frictionless. In this case the exponent in the polytropic equation is equal to k .

$$\frac{p}{\rho^k} = \text{constant} = \frac{p_2}{\rho_2^k}$$

Combining this equation with Eq. (4.7a) and integrating, we obtain

$$\frac{V_2^2}{2} + \frac{p_2}{\rho_2} \frac{k}{k-1} \left[1 - \left(\frac{p_1}{p_2} \right)^{(k-1)/k} \right] = 0$$

It will be shown in Chap. VII that the square of the sound velocity in the undisturbed stream C_2^2 is equal to $p_2 k / \rho_2$. Making this substitution, solving for p_1 / p_2 , and expanding by means of the binomial theorem one finds that

$$\begin{aligned}
 \frac{p_1}{p_2} &= \left[1 + \frac{k-1}{2} \left(\frac{V_2}{C_2} \right)^2 \right]^{k/k-1} \\
 &= 1 + \frac{k}{2} \left(\frac{V_2}{C_2} \right)^2 + \frac{k}{8} \left(\frac{V_2}{C_2} \right)^4 + \frac{k(2-k)}{48} \left(\frac{V_2}{C_2} \right)^6 + \cdots \\
 p_1 - p_2 &= \frac{p_2 k}{2} \left(\frac{V_2}{C_2} \right)^2 \left[1 + \frac{1}{4} \left(\frac{V_2}{C_2} \right)^2 + \frac{2-k}{24} \left(\frac{V_2}{C_2} \right)^4 + \cdots \right] \\
 \frac{p_1 - p_2}{(\rho_2/2) V_2^2} &= 1 + \frac{1}{4} \left(\frac{V_2}{C_2} \right)^2 + \frac{2-k}{24} \left(\frac{V_2}{C_2} \right)^4 + \cdots \quad (4.16)
 \end{aligned}$$

Equation (4.16) shows, if V_2/C_2 is small compared with unity, that $(p_1 - p_2)/(\rho_2/2) V_2^2 = 1$, which is the result obtained for an incompressible fluid. The ratio V_2/C_2 is known as the Mach number, after one of the pioneer investigators of high-speed gas flow; it will be further discussed in later chapters.

Equation (4.16) may be used to calculate the relation between the pressure difference $p_1 - p_2$, measured by a pitot-static tube, and the velocity of the undisturbed stream V_2 . In this connection the following table is of interest; it has been computed from Eq. (4.16) with $k = 1.4$ (the value for air). The table shows that for most purposes compressibility has a negligible effect on the pitot-static tube reading, if the velocity does not exceed two-tenths of the sound velocity.

$\frac{V_2}{C_2}$	0.1	0.2	0.3	0.4	0.5
$\frac{p_1 - p_2}{(\rho_2/2) V_2^2}$	1.003	1.010	1.023	1.041	1.064

4.9. Curved Streamlines. Many phenomena in fluid mechanics are marked by a whirling of the fluid in circular paths, and typical effects to be accounted for are the high discharge pressure available in a centrifugal pump, the depression in the surface of water at the center of a whirlpool, the tendency of eddies and smoke rings to persist, and the difficulty of forcing a fluid to flow around a sharp corner.

In discussing these phenomena, the concepts of irrotational and rotational motion are indispensable. These ideas will be developed in the following sections for two-dimensional continuous motion of an ideal incompressible fluid.

4.10. Irrotational Motion. The question naturally arises here as to the conditions under which the Bernoulli constant has the same value for all points in a two-dimensional flow. The answer to this question, which is developed below, leads to the very important concept of irrotational motion.

A general criterion for the uniformity of Bernoulli's constant can be developed by combining Eqs. (4.4) and (4.8). For steady flow, Eq. (4.4) reduces to

$$\frac{1}{\rho} \frac{\partial p}{\partial n} + g \frac{\partial h}{\partial n} + \frac{V^2}{R} = 0 \quad (4.4a)$$

If the Bernoulli constant, or "total head" (dimensions in foot-pounds per pound), is represented by H , Eq. (4.8) becomes

$$\frac{p}{\rho} + gh + \frac{V^2}{2} = gH$$

Differentiate this equation with respect to n , the direction normal to the streamline, bearing in mind that H depends only on n .

$$\frac{1}{\rho} \frac{\partial p}{\partial n} + g \frac{\partial h}{\partial n} + V \frac{\partial V}{\partial n} = g \frac{\partial H}{\partial n} = g \frac{dH}{dn} \quad (4.17)$$

Combine Eqs. (4.4a) and (4.17).

$$\frac{V}{R} - \frac{\partial V}{\partial n} = -g \frac{dH}{V dn} \quad (4.18)$$

Equation (4.18) shows that the necessary and sufficient condition for H to be constant is

$$\frac{V}{R} - \frac{\partial V}{\partial n} = 0 \quad (4.19)$$

The expression $(V/R) - (\partial V/\partial n)$ is called the "rotation" of the fluid at a point. Wherever Eq. (4.19) is satisfied, the motion is said to be irrotational; if it is satisfied everywhere, the entire flow is called an "irrotational flow." The reason for the name rotation is given below.

If a short segment of a fluid line is drawn parallel to V , as in Fig. 4.8a, its counterclockwise angular velocity is found to be

$$\omega_{1,2} = - \frac{V(ds/2R) + V(ds/2R)}{ds} = \frac{V}{R}$$

Similarly, for the fluid-line segment normal to V in Fig. 4.8b, the counterclockwise angular velocity is

$$\omega_{3,4} = - \frac{(\partial V/\partial n)(dn/2) + (\partial V/\partial n)(dn/2)}{dn} = - \frac{\partial V}{\partial n}$$

The rotation of the fluid at O is defined as the sum of the velocities of the two line segments.

$$\text{Rotation} = \omega_{1,2} + \omega_{3,4} = \frac{V}{R} - \frac{\partial V}{\partial n}$$

may therefore be considered as a measure of the angular velocity of the fluid at a point. It is seen that, in general, the net angular velocity may be taken as one-half of the rotation. Equation (4.19) shows that in irrotational motion the two fluid lines turn in opposite directions at equal speeds,

so that the particle as a whole is deformed but does not rotate. In other words, its net angular velocity is zero.

In the application of Bernoulli's equation to flow in ducts and channels in which friction is neglected, the fluid is tacitly assumed to issue from one large reservoir in which the velocity is negligible. The total head H is, therefore, the same for all streamlines, and the motion is irrotational.

4.11. Potential Vortex.

One of the most important examples of an irrotational flow is the potential vortex, also called a "free" vortex, since it can exist in a free flow far from any boundaries. A two-dimensional vortex is defined as a whirling mass of fluid with concentric circular streamlines. Continuity shows that the velocity is the same everywhere on one

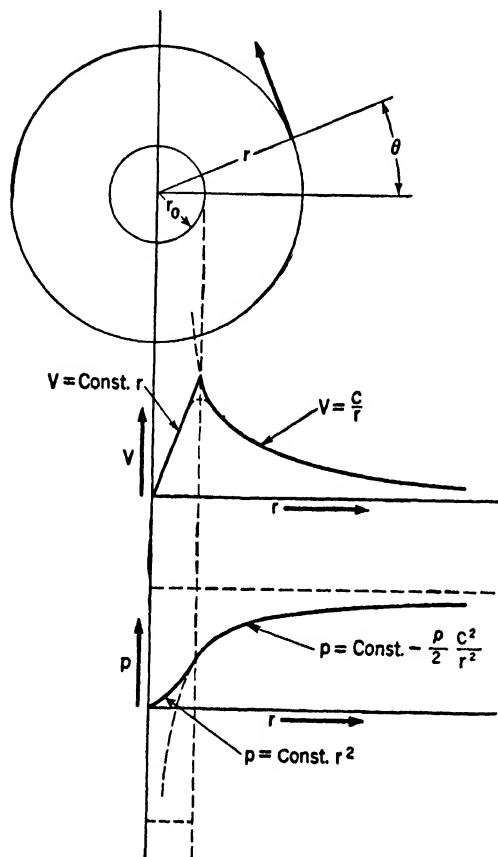


FIG. 4.9. — Potential vortex.

streamline, because the area of any stream tube is constant along its entire length. The law for the variation of velocity from streamline to streamline is found from Eq. (4.19), as follows:

At an arbitrary point r, θ , in Fig. 4.9, the radius of curvature $R = r$; and $\partial V / \partial n = -\partial V / \partial r = -dV/dr$, since $dr = -dn$ and V is a function of r only. Equation (4.19) reduces to

$$\frac{V}{R} - \frac{\partial V}{\partial n} = \frac{V}{r} + \frac{dV}{dr} = 0$$

whence

$$Vr = \text{constant} = C \quad (4.20)$$

The pressure can be obtained by combining Eqs. (4.8) and (4.20).

$$p + \frac{\rho}{2} V^2 + \rho gh = p + \frac{\rho}{2} \frac{C^2}{r^2} + \rho gh = \rho gH \quad (4.21)$$

If the streamlines lie in a horizontal plane, h is constant, and

$$p = \text{constant} - \frac{\rho}{2} \frac{C^2}{r^2} \quad (4.22)$$

These velocity and pressure distributions are shown in Fig. 4.9.

Since infinite velocities do not occur in nature, the velocity distribution for a free vortex in a real fluid cannot obey Eq. (4.20) near the origin, where friction is dominant. There is a gradual transition from the hyperbolic distribution to a linear one, characteristic of a rotating solid. The zone of transition is usually neglected and the distribution assumed to be as shown by the heavy line in Fig. 4.9. As discussed in Art. 2.19, the pressure distribution in the rotating core (radius r_0) is parabolic.

A tornado is a free vortex set up in the atmosphere. The low pressure in the core gives rise to a waterspout or a "dust devil," depending on whether the tornado moves over water or land.

As will be discussed in Chap. XI, a vortex called a "trailing" vortex is shed from the tip of an airplane wing. If atmospheric conditions are favorable, the low temperature accompanying the low pressure in the core causes condensation of water vapor, so that the core can be seen.

A trailing vortex also appears at the tip of a propeller blade. In a water tunnel for testing model ships' propellers, the low pressure in the cores of the trailing vortices causes air to come out of solution, making the vortex system visible in the water. When viewed by stroboscopic light, a silvery helix seems to spring from each apparently motionless blade tip.

The depression of the surface of a whirlpool is easily explained by use of Eq. (4.21). Atmospheric pressure p_0 exists at the free surface, so that the surface elevation h is

$$h = H - \frac{p_0}{\rho g} - \frac{1}{2g} \frac{C^2}{r^2} = \text{constant} - \frac{1}{2g} \frac{C^2}{r^2} \quad (4.23)$$

Comparison of Eqs. (4.22) and (4.23) indicates that h varies with r in the same way as the pressure at a constant level. A curve of h versus r thus has the same shape as the p versus r curve of Fig. 4.9. It is seen that the finite depth of the depression results from the finite core diameter.

4.12. Rotational Motion. The expression $(V/R) - (\partial V/\partial n)$, which is a measure of the rate of rotation of a fluid particle, is called rotation or "vorticity." The latter term arises from the fact that the angular speed of a free-vortex core, together with the core radius, determines the value of the product Vr , characterizing the vortex.

For rotation like a rigid body the value of $(V/R) - (\partial V/\partial n)$ is everywhere the same and equal to twice the angular velocity ω of the fluid. This kind of motion has already been discussed in Chap. II and the pressure distribution shown to be

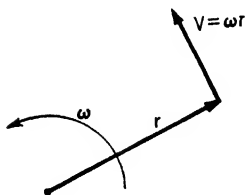


FIG. 4.10.

$$\frac{p}{\rho} - \frac{\omega^2 r^2}{2} + gh = \text{constant}$$

This relation can also be deduced from Eqs. (4.18) and (4.8) and Fig. 4.10 as follows: From Eq. (4.18),

$$\frac{V}{R} - \frac{\partial V}{\partial n} = 2\omega = -g \frac{dH}{V dn} = \frac{g}{\omega r} \frac{dH}{dr}$$

Therefore,

$$gH = \omega^2 r^2 + \text{constant}$$

Substituting this value of gH in Eq. (4.8), we get

$$\frac{p}{\rho} + gh + \frac{\omega^2 r^2}{2} = \omega^2 r^2 + \text{constant}$$

or

$$\frac{p}{\rho} + gh - \frac{\omega^2 r^2}{2} = \text{constant} \quad (4.24)$$

A practical example of such a flow occurs in a centrifugal pump with the discharge valve closed, as shown in Fig. 4.11. The blades constrain the water in the impeller to revolve with the speed ω of the shaft. Neglecting any change in level between the inner and outer radii of the impeller, we find from Eq. (4.24)

$$p_2 - p_1 = \frac{\rho}{2} \omega^2 (r_2^2 - r_1^2)$$

These concepts of vorticity and irrotational and rotational motion will be given further application in the discussions of wing theory and hydraulic machinery.

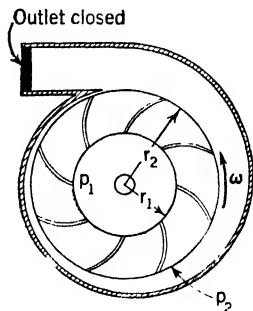


FIG. 4.11. — Centrifugal pump.

CHAPTER V

ENERGY RELATIONS FOR STEADY FLOW

The relationship involving pressure, velocity, and elevation given by Euler or Bernoulli was deduced on the assumption of a frictionless fluid, no account being taken of the frictional effects that actually occur. Nor was the possibility considered of work being done on or by the fluid through the action of moving vanes, as in a pump or turbine.

In many types of apparatus for which the mechanical engineer is responsible both these things must be taken into account. Hydraulic turbines, pumps, fans, compressors, fluid couplings, pipe lines, nozzles, and orifices are familiar examples. In a turbine the flow rotates the runner and causes work to be done on any apparatus connected to the turbine shaft. In a centrifugal pump the flow is the result of work done in turning the pump shaft. Work of this kind will be called "shaft work." In pipe lines, nozzles, or orifices no shaft work is done, but energy is dissipated by the action of viscosity.

Energy considerations are best analyzed in the light of the first law of thermodynamics, which we apply in this chapter to apparatus involving the steady flow of a real fluid. No further assumptions are made as to the nature of the apparatus or as to the character of the flow. As a result of the analysis a steady-flow energy equation is developed that will be found a useful tool in many practical problems of mechanical engineering.

5.1. First Law of Thermodynamics. This law, which, like all the generalizations of science, is based on experience, may be formulated as follows: The difference between the heat added to a system of masses and the work done by the system depends only on the initial and final states of the system.* This difference is, therefore, an attribute or property of the system and is called the "internal energy."

It should be emphasized that neither the heat added nor the work done is a property but depends on the path or process followed, as well as on the end states of the system.

The first law may be written symbolically as

$$\text{Heat} - \text{work} = E_b - E_a \quad (5.1)$$

where *heat* and *work* represent, respectively, the heat added to and work done by a system as it passes from state *a* to state *b* and $E_b - E_a$ is the corresponding change in the internal energy of the system.

* For definitions of heat and work, see, for example, reference 2 at the end of this chapter.

As it stands, Eq. (5.1) is difficult to apply to fluid-flow problems. We shall therefore change it to a more convenient form by the procedure used in Art. 3.6 for the equation of continuity.

5.2. Steady-flow Energy Equation. We apply Eq. (5.1) to a mass system defined as the matter lying within a fixed control volume \mathcal{V} at an arbitrary time t_a (Fig. 5.1a). We consider the change in state of this system

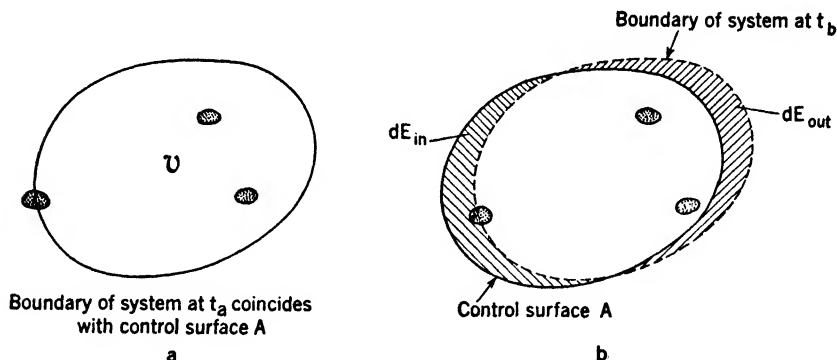


FIG. 5.1.

during a time interval $dt = t_b - t_a$. The boundary of the system at time t_b will, in general, no longer coincide with the control surface A but will be as shown by the dotted line in Fig. 5.1b.

The internal energy of that part of the system lying outside of \mathcal{V} at t_b we call dE_{out} , and the internal energy of the new matter inside of \mathcal{V} at t_b but not included in the system we call dE_{in} . Representing the internal energy of all the matter inside \mathcal{V} at any time by E' we write the initial and final energies of the system, respectively,

$$E_a = E'_a \quad \text{and} \quad E_b = E'_b + dE_{\text{out}} - dE_{\text{in}}$$

or

$$E_b - E_a = E'_b - E'_a + dE_{\text{out}} - dE_{\text{in}} \quad (5.2)$$

The change of energy of the system is thus expressed as the sum of the change inside the control volume and the net outflow of energy through the control surface.

Referring to Art. 3.6 and Fig. 3.4 we find that the flow of mass in time dt across an element dA of the control surface is $\rho V \cos \alpha dA dt$. Multiplication of this expression by the internal energy per unit mass e yields the energy carried across dA by the mass flow in time dt . Accordingly, the net outflow of energy across A is

$$dE_{\text{out}} - dE_{\text{in}} = dt \int_A \rho e V \cos \alpha dA \quad (5.3)$$

Turning next to the work term of Eq. (5.1) we assume a mechanical system, for which we can write

$$\text{Work} = \text{pressure work} + \text{shear work} \quad (5.4)$$

where the terms on the right stand for the work done by the pressure and shearing forces exerted at the boundary on the surroundings. We adopt here the point of view mentioned in Art. 4.6 and take gravity into account through the potential energy of the system. Therefore, gravity work is omitted from Eq. (5.4).

The pressure work done in time dt by a surface element of the system is seen from Fig. 5.2 to be $p dA V \cos \alpha dt$, where $p dA$ is the force on the element dA of the boundary at time t_a and $V \cos \alpha dt$ is the

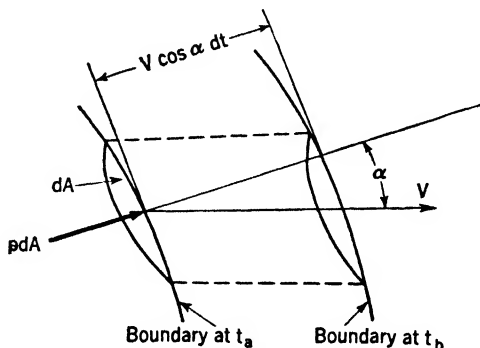


FIG. 5.2.

distance moved by this element normal to itself. The slight change in $p dA$ occurring during the motion is of higher order and may be neglected. Since dA is identical with an element of the control surface, the pressure work done by the system over its whole boundary is

$$\text{Pressure work} = dt \int_A p V \cos \alpha dA \quad (5.5)$$

Combining Eqs. (5.1) to (5.5) we get, after dividing through by dt ,

$$\frac{\text{Heat}}{dt} - \frac{\text{shear work}}{dt} = \frac{E'_b - E'_a}{dt} + \int_A \left(\frac{p}{\rho} + e \right) \rho V \cos \alpha dA \quad (5.6)$$

Experience shows that, in the absence of electricity, magnetism, and capillarity, e is the sum of three kinds of energy. Two of these, the potential energy and the kinetic energy, have already been discussed in Art. 4.6. The third kind is called the "intrinsic energy" and is denoted by u (energy/mass).^{*} We may thus write

$$e = gz + \frac{V^2}{2} + u \quad (5.7)$$

where z is the elevation above an arbitrary datum level, so that Eq. (5.6) becomes

$$\frac{\text{Heat}}{dt} - \frac{\text{shear work}}{dt} = \frac{E'_b - E'_a}{dt} + \int_A \left(\frac{p}{\rho} + gz + \frac{V^2}{2} + u \right) \rho V \cos \alpha dA \quad (5.8)$$

^{*} Changes in the intrinsic energy are explained by atomic theory as changes in the kinetic and potential energy of molecules and of atoms. Measurements of intrinsic energy changes have played an important role in the development of this theory.

Let us consider only systems for which all parts of the control surface not at fixed walls are normal to the velocity of any fluid crossing the surface and to the axis of any shaft crossing the surface. Such a system is shown in Fig. 5.3. The shear work done over the cross section of the rotating

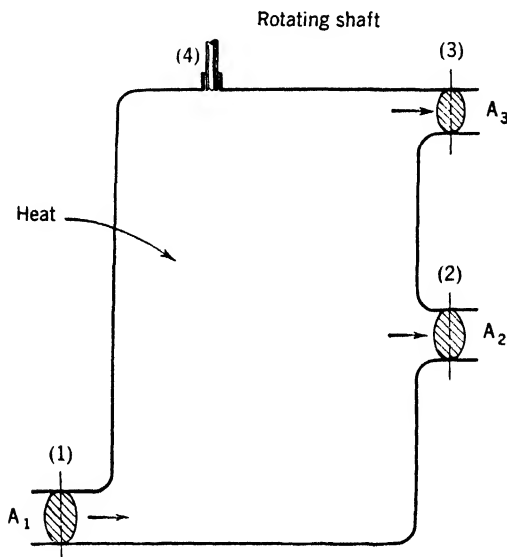


FIG. 5.3.

shaft at 4 is called the shaft work. The shear work done at all other parts of the boundary is zero, because the velocity is either zero or normal to the shearing force. For steady flow $E'_t - E'_a = 0$. Thus, from Eq. (5.8),

$$\frac{\text{Heat}}{dt} - \frac{\text{shaft work}}{dt} = \int_{A_1+A_2+A_3} \left(\frac{p}{\rho} + gz + \frac{V^2}{2} + u \right) \rho V dA \quad (5.9)$$

In the usual case, for which the flow crosses the control surface at only two areas A_1 and A_2 , over each of which $(p/\rho) + gz$, V , ρ , and u have uniform values, continuity gives $\rho_1 A_1 V_1 = \rho_2 A_2 V_2$, and Eq. (5.9) becomes

$$q - \mathfrak{W}_s = \frac{p_2}{\rho_2} - \frac{p_1}{\rho_1} + g(z_2 - z_1) + \frac{V_2^2 - V_1^2}{2} + u_2 - u_1 \quad (5.10)$$

where

$$q = \text{heat}/\rho_1 A_1 V_1 dt \quad \text{and} \quad \mathfrak{W}_s = \text{shaft work}/\rho_1 A_1 V_1 dt.$$

The symbols q and \mathfrak{W}_s thus stand, respectively, for the heat entering and the shaft work leaving the system, both being referred to unit mass of the flowing fluid.

5.3. Energy Equation for Cyclic Flow. In any machine doing positive or negative shaft work, the flow in the neighborhood of the moving blades

or pistons is cyclic, rather than steady. The state of the fluid varies periodically at any fixed point with a period T that is the same throughout the neighborhood.

Select a control surface as described above to eliminate the shear work, and assume as before that conditions are constant where the fluid crosses the control surface. Average Eq. (5.8) over a period by integrating with respect to time between the limits 0 and T and then dividing by T . Since the flow is cyclic, the term

$$\frac{1}{T} \int_0^T \frac{E'_b - E'_a}{dt} dt = \frac{E'(T) - E'(0)}{T} = 0$$

and the resulting equation will be similar to Eq. (5.9) or (5.10). These equations are, accordingly, applicable to machines in which the flow is cyclic.

5.4. Relation between the Energy Equation and the Euler Equation.

In the stream tube of ideal fluid shown in Fig. 5.4 no shaft work is done. Noting that

$$\frac{p_2}{\rho_2} - \frac{p_1}{\rho_1} = \int_1^2 d\frac{p}{\rho} = \int_1^2 \frac{dp}{\rho} + \int_1^2 p d\frac{1}{\rho}$$

where the integration is along the streamline we write Eq. (5.10) as

$$\int_1^2 \frac{dp}{\rho} + \frac{V_2^2 - V_1^2}{2} + g(z_2 - z_1) + \int_1^2 p d\frac{1}{\rho} + u_2 - u_1 - q = 0 \quad (5.11)$$

The first three terms of Eq. (5.11) may be set equal to zero by virtue of Euler's equation [Eq. (4.7)].

An observer moving along the stream tube with the fluid would see a

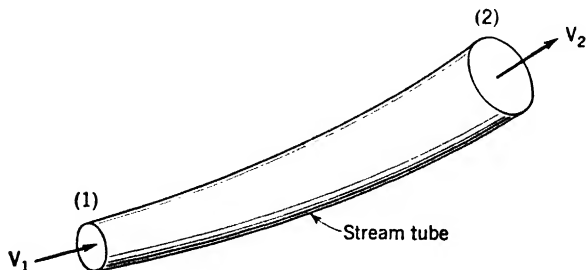


FIG. 5.4.

certain change in state of unit mass during his journey from 1 to 2. The only work done by the ideal fluid would be caused by changes in volume (or density), that is, $\int_1^2 p d(1/\rho)$. The apparent energy change would be $u_2 - u_1$, since the fluid would be at rest from the viewpoint of the ob-

server. Consequently, he would write the first law of thermodynamics for unit mass as

$$q - \int_1^2 p d \frac{1}{\rho} = u_2 - u_1 \quad (5.12)$$

which is the remainder of Eq. (5.11).

The energy equation is seen to be the sum of two independent equations, one derived from mechanics and the other from thermodynamics.

It may be noted in this connection that the more general equation, Eq. (5.8), can be derived by applying Newton's second law and the first law of thermodynamics to a particle of matter, adding the results, and integrating throughout a finite control volume.

5.5. Applications of the Energy Equation. *a. Frictionless Machine.* Consider for simplicity the type of machine shown in Fig. 5.5, to which

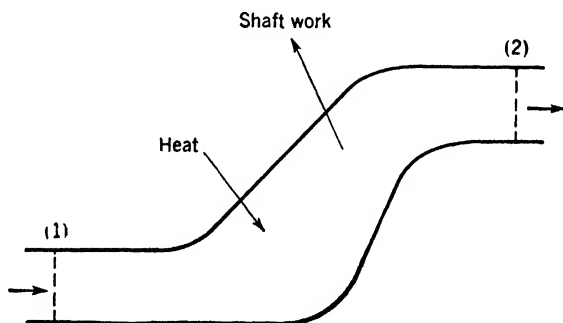


FIG. 5.5.

Eq. (5.10) applies. Breaking up the pressure-work term as in the preceding article and noting that Eq. (5.12) is valid in the absence of friction, we reduce Eq. (5.10) to the form

$$-\mathfrak{W}_s = \int_1^2 \frac{dp}{\rho} + \frac{V_2^2 - V_1^2}{2} + g(z_2 - z_1) \quad (5.13)$$

The terms on the right side are those occurring in the Euler equation. In this case, however, instead of being equal to zero, the sum of these terms is the shaft work done on the machine by external means.

It may be mentioned that Eq. (5.13) can be deduced from Newton's laws alone, without reference to the first law of thermodynamics. The derivation is, however, more complicated than the one given here.

For an incompressible fluid, $\int_1^2 dp/\rho = (p_2 - p_1)/\rho$, and Eq. (5.13) states that the shaft work equals the difference between the Bernoulli numbers at exit and entrance.

b. Machine with Real Working Fluid. For simplicity we take into account only the friction in the working fluid, neglecting, for example, any bearing friction or windage. We also assume incompressibility.

Referring to Fig. 5.6, consider first the pump, which is lifting fluid

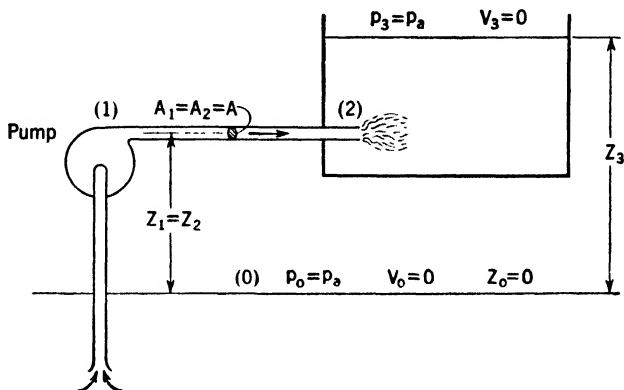


FIG. 5.6.

steadily from one reservoir to another. Equation (5.10) applied between sections 0 and 1 yields

$$-W_s = \frac{p_1 - p_a}{\rho} + \frac{V_1^2}{2} + gz_1 + u_1 - u_0 - q_{0,1} \quad (5.14)$$

From Eq. (5.12) or by comparing Eqs. (5.13) and (5.14) we see that $u_1 - u_0 - q_{0,1} = 0$ for a *frictionless* incompressible fluid. The behavior of this expression for a *viscous* incompressible fluid will now be discussed.

For any working fluid * with which we deal we assume that a property, such as internal energy or pressure, is determined when two independent properties, such as density and temperature, have given values. For the incompressible case, therefore, internal energy depends only on temperature. As the working fluid flows through the pump, it undergoes shearing deformation, since the fluid in contact with a solid surface does not slip. Shearing stresses are set up in the viscous fluid as a result of these deformations, and the temperature rises above the value it would have in frictionless flow. This temperature rise tends to increase both $u_1 - u_0$ and the heat $-q_{0,1}$ transferred to the surroundings. The expression $u_1 - u_0 - q_{0,1}$ is, therefore, positive in a flow with friction. It is often referred to as the "loss" and denoted by $g^{H_{l0,1}}$.

It is to be emphasized that these statements concerning $u_1 - u_0 - q_{0,1}$ are restricted to incompressible fluid.

* We assume the fluid to be a thermodynamically pure substance. For a definition of such a substance see reference 2 at the end of this chapter.

The efficiency of the pump is defined as the ratio of the shaft work in the frictionless case to that with friction. From Eqs. (5.13) and (5.14) we get

$$\text{Efficiency} = \eta = \frac{[(p_1 - p_0)/\rho] + (V_1^2/2) + gz_1}{-\mathcal{W}_s} = 1 - \frac{u_1 - u_0 - q_{0,1}}{-\mathcal{W}_s} \quad (5.15)$$

The efficiency is less than 1 for a real fluid and equal to 1 in the limiting case of no friction.

Turning now to the flow in the pipe between sections (1) and (2) we get from Eq. (5.10)

$$\frac{p_1 - p_2}{\rho} = u_2 - u_1 - q_{1,2} \quad (5.16)$$

The pressure work done on the fluid in the pipe is entirely used in overcoming the effects of friction.

Finally, applying Eq. (5.10) between sections 2 and 3, we find that $[(p_2 - p_3)/\rho] + g(z_2 - z_3) + (V_2^2/2) = u_3 - u_2 - q_{2,3}$. Furthermore, since the fluid is incompressible, no discontinuity in pressure occurs and the pressure of the jet emerging from the pipe must be the same as that of the surrounding fluid. Consequently, $[(p_2 - p_3)/\rho] + g(z_2 - z_3) = 0$ and

$$\frac{V_2^2}{2} = u_3 - u_2 - q_{2,3} \quad (5.17)$$

All the kinetic energy of the stream at 2 is dissipated in the tank. The surface of discontinuity in velocity that bounds the emergent jet is unstable and breaks down into large eddies, which, in turn, give rise to smaller and smaller eddies, until finally no observable motion remains.

5.6. Energy Equation for Moving Axes. So far in this chapter we have supposed the axes, or frame of reference, to be at rest. Due caution must be observed if the reference frame is moving, since the energy equation is based in part on Newton's laws, which in the form given here apply only for axes at rest or in uniform motion. The energy equations given above are, therefore, valid unless the frame of reference is accelerated.

Only one sort of accelerated frame of reference will be considered in this text, *viz.*, one that rotates at a constant speed about a fixed axis (see Art. 6.8). Applications will be made to rotating machinery.

SELECTED BIBLIOGRAPHY

1. GIBBS, J. W.: "Collected Works," Vol. I, Longmans, Green and Company, New York, 1931.
2. KEENAN, J. H.: "Thermodynamics," John Wiley & Sons, Inc., New York, 1940.
3. O'BRIEN, M. P., and G. H. HICKOX: "Applied Fluid Mechanics," McGraw-Hill Book Company, Inc., New York, 1937.
4. PLANCK, MAX: "Thermodynamik," 9th ed., Walter de Gruyter & Company, Berlin, 1930.

CHAPTER VI

MOMENTUM RELATIONS FOR STEADY FLOW

In many engineering problems, the force or torque produced on a solid body by a steadily flowing fluid is of great importance. Familiar examples are the force exerted on a body by a fluid jet; the force on a pipe bend; the lift and drag of an airplane wing; and the thrust and torque of a propeller, turbine, or centrifugal pump.

Newton's laws of motion can be put into a form known as the momentum law, which is especially convenient for dealing with steady-flow problems of this character. Heretofore we have applied Newton's laws only to a single particle of ideal fluid, in setting up Euler's equations of motion. In this chapter we shall apply them in the form of the momentum law, to mass systems including both solid bodies and a stream of fluid. No restrictions will be placed on the fluid; it may be both viscous and compressible so long as the flow is steady.

6.1. Laws of Motion. For an arbitrary direction x , Newton's second law of motion states that the resultant external x force acting on a mass particle is equal to the rate of change of x momentum of the particle. Apply this law to each of several mass particles, and sum the resulting equations. By Newton's third law, action is equal and opposite to reaction, so that any internal forces between particles of the system occur in pairs which cancel out when the forces on all particles are summed. For any mass system, therefore, the relation between force and momentum is the same as that for a single particle, and may be written

$$F_x = \frac{dM_x}{dt} \quad (6.1)$$

where F_x stands for the resultant external x force and M_x for the x momentum.

We shall now express this relationship in a form peculiarly suited to the solution of fluid-flow problems. The procedure will parallel that already used in the development of the continuity and energy equations.

6.2. Steady-flow Momentum Equation. We apply Eq. (6.1) to a mass system defined as the matter lying within a fixed control volume \mathcal{V} , at an arbitrary time t_a (Fig. 6.1*a*). For an arbitrary direction x consider the change in momentum of this system during a time interval $dt = t_b - t_a$. The boundary of the system at time t_b will in general no longer coincide with the control surface A but will be as shown by the dotted line in Fig. 6.1*b*.

The x momentum of that part of the system lying outside of \mathcal{V} at t_b we call $dM_{x_{out}}$, and the x momentum of the new matter inside of \mathcal{V} at t_b but not included in the system we call $dM_{x_{in}}$. Representing the x momentum of all the matter inside of \mathcal{V} at any time by M'_x , we see that

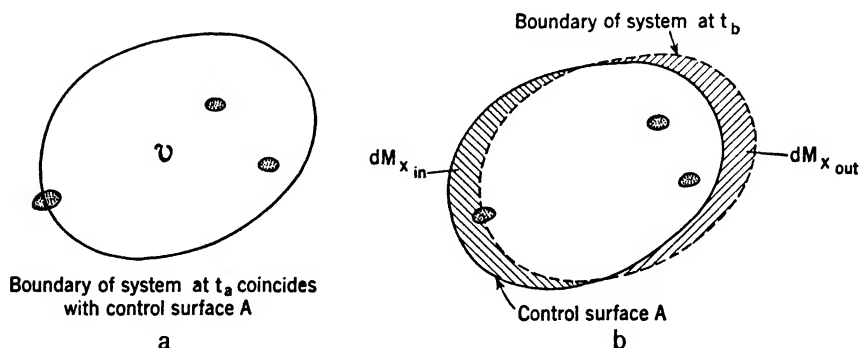


FIG. 6.1.

the initial and final x momenta of the system are, respectively, $M_{x_a} = M'_{x_a}$ and $M_{x_b} = M'_{x_b} + dM_{x_{out}} - dM_{x_{in}}$, whence

$$\frac{dM_x}{dt} = \frac{M_{x_b} - M_{x_a}}{dt} = \frac{M'_{x_b} - M'_{x_a}}{dt} + \frac{dM_{x_{out}} - dM_{x_{in}}}{dt} \quad (6.2)$$

The rate of change of x momentum of the system is thus expressed as the sum of the rate of change inside the control volume and the net rate of outflow of x momentum through the control surface.

Referring to Art. 3.6 and Fig. 3.4, we find that the flow of mass in time dt across an element dA of the control surface is $\rho V \cos \alpha dA dt$. Multiplication of this expression by the x component of velocity V_x (x momentum per unit mass) yields the x momentum carried across dA by the flow in time dt . Accordingly, the net rate of outflow of x momentum across A is

$$\frac{dM_{x_{out}} - dM_{x_{in}}}{dt} = \int_A \rho V_x V \cos \alpha dA \quad (6.3)$$

Combination of Eqs. (6.1), (6.2), and (6.3) gives the momentum equation

$$F_x = \frac{M'_{x_b} - M'_{x_a}}{dt} + \int_A \rho V_x V \cos \alpha dA \quad (6.4)$$

The resultant x force on the matter momentarily occupying the fixed volume \mathcal{V} equals the rate of change of x momentum inside \mathcal{V} plus the net rate of outflow of x momentum through the control surface.

By reasoning like that in Art. 5.3 it is seen that for steady or cyclic flow Eq. (6.4) reduces to

$$F_x = \int_A \rho V_x V \cos \alpha \, dA \quad (6.5)$$

In many problems the control volume can be so chosen that fluid enters it at an area A_1 and leaves at area A_2 , over each of which ρ , V , and $\cos \alpha$ are uniform. For such a problem, continuity gives $\rho_1 A_1 V_1 \cos \alpha_1 = \rho_2 A_2 V_2 \cos \alpha_2 = \rho_1 Q_1$, and Eq. (6.5) simplifies to

$$F_x = \rho_1 Q_1 (V_{x_2} - V_{x_1}) \quad (6.6)$$

If Eq. (6.6) is rewritten as

$$F_x - \rho_1 Q_1 V_{x_2} + \rho_1 Q_1 V_{x_1} = 0 \quad (6.6a)$$

it is seen that the system behaves as if it were in equilibrium under the action of the actual external forces F_x , a force $\rho_1 Q_1 V_{x_2}$ in the negative x direction, and a force $\rho_1 Q_1 V_{x_1}$ in the positive x direction. One can readily extend this result to show that a flux of momentum $\rho Q V$ across an area A has the same effect on the system as a force of magnitude $\rho Q V$ acting at the center of A . This force is parallel to the velocity V but always has an *inward* component, regardless of whether the flow is out or in across the area A . A steady-flow problem can thus be solved by the methods of statics if these effective forces are included with the actual external forces on the system.

6.3. Momentum Equation for Moving Axes. Equations (6.1) to (6.6) are valid when referred to axes moving without acceleration, since the usual form of Newton's laws holds under these conditions.

6.4. Application of the Momentum Equation. A real, compressible fluid flows steadily through the horizontal pipe bend shown in Fig. 6.2. It is desired to find the forces needed to hold the bend stationary. These forces will usually be exerted on the bend by the adjoining pipes and will therefore be distributed over the ends of the bend wall at 1 and 2. For simplicity, we assume that these distributed forces are equivalent to a single concentrated force R .

We choose a control volume to include the bend as well as the fluid, in order that R will be one of the external forces on the system. If the control volume included the fluid only, R would not act on the system and an additional step would be required in the solution of the problem.

In Fig. 6.2 it is seen that $V_{x_2} = V_2 \cos \beta$, $V_{x_1} = V_1$, $V_{y_1} = V_1 \sin \beta$, and $V_{y_2} = 0$. The momentum terms in Eq. (6.6) are therefore readily written down for this problem.

The resultant force on the system is caused entirely by deviations in the stress distribution over the control surface from the uniform atmospheric pressure. (The weight is normal to the plane of flow and does not enter the problem.) We have already seen that R is produced by these deviations

in stress over the ends of the pipe bend at 1 and 2. The only other deviations occur at the fluid surfaces A_1 and A_2 . From the axial symmetry of the flow at these areas it is clear that the shearing forces on either A_1 or A_2

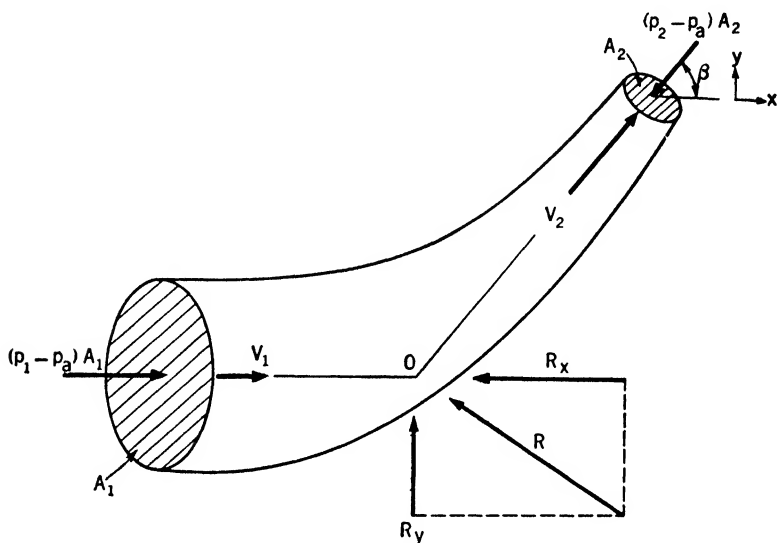


FIG. 6.2.

have a zero resultant. The excess pressure forces at A_1 and A_2 are shown in Fig. 6.2. The components of the resultant external force, therefore, are

$$F_x = (p_1 - p_a)A_1 - (p_2 - p_a)A_2 \cos \beta - R_x$$

$$F_y = R_y - (p_2 - p_a)A_2 \sin \beta$$

Substitution in Eq. (6.6) of these values of the components of velocity and force gives

$$R_x = (p_1 - p_a)A_1 - (p_2 - p_a)A_2 \cos \beta - \rho_1 A_1 V_1 (V_2 \cos \beta - V_1) \quad (6.7)$$

$$R_y = (p_2 - p_a)A_2 \sin \beta + \rho_1 A_1 V_1 V_2 \sin \beta \quad (6.8)$$

The pressure and velocity at 2 can be eliminated from these equations if incompressibility is assumed. The continuity and energy equations for incompressible flow yield

$$A_1 V_1 = A_2 V_2 \quad p_2 = p_1 - \frac{\rho}{2}(V_2^2 - V_1^2) - \rho(u_2 - u_1 - q_{1,2})$$

whence

$$R_x = (p_1 - p_a)(A_1 - A_2 \cos \beta) + \frac{\rho}{2} A_1 V_1^2 \left[2 - \cos \beta \left(\frac{A_1}{A_2} + \frac{A_2}{A_1} \right) \right] + \rho(u_2 - u_1 - q_{1,2})A_2 \cos \beta \quad (6.9)$$

$$R_v = (p_1 - p_a)A_2 \sin \beta + \frac{\rho}{2} A_1 V_1^2 \left(\frac{A_1}{A_2} + \frac{A_2}{A_1} \right) \sin \beta - \rho(u_2 - u_1 - q_{1,2})A_2 \sin \beta \quad (6.10)$$

The loss terms (on the extreme right) will be zero if the flow is assumed to be frictionless.

6.5. Angular-momentum Law. Newton's second law applied to the mass δm of Fig. 6.3 gives the following results:

$$\delta F_x = \frac{dV_x}{dt} \delta m \quad \delta F_y = \frac{dV_y}{dt} \delta m$$

where V_x and V_y are the x and y components of velocity. The counter-

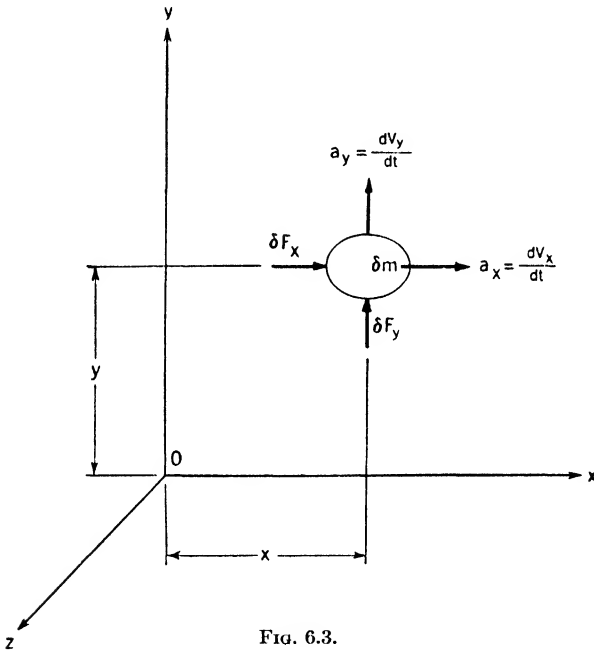


FIG. 6.3.

clockwise moment, or torque, of the external forces about an axis through O perpendicular to the x, y plane (z axis) is

$$\delta T_z = x \delta F_y - y \delta F_x = \left(x \frac{dV_y}{dt} - y \frac{dV_x}{dt} \right) \delta m$$

By the rules of differentiation

$$\begin{aligned} \frac{d}{dt} (xV_y - yV_x) &= \frac{dx}{dt} V_y - \frac{dy}{dt} V_x + x \frac{dV_y}{dt} - y \frac{dV_x}{dt} \\ &= V_x V_y - V_y V_x + x \frac{dV_y}{dt} - y \frac{dV_x}{dt} \end{aligned}$$

Therefore, since $V_x V_y - V_y V_x = 0$ and δm is constant,

$$\delta T_z = \frac{d}{dt} (x V_y - y V_x) \delta m = \frac{d}{dt} [(x V_y - y V_x) \delta m] \quad (6.11)$$

The quantity in square brackets is called the “moment of momentum” or “angular momentum” about the z axis and will be denoted by δH_z . Newton’s second law thus leads to the following statement for the mass δm : The resultant external torque about an arbitrary fixed axis (z axis) equals the rate of change of angular momentum about that axis,

$$\delta T_z = \frac{d(\delta H_z)}{dt} \quad (6.12)$$

Apply Eq. (6.12) to each of several small masses, and sum the resulting equations. By Newton’s third law the forces acting between masses of the system occur in pairs whose members are equal, opposite, and collinear. Consequently, the moment of any one internal force is canceled by that of the other member of the pair, and the resultant moment of only the external forces is obtained when the equations are summed. We thus obtain for a system of masses a result identical with Eq. (6.12)

$$T_z = \frac{dH_z}{dt} \quad (6.13)$$

where T_z represents the resultant external moment about the arbitrary fixed z axis and H_z is the z angular momentum of the system.

It will be noted that, since z is arbitrary, a torque equation for the x or y axis may be obtained from Eq. (6.13) merely by a change of subscript to x or y . The z axis is used in the above development solely because it is customary to refer the flow to the x, y plane.

There is an analogy between Eqs. (6.13) and (6.1) that enables us to write down at once an angular-momentum equation corresponding to Eq. (6.4). For F_x we substitute T_z ; for M'_x we substitute H'_z , the z angular momentum of the mass inside the control volume; and we replace the x momentum per unit mass, or x velocity, V_x , by the z angular momentum per unit mass $x V_y - y V_x$ [see Eq. (6.11)].

It is usually convenient to express $x V_y - y V_x$ in terms of V_t and r , defined in Fig. 6.4.

$$x V_y - y V_x = r \cos \theta V \sin \phi - r \sin \theta V \cos \phi = r V \sin (\phi - \theta) = r V_t \quad (6.14)$$

It is seen that the tangential velocity component V_t is defined as positive for a counterclockwise angular momentum.

Making these substitutions in Eq. (6.4), we get the angular-momentum law

$$T_z = \frac{H'_{z_b} - H'_{z_a}}{dt} + \int_A \rho r V_t V \cos \alpha dA \quad (6.15)$$

The meaning of this equation is analogous to that of Eq. (6.4): The resultant external torque on the matter momentarily occupying a fixed volume \mathcal{V} equals the rate of change of angular momentum of the matter inside of \mathcal{V}

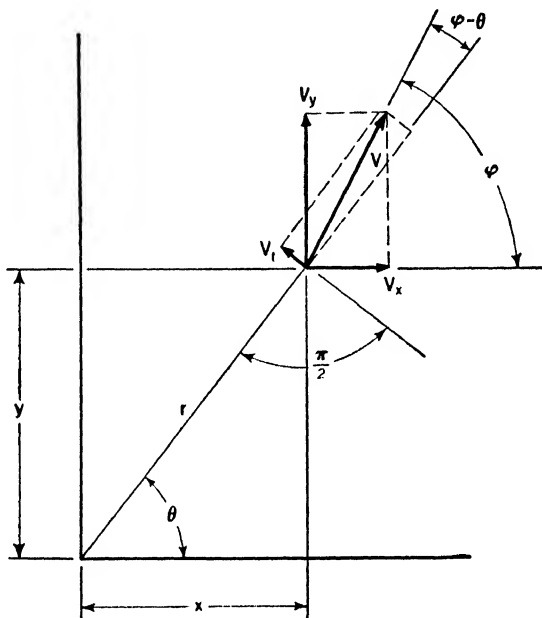


FIG. 6.4.

plus the net rate of outflow of angular momentum through the control surface.

For a steady or cyclic flow, Eq. (6.15) simplifies to

$$T_z = \int_A \rho r V_t V \cos \alpha \, dA \quad (6.16)$$

which is the analogue of Eq. (6.5).

Assume that the entire flow enters the control volume at an area A_1 and leaves at an area A_2 , over each of which ρ , V , and $\cos \alpha$ are uniform. Define $r_2 V_{t_2}$ as the mean value of $r V_t$ over A_2 and $r_1 V_{t_1}$ as the mean value over A_1 .

$$r_2 V_{t_2} = \frac{1}{A_2} \int_{A_2} r V_t \, dA \quad r_1 V_{t_1} = \frac{1}{A_1} \int_{A_1} r V_t \, dA$$

Continuity gives $\rho_1 A_1 V_1 \cos \alpha_1 = \rho_2 A_2 V_2 \cos \alpha_2 = \rho_1 Q_1$, and Eq. (6.16) becomes

$$T_z = \rho_1 Q_1 (r_2 V_{t_2} - r_1 V_{t_1}) \quad (6.17)$$

which is the analogue of Eq. (6.6).

By rewriting Eq. (6.17) in the form

$$T_z - \rho_1 Q_1 r_2 V_{t_2} + \rho_1 Q_1 r_1 V_{t_1} = 0 \quad (6.17a)$$

one can show that the moment of the momentum flux across an area A is the same as the moment of a force applied at the center of A and related to the momentum flux as described in Art. 6.2. The methods of statics are therefore applicable here as well as in the case of the linear-momentum law.

6.6. Application of the Angular-momentum Equation. In Art. 6.4 we computed the magnitude and direction of the external force R on a pipe bend. Here we shall find a point on the line of action of R .

In Fig. 6.2, take the z -axis through O , the point of intersection of the center lines of the pipes adjoining the bend. For this axis, it is obvious by inspection that $r_2 V_{t_2} = r_1 V_{t_1} = 0$. From Eq. (6.17), therefore, $T_z = 0$. Since the moments due to the pressure forces are zero, it follows that the line of action of R must pass through O .

6.7. Angular-momentum Equation for a Rotor. Equation (6.17) is

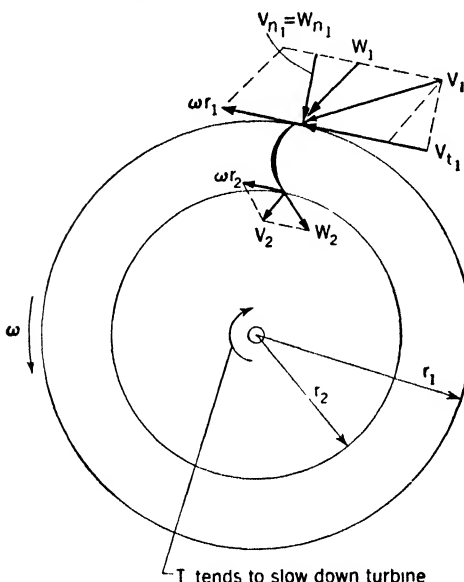


FIG. 6.5. — Velocity diagrams for a turbine runner.

applicable to the rotor of a turbine or compressor since the absolute flow in the interior of the rotor is cyclic and we may assume with fair approximation that ρ , V , and $\cos \alpha$ are uniform over the entrance section 1 and over the exit section 2 (see Figs. 6.5 and 6.6). In the figures, W refers to velocity relative to the rotor (relative velocity), and V , as usual, stands for velocity relative to the earth (absolute velocity). For clarity only one blade is shown.

If we neglect bearing friction, the drag of the fluid on the outside of the rotor, and fluid shearing stresses at 1 and 2, then the external torque T on the shaft equals the *resultant* external

torque on either system. For the turbine, however, T is clockwise, while for the compressor it is counterclockwise. Hence, for the turbine,

$$T = \rho_1 Q_1 (r_1 V_{t_1} - r_2 V_{t_2}) \quad (6.18)$$

and for the compressor,

$$T = \rho_1 Q_1 (r_2 V_{t_2} - r_1 V_{t_1}) \quad (6.19)$$

It should be emphasized that Eq. (6.16) or (6.17) is not in general applicable to rotating flows. The special case of the turbine or compressor rotor can be handled by Eq. (6.17) only because the flow satisfies the conditions listed at the beginning of this article.

An equation similar to Eq. (6.16) can be developed, however, for any rotating flow, provided merely that it be steady with respect to axes

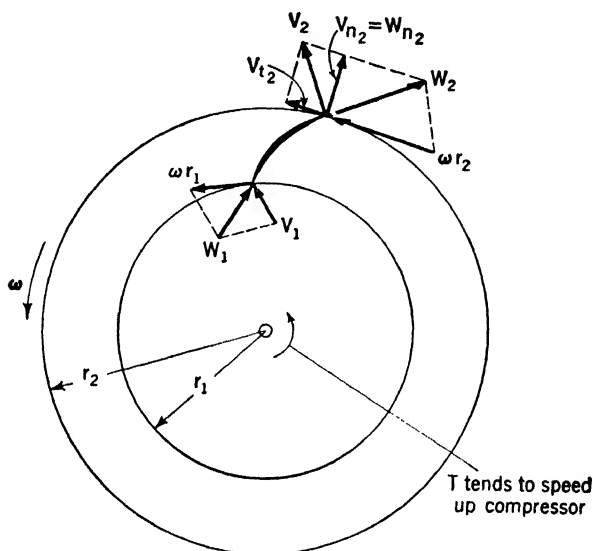


FIG. 6.6. — Velocity diagrams for a compressor or pump impeller.

rotating at a constant angular velocity about a fixed axis. This equation, which can be developed by the control-volume method of Arts. 3.6, 5.2, and 6.2, has the form

$$T_z = \int_A \rho r V_t W \cos \beta \, dA \quad (6.20)$$

where W is the velocity relative to the rotating axes and β is the angle between W and the outward-drawn normal to the element dA of a control surface that rotates with the axes. For the special case of the turbine or compressor rotor the control volume is merely an annulus concentric with the axis of rotation, so that $W \cos \beta = V \cos \alpha$ and Eqs. (6.16) and (6.20) are identical.

6.8. Energy Equation for a Rotor. To develop the energy equation for this case we retain the assumptions that the absolute flow at entrance and exit of the turbine runner of Fig. 6.5 is steady and uniform and that the absolute flow in the interior is cyclic. We also neglect any work due to fluid shear. Equation (5.10) is therefore applicable to the runner.

$$\frac{p_2}{\rho_2} - \frac{p_1}{\rho_1} + \frac{V_2^2 - V_1^2}{2} + g(z_2 - z_1) + u_2 - u_1 - q + \mathcal{W}_s = 0 \quad (5.10)$$

Note that $\mathfrak{W}_s = T\omega/\rho_1 Q_1$; whence, from Eq. (6.18), $\mathfrak{W}_s = (r_1 V_{t_1} - r_2 V_{t_2})\omega$. Substitution of this value of \mathfrak{W}_s into Eq. (5.10) gives a term $[V_2^2 - 2\omega r_2 V_{t_2} - (V_1^2 - 2\omega r_1 V_{t_1})]/2$, from which we eliminate the absolute velocities by means of the velocity diagrams of Fig. 6.5.

$$V_2^2 - 2\omega r_2 V_{t_2} = W_{t_2}^2 + (\omega r_2 - W_{t_2})^2 - 2\omega r_2(\omega r_2 - W_{t_2}) = W_2^2 - \omega^2 r_2^2$$

Similarly,

$$V_1^2 - 2\omega r_1 V_{t_1} = W_1^2 - \omega^2 r_1^2$$

Therefore, the energy equation referred to the rotor is

$$\frac{p_2}{\rho_2} - \frac{p_1}{\rho_1} + \frac{W_2^2 - W_1^2}{2} - \frac{\omega^2}{2}(r_2^2 - r_1^2) + g(z_2 - z_1) + u_2 - u_1 - q = 0 \quad (6.21)$$

A similar development for the compressor impeller shows that Eq. (6.21) applies also to that case.

If friction is negligible, Eq. (5.12) gives $\int_1^2 pd(1/\rho) + u_2 - u_1 - q = 0$, so that Eq. (6.21) becomes

$$\int_1^2 \frac{dp}{\rho} + \frac{W_2^2 - W_1^2}{2} - \frac{\omega^2}{2}(r_2^2 - r_1^2) + g(z_2 - z_1) = 0 \quad (6.22)$$

which is Euler's equation for a frame of reference rotating at a constant angular velocity.

In the special case of motion like that of a rotating rigid body ($W = 0$ everywhere), Eq. (6.22) reduces to

$$\int_1^2 \frac{dp}{\rho} - \frac{\omega^2}{2}(r_2^2 - r_1^2) + g(z_2 - z_1) = 0 \quad (6.23)$$

which has already been discussed (for incompressible fluid) in Art. 2.19.

6.9. Recapitulation. It is desirable to set down here the principal results of Chaps. III, V, and VI in order to point out the general pattern to which they all conform. This article will be restricted to a system bounded by a fixed control surface and to the steady-flow case.

The continuity equation [Eq. (3.8)] is

$$0 = \left\{ \begin{array}{l} \text{net rate of outflow of mass} \\ \text{across the control surface} \end{array} \right\} = \int_A (1)\rho V \cos \alpha \, dA$$

The energy equation [Eq. (5.6)] is

$$\left\{ \begin{array}{l} \text{Heat added} \\ \text{to system} \\ \text{per unit} \\ \text{time} \end{array} \right\} - \left\{ \begin{array}{l} \text{work done} \\ \text{by system} \\ \text{per unit} \\ \text{time} \end{array} \right\} = \left\{ \begin{array}{l} \text{net rate of out-} \\ \text{flow of energy} \\ \text{across the con-} \\ \text{trol surface} \end{array} \right\} = \int_A (e)\rho V \cos \alpha \, dA$$

The linear-momentum equation [Eq. (6.5)] is

$$\left\{ \begin{array}{l} \text{Resultant } x \text{ force} \\ \text{on system} \end{array} \right\} = \left\{ \begin{array}{l} \text{net rate of outflow} \\ \text{of } x \text{ momentum} \\ \text{across the control} \\ \text{surface} \end{array} \right\} = \int_A (V_x) \rho V \cos \alpha \, dA$$

The angular-momentum equation [Eq. (6.16)] is

$$\left\{ \begin{array}{l} \text{Resultant } z \text{ torque} \\ \text{on system} \end{array} \right\} = \left\{ \begin{array}{l} \text{net rate of outflow} \\ \text{of } z \text{ angular mo-} \\ \text{mentum across the} \\ \text{control surface} \end{array} \right\} = \int_A (rV_t) \rho V \cos \alpha \, dA$$

The factors in parentheses represent, respectively, the mass per unit mass 1, the energy per unit mass e , the x momentum per unit mass V_x , and the z angular momentum per unit mass rV_t . The product of each of these by $\rho V \cos \alpha \, dA$, the rate of mass flow across an area dA of the control surface, gives the rate of flow of each entity across dA . The algebraic sum \int_A of the elementary fluxes then gives the total flux.

It may be remarked that the Euler differential equations [Eqs. (4.3) and (4.4)], on which Chap. IV is based, can be derived from the linear-momentum law by reference to an elementary control surface.

The hydrostatic equation [Eq. (2.7)] is also a special case of the momentum law.

All the problems of steady flow discussed in this book are based on the principles outlined in this article. The method of dimensional analysis, the only other tool that will be used extensively, is presented in the next chapter.

SELECTED BIBLIOGRAPHY

1. VON MISES, R.: "Theory of Flight," McGraw-Hill Book Company, Inc., New York, 1945.
2. PRANDTL, L., and O. G. TIETJENS: "Fundamentals of Hydro- and Aeromechanics," McGraw-Hill Book Company, Inc., New York, 1934.

CHAPTER VII

DIMENSIONAL ANALYSIS AND SIMILITUDE

7.1. Dimensions. In mechanics we deal quantitatively with physical phenomena involving mass, force, momentum, energy, density, viscosity, and many other aspects of nature or entities, to which names have been given. Such an entity can be measured in terms of a selected unit amount of that entity, and we can express its quantity by an abstract number that names the number of times the unit can be contained in it.

7.2. Length. If we choose length as a primary quantity, we can construct area and volume as derived quantities. In this way we give area and volume the dimensions of $[L^2]$ and $[L^3]$. This is a symbolic notation to express the idea of dimensions.

Arithmetic deals with pure numbers, which can be added and otherwise manipulated in accordance with known rules. When we attach dimensional meaning to numbers, we may not follow the rules of arithmetic unless certain restrictions are observed.

For example, if L_1 names the length of a beam and L_0 the length of a stick, we may measure L_1 in terms of L_0 by repeated application of L_0 along L_1 . We express the result as $L_1 = nL_0$.

Here n is a pure number expressing the times L_0 is applied to L_1 . Now if L_1 and L_0 be each measured in terms of a shorter stick, or unit of length λ , we have

$$l_1\lambda = nl_0\lambda$$

where l_1 and l_0 are pure numbers that express the number of times the unit λ has been applied.

Since λ appears in both terms, $l_1 = nl_0$; and as this expression contains only numbers, the rules of arithmetic apply and we may write

$$\frac{l_1}{l_0} = n = \frac{L_1}{L_0}$$

where L_1 and L_0 are symbols or names for the lengths of two objects.

The important result of this reasoning is the realization that the ratio between two lengths is the ratio between the numbers of units which measure them, regardless of the size of the common unit of length employed.

The justification for the addition and subtraction of lengths follows by similar reasoning. A length $L_0 = l_0\lambda$ applied in continuation of a length

$L_1 = l_1\lambda$ constitutes the addition of two lengths and will be numerically expressed by $l_0 + l_1$ units of length, or

$$l_1\lambda + l_0\lambda = (l_1 + l_0)\lambda$$

We may add measures of length only when the lengths added are expressed in terms of the same unit of length.

7.3. Time. The measurement of time is more difficult than that of length. We know in nature of periodic phenomena that proceed steadily, and we can measure a time interval by counting heartbeats or by watching the sun or a clock. We can select any convenient unit of time based on some such repetition and express a time interval as a number of such units. Since we cannot directly add one time interval to another unless one interval starts when the other ends, we must assume the accuracy of clocks. We are content to add numbers of units of time so long as all time intervals are measured in the same unit.

7.4. Velocity. Velocity might be measured in arbitrary velocity units, as by the Beaufort scale of the sailor, who estimates wind velocity by the appearance of his sails. Thus 5 on the Beaufort scale is "fresh breeze, all sail drawing," and 10 is "whole gale, hove to under storm sail." The sailor has no ready means to measure velocity, and he associates velocity with force, which he can estimate.

Nature does not supply for mechanics a convenient standard unit of velocity. The speed of falling bodies is changing, and the speed of animals uncertain. The velocity of light is convenient for astronomers only. We resolve the difficulty by defining velocity in terms of length and time and making the unit of velocity the ratio between a unit of length and a unit of time. This is a new concept—to divide a length by a time and to call the quotient a velocity. We do this, not as a result of any logical analysis, but purely by our own decision. We choose to define velocity as $V = ds/dt$, where ds is the distance moved in time dt , and, as a consequence, the unit of velocity becomes a derived unit. A simple dimensional equation to express this concept is, in conventional notation,

$$[V] = \frac{[L]}{[T]}$$

where the brackets indicate that the dimensions only of the enclosed quantity are represented.

7.5. Acceleration. Like velocity, acceleration is conveniently derived from length and time, and by definition, is given the dimensions

$$[a] = \frac{[V]}{[T]} = \left[\frac{L}{T^2} \right]$$

7.6. Force. Weight is the most common force, and it is natural that force is universally measured in terms of the weight of a standard block

of material. This block is often called a "weight," and the words "force" and "weight" have become confused.

Since prehistoric times, quantities of material have been compared or measured with some form of balance, a convenient standard quantity being used for balance "weights." The convenient unit has usually been of the order of a handful of material—hence our modern pound.

Force is taken as a primary quantity in the so-called "technical" or "gravitational system," and its unit is the weight of a standard block of metal at a place where gravity has a standard value.

7.7. Mass. Mass is quantity of matter. The mass of a standard block is invariant although its weight may vary slightly with location, since gravity is not everywhere the same. The apparent weight of a given mass in an airplane when making a banked turn may be several times normal.

The distinction between weight and mass is primarily a necessity of mechanics. Newton's great generalization for the first time connected force and mass through the statement of his second law. Newton postulated mass as the fundamental entity and described force as a phenomenon whose action could be observed and measured by its effect on the state of motion of a mass. The rate of change in the quantity of motion measures the force acting. In our modern notation this is

$$\text{Force} = \frac{\text{momentum change}}{\text{time of application}} \quad \text{or} \quad F = \frac{d(mV)}{dt}$$

with a corresponding dimensional equation

$$[F] = \left[\frac{MV}{T} \right] = \left[\frac{ML}{T^2} \right]$$

which, outside of relativity regions, has been found to express a universal law of nature.

We could, with equal logic, use Newton's second law to define mass in terms of force, length, and time, thus:

$$m = \frac{F}{a} \quad \text{or} \quad [M] = \left[\frac{FT^2}{L} \right]$$

It is a matter of convenience whether we choose $[F]$ as a primary quantity and define $[M]$ in a technical system of units or choose $[M]$ as a primary quantity and define $[F]$ in a dynamic system. Both are in general use. The $[M]$ system is usually called the "absolute" system in older texts, but it is now recognized that there is nothing absolute about any system.

7.8. Moment and Work. The dimensions of these entities are symbolically similar although physically distinct. This arises because we define each in terms of a force and a length.

$$[\text{Moment}] = [FL]$$

$$[\text{Work}] = [FL]$$

For example, the moment of a 10-lb force acting with a 10-ft arm is 100 units of moment, where the unit is the moment of one pound acting with an arm of one foot.

The work done by a force of 10 lb acting through 10 ft is also 100 lb-ft. But here work is expressed in terms of a work unit, *i.e.*, the work done by one pound acting along a distance of one foot in the direction of the force. Note that the derived unit of moment is quite different as to the direction of the force with relation to the length. Moment is a vector quantity, while work is a scalar.

7.9. Zero Dimensions. There are quantities that are a ratio of two quantities of the same dimensions. Angles and trigonometric functions are pure numbers and are therefore dimensionless or of zero dimensions. For example, an angle is the ratio of an arc to its radius, which, in dimensional notation, is expressed as

$$[\alpha] = \left[\frac{L}{L} \right] = [L^0]$$

It is a peculiarity of our system of numbers that the zero can have whatever dimensions the other terms of an equation require. For example, consider the physical equation for the law of falling bodies,

$$s = gt^2/2$$

with its dimensional equivalent

$$[s] = [L] = [gt^2] = \left[\frac{L}{T^2} T^2 \right] = [L]$$

It is equally valid to write

$$s - gt^2/2 = 0$$

and its dimensional equivalent

$$[s - gt^2/2] = [L] = [0]$$

Zero in this case must have the dimensions of a length.

7.10. Properties of Materials. The dimensions of the common properties of materials can be expressed in terms of the three primary quantities in accordance with their definitions. However, density and viscosity need special attention.

The weight per unit volume of a substance (specific weight) is often erroneously called density. It is recommended to reserve the term "density" in mechanics to mean the mass per unit volume.

$$[\gamma] = \left[\frac{\text{weight}}{\text{volume}} \right] = \left[\frac{F}{L^3} \right]$$

$$[\rho] = \left[\frac{\text{mass}}{\text{volume}} \right] = \left[\frac{M}{L^3} \right]$$

Viscosity was defined by Newton as the force per unit area per unit rate of shear on adjacent layers of a moving fluid. If the thickness of an oil film is h and the relative velocity between the two sides of the film is V , V/h is the rate of shear. The coefficient of viscosity μ is then defined by $F/A = \mu V/h$, where F is the shearing force and A is the area of the oil film. There is a corresponding dimensional equation

$$[\mu] = \left[\frac{Fh}{AV} \right] = \left[\frac{FT}{L^2} \right] = \left[\frac{M}{LT} \right]$$

7.11. Dimensional Systems. A consistent dimensional system is composed of the smallest number of quantities in terms of which all entities and relations in a field of science may be expressed. For mechanics three such "primary" quantities have been found necessary and sufficient, which are usually chosen as $[M]$, $[L]$, $[T]$ or $[F]$, $[L]$, $[T]$.

For thermodynamics a fourth primary quantity is needed, generally taken for convenience as temperature $[\theta]$.

7.12. Units of Force, Weight, and Mass. We have acquired two systems of dimensions, the $[M]$ and the $[F]$, both in the metric system and in the English system.

While force is conveniently measured in terms of weight, a particular sort of force, confusion can develop when forces other than weight are involved, such as occur in dynamics. We accept without question that one pound is the force of the earth's attraction at Greenwich on a particular block of metal. This block of metal is a mass, and it is also called a pound. This "pound" block cannot be at the same time the unit of force and the unit of mass, for one quantity cannot be expressed in terms of the other alone. Their dimensions are not the same.

The difficulty comes from the fact that weight and mass are united by the special relation

$$w = gm$$

with g nearly constant. But g is not a pure number since the equivalence of w and gm would imply an impossible dimensional equation

$$[F] = \left[\frac{ML}{T^2} \right] = [g][M]$$

The two sides of this dimensional equation become reconciled only when g is an acceleration, of dimension $[L/T^2]$.

The "pound" block, if taken as a unit of mass, requires us to name another unit of force, defined from $F = ma$, as the force that gives one pound mass an acceleration of one foot per second per second. This unit of force is $1/g$ times the so-called "pound force." This unusual unit, named the poundal, has never been accepted as useful or convenient by engineers.

Man in general is constantly concerned with weight, rarely with mass. Mass is a quantity necessary to dynamics and may be considered to be a "technical" concept of historically recent origin.

American and British engineers adopt the weight of the pound block measured where $g = g_0 = 32.1739$ ft per sec per sec as the unit of weight, and a mass equivalent to 32.1739 times that of the standard pound block as the unit of mass. This was named the "slug"* by Professor Perry, with sluggishness or inertia in mind, and has been officially adopted for both British and United States government publications. A pound force gives unit acceleration to one slug of mass.

In the metric system, the same care must be taken regarding force and mass units. The unit mass is one gram, and the unit force, called a "dyne," is that force which will impart unit acceleration (in centimeters per second per second) to the gram unit of mass. The dyne corresponds to the poundal. However, the dyne is inconvenient for engineering work and the technical unit of force is taken as the weight of the gram mass measured where $g = 980.665$ cm per sec per sec; the unit of mass is 980.665 times the mass of the gram. Then a gram force gives unit acceleration to this unnamed unit of mass.

7.13. Dimensional Equations. The selection of three primary quantities, such as mass, length, and time, enables us to express the dimensions of all the other quantities of mechanics in terms of these three. The correct definition of a physical quantity implies both an algebraic equation and a dimensional equation.

Suppose a man riding in a car observes a pressure p due to the relative wind of velocity V . He has discovered a physical relation between pressure and velocity that he might assume to have the form

$$p = f(V) = KV^a$$

Since both terms must have the same dimensions, the corresponding dimensional equation, when a and K are pure numbers, would be

$$[p] = \left[\frac{F}{L^2} \right] = \left[\frac{M}{LT^2} \right] = \left[\frac{L^a}{T^a} \right]$$

The dimensional equation is out of balance, and evidently K is not a pure number but must be some function of other variables.

Suppose our experimenter were a more cautious person and assumed

* This term is applied only when the foot-pound-second system of British gravitational units is used. In many cases advantage results from using the inch instead of the foot for the linear unit, or what may be called the "inch-pound-second system." In this case the unit of mass is evidently equivalent to 32.1739×12 times that of the standard pound block.

the law of wind force might depend both on the density of the air and on the velocity. Then he would write

$$p = f(\rho, V) = K\rho^b V^a$$

and if he found by experiment that $a = 2$, the dimensional equation would now be

$$[p] = \left[\frac{M}{LT^2} \right] = \left[\frac{M^b}{L^{3b}} \right] \left[\frac{L^2}{T^2} \right]$$

Equating the exponents of M , on both sides of the equality sign, it appears that $b = 1$. Hence $p = K\rho V^2$, where K is an undetermined constant.

This experiment was made by observing the effect of but one variable, velocity; yet the dimensional analysis shows the necessary influence of another variable, density. The fact that p was found to vary as V^2 requires that p also vary as ρ .

Dimensional theory can never determine a numerical coefficient such as K , but it can give the only possible relation among the independent quantities involved. The procedure is first to deduce from dimensional considerations the general relation between the variables assumed to control the phenomenon and then by experiment to check the choice of independent variables and determine the necessary constants.

7.14. Dimensional Homogeneity. Any equation or formulation expressing a relation among physical quantities is actually an algebraic equation in which measurements, or numbers, represented by letters, imply but do not disclose the units in which each of the various quantities has been measured. There is a corresponding dimensional equation that states the dimensions of these units in each term of the algebraic equation. In dealing with physical measurements we may perform the operations of addition and subtraction only with numerical quantities of the same dimensions. The physical equation, therefore, must be dimensionally homogeneous.

This principle of dimensional homogeneity is fundamental to our whole system of physical and engineering mathematics. While pure mathematics is not concerned with dimensions, applied mathematics must deal with numbers that measure physical quantities in units of the same dimensions.

The application of this principle, first stated by Fourier, gives a test of the completeness or of the consistency of any physical equation purporting, as the result of experiment or analysis, to describe a physical phenomenon. It also furnishes a unique dimensional condition that must exist among the physical quantities involved and furnishes a clue to the form of an unknown physical equation describing it. The search for a correct dimensional form for an unknown equation is dignified by the name "dimensional analysis."

7.15. The General Form of Physical Equations. The fact that a complete physical equation must be dimensionally homogeneous can be generalized to develop a formal procedure for analysis of less simple problems. The necessity for a formal procedure arises because for mechanics there are but three primary quantities, while many mechanical relations involve more than three variables. It is not possible to determine the unknown exponents of more than three variables by means of the three simultaneous equations obtained from the exponents of M , L , and T , appearing in the corresponding dimensional equation.

Any complete physical equation expresses the relation among all of the different physical quantities that control the phenomenon in question. Let these quantities be designated by $Q_1, Q_2, Q_3, \dots, Q_n$. Then we may write the complete physical equation as an unknown function of all of the Q 's.

$$\phi(Q_1, Q_2, Q_3, \dots, Q_n) = 0 \quad (7.1)$$

Assume that Eq. (7.1) may be put in the form of an equivalent power series, each term containing all the quantities Q . A typical term will be of the form $AQ_1^{a_1}Q_2^{a_2}Q_3^{a_3}\dots Q_n^{a_n}$, where A is a numerical coefficient.

Equation (7.1) may be written as a series of such terms, the number of which may be indefinite,

$$AQ_1^{a_1}\dots Q_n^{a_n} + BQ_1^{b_1}\dots Q_n^{b_n} + \dots = 0 \quad (7.2)$$

Divide through by the first term, and obtain

$$1 + \frac{B}{A}Q_1^{b_1-a_1}Q_2^{b_2-a_2}\dots Q_n^{b_n-a_n} + \dots = 0 \quad (7.3)$$

By the principle of dimensional homogeneity, it will be observed that each term, including the zero, is dimensionless. Since the numerical coefficients are dimensionless, it follows that the products of the powers of the Q 's in each term are also dimensionless.

The dimensional equation corresponding to Eq. (7.3) will express this fact:

$$[Q_1^{x_1}Q_2^{x_2}\dots Q_n^{x_n}] = [M^0L^0T^0] \quad (7.4)$$

where x_1, x_2, \dots, x_n are unknown exponents.

The dimensional equation [Eq. (7.4)], places a restriction on the powers of the Q 's in each term of Eq. (7.3), but we cannot determine these exponents by inspection, except for very simple cases.

Since there may be a large number of Q 's, it is convenient to deal with a smaller number of products of a few Q 's taken together. Let the symbol Π represent a nondimensional product of powers of some of the Q 's, and let $\Pi_1, \Pi_2, \dots, \Pi_i$ represent all of such independent products that can be formed by using all the Q 's.

Since each Π is dimensionless, the product of any powers of the Π 's will also be dimensionless; and since the Π 's contain all the Q 's, some combination of Π 's could represent each term of Eq. (7.3). For example,

$$\frac{B}{A} Q_1^{b_1-a_1} Q_2^{b_2-a_2} \dots Q_n^{b_n-a_n} = N \Pi_1^{y_1} \Pi_2^{y_2} \dots \Pi_i^{y_i}$$

where N and y_1, y_2, \dots, y_i are pure numbers.

Therefore, we may replace the unknown function of the Q 's [Eq. (7.1)] by an unknown function of the Π 's.

$$\psi(\Pi_1, \Pi_2, \Pi_3, \dots, \Pi_i) = 0 \quad (7.5)$$

This conclusion means that a complete physical equation, expressed as a function of the physical quantities Q controlling the phenomenon, can be equally well expressed by a function of independent dimensionless coefficients or numerics formed from the Q 's. The statement that Eqs. (7.1), and (7.5) are equivalent constitutes the Π theorem.

7.16. Alternative Proof of the Π Theorem. The importance of the Π theorem in experimental fluid mechanics is considered to warrant a second proof, based on a postulate that may appeal to some readers as more nearly self-evident than the principle of dimensional homogeneity.

In order to measure any physical quantity, one must first choose a unit of measurement, the size of which depends solely on the whim of the observer. This arbitrariness of the unit size leads to the following postulate: Any equation describing a physical phenomenon can be so formulated that its validity is independent of the size of the units of the primary quantities. Such an equation is called a "complete physical equation." All the physical equations appearing in this book are assumed to be complete. A line of reasoning through which a physical equation can be simplified by virtue of its completeness is demonstrated in the example below.

A stationary sphere is immersed in a steady flow of incompressible real fluid. The sphere is far from any free surface, so that gravity has no effect on the flow pattern, the weight of every fluid particle being counterbalanced by the static buoyant force. Thus, one may assume that the independent variables determining the flow are the velocity of the undisturbed fluid V , the diameter of the sphere d , and the density and viscosity of the fluid ρ and μ . The force F , exerted on the sphere as a result of the fluid motion, will depend in some unknown way on only these four variables:

$$F = \phi(\rho, V, D, \mu) \quad (7.6)$$

Several changes of variable are now made, to put Eq. (7.6) in such form that it can be simplified through use of its assumed completeness. The immediate object of these changes is to make all the variables, except one, dimensionless in one of the primary quantities. This dimensional variable can then be deleted, as is shown below.

All the variables except ρ are first made dimensionless in mass. There is no necessity for this particular choice of density and mass, but it will be found convenient. Divide both sides of Eq. (7.6) by ρ , in order to change the dependent variable to F/ρ , which has dimensions $[MLT^{-2}/ML^{-3}] = [L^4T^{-2}]$.

$$\frac{F}{\rho} = \frac{\phi(\rho, V, d, \mu)}{\rho} = \phi_1(\rho, V, d, \mu)$$

The viscosity μ is the only independent variable (besides ρ) that has non-zero dimensions in mass. Divide μ by ρ to get a new independent variable μ/ρ , having dimensions $[ML^{-1}T^{-1}/ML^{-3}] = [L^2T^{-1}]$.

$$\frac{F}{\rho} = \phi_2\left(\rho, V, d, \frac{\mu}{\rho}\right) \quad (7.7)$$

This change from μ to μ/ρ is permissible, for ρ and μ are independent by assumption. One can therefore vary ρ without varying μ/ρ , simply by causing μ to change in proportion to ρ . The practical difficulties would be the same in either case: to keep either μ or μ/ρ constant while ρ were varied would, in general, require a change of fluid as well as a change of temperature.

These changes of variable have no effect on the completeness of the equation. The validity of Eq. (7.7) is therefore unaffected by a change in the size of the mass unit, say from slugs to grams. The value of F/ρ is unaffected by this change, so that the value of $\phi_2(\rho, V, d, \mu/\rho)$ must likewise be unaltered. The values of V , d , and μ/ρ remain the same, but the value of ρ will be different. Consequently, ϕ_2 can depend, not upon ρ , but only upon V , d , and μ/ρ . The density is therefore deleted, and

$$\frac{F}{\rho} = \phi_2\left(V, d, \frac{\mu}{\rho}\right)$$

A similar procedure gives all the remaining variables, except V , zero dimensions in time. Change F/ρ to $F/\rho V^2$, which has dimensions $[L^4T^{-2}/L^2T^{-2}] = [L^2]$; and change μ/ρ to $\mu/\rho V$, which has dimensions $[L^2T^{-1}/LT^{-1}] = [L]$.

$$\frac{F}{\rho V^2} = \phi_3\left(V, d, \frac{\mu}{\rho V}\right)$$

Deleting V by virtue of the completeness of the equation, one gets

$$\frac{F}{\rho V^2} = \phi_3\left(d, \frac{\mu}{\rho V}\right)$$

A third application of the same reasoning leads to

$$\frac{F}{\rho V^2 d^2} = \phi_4\left(d, \frac{\mu}{\rho V d}\right) = \phi_4\left(\frac{\mu}{\rho V d}\right) = \psi\left(\frac{\rho V d}{\mu}\right) \quad (7.8)$$

Equation (7.6), which involves four independent variables, has been simplified by purely dimensional reasoning to Eq. (7.8), which involves only one independent variable. It is clear that experimental data can be correlated more easily by means of Eq. (7.8) than Eq. (7.6).

Equation (7.8) is not the only form obtainable from Eq. (7.6). By operating with μ instead of ρ , or by combining the variables of Eq. (7.8) in an obvious way, one can also get

$$\frac{F}{\mu V d} = \psi_1 \left(\frac{\rho V d}{\mu} \right) \quad (7.9)$$

It is found, in most applications of these results, that Eq. (7.8) is preferable to Eq. (7.9), for $F/\rho V^2 d^2$ varies less than $F/\mu V d$ in the practical range of the independent variable $\rho V d/\mu$.

Consider now any complete physical equation relating a dependent variable to $n - 1$ independent variables:

$$Q_1 = \phi(Q_2, \dots, Q_n) \quad (7.10)$$

It is clear that the procedure used in the above example can be followed here, to yield a relationship among dimensionless products of the Q 's.

$$\Pi_1 = \psi(\Pi_2, \dots, \Pi_i) \quad (7.11)$$

where i is the number of dimensionless products, or Π 's. We thus arrive again at the Π theorem, this time by induction from an example.

To implement the Π theorem one must know how to determine the number of Π 's in any given problem. Furthermore, one should have a definite procedure for forming the Π 's, once their number has been determined. Finally, one should understand what freedom exists in the choice of alternative Π 's. These questions are considered in the following articles.

7.17. Determination of the Number of Π 's. Find by trial the largest number of Q 's that will not form a dimensionless product, and let this number be k . Usually k will be found to be the same as the number of primary quantities, which in mechanics is equal to three, M , L , and T .

Suppose now that one carries through the transformation of Eq. (7.10) to Eq. (7.11) by means of the procedure of the previous article, using (analogously to ρ , V , and d) any k of the Q 's that do not form a dimensionless product. Assume tentatively that the transformation is complete (*i.e.*, that all the products are dimensionless) after $k - 1$ steps. It is seen, however, that one of the products will contain precisely the k Q 's from which a Π cannot be made. From this contradiction it follows that at least k steps are necessary to complete the transformation. On the other hand, k steps are sufficient, for in this case every product contains $k + 1$ Q 's and is therefore dimensionless.

Referring again to the procedure of the previous article, one sees that the number of Π 's, i , is equal to the number of Q 's, n , minus the number

of steps. Since the number of steps has been shown to equal k , it follows that $i = n - k$. Equation (7.11) can thus be rewritten

$$\Pi_1 = \psi(\Pi_2, \Pi_3, \dots, \Pi_{n-k})$$

It may be observed for future reference, since the Π 's are formed by grouping the same k Q 's with each of the other Q 's in turn, that $n - k$ is not only the smallest number of Π 's which can suffice in Eq. (7.11) but also the largest number of independent Π 's which can be made from the Q 's.

In the majority of problems, one will find that k is equal to the number of primary quantities. It is easily shown that k cannot exceed this number, but it is possible for k to be less than the number of primary quantities, as in the following example:

Let a steel rod of length l and diameter d be maintained at a temperature T_1 at one end. Let the temperature of the surrounding air at a great distance from the rod be uniform and equal to T_0 . For steady conditions, one may assume that

$$q = \phi(T_1 - T_0, l, d, k_s, k_a) \quad (7.12)$$

where q is the rate of heat transfer per unit area at any point on the surface of the rod and k_s and k_a are the thermal conductivities of steel and air, respectively.

There are four primary quantities entering into the six variables of Eq. (7.12)—mass, length, time, and temperature. It is easily found, however, that the maximum number of variables which will not form a Π is only three. There are thus three Π 's in this case, rather than two. If $T_1 - T_0$, l , and k_s are chosen to play the role of ρ , V , and d in the example of the sphere, Eq. (7.12) becomes

$$\frac{ql}{k_a(T_1 - T_0)} = \psi\left(\frac{d}{l}, \frac{k_a}{k_s}\right)$$

7.18. Formulation of One Set of Π 's. The number of Π 's being known, the next step is to formulate explicitly a set of independent Π 's for the problem at hand. As already stated, one method is to combine k Q 's not forming a dimensionless product with each of the other Q 's in turn.

Referring again to the example of the sphere, we find by trial that ρ , V , and d do not form a dimensionless product and that therefore $k = 3$. The number of Q 's being $n = 5$, the number of Π 's is $n - k = 5 - 3 = 2$. One formulation of the Π 's, accordingly, is

$$\Pi_1 = \rho^{a_1} V^{b_1} d^{c_1} F$$

$$\Pi_2 = \rho^{a_2} V^{b_2} d^{c_2} \mu$$

The three unknown exponents in Π_1 are determined from the fact that Π_1 has zero dimensions in each of the three primary quantities M , L , and T . Thus,

$$[\Pi_1] = [M^0 L^0 T^0] = [(ML^{-3})^{a_1} (LT^{-1})^{b_1} (L)^{c_1} (MLT^{-2})]$$

$$[M^0 L^0 T^0] = [M^{a_1+1} L^{-3a_1+b_1+c_1+1} T^{-b_1-2}]$$

Since the unit sizes of M , L , and T can be chosen arbitrarily and independently of one another, this equation implies that

$$\begin{aligned} 0 &= a_1 + 1 \\ 0 &= -3a_1 + b_1 + c_1 + 1 \\ 0 &= -b_1 - 2 \end{aligned}$$

These three simultaneous equations in three unknowns have a unique solution, $a_1 = -1$, $b_1 = -2$, and $c_1 = -2$, so that $\Pi_1 = F/\rho V^2 d^2$. In the same way it can be shown that $\Pi_2 = \mu/\rho V d$. The result of the analysis can thus be expressed as $\Pi_1 = \psi_1(\Pi_2)$ or $(F/\rho V^2 d^2) = \psi_1(\mu/\rho V d) = \psi(\rho V d/\mu)$.

This method for determination of the exponents is rather lengthy in problems involving many Π 's, since the same process must be repeated for every Π . An alternative, quicker method is illustrated in the following example:

Suppose that the torque q which must be applied to a shaft to overcome the friction of a journal bearing depends only on the shaft diameter d ; the bearing length l ; the diametral clearance, or difference between bearing and shaft diameters, C ; the angular speed ω ; the oil viscosity μ ; the load on the shaft W ; and the volume rate of oil flow Q . Thus

$$q = \phi(d, l, C, \omega, \mu, W, Q)$$

It is readily found that d , ω , and W (for example) do not form a dimensionless product. Furthermore, there are only three primary quantities, M , L , and T . We conclude, therefore, that $k = 3$. Since $n = 8$, the number of Π 's will be $n - k = 8 - 3 = 5$. These may be formulated as

$$\begin{aligned} \Pi_1 &= \frac{q}{d^{a_1} \omega^{b_1} W^{c_1}} & \Pi_4 &= \frac{\mu}{d^{a_4} \omega^{b_4} W^{c_4}} \\ \Pi_2 &= \frac{l}{d^{a_2} \omega^{b_2} W^{c_2}} & \Pi_5 &= \frac{Q}{d^{a_5} \omega^{b_5} W^{c_5}} \\ \Pi_3 &= \frac{C}{d^{a_3} \omega^{b_3} W^{c_3}} \end{aligned}$$

To make Π_1 dimensionless, the product $d^{a_1} \omega^{b_1} W^{c_1}$ must have the dimensions of a torque; that is, $[d^{a_1} \omega^{b_1} W^{c_1}] = [ML^2 T^{-2}]$. To meet this requirement we write down the dimensions of d , ω , and W and solve for the dimensions of M , L , and T in terms of d , ω , and W .

$$\begin{aligned} [d] &= [L] & [\omega] &= [T^{-1}] & [W] &= [MLT^{-2}] \\ [L] &= [d] & [T] &= [\omega^{-1}] & [M] &= [Wd^{-1}\omega^{-2}] \end{aligned} \quad (7.13)$$

Using Eqs. (7.13), we find that

$$[ML^2 T^{-2}] = [(Wd^{-1}\omega^{-2})(d^2)(\omega^2)] = [Wd]$$

whence $\Pi_1 = q/Wd$.

For Π_2 , $[d^a \omega^b W^c] = [L]$. But, from Eqs. (7.13), $[L] = [d]$, so that $\Pi_2 = l/d$.

Similarly, it is found that $\Pi_3 = C/d$.

For Π_4 , we must have $[d^a \omega^b W^c] = [\mu] = [ML^{-1}T^{-1}]$. Equations (7.13) give $[ML^{-1}T^{-1}] = [(Wd^{-1}\omega^{-2})(d^{-1})(\omega)] = [Wd^{-2}\omega^{-1}]$, so that $\Pi_4 = \mu d^2 \omega / W$.

For Π_5 , $[d^a \omega^b W^c] = [Q] = [L^3 T^{-1}] = [d^3 \omega]$, so that $\Pi_5 = Q/d^3 \omega$.

The analysis thus leads to

$$\frac{q}{Wd} = \psi \left(\frac{l}{d}, \frac{C}{d}, \frac{\mu d^2 \omega}{W}, \frac{Q}{\omega d^3} \right)$$

This method is quick, because we determine Eqs. (7.13) but once, for Π_1 , and then use them for each of the remaining Π 's. It is unnecessary to find each exponent individually, as in the first method.

Equations (7.13) bring out the fact that d , ω , and W can themselves be used as primary quantities in this problem. It is thus seen that the greatest number of Q 's which will not form a Π is the same as the number of Q 's which can themselves be used as primary quantities in a given problem.

7.19. Formulation of Other Sets of Π 's. It has already been noted that $n - k$ is the greatest number of independent Π 's which can be made from n Q 's. If one set of $n - k$ independent Π 's be found by the methods of the preceding article, it is obvious that any other Π can be formed by multiplication of powers of two or more members of the given set. Thus all possible sets can be found from a single one. Denote by $\Pi'_1, \Pi'_2, \dots, \Pi'_{n-k}$ any such set of independent products.

Suppose that we have determined one nondimensional formulation of some problem,

$$\Pi_1 = \psi_1(\Pi_2, \Pi_3, \dots, \Pi_{n-k})$$

From this equation it follows that

$$\Pi_1 = \psi_2(\Pi_1^{a_1} \Pi_2^{a_2} \Pi_3^{a_3} \dots \Pi_{n-k}^{a_{n-k}}, \Pi_3, \Pi_4, \dots, \Pi_{n-k})$$

where $a_1, a_2, a_3, \dots, a_{n-k}$ are arbitrary exponents. Therefore,

$$\Pi_1 = \psi_2(\Pi'_2, \Pi_3, \Pi_4, \dots, \Pi_{n-k})$$

By progressing in this manner we can readily show that

$$\Pi'_1 = \psi'(\Pi'_2, \Pi'_3, \dots, \Pi'_{n-k})$$

Any set of $n - k$ independent Π products can thus be used in the nondimensional expression of a problem.

Dimensional analysis, per se, offers no clue as to which group of Π 's may be most convenient in a given problem. Aside from the obvious fact

that the dependent variable should be included in only one Π , it is necessary to rely upon previous experience and physical insight in the selection of a useful set of Π 's. Considerations of physical similitude, which are helpful in this connection, will be discussed in the next article.

7.20. Physical Similitude. Consider two systems, such as a model and its prototype, that are described by the same equation $\psi(\Pi_1, \Pi_2, \dots, \Pi_i) = 0$. Physical similitude is said to exist between two such systems if corresponding Π 's have the same value.

The identity of corresponding Π 's does not mean that corresponding Q 's must be equal but does require that they be related by scale ratios such that the Π 's which contain them are identical in the two systems.

In general, the model system and the prototype system that it represents will have corresponding quantities Q_1/Q'_1 , Q_2/Q'_2 , etc., in certain definite and constant ratios, or scales. The model scales for the several Q 's that control the phenomenon are, however, subject to the restriction of the Π theorem. These restrictions can be stated in the form of rules.

1. Provided only that they do not by themselves form a dimensionless product, k of the quantities may have any arbitrary scale ratios between the two systems.

2. The scale ratio for any of the remaining quantities is determined by the fact that the Π which contains it in the model system must equal the corresponding Π in the prototype system.

As a consequence, solid boundaries that control the flow of a fluid will be geometrically similar, and a model must be geometrically similar to its prototype. Corresponding lengths on model and prototype are related by a constant scale ratio. The locations of corresponding points in the two fields of flow can be defined as x/L , y/L , z/L and x'/L' , y'/L' , z'/L' , where L and L' are typical lengths of model and prototype. Then $x/x' = y/y' = z/z' = L/L'$. Geometrical similitude is characterized by a single and uniform scale of enlargement.

Since there is a constant scale ratio for each quantity, it follows that at all pairs of corresponding points the components of velocity bear a constant ratio to each other. Hence the resultant velocities at corresponding points are parallel, and the streamlines are geometrically similar. To transform one flow pattern to the other we need to know only the linear scale of enlargement from model to prototype.

Knowing the velocities at various points in the flow about the model, we can predict the velocities at corresponding points in the flow about the prototype by applying the proper scale of enlargement. This scale of enlargement for velocity may, for convenience, be taken as the ratio of the speeds of advance of model and prototype, V/V' .

Similar considerations lead to the conclusion that, for compressible flow, the densities at corresponding points have a constant ratio equal to

the ratio of the densities of undisturbed fluid in the two systems, ρ/ρ' . For incompressible flow, the densities are in this same ratio but are constant everywhere in each system.

In the preceding discussion, steady flow is implied. If the flow is changing with time, particles occupy corresponding positions and have corresponding velocities at corresponding times. The flow patterns will be geometrically similar only at corresponding times.

The particular form of physical similitude for which the corresponding forces have a single scale ratio is called "dynamical similitude." If there be also a single scale of temperatures at corresponding points, we have thermal similitude. For each case, geometrical similitude is a prerequisite.

The requirement of a single scale ratio for forces shows that the polygons of force on corresponding elements in the two systems are geometrically similar.

7.21. Conditions for Dynamical Similitude. In the general case of flow of a real fluid, the forces acting on an element of fluid are those due to pressure, friction, gravity, and inertia. d'Alembert's principle shows that the vector sum of these forces is zero.

$$F_p + F_f + F_g + F_i = 0$$

Similarity of corresponding force polygons in two flows is obtained if

$$F_f/F'_f = F_i/F'_i \quad \text{and} \quad F_g/F'_g = F_i/F'_i \quad (7.14)$$

since the d'Alembert equation will then ensure that $F_p/F'_p = F_i/F'_i$.

On the other hand, the criterion for dynamical similitude that is obtained directly from the Π theorem is developed as follows, for an incompressible fluid.

Let us represent the quantities controlling the fluid motion by ρ , L , V , μ , and g , where L is any characteristic length, V is the relative fluid velocity at a distance from the object disturbing the flow, ρ and μ are the density and viscosity of the fluid, and g is the acceleration of gravity. Let F represent any force, such as the lift of a wing or the resistance of a ship, whose value is desired in terms of the independent variables. Then,

$$F = f(\rho, L, V, \mu, g)$$

From the Π theorem,

$$\Pi_1 = \phi(\Pi_2, \Pi_3) \quad (7.15)$$

Since inertia forces usually predominate, it has become conventional to select the particular set of Π products beginning with a force coefficient that is independent of μ and g . Thus,

$$\Pi_1 = \rho^a L^b V^c F = \frac{F}{\rho L^2 V^2} \quad (\text{Newtonian force coefficient})$$

$$\Pi_2 = \rho^{\alpha_2} L^{\beta_2} V^{\gamma_2} \mu^{-1} = \frac{\rho V L}{\mu} \quad (\text{Reynolds number})$$

$$\Pi_3 = \rho^{\alpha_3} L^{\beta_3} V^{\gamma_3} g^{-1} = \frac{V^2}{Lg} \quad (\text{Froude number})$$

The criterion for dynamical similitude that is yielded directly from the definition at the beginning of Art. 7.20 is $\Pi_2 = \Pi'_2$ and $\Pi_3 = \Pi'_3$, or

$$\rho V L / \mu = \rho' V' L' / \mu' \quad \text{and} \quad V^2 / L g = V'^2 / L' g \quad (7.16)$$

since Eq. (7.15) then ensures that $\Pi_1 = \Pi'_1$.

From the discussion in Art. 7.20, Eqs. (7.14) and (7.16) should be equivalent. Proof of equivalence, which follows below, will shed light on the physical significance of the Reynolds and Froude numbers.

Consider an element of fluid of sides dx, dy, dz , with the x axis parallel to the streamline. The volume of the element is $\mathcal{V} = dx dy dz$. The steady velocity at the element is in the x direction and will be denoted by u .

The inertia force on this element is by definition equal to the negative of the product of mass and acceleration,

$$-F_i = \rho \mathcal{V} \frac{du}{dt} = \rho \mathcal{V} u \frac{\partial u}{\partial x}$$

since, for steady motion, $du/dt = u(\partial u/\partial x)$. The ratio of corresponding inertia forces for two systems will be

$$F_i/F'_i = \frac{\rho \mathcal{V} u (\partial u/\partial x)}{\rho' \mathcal{V}' u' (\partial u'/\partial x')} = \frac{\rho L^2 V^2}{\rho' L'^2 V'^2}$$

because corresponding lengths and velocities have the ratios L/L' and V/V' , respectively.

In Art. 1.4 the friction force F acting on the oil film in a concentric bearing was stated to be $F = \mu(V/h)A$, where V is the difference in velocity between the two sides of the film, h is the film thickness, and A is the area of the film. Experiments show that in more complicated flow patterns the friction force on a small fluid surface, such as $dx dz$, is given by a formula of this same form, but with V/h replaced by an expression having at most two terms, each of the type $\partial u/\partial y$. Since we are interested only in the ratio of the friction forces acting on corresponding elements of fluid, we may write

$$\frac{F_f}{F'_f} = \frac{\mu (\partial u/\partial y) dx dz}{\mu' (\partial u'/\partial y') dx' dz'} = \frac{\mu V L}{\mu' V' L'}$$

Also, the ratio of corresponding gravity forces is seen to be

$$\frac{F_g}{F'_g} = \frac{\rho g \mathcal{V}}{\rho' g' \mathcal{V}'} = \frac{\rho g L^3}{\rho' g' L'^3}$$

Substitution of these values into Eqs. (7.14) shows that they are equivalent to Eqs. (7.16).

We see in addition that

$$\frac{F_i/F_f}{F'_i/F'_f} = \frac{\rho VL/\mu}{\rho' V'L'/\mu'} \quad \text{and} \quad \frac{F_i/F_g}{F'_i/F'_g} = \frac{V^2/Lg}{V'^2/L'g}$$

The Reynolds number is thus a measure of the ratio of inertia to friction ratio at any point in the flow, while the Froude number measures the force of inertia to gravity force.

7.22. Friction Forces. The coefficient $\Pi_2 = \rho VL/\mu$ is known as the Reynolds number, in honor of Osborne Reynolds, who first discovered its importance in his classical study of the flow of viscous fluid through pipes.

In order to conduct experiments with a small pipe of diameter D' to predict the flow through a large pipe of diameter D we must arrange to have $\rho VD/\mu = \rho' V'D'/\mu'$. For the same fluid the velocity in the small pipe must be higher than the velocity specified for the large pipe in the ratio D/D' . If this were impracticable, it would be permissible to use some other fluid of much lower viscosity for the model experiment. By the use of the Reynolds number, experiments on smooth pipes (geometrically similar) with various liquids and gases have been reduced to a single curve of $\Pi_1 = f(\Pi_2)$, or

$$\frac{F}{\rho D^2 V^2} = f(R)$$

where F is the resistance to flow and R is the Reynolds number.

It is of practical interest to observe further that for an experiment with a model airplane in air $\rho/\rho' = \mu/\mu' = 1$, $VL = V'L'$. This means that a 5-ft model of a 50-ft wing, expected to operate at 100 mph, should be tested in a wind tunnel at 1,000 mph if frictional effects are to be truly represented. This is clearly impracticable; but if the wind-tunnel air is compressed to 5 atm, the test velocity required for constant R is reduced to 200 mph.

The Reynolds number is frequently written in the form $R = VL/\nu$, where $\nu = \mu/\rho$ is called the "kinematic viscosity" of the fluid. Although water is some 800 times as dense as air, the viscosity of air at ordinary temperatures is relatively high and its kinematic viscosity is some 14 times as great as that of water.

A constant relation between inertia and frictional forces in a given set of experiments is seen to be preserved by constancy of the Reynolds number, but other considerations determine the relative importance of friction in practical cases. Where experiments show that forces vary as $\rho V^2 L^2$, it is permissible to neglect the effect of the Reynolds number. For example, the resistance of a thin plate held normal to a flow is almost entirely due to inertia forces, while the same plate held edgewise to the

flow experiences a frictional force due to fluid shear over its wetted surface. In the former position the resistance is independent of the Reynolds number, while in the latter it is not.

The performance of propellers and hydraulic turbines and pumps is found to be mainly dependent on inertia forces. This fact is not unexpected because of the great mass of fluid flowing through the machine and the relatively small wetted surface.

The trajectory of a heavy bomb falling through air or water is largely determined by inertia forces because of the high ratio of mass to surface. On the other hand, the settling of fog particles through air or of sediment through water is controlled by frictional forces because of the low ratio of mass to surface of the individual particles.

7.23. Gravity Forces. Where surface waves are formed, gravity forces are involved, for the weight of an element of fluid near the free surface is not completely counterbalanced by buoyancy, as for one far below the surface. As we have previously seen, the coefficient $\Pi_3 = V^2/Lg$ measures the ratio of inertia to gravity force. This coefficient is known as the Froude number, from the law of comparison discovered by William Froude in 1870 in connection with his pioneering experiments with ship models.

7.24. Compressibility. Similitude between two flows of compressible fluid implies in general not only dynamic similarity but also thermal similarity. Extended consideration of thermal effects is avoided if pressure may be considered a function only of density. This assumption is usually permissible in high-speed flows of technical importance. In such flows one may assume that the changes in density are adiabatic and are uninfluenced by friction (isentropic). It is known that under these conditions there is a relation between pressure and density of the form $p/\rho^k = \text{constant}$, where the exponent k is constant for a given fluid.

If a small mass of fluid, with initial volume equal to \mathfrak{V} , is compressed isentropically, the first law of thermodynamics shows that its increase in intrinsic energy dU is equal to the work done by the pressure in decreasing the volume,

$$\begin{aligned} 0 &= p \, d\mathfrak{V} + dU \\ dU &= -p \, d\mathfrak{V} \end{aligned}$$

Consider now the change in intrinsic energy dU and the accompanying change in kinetic energy $d(KE)$ as a small fluid mass moves an infinitesimal distance in a high-speed flow. If similarity is to be preserved in a model of this flow, it is necessary that the ratio $dU'/d(KE)'$ for the corresponding mass moving between corresponding points in the model flow be equal to $dU/d(KE)$. This condition may be written

$$\frac{d(KE)}{d(KE)'} = \frac{dU}{dU'} \quad (7.17)$$

Equation (7.17) is a further restriction on the model flow, additional to those given by Eqs. (7.14) or (7.16).

Alternatively, the conditions for similitude in case of compressibility may be developed from the Π theorem if the independent variables controlling the compressibility phenomena are correctly chosen. It is customary to assume that the sound velocity in the undisturbed fluid C is the only variable that need be considered in addition to ρ , L , V , μ , and g . The primary quantities of mechanics thus suffice, and four Π products are indicated. Forming Π_4 in the same way as above, we find that $\Pi_4 = \rho^a L^b V^c C^{-1} = V/C$, Mach number. If the assumption regarding C is correct, we should expect to find that Eq. (7.17) is reducible to

$$\frac{V}{C} = \frac{V'}{C'} \quad (7.18)$$

If this reduction is possible, it will clarify the physical significance of the Mach number. The relationship between Eqs. (7.17) and (7.18) will now be developed.

The change in kinetic energy of a small mass $\rho\mathfrak{U}$ as its velocity changes from u to $u + du$ will be

$$d(KE) = \rho\mathfrak{U} \left[\frac{(u + du)^2}{2} - \frac{u^2}{2} \right] = \rho\mathfrak{U} u \, du$$

The ratio of corresponding kinetic-energy changes will be

$$\frac{d(KE)}{d(KE)'} = \frac{\rho\mathfrak{U} u \, du}{\rho'\mathfrak{U}' u' \, du'} = \frac{\rho L^3 V^2}{\rho' L'^3 V'^2}$$

To evaluate the ratio of intrinsic-energy changes we must develop the relations between the sound velocity, pressure, density, and fluid velocity. Consider a small plane pressure wave propagating from right to left with

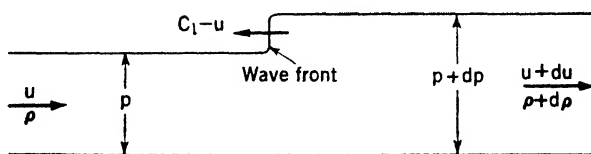


FIG. 7.1.

a velocity C_l relative to the fluid in front of it. If the velocity u of this fluid is toward the right, the absolute speed of the wave will be $C_l - u$ toward the left, as shown in Fig. 7.1. Conditions in the fluid will appear steady to an observer moving with the velocity of the wave front. From this point of view the velocities will be as indicated in Fig. 7.2.

For a stream tube of unit cross-sectional area the equation of continuity yields

$$\begin{aligned}\rho C_1 &= (\rho + d\rho)(C_1 + du) \\ C_1 d\rho + \rho du &= 0\end{aligned}\quad (7.19)$$

Likewise, the momentum equation gives

$$p - (p + dp) = -\rho C_1^2 + (\rho + d\rho)(C_1^2 + 2C_1 du + du^2)$$

whence, combining with Eq. (7.19), we get

$$\begin{aligned}dp &= -2\rho C_1 du - C_1^2 d\rho = 2C_1^2 d\rho - C_1^2 d\rho = C_1^2 d\rho \\ \frac{dp}{d\rho} &= C_1^2\end{aligned}\quad (7.20)$$

From the assumed relation between p and ρ , namely $p/\rho^k = \text{constant}$,

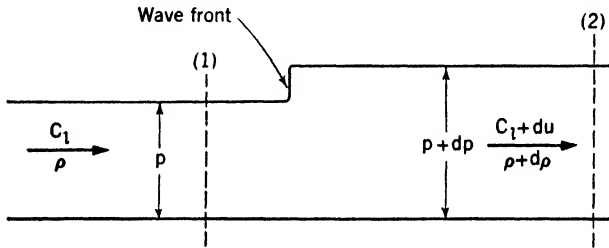


FIG. 7.2.

we find by differentiation that $dp/d\rho = kp/\rho$. Hence, from Eq. (7.20),

$$C_1^2 = \frac{kp}{\rho} \quad (7.21)$$

The change in intrinsic energy of a mass $\rho \mathcal{V}$ has been shown above to be

$$dU = -p d\mathcal{V}$$

But, since the mass $\rho \mathcal{V}$ is constant, its differential is equal to zero, or

$$-d\mathcal{V} = \mathcal{V} \frac{d\rho}{\rho}$$

Therefore, from Eqs. (7.19) and (7.21),

$$dU = p \frac{d\rho}{\rho} \mathcal{V} = -\frac{\rho C_1^2}{k} \frac{du}{C_1} \mathcal{V} = -\frac{\rho C_1}{k} \mathcal{V} du$$

Letting p_0 , ρ_0 , and C represent values in the undisturbed stream, we find that

$$C_1^2 = C^2 \frac{p}{p_0} \frac{\rho_0}{\rho} = C^2 \left(\frac{\rho}{\rho_0} \right)^{k-1}$$

whence

$$dU = -\rho \mathfrak{U} du \frac{C}{k} \left(\frac{\rho}{\rho_0} \right)^{(k-1)/2}$$

and

$$\begin{aligned} \frac{dU}{dU'} &= \frac{\rho \mathfrak{U} du C}{\rho' \mathfrak{U}' du' C'} \left(\frac{\rho}{\rho_0} \right)^{(k-1)/2} \left(\frac{\rho_0'}{\rho'} \right)^{(k'-1)/2} \frac{k'}{k} \\ &= \frac{\rho L^3 VC}{\rho' L'^3 V' C'} \left(\frac{\rho}{\rho_0} \right)^{(k-1)/2} \left(\frac{\rho_0'}{\rho'} \right)^{(k'-1)/2} \frac{k'}{k} \end{aligned}$$

Equating these expressions for the kinetic-energy ratio and intrinsic-energy ratio, in accordance with Eq. (7.17), we get

$$\frac{V}{C} = \frac{V'}{C'} \left(\frac{\rho}{\rho_0} \right)^{(k-1)/2} \left(\frac{\rho_0'}{\rho'} \right)^{(k'-1)/2} \frac{k'}{k} \quad (7.22)$$

It is seen that Eqs. (7.17) and (7.18) are equivalent only if $k = k'$.

Furthermore, if this condition is fulfilled,

$$\frac{d(KE)/dU}{d(KE')/dU'} = \frac{V/C}{V'/C'}$$

and the Mach number is a measure of the ratio of kinetic-energy change to intrinsic-energy change, just as the Reynolds or Froude number measures the ratio of certain forces.

The nondimensional quantity k should be included in the general equation as an additional Π . This example illustrates that dimensional analysis is not infallible; if a variable is omitted, the Π theorem cannot indicate the omission unless there are too few quantities to form even one Π product. Ordinarily, k is left out of consideration because model experiments on high-speed flow are usually performed with the same fluid as for the prototype. It is clear that k is important, for it controls the relation between pressure and density. The relation between compressible flows having different values of k may be likened to that between the motions of a linear and a nonlinear spring.

In practice, compressibility is found to be important for high-speed phenomena having Mach numbers exceeding 0.7. Examples are ballistics, rotary compressors, propellers, and high-speed airplanes.

7.25. Special Forms of the Dimensional Equation for Fluid Motion.

From the preceding discussion, it will be seen that it is impractical to arrange model experiments to preserve a constant Reynolds number, Froude number, and Mach number. The experimenter, however, is helped by the fact that in practical cases some of the quantities may be neglected.

For example, airplane-model experiments may omit consideration of the Froude number since no free liquid surface is involved and for moderate speeds may ignore the Mach number. However, the drag does involve the Reynolds number, since flight Reynolds numbers are very large.

Efforts are made to test airplane models at as high a Reynolds number as possible by use of compressed air.

For the lift of airplane wings, thrust of propellers, and the delivery of pumps and fans it is found that the effect of friction is much less important than the effect of inertia, and consequently the Reynolds number can be ignored for a good approximation.

The general dimensional equation is therefore not used in complete form but breaks down into

$$\frac{F}{\rho L^2 V^2} = \Pi_1 = \text{constant}$$

where inertia predominates;

$$\Pi_1 = \phi \left(\frac{\rho V L}{\mu} \right)$$

where friction is appreciable;

$$\Pi_1 = \phi \left(\frac{\rho V L}{\mu}, \frac{V^2}{Lg} \right)$$

for ship models;

$$\Pi_1 = \phi \left(\frac{V}{C} \right)$$

for high-speed flows and ballistics. It is to be noted that ship-model experiments require both the Reynolds number and the Froude number to be constant. This, however, is impossible to accomplish.

The naval architect subtracts from the observed model resistance that part due to skin friction, as computed from tests of smooth plates moved edgewise through the water at the Reynolds number of the model test. The remaining, or "residual," resistance F_1 is considered to include the "wave-making" and pressure resistance of the model and to follow Froude's law

$$\frac{F_1}{\rho L^2 V^2} = \phi \left(\frac{V^2}{Lg} \right)$$

When the model is towed at the same value of the Froude number as the ship, or at the "corresponding speed" (proportional to the square root of the length), the ship's residual resistance can be scaled up from the model by the relation

$$\frac{F_1}{F'_1} = \frac{L^2 V^2}{L'^2 V'^2}$$

where primed symbols refer to the model and unprimed ones to the prototype. At this speed the pattern of surface waves made by the model is geometrically similar to the pattern of surface waves created by the ship. Naval architects photograph the wave patterns made by models run at corresponding speeds in order to judge the effect of changes in design.

A 20-ft model of a 500-ft ship, expected to steam at 25 knots, should be towed at a corresponding speed of 5 knots to hold the Froude number constant. Since g in the Froude number is practically constant, naval architects ignore it and use simply the "speed-length ratio" V/\sqrt{L} .

Flying boats that do not begin to plane until sufficient speed has been reached must pass through a critical, or "hump," speed where the wave-making resistance is a maximum. This critical speed is a function of the Froude number and can be predicted from model tests. It cannot be computed from first principles.

7.26. Conclusions. The method of dimensional analysis indicates that in experimental and test work the quantities involved may be grouped into a definite number of independent dimensionless coefficients and the results of observation expressed in terms of such coefficients.

For model experiments designed to represent the operation of a prototype, it is necessary to have some of these coefficients numerically equal for model and prototype.

There appear to be three main uses for dimensional analysis.

1. To obtain comprehensive engineering data from model experiments where only a few of the variables can be changed.
2. To state the conditions, in terms of a few nondimensional coefficients, under which experimental results may be generally applicable.
3. To check the completeness or validity of a physical relation found by experiment or deduced by analysis.

Dimensional analysis is primarily the tool of the designer and the test engineer. Its applications to naval architecture by Froude, to aeronautics by Rayleigh, and more recently to heat transfer, lubrication, and hydraulics have revolutionized these branches of engineering. It is unnecessary to wait for the analytical solution of a problem if a controlled experiment can be arranged to satisfy the conditions of similitude.

SELECTED BIBLIOGRAPHY

1. BRIDGMAN, P. W.: "Dimensional Analysis," 2d ed., Yale University Press, New Haven, 1931.
2. BUCKINGHAM, E.: On Physically Similar Systems, *Phys. Rev.*, vol. 4, ser. 2, pp. 345-376, 1914.
3. BUCKINGHAM, E.: Model Experiments and the Form of Empirical Equations, *Trans. Am. Soc. Mech. Engrs.*, vol. 37, pp. 263-296, 1915.
4. GIBSON, A. H.: The Principles of Dynamical Similarity, *Engineering* (London), vol. 117, pp. 325-327, 357-359, 391-393, 422-423, 1924.
5. RAYLEIGH, LORD: The Principle of Similitude, *Nature*, vol. 95, pp. 66-68, 1915.
6. WEBER, M.: Das allgemeine Aehnlichkeitsprinzip der Physik, *Jahrb. Schiffbautechn. Ges.*, vol. 31, pp. 274-354, 1930.

CHAPTER VIII

INCOMPRESSIBLE FLOW IN CLOSED CONDUITS

Study of fluid flow in pipes not only has yielded information of practical value to the designer of pipe lines but also has broadened our basic knowledge of the mechanism of fluid motion in general.

It has long been known that two distinct kinds of pipe flow occur. The simpler of these, laminar flow, is characterized by motion of the fluid in layers, or laminae, parallel to the pipe axis. The path followed by any small mass of fluid is a straight line. Conditions favorable for laminar flow are high viscosity μ , low density ρ , low mean velocity V , and small pipe diameter D .

Laminar flow in a tube of circular cross section was studied experimentally by Hagen, who published his results in 1839, and independently by Poiseuille, whose work was published between 1840 and 1846. Each deduced from his tests that the volume rate of flow is directly proportional to the pressure drop and to the fourth power of the radius and inversely proportional to the tube length. On this account, the equation relating these quantities to the viscosity is called the "Hagen-Poiseuille law."

In the majority of engineering applications the flow is not laminar but turbulent. In this type of flow only the average motion of the fluid is parallel to the tube axis. The movement of any small fluid mass is highly irregular, random fluctuations being superposed on the average velocity. In a smooth pipe, however, the transverse fluctuations necessarily approach zero in the vicinity of the wall, so that even in a highly turbulent flow a thin laminar film exists next to the wall.

A laminar flow becomes unstable and tends to become turbulent as the mean velocity is increased, other things being equal. Osborne Reynolds, in 1883, showed that the transition from laminar to turbulent motion depends not only on velocity but more generally on the dimensionless quantity $\rho VD/\mu$, which is now known as the Reynolds number R . He showed that if R is below the critical value of about 2,000 the flow is laminar, while at higher values the flow tends to become turbulent. Reynolds also laid the groundwork for the present statistical theory of turbulence.

The twentieth-century developments in our knowledge of pipe flow are in large measure due to Prandtl and von Kármán, and their students. These men, by a remarkable combination of physical intuition, experimental skill, and analytical ability, have developed greatly the theory of turbulent flow in both smooth and rough pipes.

8.1. Entrance and Fully Developed Flow Regions. If an incompressible fluid flows steadily through a horizontal pipe of uniform diameter,

the velocity distribution over a cross section will be found to vary with distance from the entrance as shown in Fig. 8.1. In the tank the velocity is negligible, but in the rounded entrance it increases gradually to give the practically uniform distribution shown at section *a*. At the wall the

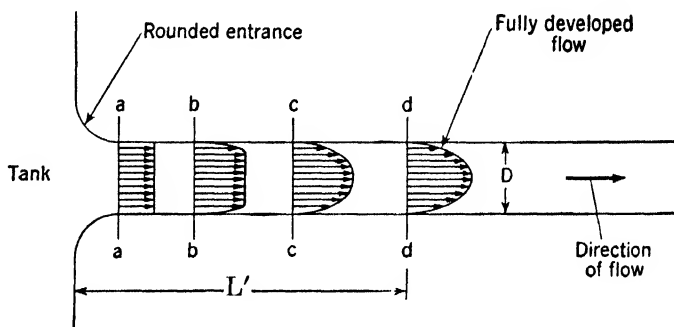


FIG. 8.1. — Development of flow in the entrance length of a pipe.

velocity is zero on account of the viscosity, but the layer of fluid affected by friction is still very thin at *a*. This boundary layer grows as the fluid moves along the tube. Somewhat upstream from section *c* its thickness is seen to equal the radius of the tube. The velocity distribution approaches the fully developed form asymptotically, but at section *d*, a distance L' from the entrance, the maximum velocity has reached 99 per cent of the ultimate value. This distance is called the “length of transition.”

It is found that in laminar flow the ratio L'/D is a function of R . The theoretical formula

$$\frac{L'}{D} = 0.058 \frac{\rho V D}{\mu} = 0.058 R \quad (8.1)$$

due to Langhaar, agrees well with observation. For $R = 1,000$, L'/D is seen to be about 58.

In a turbulent flow it is found that L'/D is less dependent on R than in laminar flow. Experiments by Nikuradse show that the value of L'/D lies between 25 and 40.

The pressure distribution over a cross section in the entrance length is not uniform, since fluid is being moved toward the center of the pipe.

In fully developed laminar flow the pressure varies hydrostatically over any cross section; in fully developed turbulent flow there is also some variation, but it may not be hydrostatic. In either case it can be shown that a correct result is obtained for the axial force on a cross section by assuming the pressure to be constant over the section. It will be convenient to define the symbol p^* as

$$p^* = p + \rho g z \quad (8.2)$$

where z is the elevation of the pipe axis above an arbitrary datum.

In a fully developed flow the momentum law yields a relationship between p^* and the apparent shearing stress acting on a cylindrical surface concentric with the axis. In Fig. 8.2 are shown the external forces acting on the fluid within a cylindrical control surface of cross-sectional area πr^2 and length dx . The apparent shearing stress τ_{app} acting on the lateral surface may be partly real and partly fictitious. The real part is due to

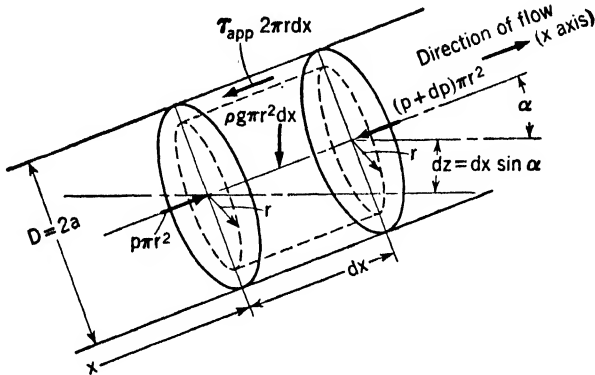


FIG. 8.2. — Forces on a cylindrical mass of fluid.

the viscous stresses exerted by the adjacent fluid, and the fictitious part is actually the net efflux of x momentum per unit area through the lateral surface. Such an efflux will occur only because of turbulent fluctuations; there will be none in a laminar flow. Since the flow is fully developed, there is no net momentum flux through the ends of the cylinder. The momentum law gives

$$p\pi r^2 - (p + dp)\pi r^2 - \rho g dx \sin \alpha \pi r^2 - 2\tau_{app}\pi r dx = 0$$

or

$$-(dp + \rho g dz)\pi r^2 = -dp^*\pi r^2 = 2\tau_{app}\pi r dx$$

or

$$-\frac{dp^*}{dx} \frac{r}{2} = \tau_{app} \quad (8.3)$$

Since the flow is fully developed, τ_{app} is independent of x and Eq. (8.3) can be integrated with respect to x , say from $x = x_1$ to $x = x_2 = x_1 + L$.

$$-(p_2^* - p_1^*) \frac{r}{2} = \tau_{app} (x_2 - x_1) = \tau_{app} L$$

or

$$\frac{p_1^* - p_2^*}{L} \frac{r}{2} = \tau_{app} \quad (8.4)$$

If we choose $r = a$, the radius of the tube, τ_{app} becomes equal to the shear stress at the wall, τ_0 .

$$\frac{p_1^* - p_2^*}{L} \frac{a}{2} = \frac{p_1^* - p_2^*}{L} \frac{D}{4} = \tau_0 \quad (8.5)$$

It is to be noted that all the quantities on the left side of Eq. (8.5) can be readily measured. The equation thus provides a simple means of finding the wall shear stress.

By combining Eqs. (8.4) and (8.5) we find that the apparent shearing stress varies linearly from zero at the pipe center to a maximum at the wall.

$$\tau_{app} = \frac{r}{a} \tau_0 \quad (8.6)$$

8.2. Friction Factor. The motion of a particle of fluid along the tube is independent of gravity because the fluid is incompressible and there is no free surface. Under these conditions the weight of each particle is exactly counterbalanced by the static buoyant force exerted on it by the surroundings. The flow pattern is therefore independent of g , and we may assume for a fully developed flow that τ_0 is a function only of V , D , ρ , μ , and the wall roughness (which is assumed to be uniform everywhere).

Application of the Π theorem to the equation $\tau_0 = \phi_1(V, D, \rho, \mu, \text{roughness})$ shows that we may write

$$\frac{\tau_0}{\rho V^2} = \phi_2\left(\frac{\rho V D}{\mu}, \text{roughness}\right) \quad (8.7)$$

Here ϕ_1 and ϕ_2 represent unknown functions, and the roughness is assumed to be dimensionless. The roughness can be expressed, for example, by a sequence of ratios of various lengths to the diameter D .

Equation (8.7) forms the basis on which pipe-flow measurements have been correlated. So important is it that the dimensionless ratio $\tau_0/\rho V^2$ has been given a name—the friction factor, denoted by f . Usually a numerical coefficient, 2 or 8, is included in the definition of the friction factor. In this text we shall define f as

$$f = \frac{8\tau_0}{\rho V^2} \quad (8.8)$$

The reason for choosing 8 is seen if τ_0 is eliminated from Eqs. (8.5) and (8.8).

$$f = \frac{p_1^* - p_2^*}{L} D \frac{1}{(\rho/2)V^2} \quad (8.9)$$

Equation (8.9) gives f in terms of quantities that are readily measured and contains the familiar factor $(\rho/2)V^2$. It is more convenient for general use in pipe-flow computations than is Eq. (8.8), but the latter should be regarded as defining f , since it shows the intimate connection between the friction factor and the frictional stress on the tube wall.

Equation (8.7) may be written as

$$f = \phi(R, \text{roughness}) \quad (8.10)$$

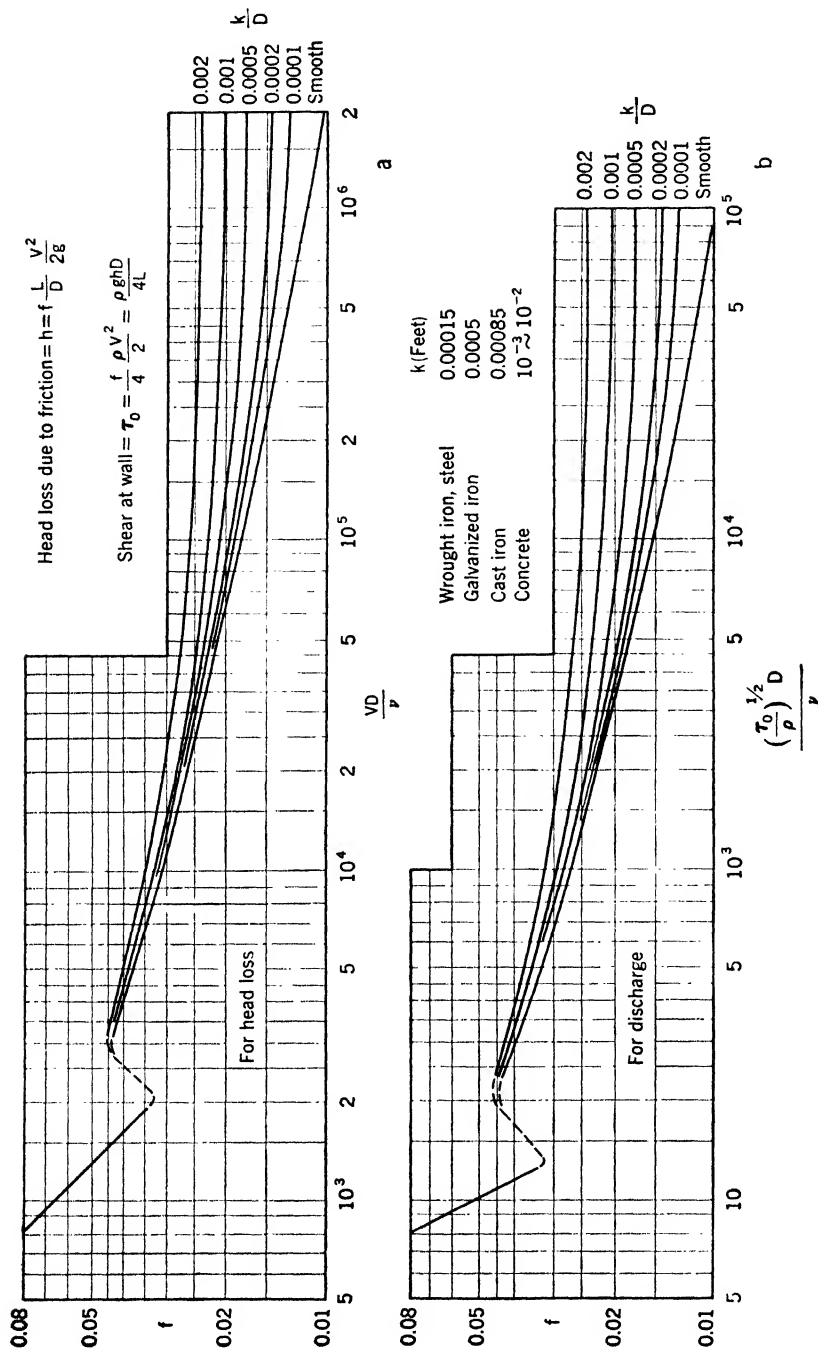


FIG. 8.3. — Relation between friction factor and other dimensionless parameters for pipes having various values of relative roughness. (After Moody, reference 10, by permission of American Society of Mechanical Engineers.)

where R is the Reynolds number $\rho VD/\mu$. This equation has been verified experimentally by many workers. Figure 8.3a shows graphically the form of the relationship for both laminar and turbulent conditions and for smooth tubes and new commercial pipe of various relative roughnesses. It is seen that moderate wall roughness has no effect on f if the flow is

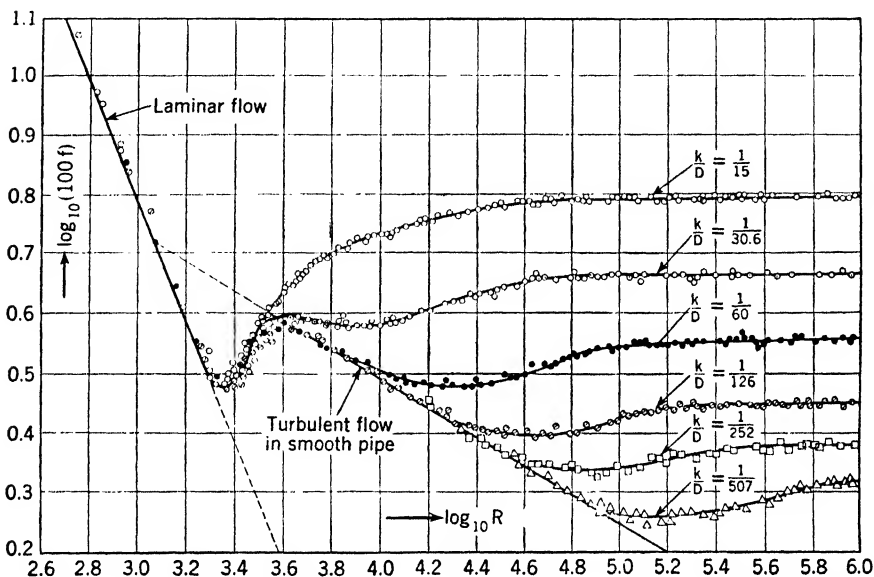


FIG. 8.4. — Relation between friction factor and Reynolds number for artificially roughened pipes.

laminar but has considerable influence for turbulent flow. The curve for laminar flow and the curve for turbulent flow in a smooth pipe are plotted from theoretical equations that will be developed later. The laminar theory is complete, but the turbulent theory requires the experimental determination of several constants whose value the theory cannot yet predict.

Nikuradse [12]* made tests on pipe artificially roughened by a coating of sand grains of uniform size. His results for different values of the relative roughness, k/a , the ratio of sand-grain diameter to pipe radius, are given in Fig. 8.4. In these tests the roughness was adequately described by a single ratio, k/a , as shown by the absence of scatter in the experimental points. The roughness was completely uniform and quite unlike that for commercial pipes.

In Fig. 8.3a are shown curves for commercial pipe of various relative roughnesses. These curves resemble those for the sand-coated tubes of Fig. 8.4, in that they become horizontal at sufficiently large values of R .

* Numbers in [] refer to the bibliography at the end of the chapter.

The value of k/a assigned to any kind of commercial pipe is obtained by a direct comparison of the horizontal parts of the curves in Fig. 8.3a with the horizontal parts of Nikuradse's curves.

In the intermediate region in which f depends on both R and k/a the curves for commercial and sand-coated pipes are very different, and one might question whether the roughness of the former can be adequately described by a single parameter k/a . The justification for this procedure is given below in Art. 8.11.

The alternative form of plot shown in Fig. 8.3b can be justified either by Eq. (8.7) and the Π theorem or by suitable intermultiplication of the variables of Eq. (8.10). This plot is useful in case the wall shearing stress (or head loss) is known and the velocity is not.

In the solution of many pipe-flow problems the steady-flow energy equation is useful. In case the fluid is incompressible, as is assumed throughout this chapter, the energy equation [Eq. (5.10)] takes the form

$$\mathcal{W}_s + \frac{p_2 - p_1}{\rho} + \frac{V_2^2 - V_1^2}{2} + g(z_2 - z_1) + gH_{l,2} = 0$$

where $H_{l,2}$ stands for $(u_2 - u_1 - g_{1,2})/g$, the energy dissipated per unit weight of flowing fluid.

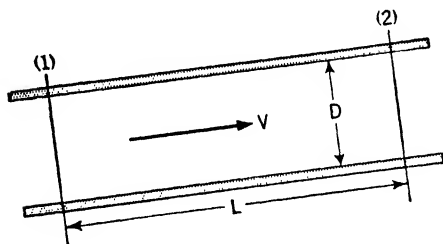


FIG. 8.5.

If sections 1 and 2 are taken in the fully developed flow region of a pipe (Fig. 8.5) $\mathcal{W}_s = 0$ and $V_2 = V_1 = V$, so that

$$\frac{p_2 - p_1}{\rho g} + z_2 - z_1 + H_{l,2} = 0$$

or

$$\frac{p_1^* - p_2^*}{\rho g} = H_{l,2} \quad (8.11)$$

Combination of Eqs. (8.9) and (8.11) gives the relation between the friction factor and the energy dissipated by friction in the length L of straight pipe.

$$H_{l,2} = f \frac{L}{D} \frac{V^2}{2g} \quad (8.12)$$

In complicated problems involving other losses besides those in a straight pipe only that part of the total loss which is due to pipe friction is given by Eq. (8.12). The other losses are added to this part to obtain the total.

8.3. Fully Developed Laminar Flow. The apparent shearing stress in a laminar flow is the actual viscous shearing stress τ , since turbulent transfers of momentum do not occur. Accordingly, Eq. (8.4) reduces to

$$\tau = \frac{p_1^* - p_2^*}{L} \frac{r}{2} \quad (8.4a)$$

In order to make further progress we must assume a relation between τ , μ , and the velocity distribution. We base our assumption on the experiment described in Art. 1.4, in which the formula $\tau = \mu V/h$ was found to hold. This formula applies to a thin fluid film of uniform thickness h , between two concentric cylinders, one fixed and one having a peripheral velocity V . In this apparatus the velocity is found to vary linearly across the film, so that at any point in the film $\partial u/\partial y = V/h$, where $\partial u/\partial y$ is the rate of change of velocity with distance from the surface (Fig. 8.6). The constant shear stress is in this case equal to $\mu(\partial u/\partial y)$.

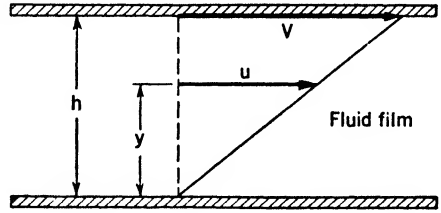


FIG. 8.6. — Linear velocity distribution in a thin film between concentric cylinders (or parallel plates).

For the laminar flow in a pipe we assume that, although the shear stress is not constant, nevertheless it is given by the formula

$$\tau = \mu \frac{\partial u}{\partial y} = -\mu \frac{\partial u}{\partial r} \quad (8.13)$$

where y is the distance from the pipe wall, as shown in Fig. 8.7. Since τ varies linearly with r , Eq. (8.13) will lead to a parabolic velocity distribu-

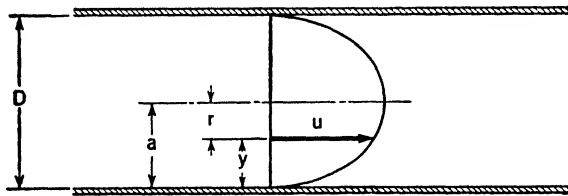


FIG. 8.7. — Nonlinear velocity distribution in a pipe.

tion. Combine Eqs. (8.4a) and (8.13), and integrate with respect to r , noting that $u = 0$ at $r = a$.

$$\begin{aligned} -\int_{u=u}^{u=0} \frac{\partial u}{\partial r} dr &= \frac{p_1^* - p_2^*}{2\mu L} \int_r^a r dr \\ u &= \frac{p_1^* - p_2^*}{4\mu L} a^2 \left(1 - \frac{r^2}{a^2}\right) \end{aligned} \quad (8.14)$$

and

$$u_{\max} = \frac{p_1^* - p_2^*}{4\mu L} a^2 \quad (8.15)$$

It is relatively hard to measure velocity distribution, so that an accurate experimental check on Eq. (8.14) is not easily obtained. We can,

however, get an expression for the volume discharge rate Q by using Eq. (8.14).

$$\begin{aligned}
 Q &= \pi \int_0^a u \, d(r^2) = \pi a^2 \int_0^1 u \, d\left(\frac{r}{a}\right)^2 \\
 &= \frac{\pi a^4}{4\mu L} (p_1^* - p_2^*) \int_0^1 \left[1 - \left(\frac{r}{a}\right)^2\right] d\left(\frac{r}{a}\right)^2 \\
 &= \frac{\pi a^4}{8\mu L} (p_1^* - p_2^*)
 \end{aligned} \tag{8.16}$$

Equation (8.16), which agrees with the measurements of Hagen and Poiseuille as well as with those of more recent investigators, is called the Hagen-Poiseuille law. The accord between Eq. (8.16) and the experimental data justifies the assumption that $\tau = \mu(\partial u/\partial y)$.

Since the mean velocity V is defined as $V = Q/\pi a^2$, it follows from Eqs. (8.15) and (8.16) that in laminar flow

$$V = \frac{u_{\max}}{2} \tag{8.17}$$

Combination of Eqs. (8.9), (8.15), and (8.17) yields the formula for the friction factor in laminar flow, which is plotted in Fig. 8.3.

$$f = \frac{64\mu}{\rho V D} = \frac{64}{R} \tag{8.18}$$

An important engineering application of these equations for laminar flow is the measurement of viscosity. The Hagen-Poiseuille law applied to the apparatus of Fig. 8.8 provides an absolute method of viscosimetry. All the quantities appearing in Eq. (8.16), except μ , are known for the viscometer of Fig. 8.8. Consequently, μ can be calculated. In order that

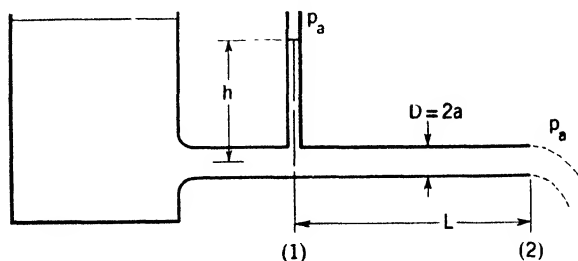


FIG. 8.8. — Capillary-tube viscometer.

Poiseuille's law be applicable it is necessary to measure the pressure difference between two points both of which lie in a region of fully developed flow. Hence, point 1 must be a sufficient distance from the pipe entry [see Eq. (8.1)].

It is difficult to install a manometer in a fine capillary tube such as

must be used to ensure laminar flow. Further, it is hard to measure accurately the diameter of such a tube. Since the fourth power of the radius occurs in Eq. (8.16), a small error in radius will cause a large error in the computed value of μ . For these reasons, this type of viscometer is not widely used for routine measurements; instead, the Saybolt viscometer is ordinarily employed in this country.

This instrument, shown schematically in Fig. 8.9, consists essentially of a reservoir in the bottom of which is a short vertical tube. These are surrounded by a constant-temperature oil bath. A viscosity determination

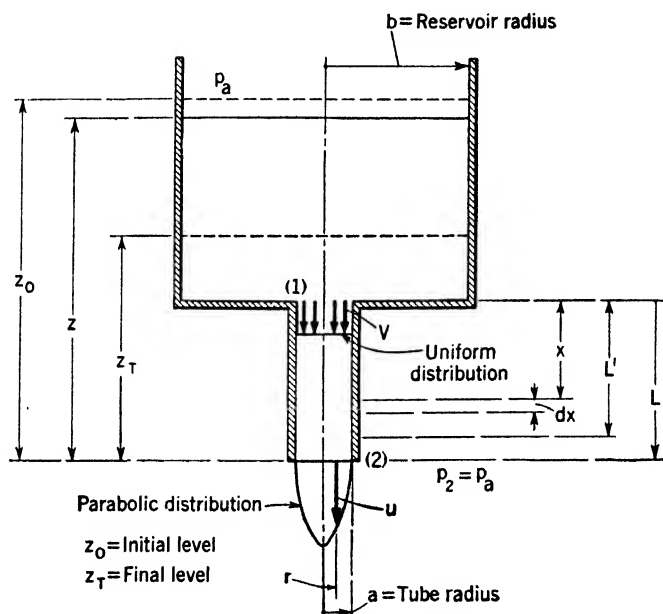


FIG. 8.9. — Essential features of a Saybolt viscometer.

is made by measuring the time required for 60 cu cm of fluid at a known temperature to flow out of the reservoir through the tube, the initial level of the fluid in the reservoir having been previously adjusted to a standard height. From the time measurement (Saybolt seconds) the kinematic viscosity $\nu = \mu/\rho$ of the fluid can be determined through the use of empirical formulas.

It is possible to deduce theoretically a formula that is in fair agreement with the empirical ones. The theory is of interest because it involves both the development of laminar flow in the entrance section of the tube and unsteady flow conditions. It will be given in the next article.

8.4. Development of Laminar Flow. Using the notation of Fig. 8.9, we may write the energy equation for the fluid in the reservoir and tube as

$$z = \frac{1}{\rho g V \pi a^2} \int_{r=0}^{r=a} \frac{\rho u^2}{2} u d(\pi r^2) + H_{l_{0,2}} \quad (8.19)$$

where z is the height of the free surface at any instant. In writing Eq. (8.19) we neglect local changes with respect to time in comparison with space rates of change.

Equations (8.14), (8.15), and (8.17) enable us to express the kinetic-energy term in the simple form V^2/g , but an accurate evaluation of $H_{l_{0,2}}$ is difficult. We neglect losses occurring in the reservoir and consider the only loss to be that in the tube. If we assume the losses there to be the same as in fully developed flow, Eqs. (8.12) and (8.18) give

$$H_{l_{0,2}} = \frac{32\mu}{\rho V a} \frac{V^2}{2g} \frac{L}{2a} = \frac{8\nu L V}{g a^2} \quad (8.20)$$

Since, however, the flow is developing between 1 and 2 in Fig. 8.9, the loss in the transition length will be greater than that for fully developed flow and Eq. (8.20) is an underestimate. Langhaar [7] has developed a satisfactory theory of the laminar transition flow by which one can compute

$$H_{l_{0,2}} = \frac{8\nu L V}{g a^2} + 0.14 \frac{V^2}{g} \quad (8.21)$$

Equation (8.19) now becomes

$$z = \frac{8\nu L V}{g a^2} + 1.14 \frac{V^2}{g} \quad (8.22)$$

The equation of continuity applied to the viscometer gives

$$-\pi b^2 \frac{dz}{dt} = \pi a^2 V$$

or

$$V = -\frac{b^2}{a^2} \frac{dz}{dt} \quad (8.23)$$

where t is the time. Combination of Eqs. (8.22) and (8.23) yields a second-degree differential equation for z , which can be solved for dz/dt in the usual manner for a quadratic. Finally we obtain, after separating the variables,

$$\frac{dz}{1 - \sqrt{1 + (4\beta/\alpha^2)z}} = \frac{\alpha}{2\beta} dt$$

where $\alpha = 8\nu L b^2/ga^4$ and $\beta = 1.14b^4/ga^4$. This equation is readily integrated to

$$T = \alpha \left(\ln \frac{y_0}{y_T} + y_T - y_0 \right) \quad (8.24)$$

where T = total efflux time

$$y_0 = 1 - \sqrt{1 + \frac{4\beta}{\alpha^2} z_0}$$

$$y_T = 1 - \sqrt{1 + \frac{4\beta}{\alpha^2} z_T}$$

The dimensions of a Saybolt universal viscometer are $a = 0.0883$ cm, $b = 1.488$ cm, $L = 1.225$ cm. The initial height of the fluid $z_0 = 12.50$ cm. The final height is computed from the area of the reservoir and the fact that 60 cu cm flows out: $z_T = 3.86$ cm. The following table shows the theoretical and empirical values of T for different values of ν :

ν , cm ² /sec	T [from Eq. (8.24)], sec	T (empirical), sec
0.02	35.2	32.6
0.07	49.3	48.7
0.1	59.2	58.8
1.0	435	462
10.0	4310	4620

For values of ν less than about 0.07 sq cm per sec the computed value of T is too large. This fact can be explained by computation of the average transition length from Eq. (8.1). It is found that the transition length is greater than the length of the tube for $\nu < 0.07$ sq cm per sec. Equation (8.24) is thus an overestimate of T in this range.

For large values of ν , Eq. (8.24) gives a value of T that is too small. This fact is probably due to neglect of friction before the fluid enters the tube.

It is also of interest to determine the amount by which the average wall shearing stress in the transition length exceeds that in fully developed flow. The momentum equation applied to the fluid inside the tube gives

$$\pi a^2(p_1 - p_a + \rho g L) - \int_0^L \tau_0 2\pi a \, dx = \int_{r=0}^{r=a} \rho u^2 \pi \, d(r^2) - \pi a^2 \rho V^2$$

where τ_0 is the wall shear stress at any point in the tube. The Bernoulli equation can be applied from the free surface to point 1, since friction is neglected there. Hence, $p_1 - p_a + \rho g L = \rho g z - (\rho/2) V^2$. We combine these last two equations and evaluate the integral for momentum efflux and obtain, finally,

$$\rho g \pi a^2 \left(z - \frac{V^2}{2g} \right) - \int_0^L \tau_0 2\pi a \, dx = \pi a^2 \frac{\rho}{3} V^2$$

Let τ'_0 be the average value of τ_0 in the transition length L' , and note from Eqs. (8.8) and (8.18) that in fully developed laminar flow

$\tau_0 = 4\mu V/a$. Then

$$\tau'_0 - 4\mu \frac{V}{a} = \frac{\rho g a}{2L'} \left(z - \frac{5V^2}{6g} - \frac{8\nu VL}{ga^2} \right)$$

Eliminate z and L' by use of Eqs. (8.22) and (8.1).

$$\tau'_0 - 4\mu \frac{V}{a} = \frac{0.31\rho a V^2}{2L'} = \frac{0.31}{2 \times 0.23} \frac{\mu V}{a}$$

Therefore, the percentage excess of wall shear stress in the transition length over that in fully developed laminar flow is constant and equal to

$$\frac{\tau'_0 - 4\mu V/a}{4\mu V/a} \times 100 = \frac{0.31 \times 100}{2 \times 0.23 \times 4} = 17\% \quad (8.25)$$

8.5. Turbulence. Osborne Reynolds [13] first showed that the Reynolds number VD/ν is the criterion for the flow condition in a tube. His apparatus is shown schematically in Fig. 8.10. A fine filament of dye was introduced into the glass tube near its smoothly rounded, trumpet-shaped entrance. At low rates of flow the filament of dye appeared as a straight

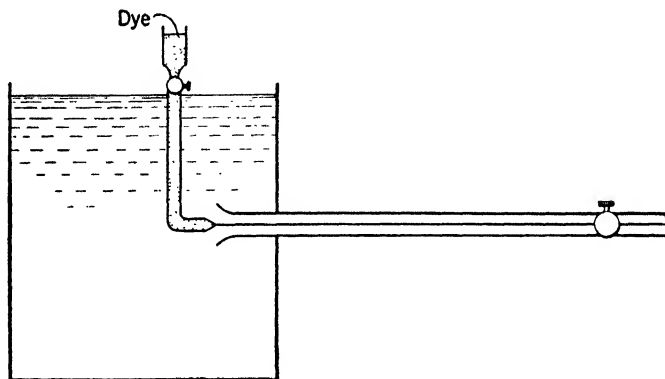


FIG. 8.10. — Reynolds' apparatus for demonstration of laminar and turbulent flow.

line parallel to the tube axis (laminar flow). At a certain critical velocity a sudden breakdown of the laminar motion occurred; the water in the tube became evenly colored by the dye throughout its entire length, except for a portion near the entry.

By performing this experiment with tubes of different sizes and with water at various temperatures Reynolds established the fact that turbulence sets in at a certain value of R . This value he found to be very sensitive to initial disturbances of the water. By allowing the water in the tank to remain undisturbed for some hours before the experiments he obtained the critical value of $R = 13,000$. Other experimenters, by taking elaborate

precautions to avoid entry disturbances, have pushed the critical R as high as 40,000.

While there appears to be no definite upper limit to the critical value of R , all experimenters agree that a lower limit exists and that its value is approximately 2,000. If R is below this lower limit, all initial disturbances, no matter how severe, are damped out and the motion becomes laminar at a sufficient distance from the entry. Filaments of dye cannot be used in determining the lower critical R . Reynolds and most of his successors measured the pressure drop in a length far from the pipe entrance and the corresponding rate of discharge.

These results indicate that the laminar motion is unstable if R exceeds 2,000 and that a suitable disturbance will cause the onset of turbulent flow. Reynolds speculated as to the nature of turbulence and suggested that it was a completely random fluctuating motion.

Dryden [4] and others have shown experimentally that Reynolds' assumption of random velocity fluctuations in a turbulent flow corresponds to the facts. These experiments were carried out with a hot-wire anemometer, which consists of a very fine electrically heated platinum wire placed in the fluid stream. Since any change in speed alters the rate at which the wire is cooled, the temperature and consequently the electrical resistance of the wire are changed, so that the voltage drop through the wire varies in a definite way with the local velocity. After amplification, this fluctu-

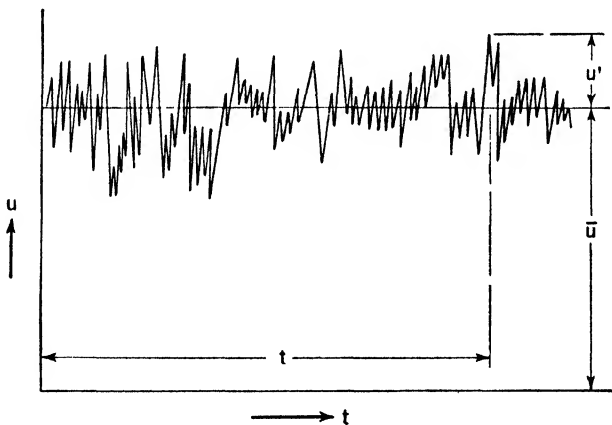


Fig. 8.11. — Random velocity fluctuations in turbulent flow.

ating voltage is applied to a cathode-ray oscillograph. A record of velocity as a function of time can thus be made on a moving photographic film and studied at leisure (Fig. 8.11).

A single hot wire set transversely to the flow will respond primarily to fluctuations parallel to the mean velocity; transverse fluctuations produce

only second-order effects. A properly oriented, X-shaped arrangement of two hot wires is needed to measure the transverse fluctuations in a given direction. Fluctuations of the type u' , discussed below, are the ones that were first measured by the hot-wire technique.

Let u, v, v_θ be the instantaneous velocity components at any point in a pipe in which the turbulent flow is fully developed. The component u is

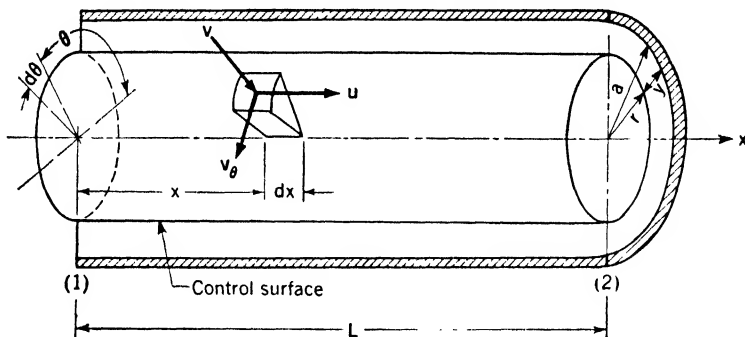


FIG. 8.12.

parallel to the mean flow (x axis); v is parallel to y , where y is measured normal to the wall and increases toward the center of the pipe; v_θ is perpendicular to both u and v . (Fig. 8.12). A photographic record of u , for example, as a function of time would look somewhat like the schematic curve of Fig. 8.11, which is meant to represent a random fluctuation u' , superposed on a constant mean value \bar{u} . The essential characteristic of u' is that its mean value $\overline{u'}$ is equal to zero. The velocity components v and v_θ are likewise subject to random fluctuations. Therefore, at an arbitrary time t

$$\left. \begin{aligned} u &= \bar{u} + u' \\ v &= \bar{v} + v' \\ v_\theta &= \bar{v}_\theta + v'_\theta \end{aligned} \right\} \quad (8.26)$$

where $\overline{u'} = \overline{v'} = \overline{v'_\theta} = 0$.

Obviously, for flow in a pipe of uniform diameter, $\bar{v} = 0$. Also, since we assume there is no spiraling of the flow, $\bar{v}_\theta = 0$.

8.6. Apparent Shearing Stress. In Art. 8.1 the concept of apparent shearing stress τ_{app} was introduced. It was there implied that part of this apparent stress is the average laminar stress and the rest is actually a momentum exchange.

At any surface element, $r d\theta dx$ of the cylindrical control surface shown in Fig. 8.12 the instantaneous efflux of x momentum is $-\rho u v r d\theta dx$. Substitute for u and v from Eq. (8.26), noting that $\bar{v} = 0$, and take the average value: $-\rho \overline{u v} r d\theta dx = -\rho (\overline{u v'} + \overline{u' \bar{v}}) r d\theta dx$. The average value of $\overline{u v'} = \bar{u} \overline{v'} = 0$, but $\overline{u' v'}$ will not be zero if a correlation exists between u'

and v' . Such a correlation is to be expected for flow in a pipe, as will be shown below. Since the flow is fully developed, $\overline{u'v'}$ is independent of x , while by symmetry it does not depend on θ . Therefore, $\overline{u'v'}$ is a function of r (or y) only and is constant over the entire cylindrical control surface.

It may be seen in Chap. VI that an efflux of momentum has the same effect as a force of the same magnitude, applied at the control surface where the efflux occurs, and opposed to the direction of the momentum. Therefore, we can consider $-\rho\overline{u'v'}$ as equivalent to a fictitious shear stress. This fictitious stress is called either the turbulent shear stress τ_{turb} or the Reynolds stress, after Osborne Reynolds, who first pointed out the existence of turbulent momentum transfers. The Reynolds stress is one part of the apparent shear stress τ_{app} .

The other part of τ_{app} is the average laminar shearing stress τ , which, as in laminar flow, is given by the product $\mu(\partial\bar{u}/\partial y)$. In laminar flow there are no fluctuations, so that $\bar{u} = u$.

The apparent shear stress is thus

$$\begin{aligned}\tau_{\text{app}} &= \tau + \tau_{\text{turb}} \\ \tau_{\text{app}} &= \mu \frac{\partial\bar{u}}{\partial y} - \rho\overline{u'v'}\end{aligned}\tag{8.27}$$

It should be pointed out that the laminar shear stress is actually a momentum transfer on a molecular scale. τ_{app} is thus the sum of two momentum transfers, one on a molecular scale, the other on a scale that is appreciable compared with the diameter of the tube. Since in fluid mechanics we ignore molecules and treat fluids as continua, we are content not to delve into the nature of the laminar shear stress. The case of the turbulent shear stress is different, however, for the mechanism of turbulent momentum exchange is one of the fundamental problems of fluid mechanics.

8.7. Zones of Flow in a Pipe. If the pipe wall is smooth, both u' and v' approach zero near the wall, so that there is a thin layer of fluid next to the wall in which τ_{turb} is negligible compared with τ . This layer is called the "laminar sublayer" and its thickness will be denoted by δ . Experiment shows that δ is so small in comparison with the pipe radius that $\partial\bar{u}/\partial y$ may be considered constant for $y \leq \delta$. The laminar parabolic velocity distribution in the sublayer is indistinguishable from a straight line, and $\tau = \mu(\partial\bar{u}/\partial y)$ is a constant.

For values of y that are larger than δ but still small relative to the pipe radius, $\mu(\partial\bar{u}/\partial y)$ decreases rapidly. From Eq. (8.4), however, τ_{app} decreases only linearly as y is increased, so that $-\rho\overline{u'v'}$, the turbulent part of τ_{app} , must become appreciable in this range of y values. Direct experiment thus shows that $\overline{u'v'}$ is different from zero and negative in this region. A correlation must, therefore, exist between u' and v' . Such a correlation

is to be expected where $\partial \bar{u}/\partial y$ is different from zero, as in this case, for a particle of fluid having a positive v' will move to a region where the mean velocity \bar{u} is greater than that at its first position. Consequently, a negative u' will tend on the average to be associated with a particle having a positive v' , and vice versa. At the center of the pipe where $\partial \bar{u}/\partial y = 0$, u' and v' will be uncorrelated.

At some value of y , say $y = \lambda$, the value of $\partial \bar{u}/\partial y$ will be small enough to make $\mu(\partial \bar{u}/\partial y)$ completely negligible with respect to $-\rho \bar{u}'v'$. It is found that λ is small compared with the radius of the pipe.

From the foregoing we are justified in breaking down the flow in a smooth pipe into three zones, as follows:

1. A laminar sublayer lying next to the wall and in which turbulent effects are negligible. ($0 \leq y \leq \delta$.)
2. A transition zone in which the effects of turbulence and of viscosity are of the same order of magnitude. ($\delta \leq y \leq \lambda$.)
3. A turbulent core comprising the bulk of the fluid and in which the effect of viscosity is negligible. ($\lambda \leq y \leq a$.)

For a rough pipe the flow conditions near the wall are in general affected both by viscosity and by roughness. In this case we shall merely distinguish between a wall region and a turbulent core. We shall assume that the turbulent fluctuations in the core are independent of both viscosity and wall roughness.

8.8. Wall-velocity Law. On the basis of experience we may assume that \bar{u} (which from now on will be written u , without the bar) depends on six independent variables, ρ , μ , a , y , wall roughness, and one other. For this sixth variable we might select V , Q , $(p_1^* - p_2^*)/L$, or τ_0 . Of these, τ_0 is the best choice. Accordingly, we assume that $u = f(\rho, \tau_0, a, \mu, y, \text{roughness})$. With ρ , τ_0 , and a common to the four independent Π products obtainable from this equation, the Π theorem yields

$$\frac{u}{\sqrt{\tau_0/\rho}} = \phi \left(\frac{\sqrt{\tau_0/\rho} a}{\nu}, \frac{y}{a}, \text{roughness} \right) \quad (8.28)$$

where ν is the kinematic viscosity μ/ρ . The roughness is assumed to be dimensionless, as in Art. 8.2. Since $\sqrt{\tau_0/\rho}$ has the dimensions of a velocity, it is convenient to define $u^* = \sqrt{\tau_0/\rho}$, and $R^* = \sqrt{\tau_0/\rho} a/\nu$. The ratio y/a will be denoted by ξ . Equation (8.28) becomes

$$\frac{u}{u^*} = \phi(R^*, \xi, \text{roughness}) \quad (8.28a)$$

Equation (8.28a) holds for all values of ξ (or y).

For a smooth pipe it is easy to show that, within the laminar sublayer, the pipe radius a plays no part in determining u . One might, therefore, assume for any type of wall that a has negligible effect also at greater

distances from the wall, even as far as the outer part of the turbulent core. An equivalent assumption is that $u = f(\rho, \tau_0, \mu, y, \text{roughness})$. Whence

$$\frac{u}{u^*} = \chi \left(\frac{u^* y}{\nu}, \text{roughness} \right) = \chi(R^* \xi, \text{roughness}) \quad (8.29)$$

Equation (8.29), which is called "Prandtl's wall-velocity law," agrees well with experiments. We shall assume that Eq. (8.29) holds in the range $0 \leq \xi \leq \xi_1$, where ξ_1 is only slightly greater than λ/a . The function χ will, in general, have different forms in the wall layers and in the outer part of the turbulent core.

8.9. Velocity-defect Law. The difference between the maximum velocity U at the center of the pipe and the velocity anywhere else in the core is called the "velocity defect." From the preceding article it is seen that this defect $U - u$ depends at most on ρ , τ_0 , a , μ , y , and roughness. $U - u$ will be determined, however, by the turbulent fluctuations in the core, which have been assumed independent of μ and roughness. Hence $U - u = f(\rho, \tau_0, a, y)$, or

$$\frac{U - u}{u^*} = \psi(\xi) \quad (8.30)$$

Equation (8.30) is called the "velocity-defect law."

This equation is amply corroborated by experiments, notably those done by Fritsch [2] while working with von Kármán. Fritsch's velocity-distribution curves for a given value of u^* but for walls of different roughness are reproduced in Fig. 8.13. Curve 1 is for a smooth wall, and curve 6 is for a very rough wall, the other curves being for intermediate roughnesses. Fritsch found that, if the points of maximum velocity are superposed, all the curves are congruent, except in a narrow region near the wall.

If we assume that Eq. (8.30) applies over the whole cross section of the pipe, we find by integration that

$$\frac{U - V}{u^*} = \text{constant} \quad (8.31)$$

where V is the mean velocity. Experiment shows the wall layers to be so thin that Eq. (8.31) may be used without appreciable error.

8.10. Resistance Law for a Smooth Pipe. From Eq. (8.8), $V/u^* = \sqrt{8/f}$, whence Eq. (8.31) becomes

$$\sqrt{\frac{8}{f}} = \frac{U}{u^*} - \text{constant} \quad (8.32)$$

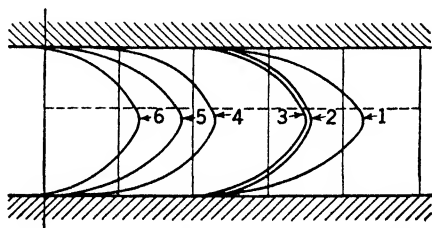


FIG. 8.13. — Turbulent-velocity-distribution curves for pipes having different wall roughness. Curve 1 is for smooth pipe and curves 2 to 6 are for rough pipes. The roughness increases in the order of the numbers of the curves.

Equation (8.28a) indicates that for a smooth pipe

$$\frac{U}{u^*} = \phi(R^*, 1) = \Phi(R^*) \quad (8.33)$$

We can, therefore, get f by finding $\Phi(R^*)$.

In the outer part of the turbulent core, where $\lambda/a \leq \xi \leq \xi_1$, both Eqs. (8.29) and (8.30) are valid. Eliminating u/u^* , we find, for a smooth pipe,

$$\chi(R^*\xi) = \frac{U}{u^*} - \psi(\xi) = \Phi(R^*) - \psi(\xi) \quad (8.34)$$

Differentiation of Eq. (8.34), first with respect to R^* and then with respect to ξ , yields two expressions for $d\chi/d(R^*\xi)$ (which we shall denote by χ').

$$\begin{aligned} \chi'\xi &= \frac{d\Phi}{dR^*} \\ \chi'R^* &= -\frac{d\psi}{d\xi} \end{aligned}$$

provided that $\lambda/a \leq \xi \leq \xi_1$. From the first of these equations χ' must have the form $f(R^*)/\xi$, since $d\Phi/dR^*$ is independent of ξ . From the second equation χ' must be of the form $f(\xi)/R^*$, since $d\psi/d\xi$ is independent of R^* . Both these requirements can be fulfilled only if $f(\xi) = \text{constant}/\xi$ and $f(R^*) = \text{constant}/R^*$, that is, only if $\chi' = \text{constant}/R^*\xi = A/R^*\xi$, where A is an unknown constant. We thus are led to the following equations:

$$\Phi(R^*) = A \ln R^* + \text{constant} \quad (8.35)$$

$$\psi(\xi) = -A \ln \xi + \text{constant} \quad (8.36)$$

$$\chi(R^*\xi) = A \ln (R^*\xi) + \text{constant} \quad (8.37)$$

Combination of Eqs. (8.32), (8.33), and (8.35) gives

$$\sqrt{\frac{8}{f}} = A \ln (R^*) + \text{constant}$$

Recalling that

$$R^* = \frac{u^*a}{\nu} = \frac{2aV}{\nu} \frac{u^*}{2V} = \frac{DV}{\nu} \frac{\sqrt{f}}{4\sqrt{2}} = \frac{R\sqrt{f}}{4\sqrt{2}}$$

we finally obtain the formula,

$$\frac{1}{\sqrt{f}} = A_1 \log_{10} (R\sqrt{f}) + A_2 \quad (8.38)$$

where A_1 and A_2 are constants to be determined experimentally. Data obtained by Nikuradse, which are plotted in Fig. 8.14, agree exactly with

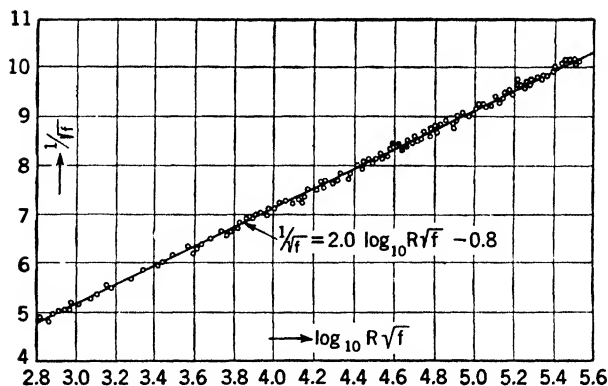


FIG. 8.14. — Resistance law for a smooth pipe.

the straight-line relationship predicted by Eq. (8.38) and lead to the final formula

$$\frac{1}{\sqrt{f}} = 2.0 \log_{10} (R\sqrt{f}) - 0.8 \quad (8.38a)$$

8.11. Resistance Law for Rough Pipe. If we assume the roughness is so great that viscosity does not affect the flow, and that the roughness depends only on a single length k , a development like that of the last article is possible for rough pipe.

Equation (8.28a) yields in this case, where the nondimensional roughness term is the single ratio k/a ,

$$\frac{U}{u^*} = \phi\left(1, \frac{k}{a}\right) = \Phi\left(\frac{k}{a}\right) \quad (8.39)$$

The wall-velocity law [Eq. (8.29)] becomes

$$\frac{u}{u^*} = \chi\left(\frac{k}{y}\right) = \chi\left(\frac{k}{a} \frac{1}{\xi}\right) \quad (8.40)$$

so that, in the range $\lambda/a \leq \xi \leq \xi_1$ Eqs. (8.31), (8.39), and (8.40) yield

$$\chi\left(\frac{k}{a} \frac{1}{\xi}\right) = \Phi\left(\frac{k}{a}\right) - \psi(\xi) \quad (8.41)$$

Since $\psi(\xi)$ must have the same form as for a smooth pipe, Eq. (8.41) leads to

$$\Phi\left(\frac{k}{a}\right) = -A \ln \frac{k}{a} + \text{constant} \quad (8.42)$$

$$\psi(\xi) = -A \ln \xi + \text{constant} \quad (8.43)$$

$$\chi\left(\frac{k}{a} \frac{1}{\xi}\right) = -A \ln \left(\frac{k}{a} \frac{1}{\xi}\right) + \text{constant} \quad (8.44)$$

Combination of Eqs. (8.32), (8.39), and (8.42) yields

$$\frac{\sqrt{8}}{\sqrt{f}} = -A \ln \frac{k}{a} + \text{constant} = A \ln \frac{a}{k} + \text{constant}$$

or

$$\frac{1}{\sqrt{f}} = A_1 \log_{10} \frac{a}{k} + A_3 \quad (8.45)$$

where A_1 should theoretically have the same value as in Eq. (8.38) and A_3 is an unknown constant.

Nikuradse's experiments on pipe artificially roughened by a coating of sand grains of uniform diameter indicate that the grain diameter k completely characterizes this type of roughness and that for sufficiently large Reynolds numbers

$$\frac{1}{\sqrt{f}} = 2.0 \log_{10} \frac{a}{k} + 1.74 \quad (8.45a)$$

The experiments bear out the prediction that the constant A_1 should have the same value for both smooth and rough pipes.

Nikuradse's results, which are plotted in Fig. 8.4, show that the limiting value of R at which f becomes independent of R varies with a/k . This fact is readily understood if we bear in mind that the importance of the roughness is determined by the ratio k/δ of the grain diameter to the thickness of the laminar sublayer. It will be shown below that δ depends only on R and that $\delta u^*/\nu = 5$. Hence

$$\frac{k}{\delta} = \frac{1}{5} \frac{u^* k}{\nu} = \frac{1}{5} \frac{u^*}{V} \frac{VD}{\nu} \frac{k}{2a} = \frac{1}{10} \frac{\sqrt{f}}{\sqrt{8}} R \frac{k}{a}$$

A plot of Nikuradse's results for $[(1/\sqrt{f}) - 2.0 \log_{10} (a/k)]$ versus k/δ is given in Fig. 8.15. This curve shows that if $k/\delta < 0.8$ the roughness has no effect, that if $0.8 \leq k/\delta \leq 12$ both viscosity and roughness are important, and that for $k/\delta > 12$ viscosity has no further influence.

It is remarkable that data from numerous sources [10] for new commercial pipes fall approximately on a single curve, as shown in Fig. 8.15. The roughness of any of these pipes is thus adequately described by a single parameter k . At one end this curve approaches asymptotically the straight line for smooth pipes and at the other the horizontal straight line for rough pipes. The formula for this transition curve was suggested by Colebrook [10] and is

$$\frac{1}{\sqrt{f}} = 1.74 - 2.0 \log_{10} \left[\frac{k}{a} \left(1 + 0.658 \frac{\delta}{k} \right) \right]$$

If $\delta/k \ll 1$, this expression reduces to Eq. (8.45a), while if $\delta/k \gg 1$ it becomes $1/\sqrt{f} = 1.74 - 2.0 \log_{10} (0.658\delta/a)$, which, with $\delta = 5\nu/u^*$, is readily seen to be identical with Eq. (8.38a).

In the case of commercial pipes the roughness is seen to affect the friction factor over a much wider range of k/δ than in the case of the sand-coated tubes. The sand grains, being of uniform size and distribution, are all immersed simultaneously in the laminar sublayer and cease to affect

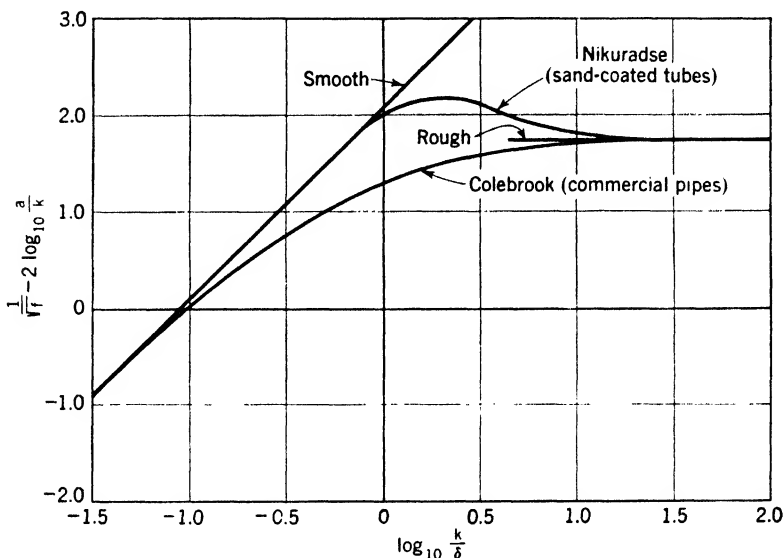


FIG. 8.15. — The friction factor for rough pipes depends on the ratio k/δ of roughness diameter to the laminar-sublayer thickness.

the flow if k/δ is less than about 0.8. The roughness of a commercial pipe, on the other hand, is nonuniform. When most of the irregularities are submerged, occasional large projections may rise clear of the sublayer and exert appreciable influence on f .

8.12. Turbulent Velocity Distribution. Equations (8.29) and (8.37) give the velocity distribution near a smooth wall.

$$\begin{aligned} u/u^* &= \chi(R^*\xi) = A \ln(R^*\xi) + \text{constant} \\ &= A \ln\left(\frac{u^*y}{\nu}\right) + \text{constant} \end{aligned} \quad (8.46)$$

Equation (8.46) would be expected to hold only in the outer part of the turbulent core, that is, for $\lambda/a \leq \xi \leq \xi_1$, but experiments by Nikuradse yield the surprising result that the equation is valid nearly to the center of the pipe. The data are plotted on a semilogarithmic scale in Fig. 8.16, from which one finds that in the turbulent core

$$\frac{u}{u^*} = 5.75 \log_{10}\left(\frac{u^*y}{\nu}\right) + 5.5 \quad (8.46a)$$

It is seen that the points begin to deviate from the straight line of Eq. (8.46a) at a value of $u^*y/\nu = 30$. This value marks the division between transition zone and turbulent core, that is, $u^*\lambda/\nu = 30$.

In the laminar sublayer $\tau_0 = \tau = \mu(du/dy) = \mu(u/y)$, since, as already

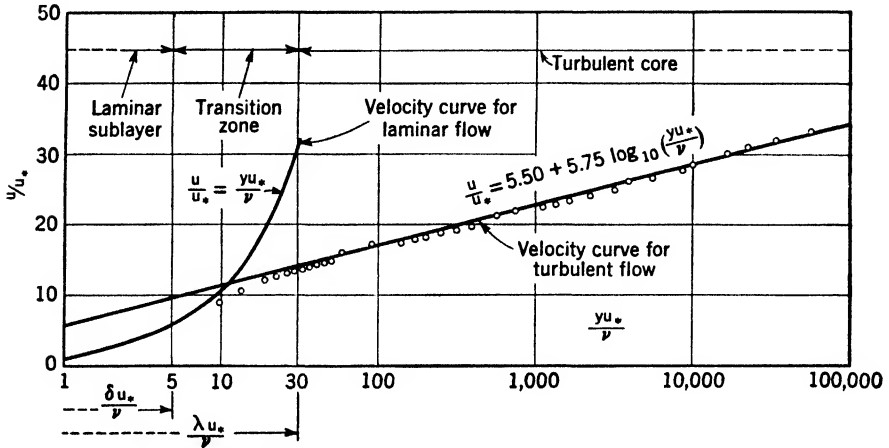


FIG. 8.16. — Velocity distribution in a smooth pipe.

stated, the velocity varies linearly with y . From this equation it follows at once that

$$\frac{u}{u^*} = \frac{u^*y}{\nu} \quad (8.47)$$

provided that $0 \leq y \leq \delta$. This equation is plotted in Fig. 8.16. Extrapolation of the trend of the test points toward smaller values of yu^*/ν indicates that the limit of the laminar sublayer corresponds to $yu^*/\nu = 5$, that is, $\delta u^*/\nu = 5$.

For roughened pipes Eqs. (8.29) and (8.44) combine to give

$$\frac{u}{u^*} = A \ln \frac{y}{k} + \text{constant} \quad (8.48)$$

for the outer part of the turbulent core. Nikuradse's tests proved, however, that this formula applies from a value $y/k = 1$ practically to the center of the pipe. His data yield

$$\frac{u}{u^*} = 5.75 \log_{10} \left(\frac{y}{k} \right) + 5.85 \quad (8.48a)$$

8.13. Mechanism of Turbulence in Pipes. The above development, which is due to Millikan [9], of the formulas for friction factor and velocity distribution brings out clearly that only two principal assumptions are involved, *viz.*, that the velocity near the wall is independent of the pipe

radius and that the velocity defect in the turbulent core is independent of the wall roughness and viscosity. A third assumption, that the wall layers are thin compared with the radius of the turbulent core, is used in justifying Eq. (8.31). Since no detailed picture of the turbulence mechanism is used, the theory cannot be expected to give complete results. Thus, in the formulas for f and u two unknown constants appear. One of these, the constant A , is common to all the formulas and appears to be of a universal nature, but the integration constants are different in every case. Further, the fact that the logarithmic velocity formulas apply nearly to the center of the pipe is entirely unexplained.

Prandtl first proposed a logarithmic velocity distribution law, developing his formula from the following conception of the turbulent process: He idealized the actually continuous mixing by assuming that a mass of fluid retained its original x velocity until it had moved transversely a certain distance l_1 and that it then mixed suddenly and completely with the surrounding fluid. He reasoned that the root-mean-square (rms) of the x velocity fluctuation, $\sqrt{\overline{u'^2}}$, would be proportional to this distance times the average velocity gradient.

$$\sqrt{\overline{u'^2}} \sim l_1 \frac{\partial u}{\partial y}$$

Also, because of the correlation between u' and v' ,

$$\sqrt{\overline{v'^2}} \sim l_1 \frac{\partial u}{\partial y}$$

The definition of the correlation coefficient is

$$\beta = \frac{\overline{u'v'}}{\sqrt{\overline{u'^2}} \sqrt{\overline{v'^2}}} \quad (8.49)$$

from which the Reynolds stress can be written

$$\tau_{\text{turb}} = -\rho \overline{u'v'} = -\rho \beta \sqrt{\overline{u'^2}} \sqrt{\overline{v'^2}}$$

Prandtl's picture of turbulence thus leads to

$$\tau_{\text{turb}} \sim -\rho \beta l_1^2 \left(\frac{\partial u}{\partial y} \right)^2$$

Prandtl suggested that the factor of proportionality and $-\beta l_1^2$ be absorbed into a single factor.

$$\tau_{\text{turb}} = \rho l^2 \left(\frac{\partial u}{\partial y} \right)^2 \quad (8.50)$$

Since l is a measure of the distance moved by a particle before mixing, Prandtl called it the "mixing length."

In the turbulent core $\tau_{\text{turb}} = \tau_{\text{app}} = \tau_0(r/a) = [(p_1^* - p_2^*)/L] (r/2)$, so that everything in Eq. (8.50) can be determined experimentally, except l . Plots of l/a versus y/a prepared by Nikuradse from his data on pipe flow are given in Fig. 8.17.

Near the wall these curves are approximated by the formula $l = ky$.

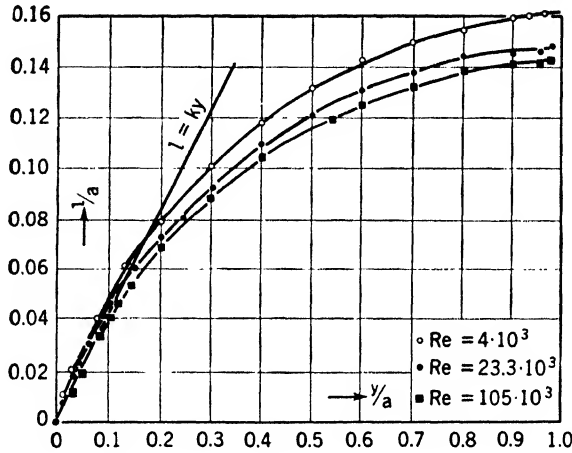


FIG. 8.17. — Mixing-length distribution in smooth and rough pipes.

Since $\tau_{\text{turb}} \approx \tau_0$ in the outer portions of the turbulent core, we get from Eq. (8.50) an approximate expression for the slope of the velocity curve.

$$\frac{\partial u}{\partial y} = \frac{1}{k} \frac{\sqrt{\tau_0/\rho}}{y} = \frac{1}{k} \frac{u^*}{y} \quad (8.51)$$

Noting that u depends only on y , we get by integration

$$\frac{u}{u^*} = \frac{1}{k} \ln y + \text{constant}$$

or, since u^*/ν is constant,

$$\frac{u}{u^*} = \frac{1}{k} \ln \frac{u^* y}{\nu} + \text{constant} \quad (8.52)$$

Comparison of Eqs. (8.46) and (8.52) shows that $A = 1/k$.

If we substitute the exact value of τ_{turb} in Eq. (8.50), we get

$$\frac{\partial u}{\partial y} = \frac{1}{l} \sqrt{\frac{\tau_{\text{turb}}}{\rho}} = \frac{1}{l} \sqrt{\frac{\tau_0}{\rho}} \sqrt{1 - \frac{y}{a}}$$

The plot of experimental data for l given in Fig. 8.17 shows that

$$l \approx ky \sqrt{1 - (y/a)}$$

over the whole range of y values, except very near $y/a = 1$. Combination of these two expressions gives again Eq. (8.51). The surprising accuracy of Eq. (8.52) is thus partly explained, but there is of course no theoretical explanation of the experimental curves of Fig. 8.17.

In 1930 von Kármán [6] suggested that the fluctuations might be kinematically similar over most of the core. In order to use this hypothesis he assumed the fluctuations, and consequently the mixing length, to be on a small scale compared with the pipe radius. Neither of these assumptions is strictly in accord with observation, but the results he obtained are, nevertheless, of interest.

For such small-scale turbulence, according to von Kármán, the value of the mixing length l_1 at any point y_1 will be determined by the local character of the fluctuations. So also will be the change in mean velocity $u_2 - u_1$ occurring between y_1 and any near-by fixed point y_2 . Since both l_1 and $u_2 - u_1$ are thus assumed dependent on the same parameters, one may consider l_1 to be a function of $u_2 - u_1$, or vice versa. Now, since $y_2 - y_1$ is small, $u_2 - u_1$ may be represented with sufficient accuracy by a Taylor's series of only two terms, thus:

$$u_2 - u_1 = (y_2 - y_1) \left(\frac{du}{dy} \right)_1 + (y_2 - y_1)^2 \left(\frac{d^2u}{dy^2} \right)_1$$

Therefore, l_1 will be a function of only $(du/dy)_1$ and $(d^2u/dy^2)_1$, $y_2 - y_1$ being a constant previously fixed by the initial choice of y_1 and y_2 . If we assume $l_1 = f[(du/dy)_1, (d^2u/dy^2)_1]$, the Π theorem shows that

$$l_1 = \text{constant} \frac{(du/dy)_1}{(d^2u/dy^2)_1} = -k_1 \frac{(du/dy)_1}{(d^2u/dy^2)_1}$$

where the minus sign is used because $d^2u/dy^2 < 0$.

The assumption of kinematically similar fluctuations at all points in the core leads at once to the conclusion that the constant k_1 is the same everywhere. Hence for any value of y in the core

$$l = -k \frac{du/dy}{d^2u/dy^2} \quad (8.53)$$

where k is a universal constant.

Combine Eqs. (8.50) and (8.53) (noting that $\partial u / \partial y = du/dy$).

$$\begin{aligned} \sqrt{\tau_{\text{turb}}} &= \sqrt{\tau_0 \left(1 - \frac{y}{a} \right)} = \sqrt{\rho} \frac{du}{dy} \left(-k \frac{du/dy}{d^2u/dy^2} \right) \\ \frac{d(du/dy)}{(du/dy)^2} &= -\sqrt{\frac{\rho}{\tau_0}} k \frac{dy}{\sqrt{1 - (y/a)}} = -\frac{k}{u^*} \frac{dy}{\sqrt{1 - (y/a)}} \end{aligned} \quad (8.54)$$

In the outer part of the core where $\sqrt{1 - (y/a)} \approx 1$, this equation integrates to

$$\frac{dy}{du} = \frac{k}{u^*} y$$

where the value zero is chosen for the integration constant because this choice has been found to give the best agreement with observation. The equation is seen to be identical with Eq. (8.51). For any point in the core Eq. (8.54) gives

$$\frac{U - u}{u^*} = -\frac{1}{k} \left[\ln \left(1 - \sqrt{1 - \frac{y}{a}} \right) + \sqrt{1 - \frac{y}{a}} \right] \quad (8.55)$$

On the other hand, the logarithmic velocity distribution given by Eq. (8.52) yields

$$\frac{U - u}{u^*} = -\frac{1}{k} \ln \left(\frac{y}{a} \right) \quad (8.56)$$

Although Eq. (8.55) agrees fairly well with experiment, Eq. (8.56) fits the data considerably better. We are thus forced to conclude that von Kármán's hypotheses are not in entire accord with the facts and that the remarkable success of Eq. (8.52) remains to a large extent unexplained.

Burgers and Gebelein have attacked the turbulence problem from the viewpoint of statistical mechanics. More recently, Taylor, von Kármán, and others have also applied statistical methods to turbulence investigations [4]. These researches are outside the scope of this text; it must suffice to state that they have already led to a better understanding of certain turbulence phenomena.

8.14. Flow in Noncircular Conduits. The equations of motion for laminar flow have been solved for tubes of various cross sections, *e.g.*, rectangular, triangular, and annular. It is known that these equations are identical mathematically with those for the

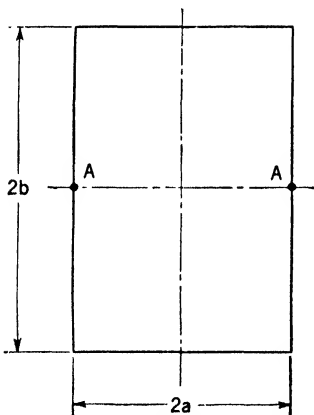


FIG. 8.18.

torsion problem for an elastic bar of the same cross section as the laminar stream. Hence the solutions of the one problem are directly applicable to those of the other [14].

This analogy leads to the following results for a tube of rectangular cross section of sides $2a$ and $2b$ as shown in Fig. 8.18. The maximum shear stress occurs at the mid-points A, A of the long sides of the cross section and has the value

$$\tau_{\max} = k \frac{p_1^* - p_2^*}{L} a$$

where $(p_1^* - p_2^*)/L$ has its usual meaning and k is a numerical factor tabulated below. The discharge rate is

$$Q = k_1 \frac{p_1^* - p_2^*}{4\mu L} (2a)^3 2b$$

where k_1 is a numerical factor given in the following table:

$\frac{b}{a}$	k	k_1	$\frac{b}{a}$	k	k_1
1.0	0.675	0.141	3	0.985	0.263
1.2	0.759	0.166	4	0.997	0.281
1.5	0.848	0.196	5	0.999	0.291
2.0	0.930	0.229	10	1.000	0.312
2.5	0.968	0.249	∞	1.000	0.333

Experimental results for laminar flow are given by Croft [3].

For turbulent flow it has been found empirically that the relation between the friction factor and the Reynolds number is practically independent of the shape of the cross section, if the proper "equivalent diameter" is used in place of D . The equivalent diameter D_e is four times the hydraulic radius. *i.e.*,

$$D_e = 4 \times \frac{\text{cross-sectional area of flow}}{\text{wetted perimeter}} \quad (8.57)$$

Croft states that for annular sections this substitution gives satisfactory results only if the ratio of inner to outer diameter does not exceed 0.3.

The turbulent fluctuations cause a secondary flow to occur if the cross section is not circular. In a rectangular duct this secondary flow takes the form of a circulation outward at the corners and inward near the mid-points of the sides. The mean velocity near the corners of the section is thus maintained at a relatively high value.

8.15. Flow in Bends. Hofmann [5] has measured the loss H_t in 90-deg bends of circular cross section. His results are plotted nondimensionally in Figs. 8.19a and b. The expression $2gH_t/V^2$ is seen to depend on the Reynolds number $R = VD/\nu$ and on the ratio of the center-line radius of the bend to its diameter r/D . The velocity V is the mean velocity of the flow through the bend.

The results of Madison and Parker [8] on losses in smooth 90-deg elbows of rectangular cross section are shown in Fig. 8.20. In this figure, "curve ratio" is the quotient of the inner radius by the outer radius of the bend, and "aspect ratio" AR is equal to the width normal to the plane of the bend divided by the difference between the outer and inner radii.

A double-spiral secondary flow occurs in bends. This flow results from

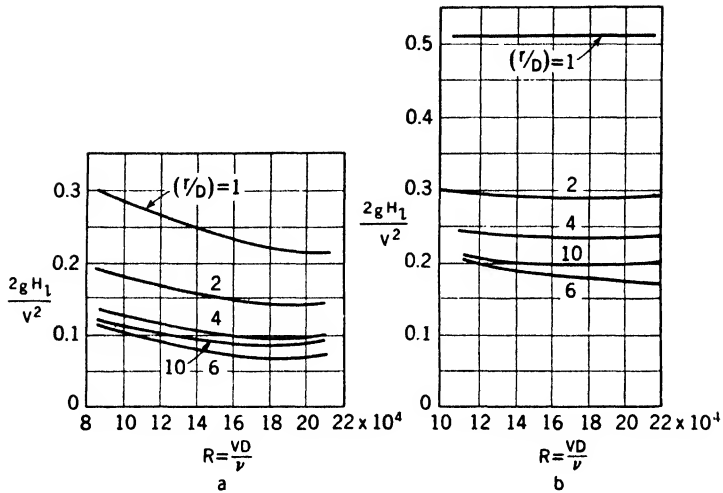


FIG. 8.19. — Loss coefficient in a 90-deg bend as a function of Reynolds number and ratio of bend radius to pipe diameter. (a) Smooth bend. (b) Rough bend. (After Hofmann, reference 5.)

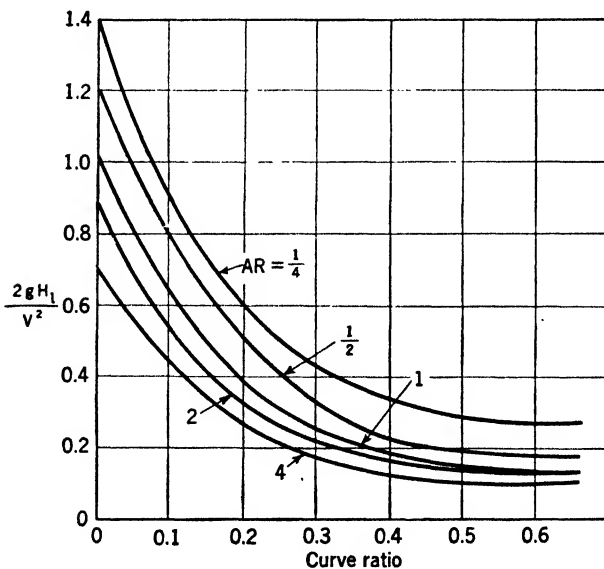


FIG. 8.20. — Loss coefficient for a smooth 90-deg bend of rectangular cross section. Curve ratio = inner radius/outer radius. AR = width normal to plain of bend/(outer radius - inner radius). (After Madison and Parker, reference 8, by permission of American Society of Mechanical Engineers.)

the fact that the fluid near the center of the cross section is moving faster than that at the sides, where friction retards it. Hence there is an outward flow in the central plane of the bend and a corresponding inward flow at each side due to the greater centrifugal force on the faster-moving fluid.

Theory shows that in a frictionless fluid rounding a bend the velocity is less at the outer streamlines than at the inner ones, just as in a potential vortex. Consequently, as fluid approaches the mid-point of a bend, the outlying fluid is decelerated and the pressure rises along the outer wall, while the fluid near the inside is accelerated. The reverse process occurs as the fluid leaves the bend, the fluid near the inside being decelerated with an accompanying increase in pressure, while that at the outside is accelerated. Wherever the pressure rises in the direction of flow, there is a rapid thickening of the boundary layer in a real fluid and a tendency for the flow to separate from the boundary. Hence, there may be separation before the mid-point of the bend at the outer wall, followed by a second separation at the inner wall downstream from the mid-point.

8.16. Loss in Pipe Fittings (Turbulent Flow). It has been found that, to a first approximation, the loss H_f in a pipe fitting such as an elbow, tee, valve, or coupling is independent of the Reynolds number of the flow. Therefore, the Π theorem shows that the loss coefficient C , defined by the equation

$$H_f = C \frac{V^2}{2g} \quad (8.58)$$

will be approximately constant. Here V is the mean velocity in the pipe to which the fitting is attached.

The loss in a fitting is also frequently expressed in terms of the length of straight pipe in which an equal loss would occur. This length is called the "equivalent length" for the fitting. Since the loss in a straight pipe is given by $H_f = f(L/D)(V^2/2g)$, the loss in a fitting is

$$H_f = f \frac{L_e}{D} \frac{V^2}{2g} \quad (8.59)$$

where L_e is the equivalent length for the fitting. For purposes of computation all that need be specified is the ratio L_e/D ("equivalent L/D ratio"). This ratio determines the loss in the fitting, provided that f is known or can be estimated. Comparison of Eqs. (8.58) and (8.59) shows that $C = f(L_e/D)$. Since f depends on R and roughness, L_e/D must also depend on the same things if C is a constant. However, the error made in considering both C and L_e/D to be constant for a given fitting is usually negligible, because the loss in the fitting is ordinarily only a small part of the total loss to be considered. Reasonable values of C and L_e/D are given in the following table:

Fitting	C	$\frac{L_e}{D}$
Standard 90-deg elbow	0.75	35
Standard 45-deg elbow	0.35	15
Open gate valve	0.15	7
Gate valve $\frac{1}{2}$ closed	4.5	200
Open globe valve	7.5	350
Open angle valve	3.8	170

8.17. Loss at a Sudden Change of Cross Section. For a sudden enlargement a theoretical expression for the loss is easily obtainable. In Fig 8.21 we take section 2 sufficiently far downstream to ensure that the

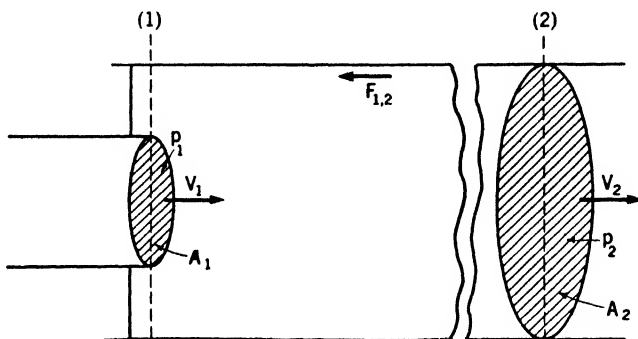


FIG. 8.21.

eddies are practically damped out when the fluid reaches 2. Apply the energy equation between 1 and 2.

$$H_{l,t} = \frac{p_1 - p_2}{\rho g} + \frac{V_1^2 - V_2^2}{2g} \quad (8.60)$$

$H_{l,t}$ is the sum of the losses due to the enlargement and to the wall friction.

The momentum equation yields

$$(p_1 - p_2)A_2 - F_{1,2} + \rho A_1 V_1^2 - \rho A_2 V_2^2 = 0 \quad (8.61)$$

where $F_{1,2}$ is the friction force exerted by the pipe wall on the fluid. The assumption is made here that the pressure is uniform over the entire area A_2 at section 1.

Eliminating $p_1 - p_2$ from Eqs. (8.60) and (8.61) and noting that $A_1 V_1 = A_2 V_2$ by continuity, we obtain for the loss due to the enlargement

$$H_l = H_{l,t} - \frac{F_{1,2}}{\rho g A_2} = \frac{V_2^2}{2g} + \frac{V_1^2}{2g} \left(1 - \frac{2A_1}{A_2} \right) = \frac{V_1^2}{2g} \left(\frac{A_1^2}{A_2^2} - \frac{2A_1}{A_2} + 1 \right)$$

or

$$H_l = \frac{V_1^2}{2g} \left(1 - \frac{A_1}{A_2} \right)^2 \quad (8.62)$$

For a sudden contraction a similar analysis can be made, but an unknown contraction coefficient appears in the result. Referring to Fig. 8.22,

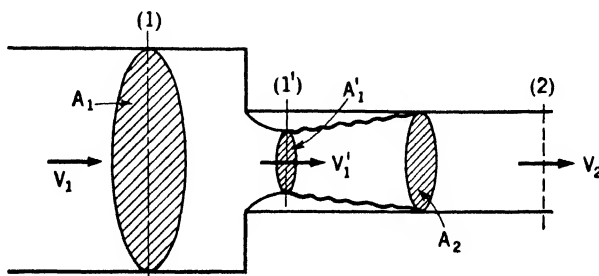


FIG. 8.22.

we can apply Eq. (8.62) between sections 1' and 2.

$$H_t = \frac{V_1'^2}{2g} \left(1 - \frac{A_1'}{A_2} \right)^2$$

Defining $C_c = A_1'/A_2$ and noting that $A_1V_1 = A_2V_2$, we get

$$H_t = \frac{V_2^2}{2g} \left(\frac{1}{C_c} \right)^2 (1 - C_c)^2 = \frac{V_2^2}{2g} \left(\frac{1}{C_c} - 1 \right)^2 \quad (8.63)$$

Values of C_c measured by Weisbach [15] and corresponding values of $[(1/C_c) - 1]^2$ are given in the following table:

$\frac{A_2}{A_1}$	0.2	0.4	0.6	0.8	1.0
C_c	0.632	0.659	0.712	0.813	1.0
$\left(\frac{1}{C_c} - 1 \right)^2$	0.34	0.27	0.16	0.05	0

Equation (8.63) might be improved by taking into account the loss between 1 and 1'. Refinement of either Eq. (8.62) or (8.63) is hardly worth while, however, since the loss at an enlargement or contraction is usually a small fraction of the total. Since variation in velocity over a cross section is neglected in Eqs. (8.62) and (8.63), they will give better results for turbulent than for laminar flow.

8.18. Venturi Meter, Nozzle, and Orifice. These three metering devices are identical in principle, each introducing into the pipe a constriction, which produces a change in pressure. The approximate relation between the pressure change and the rate of flow is easily found if the flow is considered as one dimensional.

Apply the energy and continuity equations between sections 1 and 2 of the Venturi meter shown in Fig. 8.23.

$$\frac{p_2 - p_1}{\rho g} + \frac{V_2^2 - V_1^2}{2g} + H_{l_{1,2}} = 0$$

$$A_1 V_1 = A_2 V_2$$

Combine these, and solve for V_2 , the throat velocity.

$$V_2 = \frac{1}{\sqrt{1 - (A_2/A_1)^2}} \sqrt{\frac{2(p_1 - p_2)}{\rho} - 2gH_{l_{1,2}}} \quad (8.64)$$

It is obvious that, for the same rate of flow (*i.e.*, for the same value of mean throat velocity V_2), the pressure drop $p_1 - p_2$ will be less if the loss

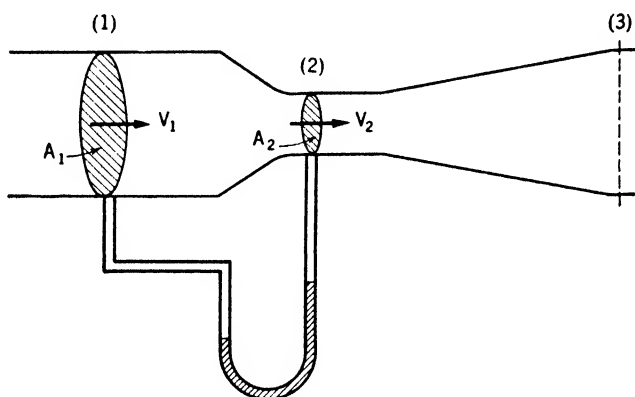


FIG. 8.23. — Venturi meter.

$H_{l_{1,2}}$ is less. The pressure drop that would be required in the limiting, idealized case of no loss would be $(p_1 - p_2)' = p_1 - p_2 - \rho g H_{l_{1,2}}$. Define a coefficient $C_v^2 = (p_1 - p_2)' / (p_1 - p_2)$, the ratio of the ideal to the actual pressure drop. Equation (8.64) can thus be written

$$V_2 = \frac{C_v}{\sqrt{1 - (A_2/A_1)^2}} \sqrt{\frac{2}{\rho} (p_1 - p_2)} \quad (8.64a)$$

The coefficient C_v is usually called the “velocity coefficient,” since it can be interpreted as the ratio of the actual velocity V_2 to that which would occur under the measured pressure drop if there were no loss. However, the interpretation of C_v as the ratio of ideal to actual pressure drop seems to be preferable, because the rate of flow is ordinarily determined by factors external to the measuring device, the pressure drop in the device being the result, rather than the cause, of the discharge rate subsisting in the pipe.

The volume rate of flow Q is equal to $A_2 V_2$; hence

$$Q = \frac{A_2 C_v}{\sqrt{1 - (A_2/A_1)^2}} \sqrt{\frac{2}{\rho} (p_1 - p_2)} \quad (8.65)$$

Since the pressure drop $p_1 - p_2$ will in general depend on Q , ρ , A_1 , A_2 , and μ , the Π theorem, together with Eq. (8.65), shows that

$$C_v = \phi_1 \left(\frac{\rho Q \sqrt{A_2}}{A_2 \mu}, \frac{A_2}{A_1} \right) = \phi \left(\frac{\rho V_2 D_2}{\mu}, \frac{A_2}{A_1} \right) \quad (8.66)$$

where D_2 is the throat diameter. The results of tests by several investigators [1] are plotted in Fig. 8.24. The ratio A_2/A_1 varied between $\frac{1}{9}$ and

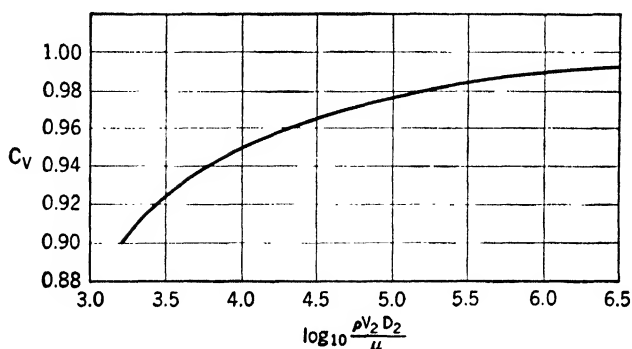


FIG. 8.24. — Coefficient for a Venturi meter as a function of Reynolds number. (From ASME report on "Fluid Meters," reference 1, by permission of American Society of Mechanical Engineers.)

$\frac{1}{4}$ in these tests, but there are not enough data available to show the effect of this variable. One is probably justified in concluding from Fig. 8.24 that C_v is independent of A_2/A_1 , at least in the range of these tests. There is some evidence from other sources that, at smaller Reynolds numbers, C_v does depend on A_2/A_1 , being larger for smaller A_2/A_1 at any given value of Reynolds number.

The purpose of the diverging cone of the Venturi meter is to minify the loss downstream from the throat, by keeping small both separation and wall-friction effects. It has been found that the sum of these two losses is a minimum for a total included angle of divergence of about 6 deg.

The total loss occurring in the Venturi meter is seen from the energy equation to equal $(p_1 - p_3)/\rho g$. The ratio $(p_1 - p_3)/(p_1 - p_2)$ usually has a value between 0.1 and 0.2.

The flow nozzle shown in Fig. 8.25 can be approximately analyzed in the same way as the Venturi meter. It will be noticed, however, that a pressure tap in the pipe wall at section 2 may not yield the pressure at the nozzle throat, because of the eddying that occurs in the dead-water region

surrounding the jet. Furthermore, the pressure at the wall upstream from the nozzle varies slightly with distance from the nozzle, owing to the

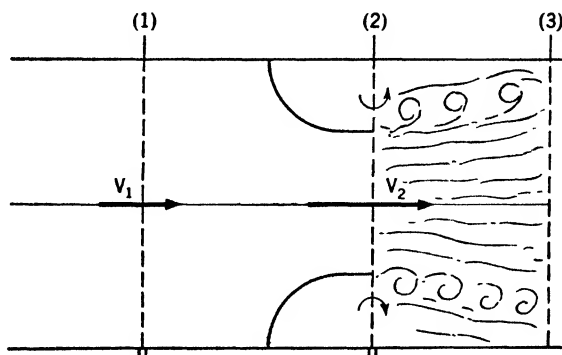


FIG. 8.25. — Nozzle.

curvature of the flow as the stream contracts. For these reasons it is preferable to replace Eq. (8.65) with

$$Q = A_2 C \sqrt{\frac{2}{\rho} \Delta p} \quad (8.67)$$

where C is called the “discharge coefficient” and Δp is the pressure difference between an upstream and a downstream tap located in any convenient way. The factor $1/\sqrt{1 - (A_2/A_1)^2}$ has for simplicity been absorbed into C .

By reasoning like that which led to Eq. (8.66) we can show that

$$C = \phi \left(\frac{\rho V_1 D_1}{\mu}, \frac{A_2}{A_1} \right)$$

provided that the shape of the nozzle and the location of the pressure taps are arbitrarily fixed.

The Verein Deutscher Ingenieure (VDI) [11] has published curves for the discharge coefficient of the German standard nozzle. The nozzle and curves are shown in Fig. 8.26. By adhering carefully to the specifications for making and installing this standard nozzle one can use it without calibration, by virtue of the curves of Fig. 8.26*b*.

A third metering device is the plate orifice, such as is shown in Fig. 8.27. The jet contracts after leaving the orifice until it reaches section 2, the vena contracta. The cross-sectional area A_2 is therefore unknown. If we define the contraction coefficient $C_c = A_2/A$, we can rewrite Eq. (8.65) for application to the orifice,

$$Q = \frac{AC_c C_v}{\sqrt{1 - C_c^2 (A^2/A_1^2)}} \sqrt{\frac{2}{\rho} (p_1 - p_2)}$$

Owing to the practical impossibility of determining C_c and C_v separately, as well as the uncertainty in locating pressure taps to measure $p_1 - p_2$, we simplify this equation to

$$Q = AC \sqrt{\frac{2}{\rho} \Delta p} \quad (8.68)$$

Equation (8.67) for the nozzle and Eq. (8.68) for the orifice have the same

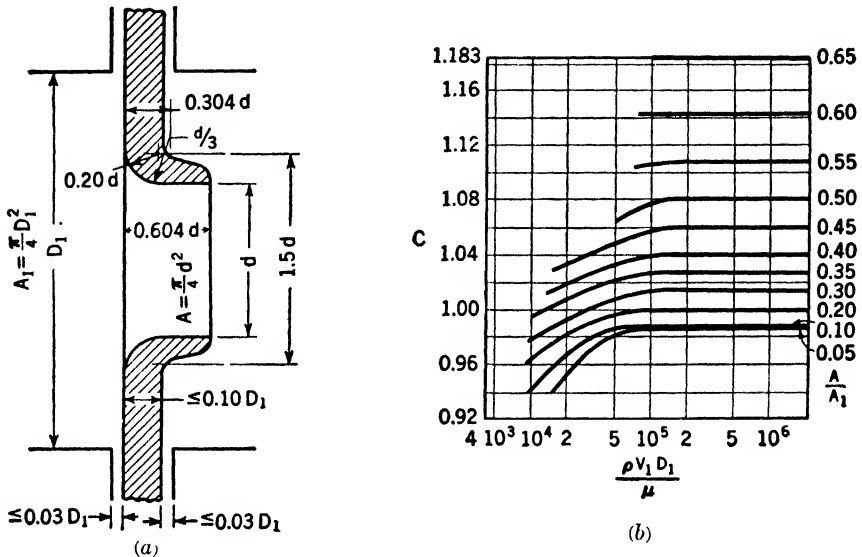


FIG. 8.26. — (a) VDI nozzle. (b) Coefficient for VDI nozzle as a function of Reynolds number and A/A_1 . (From *NACA Tech. Mem. 952*, reference 11.)

form. The discharge coefficient for the orifice, however, includes the correction for the contraction of the jet. There is no contraction in a well-designed nozzle.

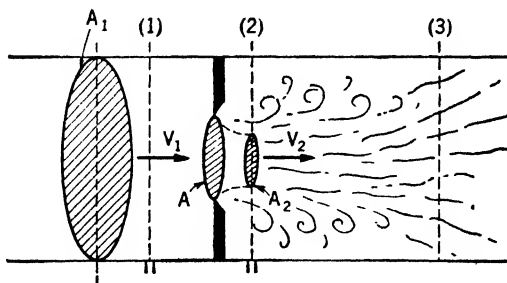


FIG. 8.27. — Thin-plate orifice.

The VDI has also developed a standard orifice, which, together with curves for discharge coefficient, is shown in Fig. 8.28.

There is no guidance of the jet downstream from a nozzle or orifice. Consequently, the over-all loss occurring in either of these instruments is larger than that for a Venturi meter. For either nozzle or orifice, the ratio $(p_1 - p_2)/\Delta p$ has a value of about 0.95 if $A_2/A_1 = 0.04$ and a value of about 0.25 if $A_2/A_1 = 0.80$. As would be expected, the loss in an orifice tends to be slightly greater than that in the corresponding nozzle.

In permanent installations, at least where the loss is a deciding factor,

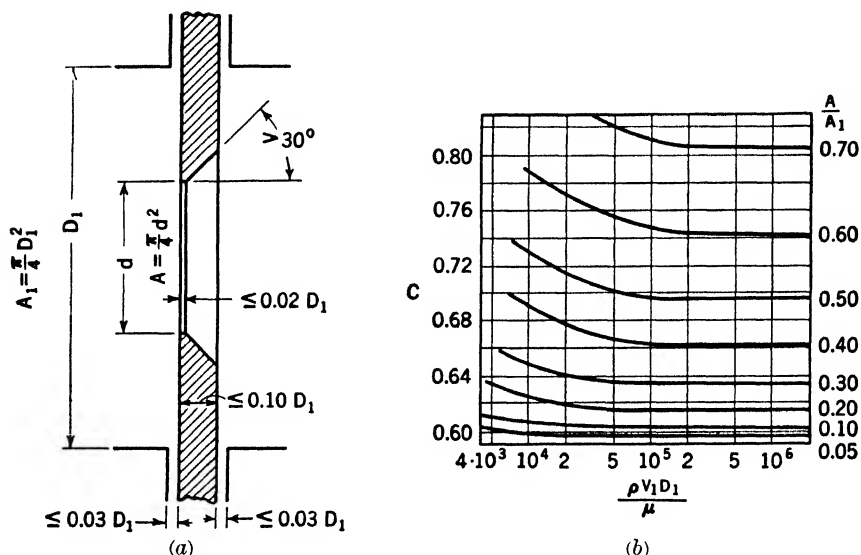


FIG. 8.28. — (a) VDI orifice. (b) Coefficient for VDI orifice as a function of Reynolds number and A/A_1 . (From NACA Tech. Mem. 952, reference 11.)

the Venturi meter is preferable to a nozzle or orifice. However, the small size and convenience of installation indicate one of the latter instruments for most other applications. The fact that a standard nozzle or orifice can be used without calibration is also an advantage.

SELECTED BIBLIOGRAPHY

1. ASME Research Committee: "Fluid Meters," 4th ed., Part I, p. 56, American Society of Mechanical Engineers, New York, 1937.
2. BAKHMETEFF, B. A.: "The Mechanics of Turbulent Flow," p. 55, Princeton University Press, Princeton, N.J., 1936.
3. CROFT, H. O.: "Thermodynamics, Fluid Flow and Heat Transmission," p. 116, McGraw-Hill Book Company, Inc., New York, 1938.
4. DRYDEN, H. L.: A Review of the Statistical Theory of Turbulence, *Quart. Applied Math.*, vol. 1, pp. 7-42, 1943.
5. HOFMANN, A.: Der Verlust in 90°-Rohrkrümmern mit gleichbleibendem Kreisquerschnitt, *Mitt. hydraul. Inst. T. H. München*, No. 3, Oldenbourg, Munich, 1929.
6. KÁRMÁN, TH. VON: Turbulence and Skin Friction, *J. Aeronaut. Sci.*, vol. 1, p. 1, 1934.

7. LANGHAAR, H. L.: Steady Flow in the Transition Length of a Straight Tube, *J. Applied Mechanics*, vol. 9, pp. 55-58, 1942.
8. MADISON, R. D., and J. R. PARKER: Pressure Losses in Rectangular Elbows, *Trans. Am. Soc. Mech. Engrs.*, vol. 58, pp. 167-176, 1936.
9. MILLIKAN, C. B.: Turbulent Flows in Channels and Circular Tubes, *Proc. Fifth International Congress for Applied Mechanics*, pp. 386-392, John Wiley & Sons, Inc., New York, 1939.
10. MOODY, L. F.: Friction Factors for Pipe Flow, *Trans. Am. Soc. Mech. Engrs.*, vol. 66, pp. 671-684, 1944.
11. N.A.C.A.: Standards for Discharge Measurement (translation of German Industrial Standard 1952), *Tech. Mem.* 952, Washington, 1940.
12. NIKURADSE, J.: Gesetzmässigkeiten der turbulenten Strömung in glatten Röhren, *VDI Forschungsheft*, 356, 1932; Strömungsgesetze in rauen Röhren, *VDI Forschungsheft*, 361, 1933.
13. REYNOLDS, O.: An Experimental Investigation of the Circumstances Which Determine Whether the Motion of Water Shall Be Direct or Sinuous, and of the Laws of Resistance in Parallel Channels, *Phil. Trans. Roy. Soc. (London)* vol. 174, 1883.
14. TIMOSHENKO, S.: "Theory of Elasticity," p. 263, McGraw-Hill Book Company, Inc., New York, 1934.
15. WEISBACH, JULIUS: "Die experimental Hydraulik," p. 133, J. S. Engelhardt. Freiberg, 1855.

CHAPTER IX

COMPRESSIBILITY PHENOMENA

Compressibility is becoming increasingly important in the problems that mechanical and aeronautical engineers are called upon to solve. There are three general types of problem in which compressibility must be taken into account. First in importance to engineers are high-speed flows, encountered, for example, in the design of aircraft, steam and gas turbines, compressors, jet- and rocket-propulsion devices, and projectiles. These high-speed flows can be divided into those which occur inside of ducts or passages between blades of machines and those which take place around bodies moving relative to the fluid. The designation "high speed" means that the velocities reached are on the order of the velocity of sound propagation through the fluid (see Art. 7.24).

The second type of problem deals with the sound waves set up by accelerated motion of a body in contact with a fluid. This type is characterized by large accelerations rather than by high velocities. Well-known engineering examples are problems in the design of rooms for specific acoustical uses, noise reduction, water hammer, and cavitation.

The third type of problem is concerned with large changes in elevation. The weight of the overlying air layers makes the density of air at ground level several times greater than that a few miles above the earth's surface.

Practical application of this type of problem is limited to meteorology.

The remainder of this chapter and later references to compressibility will deal mainly with problems of high-speed flow.

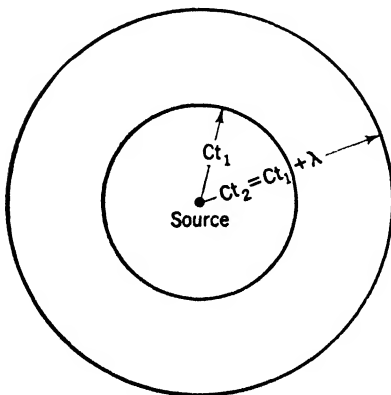


FIG. 9.1.

9.1. Motion of a Point Source of Sound. Consider a sphere the radius of which varies periodically with time and which is immersed in a compressible fluid. We assume its radius is small compared with the length of the radiated sound waves, and we call the sphere a "point source" of sound. Suppose first that the source is at rest

in the fluid, which extends indefinitely in all directions. Since the wave motion is cyclic, we can choose any convenient point in the wave as the "front." All parts of a wave front move with the same speed C relative

to the fluid. Successive wave fronts are, therefore, concentric spheres having the source as center, and each with radius Ct , where t is the elapsed time since the wave front left the source. The distance between successive

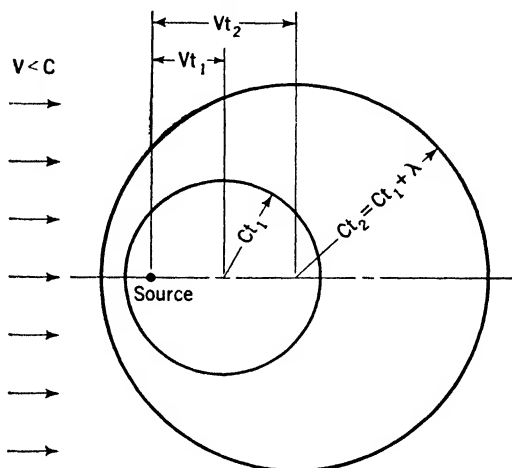


FIG. 9.2.

fronts is the wave length λ . In Fig. 9.1 are shown the circular traces of these spheres in the plane of the source.

If we now suppose that the fluid moves relative to the source with a velocity V less than C , the wave-front spheres are no longer concentric but are related as shown in Fig. 9.2. Each has as center that point in the fluid

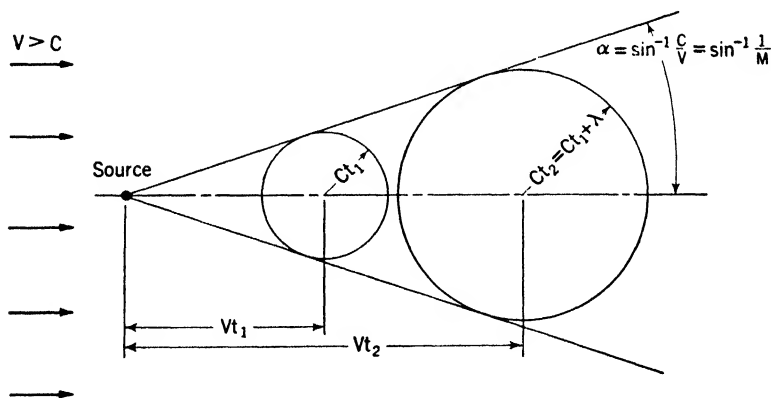


FIG. 9.3.

which coincided with the source at the instant the front left the source.

Finally, assume that V is greater than C . The velocity of wave propagation relative to the fluid is still the same, so that the wave fronts are again spheres, but they no longer surround the source (Fig. 9.3). On the

contrary, all wave-front circles are tangent to a line making the angle α with the direction of flow, such that

$$\sin \alpha = \frac{C}{V} = \frac{1}{M}$$

where M is the Mach number, referred to in Chap. VII. This line is the generator of a cone of apex angle 2α ; the line is called a "Mach line" and α the "Mach angle."

9.2. Subsonic Motion of a Body. To apply these observations to the steady motion of a rigid body of finite size, such as a projectile or airfoil, consider how the pressure and velocity fields that move along with the body are created. The final velocity of the body can be thought of as the result of a number of small impulsive increases in velocity. Each impulsive change in the motion gives rise to a pressure pulse or sound wave, which emanates from the body. The initial amplitude of the pulse will vary over the surface of the body, since the amplitude at any surface element depends on the component of the acceleration normal to the element. As the pulse passes any point in the fluid, it changes the pressure and velocity there. A positive pulse produces a velocity change having the direction of pulse propagation, while a negative pulse gives a change in the opposite direction. The new pressure and velocity will persist until another wave passes, *i.e.*, until a further acceleration of the body occurs.

A simple example is the one-dimensional motion of a piston in a long cylinder filled with fluid. If the piston is given a small increase in velocity, a pressure pulse will travel down the cylinder with velocity C relative to the undisturbed fluid. As the wave front passes, the fluid acquires the velocity of the piston. This velocity will be maintained until the piston is again accelerated, if no waves are reflected from the far end of the cylinder.

If the velocity relative to a body is everywhere subsonic, it is clear that these pulses will radiate in all directions, so that the pressure and velocity fields accompanying the body extend indefinitely toward front, rear, and sides. These fields die away gradually at some distance from the body, owing to the decrease in amplitude of each pulse as it spreads out. Steady subsonic motion of a body is, therefore, characterized by a continuous pressure and velocity distribution.

As the speed of the body approaches that of sound in the undisturbed fluid, the flow near the body becomes very complex and unsteady, because the local sound velocity is exceeded at certain points. These local disturbances may be of great importance, as, for example, in affecting lift and drag of an airfoil. These things will be discussed in Art. 10.13; here we merely note that, except for certain local regions, the flow will remain sub-

sonic so long as the speed of the body is subsonic, and therefore pressure pulses will be propagated throughout the distant field of flow.

9.3. Supersonic Motion of a Body. In a sequence of positive pressure pulses, each produces a small forward velocity in the fluid through which it has passed and each moves at sonic speed with respect to fluid between it and its immediate precursor. Each pulse, therefore, overtakes ones in front, and it can be shown analytically that the speed of the resultant steep-fronted wave exceeds the sound velocity by an amount depending on its amplitude [5].

Let a body be accelerated from a speed slightly below sound velocity to one slightly above it. The pressure pulses resulting from this small but finite velocity change coalesce into a single steep-fronted wave whose speed is slightly greater than C . Instead of moving indefinitely far ahead of the body, as in subsonic flow, this wave is halted where it reaches essentially undisturbed fluid. The limiting position of the wave marks the practical limit of the pressure and velocity fields established during the subsonic regime.

On the axis, the wave is normal to the relative velocity of the undisturbed fluid. Away from the axis, the magnitude of the wave diminishes, since these parts are farther from the source of disturbance. Hence the propagation velocity of parts farther from the axis is less than that of nearer ones; and at some distance from the axis the amplitude will be so small that the speed is equal to C . The limiting position of the wave is thus not a straight line normal to the axis but a curve that bends slightly backward and approaches a straight line making the Mach angle with the axis. Such a line is indicated in Fig. 9.4. The complex pattern behind the body, caused by the local disturbances referred to above, is suggested by the line at the rear.

If the relative velocity of body and fluid is again slightly increased, a pulse is sent out and the body will move closer to the limiting line until the pulse reaches it. This coalition increases both the size of the pressure jump and its velocity of propagation. Near the axis, the resultant pressure front moves with the speed of the body, while to the sides its amplitude and speed decrease, and it gradually curves backward to make the Mach angle with the axis

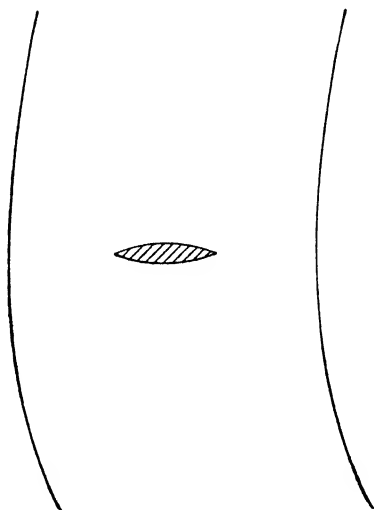


FIG. 9.4. — Wave pattern produced by a body moving at a speed slightly greater than the sound velocity.

at some distance from it. It will be noted that the Mach angle corresponding to this new state of motion is less than that previously subsisting.

As the speed is further increased, the pressure front is approached more and more closely by the body and its magnitude becomes greater. Figure

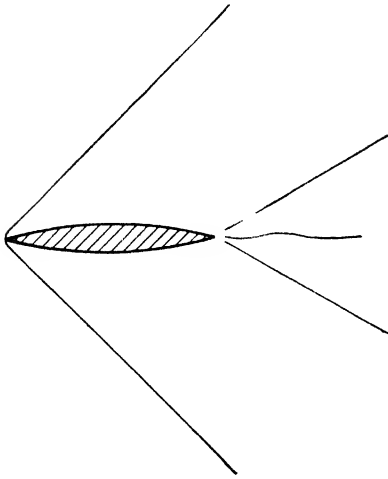


FIG. 9.5. — Wave pattern produced by a body moving faster than in Fig. 9.4.

9.5 shows the flow pattern for a tapering body at a Mach number that is considerably greater than unity. In Fig. 9.5 the forward shock is actually in contact with the body. Theory and experiment agree that, for a body with a nose angle that is not too large, there is a limiting value of M below which the nose wave does not touch the body but passes in front of it. If M is above this limit, however, the shock springs from the nose of the body.

The shock lies ahead of a body having a rounded nose or too large a nose angle, even at very high Mach numbers.

If the nose wave is detached from the body, as in Fig. 9.4, there is always at least a small subsonic region between the wave and the nose. On the other hand, if the wave springs directly from the nose, as in Fig. 9.5, there may or may not be a region of subsonic flow.

The expansion of the flow along the sides of the body takes place continuously since expansion shocks do not occur (see Art. 9.7). At the rear, however, a second compression shock is formed, where the flow bends back into a parallel stream. This shock originates in the local supersonic regions that develop at the sides of the body while the Mach number of the main flow is still less than unity. These localized shocks gradually move to the rear as the speed increases and eventually assume the form shown in Fig. 9.5. The slope of the tail shock is different from that at the front, because both the magnitude and direction of the velocity entering the shock differ from those in the undisturbed stream.

9.4. Frictionless Flow in a Convergent-divergent Nozzle. It is useful to consider in detail a one-dimensional flow, because the main features of compressibility can be brought out with the aid of relatively simple mathematics. The horizontal passage of Fig. 9.6 will be treated as a single stream tube, *i.e.*, the velocity, pressure, density, and temperature will be assumed uniform over any cross section. For any two sections separated by a distance dx , the continuity and Euler equations are

$$d(\rho A V) = 0 \quad (9.1)$$

$$\frac{dp}{\rho} + V dV = 0 \quad (9.2)$$

Equation (9.1) is readily transformed to

$$\frac{dA}{A} = -\frac{dV}{V} - \frac{d\rho}{\rho} = -\frac{dV}{V} \left(1 + \frac{V^2 d\rho}{\rho V dV}\right)$$

Substituting $dp = -\rho V dV$, from Eq. (9.2), we obtain

$$\frac{dA}{A} = -\frac{dV}{V} \left(1 - \frac{V^2}{dp/d\rho}\right) \quad (9.3)$$

It is seen that $\sqrt{dp/d\rho}$ is a critical value for the velocity. If V is everywhere less than $\sqrt{dp/d\rho}$, the fluid will speed up in the convergent passage, reach a maximum at the throat, and then slow down in the divergent passage. The compressible flow is qualitatively like an incompressible one.

It is seen further that V must be less than $\sqrt{dp/d\rho}$ until the flow reaches

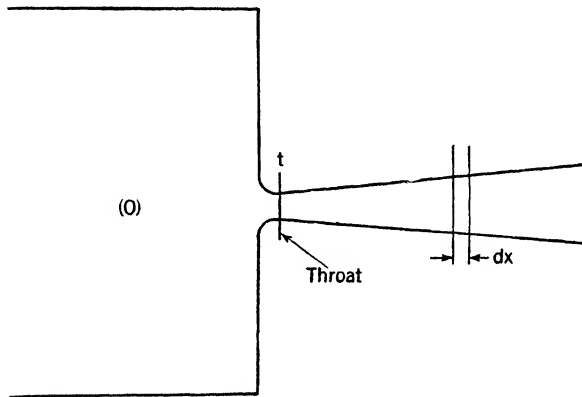


FIG. 9.6.

the throat and that the maximum velocity attainable at the throat is $\sqrt{dp/d\rho}$. If this critical speed is reached at the throat, the velocity in the divergent passage may be either sub- or supersonic. It cannot, however, be equal to $\sqrt{dp/d\rho}$. In the case of supersonic flow the velocity increases along the divergent passage—a behavior opposite to that in subsonic motion.

In Art. 7.24 it is shown, if friction be neglected, that a small plane pressure pulse in a one-dimensional flow moves relative to the undisturbed fluid with a velocity

$$C = \sqrt{\frac{\delta p}{\delta \rho}} \quad (9.4)$$

Here δp and $\delta \rho$ are the differences in pressure and density that constitute the pulse, as shown in Fig. 9.7. The changes δp and $\delta \rho$ for a gas are found to occur both frictionlessly and adiabatically; that is, $\delta p / \delta \rho$ is derivable from the relation

$$\frac{p}{\rho^k} = \text{constant} \quad (9.5)$$

where k is the so-called "isentropic exponent" and is constant over a considerable range of pressure. Thus

$$C = \sqrt{\frac{\delta p}{\delta \rho}} = \sqrt{\frac{k p}{\rho}} \quad (9.6)$$

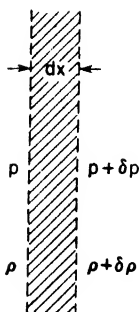


FIG. 9.7.

The sound velocity anywhere in the fluid is seen to depend on the local value of the ratio p/ρ .

If such a pulse is created by some means in the nozzle of Fig. 9.6, it will tend to move relative to the fluid with the velocity $C = \sqrt{k p / \rho}$, where p and ρ are the pressure and density at any section of the nozzle. The pulse can, therefore, be stationary only where the velocity of the fluid is equal to $\sqrt{k p / \rho}$. But the pressure-density relation in a smooth, insulated nozzle is given by Eq. (9.5), so that the critical velocity

$$\sqrt{\frac{dp}{d\rho}} = \sqrt{\frac{k p}{\rho}} \quad (9.7)$$

In this frictionless adiabatic flow the critical velocity $\sqrt{dp/d\rho}$ and the sound velocity are identical, and the pulse can be stationary only at the throat of the nozzle.

The adiabatic character of sound-wave transmission is practically independent of the temperature of the gaseous medium. That is, negligible heat transfer results from temperature differences associated with a sound wave, regardless of the bulk temperature of the gas. If, for example, the temperature of the gas flowing through a nozzle were maintained approximately constant by heat transfer through the wall, the sound velocity would, nevertheless, be given by Eq. (9.6). The critical velocity, however, would in this case be equal to $\sqrt{p/\rho}$, which is less than the sound velocity $C = \sqrt{k p / \rho}$. A sound wave could, therefore, be propagated upstream through the throat of the nozzle, even though supercritical flow velocities were attained.

With regard to the practically important case of adiabatic flow, the stream velocity can be equal to the local sound velocity only at the throat; upstream from the throat the velocity is less than the local sound speed; and downstream from the throat it may be more or less than the local sonic velocity. This kind of flow will now be further investigated.

9.5. Frictionless Adiabatic Flow in a Nozzle. Combining Eqs. (9.2) and (9.5) and integrating from section 0 in the reservoir, where the velocity is negligible, to any section of the nozzle, we get

$$V = \sqrt{\frac{2k}{k-1} \frac{p_0}{\rho_0} \left[1 - \left(\frac{p}{p_0} \right)^{(k-1)/k} \right]} \quad (9.8)$$

For given values of k and p_0/ρ_0 , the velocity depends only on the ratio p/p_0 . The maximum possible velocity, which is attained for $p/p_0 = 0$, is finite and equal to $\sqrt{[2k/(k-1)](p_0/\rho_0)}$ (see Fig. 9.8).

It is of interest to find the sound velocity at the throat C_t in terms of

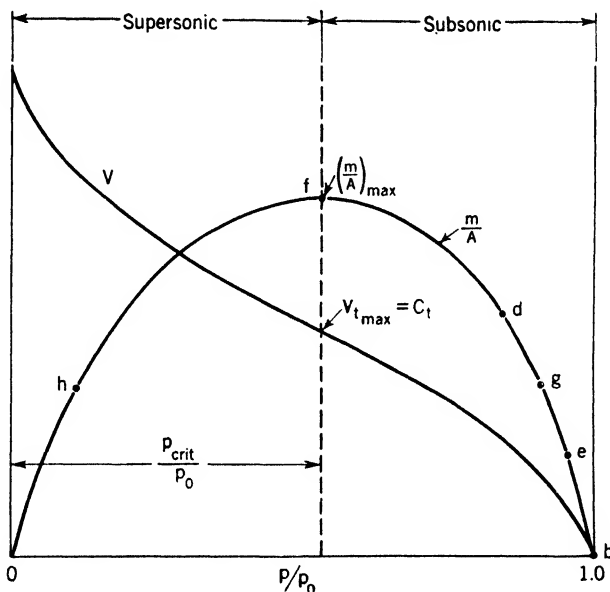


FIG. 9.8. — Velocity V and mass flow per unit area m/A versus pressure ratio p/p_0 for a frictionless adiabatic flow through a convergent-divergent nozzle.

p_0/ρ_0 and k . For this purpose consider the mass flow per unit area m/A , which by continuity equals ρV . Computing the rate of change of m/A with respect to p/p_0 and using Eqs. (9.2), (9.6), and (9.7), we get

$$\begin{aligned} \frac{d(m/A)}{d(p/p_0)} &= \frac{d(\rho V)}{d(p/p_0)} \\ &= \rho \frac{dV}{d(p/p_0)} \left(1 + V^2 \frac{d\rho}{\rho V dV} \right) \\ &= \rho \frac{dV}{d(p/p_0)} \left(1 - \frac{V^2}{C^2} \right) \end{aligned}$$

Figure 9.8 shows $dV/d(p/p_0)$ to be negative everywhere, so that $d(m/A)/d(p/p_0)$ is positive for $V > C$, zero for $V = C$, and negative for

$V < C$. Recalling that V can equal C only at the throat, we conclude that the value of p/p_0 at which m/A is a maximum is also the value at which $V = V_{t \max} = C_t$. This value of p/p_0 is called the "critical-pressure ratio." Multiplying Eq. (9.8) by ρ and using Eq. (9.5), we get

$$\frac{m}{A} = \rho V = \rho_0 \left(\frac{p}{p_0} \right)^{1/k} V = \sqrt{\frac{2k}{k-1}} \rho_0 p_0 \left[\left(\frac{p}{p_0} \right)^{2/k} - \left(\frac{p}{p_0} \right)^{(k+1)/k} \right] \quad (9.9)$$

which is plotted in Fig. 9.8. Setting $d(m/A)/d(p/p_0) = 0$, we find the critical pressure ratio to be

$$\frac{p_{\text{crit}}}{p_0} = \left(\frac{2}{k+1} \right)^{k/(k-1)} \quad (9.10)$$

The value of $V_{t \max}$ or C_t is now determined from Eqs. (9.10) and (9.8).

$$V_{t \max} = C_t = \sqrt{\frac{2k}{k+1} \frac{p_0}{\rho_0}} = \sqrt{\frac{2}{k+1}} C_0 \quad (9.11)$$

We shall now consider the theoretical pressure distribution along the divergent part of a nozzle, since it has features that show the limitations

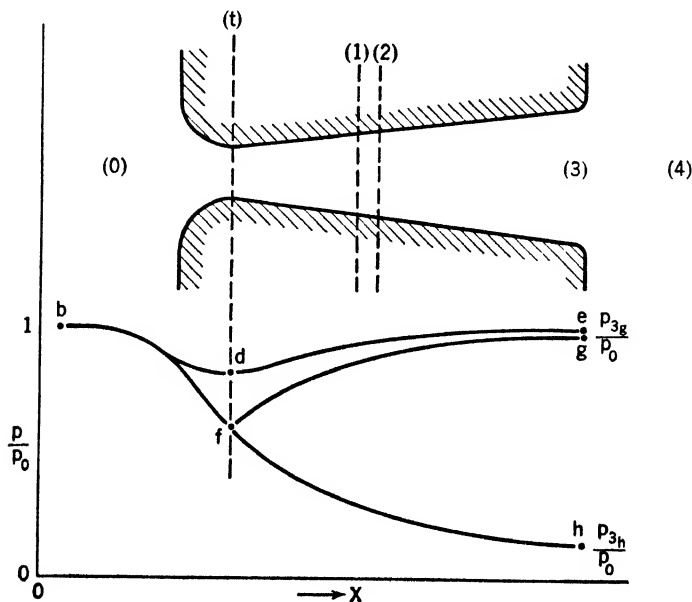


FIG. 9.9. — Pressure distribution along the axis of a convergent-divergent nozzle. (Reproduced from L. Prandtl, *The Flow of Liquids and Gases*, in "The Physics of Solids and Fluids," Blackie and Son, Ltd., London and Glasgow.)

of the one-dimensional frictionless theory and point the way to further investigation. In Fig. 9.9 are shown the pressure distributions along a

nozzle of given shape, for both sub- and supersonic flow in the divergent portion. These curves are easily obtained from the m/A curve of Fig. 9.8, since A is a known function of x for a given nozzle. Corresponding points in Figs. 9.8 and 9.9 are labeled with the same letter. If m is chosen small enough, the flow is subsonic throughout and a curve of the type bde is obtained. The maximum possible value of m is the one corresponding to $(m/A)_t = (m/A)_{\max}$, which gives either curve bfg or bfh .

It will be observed that in the subsonic regime any value of exit pressure p_3 is allowed such that $p_{3u}/p_0 \leq p_3/p_0 \leq 1$. The upper limit 1 is approached

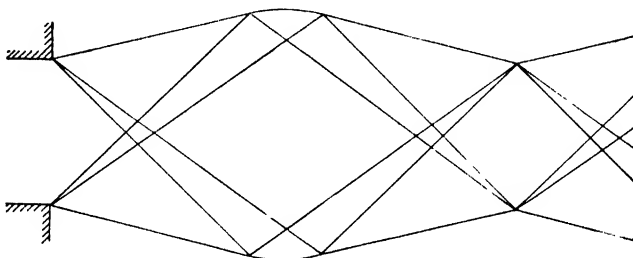


FIG. 9.10. — Wave pattern of emergent jet when receiver pressure is slightly less than at nozzle exit. (Reproduced from L. Prandtl, *The Flow of Liquids and Gases*, in "The Physics of Solids and Fluids," Blackie and Son, Ltd., London and Glasgow.)

as m becomes smaller or A_3 larger. In the supersonic region, however, only a single value of p_3 is allowed, namely, p_{3h} . The question of what happens if the receiver pressure p_4 lies between p_{3u} and p_{3h} is left unanswered by the present analysis.

Experiments show that small, oblique, standing pressure waves occur just outside the nozzle if the receiver pressure is only slightly different from

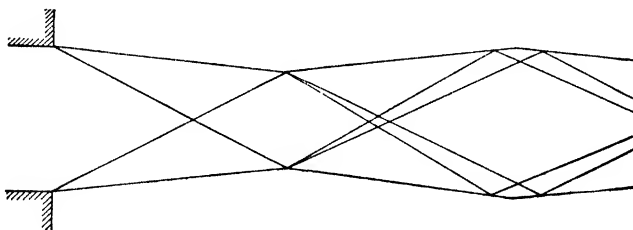


FIG. 9.11. — Wave pattern of emergent jet when receiver pressure is slightly greater than at nozzle exit. (Reproduced from L. Prandtl, *The Flow of Liquids and Gases*, in "The Physics of Solids and Fluids," Blackie and Son, Ltd., London and Glasgow.)

p_{3h} . These waves are reflected at certain parts of the boundary of the free jet where discontinuities in density occur. Figures 9.10 and 9.11 are from photographs by L. Prandtl of the flow from a two-dimensional nozzle. The first of these shows the expansion if $p_4 < p_{3h}$; the second shows the compression if $p_4 > p_{3h}$.

These pictures were made by the schlieren method, which takes ad-

vantage of the fact that a ray of light is deflected if it passes through a medium of nonuniform density. A typical apparatus is illustrated in Fig. 9.12. Light from a source at *A* is focused near the edge of a plane mirror *C*. The reflected light traverses a long path to the concave mirror *D* and back again to a second focus at the knife-edge *E*, then through a lens system to a

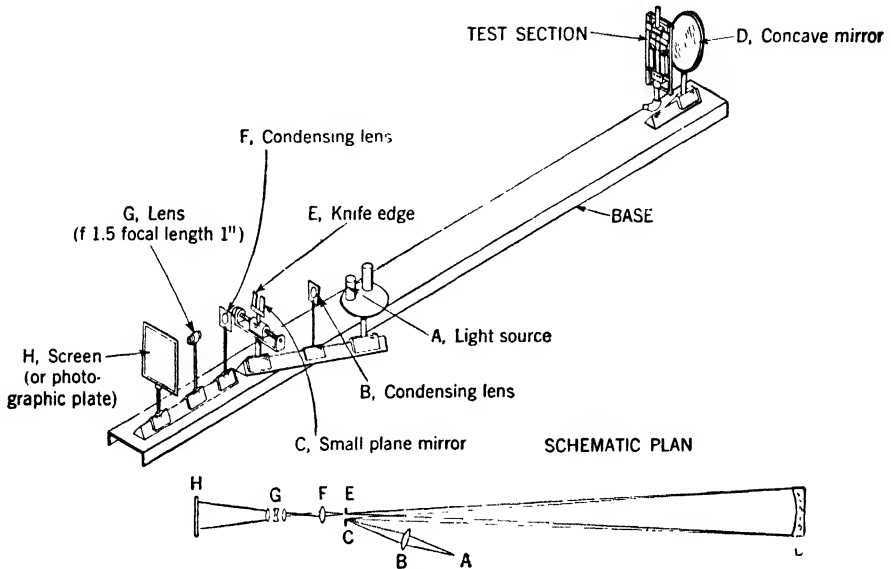


Fig. 9.12. — Schlieren apparatus. (Courtesy of F. Lustwerk.)

ground-glass screen or photographic plate *H*, where an image is formed of a two-dimensional airflow taking place in front of mirror *D*. The steep density gradients set up in the pressure waves cause the transient light to be bent slightly. Some of these bent rays are cut off by the knife-edge *E*; and others, which would normally be cut off, pass by the knife-edge and strike the screen. A region in which the density gradient is large thus appears on the screen either as very dark or very light.

A convergent nozzle is a special case of the convergent-divergent passage. If there is no divergent portion, it is readily seen that the flow will be everywhere subsonic so long as the receiver pressure is greater than the critical value. If the receiver pressure is equal to the critical, the throat pressure will also have this value and the throat velocity will be sonic. If the receiver pressure is less than the critical, the throat pressure and velocity will still have their critical values, but after leaving the nozzle the stream will expand suddenly to the receiver pressure.

9.6. Compression Shocks in a Nozzle. If the receiver pressure p_4 of Fig. 9.9 is gradually raised above p_{3h} , schlieren photographs reveal that the waves of Fig. 9.11 move upstream into the interior of the nozzle. The

shape of the waves changes also, and the flow downstream from them is considerably disturbed. Figure 9.13, taken from a schlieren photograph, shows oblique pressure waves springing from the wall, followed by a transverse wave extending over a part of the cross section. The flow appears to separate from the wall at these shocks, while downstream there are several smaller transverse shocks. It is found that the flow at the exit is subsonic and that the pressure p_3 is equal to p_4 . Upstream from the shocks, however, the flow remains supersonic and entirely unaffected by the rise in receiver pressure.

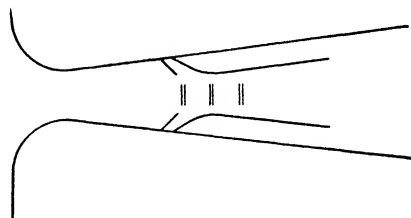


FIG. 9.13. — Disturbances in a nozzle when the receiver pressure is considerably greater than the theoretical value for unretarded flow.

If p_4 is made still larger, the disturbance becomes very concentrated and moves nearer the throat, as shown in Fig. 9.14. Very little flow separation occurs. Downstream from this transverse shock the flow is subsonic, while upstream it remains supersonic and unaffected by the changes in p_4 . Pressure measurements indicate a sudden rise in pressure at the shock, followed by a further gradual

rise to the value p_4 at the exit.

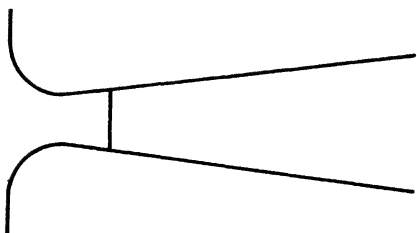


FIG. 9.14. — Transverse shock in a nozzle.

Conditions as shown in Fig. 9.13 are so chaotic that it has so far been impossible to analyze them theoretically, but the concentrated transverse shock of Fig. 9.14 is amenable to theoretical treatment. To carry through such an analysis the shock is assumed to be of infinitesimal thickness, and friction is neglected everywhere, except

in the shock itself. It is also necessary to make additional assumptions about the nature of the fluid. For simplicity we assume it to be a "perfect" gas, that is, one that obeys the gas law

$$p = \rho gRT \quad (9.12)$$

and has constant specific heats. It is shown in thermodynamics texts that, for a perfect gas, the intrinsic energy u depends only on temperature. The specific heats, therefore, are

$$c_v = \left(\frac{\partial u}{\partial T} \right)_v = \frac{\Delta u}{\Delta T} \quad (9.13)$$

$$c_p = \left\{ \frac{\partial [(p/\rho) + u]}{\partial T} \right\}_p = \frac{\Delta [(p/\rho) + u]}{\Delta T} = \frac{\Delta h}{\Delta T} \quad (9.14)$$

In these equations, R is the gas constant; T is the absolute temperature; h , defined as $(p/\rho) + u$, is the enthalpy; c_p is the specific heat at constant pressure; and c_v is the specific heat at constant volume. For a perfect gas, the ratio of the specific heats is equal to the isentropic exponent.

$$\frac{c_p}{c_v} = k \quad (9.15)$$

It is now supposed that a finite pressure jump occurs between sections 1 and 2 of Fig. 9.9. Since the thickness of this shock is assumed infinitesimal, 1 and 2 may be taken so close together that the difference in their areas and the wall friction force on the narrow strip between them are negligible. The continuity equation, therefore, is

$$\rho_1 V_1 = \rho_2 V_2 = \frac{m}{A_1} \quad (9.16)$$

and the momentum equation [Eq. (6.6)] takes the form

$$p_1 - p_2 = \rho_2 V_2^2 - \rho_1 V_1^2 \quad (9.17)$$

Since the shock is accompanied by frictional effects in the fluid, the Euler equation cannot be used between 1 and 2 but must be replaced by the more general energy equation [Eq. (5.10)], which may be written for this adiabatic flow as

$$h_1 + \frac{V_1^2}{2} = h_2 + \frac{V_2^2}{2} = h_0 \quad (9.18)$$

Here h_0 is the enthalpy in the reservoir. With the aid of Eqs. (9.12) to (9.15), the energy formula becomes

$$\frac{k}{k-1} \frac{p_1}{\rho_1} + \frac{V_1^2}{2} = \frac{k}{k-1} \frac{p_2}{\rho_2} + \frac{V_2^2}{2} = \frac{k}{k-1} \frac{p_0}{\rho_0} \quad (9.19)$$

Combination of Eqs. (9.16), (9.17), and (9.19) yields, finally, the result

$$V_1 V_2 = \frac{2k}{k+1} \frac{p_0}{\rho_0} \quad (9.20)$$

which will be recognized from Eq. (9.11) as equivalent to

$$V_1 V_2 = C_t^2 \quad (9.21)$$

The geometric mean of V_1 and V_2 is equal to the sound velocity at the throat of the nozzle.

It is now readily demonstrated that, if V_1 is supersonic, V_2 will be subsonic. The pressure ratio p_2/p_0 can be found in terms of p_1/p_0 , by use of Eq. (9.8) between 0 and 1, where the flow is frictionless, and Eqs. (9.16), (9.17), and (9.20).

definite point in the nozzle for any value of p_3 between the limits p_{3i} and p_{3e} (see Fig. 9.15). The theory does not apply if p_3 is between p_{3h} and p_{3i} .

As previously mentioned, a transverse shock is observed to occur only if p_3 is but slightly below p_{3e} . If p_3 lies in this narrow range, there is reasonable agreement between experiment and theory. For lower values of p_3 , however, the transverse shock does not fill the entire passage and is preceded by oblique shocks. These complexities are due to the interaction between friction and compressibility and are therefore not predicted by the present theory, which neglects friction except in a region of infinitesimal thickness. These phenomena will be taken up in the next chapter in the discussion of the boundary layer.

The approximate thickness of a shock wave can be calculated if the mechanism of viscous action and of thermal conduction within the shock is taken into account [5]. The thickness of a shock wave in air is estimated to lie between 10^{-5} and 10^{-4} in.

9.7. On the Impossibility of a Rarefaction Shock. Although only compression shocks are observed in nature, none of the preceding work hints at the impossibility of a shock of rarefaction. Proof of such impossibility is based on the second law of thermodynamics, a discussion of which is outside the scope of this book. It may be useful, however, to present a brief treatment of this problem, even though it is impossible to start from first principles. The existence of the entropy will be taken for granted, as well as the fact that the entropy of a system cannot decrease during an adiabatic process. The reader will find these matters discussed in texts on thermodynamics.*

For the adiabatic flow through a nozzle it will be shown that the entropy increases as the gas passes through a compression shock but would decrease in a rarefaction shock. The latter will thus be shown to be impossible.

The change in entropy of unit mass of fluid as it passes from an initial state 1 to an arbitrary final state is defined as

$$s - s_1 = \int_1 \frac{dq}{T} \quad (\text{reversible path only}) \quad (9.27)$$

where dq is the heat transfer to the unit mass during an infinitesimal change and T is the absolute temperature. The integral must be taken along a reversible path, a requirement that is fulfilled in this case if friction is supposed to be absent. The first law of thermodynamics may thus be written as Eq. (5.12), which in differential form is $dq = du + p d(1/\rho)$. The change in entropy now becomes

$$s - s_1 = \int_1 \frac{du + p d(1/\rho)}{T} = \int_1 \left(\frac{dh}{T} - \frac{dp}{\rho T} \right) \quad (9.28)$$

* See, for example, reference 3 at the end of this chapter.

Using Eqs. (9.12) to (9.15), we get

$$s - s_1 = c_p \ln \frac{T}{T_1} - c_p \frac{k-1}{k} \ln \frac{p}{p_1} \quad (9.29)$$

The change in entropy as the gas passes through a shock is found, after considerable reduction, to be

$$s_2 - s_1 = c_p \ln \left[\frac{V_2}{V_1} \left(\frac{1 - \frac{k-1}{k+1} \frac{V_2}{V_1}}{\frac{V_2}{V_1} - \frac{k-1}{k+1}} \right)^{1/k} \right] \quad (9.30)$$

It is readily shown from Eq. (9.30) that the entropy increases if $V_2 < V_1$, and vice versa. Therefore, since a decrease in entropy is not permitted, only a compression shock can occur.

Equation (9.30) is valid only for a perfect gas. Similar results can, however, be obtained as follows for any gas or vapor having known

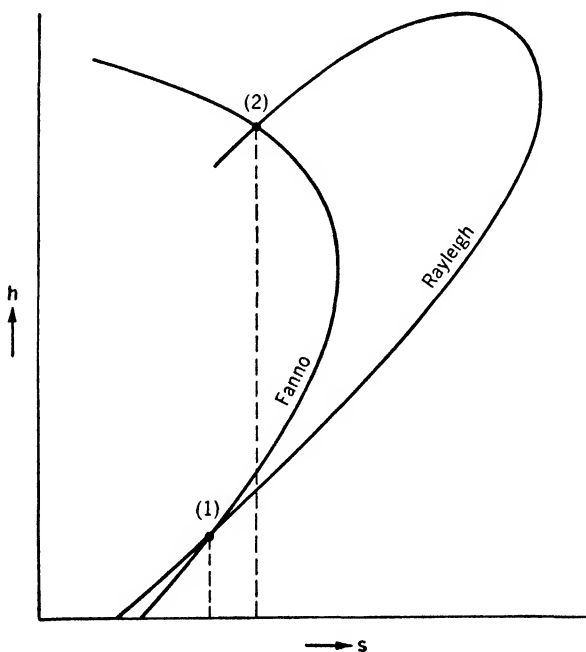


FIG. 9.16.

properties: The continuity and energy requirements of Eqs. (9.16) and (9.18) give a relation between enthalpy and density in a shock.

$$h + \frac{m_2}{2A_1^2\rho^2} = h_0 \quad (9.31)$$

Since the entropy is a known function of any two independent properties of the gas, such as enthalpy and density, we can eliminate the density by using Eq. (9.31) and obtain a relation between entropy and enthalpy that must be satisfied in the shock. Such a relation is shown schematically in Fig. 9.16, as the curve marked "Fanno line." On the other hand, the continuity and momentum requirements of Eqs. (9.16) and (9.17) yield another relation between enthalpy and density that must be satisfied in the shock. A second curve of enthalpy versus entropy can therefore be drawn independently of the Fanno line. This curve is known as a "Rayleigh line" and is indicated in Fig. 9.16. The points of intersection of the Fanno and Rayleigh lines determine the state of the gas at the beginning and end of the shock. Point 2 at higher entropy is necessarily the final state.

9.8. Adiabatic Flow in a Pipe with Friction. For simplicity we neglect gravity and assume the velocity to be uniform over any cross section.

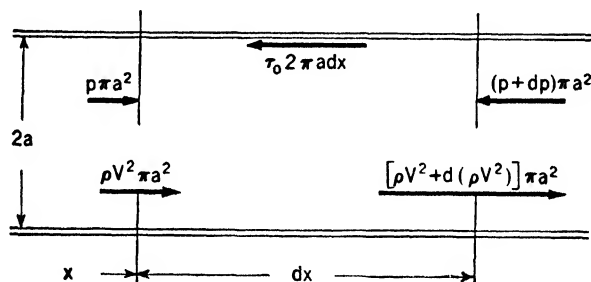


FIG. 9.17.

A relation between pressure drop and wall shearing stress τ_0 is given by the momentum equation applied between the cross sections shown in Fig. 9.17.

$$dp + \frac{2}{a} \tau_0 dx + d(\rho V^2) = 0 \quad (9.32)$$

The mass flow per unit area is constant for a pipe of uniform diameter, so that the continuity equation is

$$\rho V = G = \text{constant} \quad (9.33)$$

Combining Eqs. (9.32) and (9.33), we get

$$\frac{dp}{dx} \left(1 - \frac{V^2}{dp/d\rho} \right) = - \frac{2\tau_0}{a} \quad (9.34)$$

and

$$\frac{dV}{dx} \left(1 - \frac{dp/d\rho}{V^2} \right) = - \frac{2\tau_0}{aG} \quad (9.35)$$

Equations (9.34) and (9.35) apply to any sort of pipe flow—adiabatic, isothermal, or other—because they are based only on momentum and con-

tinuity. It is seen that $\sqrt{dp/d\rho}$ is a critical value for velocity, just as in a frictionless nozzle flow. If $V < \sqrt{dp/d\rho}$, dV/dx is positive. The velocity will therefore increase; and if it increases faster than $\sqrt{dp/d\rho}$, dV/dx will become larger and larger, approaching infinity as V approaches $\sqrt{dp/d\rho}$. If V should become equal to $\sqrt{dp/d\rho}$ and surpass it in the slightest degree, dV/dx would change from an infinite positive value to an infinite negative one. This physically intolerable fluctuation in dV/dx would persist so long as the flow continued inside the pipe. It is clear, therefore, that V will attain the value $\sqrt{dp/d\rho}$ only at the end of the pipe, if at all.

To determine the critical value of velocity we introduce the assumptions that the flow is adiabatic and the fluid a perfect gas. The energy equation may therefore be written

$$h + \frac{V^2}{2} = c_p T + \frac{V^2}{2} = h_0 = c_p T_0 \quad (9.36)$$

Equations (9.33) and (9.36) and the equation of state [Eq. (9.12)] allow p to be found in terms of ρ , so that $dp/d\rho$ can be computed.

$$p = \rho g R \left(T_0 - \frac{G^2}{2c_p \rho^2} \right) \quad (9.37)$$

$$\frac{dp}{d\rho} = gRT_0 + \frac{G^2}{\rho^2} \frac{gR}{2c_p} = \frac{p_0}{\rho_0} + V^2 \frac{k-1}{2k} \quad (9.38)$$

Equation (9.38) shows that the critical condition $V^2 = dp/d\rho$ is equivalent to

$$V^2 = \frac{p_0}{\rho_0} \frac{2k}{k+1} = C_t^2 \quad (9.39)$$

where C_t is identical with the velocity of sound at the throat of a nozzle [see Eq. (9.11)].

It is of interest to compare the velocity at any point in the pipe with the local sound velocity. For this purpose, recall from Eq. (9.6) that $C^2 = kp/\rho$, and use Eq. (9.37).

$$C^2 = \frac{kp}{\rho} = \frac{kp_0}{\rho_0} - V^2 \frac{(k-1)}{2} \quad (9.40)$$

The following inequalities are now readily established:

$$V^2 > \frac{dp}{d\rho} > C_t^2 > C^2$$

if $V > C_t$, and

$$V^2 < \frac{dp}{d\rho} < C_t^2 < C^2$$

if $V < C_t$. Wherever $V > C_t$, the flow is supersonic; and wherever $V < C_t$, it is subsonic.

The Fanno line of Fig. 9.16 applies to adiabatic pipe flow as well as to a transverse shock, for the cross-sectional area is constant in each case. Since the entropy of the fluid must increase along the pipe in a frictional adiabatic flow, the point of maximum entropy on the Fanno line can correspond only to conditions at the exit end of the pipe. At this point, the slope ds/dh is equal to zero. The differential of the entropy can be computed from Eqs. (9.28), (9.33), and (9.36).

$$ds = \frac{1}{T} \left(dh - \frac{dp}{\rho} \right) = - \frac{dp}{\rho T} \left(1 + \frac{\rho V dV}{dp} \right) = - \frac{dp}{\rho T} \left(1 - \frac{V^2}{dp/d\rho} \right) \quad (9.41)$$

If both sides of Eq. (9.41) are divided by dh and it is noted that $dp/dh\rho T \neq 0$, it is seen that $V = \sqrt{dp/d\rho}$ if $ds/dh = 0$. It follows that V can equal $\sqrt{dp/d\rho}$ only at the exit end of the pipe, if at all. This checks the previous conclusion to the same effect.

Points of higher enthalpy on the Fanno line are seen from the energy equation, [Eq. (9.36)] to correspond to subsonic flow in the pipe, and vice versa.

It has been found experimentally that disturbances like those in a nozzle may also occur in supersonic pipe flow. Oblique shocks and separation of the main stream from the wall take place, followed by one or more transverse shocks in the core, which reduce the flow to the subsonic regime.

9.9. Friction Factor for Adiabatic Pipe Flow. A friction factor may be defined for compressible flow in the same way as in Chap. VIII.

$$f = \frac{8\tau_0}{\rho V^2} \quad (8.8)$$

Dimensional analysis shows that, in a pipe carrying compressible fluid, $f = \phi(R, L/D, M)$, where the Reynolds and Mach numbers R and M may be evaluated at any convenient point in the pipe, say the entrance.

The friction factor can be determined experimentally, with the help of the equations previously developed. Substituting Eqs. (8.8) and (9.33) into Eq. (9.32), assuming f to be constant, and integrating between the limits x_1 and x_2 , we get

$$\int_1^2 \rho dp + \frac{G^2 f}{4a} (x_2 - x_1) + G^2 \ln \frac{\rho_1}{\rho_2} = 0 \quad (9.42)$$

From Eq. (9.37) we find that

$$p = \left(h_0 \rho - \frac{G^2}{2\rho} \right) \frac{k-1}{k} \quad (9.43)$$

$$\int_1^2 \rho dp = \frac{k-1}{2k} \left[h_0 (\rho_2^2 - \rho_1^2) + G^2 \ln \frac{\rho_2}{\rho_1} \right] \quad (9.44)$$

Thus, if the initial state 0 of the fluid is known, together with the mass rate of flow and the pipe diameter, measurements of p_1 and p_2 enable us to

find ρ_1 and ρ_2 from Eq. (9.43) and, hence, the friction factor from Eqs. (9.44) and (9.42).

Recent experiments on turbulent flow in a smooth pipe show that, for $L/D > 50$, f is the same function of R as in the incompressible case, regardless of whether the entrance Mach number M is greater or less than unity [4]. Values of $L/D > 50$ can rarely be attained in supersonic flow, however, so that in this case the relationship between f and L/D is of importance. The experiments appear to show that f passes through several minima and maxima in the range $0 \leq L/D \leq 50$. The relationship between f and L/D depends on R but is substantially independent of M . The value of M merely limits the maximum value of L/D attainable in supersonic flow. It may be that the relationship between f and L/D is the same as for an incompressible fluid at the same R . Data on incompressible flow are insufficient to warrant a definite conclusion.

9.10. Isothermal Flow in a Pipe with Friction. If T_1 represents the constant value of temperature everywhere in the pipe, the equation of state may be written

$$p = \rho g R T_1 \quad (9.45)$$

Therefore, $dp/d\rho = gRT_1$, so that the critical value of velocity is

$$V = \sqrt{gRT_1} \quad (9.46)$$

The local sound velocity $\sqrt{kp/\rho}$ is equal to $\sqrt{kgRT_1}$ and is constant throughout the pipe. Supercritical flow is therefore not necessarily supersonic in this case.

9.11. Stagnation Pressure in Supersonic Flow. In contrast to other aspects of the flow around an immersed body, the stagnation pressure can be found from one-dimensional considerations.

The treatment given in Art. 4.8, which is applicable only to subsonic flow, is extended here to supersonic flow, in which a transverse compression shock occurs in front of the body, as indicated in Fig. 9.18. In supersonic flow the total rise in pressure is conveniently divided into two parts, one due to the shock and the other due to the frictionless adiabatic compression between the shock and the stagnation point. Our object, just as in Art.

4.8, is to determine the quantity $(p_3 - p_1)/(\rho_1/2)V_1^2$ as a function of the Mach number of the undisturbed stream $M_1 = V_1/C_1 = V_1/\sqrt{kp_1/\rho_1}$. For this purpose, we consider the ratio p_3/p_1 , which may be broken into two factors, $p_3/p_1 = (p_3/p_2)(p_2/p_1)$, the first of which is found either from Art. 4.8 or Eq. (9.2).

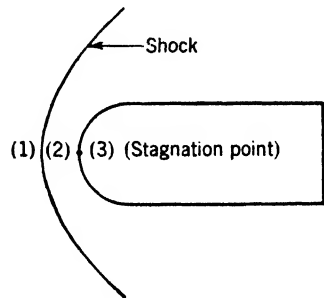


FIG. 9.18.

$$\frac{p_3}{p_2} = \left(1 + \frac{k-1}{2k} \frac{\rho_2}{p_2} V_2^2\right)^{k/(k-1)} \quad (9.47)$$

Since the cross-sectional area of the flow is the same on each side of the shock, continuity yields $\rho_1 V_1 = \rho_2 V_2$, and

$$\begin{aligned} \frac{p_3}{p_1} &= \frac{p_2}{p_1} \left(1 + \frac{k-1}{2k} \frac{\rho_1 V_1^2}{p_1} \frac{V_2}{V_1} \frac{p_1}{p_2}\right)^{k/(k-1)} \\ \frac{p_3}{p_1} &= \frac{p_2}{p_1} \left(1 + \frac{k-1}{2} M_1^2 \frac{V_2}{V_1} \frac{p_1}{p_2}\right)^{k/(k-1)} \end{aligned}$$

From Eqs. (9.20) and (9.22), V_2/V_1 and p_2/p_1 are obtained in terms of M_1 , and

$$\frac{p_3}{p_1} = \left[1 + \frac{k-1}{2} \frac{(k-1)M_1^2 + 2}{k(2M_1^2 - 1) + 1}\right]^{k/(k-1)} \left[1 + \frac{2k}{k+1} (M_1^2 - 1)\right] \quad (9.48)$$

Equation (9.48) is of course valid only if a shock occurs, that is, if $M_1 > 1$. If $M_1 \leq 1$, p_3/p_1 is obtained from Eq. (9.47) with subscript 2 replaced by 1.

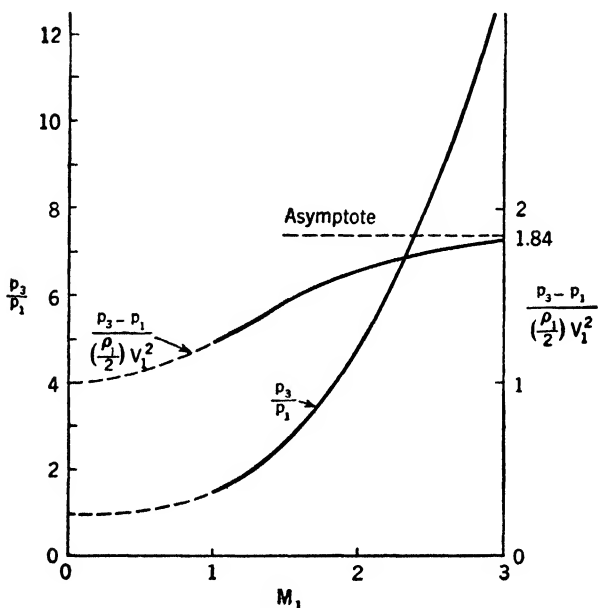


Fig. 9.19. — Stagnation-pressure coefficients for a blunt-nosed body as functions of the Mach number of the undisturbed stream M .

The stagnation-pressure ratio is plotted in Fig. 9.19. The quantity $(p_3 - p_1)/(\rho_1/2) V_1^2$ is easily computed from the formula

$$\frac{p_3 - p_1}{(\rho_1/2) V_1^2} = \frac{2}{kM_1^2} \left(\frac{p_3}{p_1} - 1\right)$$

and is also plotted in Fig. 9.19.

SELECTED BIBLIOGRAPHY

1. BINDER, R. C.: "Fluid Mechanics," Prentice-Hall, Inc., New York, 1943.
2. EWALD, P. P., TH. PÖSCHL, and L. PRANDTL: "The Physics of Solids and Fluids," Blackie & Son, Ltd., Glasgow, 1936.
3. KEENAN, J. H.: "Thermodynamics," John Wiley & Sons, Inc., New York, 1941.
4. KEENAN, J. H., and E. P. NEUMANN: Measurements of Friction in a Pipe for Subsonic and Supersonic Flow of Air, *J. Applied Mechanics*, vol. 13, pp. 91-100, June, 1946.
5. TAYLOR, G. I., and J. W. MACCOLL: The Mechanics of Compressible Fluids, in "Aerodynamic Theory," Vol. III (edited by W. F. Durand), Verlag Julius Springer, Berlin, 1935.
6. ACKERET, J.: Gasdynamik, in "Handbuch der Physik," Band VII, Verlag Julius Springer, Berlin, 1927.

CHAPTER X

DRAG

10.1. Drag and Lift. The force on a body that results from the motion of the body through a real fluid is, in general, inclined to the path direction. The component of this force parallel to the path is called the “drag,” and the normal component is called the “lift.” The drag does work as the body moves; the lift does no work. The lift is not necessarily vertical; it is defined as normal to the path, which may have any arbitrary direction.

Static buoyant force is excluded from consideration here, since it does not result from the motion of the body.

10.2. Energy and Work. Assume that a body moves at constant velocity through a large mass of fluid that is undisturbed, except by the body. The first law of thermodynamics requires that the work done by the body be equal to the increase in energy of the fluid, provided that the distant boundaries are so far away that nothing is transferred across them. If the body is partly immersed in two fluids, as a surface vessel in water and air, work is done on both fluids.

The energy imparted to the fluid may take one or more of several forms near the body, such as energy of the wake, energy of gravity waves, or energy of compression waves. Ultimately, however, the action of viscosity dissipates all these forms of energy, so that the final effect of the passage of a body is a rise in temperature of the fluid.

10.3. Dimensional Analysis—Drag Coefficient. In general, both friction and gravity forces play a role in the determination of the flow pattern around a body moving at constant velocity. Furthermore, the compressibility of the fluid may have to be taken into account. If all three of these factors are appreciable, the drag D of a body of given shape is a function of ρ , V , l , μ , g , and C , where l is a characteristic length of the body, C is the velocity of sound in the undisturbed fluid, and the other symbols have their usual meanings. Thus,

$$D = \phi(\rho, V, l, \mu, g, C) \quad (10.1)$$

One possible simplification of Eq. (10.1), by means of the Π theorem, is

$$\frac{D}{\rho V^2 l^2} = \phi_1 \left(\frac{\rho V l}{\mu}, \frac{V^2}{l g}, \frac{V}{C} \right) \quad (10.2)$$

where the independent variables are seen from Chap. VII to be, respectively, the Reynolds number R , the Froude number F , and the Mach number M .

It is customary to define the drag coefficient as

$$C_D = \frac{D}{(\rho/2)V^2A} \quad (10.3)$$

where the symbol A stands for some area pertaining to the body in question. Equations (10.2) and (10.3) combine to give

$$C_D = \psi(R, F, M) \quad (10.4)$$

Form of body	$\frac{l}{d}$	R	C_D
Disk (normal to flow)	$> 10^3$	1.12
Tandem disks (l = spacing) (normal to flow)	0	$> 10^3$	1.12
	1	$> 10^3$	0.93
	2	$> 10^3$	1.04
	3	$> 10^3$	1.54
Rectangular plate (l = length) (normal to flow)	1	$> 10^3$	1.16
	5	$> 10^3$	1.20
	20	$> 10^3$	1.50
	∞	$> 10^3$	1.95
Circular cylinder (axis parallel to flow)	0	$> 10^3$	1.12
	1	$> 10^3$	0.91
	2	$> 10^3$	0.85
	4	$> 10^3$	0.87
	7	$> 10^3$	0.99
Hemisphere:			
Hollow upstream	$> 10^3$	1.33
Hollow downstream	$> 10^3$	0.34
Circular cylinder (axis normal to flow)	1	10^3 to 10^6	0.63
	5	10^3 to 10^6	0.74
	20	10^3 to 10^6	0.90
	∞	10^3 to 10^6	1.20
	5	$> 5 \times 10^5$	0.35
	∞	$> 5 \times 10^5$	0.33
Sphere	10^3 to 10^6	0.47
	...	$> 3 \times 10^6$	0.20
Airship hull (model)	$> 2 \times 10^5$	0.040

In all problems that to date have any practical importance, at least one of the independent variables, R , F , or M , may be neglected. In the case of an immersed body moving through incompressible fluid, neither weight nor compressibility has any effect, and Eq. (10.4) reduces to

$$C_D = \psi(R) \quad (10.5)$$

The remainder of this article and several following ones will deal with the drag problems covered by Eq. (10.5). When a free surface or compressibility is to be considered, the fact will be clearly stated.

In the table on page 183 * are listed approximate experimental values of drag coefficient for various simple shapes. The approximate range of R in which these C_D values apply is also stated.

It will be noted that C_D is independent of R for each of the first five shapes listed, provided that $R > 10^3$. All these bodies have corners, from which the flow separates, and are known as bluff bodies. The next two shapes, the cylinder and sphere, are rounded and exhibit two distinct regimes of flow; that is, C_D has a large value for $10^3 < R < 10^5$ but drops abruptly at a certain critical value of R and then remains approximately constant as R increases. The airship hull is also rounded but is more "streamlined" than the cylinder or sphere and does not exhibit the sudden drop in C_D characterizing those bodies.

Examination of the table thus suggests a classification of shapes as "bluff," "rounded," or "streamlined," the drag coefficient of each class showing a certain typical behavior as the Reynolds number changes.

10.4. Pressure Drag and Friction Drag. It will be found useful to break the total drag into two components, the pressure drag D_p caused by normal stresses, and the friction drag D_f caused by tangential stresses.

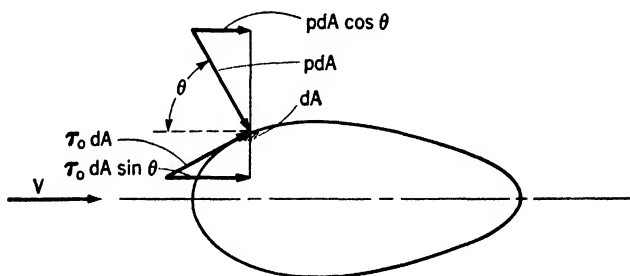


FIG. 10.1.

The normal force on a surface element dA of a body is $p dA$, and the tangential force is $\tau_0 dA$, as shown in Fig. 10.1. The components in the direction of flow of these two forces are, respectively, $p dA \cos \theta$ and $\tau_0 dA \sin \theta$, where θ is the angle between the outward-drawn normal to dA and the upstream direction. Thus the pressure and friction drags are

$$D_p = \int_A p \cos \theta dA$$

* Adapted from the tabulation in "Fluid Mechanics for Hydraulic Engineers," by Hunter Rouse, McGraw-Hill Book Company, Inc., New York, 1938.

$$D_f = \int_A \tau_0 \sin \theta \, dA$$

An example of the use of these concepts is provided in the explanation of the change in C_D with l/d ratio, for a cylinder with axis parallel to the flow (see the table, page 183). When $l/d = 0$, the pressure-drag coefficient C_{D_p} is large, and the friction-drag coefficient C_{D_f} is zero. As l/d increases, the flow separation from the corners becomes less intense and C_{D_p} gradually decreases. At the same time, however, shearing forces along the cylindrical surface are becoming appreciable, so that C_{D_f} increases. It is seen that these changes cause the over-all coefficient C_D to pass through a minimum when $l/d \approx 2$.

10.5. Drag at Small Reynolds Numbers. It will be recalled from Art. 7.22 that R is a measure of the ratio of inertia to friction force at any point in a flow. Consequently, if R is made sufficiently small, the effect of inertia on the drag may be neglected. In other words, the density of the fluid has no influence on drag at small values of R . In this case Eq. (10.1) simplifies to

$$D = \phi(V, l, \mu)$$

whence, by dimensional analysis,

$$D = \text{constant } \mu l V \quad (10.6)$$

Combining Eqs. (10.3) and (10.6), we get

$$C_D = \frac{\text{constant}}{R} \quad (10.7)$$

The unknown constant appearing in Eq. (10.6) has been evaluated theoretically for certain shapes by means of the equations of motion for a viscous fluid. In the case of a sphere, for example, Stokes found that

$$D = 3\pi\mu Vd \quad (10.8)$$

where the diameter d is taken as the characteristic length. The corresponding expression for C_D is

$$C_D = \frac{24}{\rho Vd/\mu} = \frac{24}{R} \quad (10.9)$$

Comparison of Eq. (10.9) with experimental values of C_D for a sphere indicates that Stokes' result holds only if $\rho Vd/\mu < 1.2$ (see Fig. 10.13). These equations, therefore, are valid only for extremely small spheres and velocities or for very viscous liquids. Practical applications are to dust particles in air and to water droplets occurring in fog or cloud.

The details of Stokes' analysis indicate that the pressure drag of a sphere is one-third of the total, the friction drag accounting for the remaining two-thirds.

10.6. Drag at Large Reynolds Numbers. A large Reynolds number means, in general, that inertia force predominates over friction force. It has been found experimentally that friction can be neglected everywhere in a flow with a large value of R , except in a thin layer of fluid next to the body (called the "boundary layer") and in the wake. This frictional boundary layer is formed because the relative velocity of a real fluid at the body surface is zero, while the velocity a short distance away has a magnitude comparable with that of the undisturbed stream. Consequently, close to the surface, there is a large rate of change of V with respect to n , the outward-drawn surface normal; and the shearing stress $\tau = \mu \partial V / \partial n$ is appreciable, even in a fluid of small viscosity, like air or water.

Inside the boundary layer, the fluid particles are set into rotation by the shearing forces; the motion may be roughly likened to that of rollers in a roller bearing. Outside the boundary layer, however, the friction forces are so small that the motion approximates closely to an irrotational flow of frictionless fluid.

For a streamlined body, the boundary layer remains thin over the entire surface and does not separate, the wake is small, and the streamlines and pressure distribution are nearly the same as for an irrotational flow. Theory shows that the pressure distribution over a body in an irrotational flow always yields a zero value of drag and drag coefficient. Consequently, the pressure-drag coefficient will be small for a streamlined body in a real fluid. It is found that the friction-drag coefficient is of the same order of magnitude as the pressure-drag coefficient.

The flow pattern for a bluff or rounded body differs markedly from an irrotational one, because the boundary layer separates and forms a considerable wake. Close to the body, the wake fluid experiences a violent eddying motion; the mean level of kinetic energy is higher, and the mean level of pressure is less than in the corresponding irrotational flow. Since the pressure over the portion upstream from the separation point approximates to that in irrotational flow, the pressure-drag coefficient will be large if the projected area of the wake is a large fraction of the projected area of the body.

For a bluff body the flow separates at the corners, regardless of R , provided merely that R be sufficiently large. The ratio of the projected areas of wake and body is therefore constant, and so is C_{Dp} . Since $C_{Dp} \gg C_{Df}$, the over-all coefficient C_D is likewise nearly constant.

For a rounded body, however, the separation point depends on R and also on other factors, such as the turbulence of the flow approaching the body. The sudden drop observed in C_D at a certain critical Reynolds num-

ber is caused by a sudden decrease in the area of the wake, when the boundary-layer flow becomes turbulent. This phenomenon will be discussed in more detail in Art. 10.11.

10.7. Drag in a Nonseparating Flow. In Fig. 10.2 is shown a streamlined body of revolution, together with curves of measured pressure and pressure calculated for an irrotational flow. This is one of several theo-

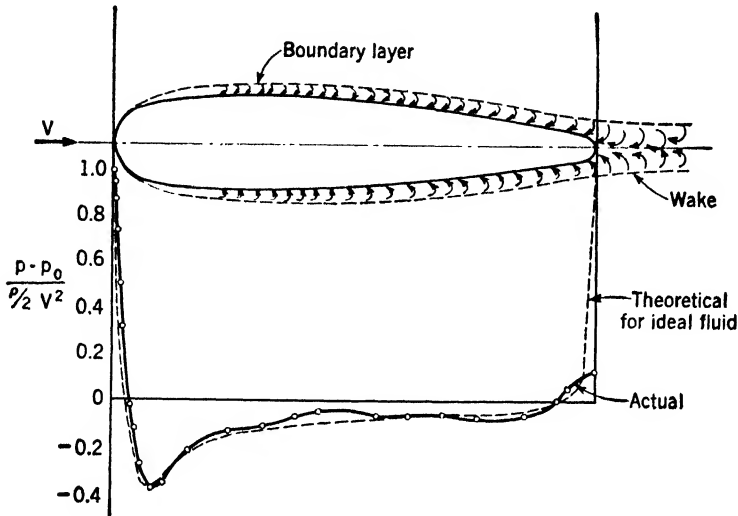


FIG. 10.2. — Theoretical and experimental pressure distributions over a body of revolution. (After Fuhrmann, reference 4.)

retically developed shapes tested by G. Fuhrmann [4] in comparing actual and theoretical flows around streamlined forms. It will be noted that the actual and theoretical pressure distributions are nearly the same, except at the tail, where the actual pressure fails to rise to the theoretical stagnation-point value.

The pressure-drag coefficient computed from the measured pressure distribution and based on the projected area of the body was found to be 0.0201. The total drag of the body was simultaneously measured and the over-all drag coefficient found to be 0.0362. The friction-drag coefficient is the difference between these two, *viz.*, 0.0161. It is seen that pressure and friction drags are of the same order of magnitude for a streamlined form.

Figure 10.2 also shows, to an exaggerated scale, the boundary layer formed on the body and the wake shed downstream. There is no appreciable separation of the main flow.

10.8. Boundary-layer Mechanics. Prandtl [6] originated the concept of the boundary layer, early in this century, and he and his associates took the lead in developing both theoretically and experimentally this branch of fluid mechanics. The demand for aircraft capable of ever higher and

higher speed has provided a constant stimulus for this development, and many workers have contributed to the field.

This article will be restricted to the simplest case of boundary-layer flow, *viz.*, that on a flat plate parallel to the flow and subject to a uniform pressure. Figure 10.3 shows the two-dimensional flow past one side of such a plate.

The basic assumption is that δ , the thickness of the boundary layer, at any point x be small compared with x . The definition of δ is somewhat arbitrary, because the friction forces die away asymptotically with distance from the surface and the velocity does not quite attain the value V of the

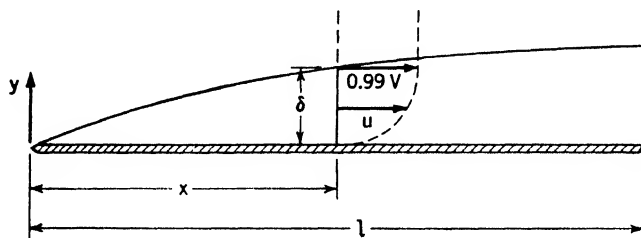


FIG. 10.3.

undisturbed flow. There is, however, practically full recovery of velocity so close to the surface that δ is usually defined as the distance at which the velocity equals 99 per cent of V .

The slowing down of the fluid close to the plate gives rise to a gradual thickening of the boundary layer and to a small velocity component in the y direction, normal to the surface. The main stream thus diverges slightly. This y velocity component is very small compared with u , the x component, and is not shown in the figures.

The main object of a boundary-layer analysis is to set up an expression for the drag coefficient of the plate, since this is the matter of greatest practical interest. Another object is to determine the thickness of the boundary layer.

In the case of a laminar boundary layer the equations of motion of a viscous fluid can be solved, thanks to the simplifying assumption that $\delta \ll x$. Formulas for C_D and δ for the laminar case were obtained by Blasius [3], an associate of Prandtl. They are

$$C_D = \frac{D}{(\rho/2)V^2bl} = \frac{1.33}{\sqrt{Vl/\nu}} = \frac{1.33}{\sqrt{R}} \quad (10.10)$$

$$\delta = \frac{5.2x}{\sqrt{Vx/\nu}} \quad (10.11)$$

where D is the drag of one side and b is the width of the plate.

The derivation of these formulas cannot be given here, but an ap-

proximation to them will be developed by means of the momentum equation. To use this momentum analysis, which is due to von Kármán [5], one must assume a form for the x -velocity distribution across the boundary layer. The analysis is, therefore, semiempirical, but it has the advantage of being applicable to a turbulent boundary layer, as well as a laminar one. Indeed, since Blasius' exact solution for a laminar layer is available, the momentum analysis is used chiefly for turbulent boundary layers, for which a reasonable velocity distribution can be assumed by analogy with pipe flow.

In Fig. 10.4 is shown an elementary portion of the boundary layer of length dx , at an arbitrary point on the plate. The boundary-layer flow may

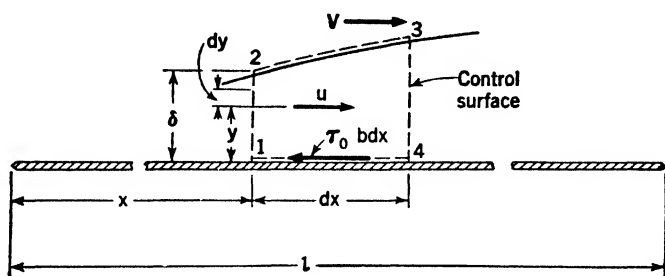


FIG. 10.4.

be either laminar or turbulent. The only external force in the x direction acting on the fluid inside the control surface 1, 2, 3, 4 is $-\tau_0 b dx$; there is no pressure force, because the pressure is assumed uniform everywhere. The momentum equation [Eq. (6.6)], gives for this case

$$-\tau_0 b dx = \text{net efflux of } x \text{ momentum from the control surface} \quad (10.12)$$

The momentum influx across boundary 1, 2 is seen to be $M = \int_0^\delta \rho u^2 b dy$; the difference between the efflux across 3, 4 and the influx across 1, 2 is written as dM . There is also a certain influx of x momentum across boundary 2, 3, which must be subtracted from dM in order to get the net efflux from the entire control surface. This momentum influx is equal to the product of the mass influx across 2, 3 and the velocity V , since 2, 3 marks the limit of the boundary layer, where the x velocity is practically equal to V . By continuity, this mass influx is equal to the difference between the mass efflux across 3, 4 and the influx across 1, 2, which may be written as dm , where m is the mass influx across 1, 2 and is equal to $\int_0^\delta \rho u b dy$.

Equation (10.12) thus becomes

$$-\tau_0 b dx = dM - V dm = d \left(\int_0^\delta \rho u^2 b dy \right) - V d \left(\int_0^\delta \rho u b dy \right)$$

which, since ρ , V , and b are constant, simplifies to

$$- \tau_0 b \, dx = \rho b V^2 d \left[\int_0^\delta \left(\frac{u^2}{V^2} - \frac{u}{V} \right) dy \right]$$

Changing the variable of integration from y to y/δ , we get

$$\frac{\tau_0}{\rho V^2} = \frac{d}{dx} \left[\delta \int_0^1 \left(\frac{u}{V} - \frac{u^2}{V^2} \right) d \left(\frac{y}{\delta} \right) \right] = \frac{d}{dx} [\delta \alpha] \quad (10.13)$$

where

$$\alpha = \int_0^1 \left(\frac{u}{V} - \frac{u^2}{V^2} \right) d \left(\frac{y}{\delta} \right) \quad (10.14)$$

The drag is the summation of the elementary friction forces on the plate.

$$D = \int_0^l \tau_0 b \, dx \quad (10.15)$$

The drag coefficient is obtained from Eqs. (10.13) and (10.15).

$$C_D = \frac{\int_0^l \tau_0 b \, dx}{(\rho/2) V^2 b l} = \frac{2}{l} \int_0^l \frac{\tau_0}{\rho V^2} dx = \frac{2}{l} \delta_l \alpha_l \quad (10.16)$$

where δ_l and α_l are the values of δ and α at $x = l$.

For a smooth plate the shearing stress at the surface is related to the velocity distribution by the formula

$$\tau_0 = \mu \left(\frac{\partial u}{\partial y} \right)_{y=0} \quad (10.17)$$

Consequently, if the distribution of velocity across the boundary layer is assumed, one can evaluate α from Eq. (10.14) and then find δ by combining Eqs. (10.13) and (10.17). Finally, the drag coefficient is computed from Eq. (10.16).

To illustrate this procedure assume a linear distribution of velocity across the boundary layer: $u/V = y/\delta$. This is a crude approximation to the actual distribution in a laminar layer. One easily finds that $\alpha = 1/6$ and that $(\partial u/\partial y)_{y=0} = V/\delta$. The differential equation for δ obtained from Eqs. (10.13) and (10.17) is

$$\frac{1}{6} \frac{d\delta}{dx} = \frac{\tau_0}{\rho V^2} = \frac{\mu}{\rho V \delta}$$

or

$$\delta \, d\delta = \frac{6\mu}{\rho V} dx$$

Noting that $\delta = 0$ at $x = 0$, we get

$$\delta^2 = \frac{12\mu x}{\rho V}$$

or

$$\delta = \frac{3.46x}{\sqrt{Vx/\nu}} \quad (10.18)$$

The drag coefficient is found from Eq. (10.16).

$$C_D = \frac{2}{l} \delta_l \alpha_l = \frac{2}{l} \frac{3.46l}{\sqrt{Vl/\nu}} \frac{1}{6} = \frac{1.16}{\sqrt{Vl/\nu}} \quad (10.19)$$

Equations (10.19) and (10.18) are to be compared with Eqs. (10.10) and (10.11), respectively, the exact formulas for a laminar layer. It is seen that the crude assumption of a linear velocity distribution leads to a value of C_D which is surprisingly near the truth.

The principal use of this momentum analysis is to establish a rational form of expression for C_D in case of turbulent flow in the boundary layer. A reasonable procedure is to assume a velocity distribution in the boundary layer based on measurements of turbulent flow in smooth pipes. In carrying over the pipe-flow data one considers V as the analogue of U , the maximum velocity at the center of the pipe, and δ as analogous to the pipe radius a .

At the time von Kármán first developed this method, it was known that a power law $u/U = (y/a)^{1/4}$ was valid for pipes in the range of Reynolds numbers which had then been investigated. Accordingly, von Kármán assumed that the velocity distribution in the turbulent boundary layer was given by

$$\frac{u}{V} = \left(\frac{y}{\delta}\right)^{1/4} \quad (10.20)$$

The value of α computed from Eqs. (10.14) and (10.20) is $7/72$.

Equation (10.20) does not apply for very small values of y , since it yields an infinite slope for the velocity curve at the plate, where $y = 0$. Actually, this slope is finite because the turbulence dies out close to the smooth surface and gives place to a thin, laminar sublayer. The value of τ_0 , therefore, cannot be computed by means of this equation; it is possible, however, to use a formula for τ_0 , due to Blasius, which is based on pressure-drop measurements in smooth pipes at moderate Reynolds numbers: $\tau_0 = 0.0228\rho U^2(\nu/aU)^{1/4}$. The analogue of this formula for a flat plate is

$$\tau_0 = 0.0228\rho V^2 \left(\frac{\nu}{V\delta}\right)^{1/4} \quad (10.21)$$

Straightforward calculations lead to the flat-plate formulas.

$$\delta = \frac{0.376x}{(Vx/\nu)^{1/2}} \quad (10.22)$$

$$C_D = \frac{0.073}{(Vl/\nu)^{1/2}} \quad (10.23)$$

It is found that these equations agree with experiments up to a Reynolds number Vl/ν of approximately 2×10^7 . Equation (10.23) is plotted in Fig. 10.5.

In the development of Eqs. (10.22) and (10.23), it was assumed that the plate was entirely covered with a turbulent boundary layer. These

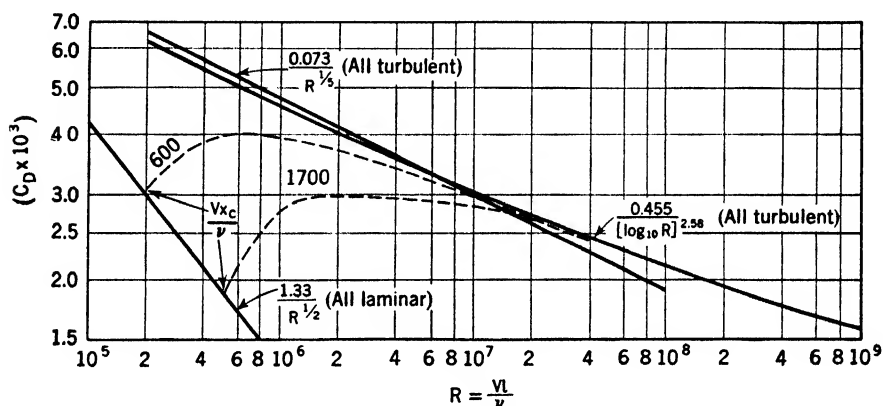


FIG. 10.5. — Drag coefficient C_D versus Reynolds number R for a flat plate parallel to the undisturbed flow.

equations will therefore be incorrect if a laminar layer covers an appreciable part of the plate. It has been found that Eq. (10.23) agrees well with experimental data for a blunt-nosed plate, on which the initial disturbance to the flow causes an early transition to turbulence in the boundary layer. Data on sharp-nosed plates, however, gradually break away from the all-turbulent curve of von Kármán as the Reynolds number decreases, and eventually reach the all-laminar curve of Blasius. An empirically corrected formula that applies in this Reynolds-number range is

$$C_D = \frac{0.073}{(Vl/\nu)^{1/2}} - \frac{\text{constant}}{Vl/\nu} \quad (10.24)$$

The constant is determined by the value of Vl/ν at which transition to turbulence occurs at the trailing edge of the plate. This value of Vl/ν is called the “critical Reynolds number” and, for a sharp-nosed plate, depends primarily on the turbulence present in the approaching flow.

With the growth of knowledge about pipe flow, it was found that the power law of Eq. (10.20) did not represent the turbulent velocity distribution at higher Reynolds numbers, and the logarithmic distribution discussed in Chap. VIII came to be accepted as substantially correct. Th. von Kármán repeated his calculations for C_D , using the logarithmic velocity-distribution law and the corresponding expression for τ_0 . Since the resulting formula is awkward for numerical computations, an empirical interpolation formula has been developed by Prandtl and Schlichting that agrees with von Kármán's equation up to $Vl/\nu = 10^9$. The Prandtl-Schlichting formula is

$$C_D = \frac{0.455}{[\log_{10}(Vl/\nu)]^{2.58}} \quad (10.25)$$

Equation (10.25) applies only if the boundary layer is all turbulent. To extend its range down to the critical value of Vl/ν , at which the last vestige of a turbulent layer disappears and the plate is completely covered by a laminar layer, the same empirical correction is made as above.

$$C_D = \frac{0.455}{[\log_{10}(Vl/\nu)]^{2.58}} - \frac{\text{constant}}{Vl/\nu} \quad (10.26)$$

The remarks concerning the constant of Eq. (10.24) apply also to this formula.

10.9. Factors Affecting Transition. If the value of Vl/ν is less than the critical, the boundary layer on a flat plate is entirely laminar. If the value of Vl/ν is above the critical, the laminar boundary layer will persist only to a distance x_c back from the leading edge. At this critical distance, transition to turbulence sets in, and the rest of the plate is covered by a turbulent layer. It is found, for a given plate, for given initial turbulence, and in the absence of disturbances, that the value of Vx_c/ν is constant and equal to the critical value of Vl/ν . Thus, as might be expected, the flow at any point is independent of the extent of the plate downstream from that point.

The practical importance of a large value of Vx_c/ν is apparent from Fig. 10.5, in which it is seen that an increase in the fraction of the surface covered by a laminar layer causes a decrease in C_D .

The values of Vx_c/ν indicated in Fig. 10.5 are on the order of 5×10^5 . These data were all obtained, however, in wind tunnels having a considerable degree of turbulence. In the motion of a surface through still fluid, as for an airplane wing, the initial turbulence is very small, and the value of Vx_c/ν is larger than that found in a turbulent wind tunnel. For this reason it is important to investigate the behavior of Vx_c/ν under conditions of low initial turbulence and to determine the effect of disturbances on the stability of the laminar layer.

Dryden [2] and his associates [11] at the U.S. Bureau of Standards have developed a tunnel having a very low turbulence. The ratio of the rms of the turbulent component of velocity to the average velocity is used as a measure of the turbulence; the lowest value reached by this ratio is about 0.02 per cent. At this value it is found that Vx_c/ν is approximately 2.8×10^6 , while, for a turbulence of 0.32 per cent, Vx_c/ν drops to 1.5×10^6 .

The Bureau of Standards group has detected the presence of fluctuations in the laminar boundary layer, which grow until a breakdown of laminar motion takes place. They have found, further, that fluctuations produced artificially by a vibrating metal ribbon are amplified only within a certain band of frequencies. Waves having frequencies outside this range die away without producing turbulence. The existence of such unstable frequency bands was predicted from theoretical considerations of the viscous forces by Tollmien and Schlichting several years before techniques were available for their experimental observation. The experiments have beautifully verified the theory.

It is clear from these results that, for low drag, one should avoid the introduction of vibrations of certain frequencies into the laminar boundary layer. Use of smooth, nonwavy surfaces braced against vibration is indicated. Even engine or propeller noise may promote turbulence, if it contains intense components of the proper frequency.

The above results relate to a flat surface subject to a uniform pressure, whereas in technical applications (*e.g.*, airfoils), the pressure is not uniform. An adverse pressure gradient on a flat surface has been found to widen the band of unstable frequencies and to increase the amplification of the Tollmien-Schlichting viscous waves. Furthermore, dynamic instability is introduced, because the velocity profile develops a reversed curvature or inflection point. By "dynamic instability" is meant one that would be operative even in the absence of friction—in contrast to the viscous instability of Tollmien and Schlichting. The over-all result is that Vx_c/ν is no longer independent of x_c but decreases as x_c is increased.

On the other hand, if the pressure decreases in the direction of flow, it appears that a stabilizing effect is produced and Vx_c/ν may increase with an increase in x_c .

The effect on transition of curvature of the surface has also been studied, with the following general results: In the absence of a pressure gradient, Vx_c/ν appears to be uninfluenced on a slightly convex surface but to be decreased on a concave surface. The destabilizing effect of the latter is due to the introduction of a dynamic instability, and not to viscous instability.

10.10. Low-drag Airfoils. The discussion in the preceding article indicates the desirability of a laminar boundary layer on a body designed for low drag. The National Advisory Committee for Aeronautics (NACA)

has developed airfoils that, under test conditions approximating free flight at useful Reynolds numbers, may have a laminar boundary layer over approximately 0.6 of the chord. The minimum drag coefficients obtainable are on the order of 0.003 at a value of $R = (Vl/\nu) \approx 6 \times 10^6$, where l is the chord. Insertion of these values into Fig. 10.5 shows that C_D for these airfoils is down near the value given by Blasius' curve for a flat plate covered by a laminar layer. The minimum C_D for a conventional airfoil is on the order of 0.007.

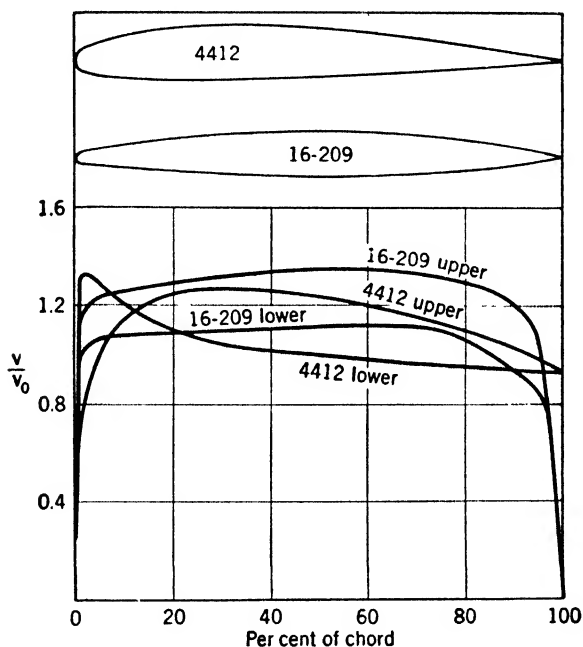


FIG. 10.6a. Velocity distributions over a conventional and a low-drag airfoil, both at a lift coefficient of 0.2.

In Fig. 10.6a is shown one of these "laminar" airfoils, NACA 16-209, together with the theoretical velocity distribution over it at the design lift coefficient of 0.2. For comparison, a conventional airfoil, NACA 4412, is also shown, together with the measured velocity distribution over it at an angle of attack $\alpha = -2$ deg, corresponding to $C_L = 0.2$. It is seen that the NACA 16-209 has the maximum thickness much farther aft than the NACA 4412. This novel shape results in a theoretical pressure distribution that decreases gradually over about 60 per cent of the chord and then rises abruptly at the tail. (The velocity-distribution curves are such that the ordinate is a maximum at the point of lowest pressure and zero at the stagnation pressure.) Tests in a nearly turbulence-free tunnel show that this favorable pressure gradient enables the boundary layer to remain

laminar up to approximately the point of minimum pressure, where transition occurs. The formation of a turbulent boundary layer at this point is really advantageous because the air is thereby given enough momentum to follow the rest of the contour more closely than would otherwise be possible. Indeed, in some experiments at lower Reynolds number, transition was so much delayed that the laminar boundary layer separated and stayed separated, the transition coming too late to effect a return of the stream to the surface. Increased drag coefficients were the result.

In contrast to the NACA 16-209, the NACA 4412 has an unfavorable pressure gradient over practically its whole surface. The laminar boundary layer thickens rapidly, therefore, and transition occurs at about 0.3 of the chord. The minimum drag coefficient is greater than 0.007, more than twice the value of approximately 0.003 for the NACA 16-209.

In Fig. 10.6b is shown one of the newest low-drag airfoils. The ordinate, labeled "pressure coefficient," gives the value of $(V/V_0)^2$, instead of V/V_0 , as in Fig. 10.6a. For this airfoil a dropping pressure is provided over the first 60 per cent of chord, followed abruptly by a linear rise in pressure over the rest of the surface. A laminar boundary layer is maintained back

to the 60 per cent chord point, where the sudden change in pressure gradient causes a quick transition to a turbulent boundary layer. The momentum of the fluid close to the surface is so much enhanced by the turbulence that very little separation occurs.

The theory has been so far developed that it can supply the shape of airfoil to give a desired pressure distribution [12]. This can be accomplished at a useful flight Reynolds number and for a desired range of lift coefficient, provided that both the mean (or design) value of C_L and its range of variation are kept small (both on the order of 0.2). The excellent control of

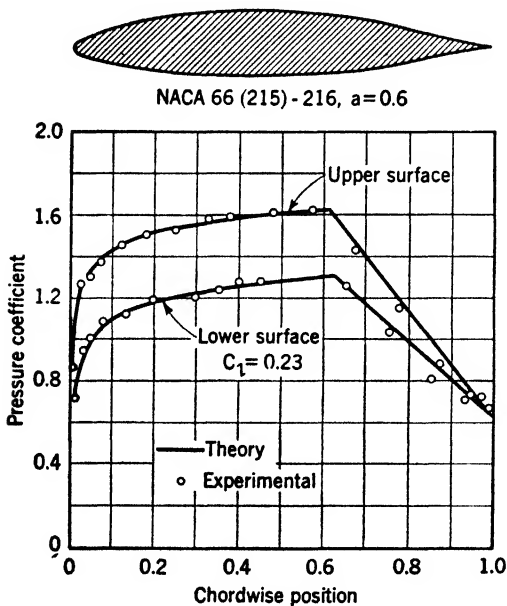


FIG. 10.6b. — Distribution of $(V/V_0)^2$ over a low-drag airfoil.

pressure distribution that is possible is illustrated in Fig. 10.6c, which shows the distribution for symmetrical airfoils having the maximum thickness (12 per cent of chord) at 30, 40, 50, and 60 per cent of chord from the lead-

ing edge. The subscript 1 indicates that this pressure distribution does not change radically in the range of lift-coefficient values, $C_{L \text{ design}} \pm 0.1$.

The advantage of the low-drag airfoil is brought out in Fig. 10.6d, which gives the C_D versus C_L curves for a conventional section and for two low-

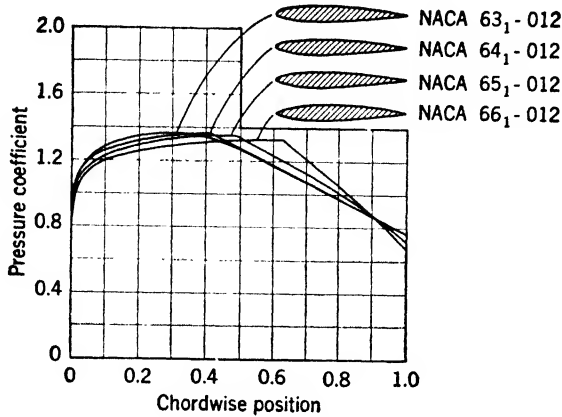


FIG. 10.6c. — Distributions of $(V/V_0)^2$ showing close relationship between point of maximum thickness and point of minimum pressure.

drag sections. The value of $C_{L \text{ design}}$ for both of the latter is 0.2. They differ, however, in the length of the laminar boundary layer, NACA 63₁-212 having 30 per cent of the chord laminar and NACA 66₁-212 having 60 per cent laminar. In the design range of C_L it is seen that NACA

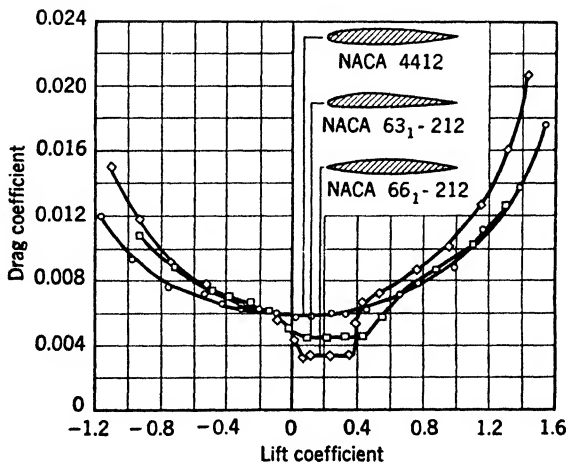


FIG. 10.6d. — Curves of drag coefficient versus lift coefficient for a conventional airfoil and two low-drag airfoils.

66₁-212 has a C_D of about half that of the conventional airfoil. Outside of this range, however, it is the least desirable of the three.

The sudden rise of C_D at each end of the "bucket" in the curve results from a forward shift in the point of minimum pressure and hence of transition.

The importance of restricting the use of a low-drag section to the design conditions is obvious from Fig. 10.6*d*. It may also be remarked that slight roughness of the airfoil surface can cause transition to occur early and completely vitiate the special low-drag design.

10.11. Drag in a Separating Flow. A flat plate set normal to the distant

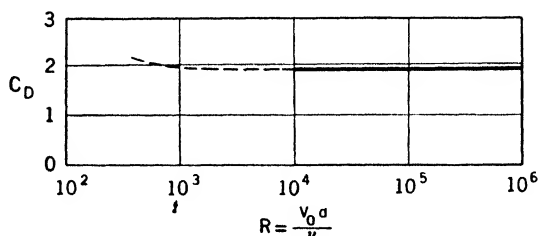


FIG. 10.7. — Drag coefficient C_D versus Reynolds number R for two-dimensional flow past a plate normal to the undisturbed flow and of breadth d . (After F. Eisner, *Das Widerstandsproblem*, Third Int. Cong. App. Mech., Stockholm, 1930.)

velocity is an extreme example of a bluff body. The flow separates at the edges for all except the smallest Reynolds numbers. The entire drag is caused by the pressure difference between the front and back of the plate, since the shearing stresses are all normal to the drag direction. Figure 10.7 gives C_D versus R for two-dimensional flow past a rectangular plate, *i.e.*, flow with negligible end effects. Figure 10.8 shows the dependence of C_D on breadth-to-length ratio d/l for rectangular plates. End effects reduce C_D because the average pressure difference over the surface is less if the flow can close in at the ends.

The drag-coefficient curve for a disk, shown in Fig. 10.9, is similar in shape to that for a square plate.

Several theoretical estimates have been made of the drag coefficient for two-dimensional flow past a plate. The assumption of a completely irrotational flow yields the obviously erroneous value of zero for the drag coefficient. This is equivalent to the assumption of a scalar "velocity potential" whose gradient at any point is the velocity vector at that point. This type of flow is therefore frequently called "potential flow." It can be shown that the drag of a body of any shape is zero in a potential flow.

Noting that the motion downstream from a plate is highly rotational, Helmholtz and Kirchhoff approximated to the actual wake by a region of

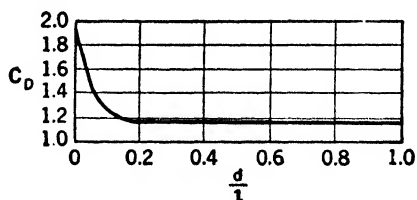


FIG. 10.8. — Drag coefficient C_D versus breadth-to-length ratio d/l for a rectangular plate normal to the undisturbed flow.

dead water or motionless fluid separated from the main stream by an infinitely thin sheet of rotating fluid particles springing from each edge of the plate. (See Fig. 10.10.) Since the fluid in such a "vortex sheet" rotates, there is a jump in velocity from zero in the wake to a finite value in the stream. For this reason the sheet is also called a "surface of discontinuity." The pressure is assumed to vary continuously across the sheet and throughout the flow. In this idealization the flow is divided by the surfaces of discontinuity into two regions, in each of which the motion is irrotational, but which have different Bernoulli numbers. Such a flow pattern cannot be more than

a first approximation to the actual one, because a vortex sheet is unstable in a viscous fluid and tends to break up into scattered vortices, owing to the intense shearing stress accompanying the large (theoretically infinite) velocity change across the sheet.

According to the Helmholtz-Kirchhoff two-dimensional theory, the value of the drag coefficient for the flat plate is

$$C_D = \frac{\text{drag per unit length}}{(\rho/2)dV_0^2} = 0.880$$

FIG. 10.10.

This value is to be compared with the experimental one of 1.8, shown in Fig. 10.7. This theory gives the right order of magnitude for C_D and is evidently a first approximation to reality.

Observation of the wake behind a body shows that under certain conditions vortices are shed alternately from first one edge and then the other at a regular frequency and that they move downstream in two approximately parallel rows. The vortices in one row are staggered with respect to those in the other. Figure 10.11a shows such a well-developed "vortex street" for a cylinder, while in Fig. 10.11b a street is starting to form behind a flat plate. Th. von Kármán has shown theoretically that such a staggered arrangement of vortices in an otherwise irrotational flow is stable only for a certain value of the ratio h/l , where h is the lateral spacing and l is the longitudinal spacing of the vortices. Photographs of actual flows show that the theoretical value of h/l approximates closely the measured ones.

Th. von Kármán has also computed the drag coefficient for this theo-

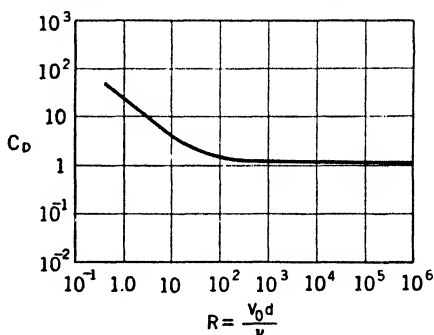


FIG. 10.9. — Drag coefficient C_D versus Reynolds number R for a disk normal to the undisturbed flow. (After Eisner, *Das Widerstandsproblem*, Third Int. Cong. App. Mech., Stockholm, 1930.)

retically stable flow in terms of the frequency with which the vortices are shed and their lateral spacing in the wake. Neither the frequency nor the spacing is predicted in the theory, but when experimental values are inserted in the theoretical equations, the computed and measured values of C_D are in good agreement.

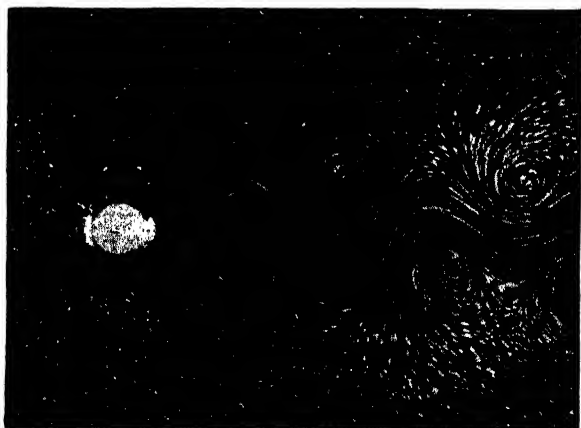


FIG. 10.11a. — Vortex formation behind a cylinder. (After Prandtl.)



FIG. 10.11b. — Vortex formation behind a plate. (After Prandtl.)

It should be emphasized that the actual wake ceases to resemble a vortex street if the value of Reynolds number $V_0 d / \nu$ exceeds about 2,500.

Measured values of the drag coefficient (based on projected area) for a cylinder with axis normal to flow and for a sphere are shown in Figs. 10.12 and 10.13, respectively. It has been pointed out in Art. 10.6 that the sudden drop in C_D at a critical value of R is associated with a change in the boundary layer from laminar to turbulent. This effect will here be further discussed for the sphere, which is a representative example of a rounded body.

Near the nose of a sphere the boundary layer is laminar on account of

its extreme thinness. Somewhat downstream from the nose the laminar-boundary-layer fluid enters a region where the pressure rises in the direction

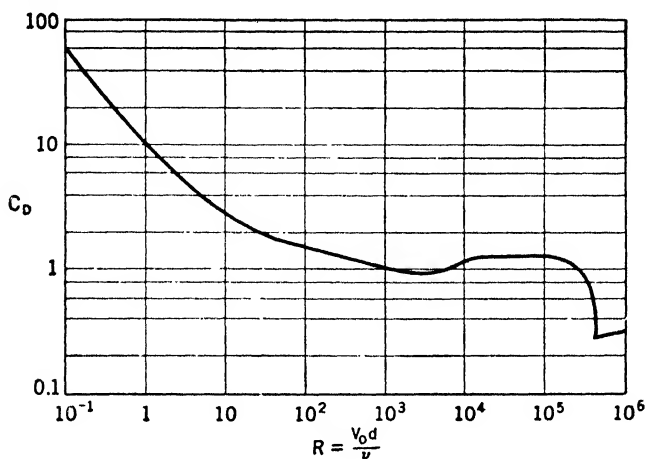


FIG. 10.12. — Drag coefficient C_D versus Reynolds number R for two-dimensional flow past a circular cylinder with axis normal to the undisturbed flow. (After Eisner, *Das Widerstandsproblem*, Third Int. Cong. App. Mech., Stockholm, 1930.)

of flow, so that the fluid is slowed down and eventually halted. Its motion is then reversed, and it is forced away from the surface. If the Reynolds

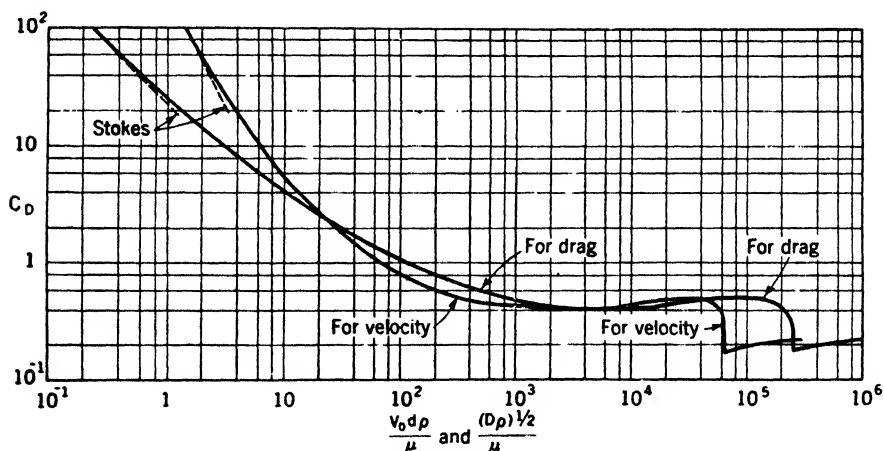


FIG. 10.13. — Drag coefficient C_D versus Reynolds number $\rho V_0 d / \mu$ and $(D\rho)^{1/2} / \mu$ for a sphere. (After Eisner, *Das Widerstandsproblem*, Third Int. Cong. App. Mech., Stockholm, 1930.)

number is below the critical value, the main stream diverges, or separates, from the body at this point, which thus becomes the separation point. If, however, R is greater than the critical value, the separated laminar layer

becomes turbulent and returns to the surface. The increased momentum of the turbulent layer enables it to progress somewhat farther before the adverse pressure again causes it to separate, this time permanently. The

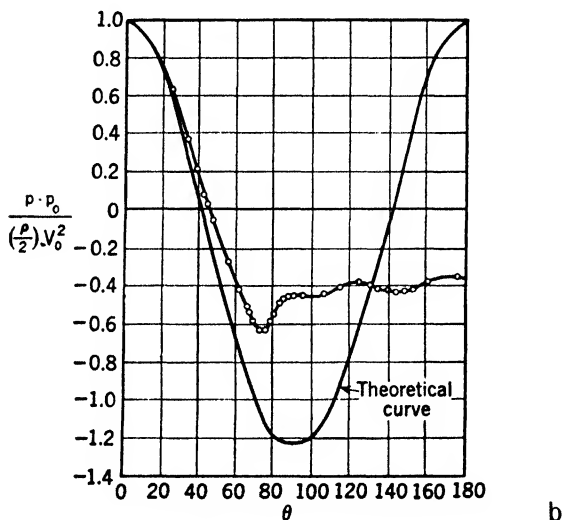
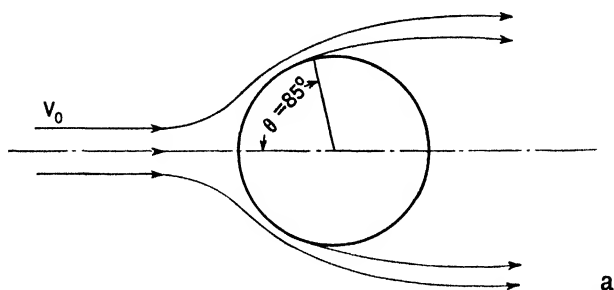


FIG. 10.14. — Measured pressure distribution for subcritical flow past a sphere. The theoretical curve for irrotational flow is also shown. [From "Modern Developments in Fluid Dynamics" (edited by S. Goldstein), courtesy of the Oxford University Press, publishers.]

transition from laminar to turbulent flow in the boundary layer thus causes the separation point to be moved toward the rear.

The critical value R_c , below which transition does not occur, depends not only on the shape of the rounded body but also on the turbulence present in the main stream. The greater the turbulence of the approaching flow, the lower the value of R_c , and vice versa.

If $R < R_c$, the separation occurs approximately at the largest cross section of the sphere, as shown in Fig. 10.14a. On the other hand, if $R > R_c$, the separation takes place farther back, where the cross-sectional area is less, as seen in Fig. 10.15a.

In Fig. 10.14b, the measured pressure distribution in subcritical flow is

compared with that for a potential flow, which, from symmetry, is seen to yield a zero drag. A similar comparison for supercritical flow is given in Fig. 10.15b. It is obvious from these figures that the pressure-drag coeffi-

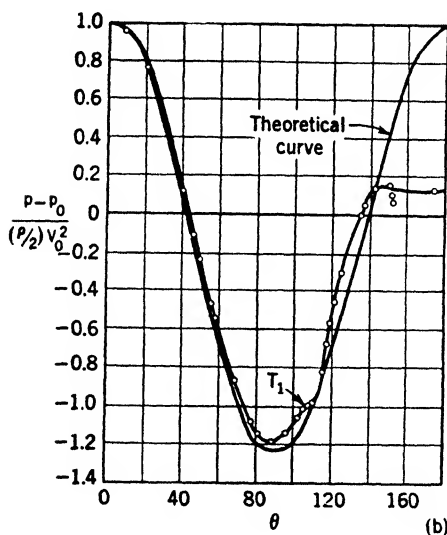
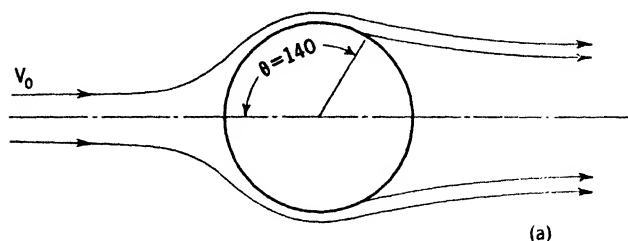


FIG. 10.15. — Measured pressure distribution for supercritical flow past a sphere. The theoretical curve for irrotational flow is also shown. [From "*Modern Developments in Fluid Dynamics*" (edited by S. Goldstein), courtesy of the Oxford University Press, publishers.]

cient is less in supercritical than in subcritical flow. Since the pressure drag predominates over the friction drag, the over-all coefficient drops as the Reynolds number surpasses the critical value.

For determination of the terminal velocity of a sphere falling through a fluid it is convenient to know the drag coefficient as a function of a dimensionless number including the drag, rather than as a function of R , because D is given, whereas V is unknown. It is seen from Art. 7.19 that the formula $C_D = \phi(R)$ can be transformed to $C_D = \phi_1(D^{1/2} \rho^{1/2} / \mu)$. This curve is included in Fig. 10.13.

10.12. Influence of a Free Surface. In this case the general equation for C_D [Eq. (10.4)] takes the form

$$C_D = \psi(R, F) \quad (10.27)$$

The principal application of Eq. (10.27) is to surface vessels, in the design of which the excess over the friction drag, or "residual drag," is an important factor. Offhand, it would appear that the naval architect could test a scale model of a proposed hull at several values of R and F and thereby determine with sufficient precision the C_D surface defined by Eq. (10.27). A difficulty arises, however, because the only practicable liquid in which to carry out towing tests on a model is water. The kinematic viscosity is therefore the same as for the full-scale hull, and it is impossible to fulfill simultaneously the conditions, $R_M = R_P$ and $F_M = F_P$, where the subscripts M and P stand for "model" and "prototype," respectively.

A satisfactory way to carry out and interpret model tests on hull forms was first suggested by William Froude in 1879, as the result of extensive experiments. Stated in modern terms, Froude's basic assumptions are (1) that the friction-drag coefficient is independent of the shape of the hull and is determined completely by the Reynolds number based on the length VL/ν , and (2) that the residual-drag coefficient is a function of only the Froude number V^2/lg . Thus, Eq. (10.27) becomes

$$C_D = C_{D_f} \left(\frac{VL}{\nu} \right) + C_{D_r} \left(\frac{V^2}{lg} \right) \quad (10.28)$$

where C_{D_f} and C_{D_r} are the coefficients of friction drag and residual drag, respectively. For the determination of the frictional component, Froude made numerous towing tests on planks, which caused practically no waves, and the drag of which was therefore nearly all due to surface friction. Froude's own friction data have now been superseded by more modern formulations of flat-plate drag, such as the Prandtl-Schlichting equation [Eq. (10.25)].

An example of the Froude method is given in Fig. 10.16. At the left is the curve of C_D for a 20-ft model, obtained from towing tests covering the range of Froude number anticipated for the prototype. Values of the Froude number $F = V^2/lg$ are spotted on this curve. The Prandtl-Schlichting curve for a smooth flat plate covered with an all-turbulent boundary layer is assumed to yield C_{D_f} for either the model or the 400-ft prototype. According to Eq. (10.28) the values of C_{D_r} obtained by subtraction of C_{D_f} from C_D for the model are independent of the Reynolds number and may therefore be added to the C_{D_f} values at the proper Reynolds numbers to get the C_D curve for the 400-ft hull. This curve appears at the right side of Fig. 10.16.

This procedure has been found reasonably satisfactory in the design of

vessels. The fact that the shape of the hull is neglected in the determination of the friction-drag coefficient does not lead to serious errors. In practice, however, a correction is added to the Prandtl-Schlichting curve for a smooth plate to take account of the roughness of the full-scale vessel. The empirical correction used depends upon the nature of the surface;

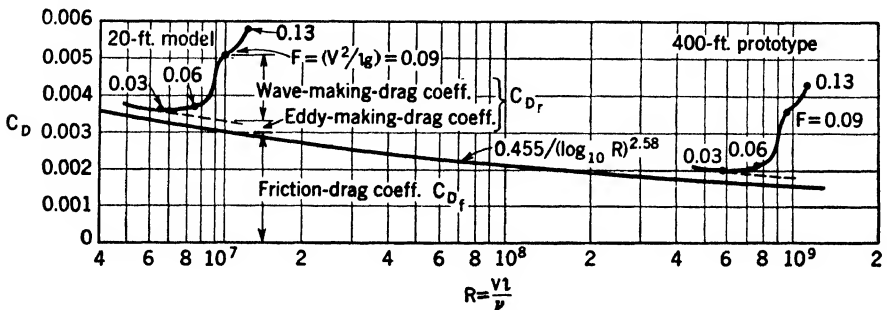


FIG. 10.16. — Drag coefficient, C_D , for a model vessel and its prototype. The dependence on both Reynolds number R and Froude number F is shown. (After Davidson, reference 10, courtesy of the author and the Society of Naval Architects and Marine Engineers.)

for example, different corrections are employed for riveted and welded hulls or for freshly painted and barnacle-covered surfaces.

The shape of the C_D curves of Fig. 10.16 is of interest in connection with the mechanism of the residual drag. At low values of Froude number ($F < 0.03$) the C_D and C_{D_f} curves are practically parallel; in other words, C_{D_r} is a constant. This fact leads one to suppose that, at low Froude numbers, the residual drag is principally form drag. In support of this conclusion is the observation that no surface waves are set up in this range of F .

The dotted line of Fig. 10.16, parallel to the Prandtl-Schlichting curve, indicates the assumed value of the form- ("eddy-making") drag coefficient at higher values of F .

The upturn in the C_D curve at $F = 0.03$ corresponds with the first appearance of surface waves created by the hull. A train of waves is shed from the bow and another at the stern, both of which increase in amplitude as F increases. The water level around the bow is raised by the presence of the bow wave, while the water level at the stern is lowered by the action of the stern wave. The pressure distribution over the hull is thus changed unfavorably, and the residual-drag coefficient is markedly increased. This increase is called the "wave-making-drag coefficient" and is indicated in Fig. 10.16.

It will be further observed in Fig. 10.16 that the C_D curve has an undulant, or "hump-and-hollow," shape and that this peculiarity is caused by variations in the wave-making coefficient. These variations have been traced to the change in phase between the bow-wave train and the stern-wave train that occurs as F is increased. When the two wave trains are in

phase, the water level at the stern is less than it would be in the absence of a bow wave, while the opposite is true when the wave trains are out of phase.

It is obviously desirable to design a hull to operate just at the base of one of the peaks of the C_D curve rather than at the crest. Otherwise, a considerable penalty is paid for a small increase in cruising speed.

10.13. Compressibility at Subsonic and Transonic Speeds. At speeds that are appreciable compared with sound velocity the general drag equation [Eq. (10.4)] takes the form

$$C_D = \psi(R, M) \quad (10.29)$$

The principal application of this equation at Mach numbers less than 1 is to aircraft. Compressibility effects on air propellers have long been recognized, and they are now important also in the flow past wings and control surfaces of high-speed airplanes. If an aircraft exceeds a certain critical velocity (as in a dive), shock waves appear on the wings and control surfaces, which then undergo not only a sudden increase in drag but also a decrease in lift and a shift in the center of pressure.

It is convenient to classify compressible flows as either subsonic or transonic. The former is defined as one in which the velocity is everywhere subsonic, while in the latter there is at least one point where sonic speed is attained or exceeded. The flow past a body moving at subsonic speed can be transonic, because near the body there are regions where the local relative velocities are higher and the local sound velocities are less than those of the distance fluid. The Mach number of the undisturbed stream at which the transition from subsonic to transonic flow occurs is known as the "critical Mach number" M_c .

In general, the Reynolds number and Mach number are both important in determining subsonic flow patterns, but in the transonic regime the Mach number predominates.

Large changes in the drag and lift coefficients of a body are observed to start if the Mach number is increased somewhat above the critical value. These changes are associated with the development of shock waves near the body, resulting from the breakdown of local supersonic flow. There is not yet a satisfactory theoretical value for the Mach number at which the shock waves first appear on a given body. The critical Mach number defined above is obviously a lower limit, since a shock wave can occur only in a supersonic flow. In certain irrotational flows that have been investigated theoretically speeds more than 50 per cent greater than the local sound velocity are attained, together with a continuous deceleration to subsonic speed farther downstream. At higher speed a so-called "limiting line" is found in the theory, beyond which the irrotational flow cannot progress. This line is interpreted as the locus of a shock wave, since these in general introduce rotation into a flow. Little is known of the stability

of these theoretical patterns, to say nothing of actual ones, which are further complicated by friction. It seems, however, that the Mach number at which a limiting line theoretically appears is a conservative upper limit to the M value at which a shock will occur in an actual flow.

For subsonic motion the Glauert-Prandtl approximate theory for slender bodies (Art. 11.32) shows that the velocities reached in compressible flow are increased by a factor $1/\sqrt{1-M^2}$ over those in incompressible flow at the same free-stream velocity. The pressure difference between any two points is also increased in the same ratio, and the drag coefficient may tend to rise, due principally to the thickening of the boundary layer by the larger adverse pressure gradient. This effect is more marked with thick airfoils than with thin ones, as is seen in Fig. 10.17. For the thin airfoil, C_D actually decreases over most of the range of M/M_c , which is attributable to the increasing R .

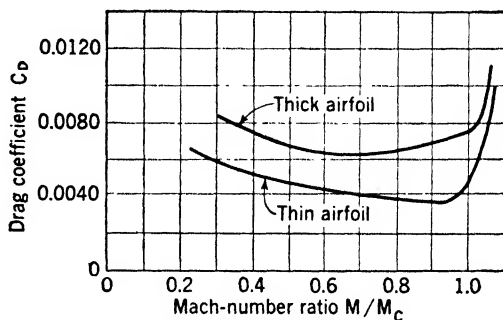


FIG. 10.17.— Drag coefficient C_D versus Mach-number ratio M/M_c for two airfoils.

Figure 10.17 also shows the rapid increase in C_D after the critical Mach number is reached. This change, which dwarfs the small compressibility

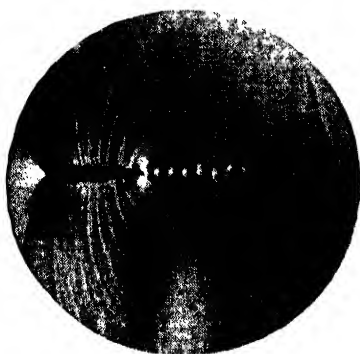


FIG. 10.18.— Schlieren photograph of NACA 0012 airfoil with tail cut off illustrating propagation of disturbances at a Mach number $M = 0.704$. (NACA photograph. Courtesy of John Stack.)

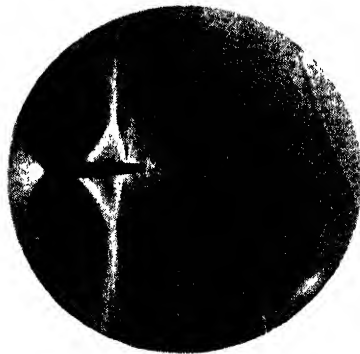


FIG. 10.19.— Schlieren photograph of NACA 0012 airfoil with tail cut off illustrating propagation of disturbances at a Mach number $M = 0.833$. (NACA photograph. Courtesy of John Stack.)

effects in subsonic flow, results from the alterations in the flow pattern produced by shock waves. Schlieren photographs of these flow phenomena are given in Figs. 10.18 and 10.19. An airfoil with the tail cut off was pur-

posely used in these experiments, so that the flow could be interpreted by observation of disturbances set up at the blunt end. These disturbances are shed alternately from one corner and the other, as is seen by their staggered arrangement. In the first picture they can progress upstream everywhere, except in a small region near the widest part of the section, where they are crowded together. The flow is therefore supersonic only in this small region. There is no separation of the stream from the surface.

The Mach number of the flow in Fig. 10.19 is higher than in Fig. 10.18, and a well-developed shock wave springs from both sides of the airfoil. Beyond the ends of the shock the tail disturbances move upstream, indicating that the supersonic region is again only local, although larger than that of Fig. 10.18. The forward end of this region is marked by oblique shocks, which coalesce with the normal shock set up at the downstream end of the region. Noticeable separation occurs, beginning under the oblique shocks and extending the length of the airfoil to form a relatively wide wake.

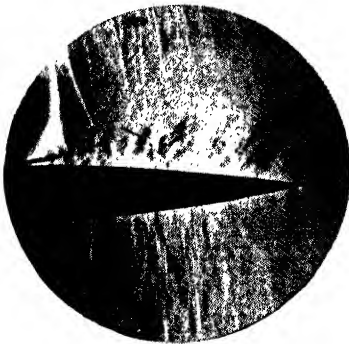


FIG. 10.20. — Schlieren photograph of separated flow for rear portion of NACA 23015 airfoil at a Mach number $M = 0.691$. Airfoil chord 5 in.; angle of attack 6 deg. (NACA photograph. Courtesy of John Stack.)

Another picture of separation is given in Fig. 10.20, which shows a transonic flow over an airfoil at a moderate angle of attack. It is clear that the separation point is just upstream from the first oblique shock. Since there would be no separation of a subsonic flow from this airfoil at this angle of attack, it seems likely that the shock is connected with the separation observed. Measurements of pressure at the surface of the airfoil show a discontinuous rise under the shock, and it is thought that this so thickens the boundary layer that separation takes place. The oblique shocks are believed to be caused by the bending of the supersonic stream into a re-

gion of higher pressure, as the supersonic stream flows over the more slowly moving fluid in the boundary layer. The dark line in Fig. 10.20 that extends downstream from the separation point may mark the boundary between sub- and supersonic flow.

The large increase in drag coefficient in the transonic regime is found to be largely due to the separation induced by the shocks, rather than to the losses in the shocks themselves. The defect in total pressure, determined by a wake traverse with an impact tube, is given in Fig. 10.21 for both sub- and transonic flow conditions. The area under each curve is a measure of the corresponding C_D . At the lower Mach number the width of the wake is small, as well as the maximum total-pressure defect. At the higher

Mach number the area under the large peak is attributed to separation and the area under the flatter parts of the curve to the shock. The former area is more than half the total.

It is of interest to compare the measured static-pressure rise on the air-

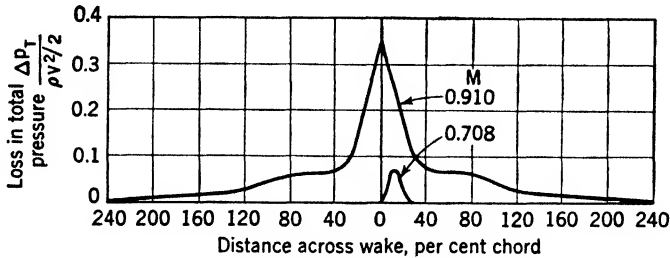


FIG. 10.21. — Wake shape and total-pressure defect as influenced by Mach number. NACA 0012 airfoil at 0-deg angle of attack. (After Stack, reference 8. Courtesy of the Institute of the Aeronautical Sciences.)

foil under the shock with the pressure rise computed from the measured total-pressure defect caused by the shock. In Fig. 10.22 are shown the measured pressure distribution over the upper surface of an airfoil and the

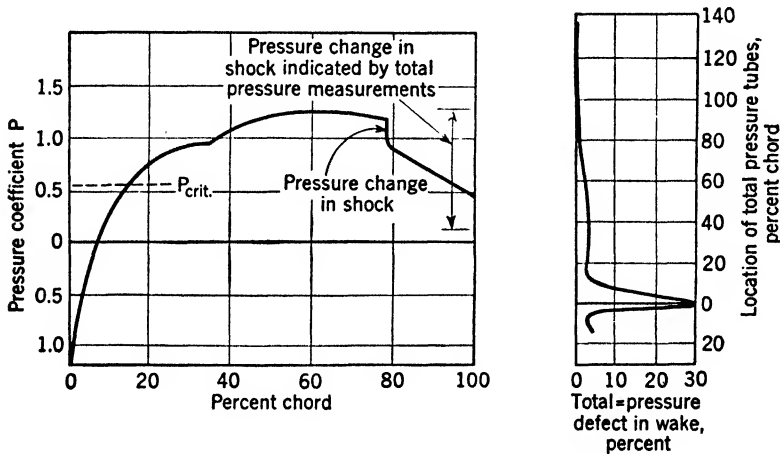


FIG. 10.22. — Measured static-pressure change through shock as compared with calculated change based on total-pressure loss in wake. NACA 4412 airfoil at $\frac{1}{4}$ -deg angle of attack. $M = 0.770$. (After Stack, reference 8. Courtesy of the Institute of the Aeronautical Sciences.)

total-pressure defect in the wake, together with the pressure jump computed from the height of the flat part of the defect curve. The latter is so much greater than the measured discontinuity that the difference cannot be accounted for by approximations in the theory. A reasonable explanation seems to be that the pressure distribution along the surface is modified by disturbances transmitted upstream through the subsonic boundary layer.

These phenomena of the transonic regime indicate the necessity of a large critical Mach number for an airfoil designed for high subsonic speeds. For a large M_c the excess of the maximum local velocity over the distant velocity must be as small as possible. This condition is met by the NACA 16 series of airfoils, each member of which is designed to have a minimum excess velocity at a definite value of the lift coefficient. In Fig. 10.6a are shown the velocity distributions for an incompressible flow over the NACA 16-209 and NACA 4412 airfoils, each at angle of attack corresponding to $C_L = 0.2$. In Fig. 10.23 are plotted the velocity distributions computed

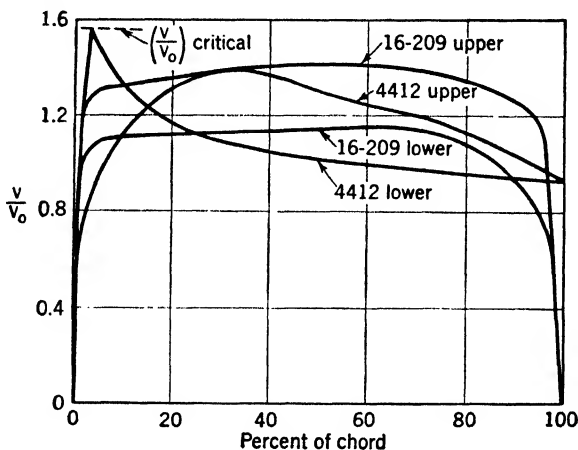


FIG. 10.23. — Velocity distributions for compressible flow over NACA 4412 and NACA 16-209 airfoils, both at the same angle of attack. Compare with Fig. 10.6a.

for a compressible flow over the same airfoils in the same attitude. The only difference between these two figures is in the Mach number: in Fig. 10.6a, $M \approx 0$, while, in Fig. 10.23, $M = 0.6$, which is the critical value for the 4412 at the given angle of attack of -2 deg. It is seen that, under these conditions, the local sound velocity is reached on the lower surface of the 4412 but that the velocity everywhere on the 16-209 is well below the sonic value. The measured critical Mach number for the 16-209 is $M_c = 0.76$.

10.14. Compressibility at Supersonic Speeds. Hitherto, this subject has been of practical importance only in the field of exterior ballistics, but the recent developments in jet and rocket propulsion foreshadow a much more widespread interest. Already, some ballisticians are using their experience with projectiles as the starting point in the rational design of low-drag forms for supersonic motion.

It will be recalled from Chap. IX that a shock wave is formed in front of a body whose velocity exceeds that of sound in the undisturbed fluid. The effect of this nose shock on the drag depends on the intensity of the shock, which in turn is greatly influenced by the shape of the front end of

the body. A relatively weak nose wave is associated with a thin airfoil or pointed projectile, while a round-nosed body sets up a bow wave of large amplitude, regardless of the tapering of the tail. A tapering, pointed nose is thus essential for low drag at supersonic speeds.

A drag-coefficient curve for an airfoil is shown diagrammatically in Fig. 10.24. The rapid dropping off of C_D beyond the transonic region is due

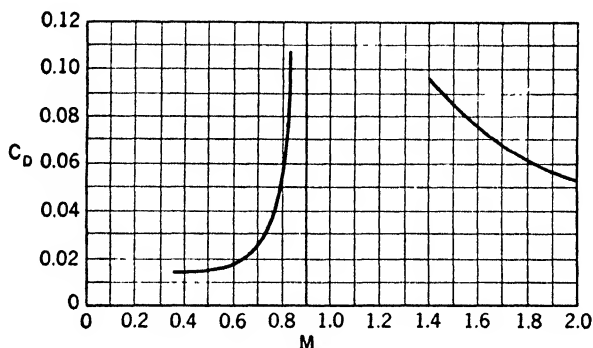


FIG. 10.24. — Diagrammatic sketch of the drag coefficient C_D versus Mach number M for an airfoil.

to the fact that shocks formed on the surface during the critical regime move off the airfoil and to the rear as M increases, the width of the wake being thus reduced. In the supersonic region, C_D is somewhat higher than at subsonic speeds, on account of the shock waves at the nose and tail.

Data on projectiles are illustrated in Fig. 10.25, in which curve a gives

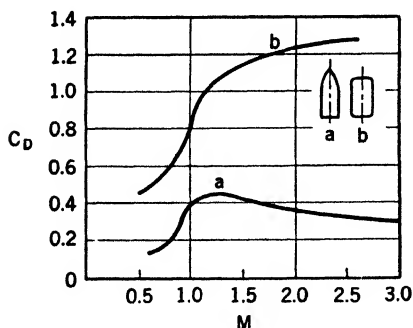


FIG. 10.25. — Drag coefficient C versus Mach number M for a sharp-nosed and a blunt projectile. (After Ackeret, reference 14.)



FIG. 10.26. — Wave pattern set up by a bullet at a speed slightly greater than the sound velocity. (After Ackeret, reference 14.)

the C_D for a pointed bullet. Critical phenomena similar to those on an airfoil cause a sharp rise in C_D beginning approximately at $M = 0.8$. The local shocks on the bullet for a Mach number slightly greater than 1, where C_D is near its maximum value, are clearly shown in Fig. 10.26.

Curve *b* of Fig. 10.25, for a blunt-nosed projectile, is quite different from that for the bullet. The effectiveness of the local shocks formed during the transonic motion in increasing the drag coefficient is less than in the previous

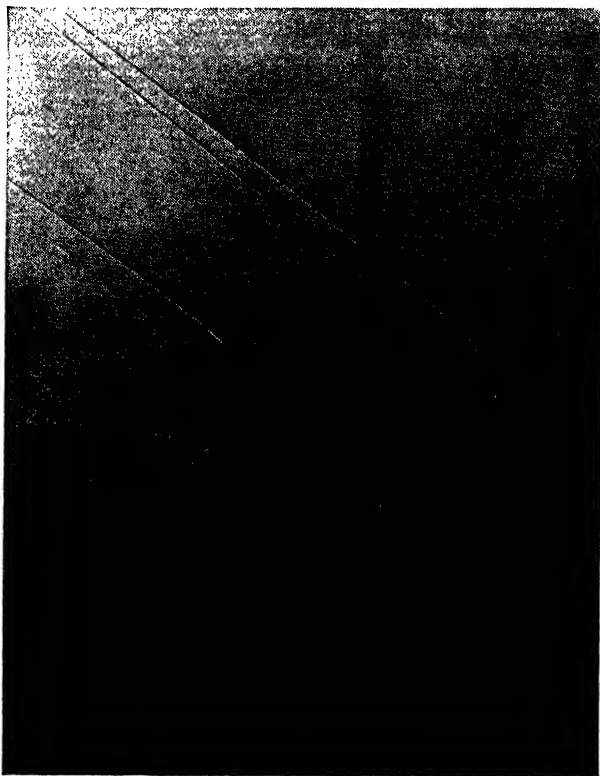


FIG. 10.27. — Wave pattern set up by a blunt-nosed bullet at a supersonic speed. (Photograph made at the Aberdeen Proving Ground. Courtesy of A. C. Charters and R. Turetsky.)

examples. The probable explanation is that the flow has already separated from the forward corners before the critical conditions are reached. Much of the rise in C_D occurs at supersonic speeds and is largely due to the increased pressure on the nose accompanying the intense head wave. There is pronounced similarity between this C_D curve and the stagnation-pressure curve plotted in Fig. 9.19.

Figures 10.27 and 10.28 are spark photographs that show the striking difference in the nose waves accompanying the blunt and pointed projectiles. It will be recalled from Art. 9.3 that the more nearly normal a shock wave is to the line of motion the greater is its intensity. The nose wave of the blunt projectile is therefore much more intense than that of the pointed one.

At high supersonic speeds the low pressure at the rear has relatively

little effect on C_D . The large pressure on the front and the surface friction are the main sources of drag. The friction increases markedly at high Mach numbers; it may amount to 75 per cent of the total drag of a well-designed body at a Mach number of 5.

The frictional heating of the boundary-layer fluid makes the wake



FIG. 10.28. — Wave pattern set up by a sharp-nosed bullet at a supersonic speed. (Photograph made at the Aberdeen Proving Ground. Courtesy of A. C. Charters and R. Turetsky.)

density less than that of the surrounding air, so that the wake is visible in the photographs.

In line with the growing interest in supersonic motion, tests have recently been made on spheres [1]. The spheres were fired in place of bullets, and spark photographs were taken at several stations along the line of flight. These photographs, made at known times, permitted the calculation of the drag-coefficient curve of Fig. 10.29. Spheres of $\frac{9}{16}$ in. diameter were used in most of the tests on which this curve is based, but a few results for $1\frac{1}{2}$ -in.-diameter spheres are also included. These fall on the same curve if $M > 0.8$, while the dotted line shows their trend at lower values of M .

It is seen that C_D starts to rise at a Mach number of about 0.5, reaches a

peak at $M = 1.5$, and then drops gradually with further increase in M . The gradual dropping off of the curve in the supersonic region suggests that the head wave may be intermediate in intensity between those for

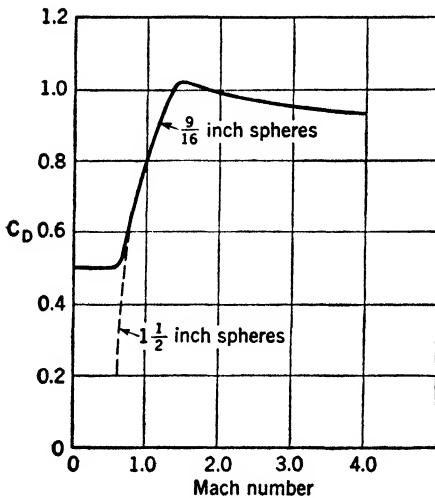


FIG. 10.29. — Drag coefficient C_D versus Mach number M for spheres. (After Charters, reference 1. Courtesy of the Institute of the Aeronautical Sciences.)

It is well known that a sphere possesses a critical Reynolds number in incompressible flow. The $\frac{9}{16}$ -in. spheres, however, showed no drop in C_D , even though R passed through the range found to be critical for large spheres under conditions of incompressibility. This fact suggests that, at sufficiently large M , the influence of R is secondary.

The dotted line in Fig. 10.29 is good evidence that the larger spheres ($1\frac{1}{2}$ in. diameter) passed through a critical R at a value of M somewhat below 0.6. The fact that the dotted line becomes coincident with the full-line curve at $M = 0.8$ strengthens the conclusion that R is unimportant at large values of M .

SELECTED BIBLIOGRAPHY

1. CHARTERS, A. C.: The Aerodynamic Performance of Small Spheres from Subsonic to High Supersonic Velocities, *J. Aeronaut. Sci.*, vol. 12, pp. 468–476, October, 1945.
2. DRYDEN, H. L.: Turbulence and the Boundary Layer, *J. Aeronaut. Sci.*, vol. 6, pp. 85–100, January, 1939.
3. GOLDSTEIN, S. (Editor): "Modern Developments in Fluid Dynamics," p. 135, Oxford University Press, New York, 1938.
4. *Ibid.*, pp. 24 and 523.
5. *Ibid.*, p. 131.
6. *Ibid.*, p. 117.
7. KÁRMÁN, TH. VON: Compressibility Effects in Aerodynamics, *J. Aeronaut. Sci.*, vol. 8, pp. 337–356, July, 1941.

pointed and blunt objects. The wave pattern of Fig. 10.30 is of interest in connection with this speculation. It is seen that the head wave follows the contour of the surface and hence is steeper (near the axis) than one for a pointed object, but not so steep as one for a blunt body.

Figure 10.31 illustrates the waves at $M = 0.992$. For steady motion there would be no head wave, but for the decelerated motion of the sphere this wave is in process of moving farther ahead and eventually disappearing. In Fig. 10.32, taken a few moments later, the head wave has moved out of the field of view. The value of M for this picture is 0.972.

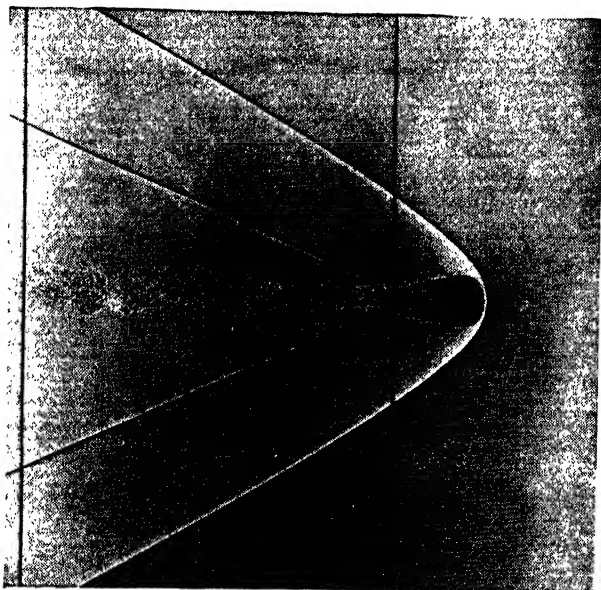


FIG. 10.30. — Wave pattern set up by a sphere at a supersonic speed $M = 2.23$. The vertical black lines are not part of the wave pattern. (Photograph made at the Aberdeen Proving Ground. Courtesy of A. C. Charters and R. Turetsky.)

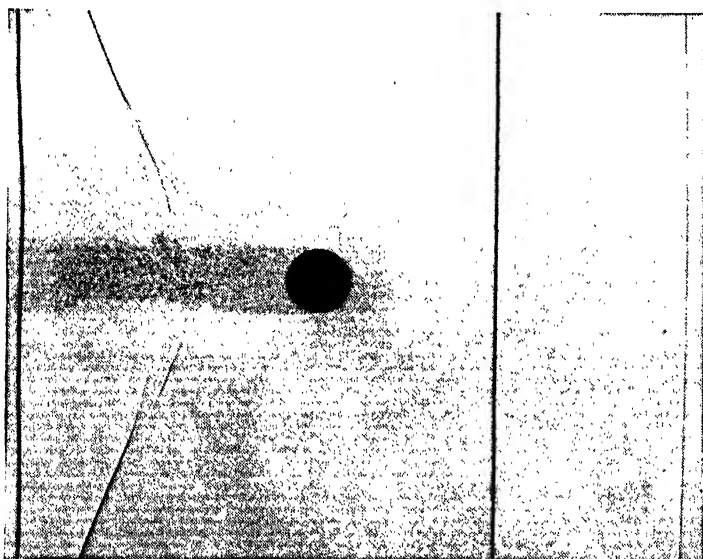


FIG. 10.31. — Wave pattern set up by a decelerating sphere at a Mach number $M = 0.992$. (Photograph made at the Aberdeen Proving Ground. Courtesy of A. C. Charters and R. Turetsky.)

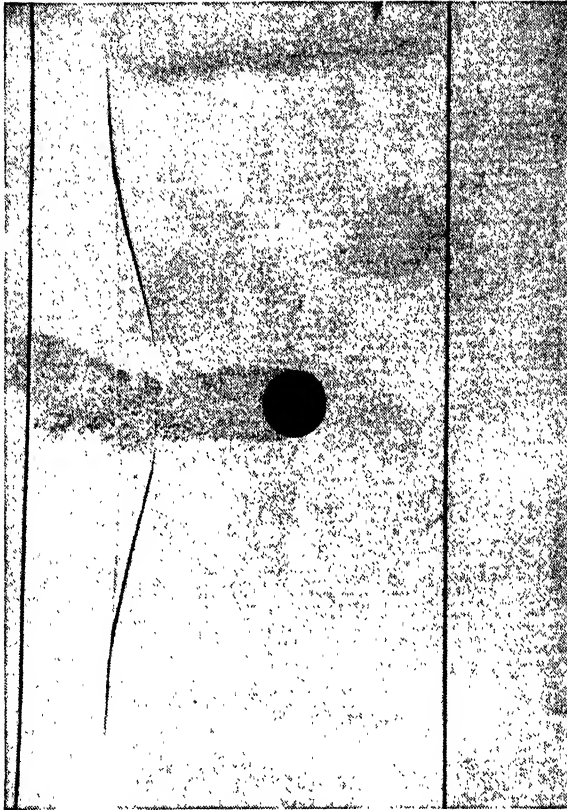


FIG. 10.32. — Wave pattern set up by a decelerating sphere at a Mach number $M = 0.972$. (Photograph made at the Aberdeen Proving Ground. Courtesy of A. C. Charters and R. Turetsky.)

8. STACK, JOHN: Compressible Flows in Aeronautics, *J. Aeronaut. Sci.*, vol. 12, pp. 127–148, April, 1945.
9. TOLLMIE, W.: “General Instability Criterion of Laminar Velocity Distributions,” *NACA, Tech. Mem.* 792, 1936.
10. DAVIDSON, K. S. M.: Resistance and Powering, Chap. II in “Principles of Naval Architecture” (edited by H. E. Rossell and L. B. Chapman), Society of Naval Architects and Marine Engineers, New York, 1939.
11. SCHUBAUER, G. B., and H. K. SKRAMSTAD: “Laminar-boundary-layer Oscillations on a Flat Plate,” *NACA Rept.*, April, 1943.
12. ABBOTT, I. H., A. E. VON DOENHOFF, and L. S. STIVERS: “Summary of Airfoil Data,” *NACA Rept.*, March, 1945.
13. DRYDEN, H. L.: “Some Recent Contributions to the Study of Transition and Turbulent Boundary Layers,” *NACA Tech. Note* 1168, April, 1947.
14. ACKERET, J.: Gasdynamik, in “Handbuch der Physik,” Band VII, Verlag Julius Springer, Berlin, 1927.

CHAPTER XI

WING THEORY

11.1. Potential Flow. The concept of a potential is familiar from its use in electricity, and in Chap. IV we discussed the potential energy in a gravity field. The potential function for an electric field has the property that its rate of change in any direction gives the magnitude of the force in that direction exerted by the field on unit charge of electricity. The gravity potential function, usually called the "gravity potential energy," has the property that its rate of change in any direction gives the magnitude of the weight force in that direction exerted on unit mass of matter. One can easily verify that the gravity potential energy P has this property, for, from Art. 4.6, P is seen to equal gh , where h is the height above an arbitrary level. The expression, $\partial P/\partial x = g \partial h/\partial x$ thus gives the negative of the weight force on unit mass in any direction x .

Each of these potential functions is seen to describe completely the force field to which it applies.

In a somewhat analogous manner, two potential functions, the stream function and the velocity potential, have been found, either of which completely describes the velocity field of a flowing fluid. The reason for introducing them is the mathematical simplification that results and the possibility of finding the theoretical flow patterns about certain shapes.

Here we confine ourselves to the steady flow of an ideal fluid and restrict the discussion to two-dimensional cases.

11.2. Equations of Motion. Any flow pattern is determined by the boundary conditions, which require the boundary streamlines to take a definite form, and by the equations of motion. These include the continuity equation, a purely kinematic relation, and a dynamic equation for each of the dimensions of space.

The continuity equation for a steady flow was shown in Chap. III to be

$$\int_A \rho V \cos \alpha \, dA = 0 \quad (3.8)$$

provided that no source of fluid is included inside the closed surface A . In this equation, α is the angle between the local velocity V and the outward-drawn normal to the surface element, dA . For two-dimensional motion the flow has no component perpendicular to the x,y plane, and the flow patterns in all planes parallel to this are the same. Consequently, the closed surface A can be thought of as a "fence" of unit height whose trace

in the x, y plane is a closed curve (Fig. 11.1). In addition to this fence, A will also include two plane-parallel surfaces forming the ends of the cylinder

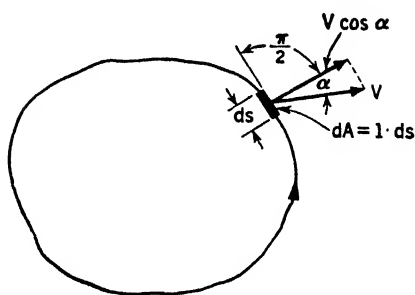


FIG. 11.1

whose side wall is the fence. These planes can be disregarded in the integration indicated in Eq. (3.8), however, since $\cos \alpha$ is zero everywhere on them. Equation (3.8) thus can be written as

$$\oint \rho V \cos \alpha \, ds = 0 \quad (11.1)$$

where \oint denotes the integral around the closed curve. By convention, one

is said to face along the curve in the positive direction if the region bounded by the curve lies on the left hand. The positive direction is indicated by the arrow on the curve in Fig. 11.1. An observer facing in the positive direction sees the local outward-drawn normal extending from left to right.

The dynamic equations for steady flow of a frictionless fluid are derived for the x and y directions just as in Chap. IV for the directions parallel and normal to the velocity. Here, however, it is convenient to neglect gravity. The components of velocity parallel to x and y are $u(x, y)$ and $v(x, y)$, respectively, and the corresponding accelerations are

$$\begin{aligned} a_x &= \frac{Du}{dt} = \frac{\partial u}{\partial x} \frac{dx}{dt} + \frac{\partial u}{\partial y} \frac{dy}{dt} = u \frac{\partial u}{\partial x} + v \frac{\partial u}{\partial y} \\ a_y &= \frac{Dv}{dt} = \frac{\partial v}{\partial x} \frac{dx}{dt} + \frac{\partial v}{\partial y} \frac{dy}{dt} = u \frac{\partial v}{\partial x} + v \frac{\partial v}{\partial y} \end{aligned}$$

The symbol D/dt denotes differentiation following the motion of the fluid; it is to be noted that here dx and dy are not arbitrary but are the components of the displacement of a particle of fluid, so that $dx = u \, dt$ and $dy = v \, dt$. The components of pressure force per unit mass in the x and y directions are $(-1/\rho)(\partial p/\partial x)$ and $(-1/\rho)(\partial p/\partial y)$, so that Newton's law yields

$$\left. \begin{aligned} -\frac{1}{\rho} \frac{\partial p}{\partial x} &= \frac{Du}{dt} = u \frac{\partial u}{\partial x} + v \frac{\partial u}{\partial y} \\ -\frac{1}{\rho} \frac{\partial p}{\partial y} &= \frac{Dv}{dt} = u \frac{\partial v}{\partial x} + v \frac{\partial v}{\partial y} \end{aligned} \right\} \quad (11.2)$$

11.3. The Stream Function. The physical principle of continuity, on which is based Eq. (11.1), states that, for a source-free, steady, two-dimensional flow, the net mass efflux across any closed curve is zero.

From Eq. (11.1) we get

$$\int_{(ACB)}^B \rho V \cos \alpha \, ds = - \int_{(BEA)}^A \rho V \cos \alpha \, ds = \int_{(AEB)}^B \rho V \cos \alpha \, ds$$

where ACB and AEB are any two curves joining the points A and B (Fig. 11.2). In words, the mass flux is the same across any curve joining A and B . The mathematical consequences are important, for since the integral $\int_A^B \rho V \cos \alpha \, ds$ is independent of the path, $\rho V \cos \alpha \, ds$ is the differential of some scalar point function. It will be found convenient to define this function by the equation

$$\left. \begin{aligned} d\psi &= \frac{\rho}{\rho_0} V \cos \alpha \, ds \\ \psi_B - \psi_A &= \int_A^B \frac{\rho}{\rho_0} V \cos \alpha \, ds \end{aligned} \right\} \quad (11.3)$$

where the constant ρ_0 is the density of the fluid at rest.

The physical meaning of $\psi(x, y)$ is immediate: The difference between the values of ψ at any two points $\psi_B - \psi_A$ is proportional to the mass flux across any curve joining the points. In the case of an incompressible fluid, $\rho = \rho_0$, and $\psi_B - \psi_A$ is the volume flux across any curve joining A and B . For this reason, ψ is called the “stream function.”

Only the difference between two values of ψ appears in the definition [Eq. (11.3)]. Therefore, the value of ψ_A , where A is any point in the flow, can be arbitrarily assigned.

The values of ψ everywhere else in the flow are then determined by Eq. (11.3).

The stream function has three properties that render it useful, especially in the synthesis of complicated flow patterns from simple ones. The first property is that ψ is constant everywhere on any one streamline. We prove this simply by choosing ds in Eq. (11.3) as an element of the streamline and noting that $\cos \alpha$ is then zero. It follows from Eq. (11.3) that $d\psi = 0$ everywhere along the streamline, or $\psi = \text{constant}$.

The second property is closely related to the first and also follows immediately from the definition. Divide both sides of Eq. (11.3) by ds , and obtain

$$\frac{\partial \psi}{\partial s} = \frac{\rho}{\rho_0} V \cos \alpha \quad (11.4)$$

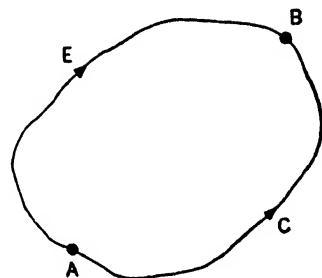


FIG. 11.2.

where the partial derivative is used to indicate that the change in ψ is that corresponding to a change in s only. The second property can be stated as follows: The rate of change of ψ with distance in an arbitrary direction is proportional to the component of velocity normal to that direction. For

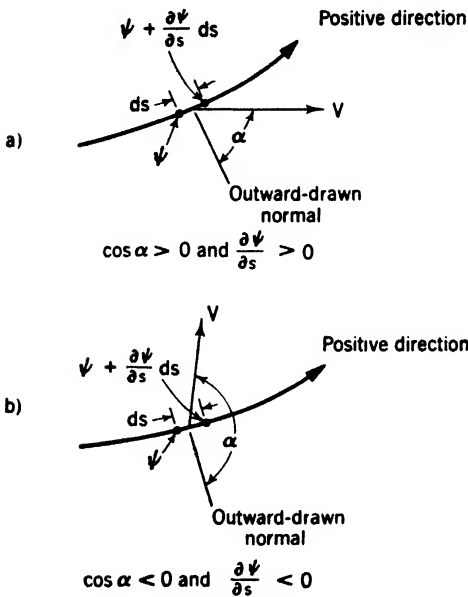


FIG. 11.3.

incompressible fluid, $\rho = \rho_0$, and $\partial \psi / \partial s$ is equal to the normal velocity component. The convention has already been stated in Art. 11.2 that an observer facing in the positive direction along a curve sees the local outward-drawn normal extending from left to right. This convention fixes the sign of $\partial \psi / \partial s$ and is illustrated in Fig. 11.3. For Cartesian coordinates x and y , Eq. (11.4) yields

$$\left. \begin{aligned} \frac{\partial \psi}{\partial y} &= \frac{\rho}{\rho_0} u \\ \frac{\partial \psi}{\partial x} &= -\frac{\rho}{\rho_0} v \end{aligned} \right\} \quad 11.5$$

To get the first of these equations, we let $ds = dy$, so that the positive x direction coincides

$$\left. \begin{aligned} \frac{\partial \psi}{r \partial \theta} &= \frac{\rho}{\rho_0} V_r \\ \frac{\partial \psi}{\partial r} &= -\frac{\rho}{\rho_0} V_\theta \end{aligned} \right\} \quad (11.6)$$

with the outward-drawn normal and $V \cos \alpha = u$. To get the second, we take $ds = dx$, so that the normal points in the negative y direction and $V \cos \alpha = -v$. Similarly for plane-polar coordinates r and θ , we get

where V_r and V_θ are the components of velocity in the directions of increasing r and θ , respectively (see Fig. 11.4). It should be pointed out that, for incompressible fluid, Eqs. (11.3), (11.4), (11.5), and (11.6) all hold (with $\rho = \rho_0$), even in an unsteady flow. This follows from the fact that, for incompressible fluid, the continuity equation has the form $\oint V \cos \alpha ds = 0$, regardless of whether or not the flow is steady [see Eq. (3.9)].

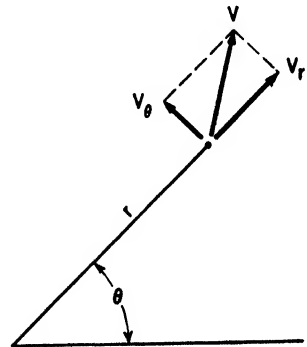


FIG. 11.4.

In this discussion of the stream function, we have so far required merely that the flow be continuous. If we add now the requirement that the fluid be incompressible and consider two flow patterns having stream functions ψ_1 , and ψ_2 , Eq. (11.4) gives

$$\frac{\partial \psi_1}{\partial s} + \frac{\partial \psi_2}{\partial s} = \frac{\partial(\psi_1 + \psi_2)}{\partial s} = V_1 \cos \alpha_1 + V_2 \cos \alpha_2$$

Since $V_1 \cos \alpha_1 + V_2 \cos \alpha_2$ is the component of the resultant velocity normal to the arbitrary direction ds , we may state the third property of the stream function as follows: The algebraic sum of the stream functions for two incompressible flow patterns is the stream function for the flow resulting from superposition of these patterns.

None of the properties of the stream function are of any practical use unless the flow patterns concerned satisfy not only the continuity requirements, but also the dynamical equations [Eqs. (11.2)]. It is possible that two incompressible flow patterns may each fulfill all of these conditions and yet, if they are superposed, their resultant may not satisfy Eqs. (11.2). It is shown below that this difficulty does not arise in case the continuous incompressible flows are assumed to be irrotational.

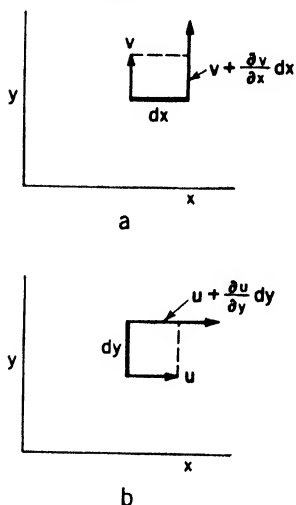


FIG. 11.5.

The rotation, or vorticity, at a point was defined in Chap. IV as the algebraic sum of the angular velocities of two mutually perpendicular line elements moving with the fluid and intersecting at the point in question. One of the pair of elements there considered was taken parallel to the velocity and the other normal to it. It may be shown, however, that the vorticity at a point is independent of the orientation of the line elements considered, so that the vorticity may be expressed in terms of elements dx and dy , for an arbitrary choice of axes x and y . Figure 11.5a shows that the counterclockwise angular velocity of fluid-line element dx is

$$\frac{v + (\partial v / \partial x) dx - v}{dx} = \frac{\partial v}{\partial x}$$

while, from Fig. 11.5b, that of dy is

$$\frac{-[u + (\partial u / \partial y) dy] + u}{dy} = -\frac{\partial u}{\partial y}$$

By convention, the counterclockwise sense is taken as positive. Consequently, the vorticity is

$$\text{Vorticity} = \frac{\partial v}{\partial x} - \frac{\partial u}{\partial y} \quad (11.7)$$

An irrotational motion is defined as one for which the vorticity is everywhere zero.

$$\frac{\partial v}{\partial x} - \frac{\partial u}{\partial y} = 0 \quad (11.8)$$

The restriction which the dynamical equations impose on the velocity components is found by elimination of p and ρ from Eqs. (11.2). Assuming ρ to be a function of p only, differentiate the first of these with respect to y , the second with respect to x , and subtract the first from the second.

$$-\frac{\partial p}{\partial y} \frac{d(1/\rho)}{dp} \frac{\partial p}{\partial x} - \frac{1}{\rho} \frac{\partial^2 p}{\partial y \partial x} + \frac{\partial p}{\partial x} \frac{d(1/\rho)}{dp} \frac{\partial p}{\partial y} + \frac{1}{\rho} \frac{\partial^2 p}{\partial x \partial y} =$$

$$\left(\frac{\partial u}{\partial x} + \frac{\partial v}{\partial y} \right) \left(\frac{\partial v}{\partial x} - \frac{\partial u}{\partial y} \right) + \frac{D}{dt} \left(\frac{\partial v}{\partial x} - \frac{\partial u}{\partial y} \right) = 0 \quad (11.8a)$$

It is obvious that, in irrotational flow, Eq. (11.8a) is everywhere satisfied.

Substitution in Eq. (11.8) of $\partial\psi/\partial y = u$ and $\partial\psi/\partial x = -v$, from Eq. (11.5), yields the differential equation that must be satisfied by ψ everywhere in the fluid.

$$\frac{\partial^2 \psi}{\partial x^2} + \frac{\partial^2 \psi}{\partial y^2} = 0 \quad (11.9)$$

Equation (11.9), known as Laplace's equation, is linear, so that the sum of two solutions is also a solution. Therefore, if two flow patterns are given, having stream functions ψ_1 and ψ_2 , each of which satisfies Eq. (11.9), the sum $\psi_1 + \psi_2$ also satisfies the same equation and thus represents the stream function for another irrotational incompressible flow. By the third property of a stream function, discussed above, this flow is the resultant of the two flows in question.

The stream function is thus a powerful tool in the study of irrotational incompressible flows, since complex patterns can be synthesized by algebraic addition of the stream functions of simple patterns. This important application of the stream function is illustrated by the examples below.

11.4. Parallel Flow. As a simple example of a stream function, assume a steady two-dimensional flow parallel to the axis of x and with velocity U . The streamlines are horizontal lines running to the right. Since $\partial\psi/\partial x = -v = 0$ and $\partial\psi/\partial y = u = U$, $d\psi = U dy$ and the stream function

$$\psi = Uy \quad (11.10)$$

completely describes the flow. Note that the x axis is the line $\psi = 0$, and larger values of y correspond to larger numerical values of ψ . If, for example, $y = 5$, $\psi = 5U$ and the discharge between this line and the x axis is $\int_0^5 d\psi = \psi_5 - \psi_0 = 5U$ per unit depth. Note that flow is positive toward the right, by our convention as to signs, so that $5U$ denotes a discharge to the right.

In this example we made the constant of integration equal to zero by arbitrarily setting $\psi = 0$ on the x axis. If we write $\psi = Uy + \text{constant}$, we do not change the flow pattern but merely change the value of ψ on every streamline by an amount equal to the constant. In any flow having a stream function the constant of integration plays the same trivial role, so that in later examples it will usually be set equal to zero.

11.5. Source and Sink. Imagine that, along a line normal to the x, y plane at the origin of coordinates, fluid is being emitted at a constant rate and that it flows away radially from this "line source." In the two-dimensional space of a layer of unit depth the source discharges at a rate of Q units of volume per unit time. At any radius r from the source the velocity V must be, from continuity considerations, $V = Q/2\pi r$. Equation (11.6) applied to this purely radial flow gives

$$\frac{\partial \psi}{r \partial \theta} = V = \frac{Q}{2\pi r} \quad \frac{\partial \psi}{\partial r} = 0$$

Therefore

$$d\psi = \frac{Q}{2\pi} d\theta$$

and

$$\psi = \frac{Q}{2\pi} \theta \quad (11.11)$$

At the origin, where all the streamlines cross, ψ can have any value whatsoever and is therefore undefined. The origin, where the source is located, is thus a singular point as far as the stream function is concerned. This is to be expected, since a source-free flow was postulated as one essential for the existence of ψ . The stream function for the source is multiple-valued, increasing by Q each time θ increases by 2π .

A sink is the reverse of a source, fluid being abstracted at a rate Q . In this case the radial velocity is $V = -Q/2\pi r$, and the stream function is

$$\psi = -\frac{Q}{2\pi} \theta \quad (11.12)$$

The streamlines for both source and sink are radial lines. The product Vr has a constant value in each case, so that the velocity varies hyper-

bolically along the radius, approaching infinity as r approaches zero and zero as r approaches infinity.

11.6. Combination of a Source and Sink. In Fig. 11.6 are shown a source at B and a sink at A . The two have the same strength Q . The value of the stream function at any point P for the resultant flow is obtained by addition of Eqs. (11.11) and (11.12), with the angles at B and A set equal to θ_1 and θ_2 , respectively.

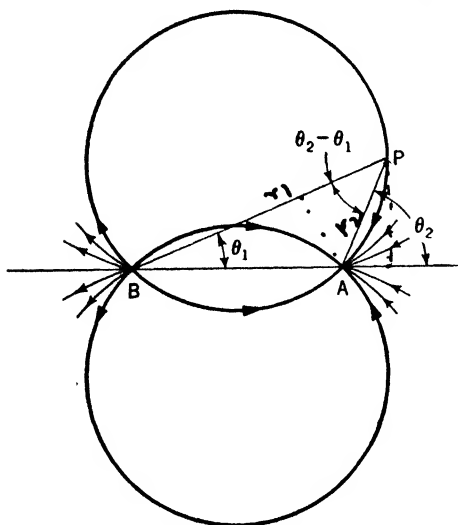


FIG. 11.6.

$$\psi = -\frac{Q}{2\pi} (\theta_2 - \theta_1) \quad (11.13)$$

Lines of constant ψ (the streamlines) are lines for which $\theta_2 - \theta_1$ is constant. Thus, by a well-known theorem in geometry, the streamlines are circles passing through A and B .

11.7. Rankine's Construction for Ship Forms. The stream

function for the combination of a source and sink with a uniform flow to the right is

$$\psi = Uy - \frac{Q}{2\pi} (\theta_2 - \theta_1) \quad (11.14)$$

The streamline $\psi = 0$ can easily be shown to be the axis of x , together with an oval enclosing all streamlines running between the source and sink.

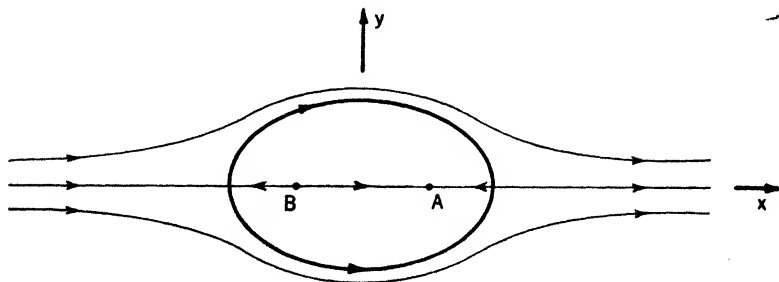


FIG. 11.7.

Outside of this oval is a field of flow consisting of streamlines extending as shown in Fig. 11.7. The oval streamline separates the fluid in the parallel flow from that flowing between the source and sink. The oval may be replaced by a solid body of the same shape, so that Fig. 11.7 may be thought

of as the pattern of frictionless flow around such a body. The restriction to frictionless flow is necessary, because the velocity at the oval is not zero. The boundary condition for a viscous fluid is thus violated.

If several sources are combined with several sinks of total aggregate strengths equal, the oval can be elongated or fish-shaped. Rankine de-

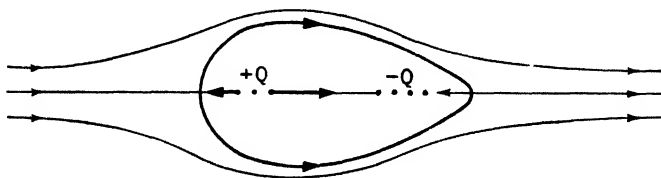


FIG. 11.8.

veloped mathematical forms for ships by this method, using two-dimensional flow, and Fuhrmann developed the forms for early Parseval airships by using a system of three-dimensional sources and sinks (see Art. 10.7).

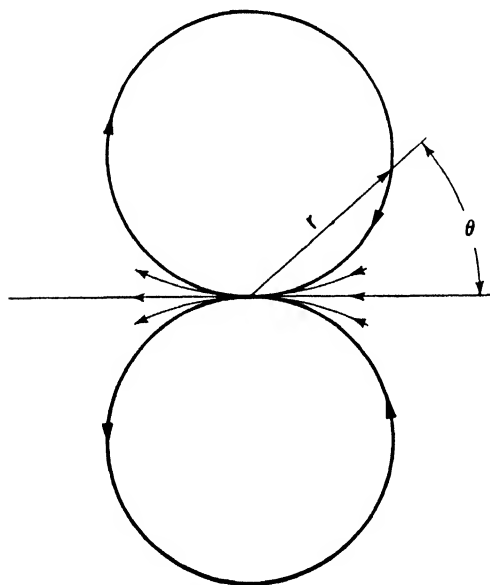


FIG. 11.9. — Streamlines for a doublet.

Such a body, as shown in Fig. 11.8, is an ideal “streamline form,” since it is bounded by streamlines in an ideal fluid.

§ 11.8. The Doublet and the Cylinder. If a source at B and an equal sink at A is moved indefinitely close together and their strengths increased so as to maintain $Q\overline{AB}$ finite and constant, the resulting flow is called a “doublet.” The streamlines will be circles tangent to the axis of the

doublet, as shown in Fig. 11.9. From Eq. (11.13) and Fig. 11.6 the stream function for a source and sink is

$$\psi = -\frac{Q}{2\pi} \frac{(\theta_2 - \theta_1)}{\sin(\theta_2 - \theta_1)} \sin(\theta_2 - \theta_1) = -\frac{Q}{2\pi} \frac{(\theta_2 - \theta_1)}{\sin(\theta_2 - \theta_1)} \frac{AB \sin \theta_1}{r_2}$$

If we let $AB \rightarrow 0$, keeping $Q\overline{AB}$ constant, $(\theta_2 - \theta_1)/\sin(\theta_2 - \theta_1) \rightarrow 1$, $\sin \theta_1 \rightarrow \sin \theta$, and $r_2 \rightarrow r$. Therefore, in the limit, the stream function for the doublet is

$$\psi = -\frac{Q\overline{AB}}{2\pi} \frac{\sin \theta}{r} = -C \frac{\sin \theta}{r} \quad (11.15)$$

where $C = Q\overline{AB}/2\pi$ is a constant. Equation (11.15) can readily be shown to yield the streamline pattern of Fig. 11.9.

If we combine a doublet with a flow parallel to the x axis, the shape enclosed by the external flow is a circle. From Eqs. (11.10) and (11.15),

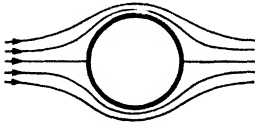


FIG. 11.10. — Combination of a doublet and a parallel flow gives the streamlines for a cylinder.

$$\psi = [Ur - (C/r)] \sin \theta$$

Let $C = Ua^2$, for convenience, so that

$$\psi = U \sin \theta \left(r - \frac{a^2}{r} \right) \quad (11.16)$$

One can readily show that Eq. (11.16) yields the flow pattern for a transverse flow disturbed by a circular cylinder, as shown in Fig. 11.10.

11.9. Pressure Distribution over a Moving Cylinder. The flow pattern about a cylinder is seen to indicate retarded flow and hence higher pressure at the front and rear of the cylinder and higher velocity and lower pressure over the top and bottom. The symmetry of the flow indicates that there is no force exerted by the pressure on the cylinder in any direction. The pressure distribution over the cylinder is obtained as follows: By Bernoulli's equation, if the pressure and velocity in the undisturbed flow are p_0 and U , we have

$$\frac{p - p_0}{(\rho/2)U^2} = 1 - \left(\frac{V}{U} \right)^2 \quad (11.17)$$

where p and V are the pressure and velocity at any point in the flow. From Eq. (11.16) the components of V are

$$\left. \begin{aligned} V_r &= \frac{\partial \psi}{r \partial \theta} = U \left(1 - \frac{a^2}{r^2} \right) \cos \theta \\ V_\theta &= -\frac{\partial \psi}{\partial r} = -U \left(1 + \frac{a^2}{r^2} \right) \sin \theta \end{aligned} \right\} \quad (11.18)$$

At the surface of the cylinder, where $r = a$, Eqs. (11.18) show that $V_\theta = -2U \sin \theta$, and $V_r = 0$. Consequently, Eq. (11.17) becomes

$$\frac{p - p_0}{(\rho/2)U^2} = 1 - 4 \sin^2 \theta \quad (11.19)$$

This equation is plotted in Fig. 11.11. It is seen that $p - p_0 = 0$ where

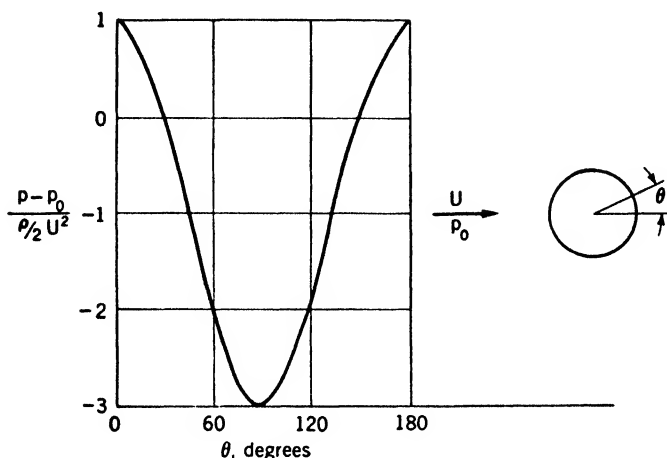


FIG. 11.11. — Pressure distribution over a cylinder.

$\sin \theta = \pm \frac{1}{2}$ and that $p - p_0$ reaches its minimum value $-3(\rho/2)U^2$ where $\sin \theta = \pm 1$.

11.10. Additional Apparent Mass. If on the flow pattern of the preceding article we superpose a general velocity $-U$ from right to left, we get a cylinder moving through a fluid that is at rest at infinity. Since the stream function for a parallel flow from right to left is $-Uy$, or $-Ur \sin \theta$, the stream function for the resultant flow is

$$\psi = U \left(r - \frac{a^2}{r} \right) \sin \theta - Ur \sin \theta = -\frac{Ua^2}{r} \sin \theta \quad (11.20)$$

The streamlines relative to the fluid are portions of circles, as can be seen by comparison of Eqs. (11.20) and (11.15), and are drawn in Fig. 11.12. The velocity at any point is given by

$$V^2 = \left(-\frac{\partial \psi}{\partial r} \right)^2 + \left(\frac{\partial \psi}{r \partial \theta} \right)^2 = \left(-\frac{Ua^2}{r^2} \sin \theta \right)^2 + \left(-\frac{Ua^2}{r^2} \cos \theta \right)^2 = \frac{U^2 a^4}{r^4}$$

Hence the kinetic energy stored in the flow pattern is

$$\int_a^\infty \frac{\rho}{2} V^2 \pi d(r^2) = \frac{\pi}{2} \rho U^2 a^4 \left[-\frac{1}{r^2} \right]_a^\infty = \frac{\pi}{2} \rho U^2 a^2 = \frac{1}{2} M' U^2 \quad (11.21)$$

The virtual mass of the cylinder is thus its own mass M plus an additional apparent mass $M' = \rho\pi a^2$ due to the energy of the flow. Any body in motion through a fluid moves with additional inertia.

Virtual mass affects the motions of balloons and airships, making them slow to accelerate. For airplanes this effect is negligible, as the displacement is relatively small. For ships and submarines virtual mass is important in mooring and docking operations.

11.11. Circulation. The circulation of fluid along any line from A to B is defined by the summation, or line integral, from A to B , at a given instant, of the component of velocity tangent to the line multiplied by

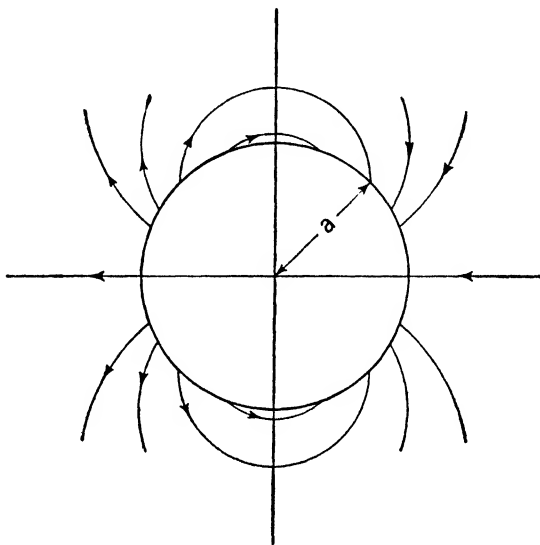


FIG. 11.12. — Streamlines for a moving cylinder.

the corresponding element ds of the line. Expressed in the symbols of Fig. 11.13, the circulation is

$$\int_A^B V \sin \alpha \, ds \quad (11.22)$$

This definition is analogous to the definition of work as the displacement times the component of force in the direction of the displacement, or

$$\text{Work} = \int_A^B F \sin \alpha \, ds$$

Now we know in mechanics that we may compute work by resolving both the force and the displacement and get, for a two-dimensional case, the work done from A to B as

$$\int_A^B (X dx + Y dy)$$

where X and Y are the force components in the x and y directions, respectively.

Similarly, the circulation along the line from A to B is the line integral,

$$\int_A^B (u dx + v dy) \quad (11.23)$$

where u and v are the components of the velocity V in the directions x and y . It should be noted that u and v are functions of x and y and that

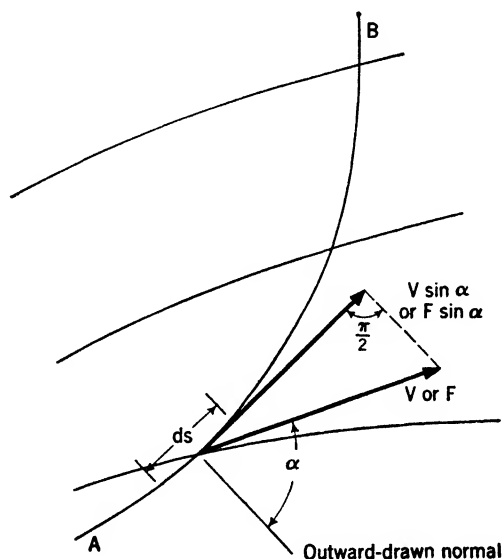


FIG. 11.13.

integration takes place along the line at a given instant. This is space integration, independent of time.

The symbol Γ is generally used to designate the circulation about a closed curve obtained by line integration indicated by the symbol \oint .

$$\Gamma = \oint (u dx + v dy) = \oint V \sin \alpha ds \quad (11.24)$$

Consider the circulation about a small rectangular element of area, defined as in Fig. 11.14.

$$\begin{aligned} d\Gamma &= u dx + \left(v + \frac{\partial v}{\partial x} dx \right) dy - \left(u + \frac{\partial u}{\partial y} dy \right) dx - v dy \\ &= \left(\frac{\partial v}{\partial x} - \frac{\partial u}{\partial y} \right) dx dy \end{aligned}$$

Thus the elementary circulation is expressed in terms of the element of area $dx dy = dA$. Any circuit will enclose a number of elementary areas dA .

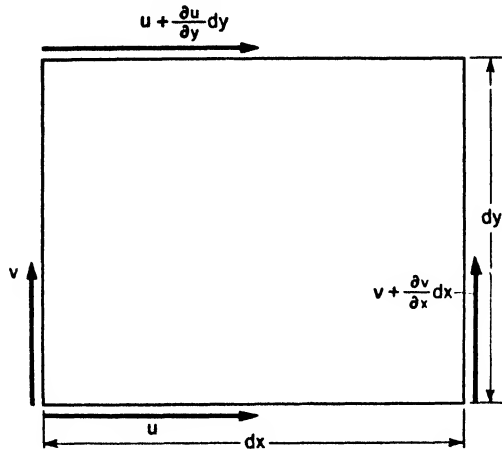


FIG. 11.14.

The sum of the circulations of all the elementary areas is obviously the circulation around the bounding circuit, because every interior line is traversed twice, in opposite directions, and all "internal records" cancel, as indicated in Fig. 11.15.

$$\Gamma = \oint (u dx + v dy) = \iint \left(\frac{\partial v}{\partial x} - \frac{\partial u}{\partial y} \right) dx dy \quad (11.25)$$

This equation is a special case of Stokes' theorem, discussed in texts on the calculus.

11.12. Velocity Potential. From Eq. (11.7) it will be recognized that $(\partial v / \partial x) - (\partial u / \partial y)$ is the rotation, or vorticity, at any point in the flow. It follows from Eq. (11.25), therefore, that the circulation is zero around any closed curve in an irrotational flow. Consequently, we see by the argument used in Art. 11.3 that the circulation from A to B is the same along any path joining these points, provided that the flow is irrotational. A scalar point function ϕ can thus be defined as

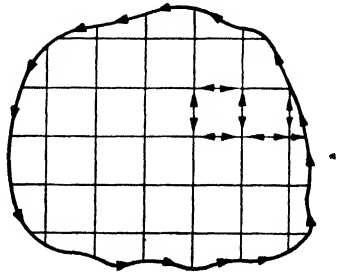


FIG. 11.15.

$$\left. \begin{aligned} d\phi &= V \sin \alpha ds \\ \phi_B - \phi_A &= \int_A^B V \sin \alpha ds \end{aligned} \right\} \quad (11.26)$$

The function $\phi(x, y)$ is called the "velocity potential."

The velocity potential has three properties that are analogous to those of the stream function and that can be demonstrated in the same way. The first property, which follows at once from Eq. (11.26), is that the lines of constant ϕ are normal to the streamlines. A plot of streamlines and equipotential lines thus appears as a mesh having all intersections at right angles.

Dividing Eq. (11.26) by ds and using the partial derivative as in Eq. (11.4), we get

$$\frac{\partial \phi}{\partial s} = V \sin \alpha \quad (11.27)$$

which gives us the second property: The space rate of change of ϕ in an arbitrary direction s is equal to the component of velocity in that direction. For x, y coordinates we thus find

$$\left. \begin{aligned} \frac{\partial \phi}{\partial x} &= u \\ \frac{\partial \phi}{\partial y} &= v \end{aligned} \right\} \quad (11.28)$$

and for plane-polar coordinates

$$\left. \begin{aligned} \frac{\partial \phi}{\partial r} &= V_r \\ \frac{\partial \phi}{r \partial \theta} &= V_\theta \end{aligned} \right\} \quad (11.29)$$

If we now consider two flow patterns having velocity potentials ϕ_1 and ϕ_2 , Eq. (11.27) gives

$$\frac{\partial \phi_1}{\partial s} + \frac{\partial \phi_2}{\partial s} = \frac{\partial(\phi_1 + \phi_2)}{\partial s} = V_1 \sin \alpha_1 + V_2 \sin \alpha_2$$

Since $V_1 \sin \alpha_1 + V_2 \sin \alpha_2$ is the component of the resultant velocity parallel to the arbitrary direction ds , we may state the third property of the potential as follows: The algebraic sum of the potentials for two irrotational flow patterns is the potential for the flow resulting from their superposition.

None of the properties of the velocity potential are of any practical use unless the flow patterns concerned are not only irrotational, but also satisfy the continuity equation [Eq. (11.1), or its equivalent, Eq. (11.4)]. It is possible that two irrotational flow patterns may each satisfy Eq. (11.4) and yet, if they be superposed, their resultant may not do so. It is readily shown, however, that this difficulty does not arise if the continuous irrotational flows are assumed to be incompressible. In this case, Eqs. (11.5), yield the condition that

$$\frac{\partial^2 \psi}{\partial y \partial x} = \frac{\partial u}{\partial x} = \frac{\partial^2 \psi}{\partial x \partial y} = - \frac{\partial v}{\partial y}$$

or

$$\frac{\partial u}{\partial x} + \frac{\partial v}{\partial y} = 0 \quad (11.30)$$

Substitution in this equation from Eqs. (11.28) shows that ϕ satisfies Laplace's equation

$$\frac{\partial^2 \phi}{\partial x^2} + \frac{\partial^2 \phi}{\partial y^2} = 0 \quad (11.31)$$

Since this equation is linear, the sum of the potentials for two different flow patterns is the potential for another irrotational incompressible flow. By the third property of a velocity potential, discussed above, this flow is the resultant of the two flows in question.

The velocity potential can thus be used in place of the stream function in the synthesis of irrotational incompressible flow patterns.

11.13. Thomson's Theorem. An important generalization is Thomson's (Kelvin's) theorem, which states that in a frictionless fluid the circulation along any closed fluid line remains constant as time goes on, provided merely that pressure depends only on density (homogeneous fluid). Consequently, if the motion starts from rest, when the vorticity is everywhere nil, the flow will be irrotational at all times. Thomson's theorem may be proved as follows:

In a continuous two-dimensional flow of fluid (unit thickness normal to xy plane) assume any closed fluid line with P and Q two points on that line: (x, y) and $(x + dx, y + dy)$. The corresponding velocity components are (u, v) and $(u + du, v + dv)$. We neglect gravity for simplicity. From Eq. (11.24) we find that the rate of change of circulation around a closed curve is

$$\frac{D\Gamma}{dt} = \frac{D}{dt} \oint (u \, dx + v \, dy)$$

where the symbol D/dt denotes the rate of change following the motion of the fluid. Since the operations D/dt and \oint are commutative,

$$\frac{D\Gamma}{dt} = \oint \frac{D}{dt} (u \, dx + v \, dy) \quad (11.32)$$

Consider now the expression

$$\frac{D}{dt} (u \, dx) = u \frac{D}{dt} (dx) + dx \frac{Du}{dt} \quad (11.33)$$

The points P, Q move with the fluid, so that the x component of the distance separating them, dx , stretches at the rate du , the x velocity of Q rela-

tive to P . Thus $(D/dt)(dx) = du$. Reference to Eqs. (11.2) shows that $Du/dt = -(1/\rho)(\partial p/\partial x)$. Therefore, Eq. (11.33) becomes

$$\frac{D}{dt}(u \, dx) = u \, du - \frac{1}{\rho} \frac{\partial p}{\partial x} dx$$

The corresponding expression in y and v is

$$\frac{D}{dt}(v \, dy) = v \, dv - \frac{1}{\rho} \frac{\partial p}{\partial y} dy$$

Substituting these expressions into Eq. (11.32), we find that

$$\frac{D\Gamma}{dt} = \oint \left[u \, du + v \, dv - \frac{1}{\rho} \left(\frac{\partial p}{\partial x} dx + \frac{\partial p}{\partial y} dy \right) \right] = \oint \left(d \frac{V^2}{2} - \frac{dp}{\rho} \right)$$

But since $p = f(\rho)$ by assumption, dp/ρ may be written as dP , where P is a function of ρ only.

$$\frac{D\Gamma}{dt} = \oint d \left(\frac{V^2}{2} - P \right)$$

The summation at a given instant around the closed path of the space differential $d[(V^2/2) - P]$ is obviously zero. Hence we obtain

$$\frac{D\Gamma}{dt} = 0 \quad \text{or} \quad \Gamma = \text{constant} \quad (11.34)$$

which was the statement to be proved.*

This proof is readily extended to include gravity and any other body force that has a potential. Consequently, irrotational flow remains irrotational, in the absence of friction, and any flow generated from rest by gravity and pressure forces alone will be irrotational.

We may justly observe that, since pressure and gravity forces cannot act tangentially, no rotation can be set up by them in any element of the fluid. Rotation requires the tangential, or shearing, force of friction, such as exists in real fluids near a solid boundary or near a surface of discontinuity of velocity. The boundary layer of real fluids is therefore rotational and turbulent, after a more or less short initial portion that may be rotational and laminar if the body be smooth and its curvature slight.

Thomson's theorem holds also for a real (viscous) fluid, provided that no vorticity crosses the fluid line. That is, if all particles comprising the fluid line are initially without rotation, the circulation around the line will remain constant so long as the motion of all particles forming the line stays irrotational.

✓ **11.14. Potential Vortex.** An important example of an irrotational flow is the potential vortex, already discussed in Art. 4.11. It will be recalled

* This may also be proved by using Eq. (11.8a).

that the streamlines are concentric circles and that the product of velocity and radius is the same for all streamlines, $Vr = \text{constant}$. From Eq. (11.24), the circulation about any streamline is

$$\Gamma = \oint V \sin \alpha \, ds = \int_0^{2\pi} Vr \, d\theta = 2\pi Vr = \text{constant}$$

Since the value of Γ is different from zero for all curves enclosing the origin, it follows that the motion at the origin is rotational. The origin is thus a singular point in an otherwise irrotational flow. The flow of a real fluid can approximate closely to a potential vortex, except in a core at the center where frictional effects predominate and the motion is like that of a rigid body. The value of Γ can be expressed in terms of the angular velocity ω and cross-sectional area of the vortex core. From the above equation we get

$$\Gamma = 2\pi Vr = 2\pi\omega r_0^2 = 2\omega\pi r_0^2$$

where r_0 is the radius of the core. Γ is thus given by twice the product of angular velocity and cross-sectional area of the core.

Since vortex motion is irrotational except for the origin, or core, a velocity potential exists outside the core. The expression for this potential is obtained by substitution in Eqs. (11.29).

$$V_r = 0 = \frac{\partial \phi}{\partial r}$$

$$V_\theta = V = \frac{\Gamma}{2\pi r} = \frac{\partial \phi}{r \partial \theta}$$

whence

$$d\phi = \frac{\Gamma}{2\pi} d\theta$$

or

$$\phi = \frac{\Gamma}{2\pi} \theta \quad (11.35)$$

where the constant of integration is arbitrarily taken as zero. The potential is a multiple-valued function that increases by Γ each time θ increases by 2π .

In a similar manner we may form the stream function for a vortex. Since $\partial\psi/\partial r = -V_\theta = -V$ and $\partial\psi/\partial\theta = 0$, we obtain

$$\frac{d\psi}{dr} = -\frac{\Gamma}{2\pi r}$$

whence

$$\psi = -\frac{\Gamma}{2\pi} \ln r \quad (11.36)$$

Figure 11.16 shows the circular streamlines and the radial equipotential lines for the vortex.

It may be remarked parenthetically that a close analogy exists between a source and a potential vortex. For comparison, the stream function and velocity potential for each are written below:

Source

$$\psi_s = \frac{Q}{2\pi} \theta$$

$$\phi_s = \frac{Q}{2\pi} \ln r$$

Potential Vortex

$$\psi_v = -\frac{\Gamma}{2\pi} \ln r$$

$$\phi_v = \frac{\Gamma}{2\pi} \theta$$

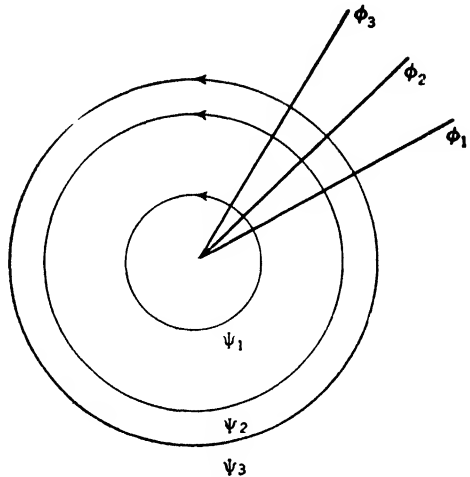


FIG. 11.16. — Streamlines and equipotential lines for a potential vortex.

It is seen that Q , the strength of the source, and Γ , the circulation, play analogous roles; Γ is frequently referred to as the strength of the vortex. The equipotential lines of the source are the streamlines of the vortex, and vice versa. ψ_s and ϕ_v , for each of which the origin is a singular point, are multiple-valued functions, but ψ_v and ϕ_s , for which all points are regular, are single-valued.

11.15. Induced Velocity. Several vortex cores or filaments may be enclosed by a fluid line, in which case the circulation along that line is the sum of the circulations, or strengths, of the enclosed vortex filaments. The velocity at a point in the continuum is the vector sum of the velocities due to each vortex present, $\Gamma_1/2\pi r_1$, $\Gamma_2/2\pi r_2$, This velocity is induced by the vortex and is called "induced velocity."

The induced-velocity field due to one or more vortices is similar to the magnetic field induced by one or more conductors carrying electric current. Current strength corresponds to vortex strength.

11.16. Conclusions of Vortex Theory. It can be shown, as by Helmholtz, that for a free potential vortex in an ideal fluid

1. The strength Γ is permanent and is constant along its length.
2. A vortex core must end on a solid boundary, form a closed loop, or extend to infinity.
3. The circulation about any closed curve is equal to the sum of the strengths of the vortex cores enclosed.
4. The velocity distributions induced by several vortices may be superimposed.

5. A vortex moves in a path prescribed by the other vortices in the region.

For example, the following sketches illustrate the nature of the velocity patterns induced by free vortices. For a single vortex, the induced velocity at any point is $V = \Gamma/2\pi r$; it is small at a great distance from the core (see Fig. 11.17a). For a pair of vortices having strengths equal and opposite, the induced velocities are equal and the pair advances, as shown in Fig. 11.17b. The eddies formed at the edges of a paddle are of this character. For a vortex pair having equal strengths, the induced velocities cause the cores to swing around a common center, as shown in Fig. 11.17c. A vortex ring advances in the direction shown in Fig. 11.17d, because of the velocity induced at each element ds by all other elements.

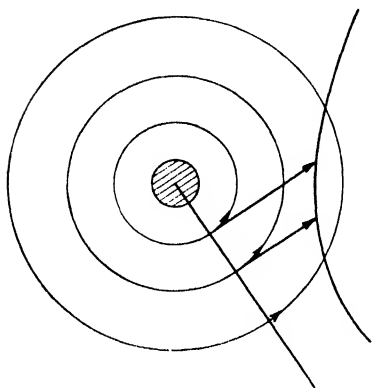


FIG. 11.17a. — Streamlines and velocity distribution for single potential vortex.

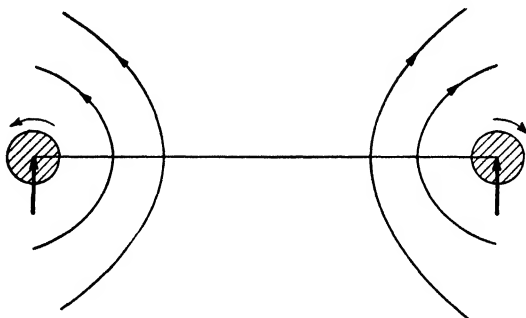


FIG. 11.17b. — Vortex pair with opposed rotations.

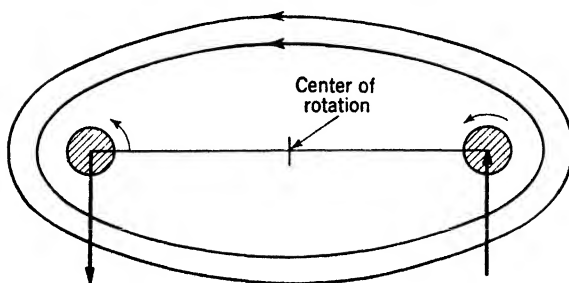


FIG. 11.17c. — Vortex pair with the same direction.

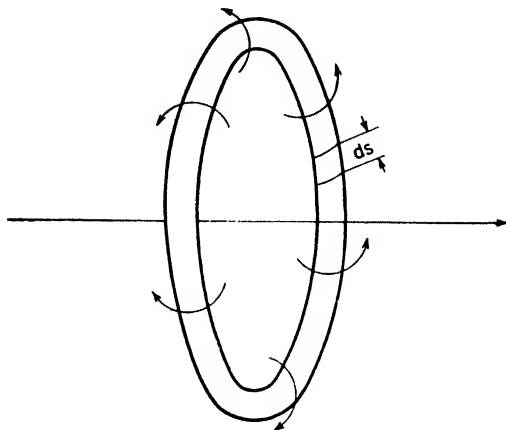


FIG. 11.17d. -- Vortex ring.

11.17. Magnus Effect. Consider a circulation about a cylinder, combined with a translation. This combination is approximated in nature by a spinning rod falling or by a sliced golf ball, cut tennis ball, or rotating rifle bullet shot across the wind. Under these conditions a transverse force is produced, known as the Magnus effect.

We have already shown how to develop the stream function defining the flow pattern about a vortex core of strength Γ and the stream function for a circular cylinder moving transversely. We have also shown that stream functions may be added to give the resultant flow. We can thus add the two stream functions and differentiate to find the velocity at any point in the combined flow.

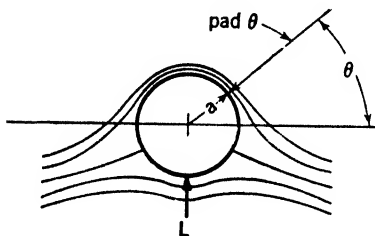


FIG. 11.18. — Combination of a doublet, parallel flow, and vortex gives the streamlines for a cylinder with circulation.

The translation of a cylinder in a perfect fluid gives rise to a symmetrical flow pattern with no resultant force on the cylinder, as shown in Fig. 11.10. However, when the flow appropriate to a clockwise vortex of stream function ψ_2 is superimposed on the flow about a cylinder in translation, given by ψ_1 , the induced velocity at every point caused by the vortex produces an unsymmetrical flow pattern, as illustrated in Fig. 11.18. From Eqs. (11.16) and (11.36) the resultant stream function is found to be

$$\psi = \psi_1 + \psi_2 = U \left(r - \frac{a^2}{r} \right) \sin \theta - \frac{\Gamma}{2\pi} \ln r \quad (11.37)$$

Since the vortex motion has been assumed clockwise, the value of Γ in

Eq. (11.37) is negative, for, by definition, a positive value of Γ is associated with a counterclockwise vortex.

The effect of adding a clockwise circulation is to speed up the flow above the cylinder and to slow it beneath the cylinder. Therefore, from Bernoulli's equation the pressure on the bottom of the cylinder is greater than on the top. Consequently, there must be a resultant upward force, or lift, due to this unsymmetrical pressure distribution. There is no drag, or resistance, to forward motion in irrotational flow, as pointed out in Art. 10.11. Note that the stagnation points S are shifted below the horizontal axis.

The lift per unit length of cylinder can be found from the distribution of pressure around the surface of the cylinder. One computes these pressures by using Bernoulli's equation, in which the velocities are given by the stream function. Differentiating Eq. (11.37) with respect to r , we find for V_θ , the velocity normal to r ,

$$V_\theta = -\frac{\partial\psi}{\partial r} = -U \left(1 + \frac{a^2}{r^2} \right) \sin \theta + \frac{\Gamma}{2\pi r}$$

At the cylinder, where $r = a$, there is no radial velocity, and

$$V_\theta = -2U \sin \theta + \frac{\Gamma}{2\pi a}$$

At the stagnation points $V_\theta = 0$, $\theta = \theta_s$, and

$$\sin \theta_s = \frac{\Gamma}{4\pi a U}$$

By Bernoulli's theorem, the pressure at a point a, θ on the cylinder is

$$\begin{aligned} p &= \text{constant} - \frac{\rho}{2} V^2 \\ &= \text{constant} - \frac{\rho}{2} \left(4U^2 \sin^2 \theta - \frac{2\Gamma U}{\pi a} \sin \theta + \frac{\Gamma^2}{4\pi^2 a^2} \right) \end{aligned} \quad (11.38)$$

From Fig. 11.18 the force on an element of area of unit length and of breadth $a d\theta$ is $pa d\theta$. The upward component of this force is an element of lift $-pa \sin \theta d\theta$. The total lift on unit length of cylinder, L , is the integral,

$$L = - \int_0^{2\pi} pa \sin \theta d\theta$$

If we substitute for p from Eq. (11.38), we obtain four terms, the first containing $\sin \theta$; the second, $\sin^3 \theta$; the third, $\sin^2 \theta$; and the fourth, $\sin \theta$. But since

$$\int_0^{2\pi} \sin \theta \, d\theta = 0 \quad \int_0^{2\pi} \sin^3 \theta \, d\theta = 0 \quad \text{and} \quad \int_0^{2\pi} \sin^2 \theta \, d\theta = \pi$$

all terms drop out except the third, and

$$L = -\rho \Gamma U \quad (11.39)$$

This is an important result and shows that the combination of a circulation with a translation produces a transverse force directly proportional to the strength of the circulation and the speed of advance. Since Γ is negative for the flow pattern of Fig. 11.18, Eq. (11.39) shows that L is positive. Usually we are interested only in the absolute value of L , the direction being obvious. The negative sign in Eq. (11.39), which results merely from the convention regarding a positive circulation, is therefore frequently omitted.

11.18. Kutta-Joukowski Law. Equation (11.39), which was developed for a cylinder, can be shown to hold, regardless of the shape of the body about which the circulation is assumed to take place. This mathematical result was endowed with a semblance of physical reality by Lord Rayleigh and soon after 1900 was given a precise application to the lift of airplane wings by the German Kutta and the Russian Joukowski. Equation (11.39) is now universally known as the Kutta-Joukowski law. It is the basis for the modern vortex, or circulation, theory of the lift of wings, the thrust of fan and propeller blades, or the transverse force on any solid body moving through a fluid in an unsymmetrical attitude.

11.19. Circulation Theory (Wing of Infinite Span). A fundamental consequence of the Kutta-Joukowski law is that, in an ideal frictionless fluid in steady two-dimensional motion, the existence of a transverse force on a wing is associated with a circulation of definite amount. The wing, for purposes of computation, can be replaced by a vortex filament of strength Γ , such that the lift per unit span is given by Eq. (11.39). This imaginary vortex filament has the properties of the free vortex of Helmholtz, except that it does not consist always of the same particles of fluid, is not a fluid line, but is "bound" to the location of the wing rather than drifting away with the transverse flow. It has no physical reality and is called a "bound vortex."

The great contribution of Kutta and Joukowski was the provision of mathematical methods to compute the lift on the wing by adjustment of Γ to give a tangential and thus a finite velocity at the trailing edge. Experiments show that the lift so computed predicts the measured lift with good approximation.

Physical intuition suggests that real fluid streams, separated at the leading edge of a wing and following the contour of the upper and lower surfaces, should join at the trailing edge and flow smoothly away. That circulation about the wing is necessary to accomplish this result is indicated

in the sketches of Fig. 11.19, which show successive stages in the development of the steady-state flow pattern around an airfoil from an initial condition of rest. Before the motion starts, the circulation is obviously zero for

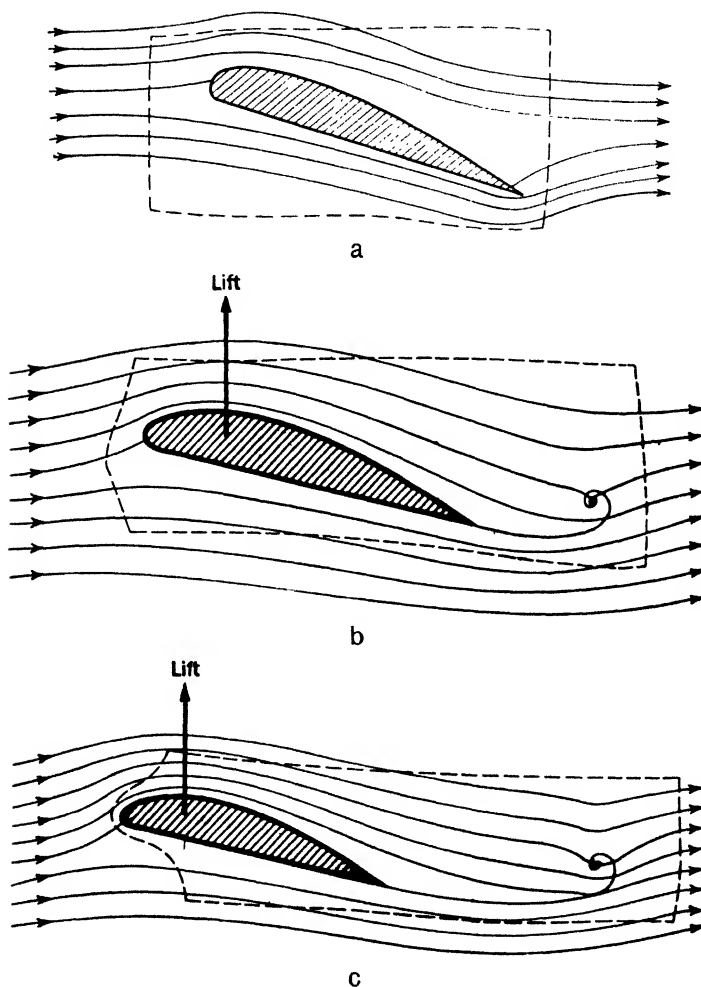


FIG. 11.19. — Development of the steady-state flow pattern about a two-dimensional wing. (a) Start of motion: no circulation, no lift, theoretically infinite velocity at trailing edge, stagnation point on back of wing. (b) Formation of starting vortex behind trailing edge (due to high friction where shearing velocity is great); circulation of starting vortex equal and opposite to that about wing. (c) Circulation established about wing sufficient to give smooth tangential flow at trailing edge.

any closed fluid line. Thomson's theorem indicates that the circulation will remain zero for the fluid line shown dotted in the sketches, because no particle in it starts to rotate during the time interval considered.

Figure 11.19a shows the flow pattern observed immediately after motion

starts. No rotating particles are yet visible in the flow. Consequently, there can be no circulation around the airfoil. The lift is zero. This flow cannot persist because of the high velocity gradients near the sharp trailing edge. Almost at once, the viscosity causes a counterclockwise vortex to spring from the airfoil, as shown in Fig. 11.19b. A single vortex (called the "starting vortex") is thus created, which has a definite strength (circulation) associated with it. But the circulation around the dotted fluid line is still zero. Hence, an equal and opposite circulation must exist around the airfoil itself, no other vortex being present in the fluid. A lift is therefore set up by virtue of the Kutta-Joukowski relation [Eq. (11.39)].

The flow pattern changes as the circulation around the airfoil increases, until the rear stagnation point has moved to the trailing edge. When this condition is reached, the high velocity gradients no longer exist in the flow, so that the starting vortex cannot continue to grow but travels on downstream, its strength remaining constant. The lift also attains a constant limiting value. This state of affairs is depicted in Fig. 11.19c.

The flow pattern around the wing (and consequently the lift) remains unchanged from this time on. The subsequent history and eventual dissipation of the starting vortex have no effect on the forces acting on the wing.

11.20. Lift Coefficient. For any wing in a two-dimensional incompressible flow, the lift per unit length of span, L , is a function of the chord c , the angle of incidence α , the distant velocity V , and the fluid properties ρ and μ . Dimensional reasoning leads to the result

$$C_L = \frac{L}{(\rho/2)V^2c} = f\left(\alpha, \frac{\rho Vc}{\mu}\right) = f(\alpha, R) \quad (11.40)$$

where C_L is called the "lift coefficient."

We can, to a good approximation, neglect frictional effects on the flow pattern for an airfoil, provided that the angle of incidence is not too large. In other words, the influence of the Reynolds number R is negligible. In this case, C_L depends only on α ; it is in fact a linear function of α , as is shown below.

It is easily seen by dimensional reasoning that, if friction is neglected, $\Gamma = Vc f(\alpha)$. Therefore, if a wing is fixed parallel to x , as in Fig. 11.20, and the velocity is assumed to be u_0 , also parallel to x , the corresponding circulation is $\Gamma_x = u_0c\Gamma_1$, where Γ_1 is a constant, because the angle of incidence (referred to the tangent to the lower surface of the wing) has the fixed value zero. Similarly, if the velocity is assumed to be v_0 , the corresponding circulation is $\Gamma_y = v_0c\Gamma_2$, where Γ_2 is a constant, because the angle of incidence has the fixed value of $\pi/2$.

If these two flow patterns are superposed, the resultant velocity will be V and the angle of incidence will be α' , as in Fig. 11.20. Furthermore,

the resultant circulation will be the algebraic sum of the component circulations, since it is a scalar defined in terms of the velocity components $\oint (u dx + v dy)$.

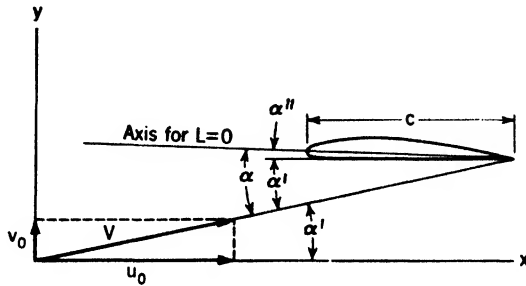


FIG. 11.20.

Thus, $\Gamma = \Gamma_x + \Gamma_y = c(u_0\Gamma_1 + v_0\Gamma_2)$. From Fig. 11.20, $u_0 = V \cos \alpha'$ and $v_0 = V \sin \alpha'$, so that

$$\Gamma = cV(\Gamma_1 \cos \alpha' + \Gamma_2 \sin \alpha')$$

Let $\tan \alpha'' = \Gamma_1/\Gamma_2$; then $\Gamma_1 = \sqrt{\Gamma_1^2 + \Gamma_2^2} \sin \alpha''$, and $\Gamma_2 = \sqrt{\Gamma_1^2 + \Gamma_2^2} \cos \alpha''$

$$\Gamma = cV\sqrt{\Gamma_1^2 + \Gamma_2^2} \sin (\alpha' + \alpha'')$$

It is seen that, for $\alpha' = -\alpha''$, $\Gamma = 0$. The angle $-\alpha''$ is thus the angle of zero lift. Since Γ_1 and Γ_2 are independent of both the magnitude of the velocity and its direction (angle of incidence), we may write, for small angles,

$$\Gamma = \text{constant } (\alpha' + \alpha'')Vc$$

and

$$L = \rho V\Gamma = \text{constant } \rho V^2 c (\alpha' + \alpha'')$$

Introducing the lift coefficient, we get

$$\begin{aligned} C_L &= \frac{L}{\rho V^2 c/2} = \text{constant } (\alpha' + \alpha'') \\ &= \text{constant } \alpha \end{aligned} \quad (11.41)$$

where α is measured from the attitude of no lift.

This analysis makes the important prediction that for small angles the lift coefficient should vary directly with the angle of incidence, and experiment verifies the prediction. A more elaborate analysis shows that the constant has the numerical value 2π , and experiment shows this to be a close approximation for actual cases. For a wing in air, it is found that

$$C_L = 2\pi\eta\alpha$$

where the correction factor for frictional effects η is of the order of 0.9 for modern airfoil sections. This result, of course, applies only to a wing of infinite span or aspect ratio (two-dimensional flow) inclined at angles well below the stalling incidence.

11.21. Circulation Theory (Wing of Finite Span). While the Kutta-Joukowski concept of a bound vortex replacing the wing predicts the lift per unit span of a wing of indefinite extent, it cannot be applied to the practical case of a wing of finite span, without modification to account for the three-dimensional flow near the tips. According to the rules of vortex motion, the bound vortex cannot end at the wing tips but must continue out into the fluid, either forming a closed loop or extending to infinity. The theory must therefore explain where the unbound portion of the vortex is located. Furthermore, the theory must account for the fact that the lift (and hence the circulation) drops off gradually to zero at the wing tips, even though the circulation of a vortex is constant along its entire length.

Lanchester first suggested that, at each wing tip, there must be a flow of air from the high-pressure region below the wing toward the low-pressure region above it. This flow sets up a vortex that is a continuation of the bound vortex of the wing. The trailing vortex shed from each wing tip is

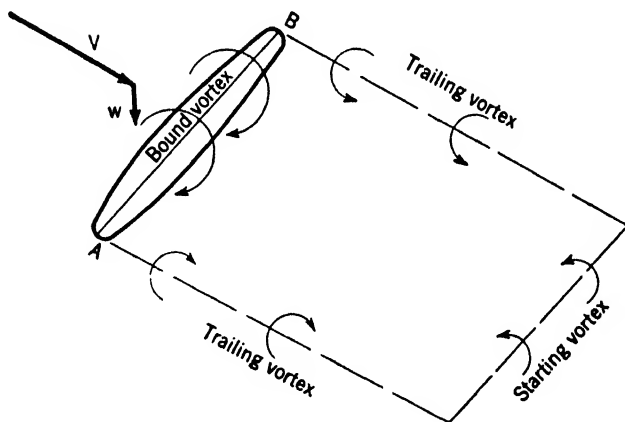


FIG. 11.21. — Vortex system of a finite wing.

thus a free vortex whose core follows the streamlines of the general flow past the wing tip. There is ample evidence of the existence of such trailing wing-tip vortices. When temperature and humidity conditions are favorable, "vapor trails" left by the wing tips of an airplane extend for miles across the sky. The lowered temperature accompanying the lowered pressure at the core of the vortex causes condensation.

The Lanchester concept of a horseshoe-shaped vortex filament extending indefinitely to the rear was developed by Prandtl into the modern

circulation theory of finite wings, by means of which great advances have been made in airplane design. In the simplest form of the theory a wing is replaced by the bound portion of a vortex of circulation Γ , which extends back from each wing tip to join the starting vortex. Thus we have a closed loop of circulation Γ at all points as the equivalent of the wing (see Fig. 11.21).

Within the loop formed by the closed vortex filament, there must be a

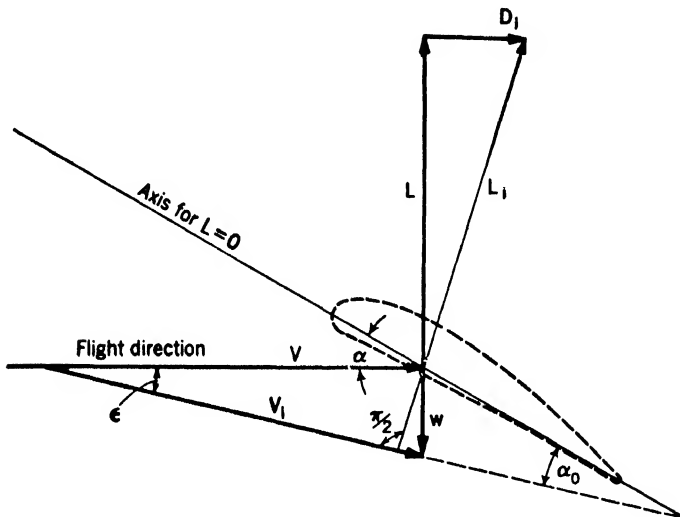


FIG. 11.22.

downward component of velocity, induced by the circulation. The downward momentum imparted to the air as the wing advances is a measure of the lift, which may be considered to be transmitted to the ground as a momentary increase of pressure, due to impact of the down-wash.

At any point along the lifting line AB , which replaces the wing, there will be a horizontal velocity V due to the forward motion of the wing and a down-wash, or vertical component, of velocity w , due to the horseshoe vortex. As the starting vortex is far distant or, in a real fluid, quickly destroyed by friction, the down-wash w is caused by the trailing vortices. If the wing span were infinite, the trailing vortices would have no effect and the only velocity would be V . This is, of course, the two-dimensional case, where the Kutta-Joukowski law applies.

For a finite wing the flow about any section takes place as in the two-dimensional case except that V has become V_i and is inclined by a small angle ϵ to the direction of V . The lift L_i , caused by the flow, is normal to the direction of V_i and is also inclined to L by the angle ϵ . The Kutta-

Joukowski law then states, for the case of the finite wing,

$$L_i = \rho V_i \Gamma$$

From Fig. 11.22, the following relations are evident:

$$\frac{w}{V} = \frac{D_i}{L} = \tan \epsilon = \epsilon$$

$$\frac{L}{L_i} = \frac{V}{V_i} = \cos \epsilon = 1 \quad L_i = L \quad V_i = V$$

$$\alpha_0 = \alpha - \epsilon = \alpha - \frac{w}{V}$$

11.22. Induced Drag. The effect of the trailing vortices is, by means of down-wash, to reduce the effective angle of attack and to rotate the transverse (lift) force vector to the rear, so that it has a component D_i in the direction to oppose the motion. D_i is, in fact, a drag and is given the name "induced drag" because of its origin. ϵ is an induced angle of incidence, and w is an induced velocity. Mathematically, w is analogous to magnetic-field strength and Γ to current strength for a horseshoe-shaped electrical circuit.

The apparent paradox of drag in a frictionless fluid must be noted. This induced drag is represented by the kinetic energy supplied to the trailing vortices as they are left behind. In a real fluid there will be an additional drag due to friction. It should be further noted that the induced drag is independent of the shape of the wing section or its chord length and depends only on the section lift. Since lift depends on angle of incidence, which in turn determines the circulation necessary to maintain smooth flow, it is apparent that the induced drag for a given wing will increase with the angle of incidence.

It is important to observe that this form of the theory only partly accounts for the objections first raised. The objection that the bound vortex must go somewhere upon reaching the wing tip has been answered by postulation of trailing free vortices. The other objection, that the lift must drop to zero at the wing tip, has not yet been met, since a single vortex filament (which must have a constant strength along its entire length) has been assumed to extend across the whole span and to turn abruptly at the wing tips.

11.23. Lift on Complete Wing. The preceding discussion must be thought of as dealing with the lift on only the central portion of the total span of a wing. To compute the lift on the complete wing, further refinement of the basic concept is required. A single vortex filament of constant circulation Γ implies a constant lift at every section out to and including

the wing tips. This is obviously impossible, as the lift must fall to zero at the wing tips. Furthermore, the down-wash w , assumed small, varies inversely as the distance from the trailing vortex and becomes large near a wing tip from which a vortex of finite strength is shed.

Prandtl resolved the difficulty by considering that, since circulations about parallel filaments may be superposed, it is immaterial to the Kutta-Joukowski law if we substitute $\int d\Gamma$ for Γ , where Γ is made up of the sum of circulations of a large number of filaments, each of infinitesimal circulation $d\Gamma$. Then he considered, instead of a single lifting line with one pair of trailing vortices, a bundle of such lifting lines of different lengths, each with its pair of trailing vortices. By adjusting the lengths of the elements one can get any desired distribution of circulation along the wing span and hence a corresponding distribution of lift. For each section, $L = \rho V \Gamma$, where Γ is a function of the distance from the axis of symmetry of the wing.

Figure 11.23 illustrates a rough distribution of circulation and lift across the span of a wing. In the limit an infinite number of vortex filaments, each of strength $d\Gamma$, can be imagined, with a trailing vortex sheet

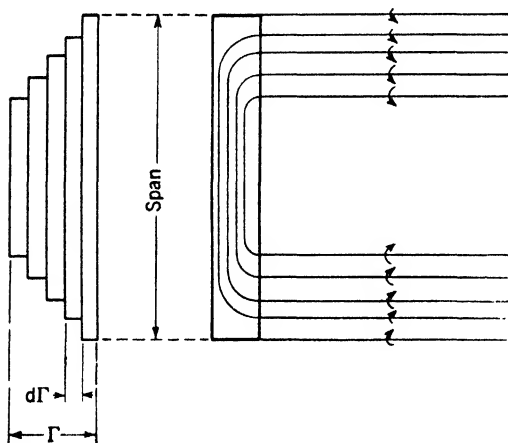


FIG. 11.23. — Diagrammatic sketch of distribution of circulation along span of finite wing.

behind the wing. Prandtl discovered that an elliptical distribution of lift for a given span gives a constant down-wash at all points along the span and that the total induced drag is a minimum for a given total lift.

This conclusion from analysis has been of the highest technical utility, as practical wings of elliptical plan form or of conventional taper are found experimentally to have an elliptical lift distribution to a very good approximation.

For constant down-wash we have similar vector triangles of velocities and forces at all points along the span. Then the induced drag on the whole wing, made up of the sum of section drags, will be

$$\frac{D_i}{L} = \frac{w}{V}$$

We introduce nondimensional lift and drag coefficients, in terms of the wing area S ,

$$L = C_L \frac{\rho}{2} V^2 S \quad D_i = C_{D_i} \frac{\rho}{2} V^2 S$$

and obtain

$$\frac{C_{D_i}}{C_L} = \frac{D_i}{L} = \frac{w}{V}$$

Computations carried out for the elliptical distribution of lift reduce to the following important relation for the necessary down-wash in terms of the aspect ratio A of a wing of span b :

$$\frac{w}{V} = \frac{C_L}{\pi A}$$

where A is defined as $A = \text{span}/\text{mean chord} = b/(S/b) = b^2/S$. Furthermore, since $\epsilon = w/V = C_L/\pi A = C_{D_i}/C_L$,

$$C_{D_i} = \frac{C_L^2}{\pi A}$$

and the effective angle of incidence

$$\alpha_0 = \alpha - \epsilon = \alpha - \frac{C_L}{\pi A}$$

where α is the geometrical angle of incidence.

An important conclusion of the theory here outlined is that the induced drag of a wing having a given C_L is reduced directly as the aspect ratio is increased. Modern long-range airplanes, consequently, have narrow wings of the greatest span that can be built in the current state of the art of materials and structural design.

The effective angle of incidence for a finite wing has been shown to be less than for a wing of infinite span by the angle of down-wash induced by the trailing vortices. For a given geometrical angle of incidence, the section lift must be correspondingly less than for the infinite wing, since the lift coefficient varies directly with the effective angle of incidence.

The slope of the lift curve for a wing of infinite span is determined by $C_L = 2\pi\alpha$ from the two-dimensional theory of Kutta and Joukowski. But for the finite wing

$$C_L = 2\pi\alpha_0 \quad \alpha = \alpha_0 + \frac{C_L}{\pi A}$$

and

$$\frac{d\alpha}{dC_L} = \frac{d\alpha_0}{dC_L} + \frac{1}{\pi A} = \frac{1}{2\pi} + \frac{1}{\pi A}$$

Therefore,

$$\frac{dC_L}{d\alpha} = \frac{2\pi A}{A+2} < 2\pi$$

The effect of aspect ratio is therefore to flatten the slope of the lift-coefficient curve, as indicated in Fig. 11.24.

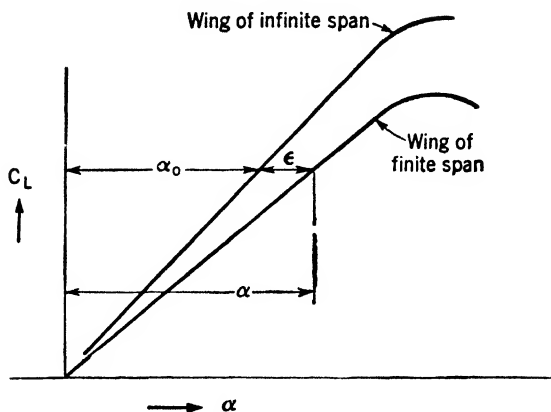


FIG. 11.24. — Diagrammatic comparison of curves of lift coefficient C_L versus angle of incidence α for wings of finite and infinite span.

11.24. Polar Diagram and Profile Drag. For a real wing in a real fluid the total drag at any given attitude is made up of the induced drag D_i , associated with the circulation and lift developed, and, in addition, a drag due to friction of the fluid and defects in the smoothness of flow around the wing section, or profile. This latter portion of the total drag is called “profile drag” because it depends on the shape, or profile, and not on the plan form or aspect ratio of the wing. For infinite span the induced drag is zero, and the total drag is the profile drag, designated by D_0 .

We may write in coefficient form,

$$C_D = C_{D_0} + C_{D_i} = C_{D_0} + \frac{C_L^2}{\pi A}$$

where

$$C_{D_0} = D_0/(\rho/2)V^2S$$

We observe that a plot of C_L versus C_{D_i} for given A will be a parabola, and we know from experimental evidence that the profile-drag coefficient C_{D_0} is substantially constant for small angles.

The relative merits of various wing profiles are conventionally displayed by plotting experimentally determined values of C_L versus C_D on a so-called “polar diagram,” together with the corresponding angle of incidence. On this polar diagram the induced-drag-coefficient parabola is plotted from $C_{D_i} = C_L^2/\pi A$ to serve as a reference to the ideal case of no friction. The curve of observed values lies to the right of the parabola by the amount of the profile-drag coefficient C_{D_0} , as shown by Fig. 11.25.

For a smooth airfoil at a small angle of incidence the profile drag is nearly equal to the skin friction on a flat plate moving edgewise. However,

when a wing or blade is held at too great an incidence or if the curvature is abrupt, the fluid cannot follow the contour, circulation is interfered with, and there is both a loss of lift and a sharp increase in profile drag, due to the formation of a large eddying wake stream. The wing is then said to be "stalled" because of flow separation.

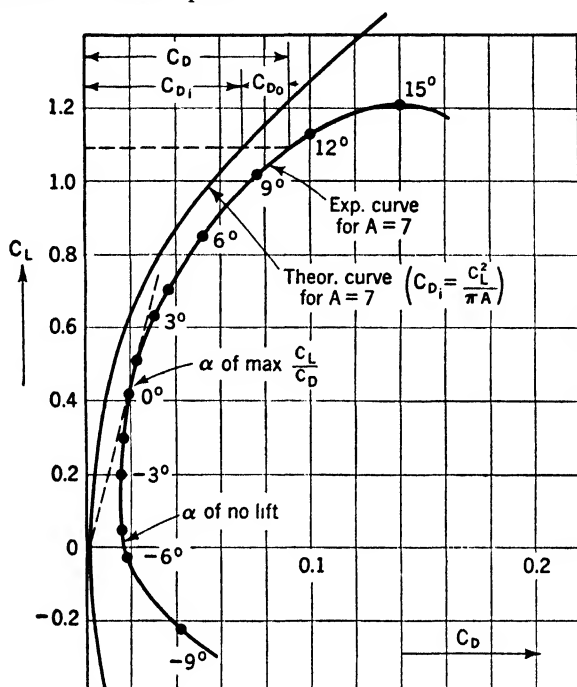


FIG. 11.25. — Polar diagram for an airfoil of finite span. (After Prandtl.)

11.25. Section Profile Drag. Airplane wings are usually tapered in plan form, not only to approximate the favorable elliptical distribution of lift and circulation, but also to save structural weight in the design of the cantilever girder. Structural considerations require a thicker wing near the root and a higher profile drag than would otherwise be chosen. Consequently, a designer frequently must estimate the profile drag of a wing having airfoil sections varying from root to tip in some regular manner. Furthermore, in actual construction, the unavoidable roughness of the surface of the wing may increase skin friction (and consequently the actual profile-drag coefficient) considerably above the values reported from wind-tunnel tests with polished models.

The "pitot-traverse" method was developed by Sir Melville Jones to estimate the section profile drag from measurements in flight. The theory is an approximation that has been found to give results within the precision of the experimental observations [5a].

Let a wing move through still air of density ρ . The relative velocity of the air is V , except in a well-defined region behind the wing, where it is less than V . This region is called the "wake" and represents a loss or defect of momentum corresponding to the profile drag. If there were no friction, there would be no wake or profile drag. The plane AA of Fig. 11.26 is normal to V and is sufficiently far behind the wing to have the

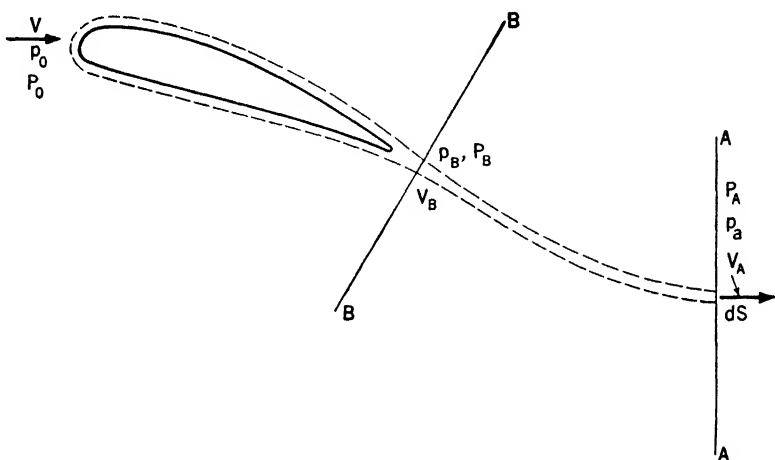


FIG. 11.26.

velocity across the plane sensibly equal to V except in the wake where it is V_A . The static pressure is sensibly equal to that in the undisturbed stream. If dS is an element of area of the plane AA and V_A is the air velocity in the elementary area, the mass of fluid passing per second through a stream tube of section dS is $\rho V_A dS$. If there were no wing friction, the velocity of this mass of fluid would be V . There has thus been a change of momentum flux equal to $\rho V_A dS(V - V_A)$. The drag of the wing causes the total momentum change in the air passing plane AA , so that

$$D = \int_S \rho V_A (V - V_A) dS$$

However, it is not possible to measure V_A in the wake at any considerable distance behind an airplane in flight. Even if we could do so, we should find that the wake had become so diffused and widened by the effects of turbulent mixing that the pitot-tube measurement of velocity differences over the plane AA would be useless. Furthermore, the wakes created by various parts of the airplane could not be identified, as each elementary stream tube leaving the trailing edge of the wing would have mixed with its neighbors.

The assumption is made that it does not matter to the wing how the

wake is diffused and that we may replace the real wake by an imaginary one in which stream tubes leaving the wing and passing the plane BB continue unmixed through AA , without further loss of total pressure. In other words, the Bernoulli constant is unchanged behind the wing in this hypothetical wake. At the plane BB , normal to the wake, the mass flow per unit time in a stream tube of section dS' is $\rho V_B dS'$. This mass when passing the plane AA has velocity V_A , and the drag of the wing must be

$$D = \int_{S'} \rho V_B (V - V_A) dS'$$

The integration is taken across the wake since no other part of the plane AA contributes to the drag. Note that we use BB , the plane of measurement, only to determine the amount of fluid ultimately discharged into the parallel wake where the static pressure is again that of the general stream.

The Bernoulli constant of the undisturbed stream is $P_0 = p_0 + (\rho/2)V^2$, where p_0 is the atmospheric pressure. In the plane of measurements BB , $P_B = p_B + (\rho/2)V_B^2$. In the plane AA the static pressure is again equal to the pressure of the undisturbed atmosphere. Since we assumed no loss of energy between BB and AA , Bernoulli's equation yields

$$P_B = p_B + \frac{\rho}{2} V_B^2 = p_A + \frac{\rho}{2} V_A^2 = p_0 + \frac{\rho}{2} V_A^2$$

whence

$$V^2 = \frac{2(P_0 - p_0)}{\rho} = \frac{2P'_0}{\rho}$$

$$V_A^2 = \frac{2(P_B - p_0)}{\rho} = \frac{2P'_B}{\rho}$$

$$V_B^2 = \frac{2(P_B - p_B)}{\rho}$$

and

$$D = \int_{S'} 2\sqrt{P_B - p_B} (\sqrt{P'_0} - \sqrt{P'_B}) dS'$$

By measuring P_B and p_B with a pitot tube at a number of points in line BB and knowing $P'_0 = (\rho/2)V^2$, one can plot values of the function $2\sqrt{P_B - p_B} (\sqrt{P'_0} - \sqrt{P'_B})$ in terms of the distance along the line BB . The area hatched in Fig. 11.27 represents the profile drag per unit of span divided by $2P'_0$, the momentum flux through unit cross section of the undisturbed stream.

The profile drag measured in a wind tunnel by the wake-survey method is found to be within 1 or 2 per cent of the profile drag obtained by subtraction of the computed induced drag from the total drag measured by the balance mechanism.

Tests in flight, made with apparatus as shown in Fig. 11.28, on actual

airplane wings usually indicate higher section profile drag than polished wind-tunnel models, owing to unavoidable roughness of manufacture. A factory-painted metal wing showed a section-profile-drag coefficient of 0.007, which was reduced to 0.005 by sanding and polishing.

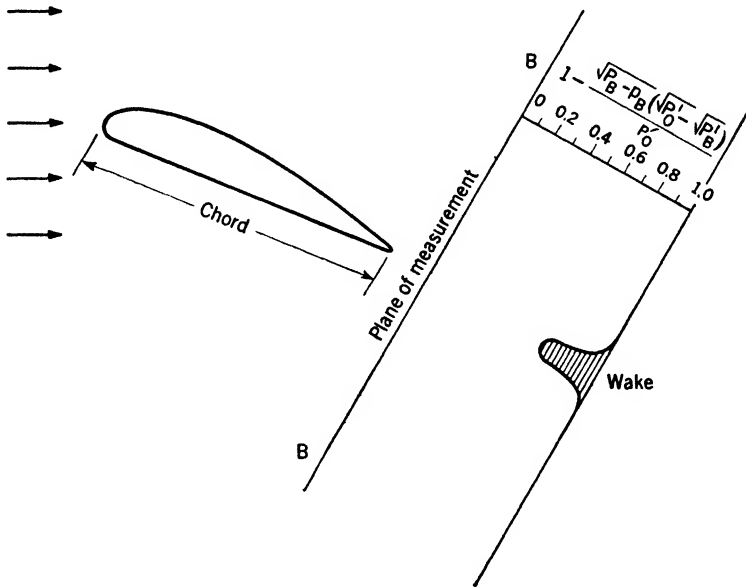


FIG. 11.27.

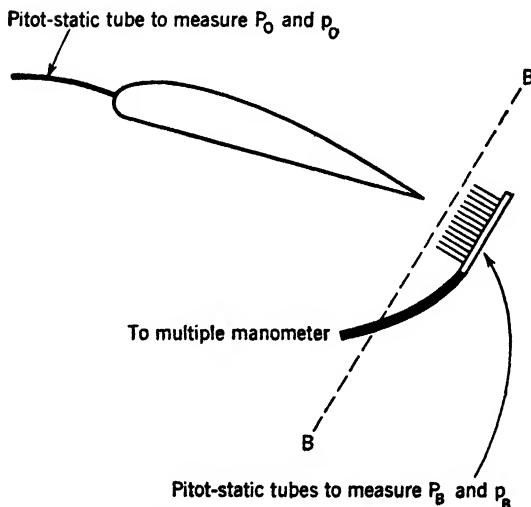


FIG. 11.28. — Diagrammatic sketch of apparatus for wake-survey measurements.

11.26. Boundary Layer. On a solid boundary a real fluid is at rest relative to the body. It was stated in Chap. X that near the boundary there is a strong velocity gradient $\partial V/\partial n$ which decreases to zero at the outside of a narrow boundary layer of fluid, where the velocity of potential flow is reached. In this boundary layer, viscous forces predominate. Outside the boundary layer, viscosity is unimportant because the velocity gradient is small.

The boundary layer is thin initially but becomes turbulent and thickens as the flow progresses along the surface. In order to prevent this layer of

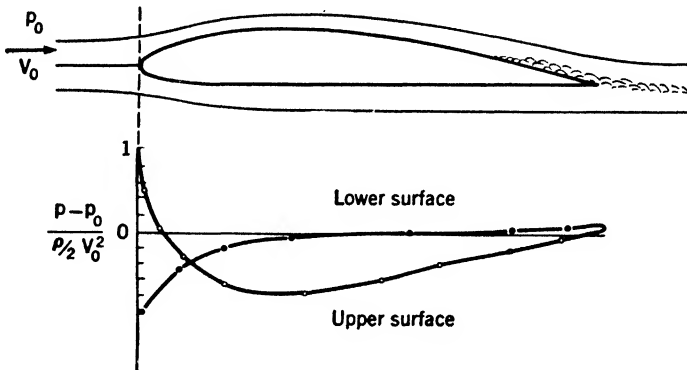


FIG. 11.29. — Pressure distribution over an airfoil at a small angle of incidence.

relatively slow-moving fluid from accumulating, there should be a fall in pressure along the surface in the direction of relative flow. Otherwise there is risk of flow separation.

Figure 11.29 shows a falling pressure at the forward end of an airfoil on the upper surface, and a gradually rising pressure over the lower surface and part of the upper one. This type of pressure distribution corresponds to an angle of incidence giving practically no lift.

11.27. Flow Separation. When the wing is turned to a sufficiently large angle of incidence, the pressure distribution assumes the form given in Fig. 11.30. The boundary layer on the upper surface then thickens and the fluid next the wall moves upstream as a result of the steeply rising pressure. Note that the main flow has separated over the back of the wing and the eddying wake stream is much broader than in Fig. 11.29. The lift of such a wing will be poor because circulation is not good, and the profile drag will be high because energy is lost in the wake.

11.28. Stalling. At a somewhat larger angle of incidence, separation will occur over the entire upper surface, and the drag will be relatively enormous. The wing is now “stalled,” as indicated by Fig. 11.31. Circulation has been further interfered with, and the lift may be even less than at a smaller incidence.

The boundary layer contains the key to flow separation and the development of eddies. The lines AB and CD represent "surfaces of discontinuity" as studied by Helmholtz and Kirchhoff. The fluid is continuous in the ordinary sense of having no voids, but the velocity is continuous only in the region outside the wake stream bounded by AB and CD . These surfaces mark a sharp discontinuity in the velocity of fluid particles.

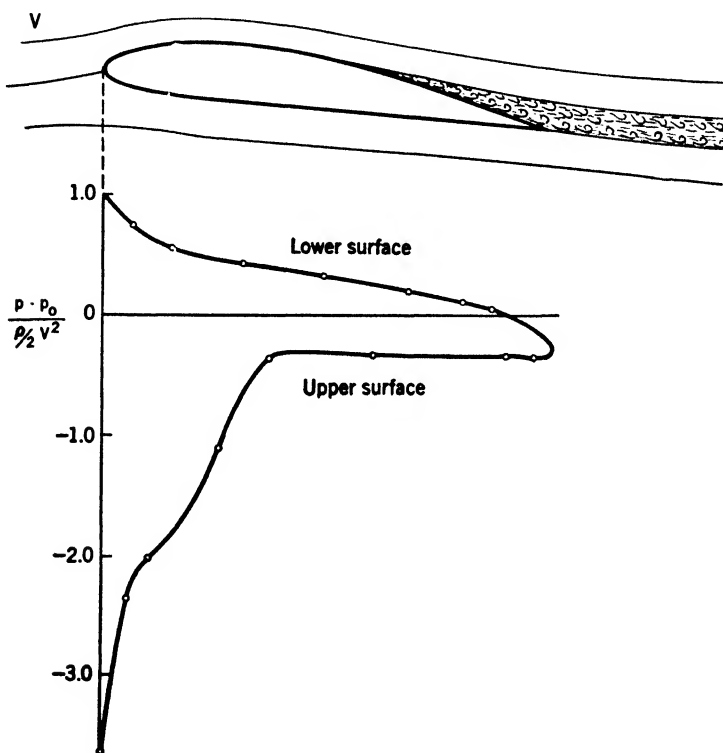


FIG. 11.30. — Pressure distribution over an airfoil at a large angle of incidence.

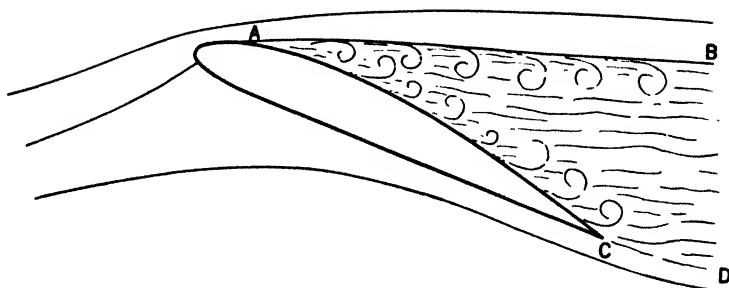


FIG. 11.31. — Streamlines around a "stalled" airfoil.

11.29. Characteristic Curves. The lift and drag at given incidence are found experimentally to vary nearly as the area of the wing, the density of the air, and the square of the velocity of the stream, *i.e.*, the lift and drag coefficients are found to be practically constant. This behavior is found in steady motion, where the velocity at no point in the flow approaches the velocity of sound. More refined experiments bear out the result of dimensional reasoning, that, at given incidence, the lift and drag

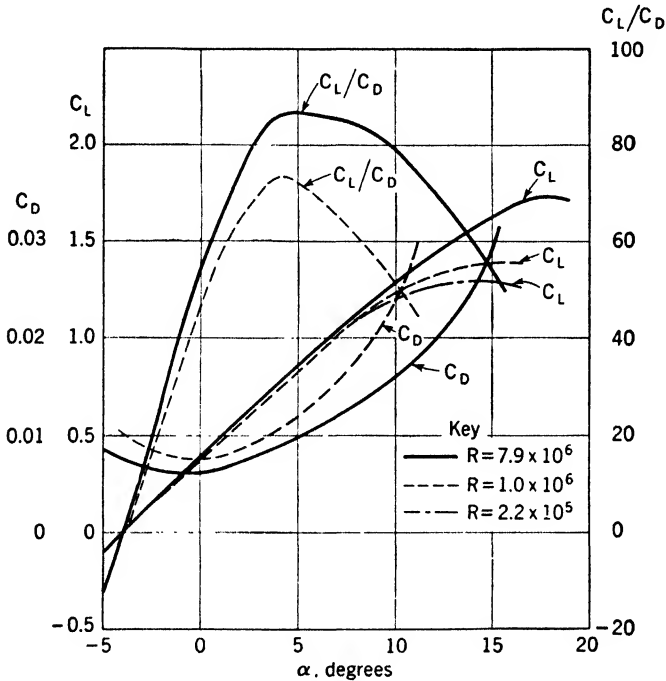


FIG. 11.32. — Characteristic curves for an NACA 4412 airfoil in two-dimensional flow. See Fig. 10.6a for the shape of this airfoil.

coefficients for any particular shape of airfoil depend on the Reynolds number Vc/ν , where c is conveniently taken as the chord. The drag coefficient C_D as a function of the Reynolds number is found to vary rather slowly. C_L for modern wings varies but little with the Reynolds number, indicating that friction plays only a small part in the maintenance of circulation. The ratio C_L/C_D is a measure of the usefulness of a wing. A typical wing has characteristics given by Fig. 11.32. Note that the wing is stalled at about a 15-deg incidence, where C_L reaches its maximum.

11.30. Airplane Mechanics. An airplane in steady level flight has its weight balanced by its lift and its drag by the propeller thrust. Thus

$$W = \text{weight} = C_L \frac{\rho}{2} V^2 A$$

$$T = \text{thrust} = (C_D + C_f) \frac{\rho}{2} V^2 A$$

where C_D is the drag coefficient for the wings and C_f is the parasite-drag coefficient for the rest of the airplane; A is the wing area. The power required is obviously

$$P_R = TV$$

The power available is the engine power P_E times the efficiency of the propeller, or

$$P_A = P_E \eta$$

For a given speed it is necessary that $C_L = 2W/\rho V^2 A$ to support the weight. To this C_L there corresponds a single value of C_D and a corre-

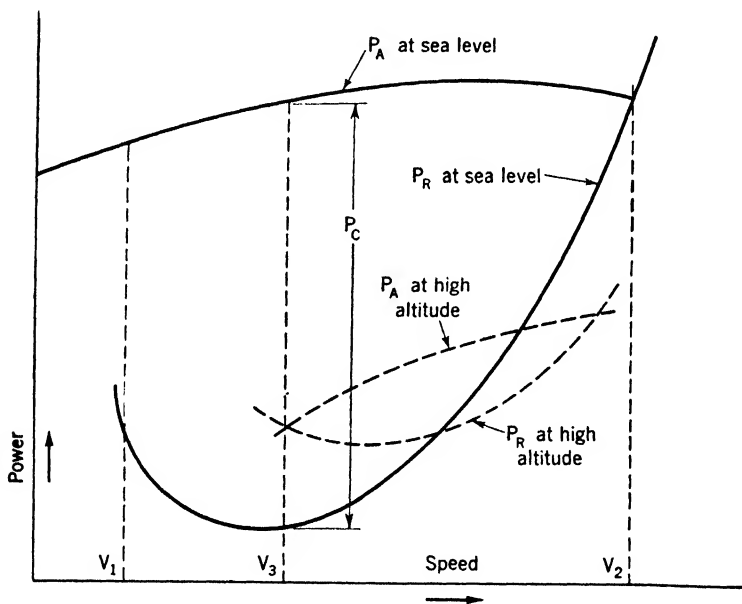


FIG. 11.33. — Power available P_A and power required P_R as functions of speed of an airplane at sea level and at high altitude.

sponding angle of incidence α , which may be found from the characteristic curve for the wing used. C_f , which is nearly independent of α , may then be added to C_D , and P_R computed. Typical speed-power curves for an airplane are given in Fig. 11.33, in which V_1 is stalling speed, V_2 is maximum speed, V_3 is speed of best climb, and P_C is power available for climb.

Note that, at high altitude, the engine power will be much lower (unless supercharged) and that the power required is higher for low speed and

lower for high speed than at sea level. For example, if the density is half that at sea level, to maintain a required C_L necessitates a doubled angle of incidence at the same speed or a 40 per cent higher speed at the same incidence. Eventually an altitude may be reached for which the curves of P_A and P_R become tangent at a certain speed. This is the absolute ceiling for the airplane with the particular engine installed.

When turning with speed V on a radius r , the airplane must be banked at an angle θ such that the centrifugal force

$$F = \frac{WV^2}{gr} = L \sin \theta$$

and the weight

$$W = L \cos \theta$$

Hence

$$\frac{F}{W} = \tan \theta = \frac{V^2}{gr}$$

The force diagram is given in Fig. 11.34.

The necessary angle of bank is greater for higher speeds and for sharper

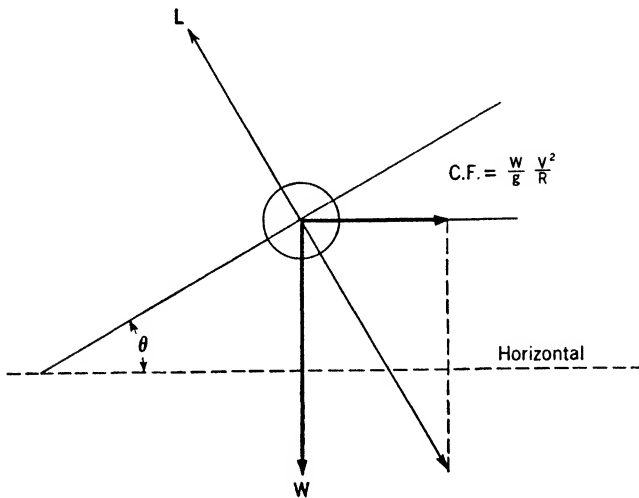


FIG. 11.34.

turns and is independent of the weight or size of the airplane. Any object, including the pilot, of weight w experiences a force opposite to the lift vector that is the vector sum of weight and centrifugal force, or

$$\text{Apparent weight} = \sqrt{\left(\frac{wV^2}{gr}\right)^2 + w^2} = w\sqrt{\tan^2 \theta + 1} = \frac{w}{\cos \theta}$$

For a sharp bank the pilot's apparent weight can be several times his normal weight, and serious structural or physiological damage may result.

In a glide with power cut off the component of the weight along the flight path balances the drag D . The lift of the wings L , normal to the flight path, balances the component of W normal to the flight path. The flight path is inclined at an angle θ to the horizon and at an angle α to the wing. For equilibrium, these three forces W , D , and L must meet at the center of gravity (see Fig. 11.35).

$$L = W \cos \theta = C_L \frac{\rho}{2} V^2 A$$

$$D = W \sin \theta = (C_D + C_f) \frac{\rho}{2} V^2 A$$

$$\tan \theta = \frac{D}{L}$$

Since for each angle of incidence α there is one value of D/L (ranging down to about $1/15$), there is also a single corresponding angle of glide θ .

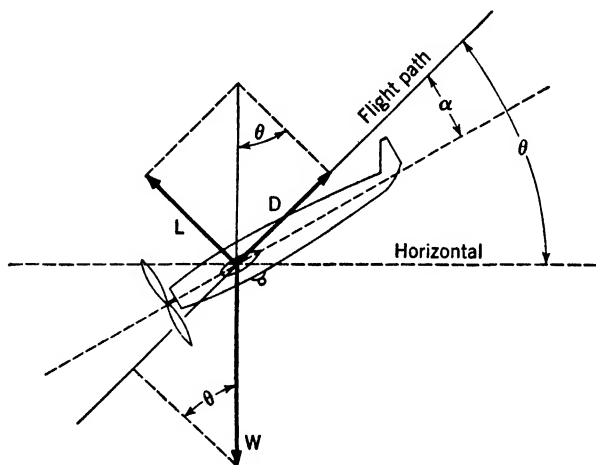


FIG. 11.35.

When $L = 0$, $\theta = 90$ deg and the glide becomes a vertical dive in which $D = W$. The speed of such a dive is called the "terminal velocity."

$$V_{\text{term}} = \sqrt{\frac{2W}{(C_D + C_f)\rho A}}$$

Modern airplanes with high wing loading W/A , low parasite resistance C_f , and flat wings of low C_D may attain dangerous speeds in such a dive.

11.31. Lift at Subsonic and Transonic Speeds. It is found in wind-tunnel tests that the lift coefficient tends to increase with increasing Mach number, other things being unchanged. This rise in C_L continues up to

the critical Mach number M_c ; but above this value C_L drops off rapidly, and C_D rises. These rapid changes in C_L and C_D are due to the formation of shock waves, as described in Art. 10.13. A typical C_L versus M curve is shown in Fig. 11.36.

This behavior of C_L is important in the flight of an airplane, not only because of the loss of lift, but also because of the changed flow around the

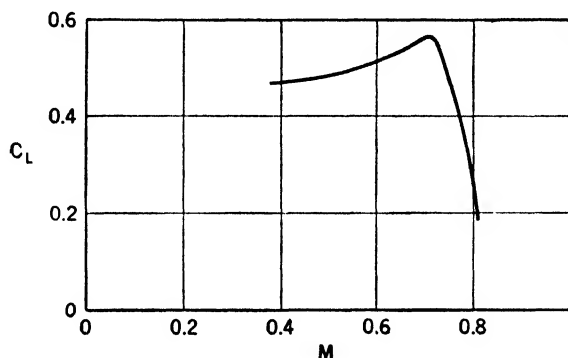


FIG. 11.36. — Lift coefficient C_L versus Mach number M .

control surfaces in the wake of the wing. The decrease in circulation around the wing results in a diminished down-wash, so that the airflow around the control planes is deflected upward from its original direction. The tail thus tends to rise and further to complicate the control problem, which may already be serious, owing to compressibility effects on the elevators themselves.

11.32. Theory of Small Perturbations for Subsonic Speeds. Glauert and Prandtl have developed an approximate theory by means of which the effect of compressibility on the pressure distribution around a thin body can be computed. The basic assumption is that the body be so thin and inclined at such a small angle as to cause only small percentage changes in the velocity of the flow. If U is the undisturbed-flow velocity and u' and v' are the additional components caused by the body, it is assumed that u'/U and v'/U are so small that their squares and products can be neglected. This assumption is obviously not fulfilled in the neighborhood of the stagnation point at the nose of a body; but if the body be thin, this region is small and so is the resultant error.

It is further assumed that pressure and density are related by the reversible adiabatic equation [Eq. (9.5)] $p/\rho^k = \text{constant}$. This, together with the additional assumption of steady irrotational flow, leads to the following equations:

$$p_1 = \left(1 - \frac{k-1}{2} V_1^2\right)^{k/(k-1)} \quad (11.42)$$

$$\rho_1 = \left(1 - \frac{k-1}{2} V_1^2\right)^{1/(k-1)} \quad (11.43)$$

$$C_1^2 = \frac{p_1}{\rho_1} = 1 - \frac{k-1}{2} V_1^2 \quad (11.44)$$

where $p_1 = p/p_0$, $\rho_1 = \rho/\rho_0$, $V_1 = V/C_0$, $C_1 = C/C_0$, and the subscript zero refers to the fluid at rest. Since we are considering only the two-dimensional case, Eqs. (11.5) apply and may be combined with Eqs. (11.28) to give

$$\left. \begin{aligned} \frac{\partial \psi}{\partial y} &= \rho_1 \frac{\partial \phi}{\partial x} \\ -\frac{\partial \psi}{\partial x} &= \rho_1 \frac{\partial \phi}{\partial y} \end{aligned} \right\} \quad (11.45)$$

Elimination of ψ from these equations, by use of the fact that $\partial^2 \psi / (\partial x \partial y) = \partial^2 \psi / (\partial y \partial x)$, gives

$$\rho_1 \left(\frac{\partial^2 \phi}{\partial x^2} + \frac{\partial^2 \phi}{\partial y^2} \right) + \frac{\partial \rho_1}{\partial x} u + \frac{\partial \rho_1}{\partial y} v = 0 \quad (11.46)$$

But from Eq. (11.43) one gets

$$\frac{\partial \rho_1}{\partial V_1} = -\frac{\rho_1 V_1}{C_1^2} \quad (11.47)$$

whence

$$\begin{aligned} \frac{\partial \rho_1}{\partial x} &= -\frac{\rho_1}{2C_1^2} \frac{\partial V_1^2}{\partial x} = -\frac{\rho_1}{C_1^2} \left(u_1 \frac{\partial u_1}{\partial x} + v_1 \frac{\partial v_1}{\partial x} \right) = -\frac{\rho_1}{C_1^2} \left(\frac{u_1}{C_0} \frac{\partial^2 \phi}{\partial x^2} + \frac{v_1}{C_0} \frac{\partial^2 \phi}{\partial x \partial y} \right) \\ \frac{\partial \rho_1}{\partial y} &= -\frac{\rho_1}{C_1^2} \left(\frac{u_1}{C_0} \frac{\partial^2 \phi}{\partial x \partial y} + \frac{v_1}{C_0} \frac{\partial^2 \phi}{\partial y^2} \right) \end{aligned}$$

Substitution of these expressions into Eq. (11.46) yields, finally,

$$\left(1 - \frac{u^2}{C^2}\right) \frac{\partial^2 \phi}{\partial x^2} - \frac{2uv}{C^2} \frac{\partial^2 \phi}{\partial x \partial y} + \left(1 - \frac{v^2}{C^2}\right) \frac{\partial^2 \phi}{\partial y^2} = 0 \quad (11.48)$$

Equation (11.48), which is nonlinear since u , v , and C depend on ϕ , must be satisfied in a compressible flow. It replaces the relatively simple linear Laplace equation [Eq. (11.31)] for incompressible fluid, to which it is seen to reduce if u and v are each very small compared with the local sound velocity C .

Introducing now the assumption peculiar to the method of small perturbations, we let

$$\begin{aligned} u &= U + u' \\ v &= v' \end{aligned}$$

where u'/U and v'/U are so small that their squares and products are negligible. The sort of flow considered is shown in Fig. 11.37. Substituting for u and v in Eq. (11.48), noting that $\partial^2\phi/\partial x^2$, $\partial^2\phi/\partial y^2$, and $\partial^2\phi/(\partial x \partial y)$ are all on the order of u' or v' , and neglecting terms of the order u'^2 , we get

$$\left(1 - \frac{U^2}{C^2}\right) \frac{\partial^2\phi}{\partial x^2} + \frac{\partial^2\phi}{\partial y^2} = 0 \quad (11.49)$$

With the aid of Eq. (11.44) it is readily found that

$$\frac{U^2}{C^2} = \frac{U^2}{C_\infty^2} \left[1 + (k-1) \frac{u'U}{C_\infty^2}\right] = M^2 \left[1 + (k-1) \frac{u'U}{C_\infty^2}\right]$$

where C_∞ is the sound velocity and M is the Mach number in the fluid having speed U . Equation (11.49) can thus be written

$$(1 - M^2) \frac{\partial^2\phi}{\partial x^2} + \frac{\partial^2\phi}{\partial y^2} = 0 \quad (11.50)$$

with negligible error (on the order of u'^2).

It will be noted that Eq. (11.50) applies to either subsonic or supersonic flow, since M may be either greater or less than 1. For the present we are concerned only with the subsonic case, for which $1 - M^2 > 0$. If we introduce a new independent variable $\eta = y\sqrt{1 - M^2}$, Eq. (11.50) reduces to the Laplace equation

$$\frac{\partial^2\phi}{\partial x^2} + \frac{\partial^2\phi}{\partial \eta^2} = 0 \quad (11.51)$$

in the x, η plane. If, then, we know the value of ϕ at any point x, η in an incompressible flow, we can assign this value of ϕ to the corresponding point x, y of a compressible flow. This procedure may be visualized with the help of Fig.

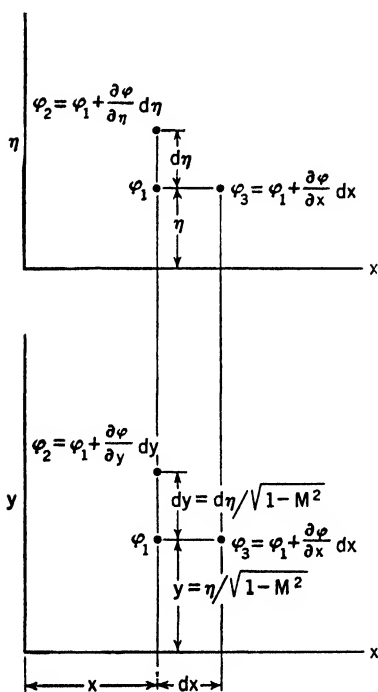


FIG. 11.38.

11.38, in which are shown three values of ϕ in the x, η plane and the same three values at the corresponding points of the x, y plane. From this figure it follows that

$$\left. \begin{aligned} \text{or} \quad \frac{\partial \phi}{\partial \eta} &= \frac{1}{\sqrt{1-M^2}} \frac{\partial \phi}{\partial y} \\ \text{and} \quad v'_i &= \frac{1}{\sqrt{1-M^2}} v'_c \end{aligned} \right\} \quad (11.52)$$

$$\left. \begin{aligned} \text{or} \quad \frac{\partial \phi}{\partial x} &= \frac{\partial \phi}{\partial x} \\ U_i + u'_i &= U_c + u'_c \end{aligned} \right\} \quad (11.53)$$

where subscripts i and c refer to incompressible and compressible flow, respectively. The ratio of the slopes of the streamlines at any pair of corresponding points is thus

$$\frac{v'_c}{U_c + u'_c} \frac{U_i + u'_i}{v'_i} = \sqrt{1-M^2} \quad (11.54)$$

It is to be noted that the boundary of the body in the incompressible flow is not mapped into a streamline of the compressible flow. The slope of the

line joining these mapped points is increased by a factor $1/\sqrt{1-M^2}$ over that in the x, η plane, while the slope of the *streamline* through any mapped point is reduced by the factor $\sqrt{1-M^2}$ below that through the original point in the x, η plane.

The curve $ABCDEF$ of Fig. 11.39 represents the surface of a body in incompressible flow, and $A'B'C'D'E'F'$ is the map of this curve in the x, y plane. The streamlines of the compressible flow obtained from the mapped values of ϕ are shown as heavy lines in the x, y plane. It is seen that between A' and F' , B' and E' , and C' and D' there are no ϕ values to map, the corresponding points in the x, η plane lying inside the body. The dotted portions of the streamlines are obtained in the following way:

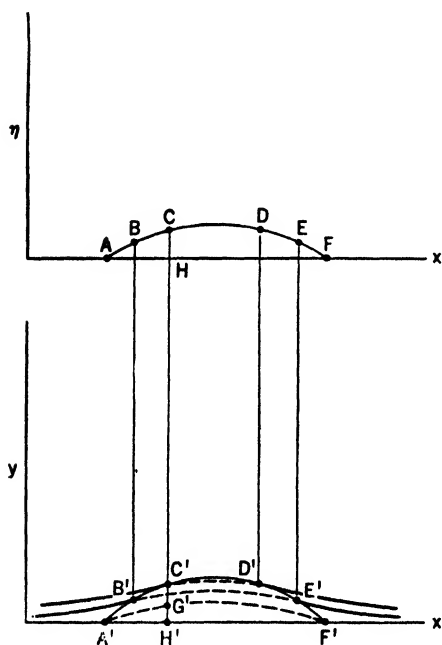


FIG. 11. 39.

Any distance, such as $G'C'$, between a point on a dotted streamline and the termination of the full streamline directly above it is on the order of δ , the thickness of the original body. This thickness, however, is measured by a mean value of the slope times the length of the body l . Hence

$$\frac{G'C'}{l} \sim \frac{\delta}{l} \sim \frac{v'_i}{U_i} \sim \frac{v'_c}{U_c}$$

Furthermore, $\partial u'_c/\partial x$ is of order u'_c/l . It follows therefore from Eq. (11.50) that $\partial v'_c/\partial y$ is also of this same order of magnitude. The difference between the values of v'_c at G' and C' is thus given by

$$\frac{\partial v'_c}{\partial y} G'C' \sim \frac{u'_c}{l} G'C' \sim \frac{u'_c v'_c}{U_c} \quad (11.55)$$

It can also be shown, from the irrotational nature of the flow, that

$$\frac{\partial u'_c}{\partial y} G'C' = \frac{\partial v'_c}{\partial x} G'C' \sim \frac{v'_c}{l} G'C' \sim \frac{v'^2_c}{U_c} \quad (11.55a)$$

Both these differences are negligible by hypothesis. Hence, at a given value of x , the slopes of all the dotted streamlines are the same as that of an adjacent full streamline.

The dotted streamline $A'G'F'$, which joins the stagnation points A' and F' , is a boundary of the compressible flow and thus may be considered as the outline of a body. It is clear from Eqs. (11.54), (11.55), and (11.55a) that any ordinate of this body, such as $H'G'$, is related to the ordinate HC at the same value of x by the equation

$$G'H' = \sqrt{1 - \bar{M}^2} CH$$

It is readily seen from this result that the approximate streamline pattern about a thin airfoil in a subsonic compressible flow can be obtained from that for an incompressible flow about an airfoil of the same length but whose thickness, angle of attack, and camber are all greater by a factor $1/\sqrt{1 - \bar{M}^2}$ than those of the first airfoil.

Practically, we are interested in knowing the relation between the lift coefficients for these two airfoils. This relation is found as follows:

The lift coefficient for the compressible flow in the x, y plane may be defined as

$$C_{L_c} = \frac{\int_0^l \Delta p dl}{\rho_\infty l U_c^2/2} = \frac{\overline{\Delta p}}{\rho_\infty U_c^2/2}$$

where l is the chord, $\overline{\Delta p}$ is the average pressure difference between the lower and upper surfaces of the profile, and ρ_∞ is the density and U_c is the velocity of the distant fluid. The Euler equation [Eq. (4.7)] reduces in this case to

$$\int_{p_\infty}^p \frac{dp}{\rho} + \frac{(U_c + u'_c)^2 + v'^2_c - U_c^2}{2} = 0$$

which, together with the formula $p/\rho^k = \text{constant}$, yields

$$\frac{p}{p_\infty} = \left(1 - \frac{k-1}{C_\infty^2} U_c u'_c\right)^{k/(k-1)} = 1 - \frac{k U_c u'_c}{C_\infty^2}$$

or

$$p - p_\infty = -\frac{k p_\infty}{C_\infty^2} U_c u'_c = -\rho_\infty U_c u'_c$$

where terms of the order $u_c'^2$ have been neglected. Therefore

$$\overline{\Delta p} = -\rho_\infty U_c \overline{\Delta u'_c}$$

and

$$C_{L_c} = -\frac{2\overline{\Delta u'_c}}{U_c} \quad (11.56)$$

The lift coefficient for the incompressible flow around the profile in the x, η plane is found by similar methods to be

$$C_{L_i} = -\frac{2\overline{\Delta u'_i}}{U_i}$$

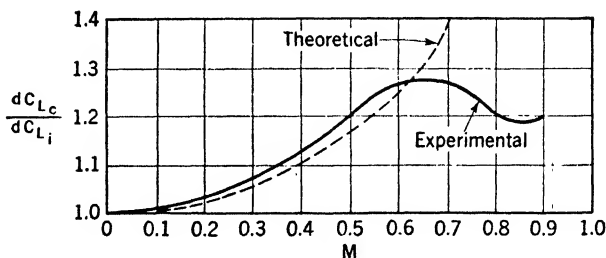


FIG. 11.40. — Ratio of the slopes of the lift-coefficient curves for compressible and incompressible flow dC_{L_c}/dC_{L_i} versus Mach number M . (After R. von Mises, reference 4.)

Thus the ratio of lift coefficients is

$$\frac{C_{L_c}}{C_{L_i}} = \frac{\overline{\Delta u'_c} U_i}{\overline{\Delta u'_i} U_c} \quad (11.57)$$

Since Eqs. (11.53) apply at all pairs of corresponding points, they hold far upstream where $u'_i = u'_c = 0$. Hence $U_i = U_c$, $u'_i = u'_c$, and $\overline{\Delta u'_i} = \overline{\Delta u'_c}$. Therefore, using Eqs. (11.55a) and (11.57), we find that

$$C_{L_c} = C_{L_i}$$

It is easily seen that the lifts and pressure distributions, also, are the same for these two airfoils, provided that ρ_∞ is the same of both.

The question now arises as to the effect of compressibility on the lift coefficient of a given profile at a given angle of attack. It is found that in this case

$$\frac{C_{Lc}}{C_{Li}} = \frac{1}{\sqrt{1-M^2}} \quad (11.58)$$

The details are left to the reader (see problem 11.19).

The theoretical formula, Eq. (11.58), is found to agree well with experiment for M less than about 0.6, as shown in Fig. 11.40. Here the measured value of dC_{Lc}/dC_{Li} is compared with that computed from Eq. (11.58), at different values of M . The computed value is, obviously, $1/\sqrt{1-M^2}$. The increasing divergence between experiment and theory for values of M greater than 0.6 is due to the fact that variations in the local Mach number and its approach to 1 in certain regions can no longer be ignored.

11.33. Lift at Supersonic Speeds. The flow pattern around a wing at supersonic speeds is characterized by the nose and tail shock waves already discussed in Art. 10.14. An idealized example, the two-dimensional flow around a thin flat plate in an unsymmetrical attitude, is given in Fig. 11.41. The approaching flow remains unaffected by the plate until the fluid reaches the lines oa and oc . On the upper side the fluid expands and turns gradually until at the line ob it is moving parallel to the plate. It then flows in a straight path to the line $o'b'$, where the stream is suddenly deflected back to its original direction. On the lower side the stream turns suddenly at the line oc , moves parallel to the surface, and then gradually returns to its original direction between $o'a'$ and $o'b'$. The pressure and velocity are constant over both the upper and lower surfaces, the pressure being greater underneath than above. It is thus a relatively simple matter to compute the lift and drag of the plate.

The theoretical flow pattern of Fig. 11.41 is based on the assumption of two-dimensional irrotational flow. It is found that a solution of the equations of motion exists which satisfies these postulates and which yields the flow patterns for the expansions around the sharp corners, *i.e.*, it gives the streamlines and pressure distributions in the wedges aob and $a'o'b'$. A second solution is known which gives the oblique shock lines oc and $o'c'$ by which the fluid is turned and suddenly compressed. Schlieren photographs of the flow of air past a plate are practically identical with the theoretical pattern.

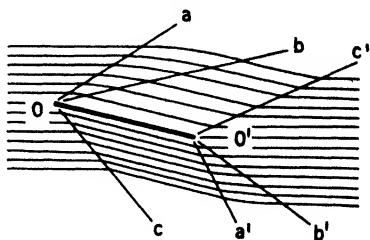


FIG. 11.41. — Supersonic flow past a flat plate at a small angle of incidence.

The occurrence of drag in this two-dimensional compressible flow is at first sight even more baffling than that in the three-dimensional incompressible flow around a wing of finite span. For the wing of finite span the origin of the drag is the continual introduction of rotation into the

fluid by the trailing vortices. In the present problem, on the other hand, the flow near the plate is entirely irrotational. It will be observed, however, that the lines oc and $o'a'$ extended will intersect. Since $o'a'$ represents a wave of rarefaction, its junction with the shock line oc will result in a decrease in the pressure jump across oc . The shock line will thus become more oblique and will eventually intersect all the rays from o' , after which it will have disappeared completely, since the pressure rise at the leading edge is exactly equal to the pressure drop at the trailing edge. It will be shown below that rotation is introduced into the flow along that part of the shock line beyond the point of intersection with $o'a'$, where the conditions cease to be the same at all points on the shock. The drag thus results from the continual input of rotational kinetic energy into the fluid at some distance from the plate.

11.34. Theory of Small Perturbations for Supersonic Speeds. As already mentioned, Eq. (11.50) of the Glauert-Prandtl theory is applicable to supersonic flow. In this case, since $M > 1$, the equation is written

$$(M^2 - 1) \frac{\partial^2 \phi}{\partial x^2} = \frac{\partial^2 \phi}{\partial y^2} \quad (11.59)$$

It is readily shown by direct substitution that a solution of this equation is

$$\phi = Ux + f(x - \sqrt{M^2 - 1}y) + F(x + \sqrt{M^2 - 1}y) \quad (11.59a)$$

where f and F are arbitrary functions of their respective arguments.

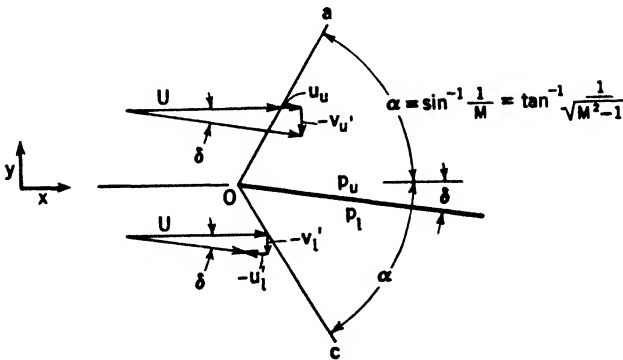


FIG. 11.42.

Equation (11.59a) will be applied to the supersonic flow around a small angle, as shown in Fig. 11.42.

Ux is the velocity potential for the undisturbed flow approaching the angle. The function $f(x - \sqrt{M^2 - 1}y)$ is the potential for an additional flow superposed on the main stream. Since the argument of f is constant along a straight line of slope $1/\sqrt{M^2 - 1}$, both f and its derivatives

$\partial f/\partial x = u'$ and $\partial f/\partial y = v'$ are also constants along such a line. Therefore, the additional velocity is normal to this line and has a constant value everywhere along it. We can accordingly build up a supersonic flow pattern that is theoretically correct by choosing suitable additional velocities to turn the stream through an angle δ when it reaches the straight lines oa and oc . The angle $\alpha = \sin^{-1} 1/M = \tan^{-1} 1/\sqrt{M^2 - 1}$ that these lines make with the x axis will be recognized as the Mach angle. The lines oa and oc , known as "Mach lines," represent standing disturbances or wavelets; the component of the approaching velocity normal to the wavelets is $U \sin \alpha$, which is equal to C_∞ , the sound velocity in the undisturbed flow.

The potential $F(x + \sqrt{M^2 - 1}y)$ gives disturbance velocities along lines of slope $-1/\sqrt{M^2 - 1}$. In the present example, however, the boundary conditions are satisfied without any such wavelets, and F must be put equal to zero.

Figure 11.42 may be considered as the flow around a flat plate. It is a simple matter to compute the lift coefficient for the plate from the theory presented above. We note that the velocity (and hence the pressure) is constant over the upper and lower surfaces of the plate. The lift coefficient is easily expressed in terms of these constant pressures: $C_L = [(p_l - p_u)/(\rho_\infty/2)U^2] \cos \delta \approx (p_l - p_u)/(\rho_\infty/2)U^2$. The Euler equation has here the form given on page 263, since terms in u'^2 are assumed negligible. Accordingly, $p_l - p_u = \rho_\infty U(u'_u - u'_l)$ and $C_L = (2/U)(u'_u - u'_l)$. The velocity diagrams of Fig. 11.42 yield the relations

$$\frac{u'_u}{U} = \frac{\delta}{\sqrt{M^2 - 1} - \delta} \quad \text{and} \quad \frac{-u'_l}{U} = \frac{\delta}{\sqrt{M^2 - 1} + \delta}$$

so that

$$C_L = \frac{4\delta}{\sqrt{M^2 - 1}} \quad (11.60)$$

The drag is equal to the resultant force multiplied by δ . Hence, the drag coefficient is $C_D = C_L \delta / \cos \delta$ or (with $\cos \delta \approx 1$)

$$C_D = \frac{4\delta^2}{\sqrt{M^2 - 1}} \quad (11.60a)$$

which is of order δ^2 and is here neglected.

The flow pattern around a thin body, such as is shown in Fig. 11.43, may be determined by the Glauert-Prandtl method if the continuously curved surface is replaced by a number of straight segments. At each corner formed by the junction of two consecutive segments a Mach line is drawn, at every point of which the velocity direction changes by the same amount. Compression occurs only at the nose and tail; along the whole surface the flow expands. It will be noted that in this approximate theory

all the Mach lines are parallel, since changes in the Mach number are assumed negligible. An exact theory must take into account the fact that

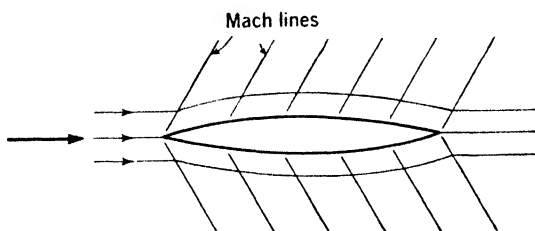


FIG. 11.43. — Glauert-Prandtl approximate supersonic flow pattern past a thin body.

neighboring Mach lines diverge in a region of expansion and converge in a region of compression.

11.35. Flow around a Corner (Expansion). To develop such a theory we observe that the Glauert-Prandtl theory is exact for an expansion of an initially parallel stream around an infinitesimal corner and that the flow downstream from the corner is again parallel but has a higher velocity and smaller Mach angle. The further expansion of this flow around another infinitesimal corner can be handled just as that around the preceding one; the new values of approach velocity and Mach angle must, however, be used. In an expanding flow, such as that over the body of Fig. 11.43, we can thus approximate as closely as we please to the exact solution, by replacing the continuously curved outline with a number of straight segments and applying the Glauert-Prandtl approximation to each corner so formed, using in every case, the appropriate velocity and Mach angle. Obviously, the greater the number of segments used, the better will be the approximation.

In a flow that is being compressed, the Mach angle increases at succes-

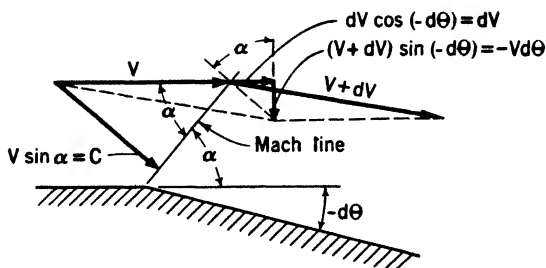


FIG. 11.44.

sive corners, and the Mach lines converge and eventually come together. Such coalescence results in the formation of a finite pressure jump, or shock, in which the changes in pressure and density are not of the reversible

adiabatic type postulated in the development of the Glauert-Prandtl theory. If, however, the total compression is small, the above method may be used with only a small error. An outline of this method, which was developed by Prandtl and Busemann, follows:

In Fig. 11.44, V is the velocity of a parallel flow approaching a corner at which the direction changes by an infinitesimal angle $-d\theta$; α is the local Mach angle; and $V + dV$ is the velocity after the flow turns the corner. By the Glauert-Prandtl theory, conditions are uniform all along the Mach line, and the disturbance velocity is normal to the Mach line. The velocity diagram of Fig. 11.44 thus yields the equation

$$\frac{dV}{V d\theta} = -\tan \alpha = -\frac{1}{\sqrt{(V^2/C^2) - 1}} \quad (11.61)$$

where C is the local sound velocity. In this equation, terms of second

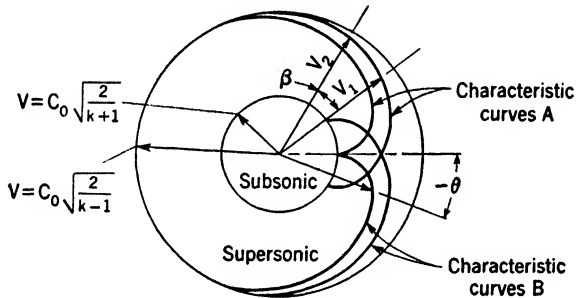


FIG. 11.45. — Characteristic curves for synthesis of supersonic flow patterns.

order are neglected. With the aid of Eq. (11.44), Eq. (11.61) can be transformed to

$$\frac{dV}{V d\theta} = -\frac{\sqrt{1 - [(k-1)/2](V^2/C_0^2)}}{\sqrt{[(k+1)/2](V^2/C_0^2) - 1}} \quad (11.62)$$

where C_0 is the sound velocity in fluid at rest.

An integral curve of Eq. (11.62) is conveniently plotted in polar coordinates for which the radius vector is the velocity V and the polar angle is the angle of turn θ . This plane is appropriately called the “hodograph plane.” It is seen from Eq. (11.62) that, in these coordinates, an integral curve is radial ($dV/V d\theta = \infty$) where $V = \sqrt{2/(k+1)}C_0$, which is the value of the local sound velocity [see Eq. (9.11)]. This lower limiting value of V is represented by a circle in the hodograph plane, as shown in Fig. 11.45. Furthermore, an integral curve is normal to V (that is, $dV/V d\theta = 0$) where $V = \sqrt{2/(k-1)}C_0$, which will be recognized from Eq. (9.8) as the maximum attainable velocity (corresponding to $p = 0$). This upper limiting value of V is given by the outer circle in Fig. 11.45. In the

supersonic region lying between these two limits it can be shown from Eq. (11.62) that an integral curve (characteristic curve) is generated by a point on a circle rolling on the inner circle and touching the outer one. The characteristics are thus epicycloids.

It is obvious that if the flow expands through a positive (counterclockwise) angle $d\theta$ we shall get Eq. (11.62) without the negative sign. There are therefore two families of characteristic curves A and B , as sketched in Fig. 11.45.

If the flow expands from any initial supersonic velocity V_1 , around a corner (or series of corners) of total angle β , the final velocity V_2 is uniquely determined by the appropriate characteristic curve (see Fig. 11.45). But from Eqs. (11.42) and (11.44) the pressure and sound velocity are determined (for given p_0 and C_0) when the velocity is known. The final condition of the flow is therefore known. It is apparent from Fig. 11.45 that there is a maximum angle through which a stream can turn and that this angle depends on the initial velocity. The greatest value of this angle, which occurs if the flow is initially just sonic, is 129.3° [9].

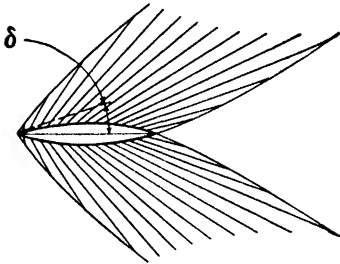


FIG. 11.46. — Shock waves and Mach lines for a supersonic flow past a thin body. (Reproduced from L. Prandtl, *The Flow of Liquids and Gases*, in "The Physics of Solids and Fluids," Blackie and Son, Ltd., London and Glasgow.)

A graphical method, based on the characteristic diagram of Fig. 11.45, has been evolved, by which supersonic two-dimensional flow patterns are readily constructed.* The flow determined by this method around the lenticular body of Fig. 11.43 is shown in Fig. 11.46. Since the nose and tail angles of the body are small, the method is satisfactory even for the compression of the flow in these regions. For example, one determines the magnitude of the velocity on the upper surface immediately downstream from the nose by following in the counterclockwise

sense through a polar angle δ the appropriate characteristic of family B of Fig. 11.45.

11.36. Flow around a Corner (Compression). If the flow is compressed and turned suddenly through an angle that is not small, the method of characteristics is not even approximately correct and a new analysis is required. It is assumed that a parallel irrotational flow of a perfect gas is turned through a finite angle by means of a straight oblique shock, along both sides of which conditions are uniform. The irreversible changes that occur as the fluid crosses the shock preclude the use of the Euler equation between points on opposite sides of the shock, and it is necessary to use the energy equation [Eq. (9.19)]. The analysis is similar to that given in

* For further information see references 1 and 9 at the end of this chapter.

Art. 9.6 for a transverse shock, the only new feature being the inclusion of a velocity component parallel to the shock.

The velocity diagrams and control surface used in the analysis [9] are shown in Fig. 11.47. The upper and lower sides of the control surface are streamlines, and the other two sides are parallel to the shock. For convenience the areas at the ends of the control surface, through which fluid enters and leaves, are taken as unity. The continuity equation thus gives

$$\rho_1 u_1 = \rho_2 u_2 \quad (11.63)$$

The momentum equation applied normal to the shock yields, when combined with Eq. (11.63),

$$p_1 - p_2 = \rho_1 u_1 (u_2 - u_1) \quad (11.64)$$

while, when applied parallel to the shock, it gives $\rho_1 u_1 (v_2 - v_1) = 0$ or $v_2 = v_1$. The energy equation [Eq. (9.19)] therefore takes the form

$$\frac{k}{k-1} \left(\frac{p_2}{\rho_2} - \frac{p_1}{\rho_1} \right) = \frac{u_1^2 - u_2^2}{2} \quad (11.65)$$

From Eqs. (11.63), (11.64), and (11.65) we obtain, finally, the expressions

$$\frac{\rho_2}{\rho_1} = \frac{(k+1)p_2 + (k-1)p_1}{(k-1)p_2 + (k+1)p_1} \quad \text{and} \quad u_1^2 = \frac{p_1}{2\rho_1} \left[(k-1) + (k+1) \frac{p_2}{p_1} \right]$$

Noting that $u_1 = V_1 \cos \beta_1$ and that the Euler equation may be applied between section 0 upstream where the velocity is zero and section 1 to give

$$V_1^2 = \frac{2k}{k-1} \frac{p_1}{\rho_1} \left[\left(\frac{p_0}{p_1} \right)^{(k-1)/k} - 1 \right]$$

we find

$$\cos^2 \beta_1 = \frac{[(k-1) + (k+1)(x/y)](k-1)}{4k [(1/y)^{(k-1)/k} - 1]} \quad (11.66)$$

and

$$\frac{\tan \beta_2}{\tan \beta_1} = \frac{(k+1)(x/y) + (k-1)}{(k-1)(x/y) + (k+1)} \quad (11.67)$$

where $x = p_2/p_0$ and $y = p_1/p_0$.

The curves of Figs. 11.48 and 11.49 are a convenient means of representing Eqs. (11.66) and (11.67). Figure 11.48 gives two values of β_1 for a given value of y and the angle of deflection $\beta_2 - \beta_1$. Only the smaller of these two values of β_1 is found to occur in experiments. This figure also shows that no solution of this type exists if the stream is turned through an angle greater than about 45 deg. It is further seen that no solution of this type exists, even for $\beta_2 - \beta_1 < 45$ deg, if β_1 is too small. This condi-

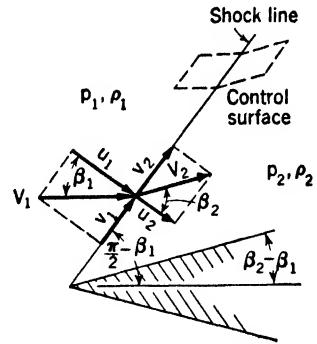


FIG. 11.47.

tion on β_1 is equivalent to the stipulation that the Mach number at 1, V_1/C_1 , cannot be too small. Experiments show that, if this type of solu-

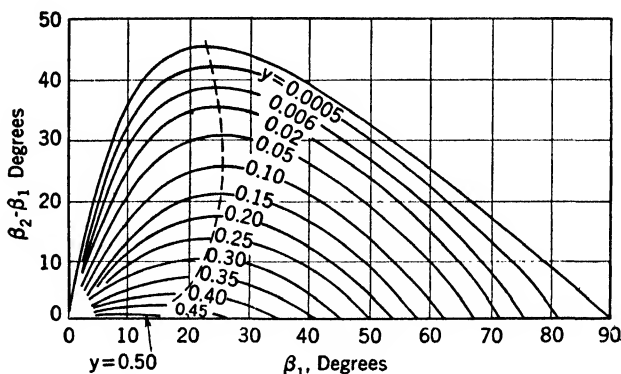


FIG. 11.48. — Curves for synthesis of a shock wave. (Courtesy of Sir Geoffrey Taylor.)

tion fails for either of these reasons (nose angle too great or V_1/C_1 too small), the shock wave does not have the shape shown in Fig. 11.47, nor does it touch the nose of the body; instead, it is curved and passes in front of the nose, as described in Art. 9.3.

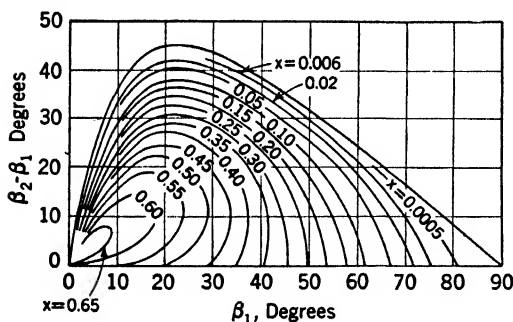


FIG. 11.49. — Curves for synthesis of a shock wave. (Courtesy of Sir Geoffrey Taylor.)

As an example of the use of these curves, suppose that the angle $\beta_2 - \beta_1$ is given, together with the flow conditions at 1 and 0. Figure 11.48 then gives the value of β_1 , from which the slope of the shock is found, while from Fig. 11.49 the value of $x = p_2/p_0$ is determined.

A similar analysis has also been made for the axially symmetrical flow over a cone [9].

11.37. Shock Waves and Rotation. In Art. 11.33 it was pointed out in connection with Fig. 11.41 that the drag on a two-dimensional object in supersonic flow results from the introduction of rotation into the fluid behind shock waves. If we refer to Fig. 11.47 it is clear that, in the region abd of Fig. 11.50, there is no rotation, since the flow conditions are uniform throughout this region. Between points b and c , however, the shock intensity gradually diminishes to a negligible value owing to the action of the rarefaction wavelets emanating from corner d . The flow downstream from this segment of the shock wave is rotational, as is shown below.

The definition of rotation given in Art. 4.12 is

$$\text{Rotation} = \frac{V}{R} - \frac{\partial V}{\partial n}$$

where R is the radius of curvature of the streamline, and the normal direction n is considered positive toward the center of curvature (Fig. 11.51). Since the fluid is assumed frictionless in this region and gravity is neglected, Euler's differential equation for the pressure change normal to the streamline [Eq. (4.4)] is valid: $(1/\rho)(\partial p/\partial n) = -V^2/R$. Furthermore, the flow is supposed to be adiabatic everywhere and to be uniform upstream from the body, so that the energy equation takes the form of Eq. (9.18): $h + (V^2/2) = \text{constant}$, or $(\partial h/\partial n) + V(\partial V/\partial n) = 0$. The expression for rotation thus becomes

$$\text{Rotation} = \frac{1}{V} \left(-\frac{1}{\rho} \frac{\partial p}{\partial n} + \frac{\partial h}{\partial n} \right)$$

This equation can, however, be expressed in terms of the entropy change normal to the streamlines, with the aid of Eq. (9.28), differentiation of which leads to $T(\partial s/\partial n) = (\partial h/\partial n) - (1/\rho)(\partial p/\partial n)$. The rotation, therefore, is

$$\text{Rotation} = \frac{T}{V} \frac{\partial s}{\partial n} \quad (11.68)$$

According to Eq. (11.68) there must be rotation downstream from segment bc of the shock, because the entropy jump through the shock is different for different streamlines.

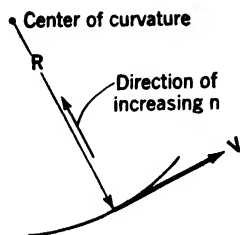


FIG. 11.51.

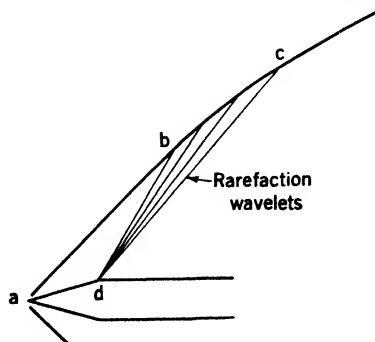


FIG. 11.50. — Shock front set up by a body with a wedge-shaped nose.

11.38. Hodograph Method. The theoretical methods so far discussed yield solutions if the flow is entirely subsonic or if it is entirely supersonic but fail if the flow contains both sub- and supersonic regions. The equation of motion for a compressible fluid in the form of Eq. (11.48) is practically impossible to handle because it is nonlinear. The Russian mathematician Chaplyguine, however, discovered that this equation becomes linear if expressed in terms of V and θ as independent variables, instead of x and y . (See Art. 11.35 for the definition of V and θ .) The great advantage of a linear equation is that solu-

tions may be added to obtain another solution, so that a technique similar to that used for an incompressible fluid can be developed. This superposition method is limited to the V, θ (hodograph) plane in the case of a compressible fluid, and a great deal of labor is involved in the transfer of the solutions to the x, y (physical) plane. The differential analyzer has been used [8] to obtain certain solutions in the hodograph plane and to transfer them to the physical plane.

Perhaps the most important result of the limited investigations so far made by the hodograph method is the fact that a continuous transition from sub- to supersonic flow and back again is possible, at least in frictionless fluid. It may be, therefore, that an airfoil can in future be designed such that over part of its surface there is supersonic flow but a complete absence of shock waves. The critical speed of such an airfoil would be considerably nearer the sound velocity than that of the best sections developed to date (see Fig. 10.23). It is, of course, impossible to avoid shocks if the speed of the airfoil itself is supersonic.

11.39. Some Factors in High-speed Flight. The flow conditions on a thin wing in actual flight approximate to those assumed in the Glauert-Prandtl theory of small perturbations (Arts. 11.32 to 11.34). The results of this theory are useful in demonstrating the adverse changes in wing characteristics that occur, say, between the flight Mach numbers of 0.8 and 1.2. Such demonstration can be expected to be only a rough guide since both these values of M are fairly close to 1.

As a simple example, consider the changes in lift coefficient C_L of a thin flat plate. Potential theory of incompressible flow [2] yields the formula $C_L = 2\pi\delta$, for a small angle of incidence δ . The effect on C_L of compressibility at subsonic speeds is given by Eq. (11.58), from which we find, for $M = 0.8$, $C_L = 2\pi\delta/\sqrt{1 - 0.64} = 10.5\delta$. In the supersonic range, on the other hand, the flow pattern has changed completely, and C_L is obtained from Eq. (11.60). It is found, for $M = 1.2$, that $C_L = 4\delta/\sqrt{1.44 - 1} = 6.0\delta$.

The change in the drag coefficient is also adverse. In subsonic motion the only source of drag in a two-dimensional flow over a plate is the skin friction, and measurements indicate that C_D is approximately 0.01 under these conditions. In supersonic motion, on the other hand, there is an additional component of drag, which is given by Eq. (11.60a). For $M = 1.2$, the incremental drag coefficient is found to be $\Delta C_D = 4\delta^2/\sqrt{1.44 - 1} = 6.0\delta^2$. If, for example, $\delta = 2$ deg (0.04 radian), $\Delta C_D = 0.009$. The drag coefficient is thus approximately doubled in the supersonic flow.

In the immediate neighborhood of $M = 1$ the Glauert-Prandtl theory is inapplicable, but the experimental results shown in Figs. 10.24 and 11.36 demonstrate the extremely undesirable changes encountered in the transonic region.

It is apparent from these two-dimensional considerations that flight at transonic or supersonic speeds offers many difficulties in connection with wing design. These difficulties are moderated, however, if a third-dimensional component is introduced into the relative flow by use of a wing swept back at an angle greater than the flight Mach angle. The basis for this improvement is the fact that the wing characteristics depend primarily on the component of flow normal to the leading edge of the wing. Thus, if the sweepback angle is greater than the Mach angle, the normal component is subsonic and the wing characteristics are nearly the same as those at this subsonic speed [11].

Consider a wing of infinite aspect ratio in a subsonic flow normal to the leading edge. It is evident, if friction be neglected, that motion of the wing parallel to its leading edge

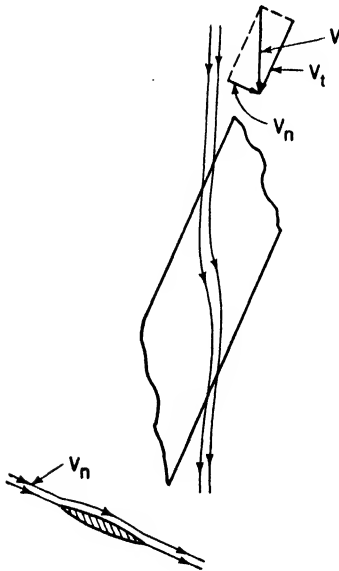


FIG. 11.53. — Streamlines near a swept-back wing in two-dimensional flow. (After Jones, reference 11.)

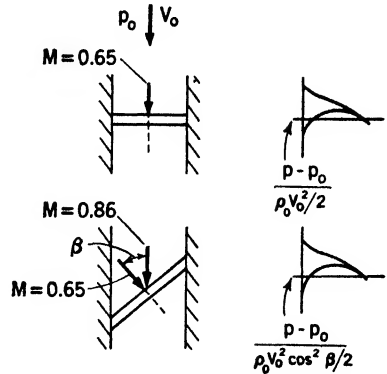


FIG. 11.52. — Experimental verification of the effect of sweep in a two-dimensional flow. Pressure distribution over mid-section depends only on normal component of flow.

will have no effect on the pattern of the normal flow. The relative velocity of air and wing can theoretically be given an arbitrarily high value without effect on the wing characteristics. Experiments made under two-dimensional conditions verify the theory, as shown in Fig. 11.52. The pressure distribution along the chord of the normal wing is seen to be practically the same as for the swept-back wing, even though the Mach numbers of the resultant flows are quite different.

The finite length of an actual wing will modify this conclusion somewhat, owing not only to the tip but also to the "wall effect" of the fuselage. The latter effect is peculiar to a swept-back wing and results from the following phenomenon:

The resultant streamlines for an infinite swept-back wing are not straight in the plan view but are slightly curved, as shown in Fig. 11.53. This bending results from the superposition of a constant velocity component V_t , parallel to the leading

edge, and a variable component V_n , normal to the leading edge. The normal component V_n is slightly reduced near the leading and trailing edges and increased near the middle of the chord, as seen from the shape of the stream tube in the sectional view of Fig. 11.53. The introduction of a wall, such as a fuselage surface, parallel to the distant flow will thus result in a changed pressure distribution, since the streamlines are thereby constrained to be parallel to the wall.

Another effect of the finite length that tends to reduce the benefit from sweepback comes into play if the Mach angle approaches the sweepback angle. In this case an air particle is undisturbed by the wing until it has practically reached the leading edge, and the flow pattern over the forward part of the wing must differ from that in subsonic motion.

These unfavorable effects of the finite length are not of first importance, however, as is evident from the fact that at supercritical Mach numbers the drag coefficient for a wing swept back at a 45-deg angle may be less than half that of an unswept wing.

The effect of sweep on stability of a wing is also important. Although, at low speed, sweep may have an unfavorable influence, at high speed it is beneficial [12]. The characteristics of control surfaces at high speed are also improved by sweepback.

In summary, it may be said that the problem of transonic and supersonic flight may not be so formidable as might be expected from the purely two-dimensional considerations of previous articles. The study of three-dimensional compressible flow is just beginning, but it has already led to important practical developments [13].

SELECTED BIBLIOGRAPHY

General:

1. EWALD, P. P., TH. PÖSCHL, and L. PRANDTL: "Physics of Solids and Fluids," 2d ed., Blackie & Son, Ltd., Glasgow, 1936.
2. GLAUERT, H.: "The Elements of Aerofoil and Airscrew Theory," Cambridge University Press, London, 1930.
3. GOLDSTEIN, S. (Editor): "Modern Developments in Fluid Dynamics," Vol. I, Oxford University Press, New York, 1938.
4. VON MISES, R.: "Theory of Flight," McGraw-Hill Book Company, Inc., New York, 1945.
5. ROUSE, HUNTER: "Fluid Mechanics for Hydraulic Engineers," McGraw-Hill Book Company, Inc., New York, 1938.
- 5a. Cambridge University Aeronautical Laboratory: "Measurement of Profile Drag by the Pitot-traverse Method," *R. and M.* 1688, Aeronautical Research Committee, London, 1936.

Compressible Flow:

6. EMMONS, H. W.: Shock Waves in Aerodynamics, *J. Aeronaut. Sci.*, vol. 12, no. 2, pp. 188-194, April, 1945.

7. KÁRMÁN, TH. VON: Compressibility Effects in Aerodynamics, *J. Aeronaut. Sci.*, vol. 8, no. 9, pp. 337-356, July, 1941.
8. KRAFT, H., and C. G. DIBBLE: Some Two-dimensional Adiabatic Compressible Flow Patterns, *J. Aeronaut. Sci.*, vol. 11, no. 4, pp. 283-298, October, 1944.
9. TAYLOR, G. I., and J. W. MACCOLL: The Mechanics of Compressible Fluids, in "Aerodynamic Theory," Vol. III (edited by W. F. Durand) Verlag Julius Springer, Berlin, 1935.
10. JACOBS, E. N.: "Preliminary Report on Laminar-flow Airfoils and New Methods Adopted for Airfoil and Boundary-layer Investigation," *NACA Rpt.*, June, 1939.
11. JONES, R. T.: "Wing Plan Forms for High-speed Flight," *NACA Tech. Note* 1033, March, 1946.
12. SOULÉ, H. A.: "Influence of Large Amounts of Wing Sweep on Stability and Control Problems of Aircraft," *NACA Tech. Note* 1088, June, 1946.
13. KÁRMÁN, TH. VON: Supersonic Aerodynamics, *J. Aeronaut. Sci.*, vol. 14, no. 7, pp. 373-402, July, 1947.

CHAPTER XII

HYDRODYNAMIC LUBRICATION

12.1. Introduction. All machinery depends for its useful operation on slippery surfaces between moving parts. The limitation on our ability to maintain slippery surfaces has always constituted an effective bar to materially higher performance. The difficulty of lubricating the hot pistons of high-powered airplane engines now limits their output, and one of the apparent advantages of the combustion gas turbine is the elimination of this restraint.

From long experience with oils and greases the term "oiliness" has come into use to indicate the slippery quality of a lubricant on a smooth surface, although no single physical property of the lubricant to measure oiliness has ever been found. It is obvious that, while maple sirup may resemble a mineral oil in appearance, it certainly does not resemble it in oiliness.

Perfect lubrication presupposes the presence of a fluid completely separating the rubbing parts and substituting fluid friction for solid friction. Perfect lubrication, therefore, becomes a matter of fluid mechanics and is often referred to as hydrodynamic lubrication. Since the solid parts do not touch, there can be no wear, and the viscosity of the fluid determines the friction. It will be shown that no oiliness consideration is required by the theory and that in special cases water or even air may afford perfect lubrication.

Hydrodynamic lubrication cannot occur if the rubbing surfaces are pressed too tightly together, as when a machine has to be started from rest. The bulk of the fluid lubricant is squeezed out in such a case and only an adherent surface film remains. This film may be only a few molecules thick but can still prevent seizure and permit sliding. The adherent film of lubricant is bound to the metal by molecular forces of great intensity and has evidently lost its fluid properties.

Under very severe conditions even the adsorbed film may be burned or scraped off. In such cases the dry friction of the metal surfaces may be avoided by the use of a solid lubricant that shears easily, such as graphite, or a chemically formed coating such as an oxide or sulfide of the metal of one of the rubbing surfaces.

Severe conditions under which perfect lubrication is impossible are classed as conditions of imperfect or boundary lubrication, and the properties of the metal surfaces in relation to the physical and chemical properties of the lubricant become of primary importance.

The limiting case of no lubricant at all implies the occurrence of dry friction and failure of the bearing. Wear, galling, and seizure are associated with dry friction. Whether or not a bearing is easily destroyed by partial or temporary failure of the lubrication has been found to depend on the combination of metals paired in the design.

Boundary lubrication is intimately concerned with the nature of the rubbing surfaces and of the lubricant, while perfect lubrication is concerned primarily with the viscosity of the lubricant. However, as a practical matter, a bearing operates sometimes under conditions of perfect lubrication and at other times under conditions of boundary lubrication. Furthermore, practical bearing surfaces are only technically smooth, clearance and alignment are not exact, the lubricant may contain abrasive dirt, and the lubricant may oxidize and change in character at high temperature. Many practical considerations combine to limit the period of perfect lubrication and to incite failure. As a result of long experience, certain metals have been found suitable for use in bearings, and other substances—fluids, plastics, and solids—have been found suitable for use as lubricants with them.

The use of ball and roller bearings avoids some of the complications of the lubrication art but introduces other difficulties inherent in high-pressure rolling contact. Rollers and balls in effect take the place of a lubricant by separating the rubbing surfaces.

12.2. Historical. The art of lubrication is at least as ancient as the greasing of Egyptian chariot wheels and axles with tallow. The launching ways of shipbuilders were greased with animal fats until very recent times. Lard oil is still used in machine shops as a "cutting" fluid to lubricate the chip coming off the tool point. Sperm oil is still highly prized by clock-makers. The early airplane engines required castor oil as a lubricant, and it was not until 1918 that the American Liberty engine demonstrated that mineral oil could be successfully employed under severe operating conditions. These references to animal and vegetable oils with good oiliness characteristics imply an empirical art in which bearing design evolved slowly with the machinery for which lubrication was essential.

The ideal, or perfect, lubrication by which moving parts are completely separated by a fluid film is a recent concept and is associated exclusively with smooth, accurate parts, continuous motion, and high speeds. In other words, the concept is associated with modern machinery.

The axle of a heavy wagon is rough and loosely fitted; the motion is slow; stopping and starting are frequent. Any lubricating fluid would be squeezed out. The case is obviously one of imperfect lubrication, and a stiff grease or even wet clay could be more effective than an oil. The pressure at the point of the cutting tool of a lathe or at the bit of a drill press is too great to permit a fluid film to separate the cutting tool from the

metal being cut. The early airplane engines already mentioned ran too hot, had inadequate bearings, and consequently suffered from imperfect lubrication. Castor oil, having superior oiliness characteristics, established tolerable boundary lubrication for a short time and helped out a defective design.

The concept of perfect lubrication evolved at about the same time, but independently, in England and Russia. Beauchamp Tower conducted

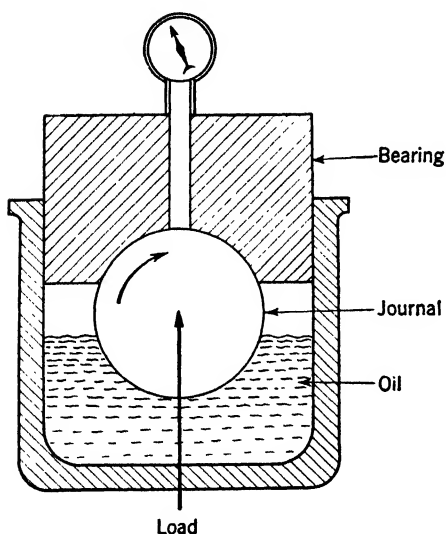


FIG. 12.1. — Schematic diagram of Beauchamp Tower's apparatus for detecting high pressure in a partial journal bearing.

between journal and bearing, reporting his results to the British Institution of Mechanical Engineers in 1885.

Professor Osborne Reynolds of the University of Manchester reported in the next year the results of his analysis of Tower's experiments. He showed that application of the principles of fluid mechanics would account for the pressures observed by Tower. His analysis was formulated as a differential equation requiring as parameters only the viscosity of the lubricant, the speed of rotation, and the dimensions. Reynolds in this paper really established the modern theory of perfect lubrication although its significance was not recognized until much later.

About this same time N. Petroff in Russia was experimenting with bearings lubricated with mineral oil from the newly opened Russian oil fields. A paper in the *St. Petersburg Engineering Journal* for 1883 indicated that Petroff also had the modern concept of perfect lubrication by means of a separating fluid film. He explained how the friction of the bearing could be entirely accounted for by shearing forces in the viscous film of lubricant.

experiments to determine the friction of the journal of a railway-car wheel. Such a journal runs in a partial bearing pressing down from above and is supplied with lubricant by a wick or pad of waste, which wipes against the journal as it turns. Tower obtained erratic results until he ran the journal in an oil bath, so ensuring a copious supply of lubricant (see Fig. 12.1). Then he observed a stream of oil being discharged from an oilhole in the top bearing. The journal and bearing acted as a pump, and attempts to hold a plug in the oil-hole indicated a very high pressure. Tower drilled other holes through the upper bearing and measured the distribution of pressure in the oil

Petroff established fluid shear as the source of frictional resistance to rotation in the form of an equation involving viscosity, speed, and the dimensions. Reynolds proved that the pressures depended on the same parameters. Reynolds's name is recalled in the Reynolds number, the non-dimensional criterion of dynamical similitude in fluid motion. Petroff is remembered by the Petroff equation for the coefficient of friction of a journal bearing.

Reynolds's theory of the journal bearing was subsequently further developed by Sommerfeld in Germany in 1904. His name is preserved in the "Sommerfeld parameter," which will later be shown to control the performance of similar bearings. Michell of Australia and Kingsbury of New Hampshire State College independently extended Reynolds's theory of the pressure-sustaining property of a converging oil film to the design of thrust bearings. A plane bearing surface was divided into separate segments, or shoes, each free to adjust itself to a small angle of inclination to the opposite rubbing surface. Because of the pressure developed in the wedges of oil so formed, metal-to-metal contact was prevented, and a large thrust load could be transmitted. These pivoted-shoe thrust bearings are necessary for large hydroelectric and marine power plants.

The theory of perfect lubrication may be considered to be in a very satisfactory state. Engineers can design bearings with full confidence in their predicted performance under specified conditions. Unfortunately, the same assertion cannot be made for boundary lubrication. Here the phenomena are much more complicated: properties of the oil other than viscosity are involved, as well as the physical and chemical condition of the surfaces.

12.3. Properties of Lubricants. Oils and greases are the most widely used lubricants. While viscosity is the most important single property involved in lubrication, in engineering applications many other properties, both physical and chemical, become important under special conditions. A voluminous literature exists regarding the specification and testing of the various properties of lubricants, but only brief mention of their nature need be made here.

12.4. Viscosity. For a fluid lubricant of Newtonian characteristics shear stress τ is directly proportional to rate of shear, that is,

$$\tau = \mu \frac{\partial u}{\partial y}$$

where μ is the coefficient of viscosity (or simply viscosity), u is relative velocity in the direction parallel to the sliding surfaces, and y is measured across the fluid film. Experiments both with bearings and with flow through capillaries indicate that Newton's law may safely be relied on for bearing design both with fatty and with mineral oils in liquid state.

Furthermore, there is abundant evidence that there is no slip between the fluid and the solid surfaces at the boundary. For extreme cold or extreme pressure, however, oils may solidify and in such condition do not behave as true fluids.

Viscosity can be measured by determining the rate of flow through a capillary tube and using Poiseuille's formula [Eq. (8.16)]. Another method is to measure the force required to rotate a cylinder mounted concentrically within an outer cylindrical shell, the space between being filled with oil. From the measured force and the rate of shear, which is known from the relative velocity and the clearance between the cylinders, viscosity can be calculated.

Common commercial practice in this country expresses the viscosity of an oil in "Saybolt universal seconds," meaning the time taken for a standard volume of liquid to flow out through the short tube of the standard Saybolt instrument. Such a measure of viscosity may be useful in purchasing oil but for engineering purposes has to be converted to absolute viscosity by means of tables.

The poise is the cgs unit of viscosity, named for Poiseuille, and is the viscosity of a fluid maintaining a shearing stress of 1 dyne per sq cm for a rate of shear of 1 cm per sec per cm thickness. The poise is thus equivalent to 1 dyne-sec per sq cm. The centipoise is one-hundredth of the cgs unit. In this country, the usual engineering unit is named after Reynolds; it is called a "reyn" and is equivalent to 1 lb-sec per sq in.

Hersey [7] gives the following conversion table:

VIScosity UNITS

1 poise, or dyne-sec/cm ²	= 1.02 × 10 ⁻² kg-sec/m ²
1 poise, or dyne-sec/cm ²	= 2.09 × 10 ⁻³ lb-sec/ft ²
1 poise, or dyne-sec/cm ²	= 1.45 × 10 ⁻⁵ lb-sec/in. ²
1 poise, or dyne-sec/cm ²	= 2.42 × 10 ⁻⁷ lb-min/in. ²

1 kg-sec/m ²	= 98 poises
1 lb-sec/ft ²	= 479 poises
1 lb-sec/in. ²	= 69,000 poises
1 lb-min/in. ²	= 4,140,000 poises

The viscosity of a gas rises slowly with increasing temperature, about as the four-fifths power of the absolute temperature. The viscosity of the common lubricating oils, like that of most liquids, falls rapidly with rising temperature and may be approximately expressed by the formula

$$\mu = \mu_0 e^{b/(T+\theta)}$$

where T is temperature and b and θ are empirical constants. θ has been found to be nearly constant for most lubricating oils.

The degree to which the viscosity depends on temperature is called the

“viscosity index” (V.I.) of the oil. Oils from Pennsylvania crudes, which show the smallest change with temperature, have been arbitrarily assigned a V.I. of 100, and those from California crudes, which show the greatest change, have a V.I. of zero. This scale has little physical significance, as additives often raise this index above 100. A high V.I. is desirable for machinery that must be started cold and is especially necessary for the working fluid of hydraulic control systems exposed to extreme ranges of temperature.

The dependence of viscosity on pressure is given by the equation

$$\mu = \mu_T e^{cp}$$

where p is the gauge pressure, μ_T is the viscosity at temperature T and atmospheric pressure ($p = 0$), and c is an empirical constant. This increase becomes appreciable at pressures greater than 1,000 lb per sq in. At a sufficiently high pressure the oil solidifies. The pressure at which this occurs for a given oil depends on the temperature. At atmospheric pressure the temperature at which solidification occurs is called the “pour point” of the oil. The effect of both temperature and pressure is more pronounced on the viscosity of mineral than fatty oils, but the fatty oils solidify more readily.

12.5. Density. The density of an oil has no direct influence on its lubricating value, but experience has indicated that, for oils made by similar methods from similar stock, viscosity increases with density. Hence there has grown up a popular classification by density of so-called “heavy” and “light” oils, although it is possible for two oils of the same density to be of substantially different viscosity.

Each industry that uses hydrometers to measure specific gravity generally devises some convenient but arbitrary scale. The petroleum industry has in the past used two so-called “Baumé scales” for liquids lighter than water but standardized in 1921 on the American Petroleum Institute (API) scale, defined by the relation

$$\text{Deg API} = \frac{141.5}{\text{specific gravity at } 60/60 \text{ F}} - 131.5$$

Degrees API are equivalent to a uniform scale of specific volume. Specific gravity is here defined as the ratio of the density of oil at 60 F to the density of water at 60 F as indicated by the symbol 60/60 F.

12.6. Acidity. The chemical test for acidity is of use to the lubrication engineer to detect deterioration of oil or to detect the presence of fatty acids as addition agents. Fatty acids in very small concentrations may be desirable for certain applications to increase oiliness but in general are dangerous in causing corrosion, sludges, and emulsions. At high temperatures the oiliness gain may be lost and several bad effects exag-

gerated. The acidity of a fatty oil will increase with decomposition at high temperature. The standard ASTM test rates acid content by a "neutralization number."

12.7. Oxidation. There is no generally accepted standard for testing the oxidizing characteristics of an oil, and recourse is usually had to testing in the actual machine for which it is intended. Carbon, gum, and varnish deposits are likely to be found in all types of internal-combustion engines where the oil is in contact with air at high temperature.

12.8. Flash Point. Though usually of no effect on lubricating value, the flash point is often cited as a characteristic of an oil. It is the temperature at which a flash appears when a test flame is placed near the surface of oil in an open vessel. It measures the degree to which light petroleum fractions have been removed in refining and should never be less than 300 F.

12.9. Emulsification. Tests of emulsification indicate the time required for an emulsion of oil and water to separate. Emulsions are undesirable for general lubrication as they retain dirt, interfere with circulation, and promote corrosion. However, for metal cutting, emulsions may be of advantage because their water content gives them a relatively large specific heat.

12.10. Foaming. Entrainment of air bubbles, bubbles of gas coming out of solution, and bubbles of water vapor may appear at high temperature and low pressure. Foaming is an especially dangerous phenomenon for airplane engines at high altitudes. The designer of the lubricating system must provide against entrainment of air and for the segregation of foam. Water in the oil tends both to increase the volume of foam and to stabilize the bubbles.

A "foam meter" is an apparatus to convert a sample of oil to foam and to note its rate of collapse. Antifoaming chemicals are frequently added to lubricating oils to cause segregated froth to collapse and submerged bubbles to coalesce. Such chemicals are generally ineffective above 212 F.

12.11. Specific Heat. This property is important in cooling a bearing by means of oil circulating through it. The specific heat of lubricating oil is about 0.45 times that of water.

The specific heat of petroleum oils, given in the following Bureau of Standards table, is calculated from the equation

$$c = \frac{1}{\sqrt{d}} (0.388 + 0.00045T)$$

in which c is the specific heat in Btu per pound per degree Fahrenheit, d is the specific gravity at 60/60 F, and T is temperature in degrees Fahrenheit. This formula does not take into account latent heat of fusion, vaporization, or reaction (cracking).

SPECIFIC HEAT OF PETROLEUM OILS
(Btu/lb deg F)

Temperature, deg F	Deg API at 60 F							
	10	20	30	40	50	60	70	80
	Specific gravity at 60/60 F							
	1.000	0.934	0.876	0.825	0.780	0.739	0.702	0.670
0	0.388	0.401	0.415	0.427	0.439	0.451	0.463	0.474
100	0.433	0.448	0.463	0.477	0.490	0.504	0.517	0.529
200	0.478	0.495	0.511	0.526	0.541	0.556	0.570	0.584
300	0.523	0.541	0.559	0.576	0.592	0.609	0.624	
400	0.568	0.588	0.607	0.625	0.643	0.661		
500	0.613	0.634	0.655	0.675	0.694			
600	0.658	0.681	0.703	0.724				
700	0.703	0.727	0.751					
800	0.748	0.774	0.799					

12.12. Thermal Conductivity. Experimental data on thermal conductivity of petroleum liquids are represented approximately by the following equation:

$$K = \frac{0.813}{d} [1 - 0.0003(T - 32)]$$

in which K is the thermal conductivity in Btu per hour per square foot per degree Fahrenheit per inch, d is the specific gravity of liquid at 60/60 F, and T is temperature in degrees Fahrenheit.

THERMAL CONDUCTIVITY OF PETROLEUM OILS
(Btu in./hr ft² deg F)

Temperature, deg F	Liquids						Solids	
	Deg API at 60 F						Asphalt	Wax
	10	20	30	40	50	60		
	Specific gravity at 60/60 F							
	1.000	0.934	0.876	0.825	0.780	0.739		
0	0.82	0.88	0.94	1.00	1.05	1.11	1.2	1.6
200	0.77	0.83	0.88	0.94	0.99	1.05	For temperature range from 32 F to melting point	
400	0.72	0.77	0.83	0.88	0.93	0.98		
600	0.67	0.72	0.77	0.82				

12.13. Perfect Lubrication. Assume two sliding surfaces separated by a film of fluid lubricant. The motion of the fluid can be considered laminar

because, although the speeds involved may be high, the thickness of the film is very small. The Reynolds number for the system stays well below the critical value. In this discussion we assume the usual boundary condition in fluid mechanics, that the relative velocity of the fluid adjacent to

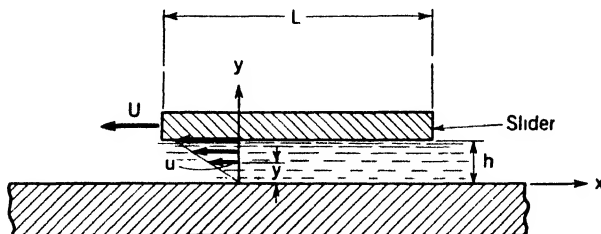


FIG. 12.2.

either solid surface is zero. We also assume the fluid to be incompressible, continuous, and of viscosity defined by the Newtonian relation

$$\tau = \mu \frac{\partial u}{\partial y}$$

Consider first the physical aspects of the problem. Let a flat slider, or slipper, of length L and width B slide on a much larger flat surface upon which is spread a copious supply of fluid lubricant as indicated in Fig. 12.2. If the two surfaces are parallel, the shear stress in the lubricant is

$$\tau = \mu \frac{\partial u}{\partial y} = \mu \frac{U}{h}$$

since experiment shows that the velocity is a linear function of y . Then the absolute value of the shearing force or friction force on the slipper will be

$$F = \tau BL = \mu \frac{U}{h} BL$$

If the two surfaces are parallel, the system will support no transverse load, since it can be shown that the pressure everywhere in the oil film equals atmospheric pressure. If, however, the surfaces are inclined to each other as shown in Fig. 12.3, a pressure is built up in the film by the motion. The upward force due to this pressure balances the normal load applied to the slider.

If the supported load W is to be large, it is necessary that the slider be wide (B/L large) to minimize the pressure-relieving effect of leakage of fluid at the sides. It is also necessary that the minimum thickness of the film be small. It is obvious that, for a given speed and fluid, the upper limit of W will be reached when the slider is pressed down to make h

vanish. Then there will be metal-to-metal contact at high spots of the plate by the heel of the slider, and imperfect lubrication with attendant wear and risk of seizure.

The velocity of the slider should be high, in order to develop sufficient pressure to support the load. In starting from rest a condition of boundary lubrication obtains until the slider reaches some minimum velocity.

It is also reasonable to conclude that high viscosity will impede the

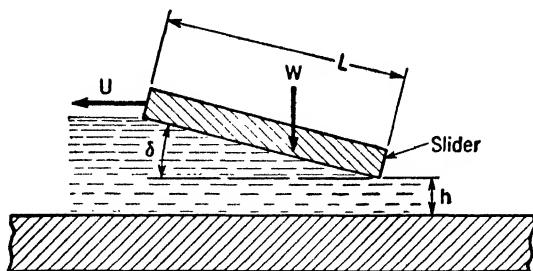


FIG. 12.3.

escape of fluid from beneath the slider and so contribute to the development of pressure in the wedge-shaped film of lubricant. Furthermore, the angle of inclination δ and the length L must play a direct part in the determination of the amount of load that can be supported.

The density of the fluid is known to be of first-order importance in the dynamic lift of airplane wings or turbine blades, but in the case of a slider inclined at a small angle and moving on a wedge-shaped film of oil the inertia effects are negligible. Density, therefore, plays no part in these phenomena.

From this consideration of the physical aspects of the problem we may name the independent variables as L , B , δ , U , μ , and h , with W as a dependent variable whose magnitude is determined by a particular set of values for the six independent quantities. Thus

$$W = \phi_1(U, B, \mu, \delta, L, h)$$

The Π theorem shows that this equation is equivalent to one involving four dimensionless products of the above variables, since there are three primary quantities. These products, or Π 's, can be chosen in any way, provided only that they are independent of one another.

Let

$$\Pi_1 = \frac{\mu UL}{W}$$

$$\Pi_2 = \frac{h}{L}$$

$$\Pi_3 = \delta$$

$$\Pi_4 = \frac{B}{L}$$

Then

$$\frac{\mu UL}{W} = \phi_2 \left(\frac{h}{L}, \delta, \frac{B}{L} \right) \quad (12.1)$$

The maximum load that can be carried safely by a bearing is of paramount importance. Equation (12.1) enables us to discuss this matter in a qualitative way. For given values of δ and B/L , $\mu UL/W$ is determined by the value of h/L . For geometrically plane surfaces, h might theoretically decrease to zero, but in actual practice there is a lower limit to h that is governed by the roughness of the surfaces and the probable size of grit and other adventitious solid particles in the lubricant. If these particles cannot pass out under the trailing edge, they will collect under the rider and score the surfaces.

This minimum value of h/L determines some corresponding minimum value of $\mu UL/W$ that, for a given slider and oil, determines a maximum value of W . This is the load capacity of the lubricated system and is of great practical importance in all design work. Since the minimum value of $\mu UL/W$ is fixed, we see that, if either viscosity or speed is doubled, the load capacity is also doubled.

If δ is increased for given h/L and B/L , the ratio of the entrance cross section to exit cross section for the oil is increased and more oil tends to collect under the slider with a resultant increase in oil pressure and load capacity.

Finally, if the slider is made quite narrow (B/L small) with δ and h/L fixed, more of the lubricant escapes from the sides and the oil pressure is decreased. This reduces the load capacity.

We have so far assumed that δ , the angle of inclination, can be fixed at will. But since δ must be small and consequently difficult to maintain accurately in practice, it is customary to pivot the slider on its support and allow it to take its own inclination. It is shown in Art. 12.16 that a pivoted slider is inherently stable.

Another point of interest in connection with a bearing is the size of the friction force. Let F be the friction force between the fluid and the supporting lower surface, when W is the total transverse load applied across the fluid film. The conventional coefficient of friction is defined as

$$f = \frac{F}{W}$$

The concept of the friction coefficient has been carried over from the study of dry friction between two solid bodies, where it has long been known

that f is essentially independent of the load and speed. Actually in fluid friction f is independent of neither. It has little fundamental significance, but long usage has made it the commonly accepted measure of performance.

We now consider f as the dependent variable and, as before, take L , B , δ , U , μ , and h as independent variables. Then

$$f = \phi_3(L, B, \delta, U, \mu, h)$$

Inspection shows that no dimensionless product can be formed with μ or U in combination with any of the other variables. The Π theorem therefore leads to

$$f = \phi_4\left(\frac{h}{L}, \delta, \frac{B}{L}\right) \quad (12.2)$$

If the flow is assumed to be two dimensional, *i.e.*, if side leakage is neglected, B has no influence on f and Eq. (12.2) becomes

$$f = \phi_4\left(\frac{h}{L}, \delta\right) \quad (12.3)$$

We shall see later what form is taken by the undetermined function ϕ_4 , but the dimensional reasoning shows that the coefficient of friction for a

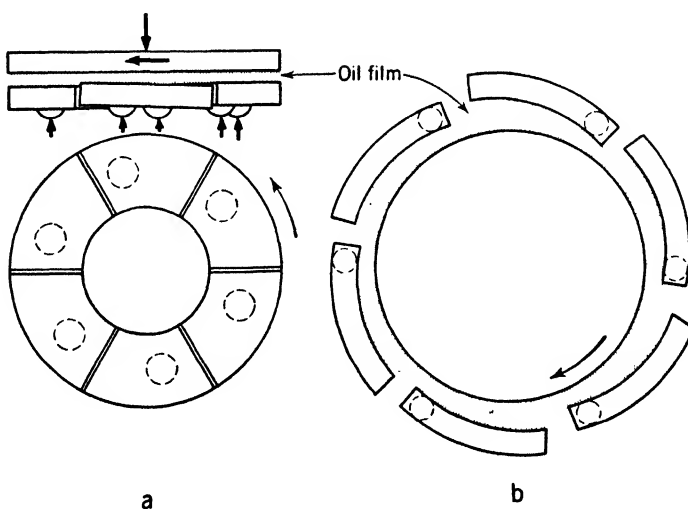


FIG. 12.4. — Schematic drawing of (a) segmental thrust bearing and (b) segmental journal bearing.

family of geometrically similar bearings (h/L , B/L constant) depends only on the inclination of the slider and is independent of speed and the kind of oil used.

A thrust bearing is designed to take an axial load on a rotating shaft. In its primitive form it consists merely of a flat plate pressing against the squared end of the shaft. Since the moving surfaces are parallel, the formation of a wedge of lubricant is impossible and the load capacity is very low. In the bearings of Michell and Kingsbury the thrust plate is cut up into segments each of which is pivoted so that it can tilt as shown in Fig. 12.4*a*. In this way a fluid wedge is formed under each segment as discussed in the case of the plane slider, and the load capacity of the bearing is increased many times. The same principle can also be applied to journal bearings as shown in Fig. 12.4*b* for unidirectional motion. Bearings can be designed so that the pivot shifts as the direction of rotation is changed.

12.14. Reynolds's Pressure Distribution. A clearer appreciation of how pressure is produced in a wedge-shaped film of fluid under the action

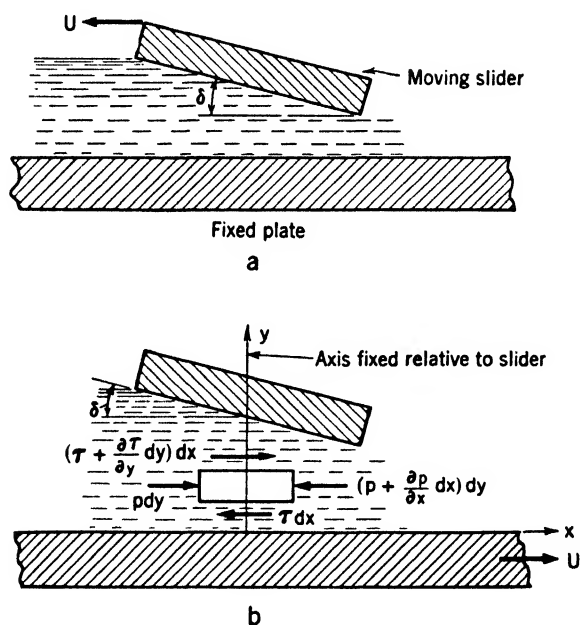


FIG. 12.5.

of viscous shear forces may be gained by a discussion of the fluid mechanics involved.

Figure 12.5 represents a slipper bearing for the two-dimensional case. It is assumed that the angle of inclination δ is small. The lubricant is a viscous incompressible fluid in laminar flow. Figure 12.5*a* shows the slider moving with a steady velocity U toward the left and the base plate fixed. In Fig. 12.5*b* the slider is at rest, and the base plate is moving toward the right with velocity U . Though the slider may actually be the moving

element, it is more convenient for purposes of analysis to consider the motion relative to the slider as shown in Fig. 12.5*b*. Newton's laws can be applied in the usual form to the relative motion because U is a constant velocity.

In Fig. 12.5*b* is shown an element of fluid of dimensions dx , dy and of unit depth normal to the x, y plane. The x forces on the element are as indicated. It can be shown that, since δ is a small angle, the pressure is independent of y and the inertia effects are negligible. Consequently, $\partial p / \partial x = dp / dx$, and the sum of the x forces is zero. The statement of the latter relation is

$$p \, dy - \left(p + \frac{dp}{dx} dx \right) dy = \tau \, dx - \left(\tau + \frac{\partial \tau}{\partial y} dy \right) dx$$

or

$$\frac{dp}{dx} = \frac{\partial \tau}{\partial y} \quad (12.4)$$

Substituting for τ from the Newtonian definition of viscosity

$$\tau = \mu \frac{\partial u}{\partial y} \quad (12.5)$$

we obtain

$$\frac{dp}{dx} = \mu \frac{\partial^2 u}{\partial y^2} \quad (12.6)$$

On integration, Eq. (12.6) becomes

$$\frac{\partial u}{\partial y} = \frac{1}{\mu} \frac{dp}{dx} y + f_1(x) \quad (12.7)$$

and

$$u = \frac{1}{2\mu} \frac{dp}{dx} y^2 + y f_1(x) + f_2(x) \quad (12.8)$$

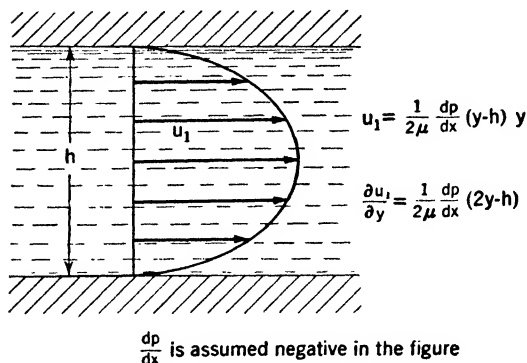
where f_1 and f_2 are functions that can be evaluated from the boundary conditions $u = U$ when $y = 0$ and $u = 0$ when $y = h$. The quantity h is the thickness of the film at x . Then $f_2 = U$, $f_1 = -(h/2\mu)(dp/dx) - (U/h)$, and

$$u = \frac{1}{2\mu} \frac{dp}{dx} (y - h)y + U \frac{(h - y)}{h} \quad (12.9)$$

The velocity at any point y in a cross section of the oil film at x is seen to consist of two terms, and we may therefore consider the velocity u of Eq. (12.9) to be made up of two components, u_1 and u_2 , such that

$$\left. \begin{aligned} u_1 &= \frac{1}{2\mu} \frac{dp}{dx} (y - h)y \\ u_2 &= U \frac{(h - y)}{h} \end{aligned} \right\} \quad (12.9a)$$

The first term u_1 represents a parabolic distribution of velocity as shown in Fig. 12.6a. Note that the velocity u_1 is zero for $y = 0$ or $y = h$,



a

FIG. 12.6a. — Parabolic velocity distribution for laminar pressure flow between fixed parallel planes.

and the flow pattern is that which would occur between stationary parallel surfaces in response to a pressure gradient dp/dx falling along the direction of the x axis.

The second term u_2 represents a linear distribution of velocity such as would occur in a layer of fluid between two parallel surfaces separated by a distance h and moving relative to each other with velocity U as indicated in Fig. 12.6b.

Let Q represent the volume rate of flow per unit width of slider. Then, from continuity, Q is the same at all cross sections. By using Eq. (12.9), we can express Q as follows:

$$Q = \int_0^h u \, dy = \frac{Uh}{2} - \frac{h^3}{12\mu} \frac{dp}{dx} \quad (12.10)$$

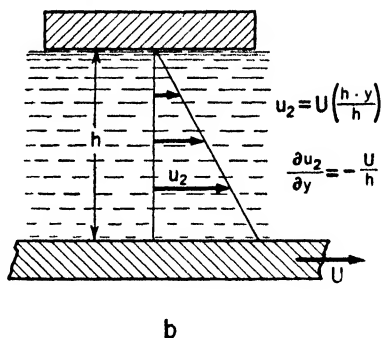


FIG. 12.6b. — Linear velocity distribution for laminar flow at constant pressure between parallel planes, one fixed and one moving.

We thus obtain a form of Reynolds's fundamental equation for the pressure gradient,

$$\frac{dp}{dx} = 6\mu U \left(\frac{1}{h^2} - \frac{2Q}{h^3 U} \right) = 6\mu U \left(\frac{1}{h^2} - \frac{k_1}{h^3} \right) \quad (12.10a)$$

Another form of this result, which is useful in some applications, is obtained by computing dQ/dx from Eq. (12.10a) and setting it equal to zero by virtue of continuity.

$$\frac{d}{dx} \left(\frac{h^3}{\mu} \frac{dp}{dx} \right) = 6 \frac{d}{dx} (Uh) \quad (12.10b)$$

The constant $k_1 = 2Q/U$ of Eq. (12.10a) can be evaluated, after an integration, from the fact that the pressures at entrance and exit are atmospheric. Note that the pressure gradient depends only on the viscosity of the lubricant μ , the speed of the slider U , and the thickness of the film h . This equation was derived without any assumption as to the shape of the surface of the slider, and, as we shall see in Art. 12.22, this equation can be applied to the developed oil film in a journal bearing.

Equation (12.10a) cannot be integrated until h is expressed as a function of x . To accomplish this in the present case the surface of the slider is taken as a plane. Let h_1 represent the film thickness under the toe, or front, of the slider, or

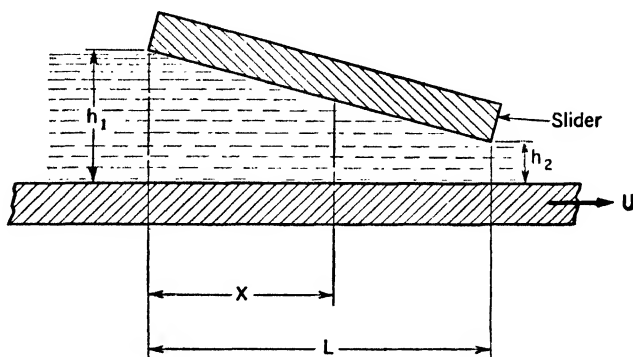


FIG. 12.7.

entrance, and h_2 the film thickness under the heel, or exit, from the slider. Let the slider be of length L in the direction of motion, and let x be measured in the direction of motion as shown in Fig. 12.7.

The film thickness h is obviously a linear function of x , with the inclination of the slider as the determining parameter. Using the method of Norton * we may write

$$h = h_1 - \frac{x}{L} (h_1 - h_2)$$

It is convenient to use, in place of x , a length coefficient $l = x/L$ such that at the toe of the slider $l = 0$ and at the heel $l = 1$. Similarly, a non-dimensional slope coefficient $s = h_1/h_2$ determines the inclination of a slider of given length. Changing the notation to correspond, one finds $h = h_2(s - sl + l)$.

Substitution of the above expression for h and Ll for x in Eq. (12.10a) yields

* See p. 72 of reference 8 of the bibliography at the end of the chapter.

$$\frac{dp}{dl} = \frac{6\mu UL}{h_2^2} \left[\frac{1}{(s - sl + l)^2} - \frac{k_1}{h_2(s - sl + l)^3} \right] \quad (12.11)$$

Integration with respect to l along the length of the slider gives

$$p = \frac{6\mu UL}{h_2^2} \left[\int_0^l \frac{dl}{(s - sl + l)^2} - \frac{k_1}{h_2} \int_0^l \frac{dl}{(s - sl + l)^3} \right]$$

and

$$p = \frac{6\mu UL}{h_2^2} \left[\frac{-1}{(1-s)(s - sl + l)} + \frac{k_1}{2h_2(1-s)(s - sl + l)^2} \right] + k_2$$

The constants of integration, which are determined from the condition

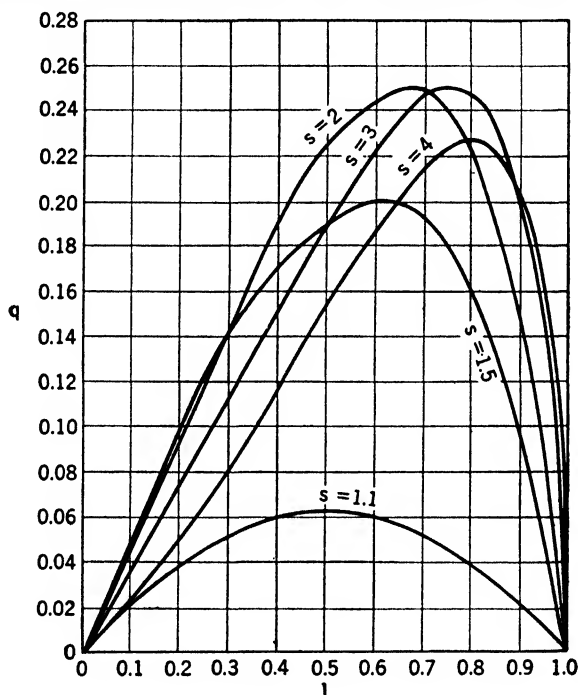


FIG. 12.8. — Theoretical pressure-distribution curves for a slipper bearing. (After Norton, reference 8.)

that $p - p_0 = 0$ (p_0 = atmospheric pressure) when $l = 0$ or 1 , are

$$k_1 = \frac{2s}{s+1} h_2 \quad k_2 = \frac{6\mu UL}{h_2^2} \frac{1}{1-s^2} + p_0$$

Substitution of the constants leads to

$$p - p_0 = \frac{\mu UL}{h_2^2} q \quad (12.12)$$

where

$$q = \frac{6(s-1)(1-l)l}{(s+1)(s-sl+l)^2} \quad (12.13)$$

The quantity $\mu UL/h_2^2$ has the dimensions of pressure, and q is a non-dimensional function called the "pressure function."

It is important to observe that, at the toe and heel of the slipper where $l = 0$ and $l = 1$, the pressure function $q = 0$. The pressure function also becomes zero when $s = 1$, indicating as would be expected that the pressure is atmospheric throughout the film when there is no inclination of the slipper.

It remains to consider how the fluid pressure is distributed in such a manner that a transverse load can be supported. The point of maximum pressure can be found by setting $dp/dx = 0$. With the nondimensional notation used before we find that this point is at

$$l_{\max} = \frac{s}{s+1} \quad (12.13a)$$

and, substituting this in Eq. (12.12),

$$p_{\max} - p_0 = \frac{\mu UL}{h_2^2} \left[\frac{1.5(s-1)}{s(s+1)} \right] \quad (12.14)$$

The distribution of pressure as given by Eq. (12.13) is shown by the computed values of the pressure function q plotted in Fig. 12.8.

12.15. Bearing Load. Any transverse load carried by the slider must be borne by hydrostatic pressure in the fluid film. Since the inclination of the slider is small, the external load can be equated to the total normal force on its surface. For a longitudinal section of unit width the total load will be

$$W = \int_0^L p \, dx = L \int_0^1 p \, dl$$

By using Eq. (12.12) for p and integrating, we find

$$W = \frac{\mu UL^2}{h_2^2} C_w \quad (12.15)$$

where

$$C_w = \frac{6}{(s-1)^2} \left[\ln s - \frac{2(s-1)}{(s+1)} \right] \quad (12.16)$$

Both W and the quantity $\mu UL^2/h_2^2$ have the dimensions of force per unit of width, while C_w is a nondimensional load factor. It is to be noted that for a given bearing the load factor depends entirely on the inclination, and where $s = 1$ no load is supported by hydrostatic pressure.

12.16. Center of Pressure. For a practical bearing it is necessary to support the slider by means of a pivot located somewhat behind the center of pressure, in order that the slider may adjust itself to an inclination appropriate to the given values of W , μ , U , L , h_2 .

Using the notation of Fig. 12.7, let x_1 be the distance of the center of pressure from the toe of the slider. Take moments about the origin, and get $x_1 W = \int_0^L x p \, dx$. Substitution of the value of p from Eq. (12.12) and W from Eq. (12.15), a straightforward manipulation, which need not be detailed here, yields $x_1 = LC_p$, where C_p represents a nondimensional support factor that is found to be a function of slider inclination alone. Calculation of C_p for a series of values of the inclination $s = h_1/h_2$ discloses that the center of pressure lies behind the mid-point of the slider and moves to the rear as the inclination is increased, as indicated in the following table:

$\frac{h_1}{h_2}$	1	2	3	4	5	Ratio of film thickness at entrance to thickness at exit
C_p	0.50	0.56	0.61	0.64	0.66	Center of pressure, % of slider length from toe

It is fortunate that the center of pressure shifts to the rear as the inclination is increased since this makes for stability. For example, suppose the pivot placed at the 56 per cent point to balance the estimated load with $h_1/h_2 = 2$. If the slider turned to a greater inclination, say to $h_1/h_2 = 3$, the center of pressure would move back to the 61 per cent point, giving a moment about the pivot tending to reduce the inclination. Correspondingly, any decrease of inclination from the equilibrium position for $h_1/h_2 = 2$ would cause the center of pressure to move ahead of the pivot and to restore the designed inclination.

12.17. Frictional Force. The force necessary to move the plate along under the slider is equal to the friction of the fluid on its wetted surface, or

$$F = \int_0^L \tau_0 \, dx \quad (12.17)$$

where F is the frictional force on the plate per unit width and τ_0 is the shear stress at the plate surface.

Combination of Eqs. (12.5) and (12.9) gives the expression for τ at any point in the fluid film. On the surface of the plate $y = 0$, $\tau = \tau_0$, and

$$\tau_0 = -\mu \left(\frac{h}{2\mu} \frac{dp}{dx} + \frac{U}{h} \right)$$

But from Eq. (12.10a) an expression for dp/dx is available. Substituting for τ_0 in Eq. (12.17) and integrating, we obtain the result in the form

$$F = \frac{\mu UL}{h_2} C_f \quad (12.18)$$

where C_f is a nondimensional friction factor that is a function of the inclination. As might be expected, the friction factor becomes somewhat smaller as the inclination increases, dropping from about 0.85 for $h_1/h_2 = 1.5$ to 0.62 for $h_1/h_2 = 5.0$.

The average coefficient of friction for the bearing as a whole can be found from Eqs. (12.15) and (12.18).

$$f = \frac{F}{W} = \frac{(\mu UL/h_2)C_f}{(\mu UL^2/h_2^2)C_w} = \frac{h_2}{L} \frac{C_f}{C_w} \quad (12.19)$$

Equation (12.19) is to be compared with Eq. (12.3), which was based on dimensional analysis. Since h_2 in Eq. (12.19) is identical with h in Eq. (12.3) and C_f/C_w is a function of $s = 1 + \delta(L/h_2)$, the two equations are in complete agreement. Dimensional reasoning alone cannot, of course, yield as complete information as the analysis leading to Eq. (12.19).

Note that the coefficient of friction is independent of the viscosity of the lubricant. This results from the fact that the transverse force W is caused by hydrostatic pressure that in turn is caused by viscous shear. [Recall that in Eq. (12.4) shearing forces were balanced against pressure forces in the horizontal plane. Since hydrostatic pressure is independent of direction, the same pressures cause an upward force on the slider to support the load W .] Hence both W and F are the direct result of fluid shear stress, owing to viscosity. Their ratio is therefore independent of the

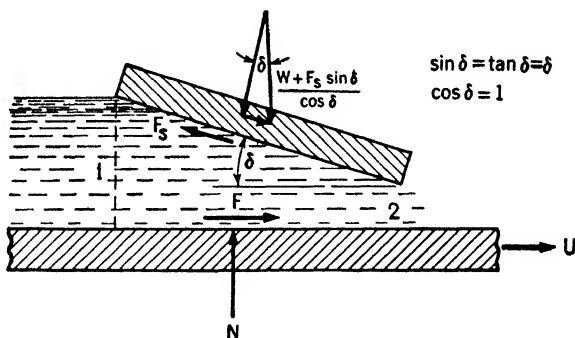


FIG. 12.9

lubricant, provided that it is a true fluid and provided that h_2 has a finite value. Obviously, if h_2 becomes zero, the load is taken by contact at the heel of the slider and the theory is invalid.

The friction force F exerted by the oil on the lower plate is equal to the force of the oil on the slider. This is true because the acceleration of the oil film is negligible. The forces acting on it are therefore in equilibrium. From Fig. 12.9

$$F_s = W\delta + F$$

$$N = W - F_s\delta = W(1 - \delta^2) - \delta F = W$$

It is permissible to let $N = W$ since $\delta^2 \ll 1$ and, from Eq. (12.19), F is on the order of $W\delta$.

It is apparent from the foregoing that the work done per second on unit width of oil film in moving either the slider or the plate at a constant speed U is equal to FU .

12.18. Energy Balance. Apply the energy equation [Eq. (5.8)] to the oil film under the slider of Fig. 12.9, assuming a steady two-dimensional flow, and neglecting heat transfer. Inertia effects and gravity are ignored, as in the rest of this chapter. Noting that the shear work per second done by the oil is $-FUB$, where B is the width of the slider, and recalling the definition of enthalpy $i = (p/\rho) + u$, we find from Eq. (5.8) that

$$FUB = (i_2 - i_1)\rho Q = \rho c\Delta TQ \quad (12.20)$$

where c is the specific heat of the oil, ΔT is its temperature rise as it passes under the slider, and Q is the volume rate of flow. Substitution of F from Eq. (12.18) yields

$$\rho c\Delta TQ = \frac{\mu U^2 LB}{h_2} C_f \quad (12.21)$$

Equations (12.9a) show that the velocity distribution across the oil film is linear at the section where $dp/dx = 0$. At this section the average velocity will be $U/2$, and consequently $Q = UBh_0/2$ where h_0 is the film thickness. Since, from Eq. (12.13a), $l_{\max} = s/(1+s)$, $h_0 = h_2(s - sl_{\max} + l_{\max}) = 2h_2s/(1+s)$. Substitution of this value of h_0 in the expression for Q gives $Q = UBh_2s/(1+s)$. From Eq. (12.21) the temperature rise is found to be

$$\Delta T = \frac{\mu UL}{\rho ch_2^2} \frac{s+1}{s} C_f \quad (12.22)$$

The quantity h_2 is, of course, extremely difficult to measure and is generally unknown. Consequently, Eq. (12.22) is of little practical interest. However, h_2 can be eliminated by substituting its value from Eq. (12.15), and we obtain in place of Eq. (12.22)

$$\Delta T = \frac{W}{L} \frac{1}{\rho c} \frac{s+1}{s} \frac{C_f}{C_w} \quad (12.23)$$

In specialized texts on lubrication,* graphs are given for values of the several nondimensional coefficients C_w , C_f and others appearing in the equations for the principal operating characteristics. These nondimen-

* See p. 76 of reference 8.

sional coefficients are each functions of the inclination $s = h_2/h_1$. The designer wishes to make the load capacity as large as possible but without letting h_2 become too small for perfect lubrication and without excessive temperature rise. Fundamentally, the designer's problem involves seven quantities of which six must be fixed to determine the seventh.

The above analysis assumed that the viscosity was constant throughout the whole extent of the film. Since the rate of shear will vary with the film thickness, the work done in shearing the oil film will vary, and hence the temperature. As a result, the viscosity will vary. Christopherson [1] has investigated this problem and solved the resulting equations, which are somewhat more complicated than those given above. Comparison of the constant-viscosity theory and of the more exact theory shows that the discrepancies are small, less than 5 per cent. It is therefore justifiable to use the constant-viscosity theory for ordinary calculations. Constant viscosity will be assumed in the remainder of this chapter.

12.19. Cylindrical or Journal Bearings. This common type of bearing is designed to take the radial load on a rotating shaft or journal. We define the following quantities (see Fig. 12.10):

D = diameter of shaft or bearing

L = axial length of bearing

C = diametral clearance, or difference in diameters of bearing and shaft

N = speed of journal in revolutions per unit time

P = load per unit projected area = W/LD

μ = viscosity of the lubricant

Q = volume rate of lubricant flow through the bearing if it has forced lubrication

By dimensional reasoning any dimensionless ratio involving the following dependent operating variables,

h_0 = minimum film thickness

e = eccentricity, or separation of the centers of shaft and bearing
= $(C/2) - h_0$

ϕ = aspect of the journal, or the angle between the line of centers and the line of the applied load

F = friction force on journal or bearing

can be expressed in terms of four Π functions.

$$\Pi_1 = \frac{\mu N}{P}$$

$$\Pi_2 = \frac{D}{C}$$

$$\Pi_3 = \frac{L}{D}$$

$$\Pi_4 = \frac{\mu Q}{C^3 P}$$

Specifically, we define

$$\eta = \frac{e}{C/2} = 1 - \frac{h_0}{C/2} = \text{eccentricity ratio}$$

$$f = \frac{F}{W} = \frac{F}{PLD} = \text{friction coefficient}$$

These quantities, together with ϕ , completely specify the system for any given conditions of operation.

12.20. Petroff Equation. If the shaft is unloaded and the speed is high, it runs concentrically, as shown in Fig. 12.10. If the shaft and bearing are absolutely concentric, the film thickness is everywhere the same and as in the case of the plane slider the bearing supports no load. However, even

in this case there is a finite friction force that can be calculated if the space between shaft and bearing is assumed to be completely filled with lubricant.

Since $C/2$, the average film thickness, is always very much less than D , the curvature in the path of flow of the lubricant can be neglected and, for laminar flow, the average shearing stress will be $\tau = \mu(V/h) = F/A$, where F is the total tangential force on the bearing of wetted area A . But V , the linear speed of the journal surface, is equal to πDN , $h = C/2$, and $A = \pi DL$.

Therefore, the friction force ex-

erted by the journal on the bearing will be $F = \tau A = \mu[\pi DN/(C/2)]\pi DL$. Hence the friction coefficient is given by the relation

$$f = \frac{F}{W} = \frac{F}{PDL} = 2\pi^2 \frac{\mu N}{P} \frac{D}{C} \quad (12.24)$$

This is generally known as Petroff's equation. Experiments verify this relation with great precision. If the shaft is *very lightly loaded* and running at high speed, it will remain *almost* concentric in its bearing so that this equation still applies.

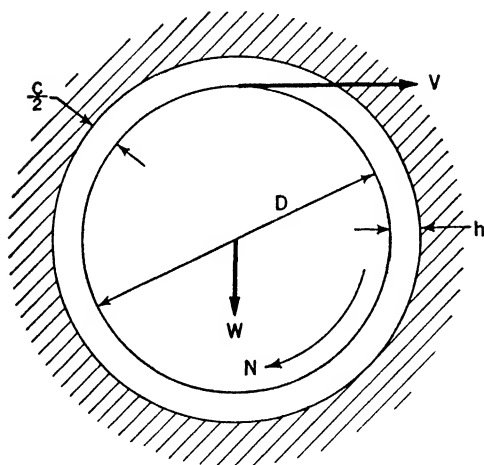


FIG. 12.10. — Definition sketch of a concentric journal bearing.

In the deduction of this equation, end effects (that is, dependence on L/D) have been ignored. However, the value of f depends on the dimensionless parameters $\mu N/P$ and D/C , identical with Π_1 and Π_2 of Art. 12.19. Petroff's formula thus agrees, as far as it goes, with the more general results of dimensional reasoning. Petroff's equation does not allow for the effect of forced lubrication as indicated by the term $\mu Q/C^3P$.

Equation (12.24) is valuable, however, aside from its historical interest in embodying the concept of hydrodynamic lubrication, because it supplies a simple means of estimating journal friction. Furthermore, the running clearance C is very difficult to measure after a bearing is assembled, and it is often better to determine the friction coefficient from a torque measurement and to compute the clearance by Petroff's equation.

12.21. Loaded Journal Bearings. If the journal and bearing are not concentric, there is a converging wedge through one-half of the oil space as shown in Fig. 12.11 and we have the necessary physical condition for building up pressure in the oil film and ability to support a transverse load. The analysis of the problem will follow exactly that of the plane slider, but the steps will only be indicated, for they are mathematically involved. We begin by recalling Eq. (12.10a).

$$\frac{dp}{dx} = 6\mu U \left(\frac{1}{h^2} - \frac{k_1}{h^3} \right)$$

giving the derivative of the pressure in the oil film at every point. We recall that this equation was derived without any assumption as to the shape of the slider. As in the case of the plane slider, in order to integrate this equation we must express the film thickness h in terms of its position x . We neglect the curvature in the direction of motion and hence develop the oil film so that the surface of the bearing is taken as plane and use its thickness as h in the above equations. Bearing in mind that both h and C are much smaller than D , we see from Fig. 12.11 that

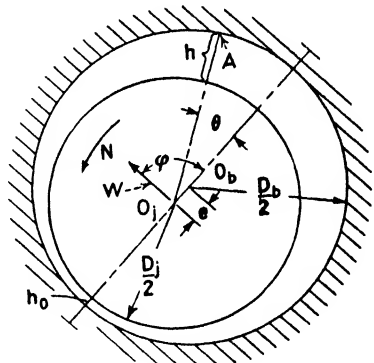


FIG. 12.11. — Definition sketch of an eccentric journal bearing.

$$O_j A = h + \frac{1}{2} D_j = \frac{1}{2} D_b + e \cos \theta = \frac{1}{2} D_j + \frac{C}{2} + e \cos \theta$$

whence $h = (C/2) + e \cos \theta$. Here θ is measured counterclockwise from the point of maximum film thickness. Also $x = \frac{1}{2} D d\theta$; whence $dx = \frac{1}{2} D d\theta$.

Substituting in Eq. (12.10a), noting that $U = \pi D n$, and integrating, we find that

$$p = p_0 + 12\pi \left(\frac{D}{C} \right)^2 \mu N \frac{\eta(2 + \eta \cos \theta) \sin \theta}{(2 + \eta^2)(1 + \eta \cos \theta)^2} \quad (12.25)$$

Here p_0 is the pressure at the point $\theta = 0$, and the constant k_1 has been determined by the condition that the pressure returns to its original value when θ has increased by 2π . This pressure distribution is plotted in Fig. 12.12, and it is seen that the pressure rise $p - p_0$ increases from zero at the point of maximum film thickness to a maximum on the converging side and then falls to zero at the point of closest approach, as in the case of the

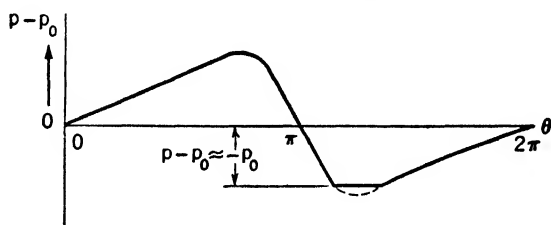


FIG. 12.12. — Theoretical pressure distribution for a two-dimensional journal bearing.

plane slider. On the diverging side the reverse is true, and the differential pressure falls to negative values. If a liquid could support a tension under the conditions existent in a bearing, the pressure would follow the dotted curve, which is symmetrical with the portion on the converging side. Actually, however, the oil film breaks near zero absolute pressure as shown by the full line. Cavitation and foaming can occur under unfavorable conditions, with consequent failure to maintain continuity of liquid in the clearance space.

This suggests a cautious approach to the question of the location of oilholes and oil grooving in a bearing. Since the maximum pressure in the oil film may be some thousands of pounds per square inch it is obviously unwise to put an oilhole for the purpose of introducing oil in the high-pressure region. The oil will probably be forced out rather than in, and the maximum pressure in the film decreased. Oilholes should preferably be located on the low-pressure, or suction, side of the bearing. Oil grooves are often used to lead fresh oil from the inlet to different parts of the bearing and are also expected to collect grit, which might otherwise lodge at the line of minimum running clearance and score the surfaces. The introduction of any oil grooves whatever should in general be viewed with suspicion. The designer should avoid connecting by grooves regions of high pressure with ones of low pressure. The oil may be drained from the high-pressure area with a resultant drop in load capacity.

To obtain the total load that can be carried by the bearing when it has an eccentricity ratio η we must integrate the pressure over the whole oil film. We shall assume that p_0 is maintained so high that the oil film is continuous and follows the dotted line in Fig. 12.12. Let us resolve the force $W = PDL$ that is exerted by the load on the journal into components parallel and normal to the line of centers. These must equal the respective

components of the film pressure integrated all around the journal. The equation for the parallel component is

$$PDL \cos \phi = \int_0^{2\pi} Lp \cos \theta \frac{D}{2} d\theta$$

where ϕ is the angle between the load direction and the line of centers, as shown in Fig. 12.11. On substituting for p from Eq. (12.25) and integrating one finds that the integral is zero. Hence $\cos \phi = 0$ or $\phi = 90$ deg. This means that the resultant force due to the film pressure is always at right angles to the line of centers; in other words, the journal so positions itself in the bearing that the line of centers is always at right angles to the direction of the load. This holds true even when the effect of side leakage is taken into account. On the other hand, it does not hold if the oil film is incomplete, if oil is fed into the bearing through an oilhole in such a manner that its pressure either partly supports or depresses the journal, or if there is any metal-to-metal contact.

To determine on which side of the load line the center of the journal will lie one should bear in mind that it is the oil pressure in the *converging* wedge which supports the load and that it is the sense of rotation of the shaft which determines the converging side. The position of the journal is then as shown in Fig. 12.11. It is to be noted that this position is opposite to that which would obtain if the bearing were dry and the journal were mechanically rolling on it.

One obtains the expression for the load component normal to the line of centers (resultant load) by substituting for p in the equation

$$PDL \sin \phi = \int_0^{2\pi} Lp \sin \theta \frac{D}{2} d\theta$$

and integrating, remembering that $\phi = 90$ deg,

$$PDL = 12\pi^2 DL \left(\frac{D}{C}\right)^2 \mu N \frac{\eta}{(2 + \eta^2)(1 - \eta^2)^{1/2}}$$

or, rearranging,

$$\frac{\eta}{(2 + \eta^2)(1 - \eta^2)^{1/2}} = \frac{1}{12\pi^2 (D/C)^2 (\mu N/P)} = \frac{1}{12\pi^2 S} \quad (12.26)$$

The dimensionless quantity S is often called the "Sommerfeld variable" after the eminent German mathematical physicist who first derived the above equation. This equation gives the journal position, or eccentricity, in terms of the operating conditions of the system and checks our dimensional result. Both η and its complement $h_0/(C/2)$ are plotted in Fig. 12.13.

It is seen that when the shaft is practically concentric, that is, when $h_0/(C/2) \approx 1$ or $\eta \approx 0$, S is very large and only a small load can be sup-

ported. When $h_0/(C/2)$ decreases, or η approaches unity, S decreases, finally becoming zero theoretically when the shaft and bearing touch. Before this point is reached, however, a limit to practical operation is set by other factors, which are difficult to take account of mathematically. Even at eccentricity ratios appreciably less than unity, metal-to-metal contact may occur owing to roughness of the surfaces, vibration, shaft deflection under load, misalignment, dirt in the oil, etc. Metal-to-metal

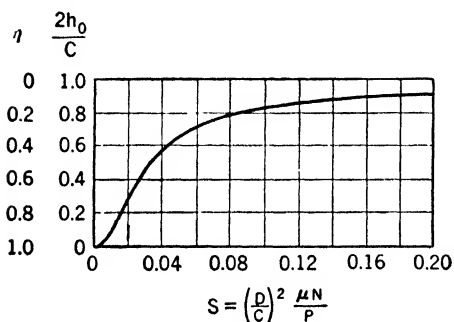


FIG. 12.13. — Eccentricity ratio η and minimum relative film thickness $2h_0/C$ versus Sommerfeld variable S for a two-dimensional journal bearing.

contact, if prolonged, will cause excessive heating and initiate a train of events leading ultimately to failure of the bearing. The eccentricity ratio at which this begins to occur therefore sets a safe limit to practical operation, which according to Fig. 12.13 sets a lower limit to S . (As we shall see below, the side leakage is also a factor in determining this value of S .) The maximum safe value of the eccentricity ratio varies greatly for different bearing assemblies and is determined largely from experience. Under the worst conditions it may be as low as 0.5; under good conditions it may be as high as 0.9.

12.22. Friction Loss in a Loaded Journal Bearing. To obtain the friction loss in a journal bearing running eccentrically we combine Eqs. (12.5) and (12.9) to obtain the shearing stress at any point in an oil film between two solid surfaces in relative motion.

$$\tau = -\frac{\mu U}{h} + \left(y - \frac{h}{2}\right) \frac{dp}{dx}$$

Substituting for dp/dx from Eq. (12.10a) and expressing h and x in terms of θ , we can integrate the shearing stress over the whole surface of the journal ($y = 0$) to obtain the friction force and hence the friction coefficient on the journal, or

$$f_i = \frac{F}{W} = \frac{1}{PDL} \int_0^{2\pi} L \tau_i \frac{D}{2} d\theta$$

When this integration is carried out and S is eliminated from the result by using Eq. (12.26), we obtain

$$\frac{D}{C} f_i = \frac{1 + 2\eta^2}{3\eta} \quad (12.27)$$

Performing the same operations at the surface of the bearing ($y = h$), we obtain for the friction coefficient on the bearing

$$\frac{D}{C} f_b = \frac{1 - \eta^2}{3\eta} \quad (12.27a)$$

Note that, as in the case of the plane slider, f depends only on the position η of the journal. Also note that the two coefficients are different. This is because the oil pressure in the converging wedge exerts a certain tangential component of force, which must be balanced. This force is responsible for the shaft's eccentric position. η can be eliminated from these expressions and Eq. (12.26) to give the friction coefficients as a function of S . The resulting equations are plotted in Fig. 12.14. The dotted line is the Petroff equation [Eq. (12.24)], which is approached by both the friction coefficients for large values of S .

12.23. Effect of Side Leakage.

In the above analysis we neglected the effect of leakage of oil from the ends of the bearing, or rather we assumed the bearing to be so long compared to its diameter that this effect was not appreciable. In most bearings, however, it is appreciable, the pressure varying in the axial direction

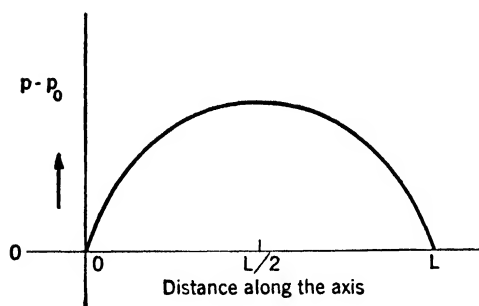


FIG. 12.15. — Diagrammatic sketch of axial pressure distribution in a three-dimensional journal bearing.

flow in the transverse, axial, or z direction, then Eq. (12.10b) becomes

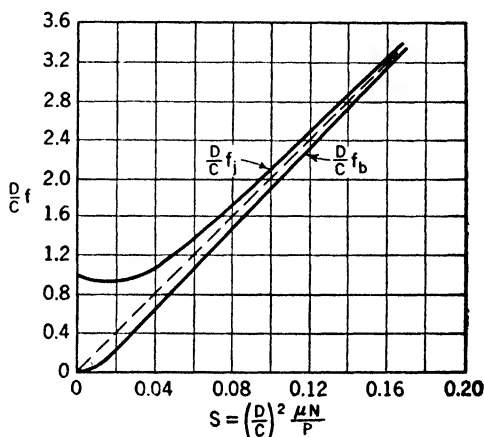


FIG. 12.14. — Friction coefficient for a journal f_j and for a bearing f_b versus Sommerfeld variable S for a two-dimensional journal bearing.

somewhat as shown in Fig. 12.15. Obviously, if this is taken into account, the load capacity is reduced since the contribution of the oil pressure near the ends is reduced; hence the same eccentricity ratio is reached at a larger value of S . The derivation in Art. 12.14 of Reynolds's equation for the pressure distribution in the oil film assumed flow only in the x direction. If in addition there is

$$\frac{\partial}{\partial x} \left(\frac{h^3}{\mu} \frac{\partial p}{\partial x} \right) + \frac{\partial}{\partial z} \left(\frac{h^3}{\mu} \frac{\partial p}{\partial z} \right) = 6 \frac{\partial}{\partial x} (hU) + 6 \frac{\partial}{\partial z} (hW)$$

where W is the velocity of the moving surface in the z direction, which in this case is zero.*

This problem is complicated mathematically but it has been attacked by Kingsbury [2] using an electrical analogy and by Muskat and Morgan [3] for a limited range of η using a method of successive approximations. The results are conveniently expressed as factors by which the value of S for the two-dimensional bearing, denoted by S_∞ , must be multiplied to give the value of S for the bearing of finite length having the same eccentricity ratio. In the table below, this factor in the form of S_∞/S is given for $\eta = 0.6$ for a number of length-diameter ratios. Obviously, $S_\infty/S = P/P_\infty$, or the relative load capacity.

$\frac{L}{D}$	$\frac{S_\infty}{S}$
0.2	0.025
0.4	0.075
0.5	0.115
0.8	0.24
1.0	0.31
1.6	0.50
2.0	0.59
3.2	0.73
4.0	0.78

While these factors vary with η , the dependence is not extreme and they can be used for the whole range of safe limiting values of η generally employed in bearings.

12.24. Journal Bearings with Dynamic Loading. In Arts. 12.19 to 12.23 we have investigated the steady-state solution of the journal bearing, assuming a constant load in a fixed direction. In a great many important practical cases, however, notably in all reciprocating engines, the load is constant neither in magnitude nor in direction. In such cases there is in addition to the pressure built up in the oil film due to the relative tangential motion of the two surfaces an additional pressure in the film produced by the relative motion of the surfaces toward and away from each other. This is the type of pressure normally developed in hydraulic recoil mechanisms and dashpots and responsible for the action of all hydraulic damping forces. Reynolds's equation [Eq. (12.10b)] must therefore be rewritten to take account of fluid velocities in the y direction,

$$\frac{\partial}{\partial x} \left(\frac{h^3}{\mu} \frac{dp}{dx} - 6hU \right) = 12V \quad (12.28)$$

where V is the velocity of any point x, h on the moving surface normal to the plane of the two surfaces. Now since the load will in general be varying

* For the derivation of this equation see any standard text on fluid mechanics, such as H. Lamb, "Hydrodynamics," 6th ed., Chap. XI, Cambridge University Press, London, 1932.

in both magnitude and direction, we can no longer assume the position of the journal center fixed with respect to that of the bearing. Hence U will no longer equal simply πDN , but both U and V will have components of motion due to the component velocities of the journal center, $(C/2)(d\eta/dt)$ and $(C/2)\eta(d\phi/dt)$. These can be evaluated; and, repeating the identical steps as for the case of a constant load, we finally arrive at expressions for the two components of the load, parallel to and normal to the line of centers. These may be written, respectively,

$$\left. \begin{aligned} \frac{1}{(1 - \eta^2)^{3/2}} \frac{1}{2\pi N_j} \frac{d\eta}{dt} &= \frac{1}{12\pi^2 S} \cos \phi \\ \frac{\eta}{(2 + \eta^2)(1 - \eta^2)^{1/2}} \left[1 - \frac{2}{2\pi N_j} \frac{d}{dt} (\phi + \alpha) \right] &= \frac{1}{12\pi^2 S} \sin \phi \end{aligned} \right\} \quad (12.29)$$

Here all the quantities are as previously defined; t is the time, and α is the instantaneous angle between the load line and some reference direction fixed with respect to bearing (see Fig. 12.16). In general, both α and S will be functions of the time depending on how the load varies. Note that the line of centers is now no longer in general normal to the load line.

It is interesting to note that even here the running position of the journal still depends on the operating variables of the system as combined in the Sommerfeld variable S , with the exception of the rotational speed of the journal N_j , which appears in addition but always in combination with the time and which would in theory at least disappear on performing the integration with respect to time and substitution of the limits. Furthermore, although we spoke of the varying load as the reason for this analysis, it was nowhere explicitly assumed and Eqs. (12.29) require only that S be a function of time.

Hence cases where the speed or the viscosity varies with time can also be solved by use of these equations. To perform the last integration of Eqs. (12.29) the dependence of S and α on the time must be known. For most cases of practical interest it is not possible to carry out the integration, and resort must be had to numerical methods. However, some quali-

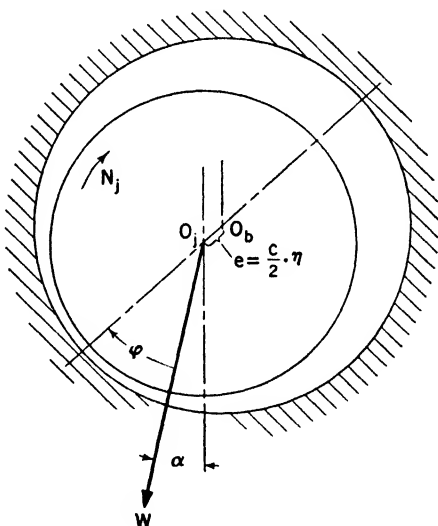


FIG. 12.16. — Definition sketch of a journal bearing with dynamic load.

tative discussion of certain of these cases is worth while. (This discussion follows in part that given by Swift [4].)

In the case of a steady state under constant load, if we take the two time derivatives to be zero, the equations reduce to the Sommerfeld equation [Eq. (12.26)].

In the case of a constant load revolving at constant speed (N_f) the equations reduce to the single one

$$\frac{\eta}{(2 + \eta^2)(1 - \eta^2)^{1/2}} \left(1 - 2 \frac{N_f}{N_j} \right) = \frac{1}{12\pi^2 S} \quad (12.30)$$

This equation is similar in form to that of Sommerfeld. If $N_f < \frac{1}{2}N_j$, the point of minimum film thickness will lie 90 deg ahead of the load line, as in the static case, but the bearing will have less load capacity (that is, a larger value of η for a given value of S) than in the static case. If $N_f = \frac{1}{2}N_j$, the bearing will support no load, which explains the phenomenon of oil whirl. If $N_f > \frac{1}{2}N_j$, the point of minimum film thickness lies 90 deg behind the load line. In particular, if $N_f = N_j$, the bearing has the same load capacity as in the static case. This is reasonable since the physical situation is the same as if the shaft were fixed and the bearing were rotating in the opposite direction. If $N_f > N_j$ or is in the opposite direction to N_j , the load capacity can become arbitrarily large as the magnitude of N_f increases.

The term $d\eta/dt$ represents the load capacity arising from a radial motion of the journal in the bearing sometimes called a "squeeze film." There will also in general be a tangential motion of the journal center, described by the term in $d\phi/dt$. If this is in the same direction as the rotation of the journal, as it generally is, it may decrease the load capacity arising from the rotation ("wedge film") alone. It is thus not generally true that dynamic loads, producing motion of the journal center in the bearing, will necessarily increase the load capacity over the static case. In fact under certain types of loading there will be a net decrease in load capacity.

For the general solution of the problem of a constant load, including the transient condition when the load is first applied, dt can be eliminated from the two original equations to yield a single differential equation in η and ϕ , which can be integrated to give

$$\sin \phi = \frac{12\pi^2 S}{5\eta(1 - \eta^2)^{1/2}} + \frac{c(1 - \eta^2)^{3/4}}{\eta} \quad (12.31)$$

where the constant c depends on the initial conditions, *i.e.*, the position of the journal when the load is first applied. This equation, together with the two original ones, shows that, even under a constant load, periodic motion of the journal center takes place. Its path is a closed orbit, surrounding the equilibrium position as given by the Sommerfeld equation. Thus during

part of its orbit the journal is nearer the bearing wall than if it were stationary in the equilibrium position. The physical existence of these orbits has not been established. If they do not exist in practice, then they must be damped out by some force, such as solid friction, not taken account of in this analysis.

A general analytical solution of these equations for any type of dynamic loading has not been possible to date, but numerical integration has been carried out for the case of a simple reciprocating load

$$P = P_0 \sin 2\pi N_f t$$

where N_f is the frequency of the loading and P_0 is its maximum value. Under this type of loading the journal center moves in a path resembling

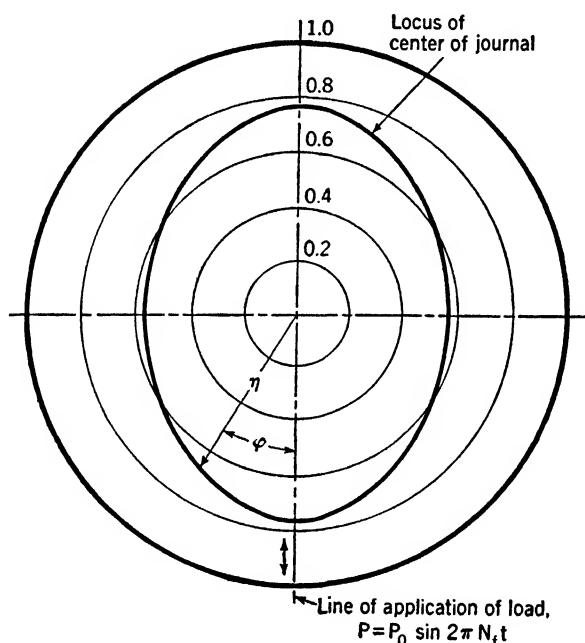


FIG. 12.17. — Eccentricity ratio η versus line-of-centers angle ϕ for a journal bearing with a reciprocating load.

an ellipse, in the same direction as the rotation of the journal as shown in Fig. 12.17. The maximum eccentricity in this path is taken to determine the load capacity. Here again, as in the case of the constantly rotating load, if $N_f < \frac{1}{2}N_j$, the maximum eccentricity is greater and the load capacity is correspondingly less than in the static case. In this instance the minor axis of the path is parallel to the line of action of the reciprocating load. If $N_f = \frac{1}{2}N_j$, there is evidence, although it has not been proved analytically, that the bearing will support no load at all. (This is of

interest since four-cycle internal-combustion engines all have a large half-period load component.) If $N_f = N_j$, which is the case of greatest practical importance, there is a definite increase in load capacity over the static case. In this case the major axis of the path is parallel to the line of action of the load, and the same maximum eccentricity is achieved with a 74 per cent greater load than under a static condition, for which bearings are conventionally designed. If $N_f > N_j$, there are even larger increases in load capacity. This 74 per cent increase in load, while quite appreciable, is smaller than that sometimes observed in bearings loaded in this manner. This may be due to the fact that the maximum eccentricity, corresponding to this load, is reached only twice every cycle. At other times the eccentricity is considerably less, so that a better measure of the load capacity might be obtained from the average eccentricity over the cycle, which would give a greater estimated load capacity. Still another explanation might be the fact that in actual unidirectionally loaded bearings the oil film is seldom complete on the unloaded side, while in the present case it may be more nearly so owing to the pumping action of the journal motion.

Finally, in the limiting case of a reciprocating load with no journal rotation, the first of the two original equations vanishes; and if ϕ is taken as 0 deg, the second one integrates to

$$\frac{\eta}{(1 - \eta^2)^{1/2}} = \frac{1}{12\pi^2 S'_0} \quad (12.32)$$

where $S'_0 = (D/C)^2(\mu N_f/P_0)$ and $P = P_0 \sin 2\pi N_f t$. Comparison of this with the Sommerfeld equation,

$$\frac{\eta}{(2 + \eta^2)(1 - \eta^2)^{1/2}} = \frac{1}{12\pi^2 S}$$

shows almost a threefold increase in the load capacity if N_f replaces N_j .

12.25. Oil Flow through a Journal Bearing. In many bearing assemblies the oil is introduced into the bearing through a hole or groove under pressure and flows through the bearing, finally emerging from the ends. A large volume of oil may thus be circulated through the bearing. Oil in excess of the amount required to keep the clearance space filled performs the useful function of carrying away the heat generated in shearing the oil film and hence keeps the bearing cool. For this reason it is useful to know the rate of oil flow through the bearing, a problem in fluid mechanics for which we have already derived the basic equations.

First consider the rate of flow circumferentially around the shaft. Equation (12.10) is the general expression for the rate of oil flow per unit width across any section of the film, which, since the fluid is incompressible, is the same across all sections. Hence for convenience we may consider the section where dp/dx or $dp/d\theta$ is zero. From Eq. (12.25) it

can be found that at this section $\theta = \cos^{-1}[-3\eta/(2 + \eta^2)]$. Then since $h = (C/2)(1 + \eta \cos \theta)$, at this point $h = C[(1 - \eta^2)/(2 + \eta^2)]$ and the expression for the total circumferential flow through a bearing of width L becomes

$$QL = \frac{\pi}{2} DLCN \frac{1 - \eta^2}{2 + \eta^2} \quad (12.33)$$

The dimensions of this flow are volume per unit time. Note that it is a maximum when the shaft and bearing are concentric and decreases with increasing eccentricity.

For flow in the axial direction we must refer to Eq. (12.9), the expression for the velocity at any point in a cross section of a viscous film. In the case of flow in the axial, or z , direction, $\partial p/\partial x$ must be replaced by $\partial p/\partial z$, and u by w . Since the relative velocity of the two surfaces in this direction is zero, $U = 0$. Equation (12.9) thus becomes

$$w = \frac{1}{2\mu} y(y - h) \frac{\partial p}{\partial z}$$

and the average velocity across the section is

$$\bar{w} = \frac{1}{h} \int_0^h w \, dy = - \frac{h^2}{12\mu} \frac{\partial p}{\partial z} \quad (12.34)$$

Consider a circumferential groove around the center of a journal bearing of which the length L is large compared with the breadth of the groove and which is supplied with oil at a pressure p_s above atmospheric. Equation (12.34) applies to this flow, which is to be thought of as superposed on the axial component of flow already described in Art. 12.23. Such superposition is legitimate because the equations of motion are linear. The symbols \bar{w} and p in Eq. (12.34) thus do not represent resultant quantities but components superposed on those already present by the addition of the circumferential source. Since the flow from this source is uniformly distributed around the periphery, the p component in Eq. (12.34) is a function of z only. Also, by virtue of continuity, \bar{w} is independent of z . Equation (12.34) thus shows that $\partial p/\partial z$ is constant. The value of this constant must be $2p_s/L$. Since $h = (C/2)(1 + \eta \cos \theta)$, the total flow due to the source out of both ends of the bearing is given by

$$\begin{aligned} Q_s &= 2 \int_0^{2\pi} \bar{w} h \frac{D}{2} d\theta \\ &= \frac{1}{48\mu} \frac{DC^3}{L} p_s \int_0^{2\pi} (1 + \eta \cos \theta)^3 d\theta \\ &= \frac{\pi}{24} \frac{DC^3 p_s}{\mu L} \left(1 + \frac{3}{2} \eta^2\right) \end{aligned} \quad (12.35)$$

The dimensions of this flow are also volume per unit time. (This should be compared with the expression for Π_4 in Art. 12.19.) Note that in this case the flow increases with increasing eccentricity and varies inversely with the L/D ratio. In Art. 12.23 it was shown that a reduction in L/D decreases the load capacity. But here we see that a reduction in L/D also increases the oil flow and hence the rate of cooling. The viscosity will thus become larger, and the reduction in load capacity with L/D will not be so great as in a bearing without forced circulation.

12.26. Criteria for Journal-bearing Operation. We are now in a position to consider the criteria for determining the safe hydrodynamic operating conditions for a journal bearing. As we have already seen, one condition is that the minimum film thickness h_0 should never be less than a certain value, which in turn determines a safe minimum value of S , denoted S_{\min} , from Eq. (12.26).

The second condition is that the operating temperature T should never exceed a certain maximum value T_{\max} ; otherwise, deterioration of the oil will be produced, corrosion of the bearing surfaces by the oil will be accelerated, and in some cases softening of the bearing materials will result.

Expressing the necessary relations analytically, we have

$$S = \left(\frac{D}{C}\right)^2 \frac{\mu N}{P}$$

whence

$$P = \left(\frac{D}{C}\right)^2 \frac{\mu N}{S} \quad (12.36)$$

(This S includes the factor to allow for side leakage.)

We also eliminate η from Eqs. (12.26) and (12.27), and obtain the friction coefficient as a function of S .

$$f = \Psi(S) \quad (12.37)$$

Now the operating temperature of the bearing is that temperature at which the sum of the rates of heat dissipation and net enthalpy efflux is equal to the power input to the bearing. Heat is carried away from a bearing by conduction through the supporting members, while the net rate of enthalpy efflux depends on the rate of oil flow and the temperature rise of the oil in the bearing. The sum of these quantities is thus

$$BA(T - T_R)^a + \rho Qc(T_2 - T_1)$$

where A is the area of the oil film πDL , T_R is the ambient or room temperature, B and a are empirical constants, Q is the rate of oil flow, ρ and c are the density and specific heat of the oil, respectively, and T_1 and T_2 are the entrance and exit temperatures of the oil. T_2 is directly dependent on the temperature of the bearing T and in many cases may be taken equal to T .

T_1 may also depend on T if the oil cooler is limited in capacity. If the oil-circulating system maintains a constant pressure, Q will depend on the viscosity and the clearance space in the bearing, according to Eq. (12.35). Both a and B have been determined empirically in some classical experiments by Lasche [5] and more recently investigated by Muskat and Morgan [6]. The value of a generally lies between 1 and 2.

Now the power input to the bearing is given by

$$FU = fPDL\pi DN$$

so that for equilibrium [compare Eq. (12.20)]

$$fPDL\pi DN = B\pi DL(T - T_R)^a + \rho Qc(T_2 - T_1) \quad (12.38)$$

In particular, if the Petroff equation is assumed,

$$FU = 2\pi^3 \frac{D}{C} \mu N^2 D^2 L$$

Finally, of course, the viscosity of the oil is markedly dependent on the temperature so that

$$\mu = \mu_0 \beta(T) \quad (12.39)$$

where μ_0 is the viscosity at some standard temperature and hence represents the grade of the oil. $\beta(T)$ is a function of the temperature that for petroleum oils is fairly independent of the grade. As pointed out in Art. 12.4, $\beta(T)$ is approximately exponential and may be expressed as $e^{b/(T+\theta)}$. It should be remembered that μ may also depend on the pressure if the latter is high.

We now have four equations [Eqs. (12.36) to (12.39)] in the quantities μ , f , S , and T . When these quantities are either eliminated or assigned limiting values, there results an expression involving the speed, the load, and the grade of oil for a given bearing. For instance, we can assume a safe minimum value for S such as S_{\min} and then eliminate μ , f , and T from the four equations and obtain a relation among P , N , and μ_0 . Alternatively, we can assume a safe maximum temperature T_{\max} , eliminate μ , F , and S , and obtain a second relation among P , N , and μ_0 . Representative curves giving the relation between P and N for a given grade of oil are shown in Fig. 12.18.

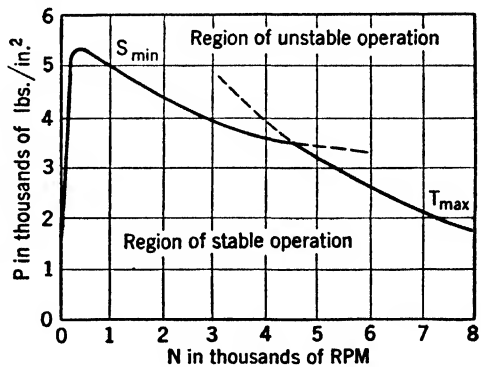


FIG. 12.18. — Plot of the two stability criteria for a journal bearing.

The region lying below the curve of constant S_{\min} corresponds to values of S which satisfy the condition that S never be less than S_{\min} . The region lying below the curve of constant T_{\max} satisfies the second condition that the operating temperature of the bearing never exceed T_{\max} . Hence, in the region lying below both curves, both conditions are satisfied, and any combination of load and speed that lies in this region represents conditions of possible operation. All the rest of the region represents impossible operating conditions. Hence the full curve in Fig. 12.18 gives the load capacity at any speed of the bearing using a given grade of oil, under the limitations originally imposed.

A similar analysis can be made to select the proper grade of oil for a bearing whose operating speed and load are known. A lighter oil will in general result in a cooler-running bearing because the rate of doing work is not so high. Indeed, it turns out in a great many practical cases that the viscosity of the light oil at its operating temperature is about the same as that of the heavy oil at its operating temperature. Hence, for a given load and speed, the value of $(D/C)^2(\mu N/P)$ is not lowered by using a lighter oil, yet the bearing will be much cooler. As a result, it is generally advantageous, under hydrodynamic operating conditions, to use the lightest possible oil.

SELECTED BIBLIOGRAPHY

1. CHRISTOPHERSON, D. G.: A New Mathematical Method for the Solution of Film Lubrication Problems, *J. Proc. Inst. Mech. Engrs.*, vol. 146, pp. 126-135, 1942.
2. KINGSBURY, A.: On Problems in the Theory of Fluid-film Lubrication, with an Experimental Solution, *Trans. Am. Soc. Mech. Engrs.*, vol. 53, pp. 59-75, 1931.
3. MUSKAT, M., and F. MORGAN: Theory of Thick-film Lubrication of Flooded Journal Bearing, *J. Applied Phys.*, vol. 10, pp. 398-407, 1939.
4. SWIFT, H. W.: Fluctuating Loads in Sleeve Bearings, *J. Inst. Civil Engrs.*, vol. 5, pp. 161-195, 1937.
5. LASCHE, O.: On Bearings for High Speeds, *Traction and Transmission*, vol. 6, pp. 33-64, 1903.
6. MUSKAT, M., and F. MORGAN: Temperature Relations in Journal-bearing Systems, *J. Applied Mechanics*, vol. 10, pp. A131-A138, 1943.
7. HERSEY, M. D.: "Theory of Lubrication," John Wiley & Sons, Inc., New York, 1936.
8. NORTON, A. E.: "Lubrication," McGraw-Hill Book Company, Inc., New York, 1942.

CHAPTER XIII

BOUNDARY LUBRICATION

The theoretical friction coefficient for a journal bearing behaves, according to Sommerfeld, somewhat as curve *A* in Fig. 13.1. However, experimental friction curves resemble *B* or *C*. They follow the theory closely in the region of perfect lubrication and high values of S but turn up sharply near some minimum value of S that depends on the particular bearing. This is the minimum permissible value S_{\min} , discussed in the preceding chapter. The region near this minimum for any particular bearing is called the region of "imperfect" or "boundary lubrication." The region to the left of the minimum, where the friction coefficient increases as S is diminished, represents unstable operation, and here bearings generally fail by seizure.

For well-designed bearings, boundary lubrication occurs in the vicinity of $S = 0.003$ and the conditions of operation here are quite different from those in the hydrodynamic range. For this condition the load is too great

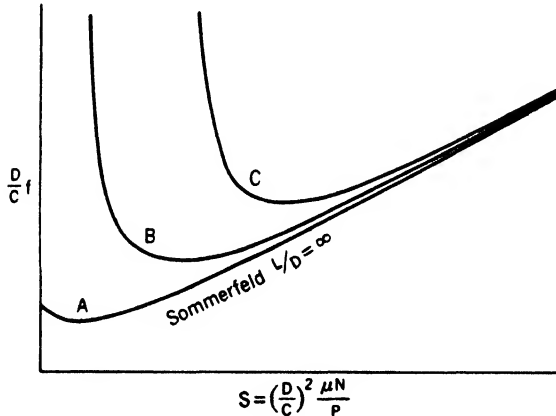


FIG. 13.1. — Schematic curves of friction coefficient f versus Sommerfeld variable S for a journal bearing.

or the speed too low to maintain fluid separation of journal and bearing by building up adequate pressure in the converging oil wedge. The load on the shaft is apparently taken on the bearing by direct contact. The viscosity of the oil is no longer of primary interest, but rather the nature of the rubbing surfaces and whatever oil film may remain to keep them slippery.

A journal operates under boundary lubrication when starting or when

the oil supply fails, but many machine elements such as gears and cams normally operate under such conditions.

Boundary lubrication is notoriously marginal, and slight variations from previously successful practice are likely to cause failure. The ability of a bearing to operate under conditions of boundary lubrication has been found to depend upon a combination of physical properties, *viz.*,

1. Nature of the lubricant.
2. Finish of the rubbing surfaces.
3. Material of the rubbing surfaces.
4. Lubricant supply.
5. Temperature.

13.1. Oiliness. Experience has indicated a marked superiority at moderate temperature in the ability of certain animal and vegetable oils to keep smooth surfaces slippery, as compared with mineral oils of the same viscosity. This ability has been called "oiliness." Despite its somewhat vague character, the term is useful in denoting that quality of a lubricant which makes it effective under conditions of boundary lubrication where viscosity is not important.

That marked differences exist in the lubricating value of various oils was recognized as early as 1902 by Kingsbury [1] in experiments on an oil-testing machine where lard oil and mineral oils were compared at loads beyond the range of effective hydrodynamic lubrication. It was found that under these conditions the lard oil ran with much less friction, qualitatively resembling curve *B* in Fig. 14.1, as compared with the mineral oil, which followed a curve similar to *C*.

Oiliness may be defined as the ability of an oil to give a lower coefficient of friction in the boundary region than another at a given value of *S*. Machines have been devised to test empirically for this so-called "property," but no physical property of a fluid has been found to correlate with the results of oiliness tests. It is therefore necessary to seek an explanation in the chemical nature of the oils in question. What follows may be somewhat speculative but appears to be consistent with observed facts.

13.2. Molecular Structure. The majority of lubricants are oils that are compounds of carbon and hydrogen with sometimes a small amount of other elements. There are two main categories, mineral oils, which are derived from petroleum, and fixed oils, which are derived from animals and vegetables. The mineral oils are composed solely of carbon and hydrogen. The molecules are generally in the shape of long chains of carbon atoms with hydrogens attached or of rings with long side chains such as are shown in Fig. 13.2.

The structure of the molecule is responsible for the properties that we generally consider typical of oil. The relatively high viscosity that oils

possess can be pictured physically as due to the entangling and intermeshing of their very long chains. Another result of their shape is a tend-

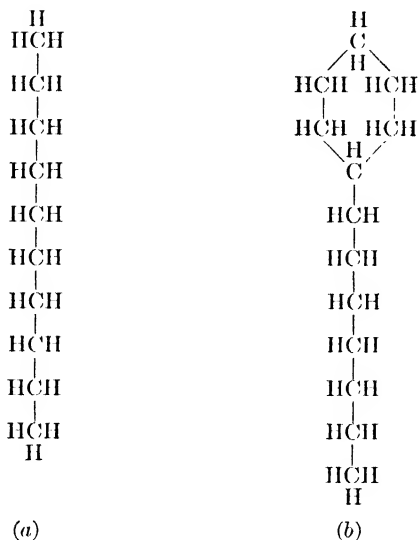


FIG. 13.2. — Structural formulas for (a) a straight-chain hydrocarbon, and (b) a ring hydrocarbon with side chain.

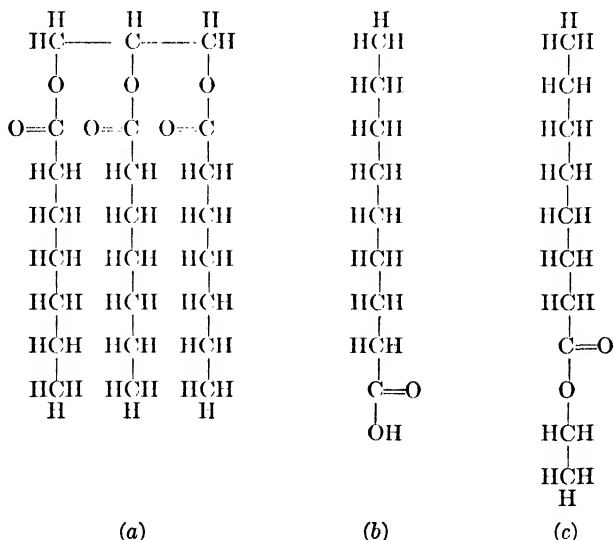


FIG. 13.3. — Structural formulas for (a) a tri-glyceride, (b) a fatty acid, and (c) an ester.

ency under certain conditions to align themselves parallel to one another and to pack closely together to form, in two dimensions, a relatively dense and rigid layer on a solid surface. This tendency is greatly accentuated

by the addition of small amounts of other types of oil to the pure hydrocarbon.

The fixed oils are a mixture of a wide variety of substances. The major portion consists of triglycerides with three long carbon chains hooked through a carboxyl linkage to a nucleus of three carbons, as in Fig. 13.3*a*, with lesser amounts of straight-chain hydrocarbons having a hydroxyl, $-\text{OH}$, or a carboxyl, $-\text{COOH}$, radical on one end, as shown in Fig. 13.3*b*. The latter are called "fatty" alcohols or acids. Other constituents are represented by the ester shown in Fig. 13.3*c*. All these compounds occur naturally in animal and vegetable oils and can be removed or concentrated by refining. There are other compounds that behave in a similar manner chemically and can be used in the same way, but they do not occur in nature and must be synthesized. They may contain a halogen, $-\text{Cl}$ or $-\text{Br}$, or an amine, $-\text{NH}_2$, radical, as shown in Fig. 13.4*a*; or the short hydrocarbon chain in Fig. 13.3*c* may be replaced by a metal atom as shown in Fig. 13.4*b* to produce a metallic soap.

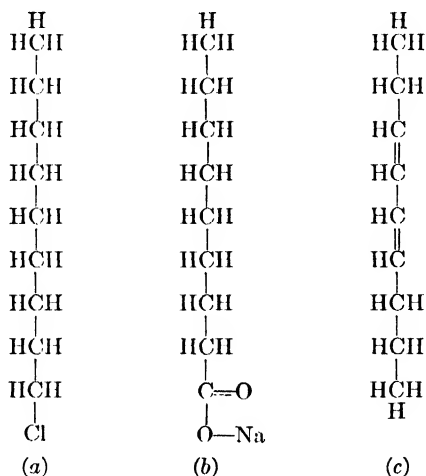


FIG. 13.4. — Structural formulas for (a) a chlorine substitution product, (b) a sodium soap, and (c) an unsaturated hydrocarbon.

Often some of the carbon atoms in the chain are not bonded to as many hydrogen atoms as possible so that double bonds between two carbons are formed, as in Fig. 13.4*c*. Such molecules are said to be unsaturated. Unsaturation often occurs in the fixed oils, while the mineral oils are more generally saturated. The region of the double bond is chemically active and will pick up other molecules, notably oxygen from the air if the oil is heated, as in an automobile engine. This activity has two results. (1) It generally produces acidity of the oil and leads to severe chemical attack of the bearing surfaces. (2) Oxidation produces gum and varnish deposits, which are generally harmful in engines.

13.3. Surface Chemistry. The above discussion of the molecular structure of the possible constituents of practical lubricants is necessary in order to elucidate their mechanism and to understand why they are made with their present-day compositions. A glance at the structures shown in Figs. 13.2 to 13.4 shows that all have the feature in common of a long chain. This point is important. As will be shown below, all these molecules tend, when in the vicinity of a solid surface, to orient themselves so that they are standing more or less normal to the surface, with one end attached to it. This being the case, it is obviously desirable to have a long chain so as to provide the maximum physical separation of the two bearing surfaces. This view has been partly substantiated in tests which show that for a homologous series of compounds, be they straight hydrocarbons, alcohols, or fatty acids, the friction within a given series decreases with increasing chain length up to a certain point.

Another property of these long-chain molecules in contact with a solid surface is their tendency to adhere in clusters. If a sufficient number is present, they will completely coat the surface with a monomolecular film of great lateral strength. This film is to all intents and purposes a solid in two dimensions. The rigidity is due to the chemical affinity between the CH_2 groups in the adjacent hydrocarbon chains. This rigid structure has been confirmed by electron-diffraction evidence.

The third structural characteristic of the molecule that is conducive to the formation of a strong adherent film is its possession of an active radical. So far we have discussed properties common to the mineral oils and the fixed oils alike, but now we reach a point of significant difference. As opposed to the pure mineral oils the molecules of a fixed oil and of a synthetic additive have an active radical on one end. This asymmetry in the otherwise symmetrical structure of the molecule, as shown in Fig. 13.3b, disarranges the normal symmetrical distribution of electric charge so that one end becomes predominantly positive and the other end negative. Such a molecule is said to be "polar."

The radical end of a polar molecule has a strong affinity for a metal surface. This end, therefore, attaches itself to such a surface, while the rest of the molecule tends to stand out more or less normal to the surface. The affinity of the active end varies both with the type of radical and with the length of hydrocarbon chain. It can be designated quantitatively as the free energy of adhesion and can be measured in a variety of ways [2]. It is a function of both the oil and the surface but is believed to depend principally on the nature of the oil. It is the work necessary to pull a unit area of oil away from a solid surface and, consequently, has the dimensions of energy per unit area. The polar and nonpolar liquids differ greatly in their energy of adhesion to metals, but a given oil has about the same energy of adhesion for all the usual bearing metals. An everyday illustra-

tion of a difference in energies of adhesion is the fact that water will stand up in droplets on a greasy surface, whereas it will spread in a thin uniform film on a clean one. The force of adhesion tends to draw the water over the surface and increase the mutual area of contact, while the surface tension of the droplet holds it back. The attraction between the water and the greasy surface is less than the surface tension and the water is held back, whereas the attraction of the clean surface is great enough to overcome the surface tension. Furthermore, the waterdrop on the greasy surface, on being rolled around, leaves a dry area behind it, so little is its attraction for the grease. On the clean surface, however, the water never recedes from an area that it has once wetted. This property of spreading, which is the result of a high adhesion energy, is obviously desirable for a boundary lubricant.

13.4. Film Formation. Long-chain molecules with lateral attraction for other chains and an active radical group at one end tend to form an adherent film on a bearing surface. Oils that have molecules of this type are superior to other fluids of the same viscosity under imperfect, or boundary, lubrication conditions. The function of the film is to separate two metal surfaces so that on rubbing they do not gall or seize. Furthermore, the film permits the surfaces to slide over each other with much less friction since the tops of the films are composed of CH_3 radicals, which are chemically saturated and have very little attraction. The situation has been likened to a stand of wheat firmly rooted to the ground. If a half-inch steel ball were magnified to the size of the earth, the thickness of the monolayer of oil on its surface would equal the height of the wheat. (This analogy to a wheat field is not quite exact since it ignores the mutual cohesive forces among the closely packed carbon chains.)

This strong monomolecular film exists only below a certain temperature, characteristic of the particular lubricant molecule *and* the particular metal surface. As the temperature increases, thermal agitation of the oil molecules decreases the attractive tendency between them. Above a certain temperature, called the "transition temperature," attraction and orientation cease entirely, and the molecules that were in the surface layer disperse themselves through the bulk lubricant much as a liquid vaporizes to a gas. This phenomenon is reversible on cooling.

Transition temperatures vary for the different classes of compounds. They are lowest for the pure hydrocarbons, which experiments by Bowden [3] and his coworkers have shown are effective as boundary lubricants only when they are solid, that is, at temperatures below their bulk melting points. As is well known, the melting point, and hence the transition temperature, increase with increasing chain length. For molecules of the same chain length the transition temperature is higher for the polar molecules since it takes more thermal agitation to tear the active radical loose from the bear-

ing surface. Some typical transition temperatures are given in Table I, taken from Bowden's work.

TABLE I.—TRANSITION TEMPERATURES OF ORGANIC COMPOUNDS

Compound	Temperature, Deg C
Docosane, $C_{22}H_{46}$	43
Octadecane, $C_{18}H_{38}$	28
Lauryl alcohol, $C_{12}H_{25}OH$	23
Octadecanol, $C_{18}H_{37}OH$	59
Lauric acid, $C_{11}H_{23}COOH$	44
Stearic acid, $C_{17}H_{35}COOH$	69
Copper laurate, $Cu(C_{12}H_{23}O_2)_2$	110
Sodium stearate, $NaC_{18}H_{35}O_2$	290

For even the most active polar compound, such as a fatty acid, there is a definite temperature above which it will not adhere to the bearing surface in a rigid monolayer. As may be seen from Table I, this temperature for the fatty acids is not so high as that often reached by high-performance automobile and aircraft engines. It was found experimentally, however, that lauric acid on copper behaved as a good boundary lubricant up to a temperature of about 100 C, while on platinum it ceased to be effective above about 43 C. Similar results have been obtained with other fatty acid-metal combinations. The explanation lies in the fact that the lauric acid reacts slightly with the copper surface to form a thin, adherent film of copper laurate, whose transition temperature is much higher than that of the pure acid. On platinum, however, the lauric acid is completely unreactive.

Such chemical reactions should be generally desirable, so long as the attack is not severe enough to change the surface contour.

13.5. Additives. We have seen that the best structure for a boundary lubricant consists of a long straight hydrocarbon chain with an active radical at one end. Compounds having such a structure occur naturally in the animal and vegetable oils, or they may be synthesized, but they do not occur in the mineral oils.

These compounds often have certain impractical aspects that make them undesirable for commercial use. For instance, the naturally occurring fixed oils, being unsaturated chemically, tend to oxidize at engine temperatures to produce acidity and chemical attack of the bearing surfaces. Further oxidation produces gummy deposits that cause stuck piston rings and clogged drains.

Fortunately, there is an easy way out of this difficulty. It has been found that a small percentage of an active polar compound when added to a straight mineral oil renders the product as efficacious a boundary lubricant as the pure additive and yet does not appreciably affect the bulk properties of the mineral oil. This is explained by the fact that the additive, having

a great affinity for the surface, migrates to it, forming its characteristic strong monolayer or chemical coating, to the exclusion of the mineral-oil molecules. Only a small fraction of 1 per cent of additive is required to coat the surface. The residue remains in solution in the mineral oil, where it is almost instantly available to repair areas of the film worn away by rubbing. In this connection Table II is of interest, which gives some measurements by Burwell [4] of the friction coefficient under boundary conditions between two ground and hardened steel surfaces for various concentrations of oleic acid in mineral oil.

TABLE II

Lubricant	Friction Coefficient
Pure mineral oil.....	0.360
2% oleic acid in mineral oil.....	0.249
10% oleic acid in mineral oil.....	0.198
50% oleic acid in mineral oil.....	0.198
Pure oleic acid.....	0.195

This table shows that although a fractional percentage of oleic acid should be sufficient to cover the surfaces completely, the friction coefficient continues to decrease up to 10 per cent concentration of the acid. Presumably, molecules of the acid are forced more rapidly to a break in the surface film if the concentration of additive is increased, but this effect is less marked at high concentration than at low.

The concentration of additive beyond which no improvement in performance is noted depends on a number of factors, notably the speed and severity of rubbing, the affinity of the additive for the bearing surface, its relative solubility in the bulk lubricant, and the difference between the temperature of operation and the transition temperature.

We conclude that a lubricant for general service where boundary conditions may be expected should consist of a mineral oil of appropriate viscosity, to which has been added a small percentage of a polar substance, preferably either a fatty acid or a metal soap. The requirements for such a "film-strength" additive are

1. The molecule should contain an active radical to give high adhesion to the bearing surfaces.
2. The molecule should be of the long straight-chain type, the active radical being at one end.
3. The additive should be present in a concentration of at least a few per cent, but not in sufficient quantity to contribute its disadvantageous bulk properties to the lubricant.
4. Either its own transition temperature or that of its reaction product with the bearing surface should be above the anticipated operating temperature.

Good commercial practice is in line with the above. Generally the active substance is added in the form of an easily procurable commercial oil, such as lard, sperm, or castor oil. A few petroleum crudes naturally contain a small fraction of such substances, and, from this standpoint, it is possible to overrefine a mineral oil. In the extreme-pressure (E.P.) lubricants used for gears, where the loading of the film is extremely high owing to the small areas of contact, the metallic soaps are generally used.

In the case of commercial oils for automobile engines where the service requirements are complicated by the necessity for exposure to extreme transient temperatures and the products of combustion, other addition agents are also used for various other purposes. Next in importance to the film-strength additives are the oxidation inhibitors. These prevent the unsaturated molecules that are inevitably present in all commercial oils from becoming oxidized. The inhibitors act principally by taking up chemically all the oxygen present and thus forming harmless materials. Other additives are employed as detergents, which enable the oil to keep in suspension finely divided solids, such as sludge and metal particles, and prevent their adhesion to the metal surfaces. Other agents are sometimes used for more specialized requirements such as raising the viscosity index and depressing the pour point.

13.6. Chemical Polishing Agents. These are used to prevent galling and seizure in the running in of new bearings. As a class, the chemical polishing agents are hydrocarbon compounds containing a metalloid atom such as sulfur, phosphorus, or arsenic. Tricresyl phosphate is an example of one that is used commercially. Beeck [5] has explained the action of these compounds as follows:

They are stable at room temperature but at elevated temperatures decompose and release the free metalloid atom. Thus they do not attack the bearing surfaces at the temperature of normal operation; but where metal-to-metal contact occurs, the local temperature rises and the resultant decomposition of the agent releases some of the metalloid, which then attacks the metal over the rubbing area to form a thin, easily sheared coating of the compound of the metal and metalloid, *e.g.*, the metal sulfide or phosphide. This coating alloys with the metal to lower its melting point, so that the high spot is worn away and the local temperature is reduced.

A chemical polishing agent ceases to function after running in is complete and the true bearing area has reached its maximum value. Hence it may be removed, and plain oil used thereafter. The film-strength additive, on the other hand, must of course be retained in the oil throughout the life of the bearing.

13.7. Other Lubricants. All the discussion so far has centered in the hydrocarbon family of compounds. However, their somewhat considerable drawbacks and the urgent requirements of the Second World War prompted

a search for other families of compounds suitable for lubricants and hydraulic fluids. To date the most interesting that have been evolved are the silicones. These are synthetic substances characterized by long chains composed of alternate silicon and oxygen linkages, as shown in Fig. 13.5.

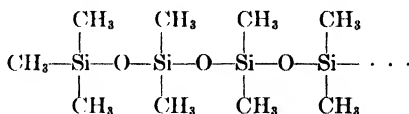


FIG. 13.5. — Structural formula for a silicone.

A silicone molecule may also contain active radicals. Silicones are superior to the hydrocarbons in having a higher viscosity index and in being noninflammable, so that they have found important use as hydraulic fluids, particularly in airplanes and naval vessels. They have not yet been developed as good boundary lubricants, but there is promise in this direction.

For specialized purposes other fluids may be used. Water is used to lubricate the rubber bearings that support the propeller shafts of vessels. Air is used for high-speed centrifuges and grinders where the clearance space is small, the speed is high, and the load is light.

Important lubricants for certain applications are the greases. They are mixtures of mineral oil and soaps either with or without a solid filler. The mixture forms a gel that is semisolid at room temperature. The base may be a sodium, a calcium, or a lead soap. Greases are never so good from a lubrication point of view as oils, but they are used under the following conditions:

1. Where the clearances are excessive, owing either to poor design or to extreme wear.
2. In dusty or dirty surroundings in order to trap dirt and grit and keep them out of the bearings.
3. In places such as weaving and food machinery where dripping oil would damage the product.
4. In inaccessible locations or where the servicing of the moving parts is likely to be infrequent.
5. At high temperatures, where the grease may be liquid at the operating temperature and behave like an ordinary oil.

For very high loads and low speeds or frequent reversals of motion a solid lubricant is effective, either alone or added to oil. The solid friction between the two metal surfaces is replaced by the friction of shearing the solid lubricant, so that galling is prevented. Graphite is advantageous since it shears easily and yet is hard enough in the direction normal to the plane of shear to support an appreciable load. There is also indication that

it is wetted by oil. It can withstand high temperatures and so can be used where ordinary oils cannot, *e.g.*, in bake-oven, glassmaking, die-casting, and other hot machinery. It is used as a colloid in either oil or water. Other solid lubricants are talc, soapstone, and mica.

13.8. Oil Supply. Wherever possible, there should be a copious supply of lubricant. Inadequate supply of oil, improperly delivered to the bearing surfaces, is probably the most common cause of bearing failure. It is always desirable to operate hydrodynamically, but this is impossible unless there is sufficient oil. Furthermore, if the oil is circulated through the bearing, a high rate of oil flow performs the very important function of cooling the bearing, as discussed in Art. 12.25. Lack of an adequate supply may in a few cases be intentional as in the case of piston rings, where it is desirable to leave as little oil on the combustion walls as possible, or in the case of textile machinery, where spoilage of the product is to be avoided.

The lubricant can be supplied to bearings and other rubbing surfaces by a number of methods. These include drop- and wick-feed oilers, hydrostatic lubricators, ring, chain, and collar oilers, mechanical force-feed oilers, and centralized appliances and circulating systems employing oil pumps and coolers. These will not be discussed further here, but reference may be made to any standard text on practical lubrication [14, 15].

13.9. Surface Finish. From the preceding discussion it follows that boundary lubrication depends largely on a joint property of the liquid and the metal surfaces, involving the maintenance of an adsorbed film over the sliding areas of contact.

Figure 13.6 indicates in a general way the nature of the contact between two supposedly flat surfaces pressed together with an oil film between them. They touch only at *A* and *B*, and the true area of contact is very

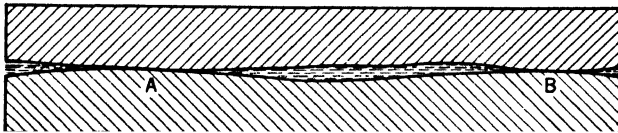


FIG. 13.6. — Schematic cross section through the contact area in boundary lubrication.

much less than the wetted area used in the theory of perfect lubrication. Boundary lubrication is characterized by the dominance of the true area of contact. As the surfaces slide over each other, they are separated at *A* and *B* by an oil film of molecular dimensions. Whether or not this oil film breaks down and metallic seizure takes place will depend on the intensity of the pressure (which in turn is governed by the areas of *A* and *B*), on the temperature rise at the local contact spots, and on whether or not the oil film is renewed from the reservoirs of oil in the hollows between contacts. Obviously the contours of the metal surfaces must determine the ability of

a given film to support the load, and hence a knowledge of surface roughness is essential.

By surface roughness is meant the small-scale geometrical profile that is imparted to bearing surfaces by the usual commercial finishing operations. It may be defined as recurrent or random irregularities in a surface that have the form of small waves or bumps. The American Standards Association (ASA) has arbitrarily set the upper limit of their spacing at about 0.01 in. This limitation excludes waviness due to looseness or chatter in the finishing machine and also dimensional deviations from shape. In these cases the wave length is relatively long and can ordinarily be measured with a dial gauge. The lower limit of height of the roughness that can be conveniently detected at present is a fraction of a wave length of light or a few millionths of an inch. This is still several hundred molecular diameters and unfortunately leaves a region of surface contour about which we know little.

There are a great many ways to measure surface roughness. One way is to take a cut perpendicular to the bearing surface, polish the section, and examine the profile under a microscope. One can also use the optical properties of the surface as a measure of its roughness or smoothness. The higher the ratio of the specularly reflected light to the diffusely reflected light from a given source, the smoother the surface. In practice, however, a mechanical-tracer type of instrument has been most commonly employed. It is similar in construction to a phonograph pickup. The vertical displacement of a stylus as it passes over the surface is amplified either by mirrors or electrically, and a magnified image of the surface profile is drawn on a moving tape. Alternatively, the electrical impulse may be fed into an a-c meter, which automatically reads the rms average of the deviations of the surface from some median plane. Surface roughness is usually specified as this rms value in microinches ($\mu\text{in.}$), or millionths of an inch. A turned surface may measure 100 $\mu\text{in.}$ or more and a ground surface about 20 $\mu\text{in.}$ Honing or superfinishing with abrading stones or lapping with loose abrasive may give 2 to 8 $\mu\text{in.}$, while metallographic polishing can give a surface profile of less than 1 $\mu\text{in.}$

It is obviously a great oversimplification to attempt completely to describe such a complex geometrical surface by a single number. This inadequacy becomes apparent if one compares the lubrication performance of two bearing surfaces having the same rms roughness but finished by different methods. It is often found that their performance differs markedly. To describe this situation better it has been suggested that a second quantity such as the rms of the first derivative of the surface, *i.e.*, its slope, be defined also.

The directional quality of surface profile is another characteristic that distinguishes surface finishes. Turned and ground surfaces possess this

quality, while honed, superfinished, and grit-blasted surfaces do not. This property is important since bearing performance depends on the relation of scratch direction to the direction of motion.

Finally, the finishing operation itself may produce metallurgical changes in the surface material. This is discussed in the following section.

That lubrication performance does in fact depend on surface roughness is illustrated by the results of two experiments, the first of which was performed under conditions of boundary lubrication. In Table III are shown values of friction coefficient for surfaces of different roughness. The rubbing surfaces were crossed cylinders in the form of standard automobile piston pins. The roughness readings are rms values and were read with a tracer-type profilometer. The interesting fact appears that the friction increases with roughness up to about 20 μ in., after which it remains essentially constant. Values for grit-blasted surfaces are appreciably less than those for ground surfaces of the same roughness. This may be the fault of the roughness measurement and may substantiate the need for a second quantity besides the rms roughness to compare surfaces prepared in different ways. It may be further noted that, the smoother the surface, the less the improvement effected by the addition agent. Possibly the incentive for producing improved addition agents in the oil industry would have been less if our rubbing surfaces had always had good surface finish.

TABLE III

Lubricant	Surface roughness, μ in., rms				
	Super-finished 2	Ground 7	Ground 20	Ground 50	Grit-blasted 55
Mineral oil.....	0.128	0.189	0.360	0.372	0.212
Mineral oil + 2% oleic acid	0.116	0.170	0.249	0.261	0.164
Oleic acid.....	0.099	0.163	0.195	0.222	0.195
Mineral oil + 2% sulfonated sperm oil.....	0.095	0.137	0.175	0.251	0.165
SAE 30 oil.....	0.119	0.252	0.253	0.192

The second category of experiments [6,7] employed full journal bearings with flooded lubrication in which journals finished in different ways to various roughnesses were run against a number of bearing metals. Under heavy loading it was found that in the region of boundary lubrication the seizure tendency was substantially reduced as the roughness of the journal was reduced from 10 down to 1 μ in. The load just prior to seizure was 400 per cent greater for the smoothest journal than for the roughest.

13.10. Materials of the Bearing Surfaces. We now consider the solid materials of which the rubbing, or bearing, surfaces are composed. Good

performance depends on certain physical and chemical properties of the surfaces as well as on a number of bulk properties of the bearing materials. Furthermore, the properties of the two surfaces must be properly matched to one other. A material that is satisfactory in rubbing against one surface may be unsuitable for use against a surface of a different material. In the case of rotating parts the shaft usually must be designed for mechanical strength, so that steel should be used for the shaft, regardless of its rubbing properties. Hence, bearings must be chosen that will operate satisfactorily against steel. Furthermore, one of the two surfaces generally wears more and must be replaced sooner. In most machinery the easier part to replace is the bearing, which further justifies the practice of making the shaft out of a hard material like steel. In other situations, such as the piston-ring-cylinder problem, there is some flexibility in the choice of materials for both surfaces.

There are several empirical rules followed in selecting materials for the two bearing surfaces. The first is that the two should not be made of similar material. If metal-to-metal contact occurs locally, two like metals tend to weld together owing to the frictional heat and pressure. When they break away, portions of one surface are left adhering to the other surface. This will in turn cause more metal pickup until the galling has become severe enough to produce failure.

In general, both surfaces should not be hard if the speed is to be high. If both are hard, the abrasion produces unnecessary friction and heat. If the speed is very low or intermittent, as in the jewel bearings of watches, two hard bearing surfaces are advantageous, as the wear is slight and little looseness develops in the parts. For the speeds that commonly occur in machinery, however, one surface should be soft enough to yield and conform to the other, to relieve the high local pressures due to misalignment. On the other hand, it must not be so soft as to yield under the normal operating load or deform under shock. Such deformation may change the shape of the converging oil wedge and impair its load-carrying capacity. A further advantage of softness is an ability to embed adventitious grit so completely that it will not scratch or grind the hard surface.

These somewhat conflicting requirements as regards hardness and strength cannot easily be achieved in a homogeneous material. As a result, practical experience has led to bearing-material compositions of a duplex nature, containing one hard constituent that mechanically supports the load and a soft constituent that conforms to the shaft and shears at a low temperature. (This mechanism is discussed further in Art. 13.11 below.) These constituents may be disposed in a number of ways. There may be hard particles embedded in a soft matrix as in the case of the babbitts; there may be soft areas in a hard matrix as in the copper-lead alloys and the lead bronzes; or the soft constituent may be a continuous thin layer

over the hard one as in the case of lead-coated and lead-indium-coated silver. This duplex structure is not universal, however, bronze and cast iron being commonly used for bearings where light loads are encountered.

An important property for bearing metals to be used in internal-combustion engines is corrosion resistance. In the airplane engine, temperatures today are high and are still increasing. In gas turbines, they may be excessive. As a result, the oil, in spite of addition agents to increase stability, often becomes partly oxidized and acidic. Lead is particularly susceptible to acid attack. While a certain amount of chemical activity on the part of bearing materials improves performance under boundary conditions, there must be a compromise between this requirement and destructive corrosion.

Whenever alternating or shock loads are present, the fatigue resistance of the materials becomes important. Alternating loads are obviously present in all reciprocating engines. For high-speed operation where the evolution of heat becomes a problem the thermal conductivity of the bearing material is important. Metals have a great advantage over non-metallic materials and coatings in this respect. Hardness is an essential prerequisite to good wear resistance.

Pure lead, tin, cadmium, and indium are the softest bearing materials and are in many cases the most satisfactory. They are given the necessary mechanical strength by coating them on steel or other strong backing materials, the layers being quite thin, often less than 0.010 in. Lead has the drawback of great susceptibility to corrosion. To increase their mechanical strength these metals may be alloyed in a number of ways. Such alloys are the babbitts, the first to be developed commercially. They originally consisted of about 90 per cent tin and the remainder copper and antimony, the latter elements forming hard crystalline intermetallic compounds with the tin, and being embedded in the soft matrix of the tin-rich eutectic. For economic and strategic reasons lead has recently been used to replace the tin, either partly or entirely. Mechanically it is just as satisfactory, but its corrosion resistance is poor. The babbitts as a class have poor fatigue resistance. The cadmium alloys are similar in structure to the babbitts and are coming into general use.

If somewhat greater mechanical strength is desired, the copper-lead alloys and lead bronzes are used. The copper-lead alloys and the lead bronzes are a dispersion of lead droplets in the copper or bronze, the lead being completely insoluble in them, even in the liquid state. On running, the lead smears over the hard matrix, which otherwise has poor resistance to galling. The depressions left by the lead serve as oil reservoirs. The copper-lead alloys still require steel backing for strength; but the bronzes, whether containing lead or not, and particularly the phosphor bronzes, are strong enough to be used as complete bushings. These are generally

used where the loads are not severe, the alignment is good, and long life without replacement is desired. Copper and its alloys may be attacked by traces of sulfurous acid left in the oil from the refining process.

A somewhat ingenious use of bronze is to form by a powder-metallurgy process a bushing containing voids. When soaked in oil, such a bushing will take up about 30 per cent of its volume and can then be used with little or no external oiling since it furnishes its own lubricant.

For more severe service, silver is coming into widespread use. It is fatigue resistant and has a low elastic modulus (10,000,000 lb per sq in.), while its low hardness (25 Brinell) affords some opportunity for grit to become embedded under its surface. Also, its thermal conductivity is high and results in a cool bearing. It has some tendency to gall and seize, possibly owing to its chemical inertness to additives, but this can be counteracted by plating a film of lead over the silver surface. The corrosion of the lead is prevented by coating it with a still thinner film of indium and diffusing it into the surface by heat treatment.

A hard metallic bearing material is cast iron. It has been in use for a long time, but only where light loads, high speeds, and good alignment are encountered. A good example is the supporting bearings for grinding-machine spindles. Superficially it would appear to violate all our rules as a good material to run against steel. It is as hard or harder than the steel shaft and chemically of the same composition. It has now been shown, however, by electron-diffraction examination that a cast-iron bearing surface after running is coated with graphite flakes, which are dragged out of the cast-iron matrix and smeared over the surface. This may account for its good operation.

Another very hard material having unique bearing properties is chromium plating. Its great chemical dissimilarity to copper and its alloys is evidenced by the chromium-copper phase diagram, which shows practically no solid solubility even at 1000 C. This lowers the tendency to gall. The smoothness of electroplated chrome surfaces is probably helpful also, although there is some indication that interrupting this smooth surface with small pits, or depressions, will improve the performance still further, particularly for engine-cylinder walls. Several processes for preparing such surfaces have been developed.

Some bearing surfaces today are chemically treated to improve their performance. This may be an oxidizing, a sulfidizing, or a phosphate treatment. It is maintained that the coating of these compounds acts as an antiwelding agent between the metal surfaces.

It is probable that bearing surfaces composed of the same material may differ in their lubrication performance owing to metallurgical differences, often produced by the forming or finishing operation. For instance, Wulff [8] has shown that grinding, honing, and lapping induce the trans-

formation from austenite to ferrite in 18-8 stainless steel. Since these differ in crystal structure, they may be expected to differ in properties that influence rubbing performance. It is well known that any such mechanical operations will distort the metal grains in the surface and reduce their size. When this is carried to an extreme degree as in a very highly polished metal surface, it has been found that such a surface is chemically more active than an undisturbed surface. Also, thermal and mechanical stresses induced in surfaces by grinding have been found greatly to increase the rate of corrosion. These surface layers may be only 0.0001 in. deep, but that is quite sufficient to change the surface properties. Shaping operations such as hot- or cold-rolling and -drawing will produce a preferred orientation of the grains, especially near the surface. It can be expected that the different crystal faces which are thus exposed may have somewhat different chemical properties with respect to the lubricant, particularly in metals the crystal structures of which are relatively anisotropic, such as zinc, antimony, or white tin. Burnishing, peening, and cold-rolling may produce high compressive surface stresses, which are advantageous for fatigue strength since they counteract the stress-raising effect of local cracks, flaws, and notches. Carburized parts also have compression in the carburized surface layer; but if this layer is removed by grinding, the new surface may be in tension and be liable to crack or check (*e.g.*, wrist pins, ball-bearing races, gear teeth).

Mention should also be made of some nonmetallic bearing materials that have value for certain special applications. The very hard wood lignum vitae has been traditionally used to line the outboard bearings that support the propeller shafts of ships. It is sufficiently hard, it will not gall the shaft, it is not injured by sea water, and there is a certain amount of natural oil in the wood. Rubber also is a very good bearing material where water is the lubricant and is gaining increasing use in ships. Certain plastic-impregnated materials such as textolite and micarta are proving satisfactory as supports for the roll necks in steel-rolling mills. Here also the antigalling property is valuable.

13.11. Dry Friction. Logically we should, proceeding still farther to the left on the curves of Fig. 13.1, next take up the phenomena of seizure and wear that occur when boundary lubrication fails. For this, it is essential that we have some knowledge of the elements of dry friction.

Results of experiments on the friction between rubbing surfaces were published by Amontons in 1699 and by Coulomb in 1779. These showed that the friction force F was proportional to the load W applied normal to the surfaces, or

$$F = kW \quad (13.1)$$

Over a large range the coefficient k was found to be independent of W , of the relative velocity of the two surfaces, and of the apparent area of contact.

It appeared at first to be a physical constant typical of the materials if the surfaces were carefully cleaned.

It was further observed that its static value, measured when the two surfaces were at rest, was almost always greater than the kinetic value when the surfaces were in relative motion. This law of proportionality at first suggested the explanation of dry friction as due to the mechanical interlocking of the asperities on the two surfaces. It can be seen from simple geometry that, if this were the case, k would equal $\tan \theta$, where θ is an average angle of slope of the asperities. The friction coefficient should, accordingly, decrease with increasing smoothness, as was found to be the case in the range of moderate roughness; but with fairly smooth surfaces the coefficient approached a constant finite value and never reached zero. This simple theory, therefore, is inadequate.

The work of subsequent investigators, climaxed by that of Bowden and his collaborators [9], of Ernst and Merchant [10], and of others, has succeeded in formulating a picture of the mechanism of dry friction which, although still tentative and with some significant gaps, does qualitatively explain most of the facts observed to date. According to this picture the total friction force consists of three terms. The first is due to the interlocking of the surface roughnesses as explained above; but since the average slope of well-ground surfaces is only a few degrees and that of honed and polished surfaces is even less, $\tan \theta$ is very small and for most cases this term is negligible.

The second term in the friction force arises when the two surfaces are of unequal hardness and is due to the plowing out of the softer material by the protuberances on the harder surface. This term is equal to the flow pressure of the softer material multiplied by a constant that is dependent on the geometric shape of the plowing protuberance. For simple geometric shapes it can be easily calculated. This may or may not be an appreciable part of the whole friction force.

The third term is based on the hypothesis that when two surfaces are in apparent contact the load is in fact carried by the few points on the surfaces which actually come into contact, as indicated in Fig. 13.6. That this area is only a small fraction of the apparent area of contact has been confirmed by measurements of the electrical conductance between two metal bodies in contact. Owing to the very small contact area, the local pressures are extremely high, so that prominences flow plastically until the local pressure no longer exceeds the flow pressure of the softer material. (In this operation the *apparent* area of contact has not changed.) It is further hypothesized that another result of these high local pressures is to cause adhesion and welding of the two surface materials over these true contact areas. Hence a portion of the friction force is due to the shearing of these junctions, which are alternately made and broken as sliding proceeds.

To the effect of pressure in forming these local welds is added that of temperature. If the sliding velocity is appreciable, the work done by this shearing component of the friction force is expended over a very small area and there is a local temperature rise. That these temperatures become appreciable has been shown in a classic experiment by Bowden and Ridler [11] in which the two rubbing surfaces were made of dissimilar metals and acted as the elements of a thermocouple. It was found that the temperature often rose to the melting point of the lower melting metal.

The third term in the friction force is equal to the shear strength of the welded junction times the true area of contact. This shear strength is difficult to calculate from the other physical properties of the materials. If the two materials are the same or similar, so that they have a high mutual solid solubility, the junction formed will generally have shear strength as great as or greater than that of the softer material and the shear will take place in the latter, thus leaving particles of the softer material adhering to the harder surface. This has been established experimentally both by electrochemical development of the foreign material on gelatine-coated paper [12] and also by making the softer surface radioactive and measuring the activity picked up by the harder material after rubbing [13]. In such cases we can use the shear strength of the softer material, which is well known, although it may be raised somewhat by work hardening. If, on the other hand, the two materials are quite dissimilar and do not tend to weld easily, the shear strength of the junction may be small.

Summarizing the above quantitatively we can say that the friction force is given by

$$F = W \tan \theta + cp + sA \quad (13.2)$$

where W is the normal force between the two surfaces, θ is the average slope of the surfaces, p is the flow pressure of the softer metal, c is a constant dependent upon the geometrical shape of the slider, s is the shear strength of the welded junction, and A is total *true* area of contact, *i.e.*, the sum of the areas of all metallic junctions.

For bearing surfaces, θ is small, and the first term can be neglected. The relative importance of the other two terms will depend on the shapes of the protuberances and the relative hardness of the two surfaces. If, for instance, the protuberances on the harder surface are imagined as spade shaped, with very little area projected on the nominal plane of contact but capable of plowing out or pushing ahead a large cross section of the softer material, then the second, or plowing, term will strongly predominate. In this case the friction may rise during the sliding owing to the softer metal piling up ahead of the spade-shaped protuberance and because p may increase owing to work-hardening. This second effect should increase with velocity, as has been found experimentally to be the case [9].

If, on the other hand, the protuberances on the harder surface are well

rounded and the materials of the two surfaces tend to form junctions of high strength, then the last term, the shearing term, will predominate. In general, the load will then determine the true area of contact by causing plastic flow of the softer metal until the true area of contact has increased to a point where the local pressure no longer exceeds the flow pressure of the metal. Hence $A = W/p$. Substitution for A in Eq. (13.2) gives for the coefficient of friction of a smooth pair of surfaces

$$\frac{F}{W} = k = \frac{s}{p} = \frac{\text{shear strength of junction}}{\text{flow pressure of softer metal}} \quad (13.3)$$

It should be noted that this makes k a function of the bulk properties of two metals, and hence k itself is a property of the metal pair. It has not been possible to find metal combinations having extremely small coefficients of dry friction (below $k = 0.1$) since for most metals s and p are somewhat proportional. Graphite, however, is an example of a material having a fairly high indentation hardness and yet a very low shear strength within itself.

Equation (13.3) provides an explanation of the observed fact that in certain instances the friction force is proportional to the applied load.

TABLE IV.—FRICTION COEFFICIENT OF A SPHERICAL STEEL RIDER
ON VARIOUS MATERIALS

<i>Material</i>	<i>k</i>
Steel.....	1.0
Copper.....	0.9
Copper film on steel.....	0.3
Lead.....	1.2
Lead film on steel.....	0.3
Lead film on copper.....	0.18
Copper-lead alloy.....	0.17
Indium.....	2.0
Indium film on steel.....	0.08
Silver.....	0.55
Indium film on silver.....	0.1

That this is due to the influence of the load on the true area of contact, and not to the load per se, has been confirmed by Bowden [9] in some ingenious experiments in which the friction coefficient of a hard slider rubbing over a soft metal in bulk was compared with that of the same slider rubbing over the same metal in the form of a thin film deposited on a very hard base. Here s , characteristic of the soft metal, remained the same, but p was much greater and hence A much less in the latter case, owing to the support of the hard base. In particular, it was found that thin films of lead and indium on copper and steel gave remarkably low coefficients of dry friction as shown in Table IV, taken from Bowden's paper.

It was concluded therefore that the friction force is actually proportional to the true area of contact and depends on the applied load only through the latter's influence on the true contact area.

This table suggests the reason for the efficacy of copper-lead bearings and lead-indium-coated silver as well as partly substantiating the old picture of the mechanism of the babbitt materials. The lead or indium provides a low shear strength, and the silver or copper has a high hardness or flow pressure.

The concept of local welding also serves to explain why static friction is usually larger than kinetic. When the surfaces are at rest, all the junctions that can form have an opportunity to do so. When the surfaces are in motion, a certain fraction (statistically speaking) of the junctions are being made and broken. If a finite time is required to form a junction, then these do not make their full contribution to the friction force. Although this explanation seems probable, it has not been positively established.

We have already seen that, by using the artifice of a thin film of a soft metal on a hard base, the value of k may be lowered. A similar effect may occur if there are foreign films present. Such a film may be adventitious as the oxide film formed on most metals in the presence of air or water vapor; or it may be due to the chemical action of a constituent of the lubricant such as sulfur, phosphorus, or arsenic; or the film may be purposely prepared for antiseizing purposes; or it may be the oiliness or boundary additive in a commercial lubricant. These films serve to reduce the shear strength at the junctions since these nonmetallic materials do not weld strongly to the metal.

At the other extreme, the static-friction coefficient of extremely clean metal surfaces that have been outgassed and measured in a vacuum may reach values as high as 6.

When the friction is due primarily to the breaking of the welded junctions and the shearing term predominates, it is generally observed that the motion proceeds intermittently. This is familiar as "chattering," or "squealing." Careful investigation has demonstrated that one surface does indeed move over the other by a series of sticks and slips. Mathematical analysis of the mechanics show that this will occur if the static coefficient of friction is higher than the kinetic, which it generally is, and if there is any elasticity in the supporting members, which is always the case. In the case of similar metals or when actual galling occurs, the motion proceeds smoothly, presumably owing to the continuous plastic deformation of the bulk material.

In the machining of metals all the conditions obtain for the welding of one surface to the other. The surface of the chip is perfectly clean and not even exposed to air at the tip of the cutting tool; the cutting edge has been

wiped free of all films by the chip rubbing over it; and there is no lubricant present at the cutting edge, the fluid being used solely for cooling. Owing to frequent starting and stopping, static friction produces incipient stick-slip action, which often results in chattering. This problem has been studied by Ernst and Merchant [10].

It need not be assumed that both materials are metallic, since friction occurs universally. However, most of the careful experimental work has been done with metals, the mechanism of local welding being most easily understood in this instance.

13.12. Seizure and Wear. The above picture of the mechanism of dry friction permits some deductions to be made about the observed phenomena of seizure and wear, since both are either extremely exaggerated instances or the integrated effect over a long period of time of the minute phenomena that contribute to dry friction under moderate conditions.

Seizure is initiated by the welding of a local junction as described above. If the two metals are similar and not too hard, they form a local weld of relatively great strength over a large area. As a result, the metal breaks, not at the weld but generally on one side or the other, so that a spot that was originally slightly high is now made higher because of metal from the other surface adhering to it. This rubs even more severely, producing higher temperatures and pressures and welding momentarily over larger areas. This process builds up until the driving force is no longer able to break the weld that has formed. Seizure is prevented by making the rubbing surfaces of dissimilar materials so that low-shear-strength junctions are formed, by keeping the true area of contact small through using hard materials or hard backing, by coating the surfaces with antiwelding films, and by use of a copious supply of a good boundary lubricant.

Wear, on the other hand, represents the long-time summation of the individual small effects of dry friction, both abrasion and welding. Another contribution to wear may be from chemical corrosion and the subsequent rubbing off of the loose compound formed, which may in itself be abrasive, as in the case of chemical polishing agent, extreme-pressure lubricants, or water vapor. Automobile-cylinder wear is thought to be due in large part to corrosion aided by moisture of condensation from the combustion products.

The same general factors that prevent seizure will also minimize wear, but with some modifications. For wear prevention the emphasis should be on hardness of both surfaces. Hence both surfaces are often made of hardened steel even though by so doing one sacrifices the desirable feature of dissimilarity of material. This difficulty can be remedied somewhat and the surfaces made even harder by carburizing, nitriding, or chrome-plating one or both surfaces. Examples are gears, cams and rollers, and piston rings and cylinders. Smooth surface finish is also important in decreasing wear by reducing the local pressures.

Antiwelding films over the hard surfaces will reduce wear so long as the films remain intact and are not in themselves abrasive. A tin or cadmium flash on new pistons is often used as a temporary antiwear agent while a permanent coating is being built up during running in.

Evaluation of wear resistance is best obtained through a simulated service test of the actual assembly or a scale model. Wear-testing machines may test the relative merits of lubricants but are generally misleading for machine design because of exaggeration of service conditions. It is better to use more precise methods of measurement than to accelerate the rate of wear.

The process of running in is generally classed as a beneficial wear phenomenon. It was originally thought that the running of newly assembled parts at reduced loads and speeds produced greater conformance of the surfaces through gradual wear of the offending high spots so that ultimately the system would be able to carry a greater load than would otherwise be the case. That a better performance will result from this practice is well established, but its explanation is not clear. Dayton [6] and others [7] have measured the metal worn off during running in, through microchemical analysis of the oil, but the amounts are either very small or quite inappreciable and disappear even while the running in is still increasing the load capacity. The changes in surface profile are too small to be measured by an instrument although the surfaces often look smooth and bright to the eye after running in. These changes can be accentuated by the use of the chemical polishing agents described in Art. 13.6. It is true, however, that a very slight smoothing of sharp roughnesses may represent a large increase in the effective load-supporting area. The improvement is generally greatest with the harder bearing materials and least with babbitt. Running in of the harder bearing materials generally produces a glazed appearance, particularly in the case of piston rings and cylinders, and there is some evidence that this appearance indicates the presence of a very thin surface layer, having altered chemical and metallurgical properties. The nature of these changes has not yet been determined.

It therefore seems probable that the beneficial effects of running in are due in part to a change in surface profile and in part to the formation of a wear-resistant layer, at least on the harder materials.

13.13. Rolling Friction. The so-called "antifriction" bearings, ball and roller bearings, substitute rolling friction for sliding friction. Rolling friction is very much less than sliding friction under any conditions of boundary lubrication, particularly in starting from rest; but where perfect fluid lubrication can be assured, the coefficient of friction of a plain journal bearing can be made lower than that of ball or roller bearings.

Rolling friction arises entirely from the elastic deformation of the two surfaces. It is distinguished by the fact that the maximum stress in the

metal is at a small but finite depth below the surface and failure is due, not to surface adhesions or galling or wear, but to fatigue cracks starting in the region of maximum stress and causing small pieces of the surface to flake, or spall, out. A metal of high fatigue resistance is important here. Where sliding is added to the rolling, as in the case of gear teeth, the region of maximum stress is raised nearer the surface. The total stress may be increased, but the wear is more of the surface type, a less harmful kind. Extreme-pressure lubricants cut down the sliding or surface wear but can do nothing for the subsurface or fatigue type of failure.

The use of any large quantity of fluid lubricant in antifriction bearings is to be avoided. A fluid can have no effect on the fatigue of a metal, and the churning of the oil by the balls or rollers will increase the friction and operating temperature. Hence there is no real lubrication problem for these bearings except between the balls or rollers and their cages. However, grease should be used to keep out dust and grit, which are extremely harmful, and also to prevent rusting of the surfaces.

13.14. Lubrication of Piston Rings and Cylinders. The lubrication of the pistons and piston rings of high-duty internal-combustion engines presents today the most critical problem of boundary lubrication. A combination of conditions unfavorable to lubrication conspires to defeat the designer's efforts to develop more power per unit of piston displacement.

The piston rings are subjected to high temperature, a doubtful supply of lubricant, high gas pressure behind the rings, and intermittent motion. The lubricant trapped in the rings is liable to break down chemically under high piston temperature and to deposit carbon, gum, and hard varnish. The usual oiliness agents are ineffective at such high temperatures, but chemical addition agents are frequently used as oxidization inhibitors and as detergents.

The case of the piston is peculiar in that the side thrust of the connecting rod is taken on a line contact with the cylinder wall, with motion in the direction of the line. Gear teeth also make line contact, but the rubbing is transverse to the line, and there is some chance to form an oil wedge. The lubrication of gears is also favored by the generally continuous nature of the motion.

Piston rings are usually made of cast iron and are carefully run in against a smooth cylinder liner of hard steel, sometimes nitrided. Where dust and grit are present, as in desert operation, wear is rapid. Chromium-plated steel rings, grooved rings, and other expedients to minimize wear are active subjects of research. Cast-iron pistons have a distinct advantage for boundary lubrication from the graphite content but are too massive for very high-speed engines because of high dynamic forces.

High-speed diesel engines often use thin-walled steel pistons designed to block the flow of heat from the crown to the rings. Airplane engines

generally use thick-walled aluminum-alloy pistons, which, although light, are especially unfavorable to lubrication since they conduct heat too well from the crown to the rings. The lubricant, therefore, must be copiously supplied to the inside of the pistons, to cool them, thus necessitating oil radiators and an elaborate circulating system. Extreme precautions are taken in running in new pistons to avoid seizure before good boundary-lubrication conditions are established.

13.15. Summary. We may summarize this chapter by the statement that the performance of sliding surfaces operating under conditions of imperfect, or boundary, lubrication depends on a large number of factors, many of which are difficult to evaluate. Some of them are

The molecular structure of the lubricant and its addition agents.

The chemical properties of the lubricant and its addition agents.

The supply of lubricant.

The surface properties of the bearing materials.

The bulk properties of the bearing materials.

The physical structure of the bearing materials, *i.e.*, whether homogeneous, duplex, or thin film.

The roughness of the surfaces.

The problem of selecting the best materials for boundary operation is one that can be treated only qualitatively at the present time and usually requires some compromise among the factors listed above. Further investigation of the mechanism of dry friction and of the physics and chemistry of the metal-lubricant interface is needed to give a better understanding of the subject.

SELECTED BIBLIOGRAPHY

1. KINGSBURY, A.: A New Oil-testing Machine and Some of Its Results, *Trans. Am. Soc. Mech. Engrs.*, vol. 24, pp. 143-160, 1903.
2. ADAM, N. K.: "The Physics and Chemistry of Surfaces," 2d ed., Chap. V, Oxford University Press, New York, 1938.
3. BOWDEN, F. P., J. N. GREGORY, and D. TABOR: Lubrication of Metal Surfaces by Fatty Acids, *Nature*, vol. 156, pp. 97-101, 1945.
4. BURWELL, J. T.: Role of Surface Chemistry and Profile in Boundary Lubrication, *S.A.E. J. (Trans.)*, vol. 50, pp. 450-457, 1942.
5. BEECK, O., J. W. GIVENS, and E. C. WILLIAM: Wear Prevention by Addition Agents, *Proc. Roy. Soc. (London)*, ser. A, vol. 177, pp. 103-118, 1940.
6. DAYTON, R. W., H. R. NELSON, and L. H. MILLIGAN: Surface Finish of Journals, *Mech. Eng.*, vol. 64, pp. 718-726, 1942.
7. BURWELL, J. T., J. KAYE, D. W. VAN NYMEGEN, and D. A. MORGAN: Effects of Surface Finish, *J. Applied Mechanics*, vol. 8, pp. A49-A58, 1941.
8. WULFF, J.: Proc. MIT Summer Conferences on Friction and Surface Finish, June, 1940, p. 13.
9. BOWDEN, F. P., A. J. W. MOORE, and D. TABOR: Ploughing and Adhesion of Sliding Metals, *J. Applied Phys.*, vol. 14, pp. 80-91, 1943.

10. ERNST, H., and M. E. MERCHANT: ASM Symposium on Surface Treatment of Metals, October, 1940, p. 299.
11. BOWDEN, F. P., and K. E. W. RIDLER: The Temperature of Sliding Metals and Lubricated Surfaces, *Proc. Roy. Soc. (London)*, ser. A, vol. 154, pp. 640-656, 1936.
12. BOWDEN, F. P., and A. J. W. MOORE: Adhesion of Lubricated Metals, *Nature*, vol. 155, pp. 451-452, 1945.
13. SAKMANN, B. W., J. T. BURWELL, and J. W. IRVINE: Measurements of the Adhesion Component in Friction, *J. Applied Phys.*, vol. 15, pp. 459-473, 1944.
14. CLOWER, J. I.: "Lubricants and Lubrication," McGraw-Hill Book Company, Inc., New York, 1939.
15. THOMSEN, T. C.: "The Practice of Lubrication," 3d ed., McGraw-Hill Book Company, Inc., New York, 1937.

CHAPTER XIV

HYDRAULIC TURBINES

The purpose of a hydraulic turbine is to convert gravity potential energy of water into shaft work. Experience teaches that all such energy could be so converted by an ideal turbine in which friction was absent. An actual turbine is arranged by artifices of design to alter the momentum of a stream of water as it passes through some sort of wheel having buckets or vanes. The forces resulting from this sustained momentum change cause the wheel to turn against an external load and thus perform work. The inevitable friction causes such a machine to fall somewhat short of the ideal, but the modern hydraulic turbine is one of the most efficient prime movers in existence.

The difference between the initial and final water levels, known as the "head," differs greatly from one installation to another. In mountainous country a head amounting to many hundred feet may be available, while elsewhere the head may be as low as 10 ft or even less. The amount of water available also depends on location and in general is small for high heads and large for low heads. These natural differences in the conditions of operation have given rise to three principal types of turbine, the impulse turbine, the radial- and mixed-flow reaction turbine, and the axial-flow, or propeller, reaction turbine. The first type is suited to high head and small discharge, the second covers the intermediate range, while the third handles a large volume under low head.

In an impulse turbine one or more nozzles direct jets of water at atmospheric pressure against buckets on the rim of a wheel. Most of this kinetic energy is utilized by the wheel, the discharge having just enough velocity left to move clear of the buckets before falling into the low-level reservoir, or "tail water." The water thus loses kinetic energy as it passes through an impulse wheel but enters and leaves at the same pressure.

In a reaction turbine, on the other hand, the flow through the wheel, or runner, is completely enclosed, and both the pressure and velocity at exit are different from those at entrance. The terms "radial flow" and "axial flow" refer to the direction of water movement through the runner.

14.1. Impulse Turbine. The impulse turbine is represented by the Pelton wheel, shown in Fig. 14.1, developed in California about 1880 to utilize the high heads available in the mountains. As already stated, the head of the supply water is converted into one or more high-velocity free jets which are directed against buckets mounted on the rim of a wheel.

These buckets are spoon shaped, with a central ridge dividing the impinging jet into halves, which are deflected backward relative to the bucket through an angle of about 165 deg. The spouting velocity of the water is very high for high heads, but with a large-diameter wheel only moderate speeds

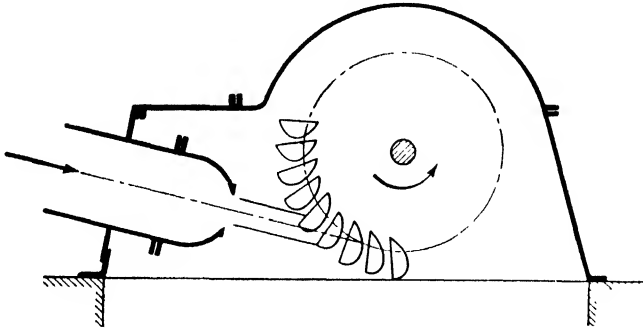


FIG. 14.1. — Impulse turbine.

of rotation are required. Present practice, for heads greater than 1,000 ft, is to use the Pelton turbine exclusively. It is also frequently employed for lower heads where insufficient water is available to operate any other type of turbine at good efficiency. Since the maximum practicable jet diameter is limited, the volume of water that can be handled under a low head is much less than that for a reaction turbine. Hence the Pelton wheel is essentially a high-head low-discharge machine. The highest head so far used is 5,800 ft in Switzerland, where a wheel with a single jet develops 30,000 hp. There are numerous installations in California, one of which has two double units, each of 56,000 hp. The highest efficiency obtained to date with a Pelton turbine is approximately 91 per cent, but for most installations the efficiency is between 85 and 90 per cent.

The runaway speed of an impulse turbine may be nearly double the normal operating speed. The runner and any machine connected to the turbine should be built to withstand the centrifugal stresses caused by removal of the load.

The resultant external torque on the system comprising the wheel and shaft and the water between sections 2 and 3 of Fig. 14.2 can be computed by means of the angular-momentum law. For this purpose we refer to the velocity diagrams of Fig. 14.2*b*, which gives an end view of a single bucket, such as would be presented to an observer in the plane of the wheel and looking toward the axis of rotation. We assume (1) that the absolute velocities V_2 and V_3 are uniform over sections 2 and 3 and are independent of time, (2) that the absolute flow on the buckets is cyclic, and (3) that the tangential velocity components V_2 and V_t have the same moment arm r . Equation (6.17) thus yields

$$\text{Resultant clockwise torque} = \rho Q r (V_2 - V_t)$$

This resultant exceeds the useful shaft torque T by the amount of the torques due to bearing friction and windage. It is therefore convenient

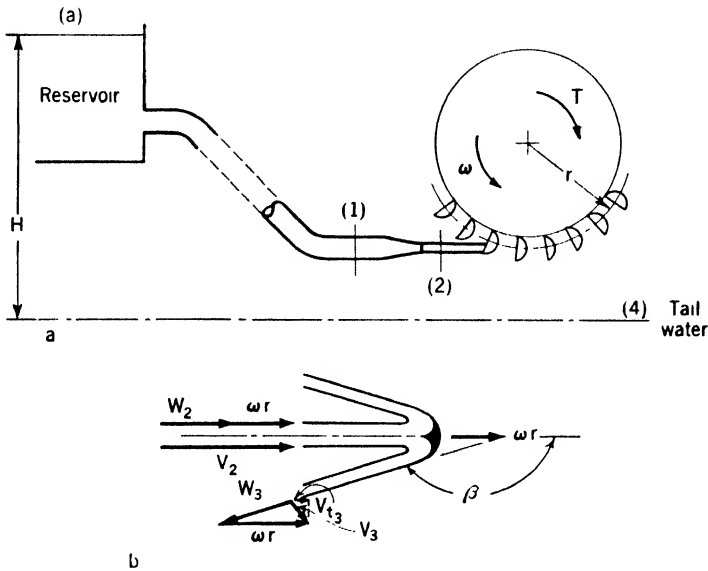


FIG. 14.2. — (a) Schematic side elevation of impulse turbine. (b) Section through bucket; sectioning plane normal to radius at radius r .

to define a mechanical efficiency η_m by the formula

$$\eta_m = \frac{\omega T}{\omega(\text{resultant torque})} \quad (14.1)$$

so that

$$T = \eta_m \rho Q r (V_2 - V_{t_2}) \quad (14.2)$$

Equation (14.2) can be put into a more useful form with the aid of the energy equation. Since we have assumed the absolute flow to be cyclic, we could use Eq. (5.10), which refers to fixed axes. It is much simpler, however, and the same result is obtained if the relative flow is assumed steady during the time each bucket is operative and Eq. (6.22), for rotating axes, is employed. Neglecting fluid friction on the buckets and any change in level between 2 and 3, we thus find that $W_2 = W_3$. This relation, together with the velocity diagrams of Fig. 14.2b, permits the torque to be expressed as

$$T = \eta_m \rho Q r (V_2 - \omega r)(1 - \cos \beta) \quad (14.3)$$

The output power P is equal to ωT ; hence, by Eq. (14.3),

$$C_P = \frac{P}{(\rho/2)QV_2^2} = \eta_m 2x(1-x)(1 - \cos \beta) \quad (14.4)$$

where $x = \omega r/V_2$ and C_P is a dimensionless power coefficient. If, as a first approximation, η_m is assumed to be a constant, Eq. (14.4) shows that, for any given value of β , C_P is a maximum for $x = \frac{1}{2}$, and that

$$C_{P_{\max}} = \eta_m \frac{1 - \cos \beta}{2} \quad (14.5)$$

In an actual turbine, the optimum value of x is about 0.45, instead of $\frac{1}{2}$, owing, in large measure, to the variation of η_m with x and, to a lesser extent, to friction in the flow over the buckets.

The efficiency of any hydraulic turbine is defined as the ratio of the actual shaft work to that which could be done in a frictionless machine. The frictional effects in the inlet duct are omitted in this definition, the inlet duct not being considered part of the turbine. Furthermore, in the case of the Pelton turbine, the slight difference in level between the nozzle exit 2 and the tail-water level 4 is disregarded. The energy equation [Eq. (5.10)] gives $\mathfrak{W}_s = gH - (u_4 - u_0 - q_{0,4})$, where, since the fluid is incompressible, $u_4 - u_0 - q_{0,4}$ is the energy dissipated by friction. Using the notation introduced in Chap. VIII, namely, $gH_{i,4} = u_4 - u_0 - q_{0,4}$, we have $\mathfrak{W}_s = g(H - H_{i,4}) - gH_{l,4}$. The efficiency is thus

$$\eta = \frac{\mathfrak{W}_s}{g(H - H_{i,4})} = \frac{\mathfrak{W}_s}{\mathfrak{W}_s + gH_{l,4}} \quad (14.6)$$

where $H - H_{i,4}$, the total head minus the loss in the inlet pipe, is called the "effective head."

We obtain an expression for efficiency that is more useful in the present case, by writing Eq. (5.10) between sections 1 and 4 (neglecting the slight difference in height between these two sections).

$$\mathfrak{W}_s = \frac{p_1 - p_4}{\rho} + \frac{V_1^2}{2} - gH_{l,4} \quad (14.7)$$

Noting that $\mathfrak{W}_s = P/\rho Q$, we find from Eqs. (14.6) and (14.7)

$$\eta = \frac{\mathfrak{W}_s}{[(p_1 - p_4)/\rho] + (V_1^2/2)} = \frac{C_P}{[2(p_1 - p_4)/\rho V_2^2] + (V_1^2/V_2^2)} \quad (14.8)$$

This equation is true in general and is not restricted by the assumption of frictionless flow over the buckets or through the nozzle. It is interesting to note that, in case the nozzle is assumed frictionless, the denominator of Eq. (14.8) reduces to 1 and $\eta = C_P$. If, further, friction of the water on the buckets is neglected, Eq. (14.4) may be used, and

$$\eta = \eta_m 2x(1 - x)(1 - \cos \beta) \quad (14.9)$$

Under these idealized conditions, the maximum value of η is equal to $\eta_m [(1 - \cos \beta)/2]$, η_{\max} being less than η_m solely because β must be less than

π to enable the flow to clear the buckets. For $\beta = 165^\circ$ and $\eta_m = 0.97$, $\eta_{\max} = 0.953$. As already mentioned, the maximum efficiency attained in practice is approximately 0.91.

The relationship between the efficiency and the output power measures the performance of a turbine over a range of operating conditions. According to the idealized equation (14.9), the efficiency of an impulse turbine of given blade angle β depends only on the ratio $x = \omega r / V_2$, regardless of the power output. Actually, there is some variation of η as P is changed with x constant. The discharge rate and hence P are usually controlled by means of a needle valve, which changes the effective cross-sectional area of the nozzle without much change in the velocity. Figure 14.3 gives an example of such an η versus P curve.

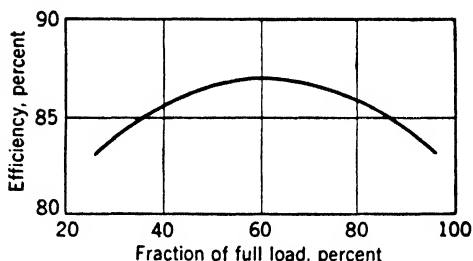


FIG. 14.3. — Efficiency versus output power for an impulse turbine.

14.2. Radial- and Mixed-flow Turbines. A turbine of this type is shown in Fig. 14.4. The flow, which is totally enclosed, enters the guide vanes directly from the inlet duct. These guides impart a tangential velocity and hence angular momentum to the water before it enters the revolving runner, in which its angular momentum is reduced. This change in angular momentum of the water as it passes through the runner gives rise to the driving torque of the turbine. From Fig. 14.4 it is clear that this type of turbine, known as the Francis turbine after J. B. Francis, who developed it in 1849, can handle a greater volume of flow than can an impulse turbine. Individual designs of runner include not only the purely radial-flow type, which is suited to relatively small volumes and high heads, but also the mixed-flow types shown in Fig. 14.5, which work efficiently with larger volumes and lower heads. On account of these wide design variations it has been possible to build Francis turbines to run at heads as low as 15 ft and as high as 750 ft. Installations up to 150,000 hp have been made, with efficiencies in the neighborhood of 94 per cent.

The resultant external torque on the system comprising the runner and shaft and the water inside the runner between sections 2 and 2' of Fig. 14.4 can be computed from the angular-momentum law [Eq. (6.17)].

$$\text{Resultant clockwise torque} = \rho Q(r_2 V_{t_2} - r_2' V_{t_2'})$$

This resultant exceeds the useful shaft torque T by the amount of the torques due to bearing friction and the water drag on the shroud of the runner. Defining the mechanical efficiency as in Eq. (14.1), we get

$$T = \eta_m \rho Q(r_2 V_{t_2} - r_2' V_{t_2'}) \quad (14.10)$$

In the case of the radial-flow turbine of Fig. 14.4, r_2 and V_{t_2} are both uniform over $2'$, so that Eq. (14.10) has a definite meaning. On the other hand, for mixed-flow runners as in Fig. 14.5, both r_2 and V_{t_2} vary over $2'$, and the meaning of Eq. (14.10) is not clear. There is no difficulty, however, if we consider only operating conditions near the design point, where the

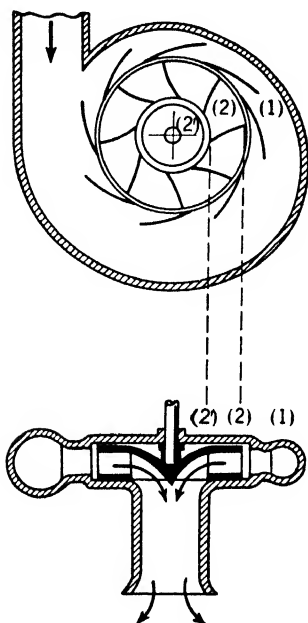


FIG. 14.4. — Radial-flow turbine.

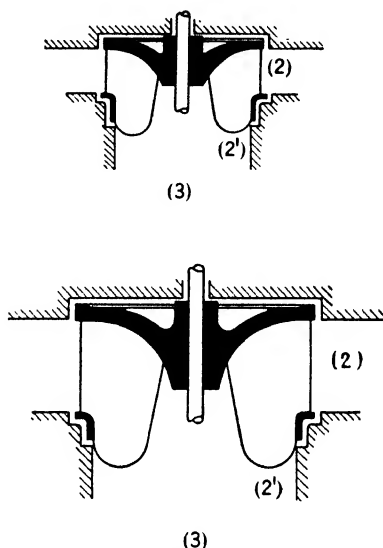


FIG. 14.5. — Mixed-flow runners.

maximum efficiency obtains. Under these conditions it is shown below in Art. 14.4 that the blades must be designed to make $V_{t_2} = 0$ everywhere, so that Eq. (14.10) reduces to $T = \eta_m \rho Q r_2 V_{t_2}$. For operation away from the design point it is desirable that $r_2 V_{t_2} = \text{constant}$ everywhere, but this condition is practically impossible to fulfill with a mixed-flow runner. Further discussion is deferred to Art. 14.4.

We define the efficiency as in Eq. (14.6), including as part of the turbine everything between sections 1 and 5 of Fig. 14.6. Noting that $\mathcal{W}s = T\omega/\rho Q$, we combine Eqs. (14.6) and (14.10), to get

$$\eta = \eta_m \frac{\omega(r_2 V_{t_2} - r_2' V_{t_2}')}{g(H - H_{v,1})} \quad (14.11)$$

which is sometimes referred to as Euler's turbine equation; it is of basic importance in turbine design.

Referring to Fig. 14.6, we break up the losses into several kinds.

- a. Friction losses between 0 and 1 in the inlet pipe.
- b. Friction losses between 1 and 2 in the guides.
- c. Entrance losses and friction losses between 2 and 3 in the runner.

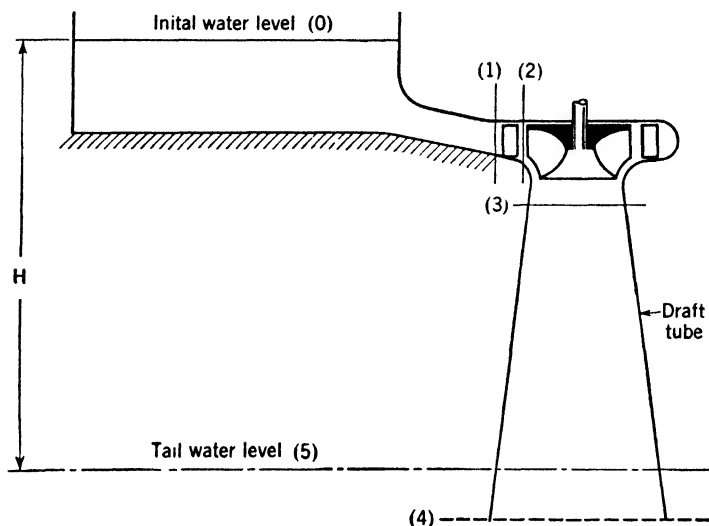


FIG. 14.6. — Schematic side elevation of a mixed-flow turbine.

Entrance losses occur if the speed, discharge rate, and guide-vane setting are improperly related, causing the relative velocity at 2 not to be tangent to the leading edge of the runner blade.

The condition shown in Fig. 14.7a is corrected in Fig. 14.7b by a de-

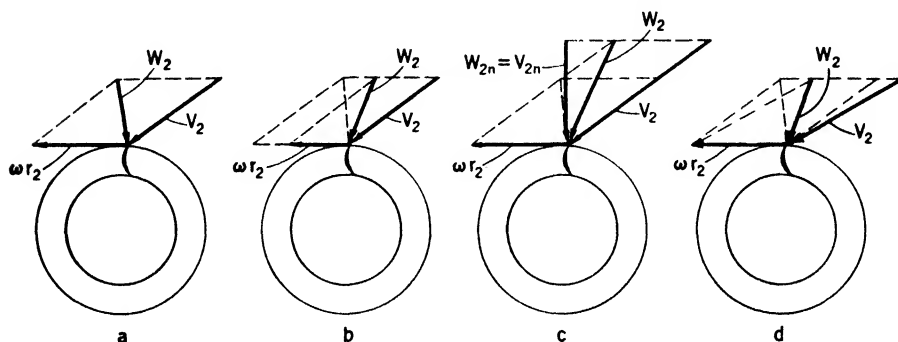


FIG. 14.7.

crease in ω , in Fig. 14.7c by an increase in Q ($= 2\pi r_2 b_2 V_{n2}$, where b_2 is the thickness of the runner at its periphery), and in Fig. 14.7d by a change in the setting of the guides, which control the direction of V_2 .

- d. Friction and separation losses between 3 and 4 in the draft tube.

e. Shock losses between 4 and 5 produced by the sudden enlargement of the cross-sectional area of the flow at the draft-tube exit. Since the area changes from a finite value at 4 to a practically infinite one, it is clear that all the kinetic energy of the flow at 4 will be dissipated by viscosity in the tail water. This conclusion can be checked by reference to Eq. (8.62).

14.3. Draft Tube. The purpose of the divergent draft tube is to make the sum of the losses between sections 3 and 5 of Fig. 14.6 smaller than would otherwise be possible. Both the exit loss and the loss in the draft tube depend on the area ratio A_4/A_3 . Since the exit loss is merely the kinetic energy of the flow at 4, we may define an exit-loss coefficient as $C_{4,5} = 2gH_{t_{4,5}}/V_3^2 = V_4^2/V_3^2$. By continuity,

$$C_{4,5} = \frac{V_4^2}{V_3^2} = \frac{A_3^2}{A_4^2} \quad (14.12)$$

The combined friction and separation loss in a conical diffuser has been studied experimentally by several investigators. Their results [3] are

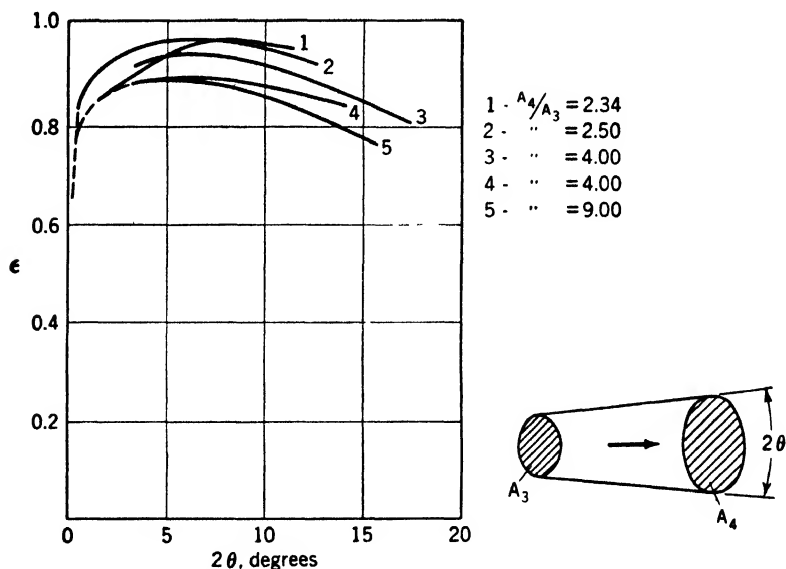


FIG. 14.8. — Diffuser efficiency ϵ versus diffuser angle 2θ for various exit-to-entrance-area ratios. (After Patterson, reference 3. Courtesy of Aircraft Engineering.)

conveniently expressed in terms of a diffuser efficiency ϵ , defined as $\epsilon = [p_4 - p_3 + \rho g(z_4 - z_3)]/(\rho/2)V_3^2[1 - (A_3/A_4)^2]$. Experimental values of ϵ as a function of the diffuser angle 2θ and the area ratio A_4/A_3 are plotted in Fig. 14.8. It is seen that, to a first approximation, the maximum value of ϵ is 0.9 for all values of A_4/A_3 tested and that it occurs at a value of 2θ approximately equal to 6 deg. The shape of these curves is easily

accounted for in terms of familiar concepts. For any given area ratio the length of the diffuser becomes so great at small values of θ that the flow is essentially like that in a straight tube and the wall friction is excessive. As the angle of flare increases beyond the optimum value, however, the adverse pressure gradient associated with the deceleration of the fluid becomes big enough to cause a rapid thickening of the boundary layer and

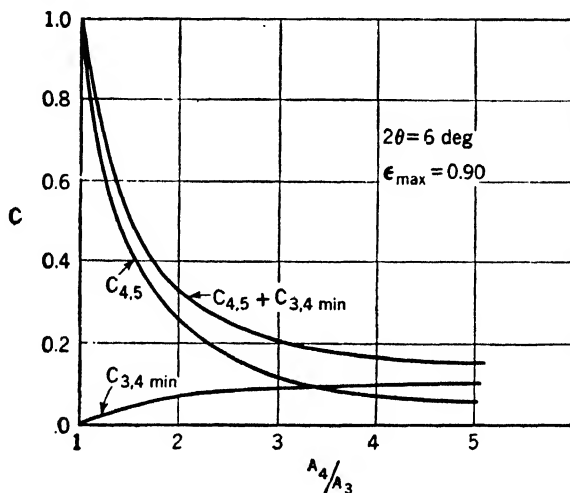


FIG. 14.9. — Loss coefficient C versus ratio of exit to entrance area A_4/A_3 for a diffuser.

separation of the flow from the wall. From the definition of ϵ , the equation of continuity, and Eq. (5.10), we find that

$$\epsilon = 1 - \{2gH_{l_{3,4}}/V_3^2[1 - (A_3/A_4)^2]\}.$$

Defining the loss coefficient for a diffuser (draft tube) as $C_{3,4} = 2gH_{l_{3,4}}/V_3^2$, we get

$$C_{3,4\min} = \frac{2gH_{l_{3,4\min}}}{V_3^2} = (1 - \epsilon_{\max}) \left[1 - \left(\frac{A_3}{A_4} \right)^2 \right] \quad (14.13)$$

Values of $C_{4,5}$ and $C_{3,4\min}$, computed from Eqs. (14.12) and (14.13), respectively, are plotted against A_4/A_3 in Fig. 14.9. It is seen that the sum of the draft-tube and exit-loss coefficients decreases rapidly as A_4/A_3 is increased from 1 to 3 but that little is gained by use of a larger area ratio. If an area ratio $A_4/A_3 = 3$ is used, the corresponding diameter ratio is $d_4/d_3 = 1.7$; and the length-diameter ratio is $(z_3 - z_4)/d_3 = 6$, since the total flare angle $2\theta = 6$ deg.

14.4. Conditions for Efficient Operation. There are two conditions of operation that must be met if the efficiency of a turbine is to be a maximum. (1) The speed, discharge, and guide setting must be adjusted to ensure shockless entry of the water into the runner. (2) The outflow from

the draft tube must have no tangential velocity component. Such a component is undesirable since it plays no role in getting the water out of the draft tube but merely increases the kinetic energy of the outflow and thus the exit shock loss. To translate this condition into one that applies at section 2' of Fig. 14.6, we neglect friction and use the angular-momentum equation between sections 2' and 4. Since the efflux of angular momentum at 4 is zero by assumption and no torque acts on the fluid, the angular momentum crossing 2' must also be zero, that is, V_t must be zero everywhere over section 2'. This requirement can be fulfilled at the design conditions of operation by use of properly shaped runner blades.

For operating conditions away from the design point there will be non-zero values of V_t at section 2' and, consequently, everywhere in the draft tube, angular momentum being conserved. In order that this tangential velocity may not, through centrifugal effects, cause intermingling of the stream tubes and thus give rise to eddy losses, it should be distributed in a definite way along the radius. To determine this distribution, we consider first section 3 and assume that there the axial velocity component is uniformly distributed and the radial component is zero. We also neglect friction and assume the blades to be so shaped that any element of the discharge dQ flows through a vase-shaped stream tube, as in Fig. 14.10,

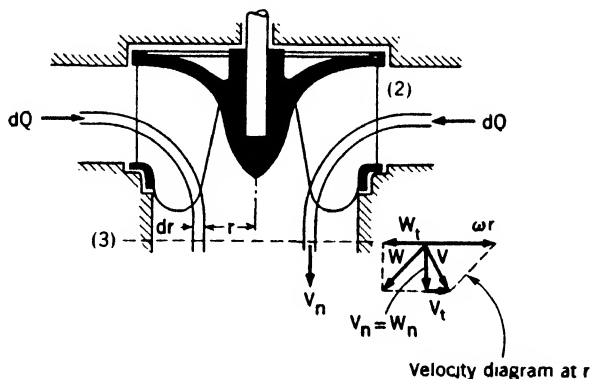


FIG. 14.10.

not mingling with other elements. In the figure, dQ is the volume that at 3 passes through the annulus of radius r and width dr . Neglecting for simplicity any change in level between 2 and 3, we may write the energy equation for rotating axes [Eq. (6.22)] in the form

$$p + \frac{\rho}{2} W^2 - \frac{\rho}{2} \omega^2 r^2 = p_2 + \frac{\rho}{2} W_2^2 - \frac{\rho}{2} \omega^2 r_2^2$$

where the symbols without subscript refer to any point of section 3. Conditions are assumed uniform at 2, so that the right-hand side of the equation is the same for all stream tubes and

$$p + \frac{\rho}{2} W^2 - \frac{\rho}{2} \omega^2 r^2 = \text{constant} \quad (14.14)$$

The further condition, that the radial pressure change balance the centrifugal force at 3, is obtained from Eq. (4.4) by the substitution of $-\partial p/\partial r$, V_t , and r in place of $\partial p/\partial n$, V , and R , respectively.

$$\frac{\partial p}{\partial r} = \rho \frac{V_t^2}{r} \quad (14.15)$$

Differentiate Eq. (14.14) with respect to r , substitute for $\partial p/\partial r$ from Eq. (14.15), and use the fact that $W^2 = W_t^2 + W_n^2 = (\omega r - V_t)^2 + V_n^2$.

$$\rho \frac{V_t^2}{r} + \frac{\rho}{2} \frac{\partial}{\partial r} [(\omega r - V_t)^2 + V_n^2] - \rho \omega^2 r = 0$$

Since V_n is independent of r by assumption, we finally get

$$\left(\frac{V_t}{r} + \frac{\partial V_t}{\partial r} \right) (V_t - \omega r) = 0 \quad (14.16)$$

For blades designed to give $V_t = 0$ at the design point the second factor of Eq. (14.16) is in general not equal to zero. It is therefore necessary that the first factor be zero. The differential equation thus obtained is

$$\frac{1}{V_t} \frac{\partial V_t}{\partial r} dr + \frac{dr}{r} = 0$$

which integrates to $rV_t = \text{constant}$. It thus appears that, if V_t is not everywhere zero, it should be distributed like the velocity in a potential vortex, so that the resultant flow at 3 is the sum of an axial motion and a vortex motion with its axis at the center of rotation (see Arts. 4.11 and 11.14). In the absence of friction the angular momentum of the fluid is conserved, and the circulation, or strength, of this vortex, $\Gamma = 2\pi rV_t$, will be constant throughout the draft tube.

It may be remarked that the stability condition $rV_t = \text{constant}$ is not in general fulfilled in a mixed-flow turbine, except for a limited range of operating conditions. In a purely radial-flow turbine, however, this condition is satisfied if the entrance to the draft tube is properly designed. For in this case the flow is assumed uniform at the runner

exit at radius r_2' (Fig. 14.11). In the absence of friction, no torque is exerted on the fluid in any stream tube between sections 2' and 3, so that the angular-momentum law [Eq. (6.17)] gives $dT = 0 = \rho dQ(rV_t - r_2'V_{t_2})$ or $rV_t = r_2'V_{t_2} = \text{constant}$.

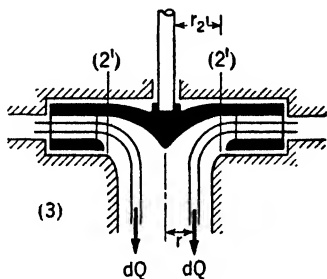


FIG. 14.11.

14.5. Axial-flow Turbine. An axial-flow (or propeller) turbine, such as is shown in Fig. 14.12, is able to handle a larger volume on a given diameter than other types, since the discharge is relatively unrestricted by the

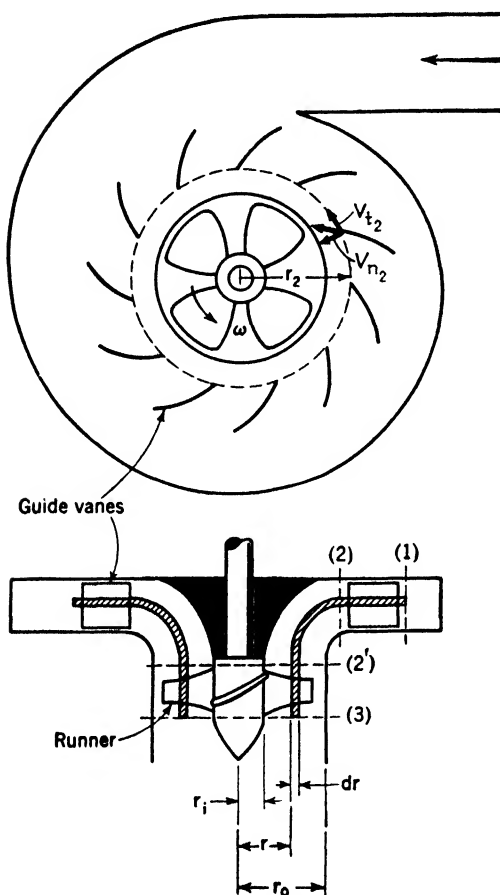


FIG. 14.12. — Diagrammatic sketch of an axial-flow turbine.

the stream turns through a right angle and is assumed to have no radial velocity component as it passes through the runner. It is further assumed that the axial component of velocity is uniformly distributed over the cross-sectional area of the stream at sections 3 and 4. Both these assumptions can be realized by suitable design of the passages and runner blades.

The resultant external torque on the system comprising the runner, the shaft, and the fluid between sections 2' and 3 is readily obtained by familiar methods. The argument of the last paragraph of Art. 14.4 can be applied

wheel. The modern low-head turbine of the propeller type is usually fitted with blades that can be adjusted to suit operating conditions, a feature due to Dr. Viktor Kaplan of Czechoslovakia. It is of more compact construction than the Francis type, runs faster, and has a higher partial-load efficiency, owing to the adjustable pitch of the blades. The Francis wheel may have some 16 blades and an outer shroud ring. The Kaplan turbine usually has but 4 to 6 blades and no shroud ring, so that the surface subjected to high water speeds is comparatively small, and so are the frictional losses. An efficiency above 92 per cent is practical with units up to 60,000 hp capacity.

As shown in Fig. 14.12, the guide vanes for a Kaplan turbine are arranged in the same way as for a Francis turbine and serve the same purpose, *viz.*, to impart angular momentum to the flow. Before entering the runner, however,

between sections 2 and 2' of Fig. 14.12 to show that, at 2', $rV_t = \text{constant} = r_2V_{t_2}$. Furthermore, the analysis leading to Eq. (14.16) is valid between sections 2' and 3 of Fig. 14.12 and indicates that the blades should be designed to give, at 3, $rV_t = \text{constant}$ (preferably zero). From the angular-momentum law we thus get

$$\text{Resultant torque} = \rho Q(r_2'V_{t_2'} - r_3V_{t_3})$$

and if the mechanical efficiency is defined as in Eq. (14.1), the useful shaft torque is

$$T = \eta_m \rho Q(r_2'V_{t_2'} - r_3V_{t_3}) \quad (14.17)$$

The discussion of efficiency, losses, and draft tube given in connection with the Francis turbine is equally valid for a Kaplan turbine.

A rational method of blade design, based on wind-tunnel data on air-foils, is possible for an axial-flow machine. Since the flow is assumed to follow annular stream tubes, as in Fig. 14.12, the blade elements of length dr in one stream tube can be designed without reference to adjoining elements. The essentially two-dimensional flow over a blade element at radius r is conveniently represented by unrolling of the annular stream tube onto a plane, as in Fig. 14.13. The local velocity diagrams are determined by over-all requirements of head, discharge, efficiency, speed, and hub and casing diameters, together with the condition that the product rV_t be independent of radius. If, in addition, the lift and drag coefficients for two-dimensional flow over the profile are known, it is not difficult to determine with a useful degree of accuracy the chord length and angle of the element. A detailed discussion of the theory is deferred to Chap. XV; for the present it is sufficient to remark that the blade angle must decrease toward the blade tip.

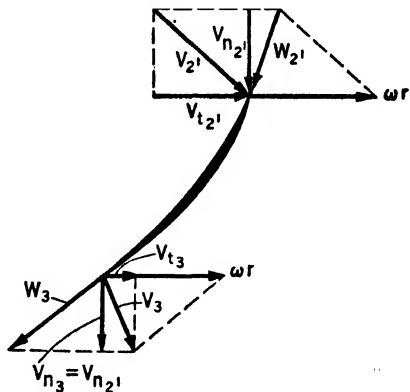


FIG. 14.13. — Velocity diagram at radius r of an axial-flow turbine.

14.6. Dimensional Analysis of a Turbine. Two important uses of dimensional theory in connection with a turbine are (1) to determine what type of turbine will operate most efficiently under given conditions of head, speed, and power; and (2) to predict the performance of a prototype from tests on a model.

We begin the analysis by listing, on the basis of experience, the independent variables ρ , μ , g , H , Q , D , and ω , for a turbine of given design. The runner diameter D is here chosen as a convenient measure of size.

This list can be simplified if we notice that the incompressible flow in a reaction turbine is totally enclosed, except at the surfaces of the initial and tail-water reservoirs. The gravity field, therefore, affects the flow only in connection with the over-all potential-energy change gH , the flow pattern being otherwise independent of g . The same is true also of an impulse turbine, because the velocity of the free jet is so high that g has no influence on it (see Art. 4.7a). We may accordingly express the output power and efficiency as functions of six independent variables.

$$P = f_1(\rho, D, \omega, Q, gH, \mu) \quad (14.18)$$

$$\eta = f_2(\rho, D, \omega, Q, gH, \mu) \quad (14.19)$$

At this stage it is advisable to test whether the variables in parentheses are really independent, as assumed. Consider, for example, a change in gH . By suitably readjusting a valve, or gate, in the system and changing the load, we can keep ω and Q constant. The other variables will be unaffected, except possibly by slight temperature changes, which are disregarded. Similarly, it can be shown that each variable can be altered independently of the other five. That no important variable has been omitted can only be decided by experiment or detailed analysis.

Applying the Π theorem to Eqs. (14.18) and (14.19) and including ρ , D , and ω in each of the four independent Π products, we get

$$\frac{P}{\rho\omega^3D^5} = f_3\left(\frac{Q}{\omega D^3}, \frac{gH}{\omega^2 D^2}, \frac{\rho\omega D^2}{\mu}\right) \quad (14.20)$$

$$\eta = f_4\left(\frac{Q}{\omega D^3}, \frac{gH}{\omega^2 D^2}, \frac{\rho\omega D^2}{\mu}\right) \quad (14.21)$$

Experiments show that, in the usual range of speed and size, the flow is highly turbulent and the viscosity has only a secondary influence on the behavior of a turbine. Variations in speed or size large enough to cause a change from turbulent to laminar conditions must of course be ruled out if μ is to be neglected. Subject to this restriction, we may write

$$\frac{P}{\rho\omega^3D^5} = f_3\left(\frac{Q}{\omega D^3}, \frac{gH}{\omega^2 D^2}\right) \quad (14.22)$$

$$\eta = f_4\left(\frac{Q}{\omega D^3}, \frac{gH}{\omega^2 D^2}\right) \quad (14.23)$$

Equations (14.22) and (14.23) are useful in the application of test data from a model to a prototype. Model data plotted in terms of these dimensionless quantities are immediately applicable to a prototype, provided that the influence of viscosity is negligible, as we have assumed. These equations also show that, if H , ω , ρ , and D are all constant (*i.e.*, if the head

and speed of a given hydraulic turbine are held fixed), P and η are functions of Q only, so that Q may be eliminated and η plotted against P . Such a curve for a Pelton turbine is given above in Fig. 14.3, while curves for several reaction turbines are shown in Fig. 14.14. The efficiencies of the fixed-blade machines, especially the Francis turbine, are seen to be excellent at the design point, but they drop off rapidly if the load changes, because the blade shape is then incorrect, the flow is much disturbed, and eddy

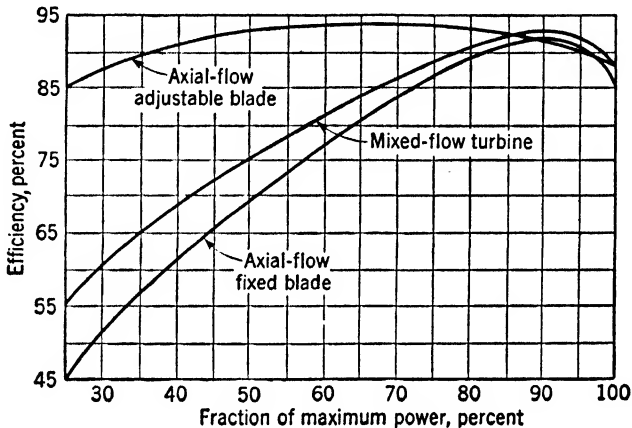


FIG. 14.14. — Curves of efficiency versus power for mixed- and axial-flow turbines. (Courtesy of G. E. Russell.)

losses occur. The efficiency of the Kaplan turbine, however, is maintained nearly constant over a wide range of load by means of a hydraulic servomotor that automatically adjusts both the guides and blades to the optimum setting.

The behavior of geometrically similar turbines operating at maximum efficiency is of interest, especially in connection with the choice of a turbine to run under given conditions of head, speed, and power. It is found that the efficiency is a maximum for only one pair of values of the two independent variables of Eq. (14.23). Thus, if $\eta = \eta_{\max}$,

$$\frac{Q}{\omega D^3} = \text{constant} = C_1 \quad (14.24)$$

$$\frac{gH}{\omega^2 D^2} = \text{constant} = C_2 \quad (14.25)$$

where the values of C_1 and C_2 depend on the design of the turbine. Equation (14.22) then yields

$$\frac{P}{\rho \omega^3 D^5} = \text{constant} = C_3 \quad (14.26)$$

These three equations indicate the effect of changes in ρ , ω , or D on Q , H , and P of a given type of turbine running at maximum efficiency. Furthermore, Eqs. (14.25) and (14.26) are the basis of the widely used "specific speed," which is discussed below.

Eliminate D from Eqs. (14.25) and (14.26), and get

$$\frac{\omega P^{1/2}}{H^{5/4}} = \frac{C_3^{1/2}}{C_2^{5/4}} \rho^{1/2} g^{5/4} \quad \text{or} \quad \frac{NIP^{1/2}}{H^{5/4}} = \frac{C_3^{1/2}}{C_2^{5/4}} \rho^{1/2} g^{5/4} \frac{60}{2\pi} \frac{1}{550^{1/2}}$$

where N is the speed in rpm, IP is the output horsepower, and H is the head in feet. The right-hand side of this equation has a definite constant value for a turbine of given design operating on water. This constant is called the specific speed N_s , so that

$$N_s = \frac{NIP^{1/2}}{H^{5/4}} \quad (14.27)$$

The name specific speed comes from the fact that, if a "specific turbine" be imagined that at maximum efficiency develops 1 hp under a 1-ft head, N_s is numerically equal to the speed, in rpm, of this turbine. The specific speed is used in the selection of the type of turbine best suited to operate at a given speed under a given head and produce a given horsepower. These three factors are determined by the characteristics of the site chosen for the installation and by the use to which the turbine is to be put. Experience shows that the range of allowable values for each of the principal types of turbine is as follows:

Kind of Turbine	Specific Speed N_s
Pelton (single jet).....	Not over 6
Pelton (multiple jet).....	Not over 10
Francis.....	10-110
Kaplan.....	100-215

Computation of the specific speed is thus the first step of the designer. He is then able to decide on the general type of turbine required for an efficient installation and can proceed with the details of the design.

14.7. Cavitation. The pressure everywhere in a turbine must be above a certain critical value if the continuity of the liquid is to be preserved. Otherwise, cavities of air and vapor will form, and the flow conditions will change, to the detriment of the efficiency. It has been found by tests on model turbines [6] that the formation of bubbles of air brought out of solution through lowering of the pressure has but a slight effect on the efficiency. The efficiency begins to be seriously affected only after bubbles of vapor start to form, *i.e.*, only after the vapor pressure has been reached somewhere in the flow. In the following discussion, the critical pressure will, accordingly, be identified with the vapor pressure:

The formation of vapor bubbles in a liquid through lowering of the pressure is called "cavitation." It is inherently an unstable phenomenon. In a flowing liquid, vapor bubbles form, grow and simultaneously move downstream, and ultimately collapse upon reaching a zone of higher pressure. The collapse causes a pressure wave, which spreads outward with the speed of sound relative to the liquid. If the zone of collapse is close enough to the place where the cavities form, the wave raises the pressure there above the critical value and cavitation ceases momentarily. The wave dies away very quickly, however, so that the phenomenon is repeated with a frequency that may be as high as several thousand cycles per second, depending on the apparatus involved. There may be no regular frequency associated with the cavitation if the collapse point is far downstream from the point of formation.

Cavitation is undesirable for two reasons. (1) The efficiency η decreases if a sufficient volume of cavitation is present. (2) Even though there may not be enough cavitation to affect η , the collapse of localized cavitation produces repeated impacts so intense that the blades may be seriously damaged. With this mechanical damaging action may be combined electrochemical effects, which accelerate the destruction.

According to the first paragraph of this article, the occurrence of cavitation depends on the value of the expression $p_m - p_v$, where p_m is the minimum pressure in the turbine and p_v is the vapor pressure of the water at the operating temperature. If $p_m - p_v > 0$, cavitation will not take place; but if $p_m - p_v = 0$, cavitation will, in general, occur. The efficiency thus depends on $p_m - p_v$ in addition to the other independent variables listed in Eq. (14.19).

$$\eta = f_1(\rho, D, \omega, Q, gH, \mu, p_m - p_v) \quad (14.28)$$

Measurement of p_m is ordinarily not feasible, since it usually occurs on the runner blades. It is therefore necessary to express p_m in terms of measurable quantities. This is done by means of the energy equation, as follows: Referring to Fig. 14.6 and using Eq. (5.10), for fixed axes, we find

$$p_2 - p_0 + \frac{\rho}{2} (V_2^2 - V_0^2) + \rho g(z_2 - z_0) + \rho gH_{l_{0,2}} = 0$$

and from Eq. (6.21), for rotating axes,

$$p_m - p_2 + \frac{\rho}{2} (W_m^2 - W_2^2) + \rho g(z_m - z_2) + \rho gH_{l_{2,m}} + \frac{\rho}{2} \omega^2(r_2^2 - r_m^2) = 0$$

Combining these equations, noting that $V_0 = 0$ and $p_0 = p_a$, we get

$$p_m - p_a + \frac{\rho}{2} [W_m^2 - W_2^2 + V_2^2 + \omega^2(r_2^2 - r_m^2)] - \rho g(H - h) + \rho gH_{l_{0,m}} = 0$$

where $h = z_m - z_b$, the height of the minimum-pressure point above the tail-water level. Since the velocities and frictional effects upstream from

the point m , where cavitation starts, depend only on ρ , D , ω , Q , and μ , the last equation can be written

$$p_m = p_a - \rho gh + f(\rho, D, \omega, Q, gH, \mu) \quad (14.29)$$

Equation (14.28) thus becomes

$$\eta = f_2(\rho, D, \omega, Q, gH, \mu, p_a - p_v - \rho gh)$$

Neglecting μ , as in Art. 14.6, and applying the Π theorem, we find as one possible rearrangement of this equation

$$\eta = f_3\left(\frac{Q}{\omega D^3}, \frac{gH}{\omega^2 D^2}, \frac{p_a - p_v - \rho gh}{\rho \omega^2 D^2}\right)$$

or, alternatively,

$$\eta = f_4\left(\frac{Q}{\omega D^3}, \frac{gH}{\omega^2 D^2}, \frac{p_a - p_v - \rho gh}{\rho gH}\right) \quad (14.30)$$

The form of the cavitation number, $(p_a - p_v - \rho gh)/\rho gH$, given in Eq. (14.30) is due to D. Thoma of Munich and is in general use as a cavitation criterion for hydraulic machinery [5]. It is denoted by the symbol

$$\sigma = \frac{p_a - p_v - \rho gh}{\rho gH} \quad (14.31)$$

We should expect σ to have no effect on η , so long as $\sigma > \sigma_c$, a critical value corresponding to the starting condition for cavitation. This expectation

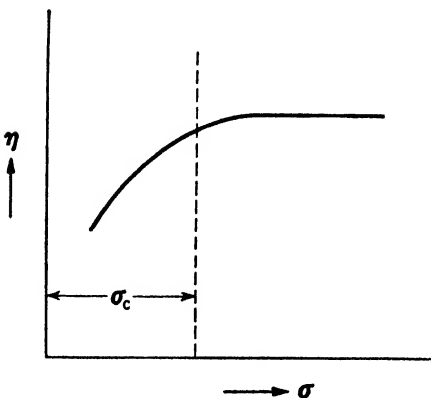


FIG. 14.15. — Schematic curve of turbine efficiency η versus cavitation number σ .

is borne out by experiments, as shown schematically in Fig. 14.15. Since the value of σ_c determined from tests on a model turbine is equal to that for a prototype, the turbine builder can tell whether or not a certain design will be free from cavitation under all operating conditions.

The obvious means to eliminate cavitation is to reduce the height h of the turbine above tail water, since, as shown by Eq. (14.29), reduction of h increases p_m . Lowering of the turbine is, however, frequently impossible for reasons of accessibility or structural soundness. In such a case improved blade design may serve to increase p_m above the danger point. For example, in Kaplan turbines, which employ blades of airfoil section, it is common practice to use a profile that has a practically uniform pressure

distribution along the chord. A small region of excessively low pressure is thus avoided. A profile of this type developed by the NACA for other applications is shown in Fig. 10.6a.

Even with the most advanced design it may be impossible to avoid cavitation under all operating conditions, such as, for example, an excessively low tail-water level at certain seasons of the year. In such a case, damage to the blades can be reduced if the endangered areas are coated with a welded-on layer of resistant material like stainless steel.

SELECTED BIBLIOGRAPHY

1. ADDISON, H.: "Applied Hydraulics," 2d ed., John Wiley & Sons, Inc., New York, 1938.
2. LOWY, R.: Efficiency Analysis of Pelton Wheels, *Trans. Am. Soc. Mech. Engrs.*, vol. 66, pp. 527-538, Aug., 1944.
3. PATTERSON, G. N.: Modern Diffuser Design, *Aircraft Eng.*, vol. 10, pp. 267-273, 1938.
4. RUSSELL, G. E.: "Hydraulics," 5th ed., Henry Holt and Company, Inc., New York, 1942.
5. THOMA, D.: Experimental Research in the Field of Water Power, *Trans. 1st World Power Conf.*, vol. 2, pp. 536-551, Lund Humphries, London, 1925.
6. VUSKOVIC, I.: Experiments on the Influence of Air Content on Cavitation (German), *Escher Wyss Mitt.* vol. 13, pp. 83-90, 1940; (English) *R.T.P. Translation 2387*, reprinted by Durand Reprinting Committee, California Institute of Technology, Pasadena, Calif.

CHAPTER XV

PUMPS, FANS, AND COMPRESSORS

The purpose of a pump, fan, or compressor is to convert mechanical work into energy of a fluid; it is thus the inverse of a turbine. In this chapter we shall discuss only hydrodynamic machines, leaving positive-displacement apparatus out of consideration. Hydrodynamic machines are divided into radial-flow, or centrifugal, and axial-flow types, according to the motion of the fluid as it passes through the impeller. In a pump the working fluid is a liquid, while in a fan or compressor it is a gas. Fans are distinguished from compressors by the fact that, in the former, the working fluid suffers no appreciable density change, while in the latter the density is considerably increased.

15.1. Centrifugal Pump and Fan. A centrifugal pump consists essentially of a bladed wheel, the impeller, which rotates inside a casing, as shown in Fig. 15.1. Liquid enters the impeller near the axis and flows

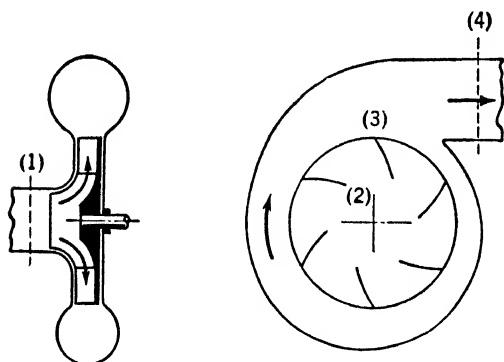


FIG. 15.1. — Centrifugal pump.

normal to the axis out along the blades into the casing and thence to the discharge pipe. Centrifugal force acting on the revolving liquid in the impeller produces the flow.

Tangential velocity is necessarily imparted to the liquid by the impeller, since the applied torque gives rise to a flux of angular momentum. The tangential velocity plays no part in transporting the liquid

into the discharge pipe and is dissipated in shock losses unless guide vanes or a vortex chamber be fitted to reduce the whirl gradually. A pump with guide vanes, known as a turbine pump, has a high efficiency over only a limited range of speed and discharge and is more expensive than one without guides. A vortex chamber, which reduces the tangential velocity simply by allowing the fluid to move farther from the center of rotation before entering the outflow pipe, adds to the over-all diameter of a pump. For these reasons the type most widely used is the simple volute pump, illustrated in Fig. 15.1.

The maximum head against which a single impeller works is ordinarily

about 300 ft of water, although several single-stage pumps have been built to pump against heads as high as 2,000 ft. If a high head is needed, it is

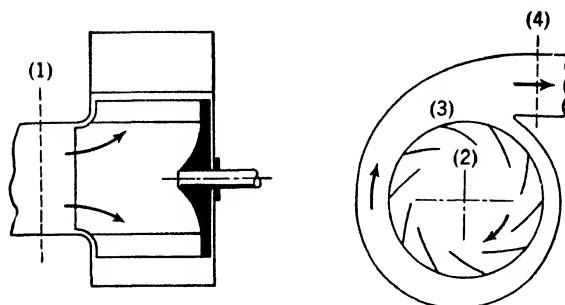


FIG. 15.2. — Centrifugal fan.

usual to build a pump with several impellers connected in series. Six such stages is the normal maximum number. Discharge rate and power vary between wide limits. The maximum efficiency of a centrifugal pump has been made as high as 92 per cent but is usually about 85 to 88 per cent.

A centrifugal fan (Fig. 15.2) is essentially the same as a centrifugal pump as long as the pressure rise is limited to 10 or 15 in. of water. Otherwise the density change in the air being handled becomes appreciable and the machine must be treated as a centrifugal compressor or supercharger, under quite different design procedures.

The resultant torque on the impeller and on the fluid between sections 2 and 3 of Fig. 15.1 or 15.2 is obtained from the angular-momentum equation [Eq. (6.19)].

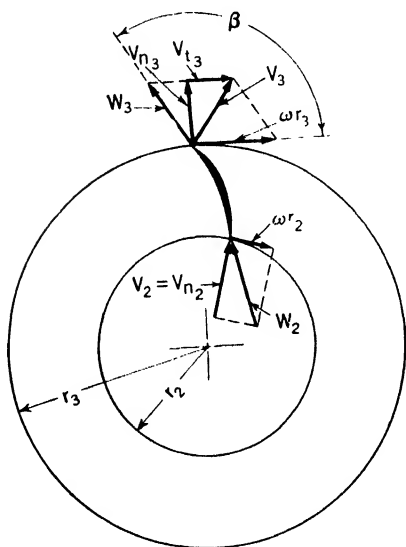


FIG. 15.3. — Velocity diagrams for a centrifugal pump or fan.

the applied torque T' of the driving motor, as well as the torques due to bearing friction and the drag of the fluid on the shroud. We define the mechanical efficiency as

$$\text{Resultant torque} = \rho Q(r_3 V_{t_3} - r_2 V_{t_2})$$

where Q is the volume rate of flow and the velocities and radii are as shown in Fig. 15.3. This resultant includes

$$\eta_m = \frac{\omega(\text{resultant torque})}{\omega T} \quad (15.1)$$

and get

$$T = \frac{\rho Q(r_3 V_{t_3} - r_2 V_{t_2})}{\eta_m}$$

The flow at 2 has no tangential component if the inlet piping has bends in only one plane or if a suitable straightener is installed near the entrance. For this reason, the expression for T is simplified to

$$T = \frac{\rho Q r_3 V_{t_3}}{\eta_m} \quad (15.2)$$

The efficiency η is defined as the ratio of the input power that would be needed for a frictionless machine to that actually required. Since the flow is incompressible, the steady-flow energy equation [Eq. (5.10)] can be written between the entrance and exit sections in the form

$$-\mathfrak{W}_s = \frac{p_4 - p_1}{\rho} + \frac{V_4^2 - V_1^2}{2} + g(z_4 - z_1) + gH_{l,4}$$

where $-\mathfrak{W}_s$ is the work done by the driving motor per unit mass of fluid and $H_{l,4}$ is the sum of all the losses between sections 1 and 4 of Fig. 15.1 or 15.2. The efficiency is thus

$$\eta = \frac{\rho Q(-\mathfrak{W}_s - gH_{l,4})}{\rho Q(-\mathfrak{W}_s)} = \frac{[(p_4 - p_1)/\rho] + [(V_4^2 - V_1^2)/2] + g(z_4 - z_1)}{-\mathfrak{W}_s} \quad (15.3)$$

Noting that $-\mathfrak{W}_s = \omega T / \rho Q$ and combining Eqs. (15.2) and (15.3), we get Euler's equation for a pump or fan.

$$\eta = \eta_m \frac{[(p_4 - p_1)/\rho] + [(V_4^2 - V_1^2)/2] + g(z_4 - z_1)}{\omega r_3 V_{t_3}} \quad (15.4)$$

The head developed is defined as the shaft work that would be needed in the frictionless case per unit weight of fluid. Thus the head is

$$H = \frac{p_4 - p_1}{\rho g} + \frac{V_4^2 - V_1^2}{2g} + z_4 - z_1 \quad (15.5)$$

Equation (15.4) is frequently written in terms of H .

$$\eta = \eta_m \frac{gH}{\omega r_3 V_{t_3}} \quad (15.6)$$

This equation is analogous to Eq. (14.11) for a turbine.

The losses in a pump or fan are similar to those in a turbine but are necessarily larger, for the flow takes place against an increasing pressure. The adverse pressure gradient leads to thicker boundary layers and possibly to separation.

It should be mentioned that Eq. (15.3) is a slight overestimate of the efficiency, for in practice some recirculation of fluid occurs through the clearance spaces between shroud and casing. This effect, which results from the adverse pressure gradient, will be disregarded here.

To determine whether a pump or fan will suit a particular application it is useful to have an experimental characteristic curve, *i.e.*, a curve of H versus Q . Several common shapes of characteristic curve are shown in Fig. 15.4. The shape depends on whether the blades are radial or curved, as will be shown below. The characteristic curve also depends on the speed ω , so that several curves are needed to show the performance over a range of speed.

The head required to force a given quantity Q through the pipe, or duct, system to which the machine is attached is, in general, roughly proportional to Q^2 , since the Reynolds number is usually high. It is clear that the pump or fan should be chosen so that its characteristic curve will intersect the head-required curve at the desired value of Q . A typical head-required curve is shown dotted in Fig. 15.4.

In the range of discharge values for which the efficiency is approximately constant, the slope of the characteristic curve depends on the value of β , the blade angle at the exit from the impeller (Fig. 15.3). Using the velocity diagrams of Fig. 15.3, we get H from Eq. (15.6) in the form

$$H = \frac{\eta}{\eta_m} \frac{\omega^2 r_3^2}{g} \left(1 + \frac{V_{n_3}}{\omega r_3 \tan \beta} \right) \quad (15.7)$$

Since V_{n_3} is proportional to Q , it follows that, at constant speed, H would vary linearly with Q , provided that η/η_m were constant. Since the latter varies somewhat, the actual curves are like those of Fig. 15.4. The general trend over the operating range is seen to depend on β , but all three curves drop off at both ends of the diagram, owing to the decrease in η/η_m .

Backward-curved blades are preferred in many applications, for the following reasons: (1) The absolute exit velocity is less than for other blade shapes, so that the shock loss at impeller exit can be kept small without the use of a large-diameter casing or guide vanes. (2) The negative slope of the characteristic curve over a large range of discharge rate makes possible the stable operation of two machines in parallel over this range.

It is also useful to have curves of efficiency and input power versus

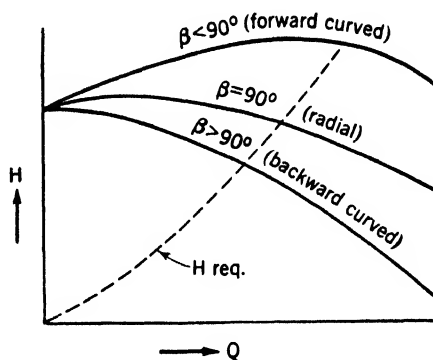


FIG. 15.4. — Characteristic curves for centrifugal machines. β is the blade angle at exit from the impeller (see Fig. 15.3).

discharge rate, so that the power requirements can be easily determined. A typical set of curves for a pump with backward-curved blades is shown in Fig. 15.5.

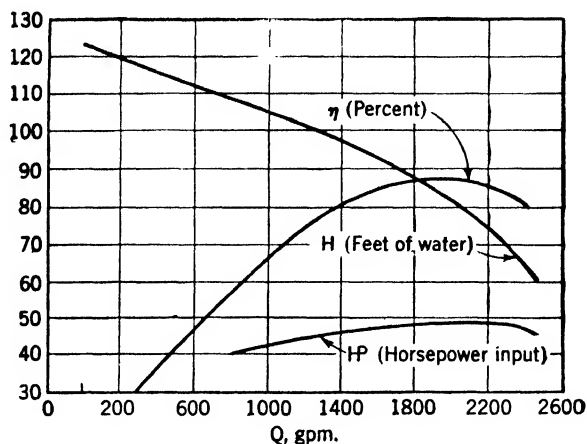


FIG. 15.5. — Head H , efficiency η , and input horse-power IP versus discharge rate Q , for a centrifugal pump with backward-curved blades.

15.2. Axial-flow Pump and Fan. Axial-flow pumps are built in a wide variety of sizes for use where a large discharge rate is required under a relatively low head. The unrestricted passage through such a pump adapts it to handling solids in suspension. Typical applications are to sewage disposal, irrigation, and drainage.

Axial-flow fans, like pumps, are best adapted to delivering a large volume under a low head. These fans are used for many ventilating applications, such as in mines, buildings, and vessels.

The fan shown in Fig. 15.6 is mounted at the entrance to a duct, but it is obvious that such a unit can be mounted anywhere in a duct system. The guide vanes shown in the figure serve their usual purpose, *viz.*, to remove from the fluid the angular momentum imparted by the impeller, thus eliminating the superfluous tangential velocity and increasing the pressure rise through the fan.

The blades and guides are designed so that no radial flow occurs between sections 1 and 3 of Fig. 15.6. The bell mouth and the hub fairing are shaped to give a uniformly distributed, purely axial velocity at 1. Since the casing and hub diameters are uniform between 1 and 3 and no radial flow occurs, continuity requires a uniform distribution of axial velocity at 3. There is no tangential velocity at 3. The tapering of the hub increases the cross-sectional area of the flow, thus reducing the velocity and increasing the pressure. Section 4, at which the diffusing action is complete and conditions are uniform across the duct, is taken as the downstream end of the fan.

The resultant torque on the blade elements and fluid within the annular stream tube between 1 and 2 at radius r is found from the angular-momentum law [Eq. (6.19)] to be

$$\text{Resultant torque} = \rho r (V_{t_2} - V_{t_1}) dQ$$

where dQ is the volume flow through the stream tube, and V_{t_2} and V_{t_1} are the tangential velocity components at radius r at 2 and 1, respectively. If

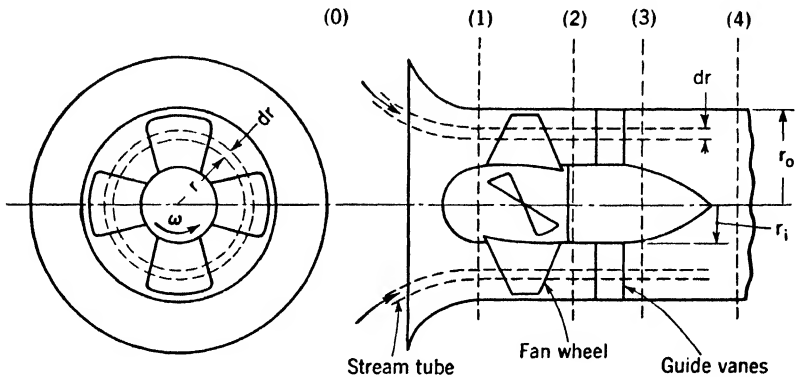


FIG. 15.6. — Axial-flow fan.

we neglect friction, we can show by the method of Art. 14.4 that the product rV_t is constant over section 2; and, by assumption, $V_{t_1} = 0$. Summing over the entire cross section, we get, therefore

$$\text{Resultant torque} = \rho Q r V_{t_2}$$

Introduction of the mechanical efficiency from Eq. (15.1) leads to

$$T = \frac{\rho Q r V_{t_2}}{\eta_m} \quad (15.8)$$

where T is the torque applied to the shaft by the driving motor. This equation is identical with Eq. (15.2) for a centrifugal machine.

The efficiency and head are defined just as for a centrifugal fan and can be expressed by Eqs. (15.3) to (15.6). It is customary, however, in the case of a fan mounted at the entrance to a duct, to include the bell mouth as part of the fan. If this is done, the expression for the head becomes

$$H = \frac{p_4 - p_0}{\rho g} + \frac{V_4^2}{2g} + z_4 - z_0 \quad (15.9)$$

section 0 being taken in front of the fan where the velocity is zero. Since the losses between 0 and 1 are small, there is practically no difference between Eqs. (15.5) and (15.9).

The characteristic curve of H versus Q is useful for an axial-flow

machine, just as for a centrifugal one. A typical curve, together with curves of power input and efficiency, is shown in Fig. 15.7. The dip in the characteristic curve is caused by "stalling," *i.e.*, by separation of the flow from the blades. This separation begins near the hub, where the operating

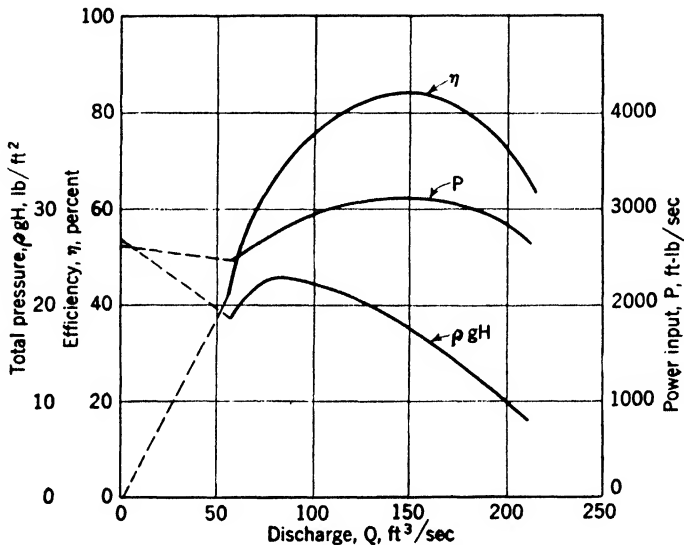


FIG. 15.7. — Total pressure, efficiency, and input power versus discharge rate for an axial-flow fan. (After Keller, reference 7.)

conditions are less favorable than near the blade tips, owing to the lower speed at the hub.

15.3. Dimensional Analysis of a Pump or Fan. Dimensional analysis is used in the same way for these machines as for a hydraulic turbine (see Art. 14.6).

Three important quantities in connection with the design or selection of a pump or fan are the head produced H , the power input required P , and the efficiency η . For a machine of given design, each of these is a function of the following independent variables: ρ , ω , D , Q , and μ . Here D represents the impeller diameter, chosen as a convenient length characteristic of the machine. The head H depends also on g , since H represents shaft work per unit *weight* of fluid. The product gH , however, or the shaft work per unit *mass* of fluid, is independent of g , because the flow through the machine is totally enclosed and the fluid incompressible. Accordingly, we write, for a given design,

$$gH = f_1(\rho, \omega, D, Q, \mu)$$

$$P = f_2(\rho, \omega, D, Q, \mu)$$

$$\eta = f_3(\rho, \omega, D, Q, \mu)$$

Applying the Π theorem and letting ρ , ω , and D be common to the three independent Π products of each of these equations, we get

$$\begin{aligned}\frac{gH}{\omega^2 D^2} &= f_4 \left(\frac{Q}{\omega D^3}, \frac{\rho \omega D^2}{\mu} \right) \\ \frac{P}{\rho \omega^3 D^5} &= f_5 \left(\frac{Q}{\omega D^3}, \frac{\rho \omega D^2}{\mu} \right) \\ \eta &= f_6 \left(\frac{Q}{\omega D^3}, \frac{\rho \omega D^2}{\mu} \right)\end{aligned}$$

Experiment shows, as for turbines (Art. 14.6), that the viscosity has only a secondary effect on the performance of a pump or fan. Hence, for a given design,

$$\frac{gH}{\omega^2 D^2} = f_4 \left(\frac{Q}{\omega D^3} \right) \quad (15.10)$$

$$\frac{P}{\rho \omega^3 D^5} = f_5 \left(\frac{Q}{\omega D^3} \right) \quad (15.11)$$

$$\eta = f_6 \left(\frac{Q}{\omega D^3} \right) \quad (15.12)$$

Equation (15.10) indicates that the characteristic curves at various speeds for a series of geometrically similar machines will all coalesce into a single curve when plotted nondimensionally, with $gH/\omega^2 D^2$ as ordinate and $Q/\omega D^3$ as abscissa. Similar conclusions can be drawn from Eqs. (15.11) and (15.12) regarding the power and efficiency. These statements are of course valid only over the range of size and speed for which changes in Reynolds number $\rho \omega D^2/\mu$ have a negligible effect on the flow.

Equations (15.10) to (15.12) are useful also in indicating the effect of changes in size or speed on the performance at maximum efficiency η_{\max} . If $\eta = \eta_{\max}$, Eq. (15.12) shows that $Q/\omega D^3$ has a definite constant value. Therefore,

$$\frac{Q}{\omega D^3} = C_1 \quad (15.13)$$

$$\frac{gH}{\omega^2 D^2} = C_2 \quad (15.14)$$

$$\frac{P}{\rho \omega^3 D^5} = C_3 \quad (15.15)$$

In words, Q is proportional to ωD^3 , H is proportional to $\omega^2 D^2$, and P is proportional to $\rho \omega^3 D^5$.

The concept of specific speed is applied in the selection of a pump to

satisfy known operating conditions, just as in the case of a hydraulic turbine (Art. 14.6). The discharge Q , the head H , and the speed ω are usually required to have certain values in any proposed installation. A dimensionless product of these quantities that has a definite value for a machine of given design operating at maximum efficiency is obtained from Eqs. (15.13) and (15.14).

$$\frac{\omega Q^{1/2}}{(gH)^{3/4}} = \frac{C_1^{1/2}}{C_2^{3/4}} = \text{constant}$$

For pumps, the speed N is usually expressed in rpm and the discharge in gallons per minute (gpm). The head H is expressed in feet. From the above relation we can define

$$N_s = \frac{N(\text{gpm})^{1/2}}{H^{3/4}} \quad (15.16)$$

where N_s , the specific speed, has a definite value for a pump of given design operating at maximum efficiency. For single-stage centrifugal pumps the values of N_s range between 500 and 5,000, while for single-stage axial-flow pumps N_s lies between 5,000 and 10,000.

A similar definition of N_s can be used in connection with fans. The discharge, however, is measured in cubic feet per second instead of gpm.

15.4. Design of an Axial-flow Machine. The blades and guide vanes of an axial-flow machine can be rationally designed if it be assumed that wind-tunnel data on lift and drag coefficients C_L and C_D are applicable to each element of a blade or guide vane. In the analysis leading to the design equations we consider only that part of the machine between sections 1 and 3 of Fig. 15.6. In case two or more stages are required, we consider only the part between the entrance to the first and the exit from the last stage and assume the pressure rise through each stage to be $\Delta p/N$, where Δp is the total pressure rise and N is the number of stages.

The given quantities on which a design is to be developed are (1) the discharge Q , (2) the pressure rise Δp , (3) the speed ω , (4) the radius of the casing r_o , (5) mechanical efficiency η_m , and (6) one or more blade forms having known values of ϵ ($= C_D/C_L$) and C_L . We wish to determine the required number of stages N , a hub radius r_i that will give a high value of efficiency, and the width and angle of the blades and guides at any radius. We begin by discussing, for a single stage, the blade and guide-vane elements of length dr at an arbitrary radius r , as follows:

Differentiation of Eq. (15.8) with respect to r gives (since rV_{t_1} is independent of r)

$$\eta_m dT = \rho r V_{t_2} dQ$$

where $\eta_m dT$ is the external torque transmitted from the shaft through the blades to the blade elements, or, since these elements move at constant speed, the torque exerted on the fluid by them. Since the velocity V_1 at section 1 is assumed axial and uniform, $dQ = V_1 2\pi r dr$, and

$$\eta_m dT = Z dF_t r = \rho r V_{t_2} V_1 2\pi r dr \quad (15.17)$$

where Z is the number of blades and dF_t is the tangential component of the force acting between one blade element and the fluid, as in Fig. 15.8. Application of the momentum principle [Eq. (6.6)] to the control volume

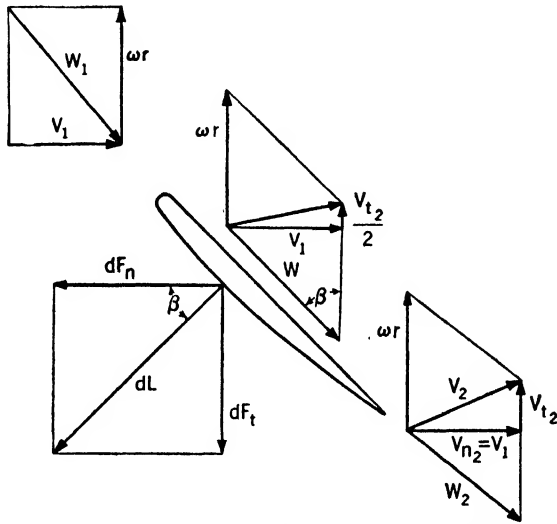


FIG. 15.8. — Velocity and force diagrams for a blade element at radius r .

formed by the annular stream tube and sections 1 and 2 of Fig. 15.6 yields

$$Z dF_n = (p_2 - p_1) 2\pi r dr \quad (15.18)$$

where dF_n is the axial component of the force acting between the fluid and blade element.

In the idealized frictionless case, the resultant force on the blade element is the lift dL , which makes an angle β with the axial direction (Fig. 15.8). To determine β , we use Eqs. (15.17) and (15.18).

$$\tan \beta = \frac{dF_t}{dF_n} = \frac{\rho V_1 V_{t_2}}{p_2 - p_1}$$

The energy equation for rotating axes [Eq. (6.22)] yields

$$p_2 - p_1 = \frac{\rho}{2} (W_1^2 - W_2^2)$$

since $r_1 = r_2 = r$ and changes in level are ignored. The velocity diagrams of Fig. 15.8 give

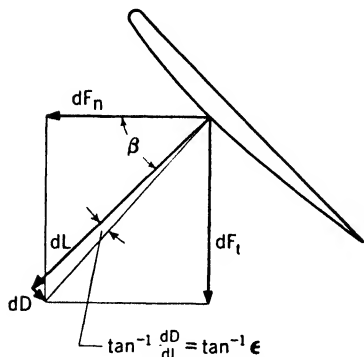
$$W_1^2 - W_2^2 = W_t^2 + W_{n1}^2 - W_{t2}^2 - W_{n2}^2 = \omega^2 r^2 - (\omega r - V_{t2})^2 = 2V_{t2} \left(\omega r - \frac{V_{t2}}{2} \right)$$

and, therefore,

$$\tan \beta = \frac{V_1}{\omega r - \frac{V_{t2}}{2}} = \frac{\phi}{1 - \lambda} \quad (15.19)$$

where $\phi = V_1/\omega r$ and $\lambda = V_{t2}/2\omega r$.

The diagram for the mean relative velocity W based on this value of β is shown in Fig. (15.8). It will be assumed that wind-tunnel data on single airfoils can be applied to the fan-blade element if the lift and drag coefficients are referred to this relative velocity W . Thus,



$$\left. \begin{aligned} dL &= C_L \frac{\rho}{2} t W^2 dr \\ dD &= C_D \frac{\rho}{2} t W^2 dr \end{aligned} \right\} \quad (15.20)$$

FIG. 15.9. — Forces exerted by the fluid on a blade element at radius r .

where t is the chord of the element. The data should, of course, be corrected to conditions of two-dimensional flow, since

no trailing vortices are shed from the element (see Art 11.21). In the actual case of flow with friction the forces are thus as shown in Fig. 15.9, and the ratio of tangential to normal force is

$$\frac{dF_t}{dF_n} = \tan(\beta + \tan^{-1} \epsilon) = \frac{\rho V_1 V_{t2}}{p_2 - p_1} \quad (15.21)$$

A similar analysis for the corresponding element of the guide vane (Fig. 15.10) yields

$$\tan \beta_v = \frac{2V_1}{V_{t2}} = \frac{\phi}{\lambda} \quad (15.22)$$

$$\frac{dF_{t_v}}{dF_{n_v}} = \tan(\beta_v + \tan^{-1} \epsilon_v) = \frac{\rho V_1 V_{t2}}{p_3 - p_2} \quad (15.23)$$

The efficiency η' of the blade and guide-vane elements combined is obtained by application of the energy equation between sections 1 and 3.

$$\eta' = \frac{1}{\eta_m} \frac{\text{shaft work (frictionless)}}{\text{shaft work (actual)}} = \frac{p_3 - p_1}{\eta_m \rho (-\mathfrak{W}_s)} = \frac{\Delta p}{N \rho (-\mathfrak{W}_s) \eta_m}$$

But since $-\mathfrak{W}_s = \omega dT/\rho dQ = \omega r V_{t2}/\eta_m$,

$$\eta' = \frac{\Delta p}{N \rho \omega r V_{t2}} = \frac{p_3 - p_1}{\rho \omega r V_{t2}} = \frac{p_3 - p_2}{\rho \omega r V_{t2}} + \frac{p_2 - p_1}{\rho \omega r V_{t2}} \quad (15.24)$$

By use of Eqs. (15.21) and (15.23)

$$\eta' = \frac{V_1}{\omega r} \left[\frac{1}{\tan(\beta + \tan^{-1} \epsilon)} + \frac{1}{\tan(\beta_g + \tan^{-1} \epsilon_g)} \right] \quad (15.25)$$

and from Eqs. (15.19) and (15.22)

$$\eta' = \phi \left[\frac{1 - \lambda - \epsilon\phi}{\phi + \epsilon(1 - \lambda)} + \frac{\lambda - \epsilon_g\phi}{\phi + \epsilon_g\lambda} \right] \quad (15.26)$$

For simplicity we assume that the drag-lift ratio is the same for both blade

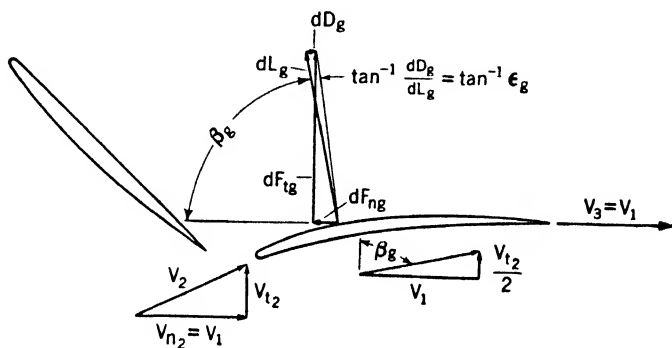


FIG. 15.10. — Velocity and force diagrams for a guide-vane element at radius r .

and guide-vane elements, that is, $\epsilon_g = \epsilon$. The efficiency is thus a function of three independent variables ϕ , λ , and ϵ .

Substitution of $\epsilon_g = \epsilon$ and reduction of Eq. (15.26) yield

$$\eta' = \frac{\phi[\phi(1 - \epsilon^2) + 2\epsilon(\lambda - \lambda^2 - \phi^2)]}{\phi^2 + \phi\epsilon + \epsilon^2(1 - \lambda)\lambda} \quad (15.27)$$

differentiation of which with respect to λ and setting of $\partial\eta'/\partial\lambda = 0$ show that the optimum value of λ is $1/2$. It will be shown below that, if wind-tunnel data on single airfoils are to be applicable, λ should not exceed about $1/4$. The conclusion is, therefore, that λ should be kept as near this upper limit as possible.

Since ϵ is small (usually about 0.025) and since ϕ is on the order of unity ($\phi = V_1/\omega r$), Eq. (15.27) can be written with good approximation as

$$\eta' = \frac{\phi + 2\epsilon(\lambda - \lambda^2 - \phi^2)}{\phi + \epsilon} \quad (15.28)$$

where terms in ϵ^2 have been omitted. In Fig. 15.11, which is computed from Eq. (15.28), η' is plotted against ϕ for several values of λ and ϵ . It will be observed that the η' curves are practically flat in the range $0.5 < \phi < 0.7$ and that, within this range of ϕ and for $0.10 < \lambda < 0.25$,

η' can be maintained constant by means of small variations in ϵ . This is a fortunate circumstance, since Eq. (15.24) shows that η' must be the same at all radii, both $p_3 - p_1$ and rV_t being assumed independent of r . Values of ϵ will therefore be chosen to give a uniform distribution of η' along the radius.

As the first step in the design it is convenient to select a value of ϕ

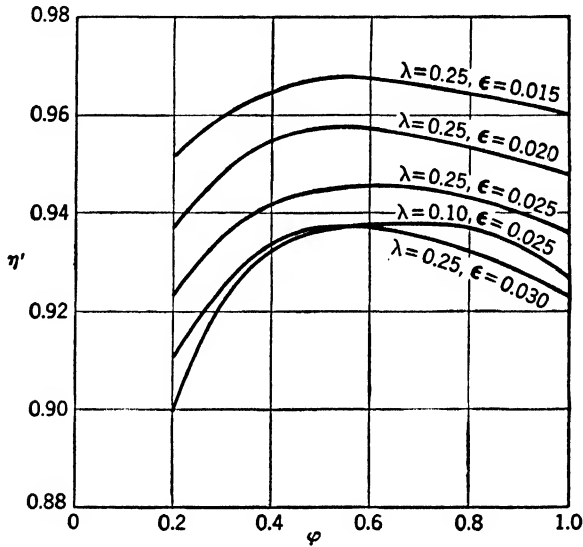


FIG. 15.11. — Efficiency of blade and guide-vane element combined η' versus flow coefficient ϕ for various values of the rotation and friction parameters λ and ϵ .

in the neighborhood of 0.5 to apply at the outer radius r_o . Let this value be ϕ_o . The hub radius r_i is next found from the relation

$$\frac{Q}{\pi(r_o^2 - r_i^2)} = V_1 = \phi_o \omega r_o \quad (15.29)$$

A tentative value of η' is then chosen, based on inspection of Fig. 15.11.

Before further progress can be made, a maximum allowable value for λ must be selected. A criterion for this choice is developed as follows:

It is found from experience that the "solidity" $Zt/2\pi r$ should not exceed about 1.1, if wind-tunnel data on single airfoils are to apply to the blade elements. We obtain a relation between the solidity and ϕ , ϵ , and λ by using Eqs. (15.17) and (15.20) and Figs. 15.8 and 15.9.

$$dF_t = \rho V_1 V_t \frac{2\pi r dr}{Z} = dL (\sin \beta + \epsilon \cos \beta)$$

$$dL = C_L \frac{\rho}{2} t W^2 dr = C_L \frac{\rho}{2} t \frac{V_1^2}{\sin^2 \beta} dr$$

whence, after considerable reduction,

$$C_L \frac{Zt}{2\pi r} = \frac{2V_{t_2}}{V_1} (\sin \beta + \epsilon \cos \beta) = \frac{4\lambda}{\sqrt{\phi^2 + (1-\lambda)^2} [1 + \epsilon(1-\lambda)/\phi]} \quad (15.30)$$

By substitution of simultaneous values of ϕ and ϵ from Fig. 15.11 it is easily shown that $C_L(Zt/2\pi r) \approx 1$ for $\eta' \approx 0.94$ and $\lambda = 1/4$. The solidity $Zt/2\pi r$ will be approximately unity also, since $C_L \approx 1$. The maximum allowable value for λ is therefore about $1/4$. The maximum value of λ will occur at the hub, since $\lambda = rV_{t_2}/2\omega r^2 = \text{constant}/r^2$. The value of λ at the hub is denoted by λ_i .

Having chosen a tentative value for λ_i , we can determine the number of stages N by using the definition of η' [Eq. (15.24)].

$$\eta' = \frac{\Delta p}{N\rho\omega r V_{t_2}} = \frac{\Delta p}{2N\rho\omega^2 r_i^2 \lambda_i}$$

whence

$$N = \frac{\Delta p}{2\rho\omega^2 r_i^2 \lambda_i \eta'} \quad (15.31)$$

The value of λ_i is to be adjusted to make the right-hand side of Eq. (15.31) equal to an integer.

The use of airfoil data begins at this point. The values of η' , ϕ_i , and λ_i being known, ϵ_i can be found from Fig. 15.11 or Eq. (15.28). The data plotted in Fig. 15.12 give ϵ versus C_L for the NACA 4412 airfoil, at various values of Reynolds number $R = Wt/\nu$. Figure 15.12 is to be used in conjunction with Eq. (15.30) to determine reasonable values for t_i and Z . Two conditions are to be fulfilled: (1) $Zt_i/2\pi r_i$ should be less than 1.1; and (2) ϵ_i , C_{L_i} , and Wt_i/ν should correspond to a single point in Fig. 15.12.

To illustrate this procedure let the following numerical values be given, on the basis of which it is required to design a suitable fan wheel.

$$Q = 200 \text{ ft}^3/\text{sec}$$

$$\Delta p = 20 \text{ lb}/\text{ft}^2$$

$$\omega = 180 \text{ radians}/\text{sec}$$

$$r_o = 1.00 \text{ ft}$$

$$\rho = 2.3 \times 10^{-3} \text{ lb-sec}^2/\text{ft}^4$$

$$\nu = 1.6 \times 10^{-4} \text{ ft}^2/\text{sec}$$

Assuming $\phi_o = 0.50$, we find from Eq. (15.29) that $r_i = 0.540 \text{ ft}$. Since this appears to be a reasonable hub radius, we proceed, assuming tentatively, on inspection of Fig. 15.11, that $\eta' = 0.95$. From Eq. (15.31) it is then found that, if N be chosen as 2, $\lambda_i = 0.243$. Referring to Fig. 15.11 we find that $\epsilon_i \approx 0.020$, whence, from Eq. (15.30), $C_{L_i} Zt_i/2\pi r_i = 0.805$.

Assuming now that $C_{L_i} = 0.80$, we see that $Zt_i/2\pi r_i = 1.01$, which is less than the allowable maximum of 1.1. To determine t_i we note from

Fig. 15.12 that the Reynolds number at the hub $Wt_i/\nu \approx 3 \times 10^5$, from which it follows that $t_i \approx 0.36$ ft. It is now readily found that $t_i = 0.38$ ft if $Z = 9$. Both these values appear to be satisfactory.

At the outer radius $r_o = 1.00$ ft, the value of ϵ_o is found from Eq. (15.28)

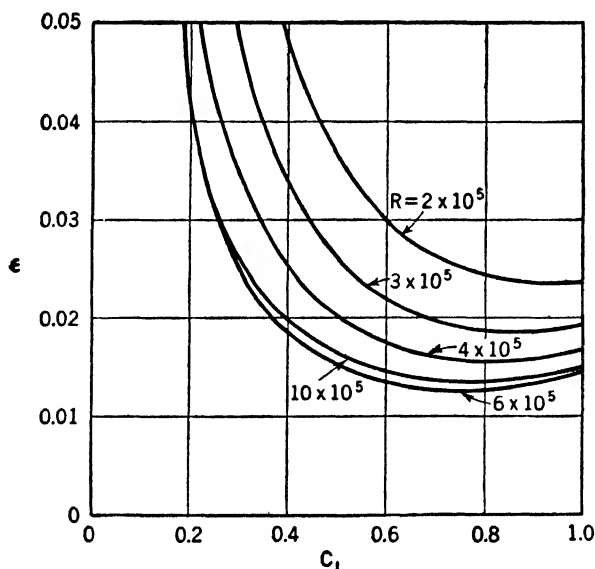


FIG. 15.12. — Drag-lift ratio ϵ versus lift coefficient C_L , for the NACA 4412 airfoil. The Reynolds number is defined as $R = Wt/\nu$.

to be 0.019, since $\eta' = 0.95$ and $\lambda_o = \lambda_i(r_i/r_o)^2 = 0.071$. Equation (15.30) yields $C_{L_o}t_o = 0.179$. A tentative value of t_o may now be assumed and the corresponding value of Reynolds number computed. If the values of C_{L_o} found from Eq. (15.30) and Fig. 15.12 do not agree, the process is repeated until a check is obtained.

A preferable method of determining t and C_L is to consider the behavior of the fan in the *neighborhood* of the design point [5]. We have seen that for stability it is necessary that the product rV_{t_i} be independent of radius, not only at the design point, but for all operating conditions. In order to fulfill this requirement, at least for a small range of speed near the design value, the chord t must be a definite function of r . To find this relation between t and r we assume that the velocity at entrance V_1 is held constant and uniform while ω is allowed to vary. In this approximate analysis we neglect friction and rearrange Eq. (15.30) to get

$$rV_{t_i} = \frac{tZV_1}{4\pi} \frac{C_L}{\sin \beta} \quad (15.30a)$$

The restriction which we wish to impose is that the rate of change of rV_{t_i} with respect to ω be the same at all radii. This will ensure that rV_{t_i} is

constant over the fan disk at values of ω near the design point. Noting that

$$\frac{\partial(rV_{t_2})}{\partial\omega} = \frac{\partial(rV_{t_2})}{\partial\beta} \frac{d\beta}{d(\tan\beta)} \frac{\partial(\tan\beta)}{\partial\omega}$$

we find

$$\begin{aligned} \frac{\partial(rV_{t_2})}{\partial\beta} &= \frac{tZV_1}{4\pi} \frac{1}{\sin\beta} \left(\frac{\partial C_L}{\partial\beta} - \frac{\cos\beta}{\sin\beta} C_L \right) \\ \frac{d\beta}{d(\tan\beta)} &= \cos^2\beta \\ \frac{\partial(\tan\beta)}{\partial\omega} &\approx \frac{\partial(V_1/\omega r)}{\partial\omega} = -\frac{V_1}{\omega^2 r} \end{aligned}$$

The expression $\partial C_L/\partial\beta$ can be rewritten as $\partial C_L/\partial\beta = (dC_L/d\alpha)(\partial\alpha/\partial\beta)$, which, since the blade angle $\alpha + \beta$ remains fixed, can be expressed as $\partial C_L/\partial\beta = -dC_L/d\alpha = -C'_L$. This substitution is advantageous, because C'_L is practically constant over the useful range of angle of attack.

We thus get

$$\frac{4\pi\omega^2 r \tan\beta}{ZV_1^2} \frac{\partial(rV_{t_2})}{\partial\omega} = t \cos\beta \left(C'_L + \frac{\cos\beta}{\sin\beta} C_L \right)$$

The approximation used above, namely, $\tan\beta \approx V_1/\omega r$, is equivalent to the assumption that $r \tan\beta$ is independent of r . The right-hand side of the last equation can thus be considered independent of r , so that

$$t \cos\beta \left(C'_L + \frac{\cos\beta}{\sin\beta} C_L \right) = t_i \cos\beta_i \left(C'_L + \frac{\cos\beta_i}{\sin\beta_i} C_{L_i} \right)$$

The unknown C_L can be eliminated by means of the relation $tC_L/\sin\beta = t_i C_{L_i}/\sin\beta_i$, which follows from Eq. (15.30a). The final result is

$$\frac{t}{t_i} = \frac{\cos\beta_i}{\cos\beta} + \frac{C_{L_i}}{C'_L} \frac{\cos\beta}{\sin\beta_i} \left(\frac{\cos^2\beta_i}{\cos^2\beta} - 1 \right) \quad (15.32)$$

Values of t and C_L at several stations along the blade are to be determined from Eqs. (15.30) and (15.32). The angle of attack α can then be found from airfoil data, such as Fig. 11.32, and the total blade angle determined as the sum $\alpha + \beta$.

We are now able, by means of Eq. (15.32), to determine the width of the blade tip for the example discussed above. Recalling that $\tan\beta \approx V_1/\omega r$, we get $\cos\beta_i \approx \omega r_i/\sqrt{V_1^2 + \omega^2 r_i^2} = 0.737$, $\sin\beta_i \approx V_1/\sqrt{V_1^2 + \omega^2 r_i^2} = 0.682$, and $\cos\beta_o \approx \omega r_o/\sqrt{V^2 + \omega^2 r_o^2} = 0.895$. From Fig. 11.32 an approximate value of C'_L is seen to be $C'_L \approx 0.095$ per deg = 5.45 per radian. Substitution in Eq. (15.32) yields $t_o/t_i = 0.763$; whence $t_o = 0.290$ ft. From the previous result that $C_{L_o}t_o = 0.179$ it follows that $C_{L_o} = 0.617$.

A check on the value of ϵ_o is obtained by computation of $W_o t_o/\nu$, which

is found to be 3.65×10^5 . Reference to Fig. 15.12 shows that these values of C_L and W_{ol}/ν correspond to $\epsilon_o \approx 0.019$, the value previously found. Failure to check approximately here would indicate either a different airfoil at the tip or a new start on the entire computation.

Values of β at root and tip are obtained from Eq. (15.19), and the values of α corresponding to the known values of C_L are found from Fig. 11.32.

The following table gives the results already discussed, together with values at an intermediate radius:

Given: $Q = 200 \text{ ft}^3/\text{sec}$	$\nu = 1.6 \times 10^{-4} \text{ ft}^2/\text{sec}$
$\Delta p = 20 \text{ lb}/\text{ft}^2$	$\rho = 2.3 \times 10^{-3} \text{ lb-sec}^2/\text{ft}^4$
$\omega = 180 \text{ radians}/\text{sec}$	4412 airfoil
Results: Number of stages $N = 2$	
Number of blades $Z = 9$	

r , ft	C_L	t , ft	β , deg	α , deg	$\alpha + \beta$, deg
0.54 (root) . .	0.80	0.36	50.7	4.5	55.2
0.80	0.70	0.31	35.1	3.3	38.4
1.00 (tip) . . .	0.62	0.29	28.1	2.5	30.6

The design of the guide vanes can be carried out by a similar method.

For fans in which the solidity $Zt/2\pi r$ is somewhat in excess of unity the same method can be used, but data on airfoil grids must be substituted for those on single airfoils. The chief effect of the increased solidity is found to be a reduction in C_L below the value measured for a single airfoil [6]. This reduction is largely attributable to the decrease in relative velocity of the fluid as it passes through the grid.

15.5. Centrifugal Compressor. These machines are widely used to compress air and other gases; they are simple in construction and can be built to operate under a wide variety of conditions. The ratio of outlet to inlet pressure does not ordinarily exceed a value of about 3, for a single stage. Efficiencies on the order of 75 per cent are commonly reached.

Referring to Fig. 15.1 or 15.2, we express the driving torque as in Eq. (15.2).

$$T = \frac{mr_3 V_{t_3}}{\eta_m} \quad (15.33)$$

where ρQ is replaced by m , the constant mass flow through the machine.

The efficiency is defined as the ratio of the power input for a frictionless compression to the actual power input. If leakage is neglected, the efficiency can be written as the ratio of the shaft works. If gravity is ignored, the energy equation for the frictionless case [Eq. (5.13)] reduces to

$$-W_s = \int_1^3 \frac{dp}{\rho} + \frac{V_3^2 - V_1^2}{2} \quad (15.34)$$

while, in the actual case, the energy equation gives

$$-\mathfrak{W}_{s_a} = \frac{p_3}{\rho_{3a}} - \frac{p_1}{\rho_1} + \frac{V_{3a}^2 - V_1^2}{2} + u_{3a} - u_1 - q_{1,3a}$$

where the subscript a is used to denote actual values. The pressure p_3 is considered the same in both cases, since the machine is supposed to develop an assigned output pressure. If the flow is assumed to be adiabatic, Eq. (9.5) is applicable to the frictionless case and Eq. (15.34) becomes

$$-\mathfrak{W}_s = \frac{k}{k-1} \frac{p_1}{\rho_1} \left[\left(\frac{p_3}{p_1} \right)^{1-(1/k)} - 1 \right] + \frac{V_3^2 - V_1^2}{2} \quad (15.35)$$

The actual work under adiabatic conditions is

$$-\mathfrak{W}_{s_a} = h_{3a} - h_1 + \frac{V_{3a}^2 - V_1^2}{2} \quad (15.36)$$

where the enthalpy h is defined as $(p/\rho) + u$. For adiabatic flow, the efficiency is thus

$$\eta = \frac{-\mathfrak{W}_s}{-\mathfrak{W}_{s_a}} = \frac{[k/(k-1)][(p_1/\rho_1)[(p_3/p_1)^{1-(1/k)} - 1] + [(V_3^2 - V_1^2)/2]}{h_{3a} - h_1 + [(V_{3a}^2 - V_1^2)/2]} \quad (15.37)$$

If the fluid is assumed a perfect gas, Eqs. (9.12) to (9.15) apply and Eq. (15.37) reduces to

$$\eta = \frac{c_p T_1 [(p_3/p_1)^{1-(1/k)} - 1] + [(V_3^2 - V_1^2)/2]}{c_p (T_{3a} - T_1) + [(V_{3a}^2 - V_1^2)/2]} \quad (15.38)$$

An alternative expression for the efficiency is obtained by use of Eq. (15.33), together with the fact that $-\mathfrak{W}_{s_a} = (\omega T/m)$.

$$\eta = \eta_m \frac{c_p T_1 [(p_3/p_1)^{1-(1/k)} - 1] + [(V_3^2 - V_1^2)/2]}{\omega r_3 V t_3} \quad (15.39)$$

This is the analogue of Eq. (15.4) for a pump or fan.

If we assume for the moment that both η and η_m are unity, Eq. (15.39) can be used as a guide in the development of a convenient form for the plotting of experimental results. We assume further that the compressor has blades which are radial at the exit section 3, so that $V_{t_3} = \omega r_3$. We thus have

$$\omega^2 r_3^2 = c_p T_1 \left[\left(\frac{p_3}{p_1} \right)^{1-(1/k)} - 1 \right] + \frac{V_3^2 - V_1^2}{2}$$

Furthermore, $V_3^2 = V_{t_3}^2 + V_{n_3}^2 = \omega^2 r_3^2 + V_{n_3}^2$ and continuity gives $A_3 \rho_3 V_{n_3} = A_1 \rho_1 V_1$, from which

$$V_{n_3} = V_1 \frac{A_1 \rho_1}{A_3 \rho_3} = V_1 \frac{A_1}{A_3} \left(\frac{p_1}{p_3} \right)^{1/k}$$

Therefore,

$$\frac{\omega^2 r_3^2}{2} = c_p T_1 \left[\left(\frac{p_3}{p_1} \right)^{1-(1/k)} - 1 \right] + \frac{V_1^2}{2} \left[\frac{A_1^2}{A_3^2} \left(\frac{p_1}{p_3} \right)^{2/k} - 1 \right]$$

which, by use of the equations $C^2 = (k-1)c_p T$ and $C_1^2/C_3^2 = (p_1/p_3)^{1-(1/k)}$ can be reduced to

$$M_1^2 = \left(\frac{V_1}{C_1} \right)^2 = \frac{(\omega r_3/C_3)^2 - [2/(k-1)][1 - (p_1/p_3)^{1-(1/k)}]}{(A_1^2/A_3^2)(p_1/p_3)^{1+(1/k)} - (p_1/p_3)^{1-(1/k)}} \quad (15.40)$$

Here C is the local sound velocity. The pressure ratio is thus expressed in terms of M_1 , $\omega r_3/C_3$, and A_1/A_3 . It can be shown by means of Eqs. (9.1), (9.5), and (9.8) to (9.10) that the value of M_1 determines the ratio m/m^* , where m^* is the mass flow when the sound velocity is reached at 1. The ratio m/m^* cannot exceed unity.

$$\frac{m}{m^*} = M_1 \left[\frac{k+1}{2 + (k-1)M_1^2} \right]^{1/(k-1)} \quad (15.41)$$

It thus appears that p_3/p_1 is a function of m/m^* , $\omega r_3/C_3$, and A_1/A_3 , in

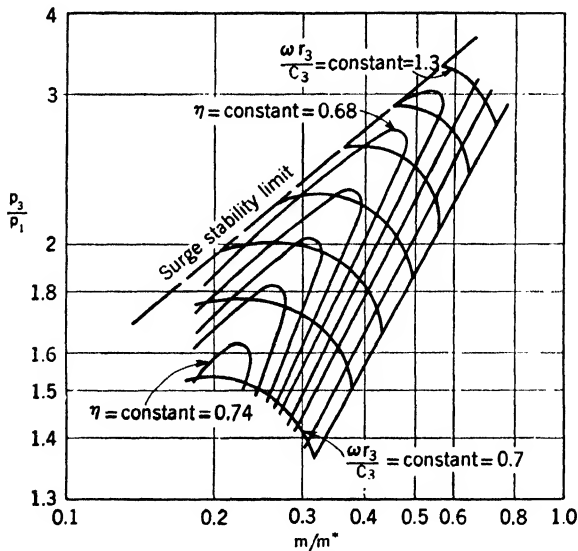


FIG. 15.13. — Pressure ratio p_3/p_1 versus relative mass flow m/m^* for a centrifugal compressor.

this idealized case. It is possible to plot experimental results in terms of these independent variables, as shown in Fig. 15.13 for a supercharger.

15.6. Dimensional Analysis of a Compressor. A form of plot similar to Fig. 15.13 can be developed by means of dimensional analysis. We assume that, for a compressor of given design, any of the three dependent

variables p_3 , η , or input power P depends only on ω ; on the impeller diameter D ; on the properties of the fluid at entrance ρ_1 , C_1 , and μ_1 ; and on the mass flow m .

The dependent quantities will, in general, be functions also of k and of the heat transfer through the casing, but these are ignored under the assumption that k is the same for all the operating fluids (diatomic gases) and that the flow is adiabatic.

It is convenient to change the independent variables ρ_1 and C_1 to p_1 and $c_p T_1$, respectively, because p_1 and T_1 are directly measured in compressor tests. These changes are legitimate, since $(k p_1 / \rho_1) = C_1^2 = c_p (k - 1) T_1$. Thus

$$p_3 = f_1(c_p T_1, D, p_1, \omega, m, \mu_1)$$

Applying the Π theorem and grouping $c_p T_1$, D , and p_1 in each of the three Π products, we get

$$\frac{p_3}{p_1} = f_2 \left(\frac{\omega D}{\sqrt{c_p T_1}}, \frac{m \sqrt{c_p T_1}}{p_1 D^2}, \frac{p_1 D}{\mu_1 \sqrt{c_p T_1}} \right) \quad (15.42)$$

Similarly, η and $P/p_1 \sqrt{c_p T_1} D^2$ are functions of the same three variables.

Experiment shows that the third independent variable of Eq. (15.42),

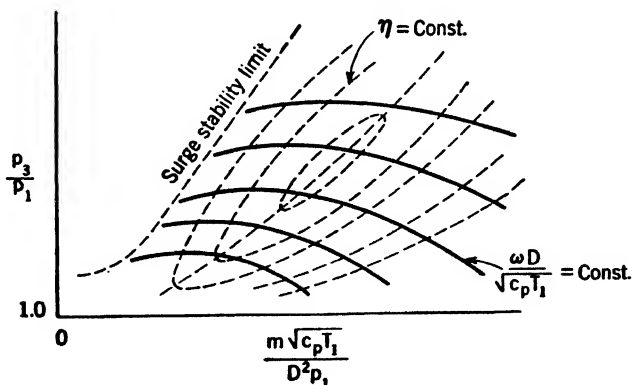


FIG. 15.14. — Dimensionless performance curves for a centrifugal pump. (After Del Mar, reference 1. Courtesy of the American Society of Mechanical Engineers.)

viz., that containing μ_1 , is of negligible importance, viscosity playing only a minor role in determining the flow through the compressor [1]. Figure 15.14 shows schematically how test results appear when plotted in these coordinates.

The “surge stability limit” marked in Figs. 15.13 and 15.14 is the locus of points at which the operation becomes unstable. Suppose that the compressor is running at a constant value of $\omega D / \sqrt{c_p T_1}$ and that m is decreasing. So long as the operating point lies to the right of the limiting line,

the pressure p_3 developed by the machine drops less rapidly with decrease in m than does the pressure characteristic of the attached system. Operation is therefore stable. To the left of the limiting line, however, the pressure p_3 drops more rapidly with decrease in m than does that of the system, and instability, or "surging," is the result.

SELECTED BIBLIOGRAPHY

1. DEL MAR, B. E.: Presentation of Centrifugal Compressor Performance in Terms of Nondimensional Relationships, *Trans. Am. Soc. Mech. Engrs.*, vol. 67, pp. 483-490, 1945.
2. KEARTON, W. J.: "Turbo-blowers and Compressors," Sir Isaac Pitman & Sons, Ltd., London, 1926.
3. PATTERSON, G. N.: "Ducted Fans: Design for High Efficiency," *Rept. ACA-7*, Australian Council for Aeronautics, July, 1944.
4. SORG, K. W.: Supersonic Flow in Turbines and Compressors, *J. Roy. Aeronaut. Soc.*, vol. 46, pp. 64-85, 1942.
5. TROLLER, TH.: Zur Berechnung von Schraubenventilatoren, *Abhandl. Aero. Inst. Tech. Hochschule Aachen*, no. 10, pp. 43-47, Verlag Julius Springer, Berlin, 1931.
6. WISLICENUS, C. F.: A Study of the Theory of Axial-flow Pumps, *Trans. Am. Soc. Mech. Engrs.*, vol. 67, pp. 451-470, 1945 (see especially the discussion by Th. Troller on p. 468).
7. KELLER, C.: "Axial-flow Fans," McGraw-Hill Book Company, Inc., New York, 1937.

CHAPTER XVI

PROPELLERS AND JETS

A propeller adds momentum to the fluid passing through it and so develops an axial force, or thrust. The fluid in the wake of the propeller is called the "race" or "slip stream," and the relative increase of velocity there is called "slip," from analogy with a screw. If a portion of propeller blade, the face of which was a helical surface of pitch p , worked in a firm nut, without slip, it would advance a distance p for one complete revolution. The helix angle at radius r would be $\tan^{-1}(p/2\pi r)$. Actually a propeller proceeding ahead at speed V advances in the time $1/n$ taken for one revolution of the propeller a distance V/n which is less than p . The slip, therefore, is $p - (V/n)$. This definition of slip is arbitrary, based on the geometry of the propeller. Its physical significance is not very clear, but for a higher-pitch propeller we should naturally expect more slip and more thrust. For no slip (when $p = V/n$) we should expect no thrust, since no fluid is accelerated. Modern propellers may have blades for which the pitch is not uniform over the face. The common practice is to have the pitch increase somewhat toward the blade tips. The pitch at three-quarters radius is usually taken as the approximate specification of the "mean geometrical pitch" of a propeller.

The common propeller-type ventilator, or fan, set in a wall or window, without an entrance pipe, operates like a propeller. Here the thrust of the fan is not the essential feature, but the velocity of flow that can be maintained. Obviously, fluid is given axial momentum by the fan. Such fans are cheap, quiet, and efficient where a large diameter can be allowed.

16.1. Momentum Theory of a Propeller. For purposes of analysis the

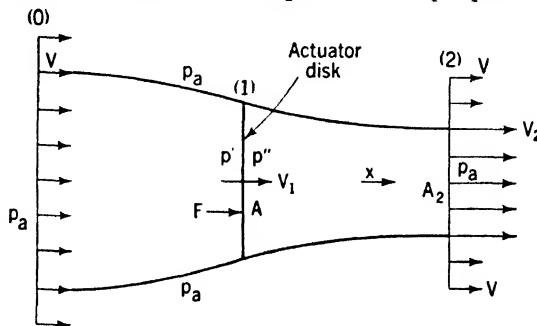


FIG. 16.1.

actual propeller is replaced by a hypothetical "actuator disk," which accelerates the flow axially without imparting any whirl to the slip stream.

The fluid is assumed to be frictionless. A surface of discontinuity in velocity is assumed to separate from the surrounding fluid the fluid that passes through the actuator, as shown in Fig. 16.1. The pressure is atmospheric everywhere on the surface, as well as at sections 0 and 2, which are stationary with respect to the disk and at which the streamlines are parallel and straight. The velocities indicated in this figure are taken relative to the disk. The undisturbed fluid is assumed to be at rest with respect to the earth, so that the actuator has an "absolute" velocity of magnitude V , from right to left.

If the actuator is considered as attached to an airplane or other load, the latter will exert a force F on the disk, as shown. This thrust is the only external x force on the system comprising the actuator and the fluid in the slip stream between sections 0 and 2. The momentum equation [Eq. (6.6)] thus gives

$$F = m(V_2 - V) \quad (16.1)$$

where m is the mass rate of flow through the actuator.

If the assumption of incompressibility is introduced here, the velocity immediately in front of the disk is seen to be the same as that just behind it, since the area of the stream is the same at both sections. The product of this velocity and the thrust, FV_1 , gives the work per second done by the actuator on the fluid. This is identical with the power input to the actuator, since the latter is assumed 100 per cent effective. The shaft work done on the actuator is found by application of the energy equation [Eq. (5.10)] to the system comprising the disk and the fluid of the slip stream between sections 0 and 2,

$$-\dot{W}_s = \frac{(V_2^2 - V^2)}{2} \quad (16.2)$$

whence

$$FV_1 = -\dot{W}_s/m = m \frac{(V_2^2 - V^2)}{2} \quad (16.3)$$

Combination of Eqs. (16.1) and (16.3) gives

$$V_1 = \frac{V + V_2}{2} \quad (16.4)$$

The velocity V_1 at the disk is thus the arithmetic mean of V and V_2 , half of the velocity change taking place upstream and half downstream from the disk.

The efficiency of the actuator is defined as the ratio of the useful work done by it to that done on it. The useful work per second (power output) is the product of the thrust and the forward speed of the disk with respect to the earth, FV , while, from Eq. (16.2), the power input to the actuator

is $m(V_2^2 - V^2)/2$. The efficiency for this idealized case, called the "ideal" or "Froude" efficiency, is thus $\eta_i = 2FV/m(V_2^2 - V^2)$, which, with the aid of Eq. (16.1), is reduced to

$$\eta_i = \frac{2V}{V + V_2} \quad (16.5)$$

or

$$\eta_i = \frac{1}{1 + (\Delta V/2V)} \quad (16.5a)$$

where $\Delta V = V_2 - V$.

It is to be noted that Eq. (16.5) or (16.5a) is based only on the definition of useful power and on Eqs. (16.1) and (16.2). All three of these are valid regardless of the compressibility of the fluid or the form of the actuator. Equation (16.5) or (16.5a), therefore, applies quite generally to any propulsive jet, whether produced by a propeller or other jet-propulsion device utilizing the atmosphere as the material of the jet.

The effect of each of the several variables on η_i is seen if a thrust coefficient is introduced, defined as $C_F = 2F/\rho V^2 A$. The efficiency is readily expressed in terms of C_F : $\eta_i = 2/(1 + \sqrt{1 + C_F})$. This relation, which is plotted in Fig. 16.2, shows that η_i increases with increase in V , ρ , or A but decreases with an increase in thrust. It is therefore desirable to make C_F small for an actual propeller, in order that the ideal upper limit to the efficiency may be high. Since the thrust, speed, and density are usually fixed by other considerations, it follows that the propeller diameter should be made as large as possible.

The ideal efficiency cannot be reached by an actual propeller, for the following reasons:

1. Some energy of whirl is left in the slip stream.
2. Tip and hub losses (eddies) always exist.
3. There are friction losses on the blades.
4. Owing to the finite number of blades the flow is not steady but pulsates.
5. The entire disk area is not utilized, there being no flow near the hub.
6. The propeller race is not an ideal jet bounded by a cylindrical surface of discontinuity but breaks up into eddies.

The actual efficiency can, however, approach the ideal quite closely, ordinarily being about 85 per cent of η_i . For airplanes, however, the actual efficiency itself may be as high as 85 per cent. For ships, owing to restrictions on diameter, efficiencies on the order of 60 per cent are more common.

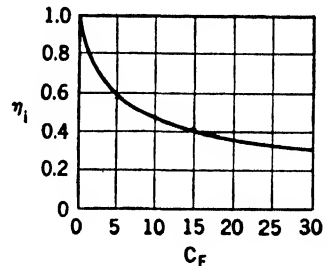


FIG. 16.2. — Ideal propeller efficiency η_i versus thrust coefficient C_F .

16.2 Blade-element Theory of a Propeller. The momentum theory of the previous article applies to an idealized actuator disk the mechanism of which is unspecified. A more detailed theory is therefore needed to investigate the performance of an actual propeller. The blade-element theory, which is commonly used for this purpose, is similar to that already described for an axial-flow fan in Art. 15.4. There are, however, certain differences between the fan and propeller, as regards both construction and purpose, which lead to modifications of the fan theory. The principal differences are pointed out below.

In the fan the product rV_{t_2} (or $Z\Gamma/2\pi$, where Γ is the circulation about one of the Z blades) is constant along the blade, since, by virtue of the housing and hub, no trailing vortices are shed. The flow immediately downstream from the fan is thus made up of a potential-vortex motion superposed on an axial translation and is irrotational (except for the frictional wakes from the blades), since the hub replaces the vortex core. The guide vanes take out the tangential velocity before the hub tapers away to zero diameter, so that no rotation appears in the flow downstream from the fan.

The flow through a propeller, on the other hand, is complicated by the absence of a housing. As already noted in the momentum theory, there is a contraction of the slipstream, which causes the relative axial velocity at the propeller to be higher than the velocity of advance. There is also a radial component of velocity near the tips, but this is so small under normal operating conditions that it is neglected in propeller theory. The principal effect of the exposed blade tips is the three-dimensional flow produced, with its accompaniment of trailing vortices, which are shed downstream in helical paths. Similar conditions exist at the blade roots. The slip stream of a propeller thus contains much rotation (even though friction on the blades be neglected). This vorticity is distributed throughout the stream but shows considerable concentration in two thin cylindrical shells, one springing from the tips and the other from the roots of the blades. The situation is similar to that on a finite wing, described in Arts. 11.21 to 11.23.

The theory of the finite wing shows that the circulation around the wing decreases toward the tip, as the trailing vortices are shed. The gradual dropping off of the circulation around the propeller blades to zero at the tips means that the thrust and torque per unit length do likewise. To see that this is so we refer to Figs. 15.8 and 15.9 and Eqs. (15.17) to (15.21), which are applicable to an element of a propeller blade.

From Eq. (15.17) we get, by substituting $rV_{t_2} = Z\Gamma/2\pi$,

$$\frac{dT}{dr} = \frac{\rho V_1 Z \Gamma}{\eta_m} r \quad (16.6)$$

while, from Fig. 15.9,

$$\begin{aligned} Z dF_n &= Z dF_t \cot(\beta + \tan^{-1} \epsilon) = \eta_m \frac{dT}{r} \cot(\beta + \tan^{-1} \epsilon) \\ &= \rho V_1 Z \Gamma \cot(\beta + \tan^{-1} \epsilon) dr \end{aligned}$$

Hence, the thrust per unit length of all the blades at radius r may be written

$$\frac{dF}{dr} = \frac{Z dF_n}{dr} = \rho V_1 Z \Gamma \cot(\beta + \tan^{-1} \epsilon) \quad (16.7)$$

Starting from Eqs. (16.6) and (16.7), one can develop expressions for dT/dr and dF/dr from which can be computed the torque and thrust distributions for a propeller of given design and size operating at a given speed of advance V and rotational speed ω [2]. The details of this development will not be given here, since they are similar to those of Art. 15.4. Typical computed curves are shown schematically in Fig. 16.3.

From Eq. (16.6) one sees, if Γ is independent of r , as for a fan in a housing, that dT/dr varies linearly with r . For comparison with a propeller such a curve is shown dotted in Fig. 16.3.

Since the purpose of a propeller is to do work at rate FV , the blade-element efficiency is defined as $\eta' = VdF/\eta_m\omega dT$, which with the aid of Eqs. (16.6) and (16.7) becomes

$$\eta' = \frac{V}{\omega r} \frac{1}{\tan(\beta + \tan^{-1} \epsilon)} \quad (16.8)$$

In contrast to that of a ducted fan, the blade-element efficiency of a propeller varies along the radius, the value at three-quarters of the outer radius ($0.75r_o$) being approximately equal to the over-all efficiency.

16.3. Dimensional Analysis of a Propeller. On account of the complexity of the flow over the blades, theory alone cannot at present indicate the most efficient design for a propeller intended to perform under specified conditions. For this reason, model experiments, correlated and interpreted by dimensional analysis, are widely used in propeller research and development.

The input power P and the efficiency η of a propeller of given design are usually desired as functions of the independent variables ρ , ω , D , V , μ , and C . Here D is the propeller diameter, V is the velocity of advance, and C is the sound velocity in the undisturbed air. (This last variable is

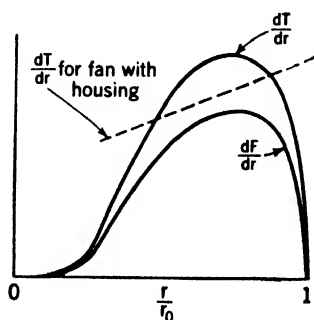


FIG. 16.3. — Schematic representation of torque and thrust grading along a propeller blade. The dotted line indicates the torque grading for a propeller in a duct.

important only in case of very high velocity of the air relative to the propeller blades. The tips are the first part of the blades to be affected by compressibility because their velocity is highest.) It is thus assumed that

$$P = f_1(\rho, \omega, D, V, \mu, C)$$

$$\eta = f_2(\rho, \omega, D, V, \mu, C)$$

Application of the Π theorem to the first of these equations, with ρ , ω , and D included in each of the four Π products, yields

$$\frac{P}{\rho \omega^3 D^5} = C_P = f_3\left(\frac{V}{\omega D}, \frac{\rho \omega D^2}{\mu}, \frac{V}{C}\right) \quad (16.9)$$

where C_P is called the "power coefficient." Similarly, it can be shown that η is a function of the same three variables.

Since $V/\omega D$ (or V/nD , where $n = \omega/2\pi$) determines how fast a given propeller is being turned relative to the speed of advance, or how actively it is being worked, it is a fair assumption to regard V/nD as the primary parameter and to expect that the effects of viscosity (in the Reynolds number $\rho \omega D^2/\mu$) and compressibility (in the Mach number V/C) are secondary and in the nature of corrections. This assumption is borne out by wind-tunnel tests. A typical set of curves for a family of geometrically similar propellers is given in Fig. 16.4.

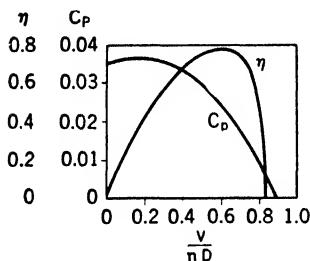


FIG. 16.4. — Power coefficient C_P and efficiency η versus slip coefficient V/nD . (After Weick, reference 2.)

The Reynolds number is found to have an appreciable effect on the efficiency curve, the maximum value of η being larger and occurring at a higher value of V/nD for a full-scale propeller than for a model.

The Mach number has little or no effect on full-scale propeller performance until values of V/C on the order of 0.7 are reached. For still higher Mach numbers the efficiency drops off rapidly, and C_P increases. The thinner the blades of the propeller, the less marked are these effects. Special thin airfoil sections have been developed for use on high-speed propellers. One of these is shown in Fig. 10.6a; they are also referred to near the end of Art. 10.13.

It is common practice to test a series of propellers that are identical, except for the ratio of pitch to diameter (pitch ratio), the pitch being measured at three-quarters radius. The effect of this change in design is indicated in Fig. 16.5, which shows that the maximum value of η increases with increase in pitch ratio. At larger values of pitch ratio than those shown the maximum efficiency is found to decrease again.

For a propeller to perform satisfactorily on a given airplane or vessel, it must fulfill definite requirements as to input power, speed, velocity of advance, and fluid density. The problem is usually to select from a series of propellers of different pitch the one that will have the highest efficiency at the given conditions of operation. The diameter D and efficiency η are to be determined as functions of ρ , V , n , P , and p , it being assumed that the effects of μ and C are negligible. The Π theorem thus leads to

$$\frac{V}{nD} = f_3\left(\frac{\rho V^5}{P n^2}, \frac{p}{D}\right) \quad (16.10)$$

$$\eta = f_4\left(\frac{\rho V^5}{P n^2}, \frac{p}{D}\right) \quad (16.11)$$

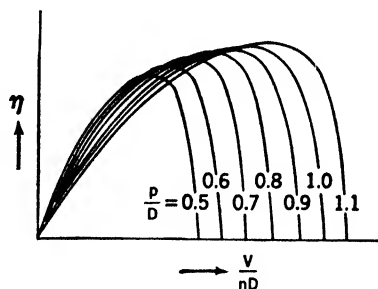


FIG. 16.5. — Efficiency η versus slip coefficient V/nD , for various values of pitch ratio p/D . (After Weick, reference 2.)

It has been found convenient to plot V/nD and η against $(\rho V^5/Pn^2)^{1/5}$, which is called the “speed-power” coefficient C_s . Typical curves for airplane propellers are shown in Fig. 16.6.

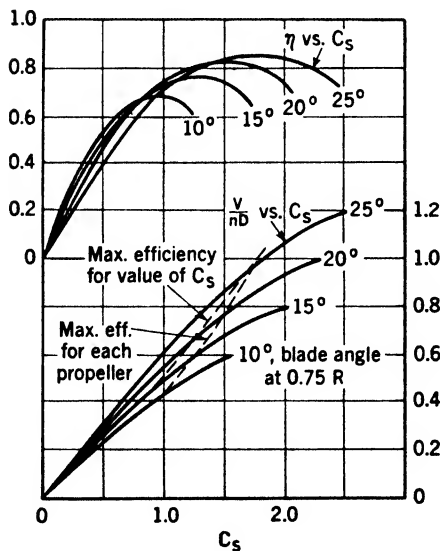


FIG. 16.6. — Design curves for a typical family of airplane propellers. (After Weick, reference 2.)

16.4. Momentum Theory of a Windmill. Just as a propeller adds momentum to a stream of fluid passing through it, a windmill takes momentum out of the wind blowing through it. From continuity considerations, the fluid passing through a propeller must form a jet of reduced diameter in the rear of the propeller. The windmill, on the contrary, has a wake, or slip stream, of reduced velocity and larger diameter.

Assuming steady flow of an ideal, incompressible fluid through a windmill, we select a control volume, with pressures and velocities as shown in Fig. 16.7. By reasoning like that for the propeller (Art.

16.1) we reach a conclusion identical with Eq. (16.4), *viz.*,

$$V_1 = \frac{V + V_2}{2} \quad (16.12)$$

The energy equation [Eq. (5.10)] shows that in this ideal machine the power output is

$$\mathfrak{W}_s \rho A V_1 = \rho A V_1 \frac{(V^2 - V_2^2)}{2}$$

The efficiency of the ideal windmill η_i is defined as the ratio of the output power to the kinetic energy, which, in the absence of the windmill, would

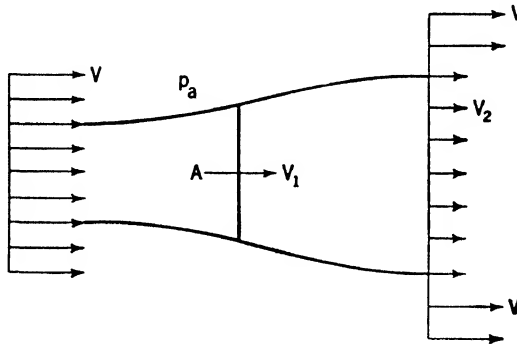


FIG. 16.7.

pass per second through an area A . Thus,

$$\eta_i = \frac{\rho A V_1 (V^2 - V_2^2)/2}{\rho A V^3/2}$$

With the aid of Eq. (16.12) the ideal efficiency can be expressed as

$$\eta_i = \frac{1}{2} \left(1 + \frac{V_2}{V} - \frac{V_2^2}{V^2} - \frac{V_2^3}{V^3} \right) \quad (16.13)$$

Differentiate Eq. (16.13) with respect to V_2/V , and set the derivative equal to zero to find the condition for a maximum of η_i : $\partial \eta_i / \partial (V_2/V) = 1/2 - (V_2/V) - 3/2 (V_2^2/V^2)$. The optimum value of V_2/V is found to be $1/3$; hence

$$\eta_{i\max} = 16/27 \approx 0.59 \quad (16.14)$$

Dutch windmills of very large diameter are said to approach 20 per cent in efficiency. Modern propeller-type windmills are more efficient.

The thrust on the windmill is, of course, of interest to the builder, and it will be zero theoretically when $V = V_2$, a condition that implies some sort of magic feathering of the blades in an ideal fluid, such that the wind is not impeded at all. On the other hand, when V_2 is very small compared with V , we have the case of a many-bladed windmill that nearly stops the wind. The thrust will then be high, and the ideal efficiency about 50 per cent. Practically, such a windmill is likely to be blown over in a storm, and means must be provided to feather the blades and govern the rotative speed.

16.5. Jet Propulsion. There are many ways to produce propulsive jets for aircraft, missiles, and rockets by means of the thrust reaction to the force required to increase the rearward momentum of a stream of gas. The conventional engine-propeller combination is a jet-propulsion device to increase the momentum of the air passing through the propeller-swept area, as shown by Eq. (16.1). Some additional thrust can be obtained by leading the engine exhaust through nozzles directed toward the rear. The additional thrust due to exhaust jets may amount to 10 per cent in a fast airplane.

If the propeller is driven by a gas turbine, the total thrust is the sum of the contributions of the propeller and of the turbine exhaust. Such a gas turbine must develop not only the power to drive the propeller but also the power necessary to drive a compressor to supply air to the combustion chamber where the fuel is burned. The relative proportions of total thrust due to the turbine exhaust and due to the propeller may be arbitrarily chosen by the designer.

For very-high-speed airplanes, where propeller efficiency is low owing to the effects of compressibility, the designer may omit the propeller and depend on the turbine exhaust entirely. This arrangement is known as a "turbojet."

The Germans, for their "buzz bombs," developed an intermittent jet that simplified the compressor-combustion chamber-turbine combination to a simple combustion chamber and tail pipe. Air, in great excess over the amount needed for combustion, is admitted through spring-closed non-return flap valves in the nose. Ignition of the fuel causes a volume increase and pressure rise, closure of the admission valves, and the ejection of hot gas as a jet. The ram pressure $\rho V^2/2$ (due to the speed of flight) then reopens the admission valves to admit a fresh charge of air. By proper tuning of the valve-closing springs and the proportions of the combustion chamber and tail pipe, firing occurs some forty times per second. This device is not effective at very low speeds and has to be launched by a powerful catapult.

A further simplification of the same idea, eliminating the admission valves and the intermittent character of the jet, can be applied at very high speeds, when the ram pressure is substantial. Such a "ram jet" takes combustion air from a forward opening through a diffuser, to decrease its relative velocity and to increase its pressure, into the combustion chamber, where fuel is burned continuously. The heated air and combustion products are ejected through the tail pipe as a steady jet.

A ram jet has certain drawbacks that partly offset its simplicity. In the first place, it has to be got up to high speed before it will operate. Furthermore, combustion is difficult to maintain, both because the flame will blow out if the local air velocity is too great and because the fuel-air

ratio near the ignition region must be kept within practical limits for a wide range of speeds and altitudes.

The rocket is the oldest as well as the simplest device for jet propulsion. The difficulties of an adequate compressed-air supply are eliminated, as well as all questions of fuel-air ratio, mixing, vaporization, flame velocity, and air flow. The rocket carries its own oxygen, so that combustion is independent of both altitude and speed. However, the penalty for these advantages is severe; for 80 to 90 per cent of the weight of the rocket propellant is due to the oxidant, and the propulsive efficiency is low, owing to the small diameter and high speed of the jet. Consequently, rocket propulsion is practicable only for a short operating time.

Applications of rocket propulsion have been made with success to the launching of airplanes and missiles, to self-propulsion of shells and bombs, and to give an airplane a short burst of speed.

The combustion of a solid propellant cannot be turned off and on, but with liquid fuel and liquid oxidant excellent control is possible. The great advantage of rocket propulsion comes from the fact that the thrust is the same at any speed and at any altitude. It has peculiar advantages under extreme conditions, *e.g.*, for a standing start or for supersonic flight in the upper atmosphere where other jet-propulsion means are relatively ineffective.

16.6. Jet-propulsion Comparisons. The utility of any type of jet propulsion depends, not only on the Froude, or ideal, efficiency of the jet proper (propulsive efficiency), but also on the thermal cycle efficiency of the means employed to create the jet. As a consequence, there appear to be certain operating conditions favoring one type and other operating conditions favoring another. As technological improvements are made, the relative merits of the various types may change. Therefore, comparisons based on the existing state of the art should be considered tentative and subject to the light of possible developments and the shadow of inherent limitations.

16.7. Ideal Efficiency of a Jet. In Art. 16.1 expressions for the ideal, or Froude, efficiency and for the thrust of a propulsive jet were given as Eqs. (16.5a) and (16.1), respectively. For easy reference these are reproduced here.

$$\eta_i = \frac{1}{1 + (\Delta V/2V)} \quad (16.5a)$$

$$F = m(V_2 - V) = m \Delta V \quad (16.1)$$

For a propeller the jet is large and ΔV small. Hence $\Delta V/2V$ is small, and the Froude efficiency rises as the speed of flight increases. For a turbojet, on the other hand, the jet is necessarily restricted, and to obtain a given thrust for a small m the velocity increase ΔV must be large. It is

apparent from the Froude efficiency equation that any small high-speed jet having a high value of $\Delta V/V$ is inherently less efficient than systems which utilize a large mass flow and a small value of $\Delta V/V$.

A propeller giving a constant thrust gains rapidly in ideal efficiency with forward speed, because m increases directly with V , causing ΔV to diminish. The result is a doubly rapid reduction of $\Delta V/V$. On the other hand, turbojets and other small high-speed jets give approximately constant ΔV . Therefore, $\Delta V/V$ diminishes with flight speed, although more slowly than for the propeller.

The straight jet, made without a propeller, can in practice closely approach its ideal efficiency even at high flight speeds, whereas the propeller is subject to additional energy losses due to rotation of the wake, nonuniformity of radial-thrust distribution, and the drag of the propeller blades. Furthermore, the blade-drag losses become serious at high speeds, as a consequence of compressibility effects. The actual efficiency of the propeller thus starts to fall off at a flight speed corresponding approximately to a Mach number $M = 0.7$; and near the speed of sound, that is, for $M = 1$, the actual propulsive efficiency of the propeller may be very low.

16.8. Engine-propeller System, Turbojet, Ram Jet. In this section, the computed efficiencies* of three types of jet propulsion at an altitude of 30,000 ft are based on the following assumptions:

Engine-propeller System:

Rotational tip speed corresponding to $M = 0.8$	
Blade-drag loss, and rotation of wake 7% at $M = 0.6$, increasing to 40% at $M = 1.0$	
Compression ratio of engine	7.5
Ideal thermal efficiency	44%
Actual thermal efficiency	25%

Turbojet:

Maximum temperature at end of combustion	1500 F abs
Compression ratio	5.0
Compressor efficiency	80%
Turbine efficiency	75%
Combustion-chamber pressure loss	8%

Ram jet:

Maximum temperature at end of combustion	2960 F abs
Effective pressure in combustion chamber	88% of ideal ram

a. Propulsive Efficiency. At flight Mach numbers up to 0.7 (476 mph at 30,000 ft) the propeller has a far higher Froude, or propulsive, efficiency than the jet units. Above $M = 0.7$, however, a rapid loss for the propeller occurs owing to compressibility effects on blade drag, while the turbojet continues to gain in efficiency with speed. Reliable test data on propeller efficiencies above $M = 0.7$ are not available, and the dotted curve of

* Made by John V. Becker of the NACA.

Fig. 16.8 is an estimate. In spite of this uncertainty, Fig. 16.8 indicates that turbojet and propeller propulsive efficiencies approach equality before $M = 1.0$.

For the ram jet at $M = 0.45$, the jet velocity becomes equal to the flight velocity, so that $\Delta V = 0$. The propulsive efficiency of 100 per cent for this case is of no significance, since the thrust is zero.

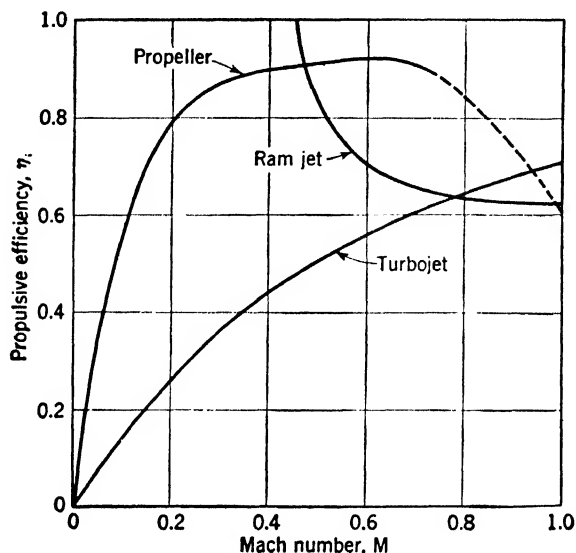


FIG. 16.8. — Propulsive efficiency η_p versus Mach number M , for propeller, turbojet, and ram jet.

b. Cycle Efficiency. The efficiency of the thermodynamic cycle of the engine is of equal importance with the propulsive efficiency in establishing the over-all or thermopropulsive characteristics of the system. Figure 16.9 shows that the thermodynamic cycle efficiency for the turbojet is not greatly lower than that of the internal-combustion engine, even at low flight speeds. Owing to the increased compression resulting from ram the turbojet cycle efficiency improves with flight speed, becoming about equal to that of the internal-combustion engine at $M = 1.0$. The cycle efficiency for the ram jet in the subsonic speed range is extremely low in comparison with the other systems. At a supersonic speed of the order of $M = 1.3$ the ram-jet cycle efficiency becomes about equal in magnitude to that of the turbojet.

c. Over-all Efficiency. The over-all efficiency is the product of the propulsive and the cycle efficiencies. Figure 16.10 indicates that the turbojet is considerably inferior to the propeller-engine system for Mach numbers up to at least 0.7, where the turbojet efficiency is only 0.13 as compared

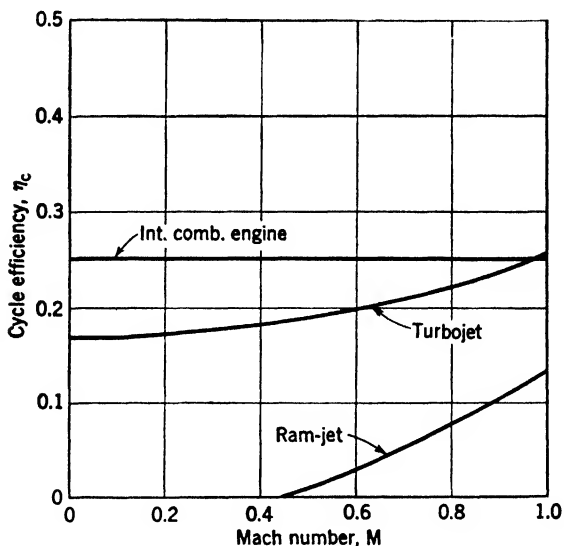


FIG. 16.9. — Cycle efficiency η_c versus Mach number M , for a conventional internal-combustion engine, turbojet, and ram jet.

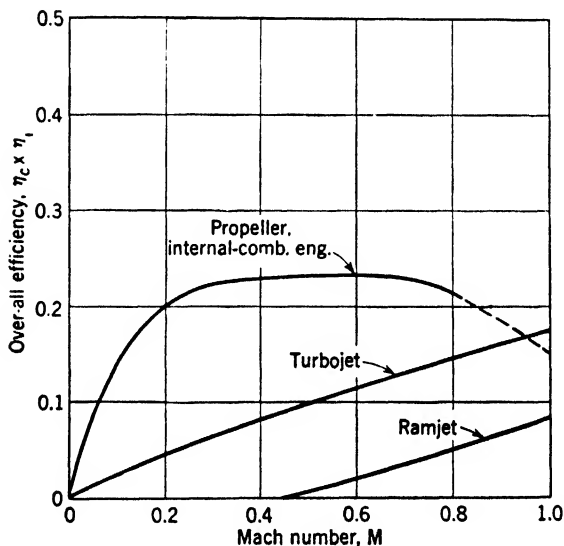


FIG. 16.10. — Over-all efficiency $\eta_c \times \eta_i$ versus Mach number M , for propeller-engine, turbojet, and ram jet.

with 0.23 for the propeller-engine system. At Mach numbers approaching unity, however, the performance of the two systems is about equal. The ram jet, because of poor cycle efficiency, has a very low over-all efficiency at subsonic speeds. The only practical advantage of this system at sub-

sonic speeds, aside from its obvious simplicity, is the absence of the maximum-temperature restriction imposed on the turbine in turbojet systems.

The increasing use of the turbojet for propulsion of aircraft whose high speed lies in the Mach-number range of 0.7 to 0.8 is justified by the feasibility of employing extremely high fuel rates. By this means, thrusts much higher than those obtainable with current engine-propeller systems can be achieved in spite of the lower over-all efficiency of the turbojet at these flight speeds. Other advantages are mechanical simplicity, light weight, and less bulk.

16.9. Trends of Development. Present airplane propellers under favorable conditions operate at an actual efficiency of the order of 85 per cent, which is close to the ideal efficiency. Research is devoted to the development of blade forms that postpone the advent of serious drag losses as the speed of sound is approached. Considerable success toward this end has been obtained by use of wide and thin blade profiles, swept-back leading edges, and other artifices. While it may be possible to retain a good efficiency up to a rotational-speed Mach number of unity, there will eventually occur a serious drop in efficiency as compressibility effects become predominant. Consequently, it is fair to state that, while the propeller as a propulsive means is highly efficient, it is inherently limited to subsonic flight speeds. There is little prospect of radical change in this situation.

The internal-combustion engine is also a highly efficient machine. With present high compression ratios and high-octane gasoline, fuel consumption may be as low as 0.4 lb per bhp-hr, and with laboratory fuels now available this figure can be further reduced. An additional gain in economy is possible by recovery of wasted power from the exhaust by use of an exhaust gas turbine geared to the crankshaft. Such a compound engine might have a fuel consumption of 0.3 lb per bhp-hr.

The great advantages of the internal-combustion engine are its high state of development and its high efficiency as a compressor and combustion device. Its disadvantages are that it is complicated and costly, limited in maximum power output, and must be used with a propeller of some form. The engine-propeller combination can be improved in over-all efficiency to a useful degree but is inherently limited to subsonic flight and to moderate altitudes.

A propeller driven by a gas-turbine unit and assisted by the exhaust jet of the turbine is lighter and simpler, but the fuel consumption may be of the order of 0.5 to 0.8 lb per bhp-hr. Since the turbine cannot withstand an excessive temperature, it is necessary to compress much more air than that necessary for the combustion of the fuel. Also, the art of compressor design limits the compression ratio. Consequently, the cycle efficiency is inferior to that of the internal-combustion engine but is sub-

ject to substantial improvement whenever higher compression ratios are feasible. By the use of regeneration, heat exchangers to permit hot exhaust gases to warm the incoming air, a gain in economy can be had at the expense of extra weight and bulk. However, the propeller-turbine combination suffers from the inherent limitations of the propeller.

16.10. Turbojets. The turbojet unit, by omission of the propeller, breaks away from the inherent propeller limitations. Here the gas turbine supplies only the power for the compressor. Such units developed for military purposes show a specific fuel consumption of about 1 lb per hr per lb of thrust. At 375 mph this corresponds to 1 lb of fuel per propulsive horsepower-hour. Since thrust is substantially independent of speed, the power economy improves with speed. A thrust of 4,000 to 5,000 lb is practicable at present, while the weight per unit thrust (specific weight) averages about 0.4.

It should be appreciated that the gas turbine was made possible by the availability of metals able to withstand high operating temperatures. The temperature of the turbine blades closely approaches the ambient-gas temperature, while in the Otto-cycle engine extremes of temperature are only momentary and the average temperature of the parts is much lower. Continuous operation at high temperature results in rapid loss of strength and high creep and corrosion rates.

Arrangements to cool the blades with compressed air entail a loss of efficiency and a higher specific fuel consumption and specific weight. German turbojets developed during the Second World War were inferior in these respects to British and American designs of the same period. German designers were short of cobalt, nickel, chromium, molybdenum, and other desirable alloying elements and resorted to somewhat elaborate cooling means. It can be expected that, as better heat-resisting alloys become available, important improvements in the gas turbine and therefore in the turbojet will follow.

Already materials are known having a useful service life at 1500 F, and other types would be usable at 3000 F if brittleness and corrosion could be overcome. Ceramics, sintered powdered metals, and their combinations have possibilities. Metallurgical research can be expected to produce improved heat-resisting materials, with a corresponding opportunity to raise the cycle efficiency of the gas turbine.

As the cycle efficiency is increased, separation and shock effects in the flow through the compressor and turbine become relatively more important. Thus, when the rate of pressure rise along a blade surface is too rapid, the boundary layer does not flow into the high-pressure region and separation takes place, with considerable energy loss. This problem of a rising pressure gradient is more serious in the compressor than in the turbine.

Adverse pressure gradients may arise from a compressibility shock with

abrupt transition from supersonic to subsonic flow and a consequent sharp pressure rise along the surface.

The fluid mechanics of flow separation for a three-dimensional rotating blade system is not well understood, nor are methods available for postponing the occurrence of compressibility shock. Consequently, the design of both compressors and turbines is based on conservative approximations, and maximum efficiency and compactness are not realized.

Owing to the fact that the turbojet requires combustion air, it is not effective above a limiting altitude. Because of expense, it is unlikely to be used to propel short-range missiles where rocket propulsion will suffice.

None of the readily available organic fuels offers the possibility of any significant improvement over petroleum products. The light combustible metals, such as magnesium, possess higher heating values per unit of weight or volume, but magnesium oxide would be discharged through the turbine. This appears to be intolerable.

In conclusion it should be pointed out that increased thrust resulting from higher combustion temperature is accompanied by decreased propulsive efficiency, with a resultant drop in over-all efficiency. Higher temperature is nevertheless desirable, because a higher power output can thus be obtained, despite the sacrifice in over-all efficiency.

16.11. Ram Jets. The intermittent ram-jet or buzz-bomb engine developed by the Germans had a specific fuel consumption of about 3 lb per hr per lb. Analysis indicates that this figure could be reduced to one-third of the above value if more rapid combustion could be achieved. To do this requires a fuel system with a burning time of a few thousandths of a second. Were such an improvement to be made, the intermittent ram jet could compete with the internal-combustion engine at subsonic flight speeds.

Since the intermittent ram-jet engine is extremely simple and cheap, it is the ideal propulsive system for an expendable missile. Its best operating speed is from 400 to 500 mph, and from the standpoint of over-all weight its range should be somewhat less than 500 miles. Operation at flight speeds greater than 600 mph is questionable because of difficulties of air supply and valving.

The true ram jet is relatively undeveloped but appears to be the most promising propulsive device for supersonic long-range missiles. Its efficiency increases with speed, as ram pressure rises. At subsonic speeds its thrust is too low to be of interest, but at supersonic speeds it should be very effective. Ram-jet missiles must use some other source of power, such as a rocket, to bring them to a flight speed above 400 mph, at which the ram jet can take over. At a flight speed corresponding to $M = 2$, a ram jet should show a fuel consumption of about 0.8 lb per hp-hr.

The supersonic ram jet presents a host of aerodynamic and combustion

problems that are not yet solved, and there appear to be two inherent limitations, *viz.*, low thrust at subsonic speeds and low thrust at low air density (high altitude).

16.12. Rocket Mechanics. The propulsion of a rocket is due to the reaction of its jet. Let the jet velocity be designated by W relative to reference axes moving with the rocket, and let e represent the energy content of the propellant per unit mass (foot-pounds per slug or square feet per square second). In this reference system, unburned propellant has no kinetic energy. The burning of propellant in the rocket will convert a fraction η_0 of its energy into kinetic energy in the jet.

$$\eta_0 e = \frac{W^2}{2}$$

or

$$W = \sqrt{2\eta_0 e} \quad (16.15)$$

Let propellant be burned at the mass rate of m slugs per sec. Then the reaction, or thrust, of the jet will be the rate of increase of momentum in the jet, relative to the moving axes,

$$T = mW = m\sqrt{2\eta_0 e} \quad (16.16)$$

Now refer to axes fixed on the earth, and let the "absolute" velocity of the rocket be V . Observe that the rocket's original energy supply is being used up at the rate of $m[e + (V^2/2)]$, as propellant of mass m is ejected every second. The useful work of the thrust in moving the rocket is done at the rate of $TV = mV\sqrt{2\eta_0 e}$. The over-all efficiency of the rocket η_R in the fixed reference system is therefore

$$\eta_R = \frac{mV\sqrt{2\eta_0 e}}{m[e + (V^2/2)]} = 2\eta_0 \frac{W/V}{(W/V)^2 + \eta_0} \quad (16.17)$$

Setting the derivative $\partial\eta_R/\partial(W/V) = 0$, one finds that η_R is a maximum if

$$\frac{W}{V} = \sqrt{\eta_0} \quad (16.18)$$

and that, consequently,

$$\eta_{R_{\max}} = \sqrt{\eta_0} \quad (16.19)$$

For perfect conversion of energy of combustion, that is, for $\eta_0 = 1$, the over-all efficiency would be 100 per cent, and W would equal V . The exhaust material would thus be ejected at rocket speed and left without kinetic energy relative to the reference system in which work was being done. Usually η_0 is found to be about 0.25, giving $\eta_R = 0.5$ as the maximum over-all efficiency. However, this efficiency is of secondary interest to the designer, who must utilize the greatest amount of energy from the initial mass of propellant.

The energy usefully applied per unit mass of propellant is

$$\eta_R \left(e + \frac{V^2}{2} \right) = V \sqrt{2\eta_0 e} \approx \frac{V}{\sqrt{2}} \sqrt{e}$$

For a given kind of propellant this quantity increases directly with rocket speed. From Eqs. (16.18) and (16.15) it is seen that, for given speed V , the highest efficiency is attained for $V = W/\sqrt{\eta_0} = \sqrt{2e}$, or $e = V^2/2$. For example, at low speed, say 400 ft per sec, the best efficiency would be obtained from a propellant having an $e = 80,000$ sq ft per sq sec. The over-all efficiency would thus be 0.5, and the useful work per unit mass would be $\eta_R [e + (V^2/2)] = 80,000$ sq ft per sq sec.

A mixture of gasoline and oxygen, on the other hand, for which $e = 3,300,000g$ would be utilized at an over-all efficiency [Eq. (16.17)] of only 2.7 per cent at this speed, but the useful energy per unit mass would be 2.96×10^6 sq ft per sq sec.

Consequently, it appears that for starting rockets, and low speeds generally the high-energy propellants are best in spite of low efficiency.

A rocket is handicapped for long range by having to carry its own oxidant as well as the fuel, but the ram jet uses the atmosphere as oxidant. The following simplified comparison brings out the advantage of the ram jet:

It can be shown for a ram jet, as in problem 16.7, that the relative kinetic energy of the jet is equal to the relative kinetic energy of the incoming air plus that part of the energy of the fuel which is converted to kinetic energy by the combustion process. Thus, under the assumption that 15 slugs of air combine with 1 slug of fuel, $16W^2/2 = (15V^2/2) + \eta_0 e$. Hence,

$$W = \frac{1}{4} \sqrt{2\eta_0 e + 15V^2} \quad (16.20)$$

Refer now to axes fixed in space. Let m_f represent the mass of gasoline burned per second. The net thrust, resulting from the burning of fuel at this rate in $15m_f$ slugs of air per second, will be

$$T = m_f W + 15m_f (W - V) = m_f (16W - 15V) \quad (16.21)$$

For a rocket burning its propellant at m_r slugs per sec, the corresponding statement is, from Eq. (16.16),

$$T = m_r \sqrt{2\eta_0 e_r} \quad (16.22)$$

where e_r is the energy per unit mass of propellant. Elimination of T from Eqs. (16.21) and (16.22) gives $m_r/m_f = (16W - 15V)/\sqrt{2\eta_0 e_r}$, while substitution for W from Eq. (16.20) yields

$$\frac{m_r}{m_f} = \frac{4\sqrt{2\eta_0 e + 15V^2} - 15V}{\sqrt{2\eta_0 e_r}} \quad (16.23)$$

Taking $c = 15 \times 10^6 g$, $e_r = 3.3 \times 10^6 g$, and $\eta_0 = 0.25$, we find the ratio of fuel rates to be

$$\frac{\text{Rocket fuel rate}}{\text{Ram-jet fuel rate}} = \begin{cases} 7.1 & \text{for } V = 800 \text{ ft/sec} \\ 5.8 & \text{for } V = 1,600 \text{ ft/sec} \end{cases}$$

The possibility of sending rockets to very great altitudes has prompted speculation about leaving the earth [9]. A very great quantity of propellant would be required, and the arrangement would have to convert quickly a large portion of the energy of the propellant into kinetic energy of the rocket. Work done in raising the weight of unburned propellant to a great height is wasted. The rocket should be accelerated to a high velocity in the shortest possible distance.

Consider the system of mass m shown in Fig. 16.11*a*, comprising a rocket and the propellant inside it at an arbitrary time. The rocket has an instantaneous upward (x) velocity V relative to the earth, and the motion of the burning propellant relative to the rocket is steady.

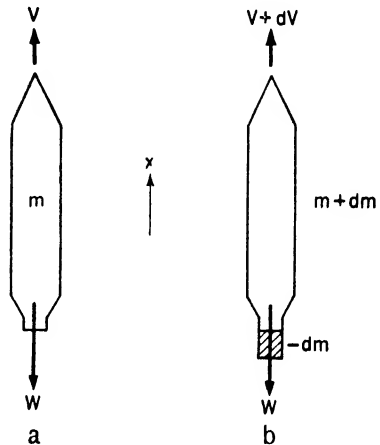


FIG. 16.11.

The constant relative velocity of the jet at exit is denoted by W .

By Newton's second law the change in x momentum of this system in time dt is equal to the product of the resultant x force F_x and dt . During this time interval an observer moving with the rocket would see a reduction $-dm$ in the mass of unburned propellant and a movement of an equal mass of gas out the tail pipe, with relative velocity W (Fig. 16.11*b*). He would see no change in the relative velocity of any part of the remaining mass, $m + dm$. The change in "absolute" velocity of this remaining mass is therefore dV , and its momentum change is $(m + dm) dV$. The initial absolute velocity of the mass $-dm$ is V , and its final velocity is $V + dV - W$. Its momentum change is therefore $-dm(V + dV - W - V)$ or $-dm(dV - W)$. The change in momentum of the entire system is thus known, and

$$F_x dt = (m + dm) dV - dm(dV - W) = m dV + W dm \quad (16.24)$$

It may be remarked parenthetically that Eq. (16.24) is equivalent to Eq. (16.16), for uniform motion of the rocket ($V = \text{constant}$). In this case, $F_x - W(dm/dt) = 0$ [which in the notation of Eq. (16.16) is $F_x + Wm = 0$]. In words, the system behaves as if, in addition to the actual external force F_x , it were acted upon by a forward thrust $T = -W(dm/dt)$.

This notion of the effective thrust T of the jet can also be applied to the accelerated system. For Eq. (16.24) can be rewritten as $F_x - W(dm/dt) = m(dV/dt)$ or $F_x + T = m(dV/dt)$. At any instant, therefore, the system behaves as if it had a constant mass m and were acted upon by a thrust T in addition to the actual external force F_x .

If now the air resistance of the rocket be neglected, the only force on the system is its weight mg , acting in the negative x direction. Equation (16.24) thus becomes $-W(dm/m) = dV + g dt$, which, with W and g constant, integrates to

$$\ln \frac{m_0}{m} = \frac{V}{W} + \frac{gt}{W} \quad (16.25)$$

where m_0 is the mass of the rocket and propellant at the start of the motion, when $V = 0$ and $t = 0$. If t be the time required to burn all the propellant, m and V will be the values of mass and velocity at "all burnt."

The jet velocity W for a given propellant and a given η_0 can be determined from Eq. (16.15). If the velocity V required to carry the rocket out of the earth's gravitational field is found, the ratio m_0/m of starting mass to all-burnt mass can be computed from Eq. (16.25). In the absence of any data on burning time, gt may, as a first approximation, be assumed negligible compared with V . Both this approximation and the neglect of air resistance tend to give a smaller value for m_0/m than the actual one; they both err on the optimistic side.

To find the initial velocity required to carry a body outside the earth's gravitational field (with air resistance neglected) we use the Newtonian law of gravitation,

$$F = -\frac{Gmm_E}{r^2} \quad (16.26)$$

where F is the force between a mass m and the earth of mass m_E , r is the distance between the earth's center and m , and G is the gravitational constant. The negative sign indicates that F acts in a direction opposite to that of increasing r .

The work done by F on m as m moves away from the earth's surface (where $r = r_E$) to infinity is

$$\int_{r_E}^{\infty} F dr = -Gmm_E \int_{r_E}^{\infty} \frac{dr}{r^2} = -\frac{Gmm_E}{r_E}$$

This work is equal to the difference between the final and initial kinetic energies of the mass m . The smallest initial kinetic energy which suffices to get the mass away from the earth is that corresponding to a final kinetic energy of zero. Thus $-Gmm_E/r_E = 0 - (m/2)V^2$. Noting that at the earth's surface $F = -mg$, we get, from Eq. (16.26), $gr_E = Gm_E/r_E$, so that

$$V = \sqrt{2gr_E} = 36,700 \text{ ft/sec} \quad (16.27)$$

where the value $r_E = 20.9 \times 10^6$ ft has been substituted.

An approximate value of m_0/m is now found, for a propellant of gasoline and oxygen ($e = 3.3 \times 10^6 g$ sq ft per sq sec) and for $\eta_0 = 1/4$, by combination of Eqs. (16.15), (16.25), and (16.27)

$$\ln \frac{m_0}{m} = \frac{1}{\sqrt{2\eta_0 e}} (V + gt) \quad (16.28)$$

$$\ln \frac{m_0}{m} = \frac{36,700 + 0}{\sqrt{3.3 \times 10^6 \times 32.2/2}} = 5.03$$

$$\frac{m_0}{m} = 155$$

$$\frac{m_0 - m}{m_0} = 0.993 \quad (16.29)$$

The mass of propellant is thus more than 99 per cent of the total, and rocket flight to other planets is impracticable with gasoline and oxygen.

The picture is completely changed, however, if one considers the eventual possibility of using a propellant such as the uranium isotope U-235, which derives energy from nuclear changes rather than from ordinary combustion. For U-235, the value of e is $2.44 \times 10^{13} g$ sq ft per sq sec [4], which is 0.74×10^7 times larger than that for gasoline and oxygen. With this value of e , Eq. (16.28) yields

$$\frac{m_0 - m}{m_0} = 0.0019 \quad (16.30)$$

The mass of propellant is only about 0.2 per cent of the initial mass and is practically negligible.

Even though a source of nuclear power is theoretically available, the problem of its utilization at a reasonable efficiency (η_0) remains to be solved. This problem is referred to again at the end of this chapter.

The feasibility of a space rocket is one aspect of the general question of the range of a simple rocket without wings. In this connection it is of interest to compare the results of Eq. (16.25) with information now available concerning the German V-2 rocket. The estimated maximum velocity V of this rocket was 3,500 mph or 5,130 ft per sec. The propellant, alcohol and liquid oxygen, should have given a jet velocity W of about 6,500 ft per sec. The burning time t was 60 sec. Equation (16.25) thus yields $m_0/m = 2.95$. The reported initial weight of the V-2 was 13.5 tons, including some 9 tons of propellant, so that actually $m_0/m = 13.5/4.5 = 3.0$.

In view of the uncertainty in several of the figures used, the very close

agreement between the actual and computed values of m_0/m is largely accidental. It is clear, however, that Eq. (16.25) gives a good approximation to the truth.

It is obvious that the V-2 type of rocket would have greater range if more fuel were burned, but this would require a vehicle of increased m_0/m ratio. In view of the necessity for at least a ton of explosive, elaborate control mechanisms, and a powerful pumping system for the liquid propellant, it would be difficult to bring this ratio much beyond 3.

Discussion of the effect of adding wings to the missile to prolong its trajectory by gliding under the pull of gravity is beyond the scope of this text.

All rocket propellants now in use have roughly the same energy per unit mass or per unit weight. The following values of energy are quoted to indicate that all are of the same order of magnitude:

Propellant	c/g , Ft-lb/lb
Hydrogen and ozone.....	5,500,000
Hydrogen and oxygen.....	4,500,000
Gasoline and oxygen.....	3,300,000
TNT.....	2,500,000
Guncotton.....	1,500,000

The merits of a propellant may also be judged on the basis of the impulse per unit weight or per unit volume, which is called the "specific impulse." The specific impulse, which is merely the thrust divided by the weight or volume of propellant burned per unit time, can be computed from Eq. (16.16). Values for several propellants are tabulated below.

Propellant	Specific impulse		W , ft/sec
	Lb-sec/lb	Lb-sec/gal	
Solid (Ballistite).....	210	2,850	6,750
Fuming nitric acid and aniline.	240	2,750	7,700
Liquid oxygen and hydrogen ..	340	1,300	11,000

Note that the oxygen-hydrogen pair is inferior, on a volume basis, because of the low density of the hydrogen.

To improve the performance of rockets substantially it would be necessary to increase jet temperature or to employ gas of lower molecular weight. Neither of these means offers great promise [8]. Temperature is already of the order of 4000 to 5000 F, and the weight of metal required to withstand the pressure is substantial. The exit nozzle is difficult to keep cool enough to prevent rapid erosion and erratic flight.

To make a major improvement in rocket missiles, some method of acceleration of the jet material other than pressure expansion is needed.

Discoveries in the field of nuclear power may some day provide means for accelerating electrons or gaseous ions, but there will still remain the problems of a material to withstand an extremely high rate of energy release in a confined space and of a working fluid to be ejected. The difficulties may be appreciated from the following comparison of the velocities involved:

The velocity W obtained with the best of the present propellants is on the order of 10^4 ft per sec. If a nuclear propellant were to be utilized at roughly the same efficiency, a velocity one thousand times greater would be attained—on the order of 10^7 ft per sec.

Present rocket research is concerned with propellants giving a high spontaneous energy release that are, at the same time, nontoxic, non-corrosive, stable in manufacture and storage, and insensitive to impurities or ordinary temperature changes. Besides the propellants mentioned previously the following have been found useful: hydrogen peroxide with permanganate catalyst, hydrogen peroxide, and hydrazine hydrate.

SELECTED BIBLIOGRAPHY

Propellers:

1. GLAUERT, H.: "Aerofoil and Airscrew Theory," Cambridge University Press, London, 1926.
2. WEICK, F. E.: "Aircraft Propeller Design," McGraw-Hill Book Company, Inc., New York, 1930.

Jets:

3. SÄNGER, E.: "Raketen Flugtechnik," R. Oldenbourg, Munich and Berlin, 1933.
4. TSIEN, HSUE-SHEN: Atomic Energy, *J. Aeronaut. Sci.*, vol. 13, pp. 171–180, April, 1946.
5. Westinghouse Electric and Manufacturing Company: The Day Dawns for Jet Propulsion, *Westinghouse Eng.*, March, 1945; also *Reprint* 4123.
6. ZUCROW, M. J.: Jet Propulsion and Rockets for Assisted Take-off, *Trans. Am. Soc. Mech. Engrs.*, vol. 68, pp. 177–188, April, 1946.
7. Various articles that have appeared during recent years in *Aviation* (see especially vols. 44 and 45, 1945 and 1946).
8. ACKERET, J.: Zur Theorie der Raketen, *Helv. Phys. Acta*, vol. 19, pp. 103–112, 1946.
9. MALINA, F. J., and M. SUMMERFIELD: The Problem of Escape from the Earth by Rocket, *J. Aeronaut. Sci.*, vol. 14, pp. 471–480, August, 1947.

CHAPTER XVII

FLUID COUPLINGS AND TORQUE CONVERTERS

Fluid couplings and torque converters are power transmissions whose operation depends on the dynamics of fluid motion. A coupling consists of only two elements, the primary, which is a centrifugal pump; and the secondary, which is a reaction turbine driven by the pump. Both these elements are enclosed in one casing, in order to make the efficiency as large as possible. Since torque is applied to the coupling only at the primary and secondary shafts, these two torques are equal under steady running conditions.

A torque converter comprises the same two elements as a coupling, but interposed between them is a set of guide vanes, fastened to the casing. By suitable design the torque reaction on these stationary vanes can be given any desired value. The output torque at starting can thus be made several times greater than the input torque.

17.1. Description of a Fluid Coupling. In Fig. 17.1 is shown a typical fluid coupling. The primary and secondary runners are identical; each

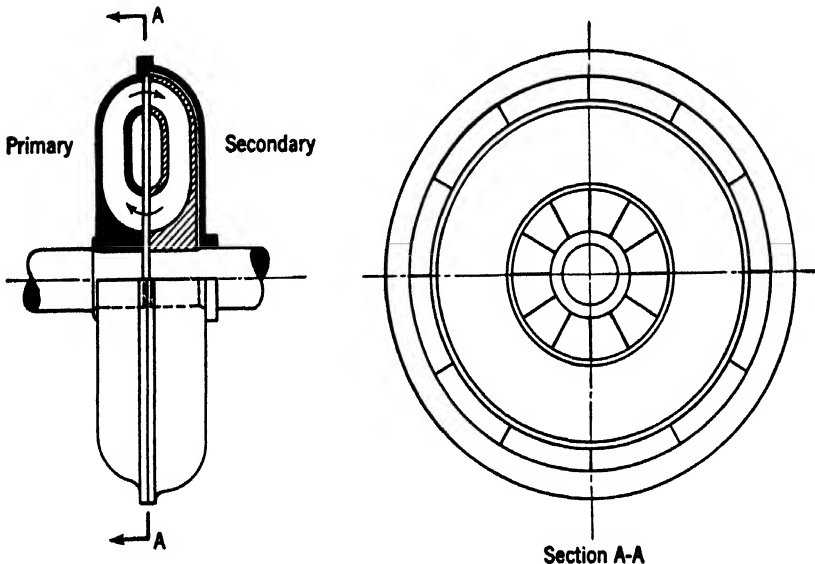


FIG. 17.1. — Fluid coupling.

has straight, radial blades so that it resembles half of an orange with the pulp removed. There is no mechanical connection between the runners.

The coupling is wholly or partly filled with liquid (usually oil), so that,

when the primary is rotated, the oil in it acquires moment of momentum about the axis and also tends to move radially outward through the passages between the blades. Oil thus flows from primary to secondary at the periphery and, by virtue of continuity, from secondary to primary at the hub. This circulation of oil continues as long as the secondary rotates more slowly than the primary, *i.e.*, as long as slip occurs. If the speeds are equal (zero slip), the centrifugal effects balance each other and no oil flows.

The moment of momentum of the oil leaving the primary is greater than that of the oil entering, for the tangential velocity is greater at the periphery than at the hub. Under steady conditions the net efflux of moment of momentum from the primary is equal to the driving torque, by virtue of Eq. (6.19). Similarly, the net influx to the secondary equals the load torque on the driven shaft. The torque transmitted by a given coupling will therefore depend both on the speed of the primary and on the slip. For zero slip, no torque is transmitted, regardless of the speed. It will be shown below that for a given slip the torque is practically proportional to the square of the primary speed. Hence a coupling is best adapted to high-speed operation.

The efficiency is defined as the ratio of output to input power. Since the power equals the product of torque and angular velocity and input and output torques are equal, the efficiency reduces to the ratio of secondary to primary speed. At normal loads and speeds the efficiency is high, usually more than 95 per cent.

The smallest couplings in use handle about 1 hp and the largest, about 36,000 hp.

The principal advantages of the fluid coupling lie in its unsteady-state characteristics. It provides low starting torques on electric motors and internal-combustion engines having high-inertia loads and smooths out torsional vibrations originating either at the prime mover or at the load.

Under steady conditions the coupling will provide a smoothly variable speed from a constant-speed prime mover. We accomplish this variation by changing the amount of oil in the coupling and thus controlling the amount of slip. By this means, flexibility is gained at the expense of efficiency, since slip and efficiency are related by the equation

$$\text{Slip} = s = 1 - \frac{\omega_s}{\omega_p} = 1 - \eta \quad (17.1)$$

where ω_s and ω_p are the secondary and primary speeds, respectively, and η is the efficiency. Such speed control is obviously unsuited to constant-power applications or to prolonged operation at reduced speed if efficiency is important.

Fluid couplings have been found particularly useful for automotive

drives; marine, railroad, and industrial diesel drives; electric-motor drives; and variable-speed conveyer operation.

17.2. Steady-state Analysis of a Fluid Coupling. A dimensional analysis of a coupling may be made, as follows: We assume that the torque T is a function only of ρ , ω_p , D , s , \mathfrak{V} , and μ , for a coupling of given design.

Here \mathfrak{V} , ρ , and μ are the total volume, density, and viscosity, respectively, of the operating fluid, ω_p is the primary speed, and D is the coupling diameter. In applying the Π theorem we may let ρ , ω_p , and D be common to all four Π products. We get

$$C_T = \frac{T}{\rho \omega_p^2 D^5} = \phi \left(s, \frac{\rho \omega_p D^2}{\mu}, \frac{\mathfrak{V}}{D^3} \right) \quad (17.2)$$

Tests at a fixed value of \mathfrak{V}/D^3 were performed at the Massachusetts Institute of Technology on an automotive type of coupling. Some of the results are shown in Fig. 17.2, from which the effect of slip is seen to be much more important than that of the Reynolds number $R = \rho \omega_p D^2 / \mu$. This behavior is not surprising, since it will be recalled from earlier chapters that the minor influence of R is typical of hydrodynamic machinery. The meaning of these curves is clarified by the following approximate analysis of the mode of operation of a coupling:

Application of Eq. (6.19) to the primary runner of the coupling of Fig. 17.3 shows that the primary torque equals the net efflux of moment of momentum from the primary. In the

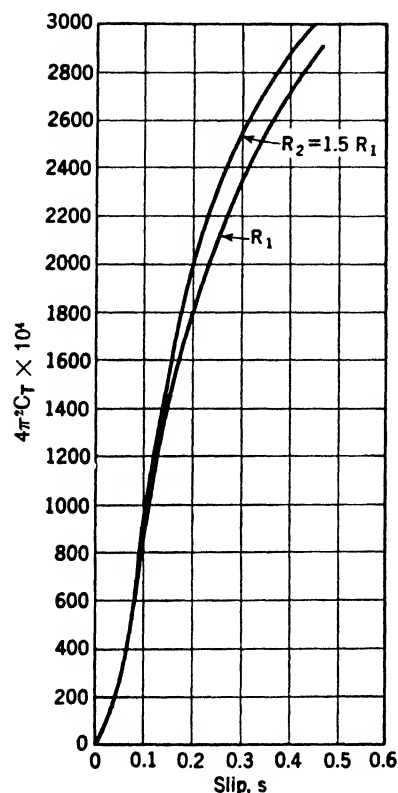


FIG. 17.2. — Torque coefficient versus slip for a fluid coupling. The measurements were made at two values of Reynolds number R , and for a constant volume of oil in the coupling.

notation of Fig. 17.3 the efflux of moment of momentum is $\rho Q \omega_p r_2^2$, and the influx is $\rho Q \omega_p r_1^2$. Thus, the torque is

$$T = \rho Q (\omega_p r_2^2 - \omega_s r_1^2) \quad (17.3)$$

To render this equation useful, we eliminate the unknown factor Q by means of the following considerations:

The difference between the input and output power $T(\omega_p - \omega_s)$ is due to the losses in the coupling, which arise in two ways.

1. As oil enters either the primary or secondary runner, the tangential velocity component of the oil suffers an abrupt change, owing to the difference between ω_p and ω_s . Eddies are thus set up because the main flow tends to separate from the leading edges of the blades. The energy of these eddies, which is called the "shock loss," is eventually dissipated

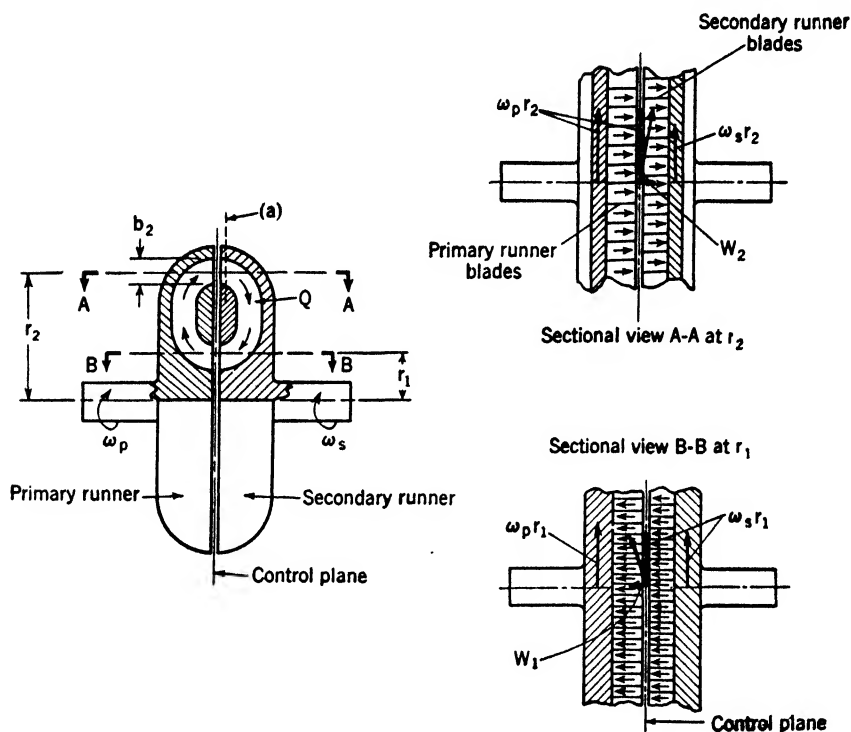


FIG. 17.3. — Velocity diagrams for a fluid coupling.

by viscosity and, under the steady conditions here assumed, appears as a heat transfer to the surroundings.

To estimate the shock loss at entrance to the secondary we use the steady-flow energy equation referred to axes rotating with the secondary [Eq. (6.21)]. In this rotating frame of reference no shaft work appears to be done on the fluid between the control plane and an adjacent section *a* just inside the secondary runner (see Fig. 17.3). Neglecting any change in pressure, we get from Eq. (6.21) that the energy of the eddies at *a* must be equal to the change in the average kinetic energy of the fluid as it moves from the control plane to *a*.^{*} In a coupling having thin, radial blades,

^{*} The momentum law shows the pressure change to be small, since the friction forces on the elementary lengths of blade are small and, by continuity, the axial momentum is constant.

practically all the tangential velocity component at the control plane $(\omega_p - \omega_s)r_2$ has disappeared at section *a*. The axial velocity is constant, by continuity, so that the energy per unit mass converted into eddies is $(\omega_p - \omega_s)^2 r_2^2 / 2$ sq ft per sq sec. Similarly, at the entrance to the primary, the energy per unit mass of the eddies is $(\omega_p - \omega_s)^2 r_1^2 / 2$ sq ft per sq sec.

The shock losses can be reduced by use of blades having well-rounded leading edges. Such refinement is not usually worth while, however, for, at the same value of ω_p , the same torque can be transmitted with equal efficiency by a coupling of slightly larger diameter and having the usual sheet-metal blades.

2. The second cause of loss in the coupling is the frictional drag of the fluid on the walls of the passages between the blades. These are similar to pipe-friction losses and may be expressed in the form $\lambda Q^2 / 2A^2$, where A is the cross-sectional area of the flow at an arbitrary point in the circuit. The ratio Q/A is thus a measure of the oil velocity relative to the passage walls. The dimensionless factor λ is analogous to the pipe-friction factor. The effect of the ratio of length to effective diameter is, however, included in λ .

With the aid of these formulas for the losses the power dissipation can be expressed as

$$T(\omega_p - \omega_s) = \frac{\rho}{2} Q \left[(\omega_p - \omega_s)^2 (r_1^2 + r_2^2) + \lambda \frac{Q^2}{A^2} \right] \quad (17.4)$$

Eliminating Q by combining Eqs. (17.3) and (17.4), we find the torque to be

$$T = \rho \omega_p^2 r_2^2 s^{1/2} \frac{A}{r_2^2} \sqrt{(2-s) \left(1 - \frac{r_1^2}{r_2^2} \right)} \frac{1 - (1-s)(r_1^2/r_2^2)}{\lambda^{1/2}} \quad (17.5)$$

This equation, in conjunction with the experimental curves of Fig. 17.2, shows that, at small values of s , λ decreases rapidly as s increases, but, at larger values of s , λ becomes approximately constant. This behavior of λ is what might be expected from the friction-factor chart (Fig. 8.3) since at small slips the flow in the coupling will be laminar, while at large slips it will be very turbulent, owing to the shock losses. In the laminar range, λ decreases rapidly as s increases, while, in the turbulent range, λ is nearly constant.

17.3. The Fluid Coupling as a Vibration Absorber. Consider an engine whose shaft has a vibratory twisting motion (torsional vibration) at the end to which a load is to be attached. To couple the driven shaft to the engine in such a way that the former turns at a uniform speed the coupling must transmit only the steady component of the driving torque and absorb the vibratory component. A *fluid* coupling is well adapted to this use. The primary runner can oscillate freely about a mean position without influencing seriously the steady circulation of oil in the coupling. The secondary thus feels an essentially steady driving torque.

Even the small fluctuating torque unavoidably transmitted may have serious effects, however, if the load system has a natural frequency close to that of the pulsating torque. In this case the coupling may be ineffective, for the small exciting torque tends to set up resonant vibrations of the load system. To remedy this situation one can obviously change the natural frequency of the load. If such change is impracticable, it will be necessary to attach the coupling to the driven system at a node, where the amplitude of resonant vibration is a minimum. The pulsating applied torque will thus have a minimum tendency to excite the system.

Sinclair [6] has described experiments in which torsiongrams were made for both primary and secondary shafts of a fluid coupling connected to a diesel engine. Even under resonant conditions, he found that the amplitude of vibration transmitted to the secondary was only about 2 per cent of the amplitude at the primary.

Eksergian [3] has analyzed in detail the vibratory characteristics of several systems involving a fluid coupling.

17.4. Description of a Torque Converter. In Fig. 17.4 is shown a side view of a torque converter. It will be seen that both primary and secondary runners lie in the left-hand half of the casing, while the entire right-hand half is taken up by the stationary guide vanes, or reaction stage. The converter illustrated has only a single-stage secondary (turbine) runner. Converters are in use that have three turbine stages and two reaction stages. These converters have a good efficiency over a wider operating range than the simpler type. The blades are not radial in a converter but are curved so as to give the desired relationships between the input and output torques and speeds.

The principle of operation of a converter is much like that of a fluid coupling. Oil is forced by centrifugal action out of the primary runner and into the turbine. From the turbine the oil enters the guide vanes, which are curved so as to alter the moment of momentum of the oil before it is discharged once more into the primary. This change in moment of momentum causes an external torque reaction on the housing. Under steady conditions the secondary torque must equal the sum of the primary and reaction torques, that is,

$$T_s = T_p + T_g \quad (17.6)$$

where the subscripts s , p , and g stand for secondary, primary, and guide vanes, respectively.

The efficiency of a converter is defined as the ratio of output to input power.

$$\eta = \frac{\omega_s T_s}{\omega_p T_p} \quad (17.7)$$

The maximum efficiency is less than that attainable in a fluid coupling on account of the greater complexity of a converter. It is usually about

85 to 87 per cent, but values as high as 89 per cent have been reported.

The first torque converters were built before 1914, by Dr. H. Föttinger of Hamburg, Germany. They had a speed ratio of 5 to 1 and were used to connect high-speed steam turbines to low-speed marine propellers. They were later displaced in this application by helical reduction gears, which

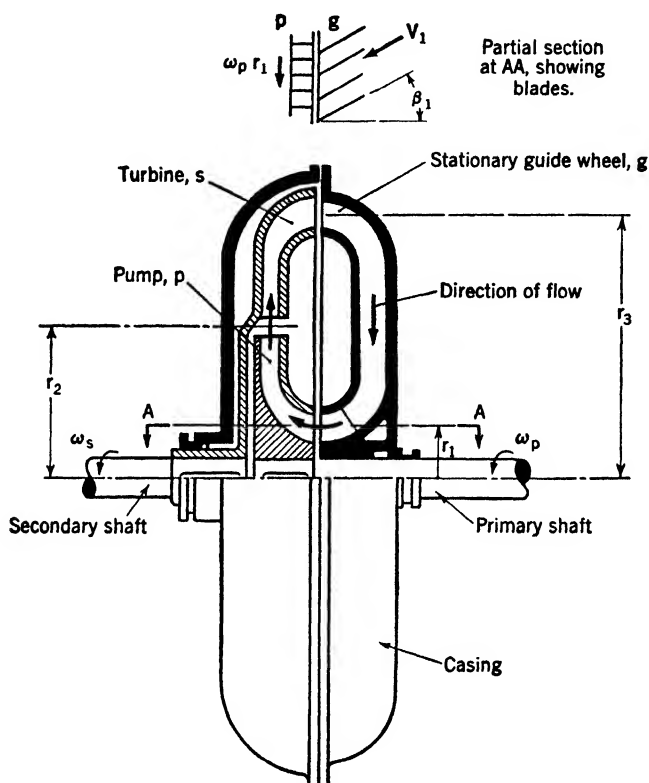


FIG. 17.4. — Torque converter.

have a higher efficiency and lower cost. In recent years, converters have come into use for automotive service, especially on trucks and busses operating in heavy traffic. The converter eliminates the frequent gear shifting that would otherwise be needed.

17.5. Analysis of a Torque Converter. For a given design of converter, filled to a fixed percentage of its total volume, we may assume that T_p , T_s , and η are functions only of ρ , ω_p , ω_s , μ , and D , the converter diameter. Application of the Π theorem leads to

$$C_p = \frac{T_p}{\rho \omega_p^2 D^5} = \phi_1 \left(\frac{\omega_s}{\omega_p}, \frac{\rho \omega_p D^2}{\mu} \right) \quad (17.8)$$

$$C_s = \frac{T_s}{\rho \omega_p^2 D^5} = \phi_2 \left(\frac{\omega_s}{\omega_p}, \frac{\rho \omega_p D^2}{\mu} \right) \quad (17.9)$$

$$\eta = \phi_3 \left(\frac{\omega_s}{\omega_p}, \frac{\rho \omega_p D^2}{\mu} \right) \quad (17.10)$$

Dividing Eq. (17.9) by Eq. (17.8), we get

$$\frac{T_s}{T_p} = \phi_4 \left(\frac{\omega_s}{\omega_p}, \frac{\rho \omega_p D^2}{\mu} \right) \quad (17.11)$$

Experiments show that, to a first approximation, the effect of the Reynolds number $R = \rho \omega_p D^2 / \mu$ can be neglected in comparison with that of the speed ratio. Typical experimental curves are plotted in Fig. 17.5.

Theoretical expressions for the torque ratio and efficiency that are in

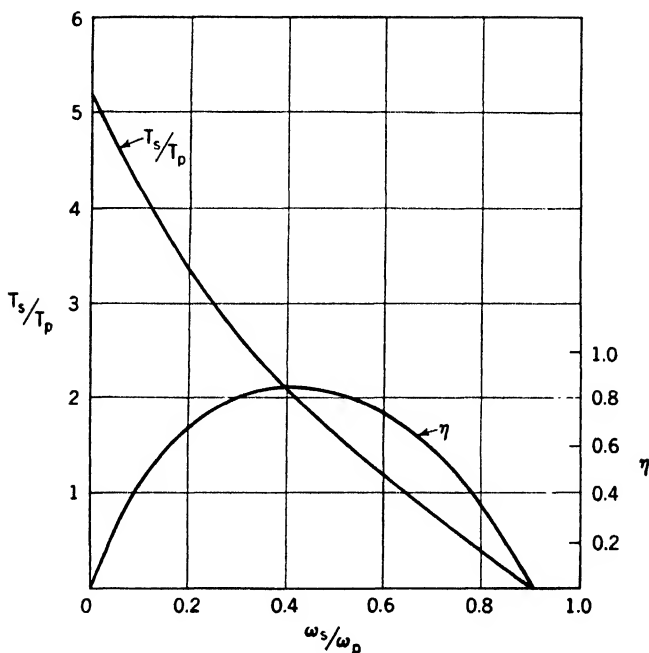


FIG. 17.5. — Torque ratio T_s/T_p and efficiency η versus speed ratio ω_s/ω_p , for a torque converter. (After Spannhake, reference 8. Courtesy of the Society of Automotive Engineers.)

substantial agreement with these curves can be set up with the aid of a few simplifying assumptions. Although the pump and turbine blades must be curved for good efficiency, we assume straight radial blades for these elements and take curvature into account only at the exit from the reaction stage. We assume also, on the basis of experience, that Eq. (17.8) will reduce to $C_p = \text{constant}$. Finally, we assume the cross-sectional area of the flow A to be the same everywhere in the circuit.

Referring to Fig. 17.4 and using Eqs. (6.18) and (6.19), we get

$$T_p = \rho Q (\omega_p r_2^2 - V_1 \sin \beta_1 r_1) \quad (17.12)$$

$$T_s = \rho Q (\omega_p r_2^2 - \omega_s r_3^2) \quad (17.13)$$

Noting that $V_1 = Q/A \cos \beta_1$, we transform these two equations to:

$$C_p = \frac{T_p}{\rho \omega_p^2 r_3^5} = \frac{Q}{\omega_p r_3^3} \left(\frac{r_2^2}{r_3^2} - \frac{Q \tan \beta_1 r_1}{A \omega_p r_3} \frac{1}{r_3} \right) \quad (17.14)$$

$$C_s = \frac{T_s}{\rho \omega_p^2 r_3^5} = \frac{Q}{\omega_p r_3^3} \left(\frac{r_2^2}{r_3^2} - \frac{\omega_s}{\omega_p} \right) \quad (17.15)$$

The torque ratio is thus

$$\frac{T_s}{T_p} = \frac{(r_2^2/r_3^2) - (\omega_s/\omega_p)}{(r_2^2/r_3^2) - (Q \tan \beta_1 / A \omega_p r_3)(r_1/r_3)} \quad (17.16)$$

and the efficiency is

$$\eta = \frac{T_s \omega_s}{T_p \omega_p} = \frac{[(r_2^2/r_3^2) - (\omega_s/\omega_p)](\omega_s/\omega_p)}{(r_2^2/r_3^2) - (Q \tan \beta_1 / A \omega_p r_3)(r_1/r_3)} \quad (17.17)$$

From the second assumption made above and from Eq. (17.14) it follows that $Q/\omega_p r_3^3$ is constant. Consequently, Eqs. (17.16) and (17.17) show that T_s/T_p is a linear function of ω_s/ω_p and that η varies parabolically with ω_s/ω_p . At maximum efficiency, T_s/T_p has one-half of its initial value.

It is clear from Fig. 17.5 that these calculated results are in approximate agreement with observation. The discrepancies between the two can be ascribed to variations in $Q/\omega_p r_3^3$ and to curvature of the pump and turbine blades. Eksergian [3] has developed a more refined theory, which takes these factors into account through an energy balance like that for the coupling, in Art. 17.4.

17.6. Torque Converter — Coupling Unit. A combination of torque converter and fluid coupling appears to offer one solution to the problem of power transmission in passenger cars. In such a combination the reaction stage is at rest so long as the primary torque is less than that required at the secondary. The unit thus functions as a converter. As soon as the primary and secondary torques become equal, however, the reaction stage automatically starts to rotate with the secondary and the unit becomes a coupling. This action is obtained through the use of two over-running clutches.

Dimensionless characteristic curves for such a unit are shown as full lines in Fig. 17.6. The broken extensions of these curves apply to the converter or coupling individually. Combination of the two elements makes it possible to use each one in a favorable operating range.

An alternative scheme is to use a torque converter for torque multiplication and to change over automatically to direct drive when the primary and secondary torques become equal [2]. With this arrangement the

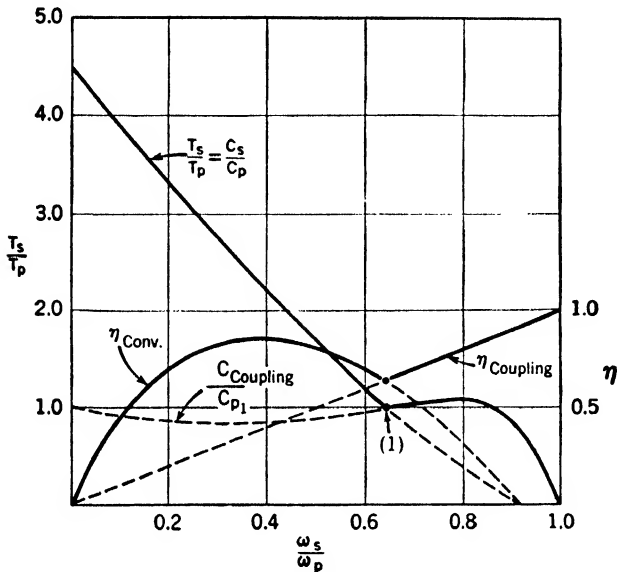


FIG. 17.6. — Torque ratio $T_s/T_p = C_s/C_p$ and efficiency η versus speed ratio ω_s/ω_p , for a combined converter and coupling. (After Spannhake, reference 8. Courtesy of the Society of Automotive Engineers.)

clutch must, of course, slip momentarily until the primary and secondary speeds are equalized.

SELECTED BIBLIOGRAPHY

1. ALISON, A. L., R. C. OLSON, and R. M. NELDEN: Hydraulic Couplings for Internal-combustion-engine Applications, *Trans. Am. Soc. Mech. Engrs.*, vol. 63, pp. 81-90, February, 1941.
2. DEIMEL, A. H.: Hydraulic Transmissions for Motor Vehicles, *S.A.E.J.*, vol. 53, pp. 10-18, January, 1945.
3. EKSERGIAN, R.: The Fluid Torque Converter and Coupling, *J. Franklin Inst.*, vol. 235, pp. 441-478, May, 1943.
4. FÖTTINGER, H.: Die hydrodynamische Arbeitsübertragung, *Jahrb. Schiffbautechn. Ges.*, vol. 31, pp. 171-214, 1930.
5. HAWORTH, H. F., and A. LYSHOLM: Progress in Design and Application of the Lysholm-Smith Torque Converter, *Proc. Inst. Mech. Engrs.*, vol. 130, pp. 193-230, 1935.
6. SINCLAIR, H.: Recent Developments in Hydraulic Couplings, *Proc. Inst. Mech. Engrs.*, vol. 130, pp. 75-190, 1935.
7. SINCLAIR, H.: Some Problems in the Transmission of Power by Fluid Couplings, *Proc. Inst. Mech. Engrs.*, vol. 139, pp. 83-182, 1938.
8. SPANNHAKKE, W.: Hydrodynamic Power Transmission for Motor Cars, *S.A.E.J.*, vol. 45, pp. 433-443, October, 1939.

CHAPTER XVIII

HYDRAULIC TRANSMISSIONS AND CONTROLS

Hydraulic positive-displacement transmissions and controls are basically different from hydrodynamic machines. In the latter the pressure and velocity are interrelated, while in the former the working fluid is confined between two pistons and maintained at an arbitrary pressure level

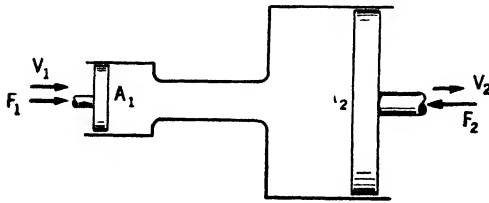


FIG. 18.1. — Elementary hydraulic transmission.

by the external forces on the pistons, regardless of the velocity. This fundamental difference is brought out by reference to Art. 17.5, in which it is stated that, for a torque converter, the primary-torque coefficient C_p is approximately constant. The input torque is

thus nearly proportional to ω_p^2 . For a hydraulic transmission, on the other hand, the input torque is substantially independent of the speed of the input shaft.

A primitive example of a positive-displacement transmission is the hydraulic press, described in Art. 2.6. The power input to the small piston is transmitted through the confined liquid to the load attached to the large piston (see Fig. 18.1). If dynamic effects and friction are neglected, the ratio of the forces equals the ratio of the piston areas.

$$\frac{F_2}{F_1} = \frac{A_2}{A_1}$$

Also, if leakage and compressibility of the liquid are neglected and the boundaries are assumed perfectly rigid, continuity requires that $A_1V_1 = A_2V_2$, or

$$\frac{V_2}{V_1} = \frac{A_1}{A_2}$$

Under these idealized conditions the input and output powers are equal ($F_1V_1 = F_2V_2$) and the efficiency is 100 per cent, regardless of the value of either F_1 or V_1 . The two components of power, force and velocity, are completely independent of each other in this ideal positive-displacement transmission.

It is frequently required to transmit power from one rotating shaft to another turning at a different speed and/or at a distance from the first. Many forms of positive-displacement transmission have been developed for this purpose, but they are all basically the same as the hydraulic press.

The single driven piston of the press is replaced by a pump that has a shaft turned by an electric motor or other prime mover and that provides a more or less continuous flow of liquid (usually oil) under pressure. This liquid flows through suitable pipes to a hydraulic motor, which replaces the single output cylinder and piston of the hydraulic press. The work done by the oil on the motor is converted by it into shaft work.

There are three principal types of pump, multiple-piston pumps, vane pumps, and gear pumps. The first two types are readily built with a variable displacement, so that the rate of oil flow can be continuously varied from a maximum in one direction to a maximum in the opposite direction. A gear pump has a fixed displacement, so that a by-pass must be used to get a controlled rate of oil flow, in one direction only.

Hydraulic motors are similar to multiple-piston or gear pumps. Vane-type motors are not used, for the vanes are held in position by centrifugal force and do not operate satisfactorily at low speeds.

These two primary elements, the pump and the motor, together with auxiliary devices, such as valves and accumulators, are connected to form a hydraulic circuit, which may take any one of a variety of forms, depending on the special function of the transmission. The design of a complex hydraulic circuit is a highly specialized task, especially when the circuit is incorporated in a servomechanism.

Hydraulic power transmission is in many respects similar to electrical. The liquid flow is analogous to the flow of electric current. Pressure may be likened to potential. Hydraulic and electrical connecting circuits are much alike. Hydraulic valves and electrical switches perform much the same functions.

Because of their similarity the two systems may be used in equivalent applications; and almost identical analyses may be applied to them. However, hydraulic transmissions have greater power-carrying capacity and greater shaft torques for given unit sizes. They also respond more exactly to control. Hydraulic-machine speeds are somewhat lower than the electrical. Distance of transmission is more limited. The efficiencies of the two types are about the same.

In consequence of certain advantages over mechanical or electrical apparatus, the hydraulic transmission is becoming a significant factor in the solution of power problems. It is applied principally to perform the following functions:

1. To provide positively controlled stepless adjustable speeds from a constant-speed prime mover.
2. To provide controlled variable driving torques or forces by manual or automatic direction.
3. To provide damping of driving shocks or pulsations.

4. To give servocontrol or power "follow-up" response to small control efforts.
5. To reduce equipment size and cost for equivalent duty.
6. To simplify design.
7. To lower maintenance costs.

Various industrial machines, such as presses, planers, and broaching machines, which require automatic speed variations during the operating cycle, are frequently fitted with hydraulic drives.

Steering engines for ships, automatic pilots for aircraft, and fire-control apparatus for naval and antiaircraft guns are among the more spectacular uses of hydraulic elements in servomechanisms.

During the war, precision-made motors and pumps of small size were developed, which handle extremely high power for their weight. One such pump or motor unit, which may easily be held in the palm of the hand, is rated at 2 hp.

18.1. Hydraulic Circuits. There are three principal types of circuit, variable speed, controlled torque, and controlled power. The first of these, shown diagrammatically in Fig. 18.2, consists of a variable-displacement

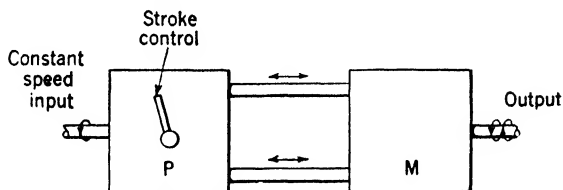


FIG. 18.2. — Variable-speed transmission with variable-stroke pump.

pump *P* connected to a constant-displacement motor *M*. For the sake of clarity, important details such as relief and replenishment valves, replenishment pump, and oil reservoir are not shown. The speed of the hydraulic motor is continuously variable from zero to a maximum in either direction. The maximum torque obtainable is independent of speed and is proportional

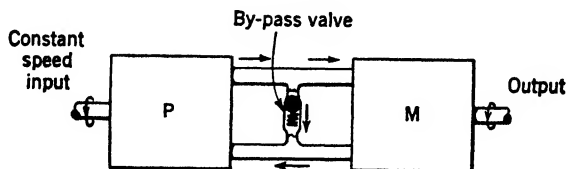


FIG. 18.3. — Variable-speed transmission with fixed-stroke pump and by-pass valve.

to the maximum pressure difference developed, which is limited by a safety relief valve. The maximum power obtainable is thus proportional to the speed.

An alternative form of this circuit, sketched in Fig. 18.3, employs a

constant-displacement pump and a by-pass valve instead of a variable-displacement pump. The arrangement shown is obviously limited to uni-directional operation. This scheme is simpler and cheaper than that of Fig. 18.2 and is usually preferred for low-power applications. For high power the low partial-load efficiency resulting from by-passing of the oil becomes important, and a variable-displacement pump is indicated.

A controlled-torque circuit is illustrated in Fig. 18.4. The displacement control of the pump is automatically adjusted to maintain a constant pres-

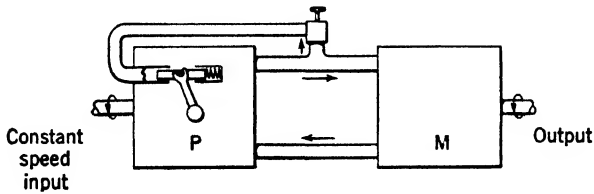


FIG. 18.4. — Controlled-torque transmission.

sure difference across the motor, and hence a constant torque, regardless of the output speed. The circuit of Fig. 18.3 will perform the same function if a spring-loaded automatic by-pass valve is employed.

The controlled-power circuit of Fig. 18.5 utilizes a constant-displacement pump and a variable-displacement motor. The output speed is

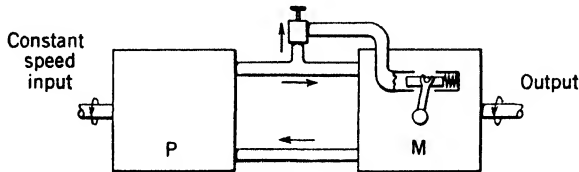


FIG. 18.5. — Controlled-power transmission.

automatically adjusted to maintain a constant pressure difference across the pump. The torque applied to the constant-speed input shaft is therefore constant, and so is the transmitted power.

It is clear that modifications of these elementary circuits can be made to give an output torque or power which is practically any desired function of speed.

18.2. Radial-piston Machines. The pistons of hydraulic machines are arranged either radially or axially. The construction of a typical radial variable-displacement pump or motor is shown in Figs. 18.6, and 18.7. The cylinder block turns on a pintle, which acts also as a porting mechanism. The outer ends of the pistons bear against a reaction ring forming part of the rotor, which is free to revolve with the cylinder block. The

center of rotation of this ring can be adjusted relative to that of the cylinder block by means of the handwheel shown in Fig. 18.6. The discharge can thus be varied from zero to a maximum in either direction. A sectional view showing the slide block in one extreme position is given in Fig. 18.7.

The pistons are free to rotate about their own axes. No sliding occurs

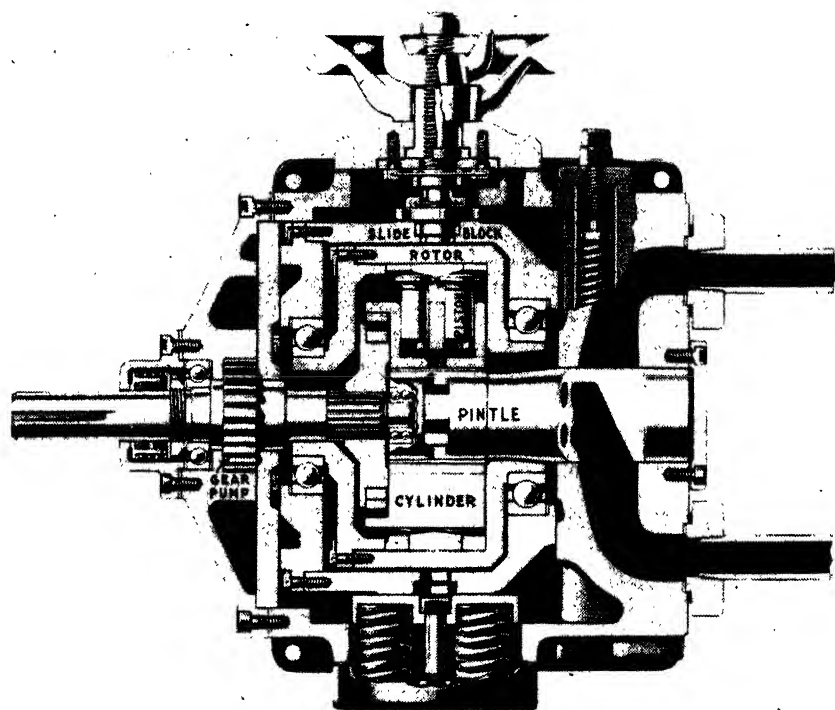


FIG. 18.6. — Radial-piston variable-stroke pump. (Courtesy of The Oilgear Company.)

between the pistons and the ring, but only a slight oscillating rotary motion of the pistons. Wear is thus reduced.

The gear pump mounted on the drive shaft is used to keep the hydraulic system full of oil and to operate hydraulic controls.

A fixed-displacement unit of the radial type is shown in Fig. 18.8. It is identical in construction with the variable-displacement unit, except for the omission of the displacement control and the auxiliary pump.

Radial pumps and motors are available in ratings between 2 and 150 hp. Pressures are usually on the order of 1,000 to 2,000 lb per sq in., but some models can operate intermittently at 3,000 lb per sq in. Maximum rotational speed is approximately 1,000 rpm.

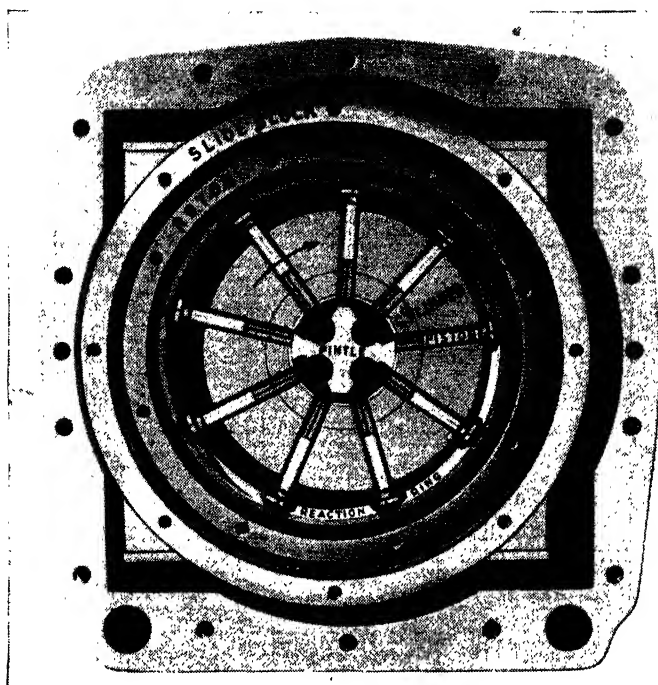


FIG. 18.7. — Radial-piston variable-stroke pump. (Courtesy of The Oilgear Company.)

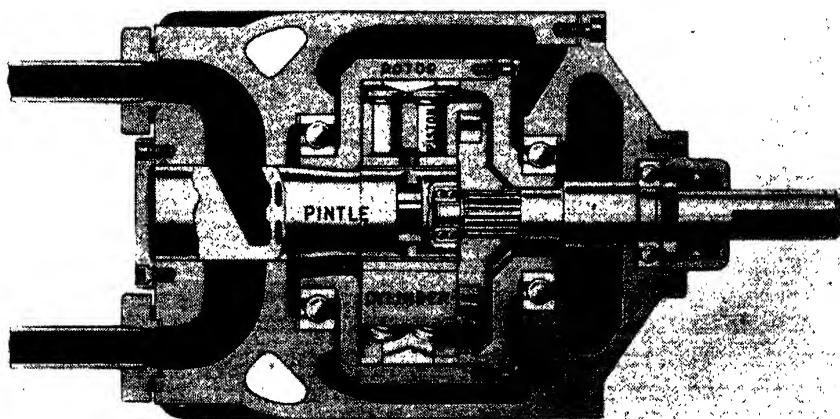


FIG. 18.8. — Radial-piston fixed-stroke motor. (Courtesy of The Oilgear Company.)

Representative performance curves are given in Fig. 18.9. It is seen that the over-all efficiency of a complete transmission exceeds 80 per cent over two-thirds of the speed range. The maximum efficiency approximates to 85 per cent.

Radial transmissions are used principally in industrial applications,

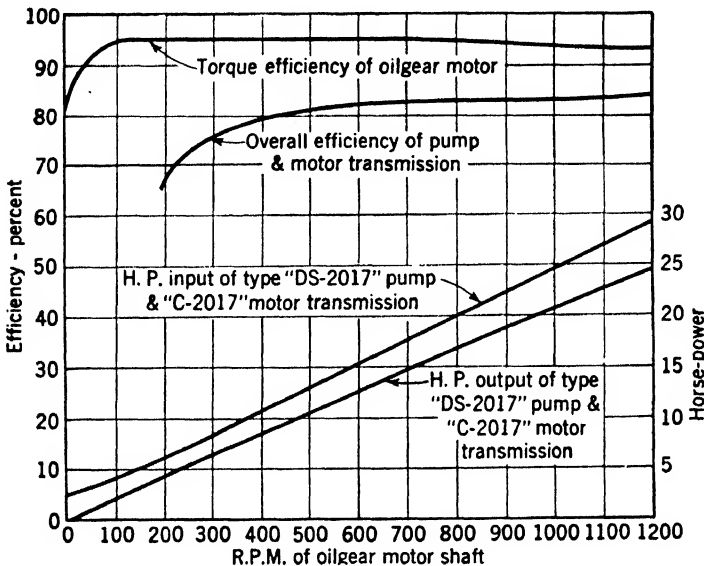


FIG. 18.9. — Performance curves for a radial-piston transmission. (Courtesy of The Oilgear Company.)

where precise control and durability are required, but where weight and bulk are not of paramount importance.

18.3. Axial-piston Machines. An example of a fixed-displacement unit of this type is given in Fig. 18.10. The cylinder block rotates about an axis set at an angle with respect to the drive shaft. The piston rods are attached by ball-and-socket joints to the pistons and to a plate carried on the drive shaft. A double universal joint serves to lock the drive shaft and cylinder block into synchronism. None of the load torque is transmitted through this shaft, only the small friction torque.

A variable-displacement unit is similar in all essentials to that just described. The cylinder block is mounted on trunnions, however, in such a way that the angularity between its axis and the drive shaft can be easily adjusted. The discharge can thus be varied at will.

Axial-piston machines are available in ratings between 2 and 300 hp. Pressures are usually on the order of 1,000 to 2,000 lb per sq in., but some models can operate at 3,000 lb per sq in. Rotational speeds for small

pumps used on aircraft may exceed 4,000 rpm; maximum speeds of large units range down to 850 rpm.

Performance curves are similar to those of Fig. 18.9 for radial-piston machines.

Axial-piston transmissions are used in numerous industrial applications. In addition, they are well adapted to use in aircraft hydraulic

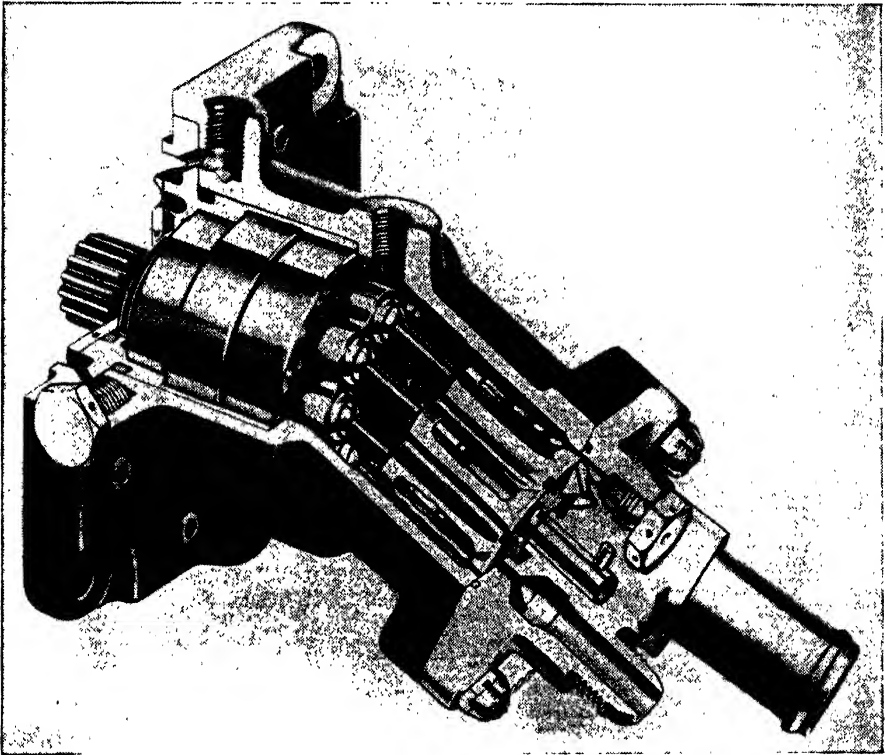


FIG. 18.10. — Axial-piston fixed-stroke pump. (*Courtesy of Vickers Incorporated.*)

systems, since the small-diameter bearings can operate at high speed and the units are compact, weighing less than 1 lb per hp.

18.4. Gear-type Machines. A hydraulically balanced gear unit is shown in Fig. 18.11. The symmetrical layout of the ports eliminates bearing loads caused by the pressure change in the machine. All gear units are of the fixed-displacement type. A gear pump must therefore be used with a by-pass valve to obtain a variable flow rate.

These machines are inherently limited to low pressure and small power, for ample clearance must be provided to prevent contact of gears and housing at all operating temperatures. The leakage can be kept within reason-

able limits only if the pressure is less than 1,000 lb per sq in. and the power is below about 25 hp. Even within these limits, the efficiency is apprecia-

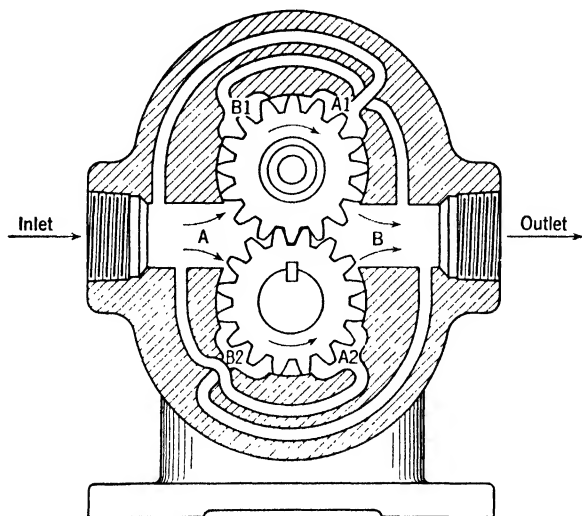


FIG. 18.11. — Hydraulically balanced gear pump. (Courtesy of Vickers Incorporated.)

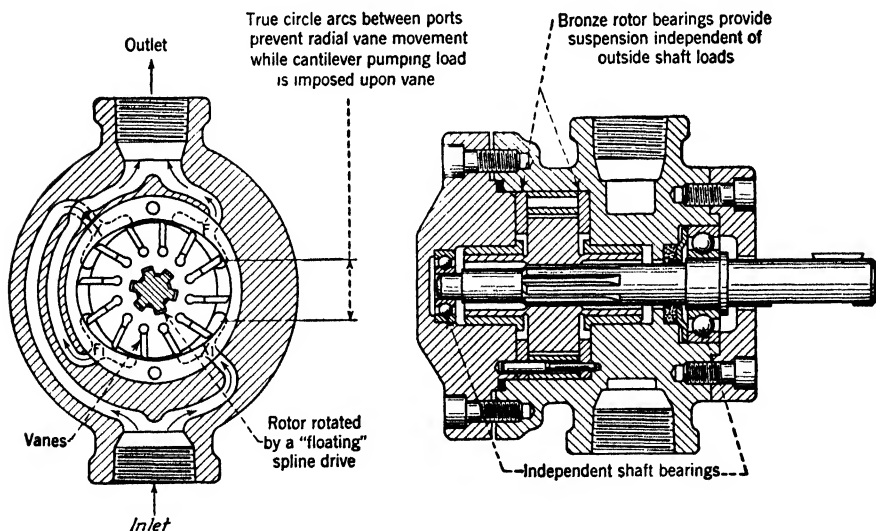


FIG. 18.12. — Hydraulically balanced vane pump. (Courtesy of Vickers Incorporated.)

bly less than that of a piston unit, but their relative simplicity and low cost justify the use of these machines in many applications.

18.5. Vane Pumps. These may be of either the fixed- or variable-displacement type, as shown in Figs. 18.12 and 18.13. The former has the

advantage of simplicity and hydraulic balance to offset its lack of flexibility.

Vane pumps are subject to the same limitations as gear units with regard to pressure and power [8, 9].

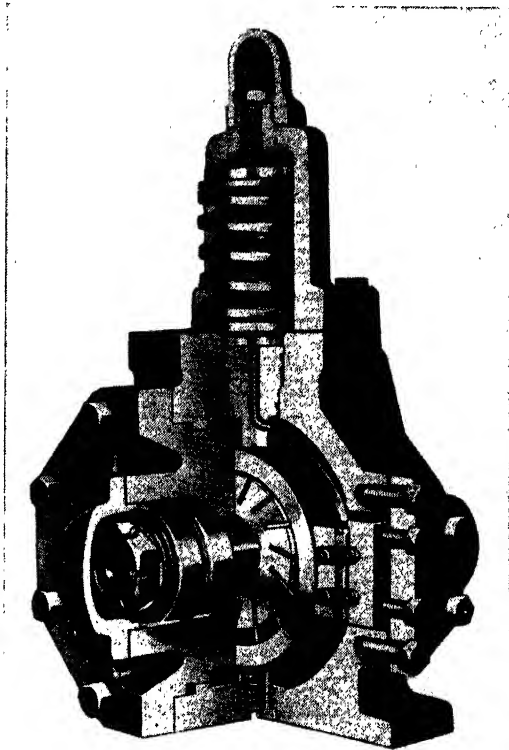


FIG. 18.13. --- Variable-stroke vane pump. The stroke setting is automatically adjusted to maintain a constant output pressure. (*Courtesy of Racine Tool and Machine Company.*)

18.6. Auxiliaries. A detailed discussion of auxiliary apparatus is beyond the scope of this book [2, 4]; all that will be attempted is a mention of the principal items.

There are many kinds of controls available for variable-displacement machines, from a simple handwheel to highly complicated automatic power control.

By-pass valves are used in conjunction with fixed-displacement pumps. Ingenious designs have been developed, by means of which any desired flow may be obtained by setting of a graduated dial. The flow is independent of pressure and temperature over a considerable range.

Relief valves are essential to any hydraulic circuit, to prevent overload. Designs range from a simple spring-loaded ball, which permits large

pressure variations around the nominal maximum, to a balanced valve, which limits the pressure accurately to a preset value, regardless of the volume handled by the valve.

Some hydraulic systems, notably in aircraft, are used only intermittently but are supplied by a constant-displacement pump, running continuously. An unloader valve and accumulator incorporated into such a circuit ensure a supply of high-pressure fluid at all times, yet permit the pump to run idle, except when the system is actually doing work or when the accumulator needs recharging [2]. An aircraft accumulator is simply a hollow steel sphere divided into halves internally by a flexible diaphragm, on one side of which is introduced compressed air at a predetermined pressure. To charge the accumulator the pump forces oil from the hydraulic system into the sphere, thus further compressing the air on the opposite side of the diaphragm. When the desired pressure has been reached, the unloader valve automatically opens a by-pass, allowing the oil to be circulated freely between pump and reservoir until the pressure in the system drops below the minimum permissible level. The unloader valve then reconnects the pump into the circuit and closes the by-pass.

The oil reservoir is an important element of a hydraulic circuit. A reservoir of sufficient capacity must be included to allow for adequate cooling of the oil and to permit air bubbles to escape. Entrained air is obviously detrimental to performance, especially where rapid and precise response is essential.

The clearances permissible in hydraulic apparatus are so small that extreme care must be taken to ensure clean operating fluid. This is especially true in small-size equipment for high pressures. A filter, usually incorporated in the reservoir, is therefore an indispensable part of a hydraulic circuit.

18.7. Hydraulic Fluids. For hydraulic service a fluid is required to be practically incompressible (*i.e.*, to be a liquid), to flow easily, to be chemically stable, and to be a good lubricant. To satisfy the last requirement, not only must the viscosity be above some lower limit, but also the other properties must be such as to prevent appreciable wear under boundary-lubrication conditions. Petroleum oils have so far best satisfied these requirements. For apparatus that operates near room temperature any highly refined turbine-type of oil is satisfactory. The kinematic viscosity of such an oil is approximately that of an SAE 20 grade (340 Saybolt universal seconds, 74 centistokes, or 0.11 sq in. per sec, at 100 F).

For equipment that is required to function over a wide range of temperature, such as that of an aircraft, the effect of temperature on viscosity is a prime consideration. A fluid that is satisfactory under normal conditions may be too thin to lubricate properly at 150 F and may congeal at -20 F. The effect of high temperature on the stability of the fluid is also

important. Some oils break down rapidly at high temperature, forming gummy deposits on working surfaces and clogging the system with sludge.

The following table gives the kinematic viscosity, in centistokes, of several hydraulic fluids as a function of temperature.

Temperature, deg F	Petroleum oil I V.I. = 101 Pour point = -20 F	Petroleum oil II V.I. = 145 Pour point = -50 F	Silicone A V.I. = 156	Silicone B V.I. = 170
210	9.5	18	30	18
130	37	57	56	36*
100	80	103	74	43*
0	8,270	2,330	275	160
-20		6,100	390	260*
-40			600	360

* Approximate value interpolated on Chart A of ASTM Standard D341.

Petroleum oil I is, by ordinary standards, an excellent oil, having a V.I. of 101, which is as good as can be obtained without special treatment (Art. 12.4.). Petroleum oil II is especially prepared for hydraulic service; its V.I. of 145 permits an extension of the operating range in both directions. The pour point is lowered to -50 F. Silicones A and B are examples of the recently developed dimethyl-silicone-polymer fluids (Art. 13.7). Silicone B is especially remarkable, having a kinematic viscosity equal to that of Petroleum oil II at 210 F but less than 5 per cent of it at -20 F.

From the viscosity-temperature standpoint, these silicones appear to be ideal hydraulic fluids. Another advantage is their noninflammability. As already mentioned, however, the boundary-lubrication characteristics of the fluid must be adequate. Recent tests on silicone A [3] have shown that it lubricates satisfactorily, provided that proper combinations of metals are used for the rubbing surfaces. Steel and bronze, for example, appear to function well, but the mating of two ferrous surfaces is to be strictly avoided. If the apparatus is suitably designed in this respect, very little wear occurs. Furthermore, the silicone fluid is exceptionally stable, showing practically no discernible change in viscosity or other properties, even after some hundreds of hours of operation.

18.8. Basic Formulas for Hydraulic Transmissions. If both friction and leakage are neglected in the pump shown schematically in Fig. 18.14, the steady-flow energy equation [Eq. (5.10)] yields

$$-W_s = \frac{p_2 - p_1}{\rho}$$

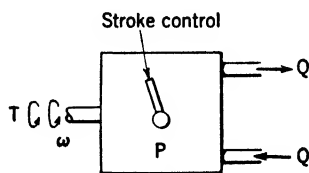


FIG. 18.14.

To obtain an expression for the ideal torque T_{ideal} applied to the pump shaft we notice that $T_{\text{ideal}} \omega = -\rho Q \omega_s$ and $Q = \omega D S$, where D is the displacement per radian at full stroke and S , the stroke setting, is the ratio of stroke to full stroke. Substitution in the energy equation gives

$$T_{\text{ideal}} = -\frac{\rho Q \omega_s}{\omega} = (p_2 - p_1) D S \quad (18.1)$$

We define the torque efficiency of the actual pump as the ratio of the ideal torque to the actual torque required to produce a given pressure rise $p_2 - p_1$.

$$\eta_{TP} = \frac{T_{\text{ideal}}}{T_{\text{actual}}} \quad (18.2)$$

Combination of Eqs. (18.1) and (18.2) gives for the actual torque

$$T_P = \frac{\Delta p_P D_P S_P}{\eta_{TP}} \quad (18.3)$$

where the pressure rise is conveniently denoted by Δp , and the subscript P indicates a pump.

The over-all efficiency of the pump is defined as the ratio of the ideal input power to the actual input power needed to produce a given pressure rise Δp_P and rate of flow Q_P . The ideal power input is readily seen to be $\Delta p_P Q_P$, while the actual power input is $\omega_P T_P$. With the aid of Eq. (18.3) the over-all pump efficiency is found to be

$$\eta_P = \frac{\Delta p_P Q_P}{\Delta p_P D_P \omega_P S_P} \eta_{TP} = \eta_{TP} \frac{Q_P}{D_P \omega_P S_P} = \eta_{TP} \eta_{VP} \quad (18.4)$$

where $\eta_{VP} = Q_P / D_P \omega_P S_P$ and is called the "volumetric efficiency" of the pump, since it is the ratio of the actual to the ideal discharge rate.

A similar development for a hydraulic motor yields the following:

$$\eta_{TM} = \frac{T_{\text{actual}}}{T_{\text{ideal}}} \quad (18.5)$$

$$T_M = \eta_{TM} \Delta p_M D_M S_M \quad (18.6)$$

$$\eta_M = \eta_{TM} \frac{D_M \omega_M S_M}{Q_M} = \eta_{TM} \eta_{VM} \quad (18.7)$$

where the subscript M indicates a motor. It will be noted that the actual output torque is less than the ideal for a given pressure drop Δp_M , so that η_{TM} is less than unity.

The torque efficiency of a radial-piston motor over a range of motor speed is shown in Fig. 18.9.

The over-all efficiency of a complete transmission is defined as the ratio of output to input power,

$$\eta = \frac{T_M \omega_M}{T_P \omega_P} \quad (18.8)$$

Substituting from Eqs. (18.3) and (18.6), we get

$$\eta = \eta_{TP} \eta_{TM} \frac{D_M \omega_M S_M}{D_P \omega_P S_P} \frac{\Delta p_M}{\Delta p_P} \quad (18.9)$$

which from Eqs. (18.4) and (18.7) becomes

$$\eta = \eta_P \eta_M \frac{Q_M}{Q_P} \frac{\Delta p_M}{\Delta p_P} \quad (18.10)$$

It is obvious that Q_M/Q_P and $\Delta p_M/\Delta p_P$ represent, respectively, the effect of leakage from and friction in the pipes connecting pump and motor.

From continuity, the total leakage from the system Q_l must equal the difference between the displacements per unit time of pump and motor.

$$Q_l = D_P \omega_P S_P - D_M \omega_M S_M \quad (18.11)$$

Equation (18.9) can thus be expressed in terms of the total leakage.

$$\eta = \eta_{TP} \eta_{TM} \left(1 - \frac{Q_l}{D_P \omega_P S_P} \right) \frac{\Delta p_M}{\Delta p_P} \quad (18.12)$$

The maximum allowable speed of a piston-type machine is limited by dynamic stresses. Assuming that, for a given design, the maximum allowable stress s_0 depends only on the density of the material, ρ_m , on ω_{\max} , and on D , we get by dimensional reasoning

$$\frac{s_0}{\rho_m \omega_{\max}^2 D^{2/3}} = \text{constant}$$

Both s_0 and ρ_m may be considered constant, to a good approximation. Experience indicates a good working rule to be

$$\omega_{\max} = \frac{187}{D^{1/3}} \quad (18.13)$$

where ω_{\max} is in radians per second and D is in cubic inches per radian.

The above relationships are useful in the discussion of various types of hydraulic circuits. In the following we shall assume, for simplicity, that $D_P = D_M = D$ and neglect the pressure drop in the connecting lines, *i.e.*, assume $\Delta p_P = \Delta p_M = \Delta p$. Consider, for example, the circuit of Fig. 18.2, which includes a variable-displacement pump and fixed-displacement motor. The continuity equation [Eq. (18.11)] enables us to plot the motor

speed as a function of S_P , the stroke setting of the pump. Noting that $S_M = 1$, we get

$$\frac{\omega_M}{\omega_P} = S_P - \frac{Q_l}{\omega_P D}$$

If we assume for the moment that $Q_l = 0$, we get the straight line aob of Fig. 18.15. Equation (18.3) shows, however, that the pressure drop across the system, Δp , varies directly with the applied torque T_P . Since in an actual system there is some leakage whenever Δp (and hence T_P) exceeds zero, the line aob is the limit approached as $T_P \rightarrow 0$.

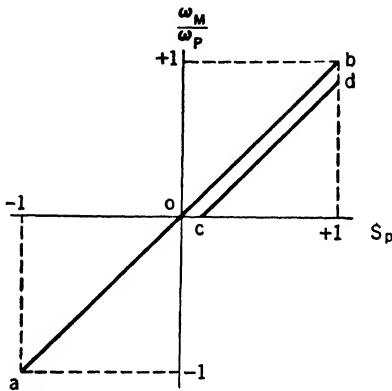


FIG. 18.15. — Speed ratio ω_M/ω_P versus pump stroke setting S_P , for the transmission of Fig. 18.2.

as this value of Δp is not exceeded. The critical value of S_P is reached at point c in Fig. 18.15. If it is assumed that Q_l remains constant as S_P is further increased, the straight line cd is followed. The horizontal distance oc between the lines ob and cd is equal to the ratio of the constant leakage to the displacement rate of the pump, $Q_l/\omega_P D_P$.

In a well-designed unworn system the clearances are small, and the leakage flow is laminar. The leakage rate is found to be very nearly proportional to the pressure drop Δp and to be essentially independent of speed. According to Eq. (18.6), therefore, $Q_l \sim T_M/\eta_{TM}$; and since η_{TM} is nearly constant over a wide range of speed, it follows that $Q_l \sim T_M$. The straight line cd in Fig. 18.15 thus corresponds approximately to the case of constant output torque.

The circuit of Fig. 18.5 is intended to yield a constant output power over a wide range of output speeds. To this end, the pressure drop Δp is automatically held constant. To analyze this circuit we apply the continuity equation [Eq. (18.11)] and find

$$\frac{\omega_M}{\omega_P} S_M = 1 - \frac{Q_l}{\omega_P D} \quad (18.14)$$

Neglecting leakage, we get $\omega_M S_M / \omega_P = 1$, the speed ratio varying hyperbolically with the motor displacement (see Fig. 18.16). From Eq. (18.6), the output power is found to be $P_M = T_M \omega_M = \Delta p D \eta_{TM} \omega_M S_M$, whence $P_M / \Delta p D \omega_P \eta_{TM} = 1$. The output power is thus approximately constant if Δp is closely regulated and variations in η_{TM} are small.

To take the laminar leakage into account it is assumed, for geometrically similar systems, that Q_l depends only on Δp , D , and μ (the viscosity). Dimensional analysis then yields

$$\frac{Q_l \mu}{D \Delta p} = \text{constant} = C_l \quad (18.15)$$

where C_l is the "leakage coefficient." From Eqs. (18.14) and (18.15),

$$\frac{\omega_M S_M}{\omega_P} = 1 - \frac{C_l \Delta p}{\mu \omega_P}$$

so that the power output becomes

$$P_M = \omega_M T_M = \Delta p D \omega_P \eta_{TM} \left(1 - \frac{C_l \Delta p}{\mu \omega_P} \right)$$

The only effect of leakage is, therefore, to reduce both the speed ratio and the power output; the character of the curves is unchanged, provided that the viscosity is constant.

18.9. Servomechanisms. A manually controlled transmission requires an operator whose function is to observe the output, note any deviation from the desired behavior, and adjust the control so as to return the output to the value wanted. He thus acts to keep small the difference between the desired output and that actually existing. This difference is called the "error."

It is possible to feed back, mechanically, electrically, or otherwise, the actual output to a device which compares it with that called for by some input signal and which automatically adjusts the control in such a way as to reduce the error. Such a feed-back linkage is an essential feature of a servomechanism. A second feature is the amplification of power achieved in a servomechanism. The power level of the input signal is usually very low compared with the output. For our purposes a servomechanism may be defined as an error-controlled power amplifier. We shall be concerned principally with hydraulic servomechanisms, but much of the following applies to other types as well.

Servomechanisms may be electrical, mechanical, pneumatic, hydraulic, or some combination of these. Their use is growing rapidly; present appli-

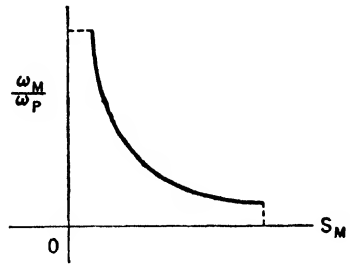


FIG. 18.16. — Speed ratio ω_M/ω_P versus motor stroke setting S_M , for the transmission of Fig. 18.5.

cations, aside from industrial, include automatic piloting of vessels and aircraft, fire control of guns, and power steering of heavy vehicles.

There are three aspects of the behavior of a servomechanism that must be considered in design or analysis. Since a source of energy for producing the power amplification is an essential part of a servomechanism, the operation may be unstable. The question of stability is therefore of primary concern.

In addition to the requirement of stability, a servomechanism must respond rapidly and accurately to the applied signal, *i.e.*, its "transient response" must be satisfactory. Under this heading are included the time lag of the output behind the input signal, the amount of overshoot, and the time required for any oscillations to die down to a given fraction of their initial amplitude.

Finally, the "steady-state error" must be taken into account, *i.e.*, the error subsisting an indefinitely long time after application of a signal. The steady-state error depends on the type of signal. For example, it may be zero for a signal consisting of a certain constant *displacement* of the input member, but this error may be finite if the input member is given a constant *velocity* or *acceleration*. Servomechanisms are sometimes described according to their steady-state error, as of the "zero-displacement-error," "zero-velocity-error," or "zero-acceleration-error" type.

There are two categories of servomechanisms, linear and nonlinear. The differential equation of a linear servomechanism is linear and has constant coefficients. The differential equation of a nonlinear servomechanism is unrestricted.

The theory of linear servomechanisms is highly developed, two methods being available for analysis or design. The transient-response method involves solution of the differential equation of the system for one or more types of input step signal. (A step signal is one that changes discontinuously from a constant zero value to some other constant value. Those usually considered are displacement, velocity, and acceleration step signals.) The behavior of the system can be completely determined by this means, but the method has two disadvantages: (1) It is tedious and cumbersome to apply to complex systems. (2) The results usually do not show how a system should be changed if its behavior deviates too greatly from a prescribed pattern.

The second method applicable to a linear system is the frequency-response method. Essentially, it involves determination of the response of a system to a sinusoidal signal of any frequency within the range of interest. It is unnecessary to obtain the general solution of the equation of the system in order to predict its behavior closely enough for design purposes. This method is relatively simple, even for complicated systems. It is especially useful in design, since the results indicate the effect on

performance of a change in any one of the design parameters. Unfortunately, its use is restricted to linear systems.

No general theory is available for nonlinear servomechanisms. The differential equation must be solved in every individual case, as outlined above for the transient-response method. This task is in general much more difficult than that of solving a linear equation with constant coefficients.

18.10. Ideal Hydraulic Servomechanism. The hydraulic transmission shown in Fig. 18.17 is assumed to have "proportional control," that is, a

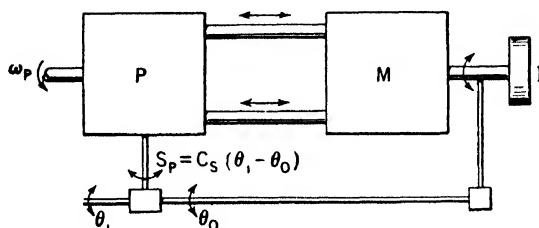


FIG. 18.17. — Hydraulic servomechanism.

feed-back linkage whereby the pump stroke control S_P is made proportional to the error. In this case the desired output-shaft position is the same as that of the signal shaft, so that the error is simply $\theta_i - \theta_o$, where θ_i and θ_o stand for the instantaneous angular displacements of the signal and output shafts, respectively. The feed-back linkage thus ensures that

$$S_P = C_s(\theta_i - \theta_o)$$

where C_s is a constant whose value depends on the nature of the linkage. If, for example, the feed-back circuit is purely mechanical, C_s will be determined by the gear ratios employed. The following additional assumptions are also made:

$$\omega_P = \text{constant}$$

$$D_P = D_M = D$$

$$S_M = 1 \text{ (fixed-displacement motor)}$$

$$Q_i = 0$$

The fluid is incompressible.

The boundaries do not deform.

The continuity equation [(Eq. (18.11))] thus gives

$$\omega_M D = \frac{d\theta_o}{dt} D = S_P \omega_P D$$

into which the expression $S_P = C_s(\theta_i - \theta_o)$ is substituted.

$$\frac{d\theta_o}{dt} + \omega_P C_s \theta_o = \omega_P C_s \theta_i \quad (18.16)$$

In order to discuss this equation we shall presuppose an elementary knowledge of the complex variable and of linear differential equations with constant coefficients.

A standard procedure for solving a linear equation with constant coefficients is to solve first for the "complementary function," which in the case of Eq. (18.16) is the solution obtained for $\theta_i = 0$. It is well known that the complementary function is the sum of exponential terms of the form Ce^{zt} , where both C and z may be complex constants.

The second step in the procedure is to determine a particular solution of the equation as originally given [that is, for a nonzero value of θ_i in Eq. (18.16)]. The complete solution is the sum of the complementary function and the particular solution. It is called "complete" because it contains just enough arbitrary constants to satisfy any given boundary conditions.

Suppose that no signal is applied to the system ($\theta_i = 0$) and that arbitrary initial conditions of displacement, velocity, etc., are imposed on the output shaft by suitable external means. (The number of initial conditions that can be arbitrarily chosen is equal to the order of the differential equation of the system. In the present case, only the initial displacement is arbitrary.) The servomechanism is said to be stable if, when the external actions on the output shaft are removed, the shaft eventually comes to rest. The stability of a linear servomechanism can be investigated by means of the complementary function since nonzero values of θ_i are not involved. The system will be stable if none of the exponents z has a positive real part, since in this case all terms of the complementary function remain finite as the time t approaches infinity. It is possible for the output shaft to oscillate indefinitely at a finite amplitude if one of the z 's is pure imaginary. In this case the system would be neither stable nor unstable. Such a neutral system is relatively unimportant and will not be further considered.

It may be remarked that an actual system is at most linear over only a certain range of motion. If the system is unstable, either the motion will build up to the point where the apparatus destroys itself or the nonlinearity will limit the motion to a safe value. This latter behavior is not to be confused with the neutral oscillations of a linear system mentioned in the previous paragraph.

To check on the stability of the ideal system of Fig. 18.17 we assume $\theta_i = 0$, $\theta_o = C_o e^{zt}$ and substitute in Eq. (18.16).

$$C_o e^{zt}(z + \omega_P C_o) = 0$$

Ruling out the trivial solution $C_o = 0$, we get

$$z + \omega_P C_o = 0 \quad (18.17)$$

from which it is obvious that the apparatus is stable, since $z = -\omega_P C_s$, which is a negative real number.*

The next question of interest is the response of the system to a step signal. Three types are commonly used in the study of servomechanisms: displacement, velocity, and acceleration step signals. We shall consider only the first type, which may be defined by

$$\left. \begin{aligned} \theta_i &= 0 & \text{for } t < 0 \\ \theta_i &= C_i & \text{for } t \geq 0 \end{aligned} \right\} \quad (18.18)$$

Substituting this expression into Eq. (18.16) we get, if $t \geq 0$,

$$\frac{d\theta_o}{dt} + \omega_P C_s \theta_o = \omega_P C_s C_i$$

A particular solution of this equation is readily seen to be $\theta_o = C_i$. The complete solution of Eq. (18.16) is thus the sum

$$\theta_o = C_o e^{-C_s \omega_P t} + C_i = C_o e^{-\alpha_0 t} + C_i$$

If the boundary condition is arbitrarily chosen as $\theta_o = 0$ at $t = 0$, $C_o = C_i$ and

$$\theta_o = C_i(1 - e^{-\alpha_0 t}) \quad (18.19)$$

The response curve is plotted in Fig. 18.18, from which it is seen that there is no overshoot and hence no oscillation. Furthermore, $\theta_o/\theta_i \rightarrow 1$ as $t \rightarrow \infty$, so that the error ultimately becomes zero.

The parameter $\alpha_0 = \omega_P C_s$, which has the dimensions of angular velocity, is seen from Eq. (18.16) to equal the ratio of the output angular velocity to the error. It is thus a measure of the speed with which the system responds. Furthermore, if a displacement step

signal is applied to the servomechanism, it follows from Eq. (18.19) that $1/\alpha_0$ is the time required for the error to drop to one eth of its initial value. α_0 is usually called the "time constant" of the system.

It is convenient to introduce the term "rise time," which is defined as the time required for θ_o/θ_i to rise from, say, 0.1 to 0.9. We observe that the rise time is reduced if the time constant α_0 is made larger. For this ideal servomechanism α_0 is the only parameter at our disposal; it should clearly be made as large as possible, to ensure a good transient response.

* C_s might, of course, be made negative, by means of a suitable feed-back linkage. The system would then be unstable.

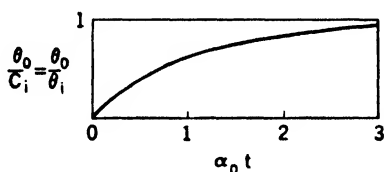


FIG. 18.18. — Response of an ideal hydraulic servomechanism to a displacement step signal.

If θ_i is assumed to be a velocity step signal, it will be found as before that there is no overshoot or oscillation, but the steady-state error will be different from zero. This type of servomechanism is therefore better adapted to positioning the output shaft than to driving it at a constant velocity. For the latter function a device with a zero velocity error would be selected.

The above method of determining the transient behavior (*i.e.*, solving the equation when θ_i is a suitable step function) is not feasible for complex systems. We shall therefore illustrate for our ideal system an alternative method of attack, the frequency-response method. For this purpose we assume that the signal θ_i is a sinusoidal function of t , having an angular frequency ω .

$$\theta_i = C_i e^{i\omega t} \quad (18.20)$$

where C_i and ω are real.* It is easily demonstrated that, for this signal, a particular solution of Eq. (18.16) is

$$\theta_o = C_o e^{i\phi} e^{i\omega t} \quad (18.21)$$

where C_o and ϕ are both real. This is the steady-state response to a sinusoidal signal, *i.e.*, the response that will obtain after the signal has been applied for a long (theoretically infinite) time.

It is well known that θ_i and θ_o can be represented as vectors drawn from a common origin and rotating at the constant angular velocity ω . The constant angle ϕ maintained between them is called the "phase angle." C_i and C_o are the lengths, or "absolute values," of θ_i and θ_o , respectively. The absolute values are also denoted by $|\theta_i|$ and $|\theta_o|$.

To show that Eq. (18.21) is a solution of Eq. (18.16), we substitute in the latter.

$$C_o e^{i\phi} e^{i\omega t} (i\omega + C_s \omega_P) = C_s \omega_P C_i e^{i\omega t} \quad (18.22)$$

$$\frac{C_o}{C_i} e^{i\phi} \left(1 + \frac{i\omega}{C_s \omega_P} \right) = 1$$

$$\frac{C_o}{C_i} \sqrt{1 + \frac{\omega^2}{C_s^2 \omega_P^2}} e^{i[\phi + \tan^{-1}(\omega/C_s \omega_P)]} = 1$$

Since the left-hand side must be real, the exponent of e is equal to zero, or

$$\tan \phi = - \frac{\omega}{C_s \omega_P} = - \frac{\omega}{\alpha_o} \quad (18.23)$$

and

$$\frac{|\theta_o|}{|\theta_i|} = \frac{C_o}{C_i} = \frac{1}{\sqrt{1 + (\omega^2/C_s^2 \omega_P^2)}} = \frac{1}{\sqrt{1 + (\omega^2/\alpha_o^2)}} \quad (18.24)$$

* The symbol i in $e^{i\omega t}$ here has its usual meaning, *viz.* $i^2 = -1$. Do not confuse this symbol with the subscript i . The latter indicates a quantity associated with the input, or signal, shaft.

C_o and ϕ are thus determined in such a way that Eq. (18.16) is satisfied. A similar demonstration can be made for any linear differential equation with constant coefficients.

The dimensionless parameter ω/α_0 represents the ratio of the angular frequency of the applied signal to the time constant of the system. When this ratio is small, it is found that the system responds more faithfully to an applied signal than when the ratio is large.

A plot of Eq. (18.24) is given in Fig. 18.19. The same qualitative information can be gleaned from this figure as from Fig. 18.18. We notice first that, since the curve exhibits no resonance peaks, the system will not oscillate at any frequency and hence cannot overshoot. Furthermore, the value of $|\theta_o|/|\theta_i|$ is close to unity only for small values of ω/α_0 . Hence the response at high frequencies will be improved if α_0 is made larger. Since a system that will not respond accurately to a high-frequency sinusoidal signal will obviously have a poor response to a step signal, we conclude that, the larger the value of α_0 , the better will be the transient response. This conclusion is rigorously justified by the theory of transients in linear systems, in which it is shown that a step signal can be considered as a suitable summation of sine waves of all frequencies.

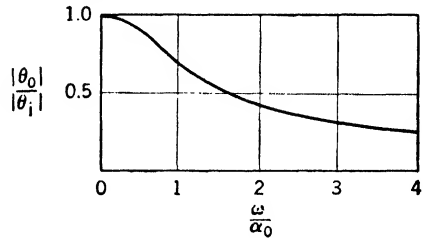


FIG. 18.19. — Amplitude response of an ideal hydraulic servomechanism as a function of frequency.

The value of the rise time cannot be determined from Fig. 18.19 alone; but if this curve is supplemented by an empirical rule, the rise time can be found with sufficient accuracy for most design purposes. This rule is

$$\omega_c t_r = \pi \quad (18.25)$$

where t_r is the rise time and ω_c is the angular frequency of “cutoff,” defined as that ω at which $|\theta_o|/|\theta_i|$ has one-half its value at zero frequency.

To determine the order of the approximation to be expected from Eq. (18.25) we compare the value of t_r computed from it with the value found from Eq. (18.19). The cutoff angular frequency is first obtained from Eq. (18.24).

$$\frac{|\theta_o|}{|\theta_i|} = \frac{C_o}{C_i} = \frac{1}{2} = \frac{1}{\sqrt{1 + (\omega^2/\alpha_0^2)}}$$

whence

$$\frac{\omega_c}{\alpha_0} = \sqrt{3}$$

Equation (18.25), therefore, yields

$$\alpha_0 t_r = \frac{\pi}{\sqrt{3}} = 1.82$$

The exact value of $\alpha_0 t_r$ is obtained from Eq. (18.19).

$$\alpha_0 t_r = \alpha_0(t_{0.9} - t_{0.1}) = \ln \frac{1}{0.1} - \ln \frac{1}{0.9} = 2.20$$

where $t_{0.1}$ and $t_{0.9}$ stand for the times at which C_o/C_i equals 0.1 and 0.9, respectively. The approximate value of $\alpha_0 t_r$ is seen to be about 20 per cent too low.

In many applications the phase angle ϕ is also important. Equation (18.23) is accordingly plotted in Fig. 18.20.

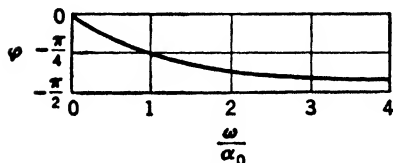


FIG. 18.20. — Phase-angle response of an ideal hydraulic servomechanism as a function of frequency.

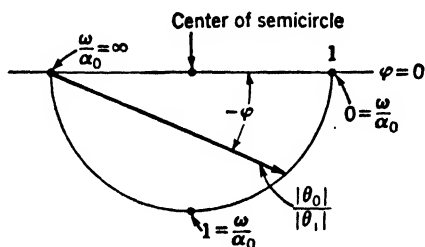


FIG. 18.21. — Vectorial form of the frequency response of an ideal hydraulic servomechanism.

The information given by Figs. 18.19 and 18.20 can be combined into the single polar curve of Fig. 18.21, in which $|\theta_o|/|\theta_i|$ is plotted as the radius vector from the origin at an angle ϕ . Values of the parameter ω/α_0 are spotted on the curve. It is readily shown by means of Eqs. (18.23) and (18.24) that in this example the curve is a semicircle of radius $1/2$ and center at $|\theta_o|/|\theta_i| = 1/2$, $\phi = 0$. The proof of this is left to the reader.

18.11. The Transfer Function. The results of the frequency-response analysis, which are presented in Eqs. (18.23) and (18.24) and plotted in Figs. 18.19 and 18.20, can also be obtained graphically, by means of the "transfer function" ζ . Use of the transfer function simplifies the analysis of complicated systems, for which the algebra leading to results corresponding to Eqs. (18.23) and (18.24) would be extremely involved. The conditions under which a system will be stable can also be easily determined by means of ζ .

The transfer function is defined, in general, as the ratio of the steady-state response to the error when a sinusoidal signal is applied. In symbols,

$$\zeta = \frac{\theta_o}{\theta_i - \theta_o} \quad (18.26)$$

where θ_o is the steady-state response and θ_i is a sinusoidal signal. Substituting into this equation the values of θ_i and θ_o from Eqs. (18.20) and (18.21), we get

$$\frac{\zeta}{\zeta + 1} = \frac{\theta_o}{\theta_i} = \frac{C_o}{C_i} e^{i\psi} \quad (18.27)$$

Or, if we put $\zeta = |\zeta| e^{i\psi}$ and $\zeta + 1 = |\zeta + 1| e^{i\chi}$

$$\frac{|\zeta|}{|\zeta + 1|} = \frac{C_o}{C_i} \quad (18.28)$$

and

$$\psi - \chi = \phi \quad (18.29)$$

It is clear from Eqs. (18.28) and (18.29) that, if ζ is known as a function of ω , C_o/C_i and ϕ can be readily determined graphically. The procedure is easily visualized from Fig. 18.22, which shows a hypothetical curve followed by the ζ vector as ω changes. For any value of ω , C_o/C_i is found from the ratio of the measured lengths of ζ and $\zeta + 1$, while ϕ is obtained from measurements of χ and ψ .

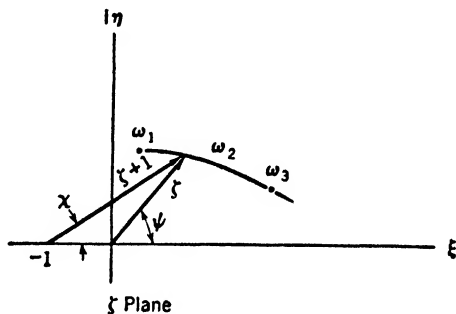


FIG. 18.22.

The problem of making a frequency-response analysis is thus reduced to that of finding the transfer function. As a simple illustration of a general method for getting ζ , revert to the ideal hydraulic servomechanism already discussed. Combining Eqs. (18.22) and (18.27), we find that

$$\frac{\zeta + 1}{\zeta} = \frac{\theta_i}{\theta_o} = \frac{C_i}{C_o e^{i\psi}} = \frac{i\omega}{C_s \omega_P} + 1 = \frac{i\omega}{\alpha_0} + 1 \quad (18.30)$$

from which $\zeta = \alpha_0/i\omega = -i\alpha_0/\omega$. Since ω is real and positive, $i\omega$ is positive imaginary and ζ is negative imaginary, as shown in Fig. 18.23. An arbitrary point g on the $i\omega$ axis of the z plane is carried over to g' in the ζ plane. The results expressed in Eqs. (18.23) and (18.24) are embodied completely in Fig. 18.23b.

Consider now a more general form of hydraulic servomechanism for which the differential equation is

$$\alpha_n \frac{d^n \theta_o}{dt^n} + \cdots + \alpha_1 \frac{d\theta_o}{dt} + \alpha_0 \theta_o = \beta_0 \theta_i \quad (18.31)$$

We now observe that Eq. (18.32) defines ζ as a function of z when z is restricted to purely imaginary values, $i\omega$, and that ζ is not yet defined for complex values of z . We may therefore extend the definition of ζ in any way that does not contravene Eq. (18.32). A useful extension is that in which $i\omega$ in Eq. (18.32) is replaced by z .

$$\frac{\zeta + 1}{\zeta} = \frac{\alpha_n z^n + \cdots + \alpha_1 z + \alpha_0}{\beta_0} \quad (18.35)$$

Comparison of this with Eq. (18.33) shows at once that the roots of the latter are also the roots of the expression $(\zeta + 1)/\zeta$. This expression can be zero, however, only when the numerator $\zeta + 1$ is zero. We thus conclude that the roots of $\zeta + 1$ are the z_1, \dots, z_n of Eq. (18.33) or (18.34). We may therefore state that, if $\zeta + 1$ has no roots with a positive real part, the servomechanism is stable.

A great simplification results from this use of ζ , for, in general, it is difficult and tedious to determine the roots of an n th-degree equation. Such determination can be avoided by use of the following theorem: Let a function $f(z)$ be analytic [that is, let $f(z)$ have a continuous derivative] for all values of z in and on the boundary of a region R , and let $f(z)$ be different from zero for all z 's on the boundary curve S . Then, if the vector z traces out S , the vector $f(z)$ will trace out a closed curve S' in the $f(z)$ plane, as indicated schematically in Fig. 18.24. It can be shown

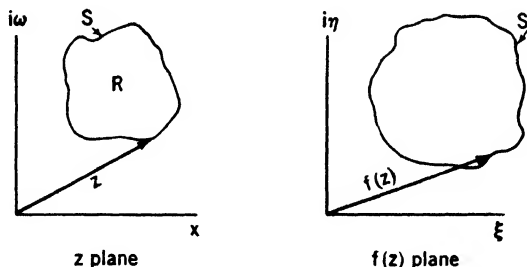


FIG. 18.24.

that the net number of counterclockwise revolutions made by the vector $f(z)$ in tracing out S' is equal to the number of roots of $f(z)$ inside the region R .*

In applying this theorem to the stability problem we take the curve S as shown in Fig. 18.25*a*, so as to include in the limit the entire right-hand half plane and thus all z 's with positive real parts. The function $f(z)$

* A proof of the theorem is outside the scope of this book. A proof is given in E. C. Titchmarsh, "Theory of Functions," 2d ed., pp. 115–116, Oxford University Press, New York, 1939.

$= \zeta + 1$ is the one to be investigated. All the expressions for $\zeta + 1$ that we shall meet satisfy the requirements for $f(z)$ listed above.

For the ideal hydraulic servomechanism, Eq. (18.32) reduces to Eq. (18.30), so that, if $i\omega$ is replaced by z , $\zeta = \alpha_0/z$. The curve S' in the ζ plane corresponding by this expression to S in the z plane is shown in Fig. 18.25*b*. The points a' and d' at the origin in the ζ plane correspond to

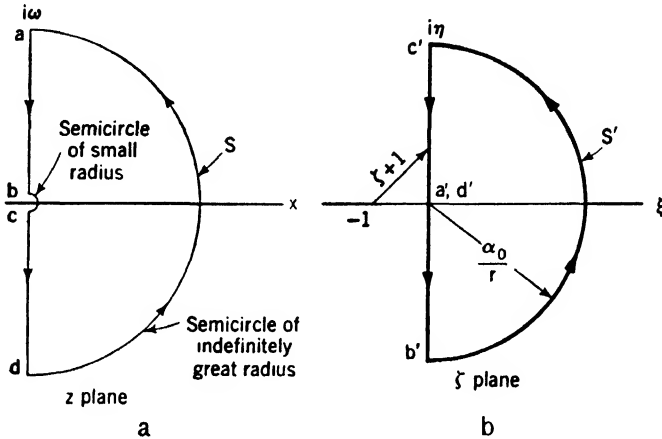


FIG. 18.25. — Stability diagram for an ideal hydraulic servomechanism.

a and d , infinitely far from $z = 0$, while the radius $\alpha_0/r \rightarrow \infty$ as $r \rightarrow 0$. It is seen therefore that, as the tip of the z vector moves around the boundary S of the right-hand half plane, the vector $\zeta + 1$ will not make a complete revolution about its point of origin -1 , and the system will be stable.

While quite superfluous in the present example, this method of investigating stability is simple and rapid, even for complex systems. It will be noted that a rough sketch of S' is sufficient, since the only information needed is the number of revolutions made by $\zeta + 1$ as it traces out the curve S' . The advantage of this method is brought out by the example of the next article.

18.12. Hydraulic Servomechanism with Leakage and Elasticity. The apparatus considered here is the same as that of Fig. 18.17. We neglect for the moment any elastic deformation of the system and deal with the leakage, which we treat as in Art. 18.8, assuming Q_l to be proportional to the pressure drop Δp .

$$Q_l = \frac{C_l D \Delta p}{\mu} \quad (18.15)$$

The continuity equation [Eq. (18.11)] thus gives

$$\frac{d\theta'_0}{dt} = \omega_P S_P - \frac{C_l}{\mu} \Delta p \quad (18.36)$$

where θ'_o represents the angular displacement of the output shaft of the rigid system.

We now take the elastic deformation of the system into account in the following approximate way: The sole effect of the elasticity is assumed to be a change in angular position of the output shaft that is proportional to the output torque T_M . Since T_M is a load torque, its effect is to compress the fluid and expand the pipes, so that the actual output-shaft position θ_o , will be somewhat less than θ'_o . The elastic constant of the system, C_e , is therefore defined as

$$T_M = C_e(\theta'_o - \theta_o) \quad (18.37)$$

The torque T_M is expressible in terms of the moment of inertia I and the angular acceleration of the load mass, by virtue of Newton's second law.

$$T_M = I \frac{d^2\theta_o}{dt^2} \quad (18.38)$$

Here it is assumed that T_M is the only external torque on the load mass.

Another expression for T_M is given by Eq. (18.6), which may be applied to nonsteady flow if the mass of all other moving parts is assumed negligible relative to the load mass.

$$T_M = \Delta p D \quad (18.39)$$

For simplicity, η_{TM} has been set equal to unity.

Combining the last four equations and introducing as before the assumption that $S_P = C_s(\theta_i - \theta_o)$ we get, after some reduction,

$$\frac{I}{C_e} \frac{d^3\theta_o}{dt^3} + \frac{C_l I}{\mu D} \frac{d^2\theta_o}{dt^2} + \frac{d\theta_o}{dt} + \omega_P C_s \theta_o = \omega_P C_s \theta_i \quad (18.40)$$

The primary question is again that of stability, to answer which we proceed as before to investigate graphically the zeros of the complementary function. Assume, as usual, that $\theta_i = 0$, $\theta_o = Ce^{zt}$, and introduce the symbols $\alpha_0 = \omega_P C_s$, $\alpha_2 = C_l I / \mu D$, and $\alpha_3 = I / C_e$. Equation (18.40) thus yields

$$\alpha_3 z^3 + \alpha_2 z^2 + z + \alpha_0 = 0$$

which will be recognized as the special form of Eq. (18.33) for this system. Comparison of Eqs. (18.31) and (18.40) shows that here $\beta_0 = \alpha_0$, so that Eq. (18.35) reduces to

$$\frac{\zeta + 1}{\zeta} = \frac{\alpha_3 z^3 + \alpha_2 z^2 + z}{\alpha_0} + 1$$

whence

$$\zeta = \frac{\alpha_0}{\alpha_3 z^3 + \alpha_2 z^2 + z} \quad (18.41)$$

It is obvious that $\zeta \rightarrow 0$ as $z \rightarrow \infty$, so that points a and d of Fig. 18.25a are mapped into the origin of the ζ plane. Also, $\zeta \rightarrow \alpha_0/z$ as $z \rightarrow 0$. Hence, if z traces out a semicircle of very small radius (Fig. 18.25a), ζ will describe a very large semicircle. The behavior of this ζ is therefore the same as that of the previous example, for either very large or very small values of z .

To determine the path followed by ζ for pure imaginary values, $z = i\omega$ (where $-\infty < \omega < \infty$), we substitute this value of z in Eq. (18.41) and get, after reduction,

$$\zeta = -\frac{\alpha_0\alpha_2}{\alpha_2^2\omega^2 + (1 - \alpha_3\omega^2)^2} - \frac{i\alpha_0(1 - \alpha_3\omega^2)}{\alpha_2^2\omega^3 + \omega(1 - \alpha_3\omega^2)^2} \quad (18.42)$$

We notice that, as ω decreases from very large positive values, the imaginary part of ζ is first positive, becomes zero at $\omega^2 = 1/\alpha_3$, and then approaches $-\infty$ as $\omega \rightarrow 0$. Furthermore, the real part of ζ [$R(\zeta)$] is never positive: $R(\zeta) \rightarrow 0$ if $\omega \rightarrow \infty$, and $R(\zeta) = -\alpha_0\alpha_2$ at $\omega = 0$. The positive imaginary axis, therefore, is mapped somewhat as shown by the full-line curve of Fig. 18.26. The rest of the boundary S of Fig. 18.25a maps into the dotted curve. The map of the negative imaginary z axis is simply the mirror image of the full-line curve with respect to the real axis of the ζ plane.

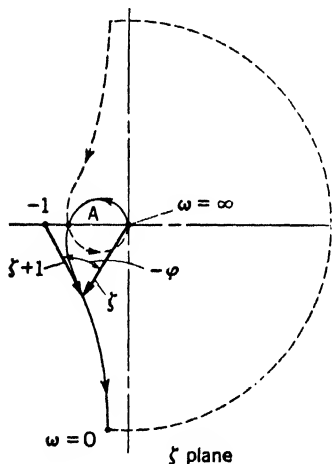


FIG. 18.26. — Transfer function for a hydraulic servomechanism with leakage and elasticity.

It will be recalled that the criterion for stability is that the vector $\zeta + 1$ make zero complete revolutions as it traces the entire closed curve of Fig. 18.26. The system will thus be stable if the point A lies to the right of the point -1 , that is, if $R(\zeta) > -1$. From Eq. (18.42) we have already seen that $\omega^2 = 1/\alpha_3$ at point A . Therefore, $R(\zeta) = -\alpha_0\alpha_3/\alpha_2$ at A , and the stability condition is

$$\left. \begin{aligned} \frac{\alpha_0\alpha_3}{\alpha_2} &< 1 \\ \text{or} \quad \frac{\omega_P C_s \mu D}{C_s C_l} &< 1 \end{aligned} \right\} \quad (18.43)$$

It was shown above for the ideal servomechanism that the larger $\omega_P C_s$, the more rapid the response. Here we see that there is actually an upper limit beyond which $\omega_P C_s$ cannot go without destroying the stability. An in-

crease in either the stiffness or the leakage coefficient C_e or C_l improves the margin of stability.

The transient response of the servomechanism is the next point of interest. Since Eq. (18.40) is of the third order, one must solve a cubic equation to get the complementary function and hence the complete solution for a step signal. This difficulty is avoided (unless exact results are necessary) by use of the frequency-response method. The value of ζ can be found from Eq. (18.41) if z is replaced by $i\omega$. Whence

$$\begin{aligned}\frac{\zeta}{\zeta + 1} &= \frac{\theta_o}{\theta_i} = \frac{C_o e^{i\phi}}{C_i} = \frac{\alpha_0}{-\alpha_3 i\omega^3 - \alpha_2 \omega^2 + i\omega + \alpha_0} \\ &= \frac{\alpha_0 / (-\alpha_3 i\omega^3 - \alpha_2 \omega^2 + i\omega)}{1 + \alpha_0 / (-\alpha_3 i\omega^3 - \alpha_2 \omega^2 + i\omega)}\end{aligned}\quad (18.44)$$

The full-line curve of Fig. (18.26) can be used to obtain graphically the value of C_o/C_i and ϕ corresponding to any given ω . In this example, however, it is relatively simple to get algebraic expressions for C_o/C_i and ϕ , so that a resort to graphical methods is unnecessary. Reduction of Eq. (18.44) yields

$$\frac{\theta_o}{\theta_i} = \frac{C_o e^{i\phi}}{C_i} = \frac{e^{-i \tan^{-1}\{(\omega/\alpha_0)[(1-\alpha_3\alpha_0^2)(\omega^2/\alpha_0^2)/(1-\alpha_2\alpha_0)(\omega^2/\alpha_0^2)]\}}}{\sqrt{[1 - \alpha_2\alpha_0(\omega^2/\alpha_0^2)]^2 + (\omega^2/\alpha_0^2)[1 - \alpha_3\alpha_0^2(\omega^2/\alpha_0^2)]^2}}$$

from which it follows that

$$\frac{C_o}{C_i} = \frac{1}{\sqrt{[1 - \alpha_2\alpha_0(\omega^2/\alpha_0^2)]^2 + (\omega^2/\alpha_0^2)[1 - \alpha_3\alpha_0^2(\omega^2/\alpha_0^2)]^2}}\quad (18.45)$$

and

$$\tan \phi = -\frac{(\omega/\alpha_0)[1 - \alpha_3\alpha_0^2(\omega^2/\alpha_0^2)]}{1 - \alpha_2\alpha_0(\omega^2/\alpha_0^2)}\quad (18.46)$$

These are seen to reduce to the corresponding equations for the ideal system [Eqs. (18.23) and (18.24)] if $\alpha_2 = \alpha_3 = 0$.

Each of the dimensionless parameters of Eqs. (18.45) and (18.46) has a physical significance. The basic parameter ω/α_0 has already been shown to represent the ratio of the forcing frequency to the time constant of the ideal system. The parameter $\alpha_3\alpha_0^2 = I\omega_p^2 C_l^2 / C_e$ is a measure of the ratio of inertia to elastic effects; the greater the stiffness of the system relative to the inertia of the load, the smaller this parameter. Similarly, $\alpha_2\alpha_0 = I\omega_p C_l / \mu D$ measures the ratio of load inertia to the viscous forces opposing leakage.

The stability criterion [Eq. (18.43)] states simply that $\alpha_3\alpha_0^2/\alpha_2\alpha_0 < 1$, or that the ratio of viscous force to stiffness must be less than a certain upper limit. It is obvious physically that, the greater the resistance to leakage relative to the stiffness of the system, the greater the tendency for continued oscillation, *i.e.*, the smaller the margin of stability.

Plots of Eq. (18.45) for several values of $\alpha_3\alpha_0^2$ and $\alpha_2\alpha_0$ are given in Fig. 18.27. Curve *a*, for the ideal case of infinite stiffness and zero leakage, is the same as Fig. 18.19.

Curve *b*, for large stiffness and low leakage, has several desirable characteristics. The resonance peak is very small and occurs at a high value

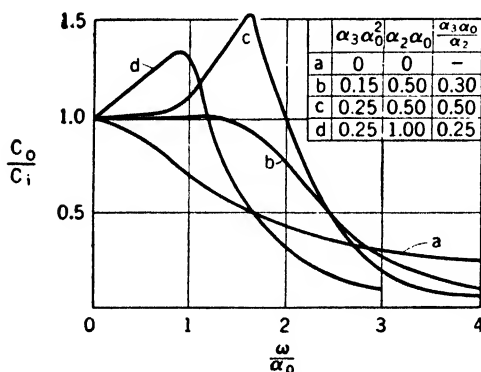


FIG. 18.27. — Amplitude response of a hydraulic servomechanism with leakage and elasticity.

of ω/α_0 , so that the amplitude response is better at high frequencies than in the ideal case.

The low value of the peak means that there will be very little overshoot in the response to a step signal. Furthermore, the occurrence of the peak at a large ω/α_0 boosts the cutoff value of ω/α_0 from about 1.8 for curve *a* to 2.4 for curve *b*. Equation (18.25) thus indicates a rise time for *b* only about 75 per cent of that for *a*. The stability number $\alpha_3\alpha_0/\alpha_2$ is well

below unity, so that the time required for oscillations to damp out should be satisfactorily small.

Curve *c* shows what happens if the stiffness is decreased without change in the leakage parameter. The amplitude ratio at resonance is 1.56, a value that is found to give undesirably large overshoot in the response to a step signal. The maximum amplitude ratio that can be tolerated is found by experience to be about 1.35. Thus, although the rise time is about the same as for *b*, curve *c* is unsatisfactory. Another count against *c* is the relatively large value of the stability number, which means decreased damping of the oscillations.

Curve *d* shows the effect of an increased leakage if the stiffness is kept the same as for *c*. The amplitude ratio at resonance drops to 1.35, which is reasonable, and the margin of stability is improved. The increased rise time, accompanying the lowered resonant frequency, may, however, be a serious drawback.

The phase-angle response corresponding to each of the curves of Fig. 18.27 has been computed from Eq. (18.46) and plotted in Fig. 18.28. The most notable feature is that the presence of leakage and elasticity increases the maximum phase shift from $-\pi/2$ to $-3\pi/2$. There is little to choose among curves *b*, *c*, and *d*, but curve *b* seems on the whole to be the best. The dotted curve is included to show that the maximum phase shift is equal to $-\pi$ if the system is assumed to be rigid but to have a finite leakage.

The results of Figs. 18.27 and 18.28 can be combined on a single polar diagram like that of Fig. 18.21. This is left as an exercise for the reader.

The steady-state error for a displacement step signal is readily seen from physical considerations to be zero, since the load has been assumed to be entirely due to inertia. For, so long as the error is different from zero, Δp cannot be zero, and hence, from Eqs. (18.38) and (18.39), the load mass will have some angular acceleration. θ_o will thus continue to change until it equals the constant value of θ_i .

The same thing can be shown theoretically from the fact that the full-line curve of Fig. 18.26 approaches infinity along the negative imaginary axis. Furthermore, if this curve approached infinity along the negative real axis, the servomechanism would have a zero velocity error [1]. Proof of these statements is beyond the scope of this book.

It is clear physically that the steady-state displacement error will not be zero if there is applied to the output shaft an external torque which does not vanish with the angular velocity or acceleration, $d\theta_o/dt$ or $d^2\theta_o/dt^2$. For, in such a case, the steady-state pressure difference across the motor must suffice to counterbalance this torque. On account of the leakage, this pressure difference cannot be maintained without a finite steady-state error.

18.13. Linear Servomechanisms: Concluding Remarks. The examples discussed above are intended to illustrate the two methods available for analysis and design of hydraulic (or other) linear servomechanisms and to bring out the relative simplicity and power of the frequency-response method.

In both these examples the feed-back circuit has been assumed to give proportional control, that is, $S_P = C_s(\theta_i - \theta_o)$. It is frequently advantageous to employ more complicated feed-back arrangements, to give, for example, "proportional plus derivative control" or "proportional plus integral control," that is,

$$S_P = C_s(\theta_i - \theta_o) + G_s \frac{d}{dt}(\theta_i - \theta_o)$$

or

$$S_P = C_s(\theta_i - \theta_o) + H_s \int_0^t (\theta_i - \theta_o) dt$$

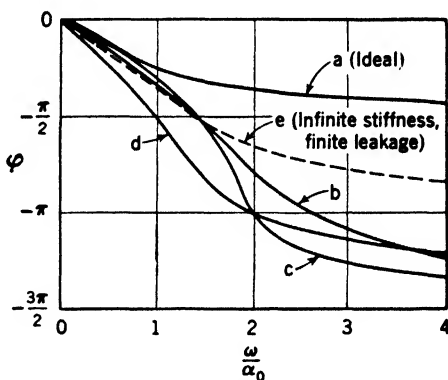


FIG. 18.28. — Phase-angle response of a hydraulic servomechanism with leakage and elasticity.

Discussion of such systems cannot be undertaken here. The reader is referred to problems 18.12 and 18.13, and to the literature [1].

18.14. Valve-controlled Servomechanisms. If a translatory motion is to be controlled by a hydraulic servomechanism, the simplest scheme is to use a hydraulic cylinder connected through a four-way valve to a source of high-pressure oil, as shown schematically in Fig. 18.29. Such an apparatus has many applications, for example, in machine tools, control of aircraft, and power steering of heavy vehicles.

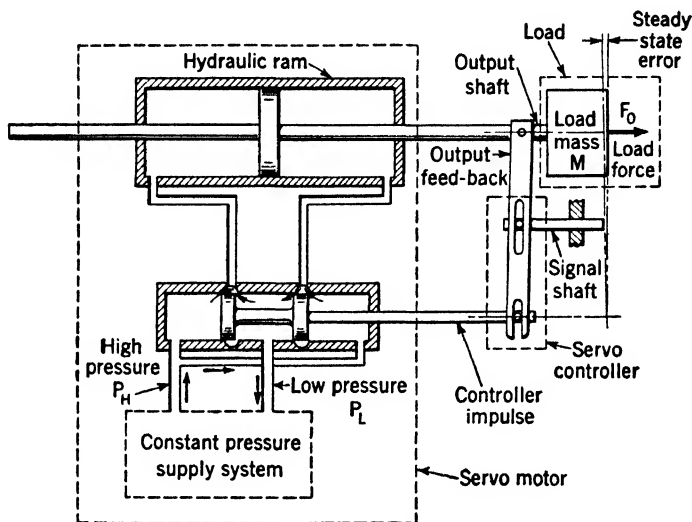


FIG. 18.29. — Schematic diagram of a valve-controlled hydraulic servomechanism. (Courtesy of C. E. Grosser.)

Study of Fig. 18.29 shows that, if the signal shaft is moved, say, to the left and then held stationary, the valve will open in such a way as to admit high-pressure oil to the right end of the cylinder and permit the low-pressure oil to flow out of the left end. The piston will then move to the left, and the feed-back link will tend to close the valve.

It will be observed that a given position of the signal shaft implies, ideally, a single corresponding position of the power shaft. Actually, however, if the mechanism is initially at rest and the signal shaft is displaced, the power-shaft position will fail momentarily to correspond to that called for, *i.e.*, an error will be produced. It is the creation of this error that opens the valve, thus causing the power shaft to move so as to reduce both the error and the valve opening.

The differential equation of a valve-controlled servomechanism is based on the energy principle [Eq. (5.6)] and will involve, *inter alia*, the hydraulic losses occurring in the system. To a first approximation, the losses in the

pipes and fittings can be neglected, as was done previously, by virtue of the assumption that $\Delta p_P = \Delta p_M = \Delta p$. The loss in the valve of Fig. 18.29 will, however, become of prime importance as the valve nears the closed position. The loss per unit mass of oil varies as the square of the oil velocity through the valve, which in turn depends on the product of the area of the valve opening and the piston velocity. The resulting equation is nonlinear and must be integrated by special methods, such as a step-by-step technique [4], or by means of a differential analyzer.

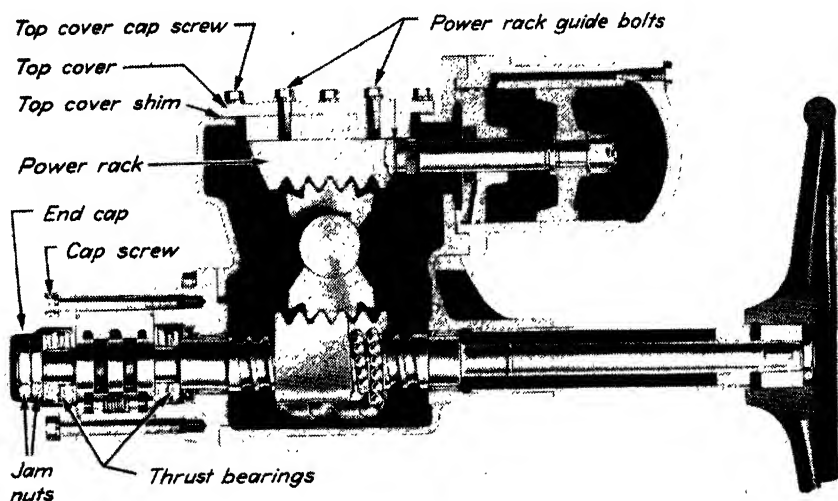


FIG. 18.30. — Valve-controlled hydraulic steering booster. (Courtesy of F. W. Davis.)

A detailed discussion of this servomechanism cannot be given here. It exhibits, however, a behavior which is qualitatively like that of a linear servomechanism, *i.e.*, if subjected to a displacement step signal, it has a certain rise time, overshoot, natural oscillation frequency, and decay time. The corresponding steady-state error is zero for a pure inertia load, as may be seen from a physical argument like that of Art. 18.12. If, however, a static force is applied to the output shaft, the leakage necessitates a slight opening of the valve to maintain the required pressure difference across the piston. A steady-state error results, which is greater the greater the leakage.

The servomechanism of Fig. 18.29 is operated from a constant-pressure source of oil. This may be supplied in several ways, for example, by a fixed-displacement pump and relief valve or unloader valve, together with an accumulator, as described in Art. 18.6.

In some applications, such as power steering of a truck, it is desirable

to dispense with the complication of the accumulator and the associated valves. This simplification has been accomplished in one type of steering booster by use of a control valve that under static conditions is open instead of closed [10]. This booster is shown in Fig. 18.30. Oil from a gear pump driven at engine speed circulates freely through the open valve unless a considerable steering effort is required. If only a small torque is needed to turn the wheels, the valve is unaffected, the booster does not operate, and steering is done manually in the usual way. If, however, the torque on the steering wheel exceeds a predetermined amount, the end thrust suffices to move the steering column slightly lengthwise, through compression of centering springs. The valve spool, which moves with the steering column, is thus displaced from its neutral position, oil is forced to the appropriate side of the piston, and the booster functions.

In addition to its relative simplicity, this type of booster has the advantage that the steering effort required of the operator is readily adjustable. Some operator effort has been found advisable for safety reasons, since a certain "feel" of the road is thereby obtained, which is absent if the entire steering load is taken by the booster.

SELECTED BIBLIOGRAPHY

1. BROWN, G. S., and A. C. HALL: Dynamic Behavior and Design of Servomechanisms, *Trans. Am. Soc. Mech. Engrs.*, vol. 68, pp. 503-524, July, 1946.
2. FIELD, HOWARD, JR.: An Introduction to Aircraft Hydraulic Systems, *Trans. Am. Soc. Mech. Engrs.*, vol. 66, pp. 569-576, October, 1944.
3. FITZSIMMONS, V. G., D. L. PICKETT, R. O. MILITZ, and W. A. ZISMAN: Dimethylsilicone-polymer Fluids and Their Performance Characteristics in Hydraulic Systems, *Trans. Am. Soc. Mech. Engrs.*, vol. 68, pp. 361-369, May, 1946.
4. GROSSER, C. E.: Hydraulic Control Affords Design Flexibility, *Machine Design*, vol. 12, pp. 37-40, 120-122, December, 1940 (see also several other related articles that appeared during 1941).
5. HERMAN, DALE: Evolution of the Hydraulic Pump as Applied to Aircraft, *Trans. Am. Soc. Mech. Engrs.*, vol. 66, pp. 583-588, October, 1944.
6. HERMAN, K. R.: Modern Hydraulic Units for Machine Tools, *Mech. Eng.*, vol. 60, pp. 823-828, November, 1938.
7. MACCOLL, L. A.: "Fundamental Theory of Servomechanisms," D. Van Nostrand Company, Inc., New York, 1945.
8. PIGOTT, R. J. S.: Some Characteristics of Rotary Pumps in Aviation Service, *Trans. Am. Soc. Mech. Engrs.*, vol. 66, pp. 615-623, October, 1944.
9. WILSON, W. E.: Rotary-pump Theory, *Trans. Am. Soc. Mech. Engrs.*, vol. 68, pp. 371-384, May, 1946.
10. DAVIS, F. W.: Power Steering for Automotive Vehicles, *S.A.E.J. (Trans.)*, vol. 53, pp. 239-256, 1945.

APPENDIX

MECHANICAL PROPERTIES OF FLUIDS

Values of fluid properties are given at several places in the text. These places are listed below for easy reference.

Art. 2.22. Bulk compression modulus of water. Specific-heat ratio, gas constant, and specific weight of gases.

Art. 8.4. Kinematic viscosity: relation between Saybolt seconds and centistokes.

Art. 12.4. Conversion factors for viscosity.

Art. 12.5. Specific gravity of oils.

Art. 12.11. Specific heat of oils.

Art. 12.12. Thermal conductivity of oils.

Art. 18.7. Kinematic viscosity of hydraulic fluids.

The following tables give the density ρ , the viscosity μ , and the kinematic viscosity ν as functions of temperature for several liquids and gases. The first two tables are for water and air, since these are the fluids most commonly used in engineering practice.

PROPERTIES OF WATER AT ATMOSPHERIC PRESSURE *

Temperature		Density		Viscosity		Kinematic viscosity	
Deg C	Deg F	G/cm ³	Slug/ft ³	Dyne-sec/cm ²	Lb-sec/ft ²	Cm ² /sec	Ft ² /sec
0	32	0.99987	1.940	1.794×10^{-2}	3.746×10^{-5}	1.794×10^{-2}	1.930×10^{-5}
4	39.2	1.00000	1.941	1.568	3.274	1.568	1.687
5	41	0.99999	1.941	1.519	3.172	1.519	1.634
10	50	0.99973	1.940	1.310	2.735	1.310	1.407
15	59	0.99913	1.940	1.145	2.391	1.146	1.233
20	68	0.998	1.937	1.009	2.107	1.011	1.088
30	86	0.996	1.932	0.800	1.670	0.803	0.864
40	104	0.992	1.925	0.654	1.366	0.659	0.709
50	122	0.988	1.917	0.549	1.146	0.556	0.598
60	140	0.983	1.907	0.470	0.981	0.478	0.514
70	158	0.978	1.897	0.407	0.850	0.416	0.448
80	176	0.972	1.885	0.357	0.745	0.367	0.395
90	194	0.965	1.872	0.317	0.662	0.328	0.353
100	212	0.958	1.858	0.284	0.593	0.296	0.318

* Data from the "International Critical Tables" (abbreviation I.C.T.), McGraw-Hill Book Company, Inc., 1930.

PROPERTIES OF AIR AT ATMOSPHERIC PRESSURE *

Temperature		Density		Viscosity		Kinematic viscosity	
Deg C	Deg F	G/cm ³	Slug/ft ³	Dyne-sec/cm ²	Lb-sec/ft ²	Cm ² /sec	Ft ² /sec
0	32	1.293×10^{-3}	2.510×10^{-3}	1.709×10^{-4}	3.568×10^{-7}	0.1322	1.427×10^{-4}
50	122	1.093	2.122	1.951	4.074	0.1785	1.921
100	212	0.946	1.836	2.175	4.541	0.2299	2.474
150	302	0.834	1.619	2.385	4.980	0.2860	3.077
200	392	0.746	1.448	2.582	5.391	0.3461	3.724
250	482	0.675	1.310	2.770	5.784	0.4104	4.416
300	572	0.616	1.196	2.946	6.151	0.4782	5.145
350	662	0.567	1.101	3.113	6.500	0.5490	5.907
400	752	0.525	1.019	3.277	6.842	0.6246	6.721
450	842	0.488	0.947	3.433	7.168	0.7035	7.570
500	932	0.457	0.887	3.583	7.481	0.7840	8.436

* Data from the I.C.T.

PROPERTIES OF LIQUIDS AT ATMOSPHERIC PRESSURE *

Temperature		Density		Viscosity		Kinematic viscosity	
Deg C	Deg F	G/cm ³	Slug/ft ³	Dyne-sec/cm ²	Lb-sec/ft ²	Cm ² /sec	Ft ² /sec
Carbon Tetrachloride							
0	32	1.633	3.170	1.34×10^{-2}	2.80×10^{-5}	0.82×10^{-2}	0.88×10^{-5}
20	68	1.594	3.094	0.97	2.02	0.61	0.65
40	104	1.555	3.018	0.74	1.54	0.48	0.52
Castor Oil							
20	68	0.960	1.863	9.86	2.059×10^{-2}	10.27	11.05×10^{-3}
40	104	0.946	1.836	2.31	0.482	2.44	2.63
Ethyl Alcohol							
0	32	0.806	1.564	1.790×10^{-2}	3.738×10^{-5}	2.221×10^{-2}	2.390×10^{-5}
20	68	0.789	1.531	1.716	3.583	2.175	2.340
40	104	0.772	1.498	1.647	3.439	2.133	2.295
60	140	0.756	1.467	1.581	3.301	2.091	2.250
Glycerol							
30	86	1.255	2.436	3.8	7.9×10^{-3}	3.0	3.2×10^{-3}
75	167	1.226	2.380	0.24	0.50	0.20	0.22
Glycol							
25	77	1.110	2.154	0.174	0.363×10^{-3}	0.158	0.170×10^{-3}
Mercury							
0	32	13.60	26.40	1.66×10^{-2}	3.47×10^{-5}	0.122×10^{-2}	0.131×10^{-5}
20	68	13.55	26.30	1.54	3.22	0.114	0.123
40	104	13.50	26.20	1.47	3.07	0.109	0.117
100	212	13.35	25.91	1.26	2.63	0.094	0.101
Methyl Alcohol							
0	32	0.810	1.572	0.808×10^{-2}	1.687×10^{-5}	0.998×10^{-2}	1.074×10^{-5}
20	68	0.791	1.535	0.593	1.238	0.750	0.807
40	104	0.773	1.500	0.449	0.938	0.581	0.625
60	140	0.753	1.462	0.349	0.729	0.463	0.498
White Mineral Oil (SAE 10)							
15.5	60	0.875	1.698	1.29	2.69×10^{-3}	1.47	1.58×10^{-3}
49	120	0.855	1.660	0.236	0.493	0.276	0.297
93.5	200	0.835	1.621	0.062	0.129	0.074	0.080
White Mineral Oil (SAE 30)							
15.5	60	0.885	1.718	3.70	7.73×10^{-3}	4.18	4.50×10^{-3}
49	120	0.865	1.679	0.414	0.864	0.479	0.515
93.5	200	0.845	1.640	0.88	0.184	0.104	0.112

* Data for castor oil from "Smithsonian Physical Tables," 8th ed., Smithsonian Institution, 1933. All other data from I.C.T., except for the white mineral oils. For these the density was furnished by the supplier, and the kinematic viscosity was measured at M.I.T.

The viscosity of a gas can be obtained from Sutherland's formula, as follows:

$$\mu = \mu_0 \frac{273 + C}{T + C} \left(\frac{T}{273} \right)^{\frac{3}{2}}$$

where μ_0 = viscosity at $T = 273\text{ }^{\circ}\text{C}$ abs

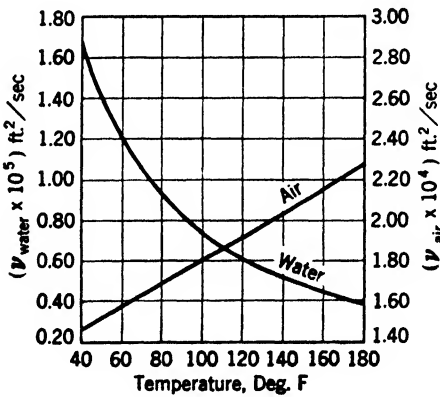
C = constant characteristic of the gas

Values of μ_0 and C for several gases are as follows:

	μ_0		C
	Dyne-sec/cm ²	Lb-sec/ft ²	
Air*.....	1.71×10^{-4}	3.57×10^{-7}	120
Carbon dioxide.....	1.42	2.97	240
Helium.....	1.89	3.95	80
Hydrogen.....	0.867	1.81	72
Nitrogen.....	1.66	3.47	110
Oxygen.....	1.89	3.97	131

* Data for air from I.C.T. All other data from "Smithsonian Physical Tables," 8th ed., Smithsonian Institution, 1933.

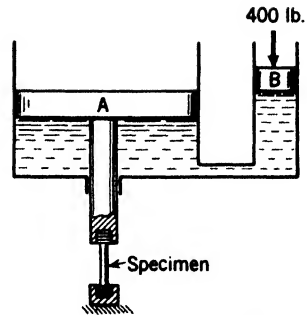
Plots of kinematic viscosity versus temperature are given below for air and water to facilitate computation of the Reynolds number.



PROBLEMS

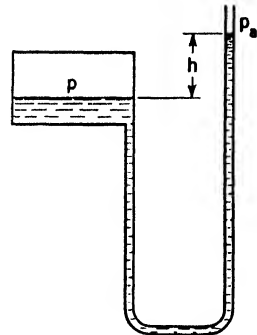
Chapter II

2.1. The motor for the hydraulic testing machine shown is capable of producing a thrust of 400 lb. It is desired to produce a stress of 150,000 lb per sq in. (based on initial area) in a standard tensile test specimen of 0.505-in. diameter. What must be the area ratio of the two pistons *A* and *B*?



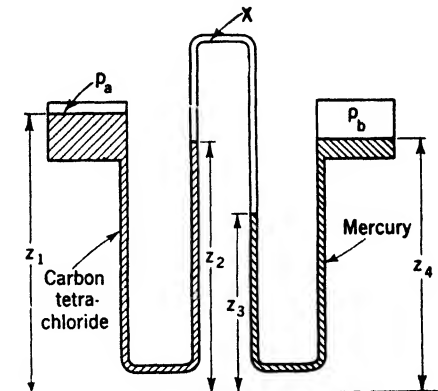
PROBLEM 2.1.

2.2. The gauge pressure $p - p_a$ at the liquid surface in the closed tank is 3.0 lb per sq in. Find h if the liquid in the tank is (a) water; (b) methyl alcohol; (c) mercury.



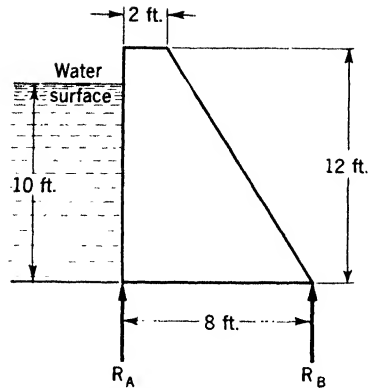
PROBLEM 2.2.

2.3. If the pressure difference between the two tanks is $p_a - p_b = 142$ lb/ft² and $z_1 = 36$ in., $z_2 = 30$ in., $z_3 = 26$ in., $z_4 = 29$ in., find the specific weight of fluid *X*.



PROBLEM 2.3.

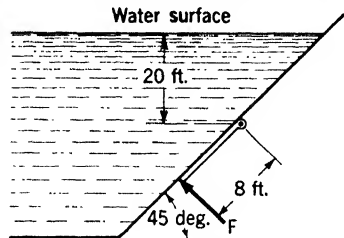
2.4. If the specific weight of concrete is 150 lb per cu ft, find the vertical reactions R_A and R_B for a unit length of the concrete dam.



PROBLEM 2.4.

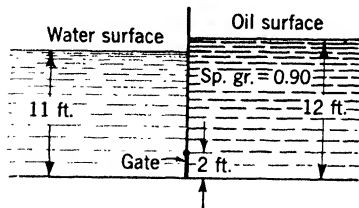
2.5. A gate 3 ft square in a vertical dam is exposed to the atmosphere on one side. It is located so far below the level of the water surface that the center of pressure is 1 in. below the center of gravity of the gate. How far is the top of the gate below the water surface?

2.6. A rectangular gate 4 by 8 ft, located in a slanting wall is held shut by a force F . If the gate weighs 500 lb, find F .



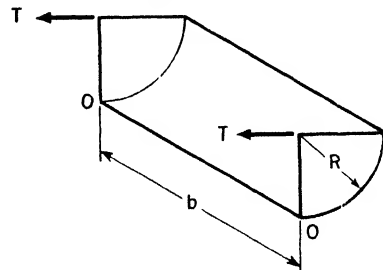
PROBLEM 2.6.

2.7. A rectangular gate 3 ft wide and 2 ft high is hinged at the top. Find the direction and magnitude of the moment tending to turn the gate about the hinge.



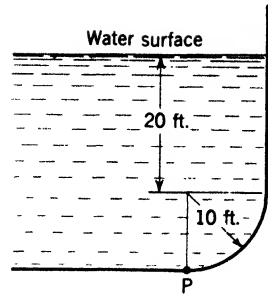
PROBLEM 2.7.

2.8. A container for liquid is made up of two hollow quarter cylinders hinged together along the edge OO and held by a strap at each end along the horizontal diameter. If the semicylindrical container is completely filled with liquid of density ρ , find the tension T in each strap.



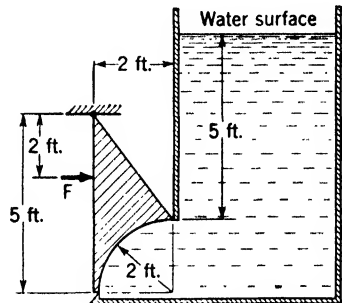
PROBLEM 2.8.

2.9. A dam is composed of a straight vertical section 20 ft high and a quadrant of 10-ft radius. Find the moment about P of the water forces on unit length of the dam.



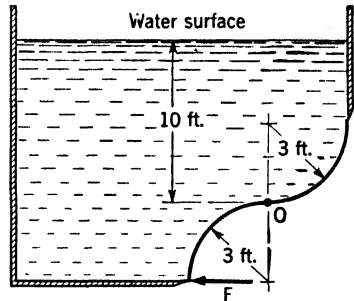
PROBLEM 2.9.

2.10. Find the force per unit length F required to keep the gate closed. Neglect bearing friction and weight of gate.



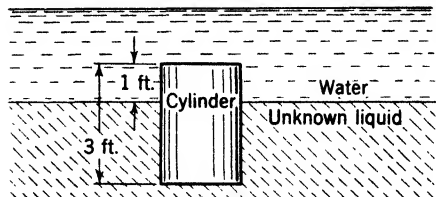
PROBLEM 2.10.

2.11. Determine the horizontal force per unit length F required to keep the S-shaped gate closed. Neglect friction in bearing O .



PROBLEM 2.11.

2.12. The specific gravity of the right circular cylinder shown is 0.9. (a) Find the specific gravity of the unknown fluid, assuming the system to be in equilibrium as shown. (b) Why is not this system in stable equilibrium? (c) When the system reaches equilibrium, where will the top of the cylinder be relative to the interface between liquids?



PROBLEM 2.12.

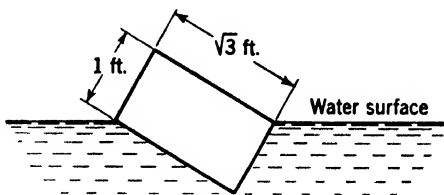
2.13. A rectangular body of specific gravity $\frac{2}{3}$ has length a , width b , and height c ($a > b > c$). Determine the maximum value of c for stable flotation in water.

2.14. A long prism (specific gravity s) the cross section of which is an equilateral triangle of side a is assumed to float in water with one side horizontal and submerged to a depth t . (a) Find t/a as a function of s . (b) Find the metacentric height for small angles of tilt if $s = \frac{3}{4}$.

2.15. A river barge of rectangular plan and cross section 60 ft long and 20 ft wide is loaded to a uniform depth of 4 ft with sand of specific weight 94 lb per cu ft. The unloaded barge weighs 50,000 lb, and its center of gravity is 2 ft above the center of its bottom. Find (a) the depth of immersion of the bottom of the barge; (b) the metacentric height for small angles; (c) the righting moment for a 1-deg angle of tilt.

2.16. A block 3 ft long, 2 ft wide, and $\frac{1}{3}$ ft high floats submerged half in water and half in oil of specific gravity 0.86. Find the specific gravity of the block and the metacentric height for small angles of tilt.

2.17. A rectangular block of specific gravity $\frac{1}{2}$ is 4 ft long and has the cross section shown. Find the righting moment when the block is tilted as indicated.



PROBLEM 2.17.

2.18. Find the pressure at an elevation of 9,000 ft if the lapse rate of the atmosphere is constant and equal to $\frac{1}{300}$ F per ft. The ground-level temperature is 60 F, and the barometer reading is 29.8 in. Hg. (The gas constant for air is 53.4 ft per deg F.)

2.19. The temperature of air at ground level $T_0 = 520$ F abs, the pressure $p_0 = 15$ lb/in.² abs (psia). The lapse rate of the troposphere $\lambda = \frac{1}{300}$ F/ft. The height of the troposphere is 7 miles. (a) Find the heights above ground level at which $p = p_0/2$ and $p = p_0/10$. (b) Find the temperature at each level asked for in part (a).

2.20. A balloon filled with hydrogen (gas constant = 767 ft/deg F) reaches a maximum height of 6 miles above the earth. The following are known:

W = weight of balloon, gondola, etc. (excluding gas), lb.	2,000
L_0 = initial lift force (or the tension in mooring cable), lb.	200
T_0 = ground-level temperature, deg F abs.	525
p_0 = ground-level pressure, psia.	15
λ = atmospheric lapse rate, deg F/ft.	$\frac{1}{300}$

Assuming that, at any elevation, the pressure and temperature of the hydrogen are the same as those of the surrounding air, find the volume of hydrogen in the balloon at take-off and at the maximum height.

2.21. A balloon 6 ft in diameter is filled with hydrogen at ground-level pressure and temperature and sealed. The weight of balloon and load is 4 lb. (a) Neglecting any

change in volume of the balloon and using the pertinent data of the preceding problem, find the maximum height reached by the balloon. (b) Assuming the temperatures of the hydrogen and air to be the same, find the difference between the internal and external pressures.

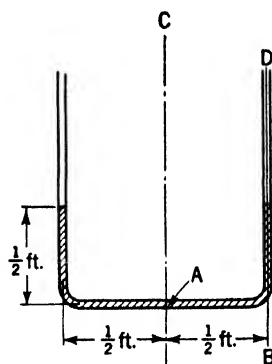
2.22. A tank containing water slides down an inclined plane under the action of gravity. The angle between the plane and the horizontal is α . Find the angle between the water surface and the horizontal (a) if the surface is frictionless; (b) if the coefficient of friction between tank and surface is μ .

2.23. An automobile manufacturer claims for his car an acceleration from 15 to 50 mph in 13 sec in high gear. If a glass U-tube with vertical legs 2 ft apart is partly filled with water and used as an accelerometer, what is the difference in level of the two legs for this constant acceleration? For an initial speed of 15 mph, how fast would the car be going at the end of 13 sec if the difference in level were $\frac{1}{2}$ in. larger? If it were $\frac{1}{2}$ in. smaller?

2.24. A vertical cylindrical tank 2 ft in diameter and 4 ft in height contains a water layer 2 ft deep and an oil layer 1 ft deep. The specific gravity of the oil is 0.86. (a) At what rotational speed will the oil just reach the rim of the tank? (b) What is then the pressure at the intersection of the wall and the bottom?

2.25. A vertical cylindrical tank 2 ft in diameter and 5 ft in height is half full of water. (a) Find the maximum speed with which it can be rotated without spilling any water. (b) If the same tank has a cover with a pinhole in the center, is completely filled with liquid of specific gravity 0.89, and is turned at 100 rpm, find the gauge pressure at the periphery of the top and bottom and at the center of the bottom.

2.26. A U-tube containing water rotates about the vertical axis CA . (a) If the atmospheric pressure is 14.7 psia, find the pressure at A for 100 rpm. (b) Assuming the vapor pressure to be zero and neglecting the volume of liquid vaporized, find the height of the liquid surface in the vertical legs at 950 rpm. (c) What are the levels in the legs if the tube rotates about axis BD at 200 rpm?

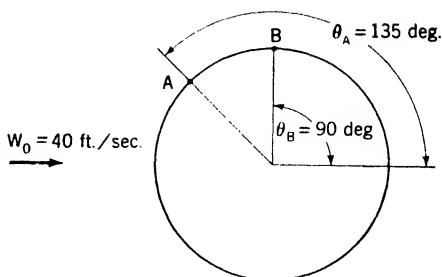


PROBLEM 2.26.

2.27. An open can 1 in. in diameter is filled with mercury to a depth of 10 in. and whirled at constant angular velocity at the end of a wire. The bottom of the can is outermost and describes a circle of 3-ft radius in a vertical plane. If the minimum tension in the wire during a revolution is equal to zero and the weight of the can is neglected, find (a) the angular velocity; (b) the location and magnitude of the minimum gauge pressure in the mercury.

Chapter III

3.1. The magnitude of the relative velocity at the surface of a cylinder in two-dimensional incompressible flow is given by $W = 2W_0 \sin \theta$, where W is tangent to the surface and W_0 is the velocity of the distant fluid. At points A and B construct the vector diagram of the relative and absolute velocities.



PROBLEM 3.1.

3.2. A pipe 10 in. in diameter carries an unsteady flow of incompressible liquid. The pipe terminates in a nozzle 6 in. in diameter. Find the velocity and acceleration of the parallel stream leaving the nozzle at the instant when the velocity and acceleration in the pipe are 12 ft per sec and 2 ft per sq sec.

3.3. A gas following the law $p = \text{constant } \rho T$ flows steadily in a horizontal pipe of constant cross-sectional area A . If the flow is isothermal and the ratio of the pressures at two sections is $p_2/p_1 = 3/4$, find the velocity ratio V_2/V_1 .

3.4. (a) Incompressible fluid flows radially outward in all directions from a point source. Assuming that the velocity depends only on r , the distance from the source, find V as a function of r . (b) Do the same for the axially symmetrical flow from a line source.

3.5. (a) A uniform parallel flow of velocity V_0 is superposed on the flow from a point source discharging at a rate Q . Where is the resultant velocity equal to zero? (b) Answer the same question if the parallel flow is superposed on a line source of strength Q .

3.6. Show that the rate of change of mass inside a control volume \mathcal{V} can be expressed as $\int_{\mathcal{V}} \frac{\partial \rho}{\partial t} d\mathcal{V}$.

3.7. Standing waves are set up in a compressible fluid contained in a rigid pipe of constant cross-sectional area A . The density is uniform over every cross section but varies with time t and distance along the pipe axis x , according to the law

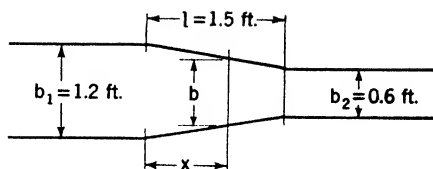
$$\rho = \rho_0 = (\rho_m - \rho_0) \sin \left(\frac{2\pi ct}{\lambda} \right) \sin \left(\frac{2\pi x}{\lambda} \right)$$

where ρ_0 is the average density, ρ_m is the maximum density, c is the velocity of wave propagation in the fluid, and λ is the wave length. Find the net rate of mass flow at any instant out of the length of pipe bounded by the planes $x = 0$ and $x = \lambda/4$.

Chapter IV

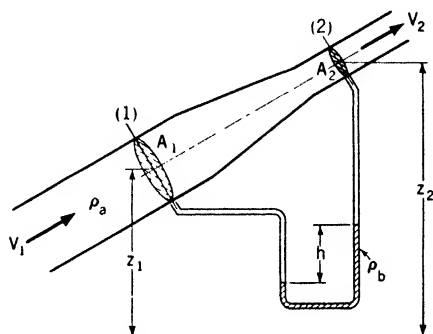
4.1. Water flows steadily at a rate of 0.6 cu ft per sec through a horizontal cone-shaped contraction the diameter of which decreases from 4.0 to 3.0 in. in a length of 1.2 ft. Assuming that conditions are uniform over any cross section find the rate of change of pressure in the direction of flow at the section 0.6 ft from the ends of the contraction.

4.2. A two-dimensional duct contains a straight-sided contraction. At a certain time the flow per unit width is 4.0 sq ft per sec and is increasing by 3.0 sq ft per sec². Assuming the velocity to be uniform over any cross section find the acceleration at the section $x = 0.75$ ft.



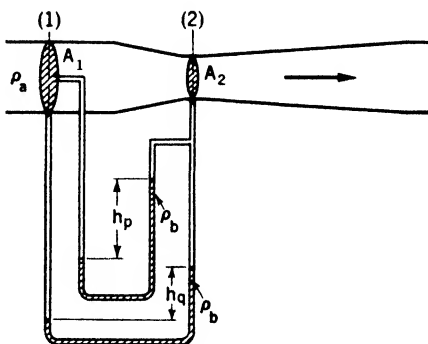
PROBLEM 4.2.

4.3. Find $p_1 - p_2$ and A_1/A_2 in terms of $z_1 - z_2$, h , ρ_a , ρ_b , and V_1 .



PROBLEM 4.3.

4.4. Air of density 2.38×10^{-3} slug per cu ft flows in the working section of a wind tunnel, in which the pressure is atmospheric. One leg of a U-tube containing alcohol of specific gravity 0.79 is attached to an impact tube inside the tunnel. The other leg of the U-tube is open to the atmosphere. Find the difference in the alcohol levels corresponding to a velocity of 90 mph in the working section.



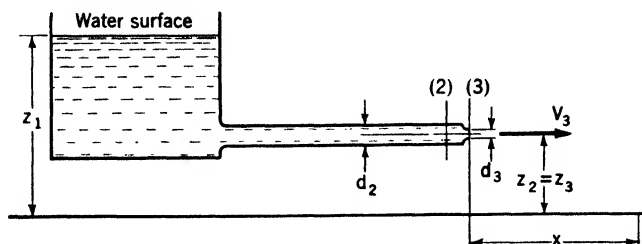
PROBLEM 4.5.

4.5. (a) Determine the ratio h_p/h_q .
(b) Repeat for a slanted pipe.

4.6. Water flows from a large open reservoir and discharges horizontally into the air, striking the ground a distance x from the nozzle.

$$\begin{array}{ll} z_1 = 30 \text{ ft} & d_2 = 5 \text{ in.} \\ z_2 = 20 \text{ ft} & d_3 = 3 \text{ in.} \end{array}$$

Neglecting friction, find (a) velocity V_3 at nozzle exit; (b) velocity V_2 and pressure p_2 in the pipe near the nozzle; (c) x (assuming parabolic path).

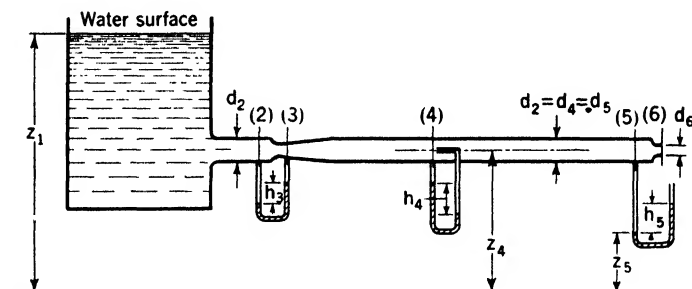


PROBLEM 4.6.

4.7. Water flows through the system shown.

$$\begin{aligned} z_1 &= 30 \text{ ft} & d_3 &= 3 \text{ in.} \\ z_5 &= 7 \text{ ft} & d_2 &= d_5 = 5 \text{ in.} \\ h_5 &= 1.6 \text{ ft} & d_6 &= 2.5 \text{ in.} \end{aligned}$$

The fluid in the manometers is mercury. Neglecting friction, find (a) discharge rate Q ; (b) h_3 ; (c) h_4 .

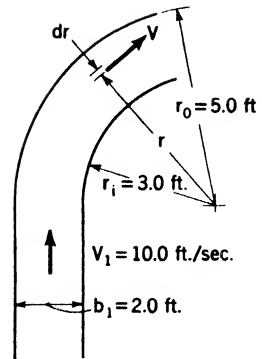


PROBLEM 4.7.

4.8. Air flows steadily from a 2-in.-diameter convergent nozzle in a large tank out into the atmosphere. The velocity in the tank far from the nozzle is negligible and the pressure there is 50 per cent greater than atmospheric pressure. The relation between pressure and density anywhere in the flow is $p/\rho^{1.4} = \text{constant}$. At the nozzle outlet, the pressure is atmospheric and equal to 14.7 psia, and the density is 2.4×10^{-3} slug per cu ft. Find the mass rate of flow through the nozzle.

4.9. Water in an open cylindrical tank 10 ft in diameter discharges into the atmosphere through a nozzle 2 in. in diameter. Neglecting friction and the unsteadiness of the flow, find the time required for the water in the tank to drop from a level 16 ft above the nozzle to the 8-ft level.

4.10. An irrotational two-dimensional flow leaves a straight duct and enters a bend of the same width. Assuming a velocity distribution in the bend like that in a potential vortex ($Vr = \text{constant}$), find the velocities at the inner and outer walls of the bend.



PROBLEM 4.10.

4.11. At a distance of 3 in. from the axis of a whirlpool the velocity is 13.1 ft per sec. At radii of 6 in. and 12 in. find the depression of the free surface below the level of the distant fluid.

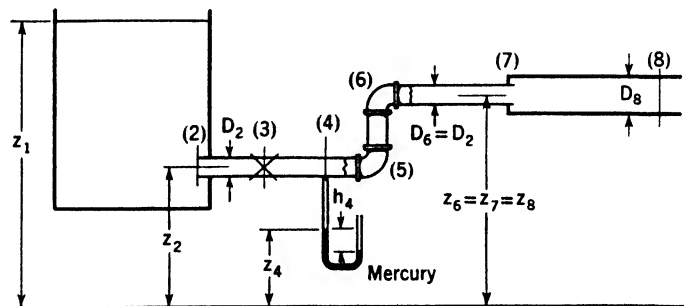
4.12. A paddle wheel 6 in. in diameter rotates at 200 rpm inside a closed circular concentric tank 2 ft in diameter completely filled with water. Assuming two-dimensional flow in a horizontal plane, considering the water inside the wheel to move as a forced vortex and that outside to move as a free vortex, find the difference in pressure between the rim of the tank and the center of the wheel.

Chapter V

5.1. Water flows through the system shown. Neglect all friction losses except those occurring at sections 2 (reentrant pipe), 3 (open globe valve), 5 and 6 (90° elbows), 7 (sudden enlargement). Each loss in head is expressed as $CV^2/2g$.

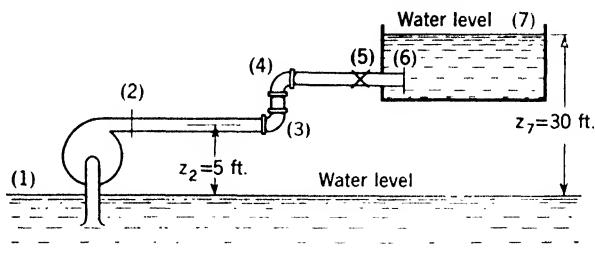
$z_1 = 20 \text{ ft}$	$D_2 = D_6 = 3 \text{ in.}$	$C_6 = 0.75$
$z_2 = 5 \text{ ft}$	$D_8 = 5 \text{ in.}$	$C_7 = 0.41$ (based on velocity
$z_4 = 2 \text{ ft}$	$C_2 = 1.0$	in 3-in. pipe)
$z_6 = 9 \text{ ft}$	$C_8 = 7.5$	$p_1 = p_8 = 15 \text{ psia}$
$h_4 = 0.8 \text{ ft}$		

Find V_8 and p_8 .



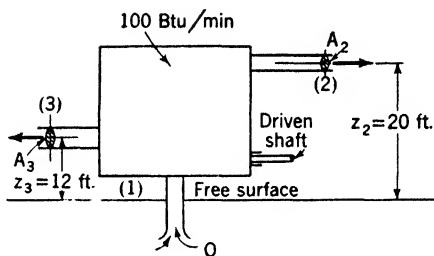
PROBLEM 5.1.

5.2. A pump discharges water at a constant rate of 0.80 cu ft per sec. The total length of pipe between 2 and 6 is $L = 600$ ft, and the uniform diameter $D = 3$ in. The loss due to friction in the straight pipe is given by $H_{l_{pipe}} = 0.02 (L/D)V^2/2g$, where V is the velocity in the pipe. The loss coefficients for the elbows and valve are the same as in the preceding problem, while the loss coefficient for the sudden enlargement at 6 is 1.0. (a) Find the gauge pressure at 2. (b) Neglecting losses in the inlet pipe and assuming a pump efficiency of 80 per cent, find the power input to the pump.



PROBLEM 5.2.

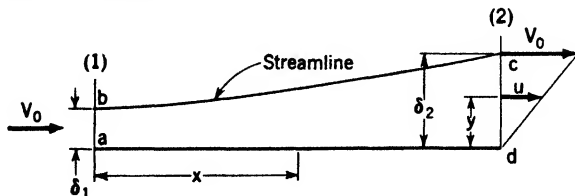
5.3. Frictionless incompressible fluid is pumped steadily at a rate of 0.8 cu ft per sec by the apparatus shown. The density of the fluid is 1.6 slug per cu ft. At section 2, the pressure is 10 lb per sq in. gauge (psig), the velocity is 9.5 ft per sec, and the area $A_2 = 0.04$ sq ft. At section 3, the pressure is 30 psig, and the area $A_3 = 0.03$ sq ft. If the heat transfer to the apparatus is 100 Btu per min (1 Btu = 778 ft-lb), find the power input at the shaft.



PROBLEM 5.3.

5.4. An axial-flow fan absorbing 0.54 hp discharges 5,000 cu ft per min of air having a specific weight of 0.0765 lb per cu ft. A water-filled manometer attached to the duct downstream from the fan shows that the static pressure at that point exceeds atmospheric by $\frac{1}{4}$ in. of water. If the air taken into the fan is drawn from a large room where the air is at rest at atmospheric pressure, find the loss upstream from the point where the manometer is attached. (Duct diameter = 2 ft.)

5.5. An incompressible fluid flows past one side of a flat plate, as shown. The velocity at the leading edge of the plate is uniform and equal to V_0 , while the x component u at the trailing edge is distributed linearly across the thickness δ_2 . Find the sum of the rates of heat transfer and intrinsic-energy transport out of the control surface $abcd$. The result is to be given in terms of ρ , V_0 , and δ_2 .



PROBLEM 5.5.

5.6. The efficiency of the hydraulic turbine η_T is defined as the ratio of the actual power output to that which would subsist if $H_{l_{BC}}$ were zero. The efficiency of the pump η_P is analogously defined in terms of $H_{l_{FG}}$.

$$\eta_P \eta_T = 0.85$$

$$Q_P = 0.354 \text{ ft}^3/\text{sec}$$

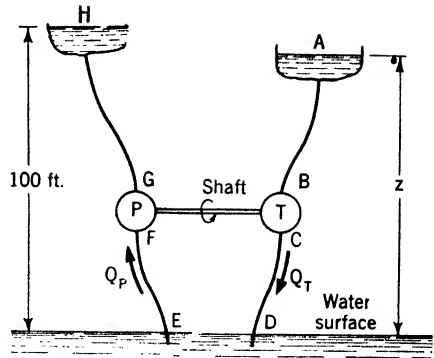
$$Q_T = 0.500 \text{ ft}^3/\text{sec}$$

$$H_{l_{AB}} = H_{l_{CD}} = H_{l_{EF}} = 5 \text{ ft}$$

$$H_{l_{FG}} = 9 \text{ ft}$$

$$H_{l_{GH}} = 3 \text{ ft}$$

Find (a) z ; (b) power output of turbine; (c) loss in the turbine, $H_{l_{BC}}$.



PROBLEM 5.6.

5.7. Water flows between the three reservoirs as shown.

$$Q_{AB} = 0.15 \text{ ft}^3/\text{sec}$$

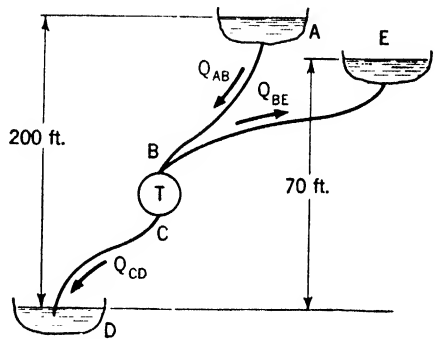
$$Q_{BE} = 0.05 \text{ ft}^3/\text{sec}$$

$$H_{l_{AB}} = 30 \text{ ft}$$

$$H_{l_{CB}} = 10 \text{ ft}$$

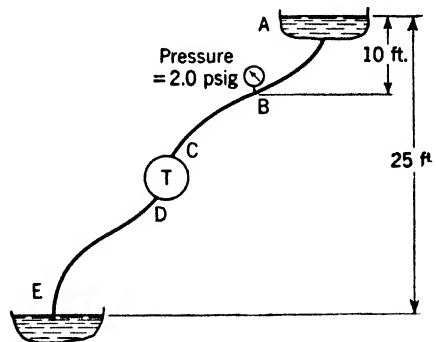
$$H_{l_{CD}} = 20 \text{ ft}$$

(a) Find $H_{l_{EB}}$. (b) What is the efficiency η_T of the turbine T ? (η_T is defined as in Prob. 5.6). (c) What is the power output of the turbine?



PROBLEM 5.7.

5.8. For the turbine installation shown $H_{l_{AB}} = H_{l_{BC}} = H_{l_{ED}} = 2 \text{ ft}$, $H_{l_{DC}} = 4 \text{ ft}$. Find (a) velocity at B; (b) power output of turbine; (c) efficiency of turbine η_T , defined as in Prob. 5.6 (all pipe 2-in. diameter).

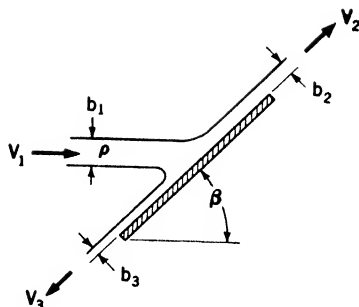


PROBLEM 5.8.

5.9. Consider the machine in Prob. 5.8 to be a pump with all losses the same and the same reading on the pressure gauge as there given. If water is pumped from E to A, find (a) velocity at B; (b) power input to pump; (c) efficiency of pump.

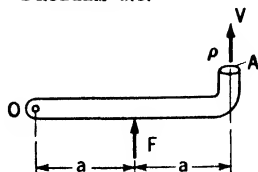
Chapter VI

6.1. A two-dimensional jet of incompressible fluid strikes a plane surface. Neglecting friction and gravity, find V_2 , V_3 , b_2 , and b_3 in terms of ρ , V_1 , b_1 , and β . Find also the direction and magnitude of the force per unit length needed to hold the plate stationary.



PROBLEM 6.1.

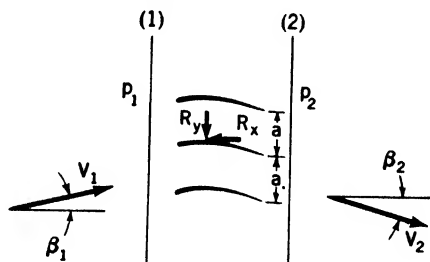
6.2. Find the force F needed to prevent rotation of this pipe about the vertical axis O .



PROBLEM 6.2.

6.3. A locomotive pulls a tender at a constant velocity $V = 59$ ft/sec. The combined wind and wheel resistance is $D = 400$ lb. Water is being scooped up at a constant rate $Q = 10$ ft³/sec from a trough between the tracks. (a) Find the pull F exerted by the locomotive on the tender. (b) Find the horsepower developed by the locomotive.

6.4. Incompressible fluid flows steadily through a two-dimensional series of fixed vanes, a few of which are shown. The velocity and pressure are constant all along sections 1 and 2. Find the reactions per unit length R_x and R_y necessary to keep one vane in its fixed position. Neglect gravity and friction.



PROBLEM 6.4.

6.5. Find R_x and R_y for the preceding problem if a loss $H_{l,2}$ occurs between sections 1 and 2.

6.6. Water flows steadily through the horizontal pipe bend shown.

$$A_1 = 0.1 \text{ sq ft} \quad \beta = 45^\circ$$

$$A_2 = 0.2 \text{ sq ft}$$

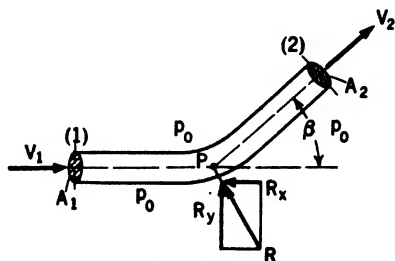
$$V_1 = 20 \text{ ft/sec}$$

$$p_1 = 20 \text{ lb/in.}^2 \text{ abs}$$

$$p_0 = 15 \text{ lb/in.}^2 \text{ abs}$$

$$H_{l,1} = 6.0 \text{ ft-lb/lb}$$

(a) Find R_x and R_y . (b) Show that, if no external moment is exerted on the pipe, R must act through P , the intersection of the lines of V_1 and V_2 .



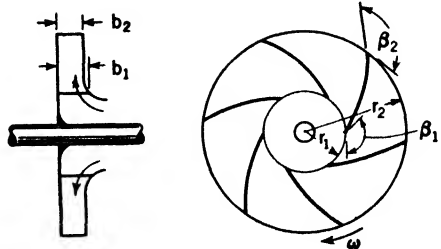
PROBLEM 6.6.

6.7. Ideal incompressible fluid of density $\rho = 1.94$ slugs/ft³ flows steadily with respect to axes rotating in a horizontal plane at a constant rate $N = 200$ rpm. The relative velocities at two points on the same relative streamline are $W_1 = 20$ ft/sec and $W_2 = 15$ ft/sec, the flow going from 1 to 2. The normal distances from the axis of rotation are $r_1 = 1.6$ ft and $r_2 = 1.0$ ft. If the two points are at the same elevation, find $p_1 - p_2$.

6.8. Repeat the preceding problem if a loss of energy $H_{1,2} = 2.50$ ft-lb/lb occurs between points 1 and 2.

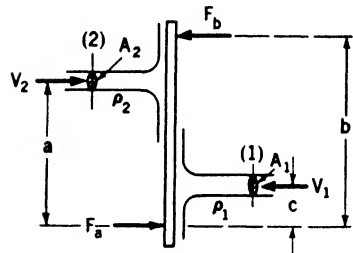
6.9. Water flows through the impeller of a centrifugal pump as shown. Find the torque exerted on the impeller and the power required to drive it. The absolute velocity of the water at the entrance has no tangential component.

$$\begin{aligned} Q &= 2 \text{ ft}^3/\text{sec} \\ \omega &= 100 \text{ radians/sec} \\ r_1 &= 2 \text{ in.} \\ r_2 &= 6 \text{ in.} \\ b_2 &= \frac{1}{2} \text{ in.} \\ \beta_2 &= 120 \text{ deg} \end{aligned}$$



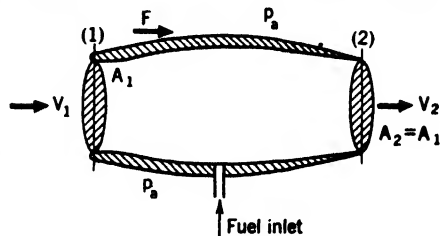
PROBLEM 6.9.

6.10. Two horizontal fluid jets strike a flat plate, which is held in equilibrium by forces whose horizontal components are F_a and F_b . Find F_b and b in terms of ρ_1 , ρ_2 , A_1 , A_2 , V_1 , V_2 , a , c , and F_a .



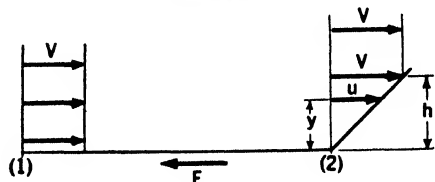
PROBLEM 6.10.

6.11. Gasoline is burned in this thrust augmentor at one-thirtieth the mass rate of air inflow at 1. The density and velocity of the air far in front of the augmentor are 2.4×10^{-3} slug per cu ft and 200 ft per sec. $A_1 = 1.5$ sq ft. The mean density of the combustion products at 2 is 0.86×10^{-3} slug per cu ft. Assuming $p_1 = p_2 = p_a$ and neglecting friction upstream from 1, find the external force F on the augmentor.



PROBLEM 6.11.

6.12. Water flows past one side of a flat plate. The velocity is uniform at the leading edge and parallel to the plate, while at the trailing edge the parallel component varies linearly with y , $u = ky$ for $y \leq h$. For $y > h$, $u = V$. Assuming steady two-dimensional flow, find F , the parallel component of the supporting force per unit width.

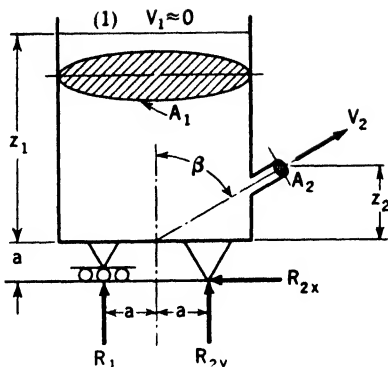


PROBLEM 6.12.

6.13. Water flows from the nozzle in this tank.

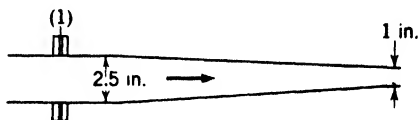
$$\begin{aligned} A_1 &= 1.0 \text{ sq ft} & z_1 &= 5.0 \text{ ft} \\ A_2 &= 0.02 \text{ sq ft} & z_2 &= 0.5 \text{ ft} \\ a &= \frac{1}{3} \text{ ft} & \beta &= 60 \text{ deg} \end{aligned}$$

Neglecting friction and the weight of the tank (but not that of the water), find the supporting forces R_1 , R_{2x} , and R_{2y} .



PROBLEM 6.13.

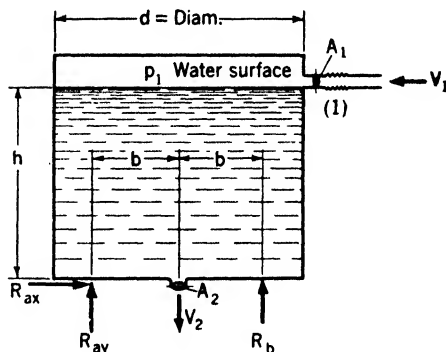
6.14. Neglecting friction, compute the axial force produced at flange 1 when water is discharged from this nozzle at 100 gpm.



PROBLEM 6.14.

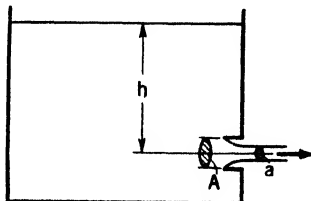
6.15. Water flows steadily through this closed tank. No force is transmitted by the flexible union at 1. Neglecting friction, find the rate of flow and R_{ax} , R_{ay} , and R_b , if

$$\begin{aligned} A_1 &= 0.03 \text{ sq ft} & b &= \frac{2}{3} \text{ ft} \\ A_2 &= 0.04 \text{ sq ft} & d &= 2 \text{ ft} \\ h &= 2 \text{ ft} & p_1 - p_a &= 10 \text{ lb/in.}^2 \end{aligned}$$



PROBLEM 6.15.

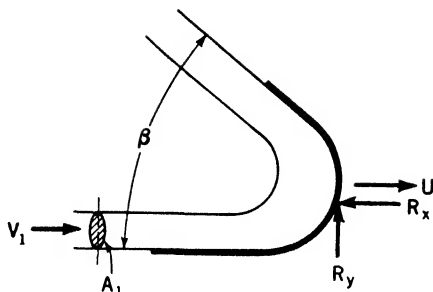
6.16. Liquid flows steadily out of the reentrant (Borda) nozzle in the wall of this tank. Neglecting friction, find the ratio of the jet area to the nozzle area a/A (contraction coefficient).



PROBLEM 6.16.

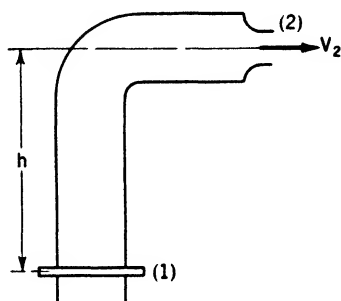
6.17. Water having a constant velocity V_1 strikes a vane moving with constant velocity U in the same direction. Neglecting friction and gravity, find R_x and R_y , the external forces on the vane, and the power output if

$$\begin{aligned} V_1 &= 40 \text{ ft/sec} & U &= 30 \text{ ft/sec} \\ A_1 &= \pi/144 \text{ sq ft} & \beta &= 20 \text{ deg} \end{aligned}$$



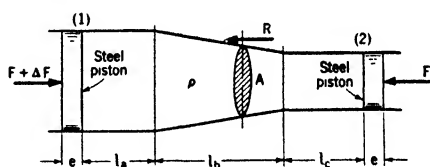
PROBLEM 6.17.

6.18. Water flows through the bend and discharges into the atmosphere at 2. Neglecting friction and gravity, find the supporting force and moment transmitted to the bend at the flange 1 if $Q = 10 \text{ ft}^3/\text{sec}$, $A_2 = 0.10 \text{ sq ft}$, $A_1 = 0.25 \text{ sq ft}$, $h = 5 \text{ ft}$.



PROBLEM 6.18.

6.19. A piston at 2 is at rest at time $t = 0$ and is accelerated toward the right by the pressure of the fluid in the cylinder. It is required that F be constant at all times. (a) Find ΔF at time $t = 1 \text{ sec}$, assuming that friction and compressibility are negligible and that the x component of velocity is uniform over any area normal to the x direction, such as A . ΔF is to be expressed in terms of



PROBLEM 6.19.

$$\begin{aligned} \text{Fluid density, } \rho &= 1.6 \text{ slugs/ft}^3 & F &= 100 \text{ lb} \\ \text{Steel density, } \rho_s &= 15 \text{ slugs/ft}^3 & \frac{dV_2}{dt} &= 10 \text{ ft/sec}^2 \\ \text{Area of piston 1, } A_1 &= 0.03 \text{ sq ft} & l_a(0) &= 2 \text{ ft}, l_b = 1 \text{ ft} \\ \text{Area of piston 2, } A_2 &= 0.01 \text{ sq ft} & l_c(0) &= 2 \text{ ft}, e = 1 \text{ in.} \end{aligned}$$

(b) Find the external supporting force R needed to hold the cylinder stationary.
(c) Compare the values for ΔF and R with those obtained for steady flow, assuming $V_2 = 10 \text{ ft/sec}$.

6.20. Air flows steadily at a rate of 1.082 slugs per sec with an upward component in a pipe 4 in. in diameter tilted at an angle of 30° to the horizontal. At section 1, the pressure is 100 psia and the density is 0.0155 slug per cu ft. At section 2, 50 ft downstream, the pressure is 98 psia, and the density is 0.0152 slug per cu ft. Assuming the average density of the air between 1 and 2 to be the arithmetic mean of ρ_1 and ρ_2 , find the friction force exerted by the air on the wall of the 50-ft length of pipe.

Chapter VII

By means of dimensional analysis simplify Probs. 7.1–7.5.

7.1. The period of a pendulum T is assumed to depend only on the mass m , the length l , the acceleration of gravity g , and the angle of swing θ .

7.2. The velocity of propagation V of surface waves on shallow liquid is assumed to depend only on the depth of the liquid h , the density ρ , and the acceleration of gravity g .

7.3. A mass m is mounted on a massless spring of spring constant k and subjected to a damping force proportional to the velocity. The damping constant is C . If the mass vibrates steadily under the action of a periodic force of amplitude F_0 and frequency f , the maximum displacement x_0 is assumed to depend only on m , k , C , f , and F_0 .

7.4. The velocity of sound propagation C in a liquid is assumed to depend only on the density ρ , the viscosity μ , and the bulk compression modulus β [see Eq. (2.11)].

7.5. The thrust T of a propeller is assumed to depend only on the diameter D , the fluid density ρ , the viscosity μ , the revolutions per unit time n , and the velocity of advance relative to the distant fluid V .

7.6. A ship 340 ft long moves in fresh water at 60 F at 30 mph. Find the kinematic viscosity of a fluid suitable for use with a model 12 ft long, if dynamical similarity is to be attained.

7.7. (a) The height h to which a liquid will rise in a small-bore tube owing to surface forces (the capillary rise) is a function of the specific weight of the liquid γ , the radius of the tube r , and the surface tension of the liquid σ . By dimensional analysis, find an expression for h involving nondimensional variables only. (b) If the capillary rise for liquid A is 1 in. in a tube of radius 0.010 in., what will be the rise for a liquid B having the same surface tension but four times the density of A in a tube of radius 0.005 in.?

7.8. A test on a 12-in.-diameter model ship propeller indicates 50 per cent increase in the relative water speed behind the screw when the towing speed is 10 ft per sec and the rotational speed is 1,000 rpm. (a) Estimate the corresponding thrust on the model propeller shaft. (b) If the prototype propeller is to operate at 200 rpm at a forward speed of 25 ft per sec, what will be the thrust on the prototype shaft when operating at the same efficiency as the model? The fluid (water) has the same density for model and prototype.

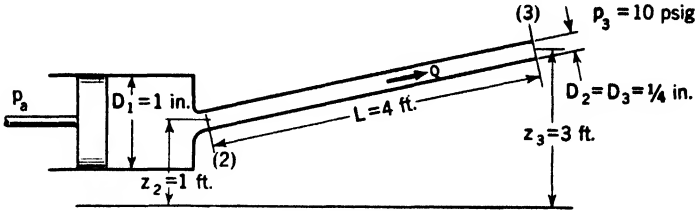
Chapter VIII

8.1. Oil of kinematic viscosity $\nu = 4 \times 10^{-4}$ ft²/sec at room temperature flows through an inclined tube of $\frac{1}{2}$ in. diameter. Find the angle α between the tube and the horizontal plane if the pressure inside the tube is constant along its length and the delivered quantity of oil $Q = 5$ ft³/hr. The flow is laminar.

8.2. Find the quantity Q , the mean velocity V , and the maximum velocity V_{max} of an oil of kinematic viscosity $\nu = 14 \times 10^{-3}$ ft²/sec at room temperature flowing through an inclined tube of 1 in. diameter when the lost head per unit of length $H_f/l = \frac{1}{2}$. The flow is laminar.

8.3. A positive-displacement pump forces oil at a constant rate $Q = 425$ in.³/min through a copper tube, as shown, and into a bearing. The pressure p_s where the oil enters the bearing is required to be 10 psig. The oil properties are $\rho = 1.6$ slugs/ft³ and

$\nu = 5.0 \times 10^{-4} \text{ ft}^2/\text{sec}$. The velocity is constant across the cylinder diameter (section 1) and across the tube diameter at entrance (section 2). Effects of friction between 1 and 2 are neglected. (a) Show that the flow in the tube is laminar. (b) Find the power output of the pump. (c) Find the percentage error in power for each of the following cases: (1) The difference in levels $z_3 - z_2$ is neglected. (2) The correction for development of the laminar flow pattern between 2 and 3 is neglected.



PROBLEM 8.3.

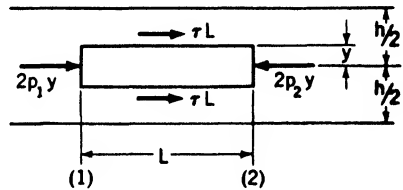
8.4. A steady laminar two-dimensional flow takes place between parallel fixed plates. (a) Assuming the velocity to be parallel to the plates, the pressure to be independent of y , and that

$$\tau = \mu \partial u / \partial y, \text{ show that}$$

$$u = \frac{p_1 - p_2}{2\mu L} \left(\frac{h^2}{4} - y^2 \right)$$

(b) Show that the volume flow per unit depth is

$$Q = \frac{h^3(p_1 - p_2)}{12\mu L}$$



PROBLEM 8.4.

8.5. A horizontal crack 0.01 in. wide and 10 in. long extends completely through a wall that is 10 in. thick. Water at 70 F stands on one side of the wall; the other side is open to the atmosphere. If the water surface is 10 in. above the crack, estimate the leakage rate through the crack.

8.6. Find Reynolds number for water at 50 F flowing (a) in a capillary tube of $\frac{1}{4}$ in. diameter with a velocity of 4 in. per sec; (b) in a pipe of 8 in. diameter with a velocity of 3 ft per sec; (c) in a pipe of 5 ft diameter with a velocity of 6 ft per sec.

8.7. What is the velocity for each of the three cases of the preceding problem when the flow changes from turbulent to laminar?

8.8. In order to obtain the same friction factor for water of 60 F flowing through a certain pipe and for air at the same temperature and at atmospheric pressure flowing through the same pipe, what must be the ratio of the volume rates of discharge?

8.9. Water flows steadily through a smooth circular pipe lying horizontally. The discharge rate is 1.5 cu ft per sec; the pipe diameter is 6 in. Find the difference in pressure between two points on the pipe separated a distance of 400 ft if the water temperature is 60 F.

8.10. Repeat the preceding problem assuming that the pipe is tilted upward in the direction of flow at an angle of 10 deg with the horizontal.

8.11. A new steel pipe 4 in. in diameter and 100 ft in length is attached to a large reservoir. The pipe slopes downward at an angle of 15 deg to its free end, which is 50 ft below the water level in the reservoir. Neglecting all losses except those due to

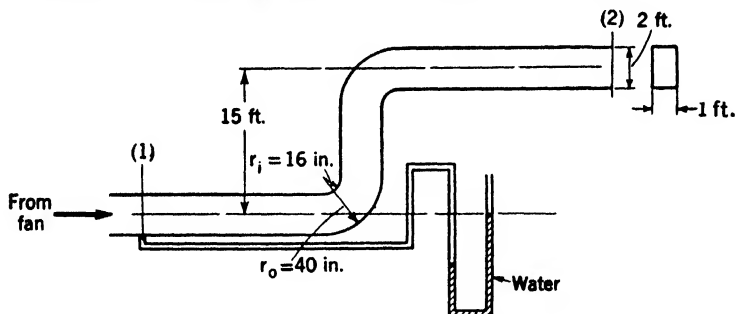
pipe friction, find the rate of discharge. The water temperature is 50 F. A trial-and-error method must be used.

8.12. A fan is required for delivering 100 cu ft per sec of air at the upper end of a vertical smooth-walled duct 18 in. in diameter and 40 ft in length. Neglecting all losses except those due to pipe friction in the duct and assuming the fan to be located in a room in which the air is at atmospheric pressure, find the necessary power input to the fan. The air temperature is 80 F. What error is made if variation of atmospheric pressure with height is neglected?

8.13. Two pipe lines are connected to a large water reservoir and have free discharge at the outlet ends. One is 6 in. in diameter and 1,000 ft in length, with outlet 12.5 ft below the reservoir water level. The other is 8 in. in diameter and 2,000 ft in length. The combined discharge rate is 2.00 cu ft per sec. Assuming that $f = 0.018$ for each pipe and neglecting entrance losses, find how far the end of the 8-in. pipe is below the water level in the reservoir.

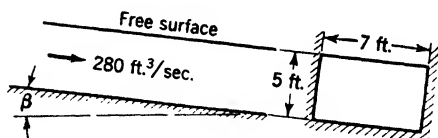
8.14. Solve the preceding problem if the 8-in. pipe is terminated by an open-gate valve and contains three standard 90-deg elbows, while the 6-in. pipe terminates in an open globe valve. The over-all discharge rate is assumed to be the same.

8.15. A smooth rectangular duct, 12 by 24 in. in cross section and 150 ft long, contains two 90-deg bends with a 16-in. inside radius. The free end of the duct is 15 ft higher than the inlet end. Find the reading (inches of water) of the water-filled U-tube, attached as shown, if the discharge rate is 75 cu ft per sec of air at 85 F.



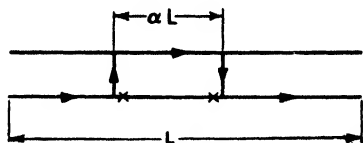
PROBLEM 8.15.

8.16. Water flows uniformly through the rectangular open channel, as shown. The channel is made of finished concrete, for which the friction factor $f = 0.0217$. Find angle of slope β .



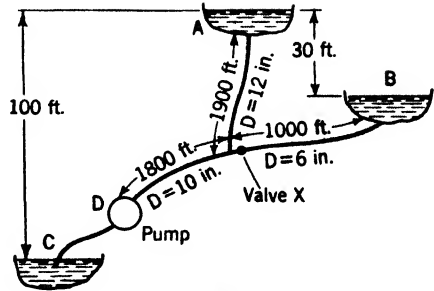
PROBLEM 8.16.

8.17. Two identical parallel pipes leave a reservoir at a distance H below the water surface. Each pipe has length L , diameter D , and friction factor f . Two cross connections are located a distance αL apart. The length αL of one pipe lying between the connections is closed, the flow being as shown in the figure. Find the percentage decrease in discharge if $D = 6$ in., $f = 0.020$, $L = 2,000$ ft, $\alpha = \frac{1}{4}$. Neglect all minor losses and losses in branches.



PROBLEM 8.17.

8.18. Water at 72 F is pumped through cast-iron pipes to reservoirs *A* and *B*. The discharge at the pump is 3 cu ft per sec, while 0.8 cu ft per sec flows into *B*. Neglect friction loss in the intake pipe *CD* and other minor losses. (a) Find the head imparted to the water by the pump. (b) Find the head lost at valve *X*.

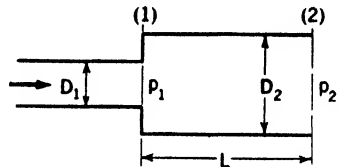


PROBLEM 8.18.

8.19. A straight 10-in. pipe 2 miles long runs between two reservoirs of surface elevations 450 ft and 200 ft. A parallel 12-in. line 1 mile long is laid from the mid-point of the 10-in. line to the lower reservoir. Neglecting all minor losses and assuming a friction factor of 0.02 in both pipes, find the increase in discharge rate caused by the addition of the 12-in. pipe.

8.20. An 18-in. pipe divides into 8- and 6-in. branches, which rejoin. If the 6-in. branch is 5,000 ft long, how long must be the 8-in. branch for the flow to divide equally when 5 cu ft per sec flow in the 18-in. pipe? The 8-in. branch is cast iron, and the 6-in. branch is smooth. The water temperature is 65 F.

8.21. The pressure p_2 at a distance L downstream from a sudden enlargement is equal to p_1 , the pressure at the enlargement. Assuming $D_2 = \sqrt{2}D_1$ and a friction factor of 0.02, find L/D_2 .

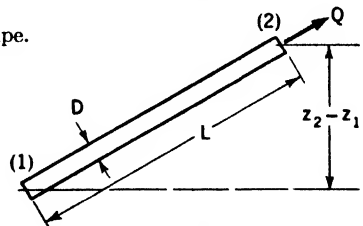


PROBLEM 8.21.

8.22. Ethanol at 65 F flows in this cast-iron pipe.

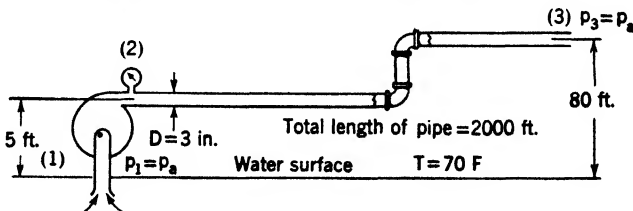
$$\begin{aligned} p_1 - p_2 &= 3,500 \text{ lb/ft}^2 \\ z_2 - z_1 &= 30 \text{ ft} \\ L &= 150 \text{ ft} \\ D &= 3 \text{ in.} \end{aligned}$$

Find Q .



PROBLEM 8.22.

8.23. A gauge at 2 reads 78 lb per sq in. The measured torque on the pump shaft is 32.8 ft-lb, and the speed is 1,625 rpm. The discharge pipe is smooth and contains two 90-deg elbows. Neglecting loss in the short entrance pipe, find the pump efficiency.



PROBLEM 8.23.

8.24. A pump that is capable of delivering any desired volume of water at 60 psig is connected by a horizontal 2-in. steel pipe 1,000 ft long to a machine requiring water at 20 psig. What is the maximum volume that can be delivered at 65 F?

8.25. An oil having a kinematic viscosity of 60 Saybolt universal seconds and a specific gravity of 0.86 flows through a 3-in. standard orifice in a 5-in. pipe. If the pressure drop across the orifice is 40 lb per sq in., find the rate of discharge.

8.26. Two horizontal pipes of equal length carry air and water, respectively, at 60 F at velocities such that the Reynolds numbers and pressure drops for each are the same. Find the ratio of the mean air velocity to that of the water.

8.27. Water flows in turbulent fashion through a smooth pipe of diameter D and a square pipe of area D^2 . In which pipe will the pressure drop per unit length be greater if the discharge rates are the same? Explain.

Chapter IX

9.1. Air leaves a reservoir in which the pressure and density are p_0 and ρ_0 and expands isentropically through a convergent-divergent nozzle. The exit velocity V_3 is 1.70 times as great as the sound velocity in the reservoir. Find the ratio of the exit diameter to that at the throat d_3/d_t , p_3/p_0 , and ρ_3/ρ_0 .

9.2. Suppose that a transverse shock occurs in the nozzle of the preceding problem at a section 2 where $d_2/d_t = \sqrt{2}$. (a) Find V_1/C_0 and V_2/C_0 , where V_1 and V_2 are the velocities immediately above and below the shock and C_0 is the sound velocity in the reservoir. (b) Find V_3/V_2 , ρ_3/ρ_0 , and p_3/p_0 , where subscript 3 refers to the nozzle exit.

9.3. Derive Eq. (9.21).

9.4. Air leaves a reservoir in which the pressure and density are p_0 and ρ_0 and expands isothermally through a convergent-divergent nozzle. The exit velocity $V_3 = 1.70\sqrt{p_0/\rho_0}$. (a) Find p_t/p_0 , the ratio of the throat pressure to that in the reservoir. (b) Find d_3/d_t , the ratio of exit to throat diameter. (c) Find d_s/d_t , where d_s is the diameter where the local sound velocity occurs.

9.5. (a) If the friction factor f is assumed to be constant in an isothermal flow of gas through a horizontal tube, show that

$$\frac{fl}{d} = \frac{2}{G} \left[\frac{p_1^2}{2GgRT_1} \left(1 - \frac{p_2^2}{p_1^2} \right) - \ln \frac{p_1}{p_2} \right]$$

where d and l are the diameter and length of the tube, G is the mass rate of flow per unit area, and subscripts 1 and 2 refer to the upstream and downstream ends of the tube, respectively. (b) If the critical velocity is reached in the tube, show that the above expression reduces to

$$\frac{fl}{d} = \frac{p_1^2}{p_2^2} - 1 + \frac{2\sqrt{gRT_1}}{p_1} \ln \frac{p_1}{p_2}$$

9.6. (a) For an isothermal flow of air through a horizontal smooth pipe 0.1 ft in diameter, $T_1 = 540$ F abs, $p_1 = 30$ lb/in.², and $p_2/p_1 = 0.5$. The critical velocity is reached in this flow. Assuming the relation between friction factor and Reynolds number to be the same as for incompressible flow, find the length of the pipe. (b) Using the arithmetic mean of the initial and final velocities, estimate the time required for a sound wave to be propagated from the downstream to the upstream end of the pipe, and vice versa.

9.7. What would be the maximum length of the pipe of the preceding problem if the mass flow per unit area were 1.5 times larger and p_1 and T_1 were unchanged?

9.8. For an isothermal flow of air through a horizontal smooth pipe 0.1 ft in diameter, $T_1 = 700$ F abs, $p_1 = 1.0$ lb/in.² abs, and $p_2/p_1 = 1.1$. Assuming the critical velocity to be reached in this pipe and that subcritical speeds do not occur in it, find the length of the pipe.

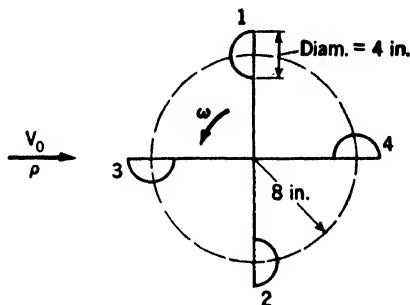
Chapter X

10.1. Find the terminal velocity of a steel sphere of specific weight $\gamma_s = 0.28$ lb/in.³ and 0.0175 in. diameter, falling freely in oil of specific weight $\gamma_o = 0.032$ lb/in.³ and viscosity $\mu = 7.0 \times 10^{-6}$ lb-sec/in.²

10.2. A solid spherical particle of radius a and density ρ_s is whirled in a horizontal circular path of radius r with a tangential velocity V_t by means of an inwardly spiraling flow of air of density ρ and viscosity μ . Assuming that Stokes's law applies, find the inward radial component of air velocity V_r . Assume that $\rho_s = 6.0$ slugs/ft³, $a = 8.0 \times 10^{-6}$ ft, $V_t = 150$ ft/sec, $\mu = 3.6 \times 10^{-7}$ lb-sec/ft², $r = \frac{3}{4}$ ft.

10.3. A disk 6 in. in diameter is set normal to the velocity of an air stream. The measured drag of the plate is 0.89 lb when the air velocity is 60 ft per sec and the air temperature is 80 F. Find the drag of a disk 15 in. in diameter similarly arranged in a flow of water having a velocity of 15 ft per sec and a temperature of 50 F.

10.4. Find the steady-state angular velocity ω of the four-cup anemometer. Consider only the position shown, that is, arm 1-2 normal to V_0 and arm 3-4 parallel to V_0 . Neglect any torque exerted by cups 3 and 4. $V_0 = 60$ ft/sec, $\rho = 2.4 \times 10^{-3}$ slug/ft³.



PROBLEM 10.4.

10.5. A rising spherical weather balloon 6 ft in diameter is filled with hydrogen of specific weight 0.00416 lb per cu ft. The specific weight of the surrounding air at that level is 0.0600 lb per cu ft. If the combined weight of the rubber envelope plus instruments is 6 lb, find the rising velocity V . (Temperature = 500 F abs.)

10.6. A sphere 8 in. in diameter is found to have a drag of 1.80 lb in air at 80 F having a relative velocity of 150 ft per sec. (a) Find the velocity at which the drag of a 2-ft sphere immersed in water at 50 F can be determined from the above data. (b) What is the drag of the 2-ft sphere for the velocity found in a?

10.7. If the vertical component of the landing velocity of a parachute is equal to that acquired during a free fall of 6 ft, find the diameter of the open parachute (hollow hemisphere), assuming the total weight to be 250 lb and an air density of 2.4×10^{-3} slug per cu ft.

10.8. A rectangular billboard 10 ft high by 50 ft long is erected on an open scaffold some distance above the earth's surface. A 100-mph gale strikes the board normally. If the air density is 2.4×10^{-3} slug per cu ft, find the total force due to wind pressure.

10.9. A bracing wire $\frac{1}{20}$ in. in diameter is found to vibrate at 930 cps when the speed of the airplane is 60 mph. If the natural frequency of the strut is 500 cps, at what speed is the amplitude of vibration likely to become dangerously large?

10.10. A flat plate 2 ft long is set parallel to a flow of air at a temperature of 70 F. The velocity of the air far from the plate is 40 ft per sec. (a) Find the maximum thickness of the boundary layer. (b) Find the over-all drag coefficient. (c) Find the total drag per unit width of the plate if the air covers both sides.

10.11. Repeat the preceding problem if the plate is immersed in water at 60 F, assuming the Reynolds number to be unchanged.

10.12. A flat plate 10 ft long is immersed in water at 60 F, flowing parallel to the plate with a velocity of 20 ft per sec. Neglect the laminar part of the boundary layer. (a) Find the approximate boundary-layer thickness at $x = 5$ ft and $x = 10$ ft, where x is measured from the leading edge. (b) Find the over-all drag coefficient. (c) Find the total drag per unit width of the plate if the water covers both sides.

10.13. A flat plate 4 ft long is immersed in air at 70 F flowing parallel to the plate at a speed of 50 ft per sec. Assume the critical Reynolds number is 5×10^5 . (a) At what distance from the leading edge does transition occur? (b) Plot the local drag coefficient $2\tau_0/\rho V^2$ as a function of Vx/ν . (c) Find the total drag per unit width of the plate.

10.14. Find the ratio of the friction drags of the front and rear halves of a plate of total length l if the boundary layer is completely turbulent and follows the one-seventh-power law of velocity distribution.

10.15. A ship 160 ft long requires 200 hp to overcome the resistance to motion at 20 ft per sec. Find the friction and residual drags if the wetted area is 4,000 sq ft. Assume $\rho = 1.94$ slugs/ft³ and $\nu = 1.2 \times 10^{-5}$ ft²/sec.

10.16. A model vessel having a submerged surface area of 8.0 sq ft and length 7.0 ft has a total drag of 0.95 lb when towed at a velocity of 5.14 ft per sec. Assume the friction drag of the submerged part of the hull to follow the same law as a flat plate of the same length, set parallel to the velocity, and covered with a completely turbulent boundary layer. The density and kinematic viscosity of the water are the same as in the preceding problem. (a) Find the friction drag of the model hull. (b) Find the total drag of a geometrically similar hull 25 times as long as the model when moving at corresponding speed.

Chapter XI

11.1. Given the stream function $\psi = Vy$. (a) Plot the streamlines. (b) Find the x and y components of velocity at any point. (c) Find the quantity flowing between the streamlines $y = 1$ and $y = 2$.

11.2. Find the stream function for a parallel flow of uniform velocity V making an angle β with the x axis.

11.3. Given the stream function $\psi = Axy$ ($A > 0$). (a) Sketch several streamlines. (b) Find the x and y velocity components at 0, 0; 1, 1; ∞ , 0; 4, 1. (c) Find the quantity crossing any line joining points 0, 0 and 1, 1; points 1, 3 and 7, 5.

11.4. Given the stream function $\psi = 3x^2y - y^3$. Express this in polar coordinates, recalling that $\sin 3\theta = 3 \sin \theta \cos^2 \theta - \sin^3 \theta$. Sketch the streamlines, and determine the magnitude of the velocity at any point.

11.5. A fluid flows along a flat surface parallel to the x direction. The velocity u varies linearly with y , the distance from the wall, that is, $u = ky$. (a) Find the stream function for this flow. (b) Determine whether or not the flow is rotational.

11.6. The flow in a laminar boundary layer on a flat plate is given approximately by the stream function

$$\psi = V_0 \left[y + \frac{(\delta - y)^3}{3\delta^2} \right] \text{ for } 0 \leq y \leq \delta$$

where V_0 is the velocity outside the boundary layer, δ is the boundary-layer thickness, and y is the coordinate normal to the plate. Variation of δ with x is neglected. (a) Sketch the streamlines. (b) Determine the velocity, rotation (vorticity), and shearing stress at any point if the viscosity is μ .

11.7. Show that in polar coordinates the rotation, or vorticity, is given by the expression

$$\frac{\partial V_\theta}{\partial r} + \frac{V_\theta}{r} - \frac{1}{r} \frac{\partial V_r}{\partial \theta}$$

11.8. Given: $V_r = \frac{A}{r}$, $V_\theta = \frac{A}{r}$ ($A > 0$). Find ψ , and sketch a few streamlines.

11.9. In Prob. 11.1 to 11.4, find the velocity potential, and sketch lines of constant ϕ .

11.10. Given the velocity potential $\phi = A\theta$ ($A > 0$). (a) Sketch lines of $\phi = \text{constant}$. (b) Find the velocity components at any point (r, θ) . (c) Find ψ , and sketch a few streamlines.

11.11. Given the stream function $\psi = (\frac{3}{2})r^{\frac{3}{2}} \sin(\frac{3}{2}\theta)$. (a) Plot the streamline $\psi = 0$. (b) Find the velocity at $r = 2$, $\theta = \pi/3$ and $r = 3$, $\theta = \pi/6$. (c) Find the velocity potential ϕ .

11.12. A two-dimensional flow of ideal incompressible fluid is composed of a parallel flow of velocity V_0 , a source of strength Q , and sink of strength $-Q$, separated by a distance b in the direction of the parallel flow, the source being upstream from the sink. (a) Find the resultant stream function and velocity potential. (b) Find the distance from the upstream stagnation point to the source.

11.13. Find the stagnation points on a cylinder of 1-ft radius if the velocity in the undisturbed stream $V_0 = 15$ ft/sec and circulation $\Gamma = -90$ ft²/sec.

11.14. (a) In order to have a lift force of 5 lb per ft of length on the cylinder of the preceding problem, how large must be the circulation if $V_0 = 15$ ft/sec and the density is 2.4×10^{-3} slug per cu ft? (b) Find the points of maximum and minimum pressure on the cylinder. (c) Plot the pressure distribution on the cylinder.

11.15. A cylinder of radius $a = 0.5$ ft is submerged in a flow of ideal fluid having a velocity $V_0 = 60$ ft/sec. If $2(p - p_0)/\rho V_0^2 = -8$ at the top of the cylinder, find the velocity at this point and the circulation.

11.16. A long cylinder of radius a is immersed in air having velocity V_0 and is rotated clockwise with an angular speed ω such that the observed flow pattern resembles the theoretical pattern in which the stagnation points coincide. (a) Find the theoretical lift coefficient. (b) Find ω , assuming that the peripheral speed of the cylinder equals the maximum theoretical velocity of the fluid at the surface of the cylinder.

11.17. In a two-dimensional flow of ideal fluid past a cylinder of radius a the maximum velocity is 6 times that of the undisturbed stream V_0 . (a) Show that the maximum

velocity occurs on the cylinder. (b) Find the circulation and the distance of the stagnation point from the center of the cylinder.

11.18. A ship having a water-drag coefficient of 3.55×10^{-3} based on the wetted area of 1,000 sq ft has (in place of sails) two identical 20-ft-high cylinders, or rotors, each of which spins about a vertical axis. The ship moves on a fresh-water lake at a constant speed V_s , which is parallel to the resultant force of the wind on the rotors. The absolute wind velocity is V . Assuming that $V_s = V/2$ and that the lift and drag coefficients based on the projected rotor area are 10 and 5, respectively, find the radius a of the rotors. Assume the density of air to be 2.38×10^{-3} slug/ft³.

11.19. Let ϕ_c and ϕ_i be the velocity potentials for compressible and incompressible flow, respectively, about a given thin profile in a given altitude; ϕ_c satisfies Eq. (11.50), and ϕ_i satisfies Eq. (11.51). (a) Show that Eqs. (11.50) and (11.51) are satisfied if $\phi_i = k\phi_c$, where k is an arbitrary constant. (b) Using the condition that the slope of a streamline at the profile surface must be the same in both compressible and incompressible flow, show that k must equal $U_i\sqrt{1-M^2}/U_c$, where U_i and U_c are the velocities of the distant fluid. (c) Verify Eq. (11.58).

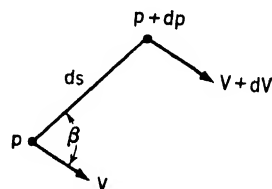
11.20. An airfoil moves with a speed of 550 ft per sec at a given angle of attack, at sea level and at a 10,000-ft altitude. Taking the gas constant for air as 53.3 ft per deg F and assuming a sea-level temperature of 50 F and a lapse rate of $1/200$ F per ft, estimate the ratio of the lift coefficients and the ratio of the lifts.

11.21. A two-dimensional parallel flow of air is deflected by a flat plate set at an angle of 20 deg to the undisturbed flow. The stagnation temperature and pressure of the air are 60 F and 14.7 psia. The Mach number of the undisturbed flow is 2.02. (a) Find the pressure of the undisturbed flow. (b) Find the pressure on the high-pressure side of the plate and the angle of the shock wave set up at the leading edge of the plate. (c) By plotting an epicycloid, as in Fig. 11.45, find graphically the velocity on the low-pressure side of the plate. (d) Find the normal force per unit area of the plate.

11.22. From Eqs. (11.2) show that

$$\frac{\partial v}{\partial x} - \frac{\partial u}{\partial y} = -\frac{(dp/\rho) + dV^2/2}{V \sin \beta ds} = -\frac{(dp/\rho) + dV^2/2}{dQ}$$

where ds and β are as shown. Explain how this result proves the rotation to be independent of the choice of axes.



PROBLEM 11.22.

11.23. (a) Using the result of Art. 11.3 that $(D/dt)[(\partial v/\partial x) - (\partial u/\partial y)] = 0$, show that, although $\psi_1 = k_1 y^3/3$ and $\psi_2 = k_2 x^2/2$ both satisfy Eqs. (11.2), their sum does not.

Chapter XII

12.1. A thrust bearing supports a total thrust of 3,000 lb. There are four slippers, each having $l = b = 3.00$ in. The point of support of each slipper is at a distance of 6 in. from the axis of the shaft and 1.83 in. from the leading edge. The shaft turns at 750 rpm, and the oil viscosity is 6×10^{-6} lb-sec per sq in. Assuming that the flow under each slipper is the same as that for a two-dimensional slipper bearing with sliding velocity equal to that under the point of support, find the angle of tilt of the slipper and the minimum film thickness.

12.2. The fixed shoe of a slider bearing is 2 in. long (in the direction of motion) and 4 in. wide and is fixed at an inclination of 4 min. The oil to be used has a viscosity of 40 centipoises at the operating temperature. The speed of the moving slider is 30 ft per sec. What load can the bearing carry if the minimum film thickness is not to be less than 0.002 in. for safe operation?

12.3. Calculate the friction coefficient and total power requirements for the two bearings of a grinder, assuming the shaft and bearings to be practically concentric. Length of each bearing is 5.00 in., shaft diameter is 2.50 in., clearance ratio is 1 part per thousand, shaft speed is 1,500 rpm, total load on both bearings is 1,100 lb, oil viscosity is 5.84×10^{-4} lb-sec per sq ft.

12.4. The load capacity for a perfectly lubricated journal bearing can be defined as the load at which the minimum film thickness is half the radial clearance between shaft and bearing. The corresponding value of the Sommerfeld variable is 0.034. What is the load capacity of each of the bearings of the preceding problem if the effect of side leakage is neglected?

12.5. A full journal bearing 6.4 in. long, 2 in. in diameter, and having 0.0018 in. diametral clearance runs at 800 rpm. If the minimum film thickness for safe operation is not to be less than 0.0005 in., what oil viscosity at the operating temperature is required to carry a load of 3,000 lb? What is the power consumption? Neglect the effect of side leakage.

12.6. If account is taken of side leakage in the bearing of the preceding problem, what oil viscosity will be required?

12.7. The following are given for a journal bearing: shaft diameter $D = 1.00$ in., bearing length $L = 2.00$ in., clearance ratio $D/C = 1,000$, speed $n = 50$ rps, room temperature $T_0 = 80$ F, specific weight of the oil $\gamma = 0.0314$ lb/in.³, specific heat of the oil $c = 193$ Btu-in./lb sec² F, oil viscosity $\mu = 0.0250/T$ lb-sec/in.², where T is oil temperature in degrees Fahrenheit. Assuming that Petroff's equation applies and neglecting any heat transfer from the bearing to the surroundings, determine the rate of oil flow needed to limit the oil temperature to 150 F. The oil enters the bearing at room temperature.

12.8. The friction coefficient for a journal bearing is given by

$$\frac{D}{C}f = 15\left(\frac{D}{C}\right)^2 \frac{\mu n}{P} + 5.0$$

provided that $(D/C)^2(\mu n/P)$ is not less than 0.006. If $(D/C)^2(\mu n/P)$ is less than 0.006, the bearing seizes. The viscosity of the oil is $\mu = 3.60/T^2$ lb-sec/ft², where T is in degrees Fahrenheit. The rate of heat transfer from the bearing is $\alpha\pi DL(T - T_0)$ Btu per sec, where T and T_0 are the temperatures of the oil and the surroundings, respectively. The following are known: $n = 15$ rps, $D = 0.17$ ft, $L = 0.12$ ft, $D/C = 1,000$, $T_0 = 80$ F, $\alpha = 1.50 \times 10^{-3}$ Btu/sec ft² F. There is no appreciable flow of oil through the bearing. Assuming the maximum allowable oil temperature to be 220 F, find the maximum allowable value of P , the load per unit projected bearing area.

12.9. The friction coefficient for a journal bearing is the same as for the preceding problem; the limits on $(D/C)^2(\mu n/P)$ are also the same. The following are known: $P = 800$ lb/in.², $n = 15$ rps, $D = 0.17$ ft, $L = 0.12$ ft, $D/C = 1,000$, $\alpha = 1.60 \times 10^{-3}$ Btu/sec ft² F, $T_0 = 70$ F, oil density $\rho = 1.73$ slugs/ft³, specific heat of oil $c = 16.1$ Btu/slug F, rate of oil flow through bearing $Q = 4.0 \times 10^{-5}$ ft³/sec. Assuming that the maximum oil temperature cannot safely exceed 180 F, find the maximum and minimum allowable values of viscosity.

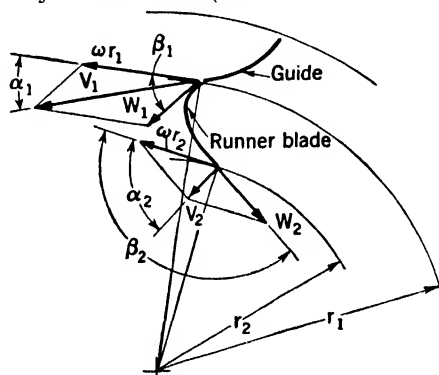
12.10. A 3-in. shaft rotating at 2,000 rpm carries an assembly that is free to rotate about it and is driven in the same direction by a 2.5-to-1 gear reduction. The assembly carries an eccentric weight that applies a centrifugal load equivalent to 5,000 lb at this speed. The oil has a viscosity of 3 centipoises at the operating temperature. How long should each of the two shaft bearings be made if the safe minimum film thickness is 0.0002 in.? Follow the usual design practice of taking the clearance ratio as 1 part in a thousand. Neglect side leakage.

Chapter XIV

Mechanical efficiency $\eta_m = 1.00$ in all problems for this chapter.

14.1. A Pelton turbine has a diameter of 78 in., a speed of 300 rpm, and a bucket angle $\beta = 165$ deg (see Fig. 14.2, page 343). The exit diameter of the nozzle is 8 in., the base diameter is 12 in., and C_v and C_c are 0.97 and 0.80, respectively. (See pages 154 and 156 for definitions of C_v and C_c .) (a) Find the maximum power output, neglecting loss at the buckets. (b) Find the efficiency of the turbine (wheel and nozzle combined).

14.2. The velocity diagrams for the runner of a Francis turbine are shown. The discharge is 159 cu ft per sec, the head is 350 ft of water, the speed is 410 rpm, $r_1 = 2.0$ ft, $\alpha_1 = 18$ deg, $V_1 = 117$ ft/sec, and the tangential component of the absolute velocity at the runner exit V_{t2} is zero ($\alpha_2 = 90$ deg). Find β_1 , the torque, the output power, and efficiency.



PROBLEM 14.2.

14.3. At 240 rpm the pressure at the entrance to a hydraulic-turbine runner is 27.5 psia, while that at exit is 4 psia. Referred to the figure of Prob. 14.2, the other data are

$$\begin{array}{lll} \alpha_2 = 90 \text{ deg} & r_1 = 3.0 \text{ ft} & W_1 = 55 \text{ ft/sec} \\ \beta_2 = 160 \text{ deg} & r_2 = 2.5 \text{ ft} & z_1 = z_2 \end{array}$$

Compute the loss in the runner $H_{l_{1,2}}$.

14.4. Referred to the figure of Prob. 14.2, the data for a Francis turbine are

$$\begin{array}{ll} Q = 113 \text{ ft}^3/\text{sec} & \omega = 4.50 \text{ radians/sec} \\ r_1 = 4.67 \text{ ft} & \text{Width of runner} = b = 0.97 \text{ ft} \\ r_2 = 4.00 \text{ ft} & \text{Loss in runner} = H_{l_{1,2}} = \frac{0.20 W_1^2}{2g} \text{ ft} \\ \alpha_1 = 12 \text{ deg} & p_2 = 5 \text{ psia} \\ & V_{t2} = 0 \end{array}$$

Find the pressure p_1 at the runner entrance, and $H_{l_{1,2}}$.

14.5. A Pelton water wheel is 10 ft in diameter and operates at 250 rpm. (a) When operating at the theoretical condition for maximum efficiency, what head of water will be required at the inlet to the nozzle if the outlet diameter of the nozzle is 6 in., $C_v = 0.98$, and $C_c = 0.85$? (b) If the specific speed of this turbine is 2.7, what is its over-all efficiency?

14.6. A Francis turbine operates under the following conditions (see the figure of Prob. 14.2):

$$\begin{aligned} W_1 &= 5 \text{ ft/sec} \\ W_2 &= 20.3 \text{ ft/sec} \\ \omega &= 5 \text{ radians/sec} \\ r_2 &= 4 \text{ ft} \\ r_1 &= 5 \text{ ft} \\ \alpha_2 &= 90 \text{ deg} \\ \text{Width of runner} &= 1 \text{ ft} \end{aligned}$$

(a) Find the flow through the turbine. (b) Find the torque.

14.7. A turbine develops 640 hp at an efficiency of 86 per cent under head of 40 ft when fitted with a cylindrical draft tube 5.0 ft in diameter. Determine the increase in power and efficiency if a conical draft tube 7.5 ft in exit diameter is substituted for the cylindrical one. Assume the discharge, head, and speed to remain the same and that the losses in both draft tubes are the same. Assume that $V_t = 0$ for each tube.

14.8. A vertical cone-shaped draft tube 23 ft long is 6 ft in diameter at the top (section 1) and 8.4 ft in diameter at the bottom (section 2). The lower end of the tube is 5 ft below the tail-water level. The discharge rate is 810 cu ft per sec. Assume the loss in the tube to be $H_{l,2} = 0.6(V_{n2}^2/2g)$ where V_{n2} is the axial velocity component at the exit. (a) If the circulation in the draft tube is zero, find the gauge pressure at the wall at 1. (b) If there is in the draft tube a free vortex with a core of constant radius r_c and a constant circulation Γ , show that the kinetic energy resulting from the tangential velocity components that crosses section 2 per unit time is

$$\rho Q \frac{\Gamma^2}{4\pi^2 r_2^2} \left(\frac{1}{4} + \ln \frac{r_2}{r_c} \right)$$

(c) Find the gauge pressure at the wall at 1 if $\Gamma = 200 \text{ ft}^2/\text{sec}$ and $r_c = 0.50 \text{ ft}$, assuming that all the kinetic energy at 2 is dissipated. Use Eq. (5.9).

14.9. A Kaplan turbine has a casing diameter of 16 ft, a hub diameter of 6 ft, a speed of 120 rpm, and a discharge of 7,000 cu ft per sec. The circulation just upstream from the runner is 240π sq ft per sec and is zero in the draft tube. (a) Assuming shockless entry of the water into the runner, find the entrance and exit blade angles at a 5-ft radius. (b) Find the power output.

14.10. What type of turbine will be required in order to develop 6,500 hp at 530 rpm under a head of 650 ft? If only 850 hp is to be developed, what type of turbine should be used?

14.11. A model of a Francis turbine one-fifth of full size develops 4.1 hp at a speed of 360 rpm under a head of 5.9 ft. Find the speed and power of the full-size turbine when operating under a head of 19 ft. Assume that both model and full-size turbine are operating at maximum efficiency.

14.12. In the development of the power of a certain river, it is found that the mean annual discharge is 6,000 cu ft per sec and the mean head is 40 ft. What type of turbine should be selected if it is to run at 180 rpm, use half of the water available, and have an efficiency of 85 per cent?

14.13. (a) Assuming that the maximum relative velocity on the blades of the turbine of Prob. 14.9. is 1.2 times as great as the relative velocity at the runner entrance, determine whether cavitation will appear first at the root or tip of the blades. (b) Neglecting the loss in the guide vanes and runner blades, assuming that the hydraulic efficiency η/η_m is 94 per cent, and taking atmospheric pressure as 14.7 psia and the

vapor pressure as zero, find the maximum allowable height of the turbine runner above the tail-water level.

Chapter XV

Mechanical efficiency $\eta_m = 1.00$ in all problems for this chapter.

15.1. The following are known for a centrifugal water pump (see figure of Prob. 6.9):

$$\begin{aligned} r_1 &= 2 \text{ in.} & r_2 &= 6 \text{ in.} \\ b_1 &= 0.75 \text{ in.} & b_2 &= 0.50 \text{ in.} \\ \beta_1 &= 120 \text{ deg} & \beta_2 &= 150 \text{ deg} \\ N &= 1,800 \text{ rpm} \end{aligned}$$

The gauge pressure is 45 lb per sq in. at a point on the discharge pipe which is 6.0 ft above the water level in the reservoir from which the pump draws water. The diameter of the discharge pipe is 6.0 in. Neglect losses in the entrance pipe, assume shockless entry of water onto the blades at 1, and take $V_{t1} = 0$. (a) Draw the entrance and exit velocity diagrams. (b) Determine the discharge rate. (c) Find the shaft horsepower. (d) What is the efficiency?

15.2. A centrifugal pump operates at 150 radians per sec and requires 294 hp. Determine the flow through the pump if the absolute velocity of the water at the entrance has no tangential component and

$$\begin{aligned} r_2 &= 8 \text{ in.} \\ b_2 &= 1 \text{ in.} \\ \rho &= 1.94 \text{ slugs/ft}^3 \\ \beta_2 &= 135 \text{ deg} \end{aligned}$$

(See figure of Prob. 6.9)

15.3. A 10-bladed axial-flow fan with guide vanes, hub, and housing draws in air from a room in which the air is at rest (see Fig. 15.6). The casing radius is 1.0 ft, the hub radius is 0.5 ft, the speed is 2860 rpm, $p_3 - p_1 = 14 \text{ lb/ft}^2$, and the air density is $2.38 \times 10^{-2} \text{ slug per cu ft}$. At a radius $r = \frac{5}{6} \text{ ft}$ the absolute tangential velocity of the air at 2, $V_{t2} = 26.3 \text{ ft/sec}$, and the angle between the relative air velocity W_1 and ωr is 15 deg. (a) Find the discharge rate. (b) Find the tangential force per unit length on one blade at $r = \frac{5}{6} \text{ ft}$. (c) Find the total torque exerted on the fan wheel. (d) What is the efficiency of the fan?

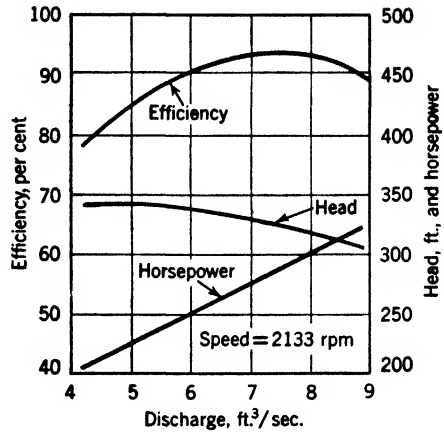
15.4. For the fan of the preceding problem, compute that part of the kinetic energy passing section 2 per second which results from the tangential velocity V_{t2} . Assume, as usual, that rV_t is independent of r . Note that, if the guide vanes are removed, all this kinetic energy will be wasted. Show then that, if friction in the guides is neglected,

$$\eta_{NG} = \eta_G - \frac{V_{t2,0}}{\omega r_o} \frac{\ln(r_o/r_i)}{1 - (r_i/r_o)^2}$$

where η_{NG} is the efficiency without guides, η_G is the efficiency with guides for the same input power and discharge, $V_{t2,0}$ is the tangential velocity at 2 at the casing, and ω is the angular velocity.

15.5. A certain water pump tested at 2,000 rpm discharges 6.0 cu ft per sec against a head of 340 ft. At this capacity, the efficiency is 88 per cent. If a geometrically similar pump of twice the size runs at 1,500 rpm, find its discharge, head, and power for the same efficiency.

15.6. The curves shown refer to a centrifugal pump *A* discharging water. A geometrically similar pump *B* having a diameter 50 per cent greater than that of pump *A* and discharging oil of specific gravity 0.84 operates at 1,750 rpm. Neglecting the effect of friction, find the head developed and the necessary horsepower input for pump *B* at its maximum efficiency.



PROBLEM 15.6.

15.7. The following test data apply to a centrifugal water pump having impeller diameter $D = 0.875$ ft and running at $n = 24.2$ rps.

Discharge, Ft³/sec	Head, Ft of water	Efficiency, %
2.23	70	72
2.67	67	77
3.12	64	84
3.57	60	88
4.02	55	86
4.46	44	78

Geometrically similar pumps having impeller diameters of 0.750 and 0.667 ft are available. Either of these can run at 29.2, 24.2, or 19.2 rps. (a) Select from among these the most suitable combination for a pump that is to produce a head of 51 ft of water at a discharge rate of 1.90 cu ft per sec. (b) Compute the power input required for the pump chosen in part a.

15.8. The following are given for an axial-flow fan: Discharge rate = 20 ft³/sec, pressure rise = 5.0 lb/ft², speed = 1,200 rpm, casing radius = 0.60 ft. Air pressure and temperature are 14.7 psia and 70 F. The blades are to have NACA 4412 sections. Assuming that blades and guide vanes have the same value of ϵ , the drag-lift ratio, determine a suitable hub radius, number of stages, number of blades, C_L , t , α , and $\alpha + \beta$ at hub and tip. (These symbols are defined in Art. 15.4.)

15.9. Derive Eq. (15.41).

15.10. Referring to the notation of Fig. 15.1, assume that a centrifugal compressor has blades which are radial at exit 3. Assume further that the flow is isentropic and the fluid a perfect gas. Using the results of Art. 15.5, plot p_3/p_1 as a function of m/m^* for several constant values of $\omega r_3/C_3$. Consider the following ranges of the variables:

$$1.4 \leq \frac{p_3}{p_1} \leq 2.0 \quad 0.7 \leq \frac{\omega r_3}{C_3} \leq 0.9$$

Take $A_3/A_1 = \sqrt{3}$ and $k = 1.4$. Compare your plot with Fig. 15.13.

Chapter XVI

16.1. A 6-ft-diameter ship propeller develops a thrust of 4,000 lb in fresh water when the velocity of the ship is 25 mph. (a) What is the ideal efficiency? (b) What is the absolute velocity of the slipstream at some distance from the propeller?

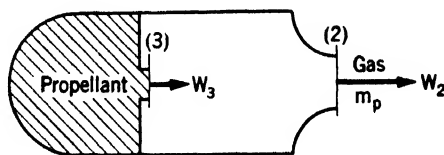
16.2. A propeller of the series shown in Fig. 16.6 is to absorb 1,000 hp at 1,200 rpm and a speed of 225 mph at sea level. (a) Determine the blade angle at the $\frac{3}{4}$ -radius point, the efficiency, and the diameter. (b) Find the thrust and ideal efficiency.

16.3. A three-bladed propeller 18 ft in diameter absorbs 3,000 hp at 800 rpm when moving at 400 mph at a 25,000-ft altitude. The efficiency is 0.81. (a) Find the thrust F_n and the torque T . (b) If, at the $\frac{3}{4}$ -radius point, $dF_n/dr = 130$ lb/ft and $dF_t/dr = 145$ lb/ft, find dL/dr and dD/dr at this point. Neglect any additional velocity caused by contraction of the stream. (c) Assuming a lapse rate $\lambda = \frac{1}{300}$ F/ft, ground-level pressure and temperature of 14.7 psia and 60 F, and a lift coefficient of 0.35, find the blade width (chord) at the $\frac{3}{4}$ -radius point. What is the drag coefficient of this blade element?

16.4. A model propeller 3 ft in diameter is tested in a wind tunnel having an air-stream speed of 300 ft per sec. The pressure and temperature of the air are 14.7 psia and 60 F. At a rotational speed of 40.5 rps, this propeller absorbs 31.8 hp and produces a thrust of 47.0 lb. (a) What is the efficiency of the propeller? (b) A geometrically similar propeller 12 ft in diameter moves at 400 ft per sec relative to the undisturbed air. At what rotational speed can the power and thrust of this propeller be computed from the above model data if friction and compressibility are neglected? (c) Find the power and thrust of the 12-ft propeller if it operates at a 25,000-ft altitude. Assume ground-level conditions as above and a lapse rate of $\frac{1}{300}$ F per ft.

16.5. Assuming steady flow with respect to a ram jet traveling at constant velocity through the atmosphere, find, by use of the momentum theorem, the force that must be exerted on the ram jet to enable it to pick up air at a constant mass rate m . What work is done on the ram jet per unit time by this force?

16.6. The velocities of liquid propellant and gaseous combustion products relative to a steadily moving rocket are shown in the figure. To a good approximation, W_3^2 can be neglected, and the heating value of the propellant e_p can be taken equal to h_3 , the enthalpy per unit mass of propellant entering the combustion chamber at 3. Show by applying the steady-flow energy equation that

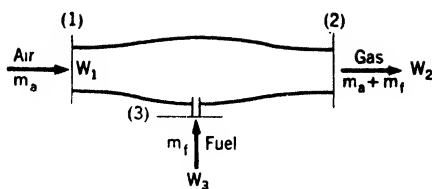


$$\frac{W_2^2}{2} = e_p - h_2 = \eta_0 e_p$$

where h_2 is the enthalpy per unit mass of (burned) propellant at 2 and η_0 is defined by the equation

$$\eta_0 = \frac{e_p - h_2}{e_p}$$

16.7. The velocities and mass rates of flow of air, gas, and liquid fuel relative to a steadily moving jet-propulsion unit are shown in the figure. To a good approximation, W_3^2 can be neglected, and $e_f m_f = h_1 m_a + h_3 m_f$ where h_1 and h_3 are enthalpy per unit mass at 1 and 3, respectively. (a) Show by applying the steady-flow energy equation that



PROBLEM 16.7.

$$\frac{W_2^2}{2} = \frac{W_1^2}{2} - \frac{m_a}{m_a + m_f} + e_f \frac{m_f}{m_a + m_f} - h_2 = \frac{W_1^2}{2} - \frac{m_a}{m_a + m_f} + \eta_0 e_f \frac{m_f}{m_a + m_f}$$

where η_0 is defined by the equation

$$\eta_0 = \frac{e_f m_f - h_2(m_a + m_f)}{e_f m_f}$$

(b) Show that this definition of η_0 is identical with that given in the preceding problem. (Note that $e_f m_f = e_p m_p$ for a given fuel.)

16.8. (a) If the efficiency η of a jet-propulsion unit is defined as the ratio of the useful power output to the energy per unit time supplied by the fuel, show (with the aid of the results of the preceding problem) that

$$\eta = 2\eta_0 \frac{(1 + \alpha)x - 1}{(1 + \alpha)x^2 - 1 + \alpha\eta_0}$$

where $x = W_2/W_1$ and $\alpha = m_f/m_a$. (b) Noting that to a good approximation α can be neglected in comparison with unity, plot η/η_0 as a function of x .

16.9. Assuming the maximum velocity of a V-2 rocket to be 5,130 ft per sec and neglecting air resistance and any variation in g , find the height to which the rocket will rise above the point where the maximum velocity is attained.

16.10. (a) Assuming that the initial and final weights of a V-2 rocket are 27,000 lb and 9,000 lb, respectively, that the relative jet velocity is constant and equal to 6,500 ft per sec, and that propellant is discharged at a uniform rate, find the height above the earth reached by the rocket at the end of the burning time of 60 sec. Neglect air resistance and variations in g . (b) What is the total height attained? (See preceding problem.)

16.11. A jet-propulsion unit uses 40 lb of air per pound of fuel at an over-all efficiency of 15 per cent when moving at a velocity of 800 ft per sec. Assuming a value of $\eta_0 = 0.25$, find the specific impulse (thrust per unit weight of fuel).

Chapter XVII

17.1. A radial-bladed fluid coupling has the characteristic curve of Fig. 17.2 corresponding to the larger value of Reynolds number. The specific gravity of the oil is 0.89. (a) What diameter must the coupling have to transmit a torque of 200 ft-lb

at 3,000 rpm and a slip of 5 per cent? (b) If the slip is doubled, what is the necessary diameter?

17.2. An automobile has the following characteristics: Total weight is 3,000 lb; maximum engine brake torque is 150 ft-lb over a speed range of 1,000 to 3,600 rpm; reduction ratio in differential is 4 to 1; tire diameter is 28 in.; a 1-ft-diameter fluid coupling having the upper characteristic curve of Fig. 17.2 is attached to the engine shaft. (a) What car speed is attained at an engine speed of 3,600 rpm if the torque transmitted is three-quarters of the maximum? (b) What is the approximate efficiency of the coupling under these conditions? (c) Assuming a constant engine speed of 3,600 rpm and that the over-all drag of the car varies as the square of the car speed, find the engine torque, coupling efficiency, and car speed when the car climbs a grade of 4 per cent.

17.3. The torque coefficient of a fluid coupling of given design is found to follow the law

$$C_T = \frac{T}{\rho \omega_p^2 D^5} = 0.0080 \left(1 - \frac{\omega_s}{\omega_p} \right)^{1/2}$$

where T is the torque, ρ is the density of the operating fluid, ω_p and ω_s are the angular speeds of the primary and secondary shafts, respectively, and D is the diameter. Find ω_p for a coupling 1 ft in diameter filled with oil of density 1.65 slugs per cu ft if the output is 15 hp and the efficiency is 98 per cent.

17.4. A fluid coupling having diameter $D = 1.20$ ft transmits a torque $T = 194$ ft-lb at a slip of 3 per cent when connected to an engine shaft turning at 2,000 rpm. A geometrically similar coupling is to be used to deliver 20,000 hp to a propeller shaft turning at 600 rpm. Find the diameter of this coupling if it operates on oil of the same density as the other.

17.5. A certain automotive hydrodynamic torque converter having the characteristics of Fig. 17.5 develops an output torque of 300 ft-lb at an output-shaft speed of 1,000 rpm when operating at maximum efficiency. (a) What are the input torque and speed under these conditions? (b) What is the efficiency? (c) If the input torque and speed are held constant and the output torque is doubled, what will be the output-shaft speed?

17.6. Two torque converters of the same design having diameters D and D' run at maximum efficiency. Both use the same kind of oil and are filled to the same fraction of the total volume. Neglect frictional effects, and assume that $\omega_p = 2\omega_s$ and $D' = D/2$. (a) How do the torque ratios T_s/T_p and T'_s/T'_p compare? (b) What is the value of T'_s/T_s ?

17.7. A torque converter is to be designed which is similar to that described in Art. 17.5 and shown in Fig. 17.4, except that the trailing edges of the primary and secondary blades are curved backward, instead of being normal to the direction of blade motion. The trailing edges of the primary vanes make an (acute) angle β_2 with the tip velocity $\omega_p r_2$. The trailing edges of the secondary vanes make an (acute) angle β_3 with the tip velocity $\omega_s r_3$. The guide vanes are the same as in Fig. 17.4. The converter is to give a torque ratio $T_s/T_p = 2.2$ when the shock losses are zero. Under these conditions it is assumed that the friction losses amount to 14 per cent of the power input, *i.e.*, the efficiency is 86 per cent. If $r_1 = 2.50$ in., $r_3 = 7.00$ in., $\beta_1 = 45^\circ$, $A = 57$ sq in., $\omega_p = 200$ radians/sec, and the specific weight of the oil is 0.0298 lb per cu in., find r_2 , β_2 , β_3 , and the input horsepower.

17.8. A torque converter is identical with that shown in Fig. 17.4 and has $r_1 = 2.50$ in., $r_2 = 5.42$ in., $r_3 = 7.00$ in., $\beta_1 = 45^\circ$, and $A = 57$ sq in. (a) Taking only shock loss into account, set up an expression for the efficiency; combine this with Eq. (17.17) to determine $Q \tan \beta_1 / A \omega_p r_3$ as a function of ω_s / ω_p . (b) What is the per-

centage variation of $Q \tan \beta_1 / A \omega_p r_s$ from a mean value? Is the assumption that this expression is constant justifiable as a first approximation in computing the optimum value of ω_s / ω_p , as in Art. 17.5? (c) Find the approximate value of the maximum efficiency.

Chapter XVIII

18.1. A rotary displacement pump is tested at constant speed and full stroke by throttling the discharge to produce different values of Δp , the pressure rise across the pump. If the friction torque T_f is constant, find the torque efficiency and power input in terms of Δp , D_P , T_f , and ω_P .

18.2. A hydraulic transmission consists of a variable-stroke pump and a fixed-stroke motor, having equal displacements, $D_P = D_M$. Assume a constant over-all torque efficiency of 90 per cent and a constant leakage rate of 5 per cent of the pump displacement per unit time ($Q_l = 0.05 D_P \omega_P$). Plot the over-all efficiency as ordinate, using as abscissa (a) pump stroke and (b) percentage of maximum motor speed.

18.3. A hydraulic transmission comprising a constant-displacement pump and variable-displacement motor is to do work at a uniform rate of 20 hp over an output-speed range of 800 to 1,800 rpm. Assuming a pressure rise of 1,700 lb per sq in. at the pump and reasonable values for the efficiencies involved, determine the approximate displacement per revolution of the hydraulic motor.

18.4. Calculate the leakage flow rate past a stationary piston if the piston length is 1.00 in., piston diameter is 1.00 in., pressure difference between the ends of the piston is 1,500 lb per sq in., viscosity of oil is 2.00×10^{-4} lb-sec per sq in., uniform radial clearance between piston and cylinder is 0.0010 in. Assume fully developed laminar flow throughout clearance space.

NOTE: Equation (12.10) is the starting point for the solution of this problem. The clearance is so small compared with the radius of the piston that the flow may be considered identical with that between parallel planes.

18.5. Solve the preceding problem if the piston has a constant velocity of 10 ft per sec in the direction of the pressure drop.

18.6. A dashpot consists of a piston of diameter D and piston rod in a closed cylinder through both end plates of which the piston rod extends. The cylinder is completely filled with oil of viscosity μ , which flows through four small holes of diameter d drilled axially through the piston, when the piston moves along the cylinder. The length of the piston is l , and its mass is m . Neglect leakage, friction force on the piston, and compressibility; and consider both the cross-sectional area of the piston rod and that of the four holes to be negligible compared with $\pi D^2/4$. (a) Assuming that Poiseuille's law applies to the flow through the holes in the piston and neglecting the mass of the oil and piston rod, set up the equation of motion of the piston under the action of an external force F_0 . (b) Show that the solution of this equation is

$$x = \frac{F_0}{m\alpha^2}(e^{-\alpha t} - 1 + \alpha t)$$

if the displacement and velocity, x and dx/dt , are both zero at $t = 0$. The constant α is to be expressed in terms of known quantities μ , l , m , d , and D .

18.7. The following are given for an elevator driven by an electric motor through a hydraulic-displacement transmission:

Limiting acceleration of cab	$= \pm \frac{g}{5}$
Limiting velocity of cab	$= \pm 500 \text{ ft/min}$
Distance between stops	$= 17 \text{ ft}$

Assume a variable-stroke pump and a fixed-stroke motor, with $D_P = D_M$. Neglect leakage. (a) What is the relation between the stroke-control setting S_P and the speed of the motor shaft, ω_M ? (b) If the hydraulic-motor shaft is automatically geared to the stroke-control shaft at a distance h before a stop, determine h and the time required for the cab to travel a distance $0.99h$. Assume that the cab is traveling initially at its limiting speed and that the initial deceleration has its limiting value. (c) Sketch the velocity-distance and velocity-time diagrams for single-floor operation.

18.8. The following additional information is given for the elevator of the preceding problem:

Weight of cab, W	2,500 lb
Weight of counterweight, W_1	2,250 lb
Radius of drum for cable, r	15 in.
Leakage constant $Q_l/\Delta p \omega_P D_P$	$5 \times 10^{-5} \text{ in.}^2/\text{lb}$
Displacement $D_P = D_M$	$3.67 \text{ in.}^3/\text{radian}$
Pump speed $N_P = \omega_P 60/2\pi$	600 rpm
Motor torque efficiency η_{TM}	1.00

(a) Find the speed of the hydraulic motor at a cab speed of descent $dz/dt = -500 \text{ ft/min}$. (b) Assuming that the cab just fails to oscillate when it is brought to rest and that the initial deceleration and velocity are $d^2z/dt^2 = 0$ and $dz/dt = -500 \text{ ft/min}$, find the value of h . (c) Compute the maximum deceleration.

18.9. Assuming that the stopping period for the elevator of the preceding problem begins at $t = 0$ and that the values of height, velocity, and acceleration at $t = 0$ are $z = h = 10.8 \text{ ft}$, $dz/dt = -500 \text{ ft/min}$, find the time required for z to reach the value $h/100 = 0.108 \text{ ft}$. Also determine the maximum deceleration during the stopping period.

18.10. An ideal displacement servomechanism with proportional control has the following characteristics: Moment of inertia of load is $0.350 \text{ lb-in. sq sec}$, pump speed is $1,800 \text{ rpm}$, displacement of pump or motor is $2.00 \text{ cu in. per radian}$, pinion to ring-gear ratio of differential is 1 to 4 , gear ratio from output shaft to differential is 1 to 1 , pump stroke-control shaft turns 30 deg from neutral to full stroke, motor has a fixed stroke. (a) Compute the time constant α_0 . (b) Plot $\alpha_0 \theta_o/\omega_i$ against $\alpha_0 t$ when a velocity step signal $d\theta_i/dt = \omega_i = \text{constant}$ is applied at $t = 0$ and maintained for all later times. Assume $\theta_o = d\theta_o/dt = 0$ at $t = 0$.

18.11. The servomechanism of the preceding problem is no longer supposed to be ideal but to have a leakage of 5 per cent of the maximum displacement of the pump when the pressure rise across the pump is $1,000 \text{ lb per sq in.}$ The viscosity of the oil is $2.0 \times 10^{-6} \text{ lb-sec per sq in.}$ (a) Compute the leakage coefficient C_l defined in Eq. (18.15). (b) Determine the value of the elastic coefficient C_e [Eq. (18.32)] at which the system becomes unstable. (c) If C_e has twice this limiting value, plot the response curve, as in Fig. 18.27.

18.12. An ideal linear hydraulic servomechanism has proportional-plus-derivative control, i.e.,

$$S_P = C_s(\theta_i - \theta_o) + G_s \frac{d}{dt}(\theta_i - \theta_o)$$

(a) Show that the transfer function ζ for this servomechanism is expressible in the form

$$\frac{1 + \zeta}{\zeta} = \frac{z/\omega_P G_s}{z + C_s/G_s} + 1$$

(b) Make a rough plot of this transfer function, similar to Fig. 18.25, and determine therefrom the stability criterion and the approximate form of the frequency-response curve. What is peculiar about the limiting value of the response as the frequency increases? (c) Compute the transient response to a displacement step function $\theta_i = C_i$.

18.13. An ideal linear hydraulic servomechanism has proportional-plus-integral control, *i.e.*,

$$S_P = C_s(\theta_i - \theta_o) + H_s \int_0^t (\theta_i - \theta_o) dt$$

(a) Show that the transfer function ζ for this servomechanism is expressible in the form

$$\frac{1 + \zeta}{\zeta} = \frac{z^2}{\omega_P(C_s z + H_s)} + 1$$

(b) Make a rough plot of this transfer function, similar to Fig. 18.25, and determine therefrom the stability criterion and the approximate form of the frequency-response curve. (c) Determine the transient response to a velocity step signal $d\theta_i/dt = \omega_i = \text{constant}$, and show that the steady-state error is zero. (Note the statement at the end of Art. 18.12 regarding steady-state error and shape of the transfer-function curve.)

INDEX

A

- Acceleration, of fluid particle, 62
 - uniform rectilinear, 41-43
- Accumulator, hydraulic, 424
- Acidity of oil, 283
- Additives for boundary lubricants, 321-323
- Airfoils, low-drag, 194-198
- Airplane mechanics, 255-258
- d'Alembert's principle, 41, 113
- Amontons, G., 331
- Anemometer, hot-wire, 135
- Angular momentum, definition of, 92
- Angular-momentum principle, 91*ff.*
- Apparent mass, 227
- Apparent shearing stress, 124, 136
- Archimedes, 14
 - principle of, 32
- Area of contact, true value for a bearing, 325
- Atmosphere, equilibrium of, 47-52
 - isothermal, 47
- Axial-flow fan, 364-366
- Axial-flow machine, design of, 368*ff.*
- Axial-flow pump, 364-366

B

- Balloons, 52
- Barometer, 23
- Bearing materials, 327-331
- Bernoulli, Daniel, 67
- Bernoulli's equation, 67
- Blade-element theory of a propeller, 384
- Blasius, H., 188, 189, 191, 192
- Boundary layer, 7
 - momentum equation for, 189
 - on a wing, 253
- Boundary-layer mechanics, 187*ff.*
- Boundary lubrication, 315*ff.*
 - definition of, 278
- Bowden, F., 320, 332-334
- Burgers, J., 148
- Burwell, J., 322
- Busemann, A., 269

C

- Cavitation, 356-359
- Cavitation number, 358
- Centrifugal compressor, 376-380
- Centrifugal fan, 360-364
- Centrifugal pump, 360-364
- Characteristic curve, for airfoil, 255
 - for axial-flow machine, 366
 - for centrifugal machine, 363
- Characteristics, method of, 269-270
- Circulation, 10
 - definition of, 228
- Colebrook, C., 142
- Compressible flow, conditions for dynamical similitude in, 116
 - around a corner, compression, 270
 - expansion, 268
 - in a nozzle, 164
 - in a pipe, 176-179
- Compressible fluid, statics of, 45-53
- Compression modulus, 45
- Compressor, centrifugal, 376-380
- Conduits, incompressible flow in, 122*ff.*
- Conservation of mass, 56*ff.*
- Continuity equation, 56*ff.*
- Continuum, 4
- Contraction, sudden, 153
- Convection, 27
- Coulomb, C., 331
- Critical Mach number, definition of, 206
 - of high-speed airfoil, 210
- Croft, H., 149
- Cyclic flow, energy equation for, 82
- Cylinder, flow pattern for, without circulation, 226
- Cylinder (of internal-combustion engine), lubrication of, 338

D

- d'Alembert's principle, 41, 113
- Dayton, R., 337
- Density, definition of, 11
 - of oil, 283
 - of various fluids, 449-452

- Diameter, equivalent, 149
 - Diffuser efficiency, 348
 - Dimensional analysis, 14, 98*ff.*
 - of compressor, 378
 - of propeller, 385
 - of pump or fan, 366
 - of turbine, 353
 - Dimensional homogeneity, 104
 - Dimensional system, 102
 - Discharge coefficient, for nozzle, 156, 157
 - for orifice, 157, 158
 - Doublet, 225
 - Down-wash velocity, 244
 - Draft tube, 348
 - Drag, definition of, 182
 - Drag coefficient for compressible flow, for
 - an airfoil, 211
 - for projectiles, 211
 - for sphere, 213
 - subsonic, 207
 - supersonic, 211–214
 - transonic, 207–210
 - for cylinder, 201
 - definition of, 183
 - for flat plate normal to flow, 198
 - for low-drag airfoil, 196–197
 - for a sphere, 201
 - for surface vessel, 204–206
 - for various bodies, 183
 - (*See also* Laminar boundary layer; Turbulent boundary layer)
 - Dry friction, mechanism of, 331–335
 - Dryden, H., 135, 194
 - Dynamical equations of ideal fluid, 62*ff.*
 - Dynamical similitude, 113
- E
- Eksergian, R., 409, 412
 - Elevation, measurement in atmosphere, 49
 - Energy, internal, 79
 - intrinsic, 81
 - Energy of adhesion, 319
 - Energy balance for a slipper bearing, 298
 - Energy equation, 80*ff.*
 - and Euler equation, 83
 - for moving axes, 86
 - for rotor, 95
 - Enlargement, sudden, 152
 - Enthalpy, definition of, 172
 - Entropy, change in a shock wave, 175, 273
 - definition of, 174
 - Equilibrium, of atmosphere, isothermal, 47
 - polytropic, 48
 - conditions for, 18
 - definition of, 15
 - dynamic, 41
 - of floating bodies, 34
 - of submerged bodies, 32
 - Equivalent diameter, 149
 - Equivalent length for a pipe fitting, 151
 - Ernst, H., 332, 336
 - Error of a servomechanism, definition of, 429
 - Euler, L., 14
 - Euler's equation, 67
 - and energy equation, 83
 - for pumps, 362
 - for turbines, 346
- F
- Fanno line, 176
 - First law of thermodynamics, 79
 - Flash point, 284
 - Floating bodies, 34–40
 - Flow, laminar and turbulent, 10
 - rotational and irrotational, 10
 - Fluid, definition of, 1
 - perfect (or ideal), definition of, 3
 - Fluid coupling, analysis of, 406–408
 - description of, 404–406
 - as vibration damper, 408
 - Fluid mechanics, definition of, 1
 - Föttinger, H., 410
 - Force, 99
 - Forces, on an element of ideal fluid, 64–66
 - Free surface, and gravity force, 116
 - Friction coefficient, values for various
 - amounts of additive, 322
 - values for various materials, 334
 - values for various surface finishes, 327
 - Friction drag, definition of, 184
 - Friction factor, for compressible flow in a
 - pipe, 178
 - definition of, 125
 - Fritsch, W., 139
 - Froude, W., 116, 121, 204
 - Froude number, physical significance of, 114
 - Froude's law, 120
 - Fuhrmann, G., 187, 225

G

Gas, definition of, 3
 Gauges, pressure, 31
 Gebelein, H., 148
 German standard nozzle, 156, 157
 German standard orifice, 157, 158
 Glauert, H., 259
 Gradient, 17
 Gravity, effect on jet, 69
 Gravity force, 15
 and free surface, 116
 Gravity potential energy, 68
 Grease, 324

H

Hagen, G., 122, 130
 Hagen-Poiseuille law, 130
 Helmholtz, H. von, 14, 198, 199, 254
 Hersey, M., 282
 Hodograph method, 273
 Hodograph plane, 269
 Hofmann, A., 149
 Hot-wire anemometer, 135
 Hydraulic accumulator, 424
 Hydraulic circuits, 416-417
 Hydraulic press, 24
 Hydraulic radius, 149
 Hydraulic transmissions, auxiliaries, 423-424
 circuits for, 416-417
 description of, 414-416
 error-controlled (*see* Servomechanisms)
 operating fluids for, 424-425
 pumps and motors for, 417-423
 theory of, 425-429
 Hydraulic turbines, 341*ff.*
 axial-flow, 352-353
 impulse, 341-345
 mixed-flow, 345-351
 Hydrodynamic lubrication, definition of, 278
 theory of, 285*ff.*
 Hydrostatic equation, 18*ff.*
 applications of, 22*ff.*
 Hydrostatic paradox, 24

I

Impulse turbine, 341-345
 Induced drag, 245

Induced velocity, 235
 Inertia force, 41
 Intermittent ram jet, 389
 Internal energy, 79
 Intrinsic energy, 81
 Irrotational motion, 73

J

Jet propulsion, 389*ff.*
 Jones, B. M. (Sir Melville Jones), 249
 Joukowski, N., 14, 239, 247
 Journal bearing, criteria for safe operation, 312
 dynamically loaded, 306
 with forced oil circulation, 310
 friction coefficient for, 304
 side leakage in, 305
 theory of, 301*ff.*

K

Kármán, Th. von, 122, 139, 147, 148, 189, 192, 199
 Kelvin, Lord, 14
 Kinematic viscosity, 126, 131
 for various fluids, 449-452
 Kingsbury, A., 281, 290, 306, 316
 Kirchhoff, G., 14, 198, 199, 254
 Kutta, W., 14, 239, 247
 Kutta-Joukowski law, 239

L

Lamb, H., 14
 Laminar boundary layer on a flat plate,
 drag coefficient for, 188
 thickness of, 188
 Laminar flow in a pipe, 128-134
 development of, 131-134
 Laminar sublayer in a smooth pipe, 137
 Lanchester, F., 14, 243
 Langhaar, H., 123, 132
 Laplace's equation, 221, 232
 Lapse rate, 48
 Lasche, O., 313
 Lift, on a cylinder, 239
 definition of, 182
 for a finite wing, 243*ff.*
 for an infinite wing, 239
 in supersonic flow, 265

Lift coefficient, for compressible flow, subsonic, 258

supersonic, 263-265

definition of, 241

Liquid, definition of, 3

Lubricants, molecular structure of, 316
monomolecular film of, 320

M

Mach angle, 162

Mach line, 162, 267

Mach number, 7, 73

physical significance of, 117-119

Madison, R., 149

Magnus effect, 237

Manometers, 23, 27-31

Mass, 100

Merchant, M., 332, 336

Metacenter, 36

Metacentric height, 37-39

Michell, A., 281, 290

Millikan, C., 144

Mixed-flow turbines, 345

Mixing length, 145

Molecular structure of lubricants, 316

Molecule and continuum, 11-12

Momentum equation for a boundary layer, 189

Momentum principle, 87*ff.*

Momentum theory, of a propeller, 381
of a windmill, 387

Monomolecular film of lubricant, 320

Morgan, F., 306, 313

Muskat, M., 306, 313

N

Newton, Isaac, 87, 100

Newton's second law of motion, 62

Nikuradse, J., 123, 142, 144, 146

Noncircular conduits, 148

Nozzle, compressible flow in, 164*ff.*

for flow measurement, 155

shock wave in, 170-176

O

Oil, specific gravity of, 283

specific heat of, 284

Oiliness, 316

Orifice, discharge from, 69

for flow measurement, 156

P

Parallel flow, 222

Parker, J., 149

Path line, 55

Pelton turbine, 341-345

Perfect fluid, definition of, 3

Perturbation theory, for subsonic flow, 259
for supersonic flow, 266

Petroff, N., 280

Petroff equation, 300

Physical similitude, 112

Pi (II) theorem, 105*ff.*

Pipe, incompressible flow in, 122*ff.*

Pipe bends, 149

Pipe fittings, 151

Piston ring, lubrication of, 338

Pitot, 70

Pitot-static tube, 71

Pitot tube, 70

Point source of sound, 160

Poiseuille, J., 122, 130, 282

Polar diagram, 248

Polar molecule, 319

Potential, gravity, 19

Potential energy, 20

Potential functions for fluid motion, 217*ff.*

Potential vortex, 76

stream function for, 234

velocity potential for, 234

Prandtl, L., 14, 122, 145, 244, 246, 259, 269

Pressure, center of, 26

definition of, 13

gauge, 22

measurement of, 27-31

static distribution in liquid, 20

on walls, 25

Pressure distribution, on a cylinder, 226

on a rounded body, 202

Pressure drag, definition of, 184

Pressure force, 15-17

Pressure gauges, 31

Profile drag, 248

Jones' method for measuring, 249-252

Propeller, blade-element theory of, 384

dimensional analysis of, 385

ideal efficiency of, 383

momentum theory of, 381

Propeller and engine, efficiency of, 391-394
 Properties of fluids, 45, 449
 Propulsive (ideal) efficiency, 383

R

Ram jet, 389
 advantages and limitations of, 396
 efficiency of, 391-394
 intermittent, 389
 Rankine, W., 225
 Rayleigh, Lord, 14, 121, 239
 Rayleigh line, 176
 Relative motion, 54
 Residual drag, 204
 Resistance law, for rough pipe, 141
 for smooth pipe, 139
 Reynolds, O., 115, 122, 134, 135, 137, 280, 282
 Reynolds number, critical value of, for a
 flat plate, 192
 for a rounded body, 201
 physical significance of, 114
 for pipe flow, lower critical value of,
 122, 135
 upper critical value of, 134
 Reynolds stress, 137
 Ridler, K., 333
 Rise time, definition of, 433
 relation to cutoff frequency, 435
 Rocket, 390
 Rocket mechanics, 397-403
 Rocket propellants, 402
 Rolling friction, 337
 Rotation, of a fluid particle, 74*ff.*, 221
 uniform, 43
 Rotational motion, 77
 Roughness of pipes, 125
 Running in, 337

S

Saybolt second, 131
 Saybolt viscometer, 131, 282
 Schlichting, H., 194
 Schlieren apparatus, 169
 Second law of motion, 62
 Secondary flow, in bends, 149
 in a rectangular duct, 149
 Seizure of a bearing, 336
 Separation, from a boundary, 10

 in compressible flow, 208
 from a rounded body, 201
 from a wing, 253
 Servomechanisms, analysis of ideal, 431-436
 analysis of nonideal, 440-445
 definition of, 429
 description of, 429-431
 types of feedback in, 445
 valve-controlled, 446
 Shearing stress, apparent, 124, 136
 Ship-model tests, 120
 Shock wave, 6
 in a nozzle, 170-176
 oblique, 270
 and rotation, 272
 thickness of, 174
 Silicone, 324
 as a hydraulic fluid, 425
 Similitude, 112*ff.*
 Sinclair, H., 409
 Sink, 223
 Slipper bearing, center of pressure for, 295
 frictional force for, 296
 load for, 295
 pressure distribution for, 294
 velocity distribution for, 291
 Solid, elastic, 3
 plastic, 3
 Sommerfeld, A., 281, 315
 Sommerfeld variable, 303
 Sound, point source of, 160
 Sound propagation in a fluid stream, 165
 Sound velocity, 117
 Source, 223
 Sources and sinks, method of, 224
 Specific gravity of oil, 283
 Specific heat of oil, 284
 Specific speed, of pump or fan, 368
 of turbine, 356
 Specific volume, 45
 Stability, of floating bodies, 36
 of submerged bodies, 33
 Stagnation pressure, in supersonic flow, 179
 effect of compressibility on, 72
 Starting vortex, 241
 Statics, 5, 15*ff.*
 Steady flow, definition of, 55
 Steady-flow equations for mass, energy, and momentum, 96

- Steering booster, 447-448
 Stokes' law, 185
 Stream function, 218*ff.*
 Stream tube, 55
 Streamline, 55
 Submerged bodies, 32-34
 Subsonic motion of a body, 162
 Sudden contraction, 153
 Sudden enlargement, 152
 Supersonic motion of a body, 163
 Surface, of discontinuity, 9
 free, of liquid at rest, 21
 Surface roughness, measurement of, 326
 Sweepback, 275
 Swift, H., 308
- T
- Taylor, G., 148
 Terminal velocity, of airplane, 258
 of sphere, 203
 Thermal conductivity of oil, 285
 Thermodynamics, first law of, 79
 Thoma, D., 358
 Thomsons' theorem, 232
 Thrust bearing, 290
 Time constant, 433
 Tollmien, W., 194
 Torque, 91
 Torque converter, analysis of, 410-412
 combined with coupling, 412
 description of, 409-410
 Torricelli, E., 69
 Torricelli's formula, 69
 Tower, B., 280
 Trailing vortex, 243
 Transfer function, 436-440
 Transition on a flat plate, 193
 Transition layer in a pipe, 138
 Transition temperature, 320
 Turbojet, 389
 advantages and limitations of, 395
 efficiency of, 391-394
 Turbulence in a pipe, 134*ff.*
 Turbulence mechanism, 144
 Turbulent boundary layer, on a flat plate,
 drag coefficient for, 192, 193
 thickness of, 192
 Turbulent core in a pipe, 138
 Two-dimensional flow, definition of, 59
- U
- Units, 102
 Uranium, 401
- V
- V-2 rocket, 401
 Velocity, critical, 6
 for leaving the earth, 400
 of sound, equations for, 117
 Velocity coefficient for a Venturi meter, 154
 Velocity distribution, in the entrance
 length of a pipe, 123
 in a pipe, laminar flow, 129
 turbulent flow, 143
 relation to shear stress, 129
 Velocity fluctuations in turbulent flow, 135
 Velocity potential, 230
 Venturi meter, 153
 Viscometer, capillary tube, 130
 Saybolt, 131
 Viscosity, definition of, 2
 of oil, 281
 of various fluids, 449-452
 Viscosity index, 283
 Vortex pair, 236
 Vortex ring, 237
 Vorticity (*see* Rotation)
- W
- Wall-velocity law for a turbulent flow, 138
 Wave length, 161
 Wear, 336
 Weight, specific, 15
 (*See also* Gravity force)
 Weisbach, J., 153
 Whirlpool, 77
 Windmill, 387
 Wulff, J., 330

